Convention on Long-range Transboundary Air Pollution

emep

Co-operative programme for monitoring and evaluation of the long-range transmission of air pollutants in Europe

STATUS REPORT 1/2016

Transboundary particulate matter, photo-oxidants, acidifying and eutrophying components

Status Report 1/2016

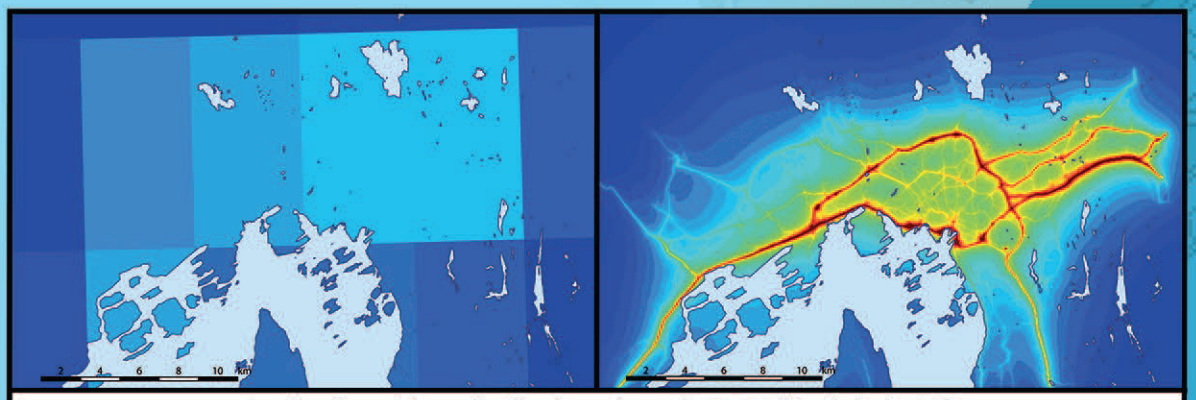

Application of the redistribution scheme "uEMEP" in Oslo for NO_2

msc-w & ccc & ceip

EMEP Report 1/2016
Date: September 13, 2016

METEOROLOGISK INSTITUTT
Norwegian Meteorological Institute

Transboundary particulate matter, photo-oxidants, acidifying and eutrophying components

EMEP/MSC-W:	Hilde Fagerli, Svetlana Tsyro, Bruce Rolstad Denby, Dirk Olivié, Ágnes Nyíri, Michael Gauss, David Simpson, Peter Wind, Anna Benedictow, Augustin Mortier, Jan Eiof Jonson, Michael Schulz, Alf Kirkevåg, Álvaro Valdebenito, Trond Iversen, Øyvind Seland, Heiko Klein
EMEP/CCC:	Wenche Aas, Anne-Gunn Hjellbrekke, Sverre Solberg, Richard Olav Rud, Kjetil Tørseth, Karl Espen Yttri
EMEP/CEIP:	Christine Brendle, Katarina Mareckova, Marion Pinterits, Sabine Schindlbacher, Melanie Tista, Bernhard Ullrich, Robert Wankmüller
CCE/RIVM:	Maximilian Posch
CNR-IMAA:	Lucia Mona
Stockholm University:	Juan-Camilo Acosta Navarro, Annica Ekman, Hans-Christen Hansson, Ilona Riipinen, Hamish Struthers, Vidya Varma

EMEP Status Report 2016; September 13, 2016

ISSN 1504-6109 (print)
ISSN 1504-6192 (on-line)

Executive Summary

This report presents the EMEP activities in relation to transboundary fluxes of particulate matter, photo-oxidants, acidifying and eutrophying components, with focus on results for 2014. It presents major results of the activities related to emission inventories, observations and modelling. The report also introduces specific relevant research activities addressing EMEP key challenges, as well as technical developments of the observation and modelling capacities.

Measurements and model results for 2014
In the first chapter, the status of air pollution in 2014 is provided, combining meteorological information with numerical simulations using the EMEP/MSC-W model together with observed air concentration and deposition data.

Altogether 36 Parties reported measurement data for 2014, from 164 sites in total. Of these, 129 sites reported measurements of inorganic ions in precipitation and/or main components in air, of which 72 sites had co-located measurements in both air and precipitation. The ozone network consisted of 138 sites, particulate matter was measured at 69 sites, of which 43 performed measurements of both PM_{10} and $PM_{2.5}$. In addition, 53 sites reported at least one of the of the components required in the advanced EMEP measurement program (level 2); however only 6 of these sites had a complete aerosol program and even fewer sites provided the required oxidant precursor measurements.

The EMEP/MSC-W model was run with meteorology and emissions data for 2014 (status run). In addition, two sets of model runs were performed; i) a 14-year trend run with meteorology and emissions data for the period 2000-2013 and ii) a 14-year climatology run using fixed 2014 emissions but varying meteorology for all the years 2000-2013. The 2014 results were then compared to the average of the climatology run and to the average of the trend run. This facilitates an assessment of how meteorology affected air pollution in 2014 and characterize the difference in the 2014 air pollution situation to the average of the 14 years before.

According to these calculations, meteorological conditions for the summer half-year of 2014 lead to average daily maximum ozone concentrations higher than the climatological mean by 1-3 ppb in parts of Russia, Norway and Spain. For Portugal and the south-eastern part of Europe, unusually low ozone levels were modelled, coinciding with lower spring/summer

temperatures. However, for most of Europe, the modelled ozone concentrations were only slightly different (ca 1 ppb) from the climatological mean. A comparison of the variations in the modeled ozone episodicity indicated that for large parts of Europe the meteorology of 2014 was generating fewer high ozone episodes than the mean meteorology (based on 2000-2013). Furthermore, when 2014 was compared to the average of the trend runs, taking into account both the variations in meteorology and emissions, only the easternmost part of the EMEP domain show higher concentrations. For most of the EMEP domain the average of daily maximum ozone concentrations were significantly lower than the 2000-2013 average. This indicates that for the last 15 years, the effect of reduced European precursor emissions is significantly more important for the ozone levels than the effect of interannual variations in meteorology.

The distribution of particulate matter concentrations in 2014, calculated by the EMEP/MSC-W model, shows large regional gradients across the EMEP domain, with the highest concentrations in the south and in some hotspot areas. Though the high PM in the south cannot be verified due to the lack of measurements, there is otherwise a relatively good agreement between the modelled and observed PM distribution. The modelled annual mean concentrations of PM_{10} and $PM_{2.5}$ were lower over central and southern Europe by 2-5 μg m^{-3} in 2014 compared to the average for the period 2000-2013. North European and Russian PM pollution were close to the average, while Ukraine, Turkey and EECCA experienced higher than average 2000-2013 PM levels. In addition to emission reductions during 2000-2013, the meteorological conditions in 2014, with enhanced precipitation, cloudy weather and positive temperature anomalies in winter in central Europe, contributed to improved air quality. In the rest of Europe, the meteorological conditions were less favourable in terms of PM pollution.

Modelled and observed annual mean concentrations were below both the EU limit values of 40 μg m^{-3} for the PM_{10} and the EU target value of 25 μg m^{-3} for $PM_{2.5}$, with the exception of the Po valley. No violations of the PM_{10} EU limit value were observed or calculated for daily concentrations at EMEP background sites, but there was a breach of the WHO air quality guidelines at 10 sites. For daily $PM_{2.5}$, violations of the WHO air quality guidelines were observed and calculated at more than half of the sites.

2014 appears to be a moderately polluted year in terms of the number of days with PM exceedances at the individual sites compared to the previous five years. Among the most prominent features of PM pollution in 2014 was a series of episodes in Central and Western Europe in the winter/early spring period.

A volcanic fissure at Holuhraun, Iceland, started at the end of August 2014 and continued for 6 months until the end of February 2015. Large amounts of SO_2 were emitted into the atmosphere (around 10,880 kt in 2014), which is more than 3 times the amount of anthropogenic SO_2 emissions from all the European Union countries for the year 2014. The volcanic eruption had episodically significant effects on SO_2 and SO_4^{2-} concentrations in air, as well as sulfur deposition in several countries, especially in Northern Europe.

Preliminary 2015 status runs have also been performed (using 2014 emissions) and are briefly presented in this report.

Status of emissions

Completeness and consistency of submitted emission data have improved significantly since EMEP started collecting information on emissions, and about 40 to 48 Parties report data regularly since 2010. In 2016, 45 out of 51 Parties (88%) submitted emission inventories. An improvement of reporting by EECCA countries has been observed in the last two years. However, the quality of submitted data differs significantly across countries, and the uncertainty in the data is considered relatively high. Furthermore, reporting of gridded data is still insufficient and covers less than 50% of the geographical EMEP domain. In total, only 29 countries reported sectoral gridded emissions for the main pollutants and PM for the year 2010.

The development in emissions in the eastern and western parts of the EMEP area seems to follow different patterns. Emissions in the western part of the EMEP area are slowly decreasing, while emissions in the east seem to fluctuate around the same level or even increase. The emissions in western parts of the EMEP area are almost entirely based on reported data, while the emissions in eastern parts often are based on so-called expert estimates (with larger uncertainty). From 2000 to 2014, the total change in emissions for the EMEP area has been: NO_x (-22%), NMVOCs (-22%), SO_2 (-23%), NH_3 (+18%), $PM_{2.5}$ (+5%), PM_{coarse} (+29%) and CO (-25%).

Ship emissions

A recent discussion with HELCOM about ship emission trends in the Baltic Sea has triggered further considerations in regard to ship emissions data sets available for air quality modelling. For international shipping emissions, EMEP/MSC-W has been using the TNO-MACC data set for 2011, i.e. no trends have been taken into account for the period since 2011. In the meantime, new emissions data have been generated by FMI based on AIS data (real ship movements tracked by the Automatic Identification System). The use of AIS data for air quality research is certainly welcome, but until now it is restricted by commercial data providers and maritime authorities, and it is not available for years before 2006. In addition, uncertainties remain on emission factors for different ship types, and on the practice of slow steaming in different European seas. Thus, also for this year's status and trend modelling EMEP/MSC-W has used TNO-MACC data for international shipping, but the question about which emission data to use will be further investigated during the second half of 2016.

Downscaling EMEP/MSC-W model results to urban resolution

There is a need for European wide exposure assessment at higher resolutions than the EMEP model is currently capable of simulating. Increasing resolution of the model down to $\sim$1-2 km would allow a more detailed assessment of urban background levels but is still not adequate for assessing exposure near emission sources, e.g. from traffic. In order to fill this gap an urban downscaling methodology, called 'uEMEP', is being developed. The methodology takes high resolution (50 m) proxy emission information from traffic, shipping and other sources and redistributes these using Gaussian dispersion theory. High resolution maps, that preserve the average EMEP model grid concentrations, provide detailed information on the sub-grid distribution. The methodology is explained and an example for the city of Oslo is provided. The results show a significant improvement against measurements in both spatial correlation and bias and provide a consistent methodology for detailed exposure assessment on the European scale.

Reduced European sulfur emissions unleashes the Arctic greenhouse warming
Using the advanced climate model NorESM1-M, the reduction of sulfate in Europe (EMEP region) between 1980 and 2005 is found to explain as much as about half of the warming observed in the Arctic during the same period. In other words, as a result of regulations on emissions in Europe to improve air quality and acidification of water and soils, a substantial portion of the dampening effect of aerosol particles has been removed, and consequently more of the actual warming of the Arctic due to increased greenhouse gas levels has emerged. Over continental Europe itself, however, the modeled warming due to the same regulations on European emissions is only a fifth of the observed warming. A redistribution of the energy input to the Arctic over the year appears to be a critical factor in explaining the stronger response in the Arctic.

Climate impact of the 2012 revision of the Gothenburg Protocol
Whereas the expected improvements for human health and ecosystem protection from the 2012 revision of the Gothenburg Protocol have been described elsewhere, we here describe the impact on climate. Three different emission scenarios for Europe were chosen as a basis for our study; a base 2005 scenario, the Gothenburg (GP) 2020 scenario and a 2020 Current Legislation (CLE) scenario. First, European emissions were combined with Europe-specific radiative forcing efficiencies for SO_2, NO_2, CO, VOC, BC, OC, and NH_3 emissions in order to generate the radiative forcing for the different scenarios. Secondly, regional response coefficients (expected temperature change in a specific region from forcing in the same or a different region) multiplied by the climate sensitivity were used to generate the temperature impact of the 3 different scenarioes for different regions. For 2005, we estimate that the European emissions cause a cooling of around –0.1 K both in the Arctic and northern mid-latitudes. In the 2020 GP scenario, the cooling in the northern mid-latitudes is halved, and even more reduced in the Arctic (–0.03 K). Due to the stronger emission reductions in the 2020 CLE scenario compared to the 2020 GP scenario, the net cooling is even more reduced in the 2020 CLE scenario; around one third of the 2005 value. The results obtained here are in line with the results of the study described in the previous subsection, i.e., that regulations of emissions in Europe to improve air quality and protect ecosystems will likely lead to a reduction of the cooling component, emphasizing the importance and urgency of rapidly reducing greenhouse gas emissions in order to mitigate further climate change.

Model improvements
A number of additional technical improvements and updates of the EMEP/MSC-W model have been carried out during 2015-2016. In order to implement GNFR sectors (which will be the standard used in the EMEP/MSC-W $0.1^\circ \times 0.1^\circ$ model calculations from next year onwards), and to generally allow for more flexibility, a new interface defining the mapping between sectors and classes has been implemented. This also allows the definitions of new classes for release height, timefactors and splits that can be assigned to specific sectors. Several modifications that affect aerosol production/modelling have been implemented; e.g. modification of the sea salt parametrisation, changes in the standard aerosol surface area and uptake rates, dust boundary conditions and an update of the split of particulate matter into elemental carbon, organic matter and the remainder. Furthermore, biogenic emissions of dimethyl sulphide (DMS) have been updated. Rather than being prescribed, DMS emissions are now calculated dynamically during the model calculation and vary with meteorological conditions.

Evaluation of vertical aerosol profiles

Providing valuable information on aerosol profiles, lidar measurements offer new possibilities for model evaluation. In this report, we present a comparison of EMEP/MSC-W model calculations to lidar measured aerosol extinction and backscatter profiles for the year 2012. A specific focus has been put on the period of the EMEP/ACTRIS dust campaign in June-July 2012, for which we could additionally evaluate the model for Saharan dust events. The model results are found to be closer to lidar observations in the mid-troposphere (between 3 and 6 km) than at the layers below and above. Also, the agreement between the model and lidar measurements was better for backscatter than for extinction, which is partly due to the larger dataset and better vertical resolution.

Development in the monitoring network and database infrastructure

The last chapter of the report presents the implementation of the EMEP monitoring strategy and general development in the monitoring programme including data submission. There are large differences between Parties in the level of implementation, as well as significant changes in the national activities during the period 2000-2014. With respect to the requirement for level 1 monitoring, 40% of the Parties have had an improvement since 2005, while 35% have reduced the level of monitoring. For level 2 monitoring there has been a general positive development in recent years. However, in large parts of Europe the implementation of the EMEP monitoring strategy is still unsatisfactory.

The complexity of data reporting has increased the latter years. To improve the quality and timeliness of data reporting a new online data submission and validation tool has been developed, which was launched in spring 2016. Along with the submission tool, new templates for reporting of surface ozone, NOx, VOC and aerosols have been developed.

Acknowledgments

This work has been funded by the EMEP Trust Fund.

The development of the EMEP/MSC-W model has also been supported by the EU FP7 projects MACC-II/MACC-III and PANDA, the Nordic Council of Ministers, the Norwegian Space Centre and the Norwegian Ministry of the Environment, and the Swedish Strategic Research project MERGE.

The upgrade of the EBAS database platform is supported within the EBAS-Online project by the Norwegian Research Council, INFRA-208473. The Norwegian Ministry of Environment has contributed with additional funding to EMEP/CCC for their work mainly related to improve the data flow of advanced aerosol measurements.

The work presented here has benefited largely from the work carried out under the four EMEP Task Forces and in particular under TFMM.

A large number of co-workers in participating countries have contributed in submitting quality assured data. The EMEP centers would like to express their gratitude for continued good co-operation and effort. The institutes and persons providing data are listed in the EMEP/CCCs data report and identified together with the datasets in the EBAS database. For developing standardized methods and harmonization of measurements, the close co-operation with participants in the EU FP7 infrastructure project ACTRIS as well as with the Scientific Advisory Groups (SAGs) in WMO/GAW are especially appreciated.

Melissa Anne Pfeffer from the volcanic hazard team at the Icelandic Met Office is acknowledged for kindly providing us with the time series of plume height observations and the SO_2 emission rate measurements from the Holuhraun fissure eruption.

Chris Heyes and Zig Klimont from EMEP CIAM/IIASA are acknowledged for provision of emission data on EC/OC and helpful discussions and advice.

Dr. Hugo Denier van der Gon (TNO, Netherlands) and Dr. Jukka-Pekka Jalkanen (FMI, Finland) are acknowledged for valuable comments on the chapter on Emissions from International Shipping.

The Working Group on Effects and its ICPs and Task Forces are acknowledged for their assistance in determining the risk of damage from air pollution. The Coordination Center for Effects (CCE) and Jean Paul Hettelingh have provided the latest data on critical loads.

The work related to climate modelling has been supported by the Research Council of Norway through the EVA (grant 229771) project as well as NOTUR project “CPU time for EVA - Earth system modelling of climate Variations in the Anthropocene” (nn2345k) and NorStore project “Storage for EVA - Earth system modelling of climate Variations in the Anthropocene” (ns2345k).

The work on model comparison with EARLINET Lidar observations has been supported by the EU FP7 ACTRIS and ACTRIS-2 projects, as well as the Norwegian Research Council project AeroCom-P3, and has been carried out in a close cooperation with researches at the CIAO Observatory in Potenza, Italy.

This work has received support from the Research Council of Norway (Programme for Supercomputing) through CPU time granted at the super computers at NTNU in Trondheim, the University of Tromsø, and the University of Bergen. IT infrastructure in general was available through the Norwegian Meteorological Institute. The CPU time made available by the ECMWF to generate meteorology has been of crucial importance for this year’s status and source receptor calculations.

Contents

CHAPTER 1

Introduction

1.1 Purpose and structure of this report

The mandate of the European Monitoring and Evaluation Programme (EMEP) is to provide sound scientific support to the Convention on Long-range Transboundary Air Pollution (LRTAP), particularly in the areas of atmospheric monitoring and modelling, emission inventories, emission projections and integrated assessment. Each year EMEP provides information on transboundary pollution fluxes inside the EMEP area, relying on information on emission sources and monitoring results provided by the Parties to the LRTAP Convention.

The purpose of the annual EMEP status reports is to provide an overview of the status of transboundary air pollution in Europe, tracing progress towards existing emission control Protocols and supporting the design of new protocols, when necessary. An additional purpose of these reports is to identify problem areas, new aspects and findings that are relevant to the Convention. The progress according to the EMEP Workplan (UNECE 2016) is also reported here. Table 1.1 give an overview of which items in the workplan that the different chapters report on.

Table 1.1: Overview of items from the EMEP workplan 2016-2017 that chapters report progress on. Other chapters report results for the mandatory work.

Chapter	Workplan item
4	1.1.1.4
6	1.3.3
8	1.1.1.20
10	1.2.1

The present report is divided into four parts. Part I presents the status of transboundary air pollution with respect to acidification, eutrophication, ground level ozone and particulate matter in Europe in 2014 (and preliminary results for 2015). Part II summarizes research activities of relevance to the EMEP programme, while Part III deals with technical developments going on within the centres.

Appendices A-C in Part IV contain basic information on 2014 emissions and emission trends in form of tables, and country-to-country source-receptor matrices with calculations of the transboundary contributions to pollution in different countries for 2014. Appendix D describes the country reports which are issued as a supplement to the EMEP status reports.

Appendix E introduces the model evaluation report for 2014 (Gauss et al. 2016b) which is available online and contains time-series plots of acidifying and eutrophying components (Gauss et al. 2016c), ozone (Gauss et al. 2016a) and particulate matter (Tsyro et al. 2016). These plots are provided for all stations reporting to EMEP (with just a few exclusions due to data-capture or technical problems). This online information is complemented by numerical fields and other information on the EMEP website. The reader is encouraged to visit the website, `http://www.emep.int`, to access this additional information.

1.2 Definitions, statistics used

For sulphur and nitrogen compounds, the basic units used throughout this report are μg (S or N)/m^3 for air concentrations and mg (S or N)/m^2 for depositions. Emission data, in particular in some of the Appendices, is given in Gg (SO_2) and Gg (NO_2) in order to keep consistency with reported values.

For ozone, the basic units used throughout this report are ppb (1 ppb = 1 part per billion by volume) or ppm (1 ppm = 1000 ppb). At 20°C and 1013 mb pressure, 1 ppb ozone is equivalent to 2.00 μg m^{-3} .

A number of statistics have been used to describe the distribution of ozone within each grid square:

Mean of Daily Max. Ozone - First we evaluate the maximum modelled concentration for each day, then we take either 6-monthly (1 April - 30 September) or annual averages of these values.

SOMO35 - The Sum of Ozone Means Over 35 ppb is the indicator for health impact assessment recommended by WHO. It is defined as the yearly sum of the daily maximum of 8-hour running average over 35 ppb. For each day the maximum of the running 8-hours average for O_3 is selected and the values over 35 ppb are summed over the whole year.

If we let A_8^d denote the maximum 8-hourly average ozone on day d, during a year with N_y days (N_y = 365 or 366), then SOMO35 can be defined as:

$SOMO35 = \sum_{d=1}^{d=N_y} \max\left(A_8^d - 35 \text{ ppb}, 0.0\right)$

where the `max` function evaluates $\max(A-B,0)$ to $A-B$ for $A > B$, or zero if $A \leq B$, ensuring that only A_8^d values exceeding 35 ppb are included. The corresponding unit is ppb.days.

POD$_Y$ - Phyto-toxic ozone dose, is the accumulated stomatal ozone flux over a threshold Y, i.e.:

$$\text{POD}_Y = \int \max(F_{st} - Y, 0)\, dt \tag{1.1}$$

where stomatal flux F_{st}, and threshold, Y, are in nmol m^{-2} s^{-1}. This integral is evaluated over time, from the start of the growing season (SGS), to the end (EGS).

For the generic crop and forest species, the suffix gen can be applied, e.g. POD$_{Y,gen}$ (or $AF_{st}1.6_{gen}$) is used for forests. POD was introduced in 2009 as an easier and more descriptive term for the accumulated ozone flux. The definitions of AFst and POD are identical however, and are discussed further in Mills and Simpson (2010). See also Mills et al. (2011a) and Mills et al. (2011b).

AOT40 - is the accumulated amount of ozone over the threshold value of 40 ppb, i.e..

$$AOT40 = \int \max(O_3 - 40 \text{ ppb}, 0.0)\, dt$$

where the `max` function ensures that only ozone values exceeding 40 ppb are included. The integral is taken over time, namely the relevant growing season for the vegetation concerned. The corresponding unit are ppb.hours (abbreviated to ppb.h). The usage and definitions of AOT40 have changed over the years though, and also differ between UNECE and the EU. LRTAP (2009) give the latest definitions for UNECE work, and describes carefully how AOT40 values are best estimated for local conditions (using information on real growing seasons for example), and specific types of vegetation. Further, since O_3 concentrations can have strong vertical gradients, it is important to specify the height of the O_3 concentrations used. In previous EMEP work we have made use of modelled O_3 from 1 m or 3 m height, the former being assumed close to the top of the vegetation, and the latter being closer to the height of O_3 observations. In the Mapping Manual (LRTAP 2009) there is an increased emphasis on estimating AOT40 using ozone levels at the top of the vegetation canopy.

Although the EMEP/MSC-W model now generates a number of AOT-related outputs, in accordance with the recommendations of LRTAP (2009) we will concentrate in this report on two definitions:

AOT40$^{\mathbf{uc}}_{f}$ - AOT40 calculated for forests using estimates of O_3 at forest-top (uc: upper-canopy). This AOT40 is that defined for forests by LRTAP (2009), but using a default growing season of April-September.

AOT40$^{\mathbf{uc}}_{c}$ - AOT40 calculated for agricultural crops using estimates of O_3 at the top of the crop. This AOT40 is close to that defined for agricultural crops by LRTAP (2009), but using a default growing season of May-July, and a default crop-height of 1 m.

In all cases only daylight hours are included, and for practical reasons we define daylight for the model outputs as the time when the solar zenith angle is equal to or less than 89°. (The proper UNECE definition uses clear-sky global radiation exceeding 50 W m^{-2} to define daylight, whereas the EU AOT definitions use day hours from 08:00-20:00.). In the comparison of modelled and observed AOT40$^{\text{uc}}_{f}$ in chapter 2, we have used the EU AOT definitions of day hours from 08:00-20:00.

The AOT40 levels reflect interest in long-term ozone exposure which is considered important for vegetation - critical levels of 3 000 ppb.h have been suggested for agricultural crops and natural vegetation, and 5 000 ppb.h for forests (LRTAP 2009). Note that recent UNECE workshops have recommended that AOT40 concepts are replaced by ozone flux estimates for crops and forests. (See also (Mills and Simpson 2010)).

This report includes also concentrations of particulate matter (PM). The basic units throughout this report are μg m^{-3} for PM concentrations and the following acronyms are used for different components to PM:

PBAP - primary biological aerosol particles describes airborne solid particles (dead or alive) that are or were derived from living organisms, including microorganisms and fragments of all varieties of living things (Matthias-Maser (1998)).

SOA - secondary organic aerosol, defined as the aerosol mass arising from the oxidation products of gas-phase organic species.

SIA - secondary inorganic aerosols, defined as the sum of sulphate (SO_4^{2-}), nitrate (NO_3^-) and ammonium (NH_4^+). In the EMEP/MSC-W model SIA is calculated as the sum: SIA= SO_4^{2-} + NO_3^-(fine) + NO_3^-(coarse) + NH_4^+.

SS - sea salt.

PPM denotes primary particulate matter, originating directly from anthropogenic emissions. One usually distinguishes between fine primary particulate matter, $PPM_{2.5}$, with dry aerosol diameters below 2.5 μm and coarse primary particulate matter, PPM_{coarse} with dry aerosol diameters between 2.5 μm and 10 μm.

$PM_{2.5}$ denotes fine particulate matter, defined as the integrated mass of aerosol with dry diameters up to 2.5 μm. In the EMEP/MSC-W model $PM_{2.5}$ is calculated as $PM_{2.5}$ = SO_4^{2-} + NO_3^-(fine) + NH_4^+ + SS(fine) + $PPM_{2.5}$ + 0.27 NO_3^-(coarse).

PM_{coarse} denotes coarse particulate matter, defined as the integrated mass of aerosol with dry diameters between 2.5μm and 10μm. In the EMEP/MSC-W model PM_{coarse} is calculated as PM_{coarse} = 0.33 NO_3^-(coarse)+ SS(coarse) + PPM_{coarse}.

PM_{10} denotes particulate matter, defined as the integrated mass of aerosol with dry diameters up to 10 μm. In the EMEP/MSC-W model PM_{10} is calculated as PM_{10} = $PM_{2.5}$+PM_{coarse}.

In addition to bias, correlation and root mean square the statistical parameter, index of agreement, are used to judge the model's agreement with measurements:

IOA - The index of agreement (IOA) is defined as follows (Willmott 1981, 1982):

$$IOA = 1 - \frac{\sum_{i=1}^{N}(m_i - o_i)^2}{\sum_{i=1}^{N}(|m_i - \bar{o}| + |o_i - \bar{o}|)^2} \tag{1.2}$$

where $\overline{o}$ is the average observed value. Similarly to correlation, IOA can be used to assess agreement either spatially or temporally. When IOA is used in a spatial sense, N denotes the number of stations with measurements at one specific point in time, and m_i and o_i are the modelled and observed values at station i. For temporal IOA, N denotes the number of time steps with measurements, while m_i and o_i are the modelled and observed value at time step i. IOA varies between 0 and 1. A value of 1 corresponds to perfect agreement between model and observations, and 0 is the theoretical minimum.

1.3 The EMEP extended domain

The EMEP domain defines the area where information on long-range transboundary air pollution is available from the EMEP centres. The information available concerns emissions, observations and modelling results. In 2007, the Steering Body adopted an extension of the EMEP domain to facilitate the inclusion of countries in Eastern Europe, Caucasus and Central Asia (EECCA) in the EMEP calculations (ref. ECE/EB.AIR/GE.1/2007/9). Thus, in 2008, the old 50×50 km^2 polar stereographic EMEP grid was extended from 132×111 to 132×159 grid cells, following Stage 1 in ECE/EB.AIR/GE.1/2007/9. In geographical projection this led to an eastward extension. The extended EMEP domain is presented in Figure 1.1.

One of the drawbacks of the current extended EMEP domain is that it only partly covers the Russian Federation. It is also recognized that results on air pollution in central Asian countries are highly dependent on sources outside the calculation domain. Countries in Central Asia are contiguous with other Asian countries, like China, India, Pakistan and Iran, that significantly affect pollution levels over the EECCA territories but are not included directly in the calculations. Consequently, the current EMEP modelling capacity for EECCA countries and the related grid domain is only an interim solution.

At the 36^{th} session of the EMEP Steering Body the EMEP Centres suggested to change the spatial resolution and projection of reported emissions from the 50×50 km^2 polar stereographic EMEP grid to $0.1^\circ \times 0.1^\circ$ longitude-latitude grid in a geographic coordinate system (WGS84). The new EMEP domain will cover the geographic area between 30°N-82°N latitude and 30°W-90°E longitude. This suggestion represents a balance between political needs, scientific needs and technical feasibility. Countries are invited to report in the new system as soon as possible (on voluntary basis), but latest in 2017.

The extension of the old EMEP domain made it necessary to introduce new codes for the new countries and areas now included in the extended EMEP domain. The new country codes and their rationale are explained below.

Kyrgyzstan and Tajikistan were not included in the old EMEP domain in any part. These two countries are now included with their full area inside the extended EMEP domain. For these two countries, following UNECE nomenclature, ISO2 country codes are used. The codes are 'KG' for Kyrgyzstan and 'TJ' for Tajikistan.

In the case of the Russian Federation and Kazakhstan, their respective ISO2 codes, 'RU' and 'KZ', previously referred to the parts of their territories inside the old EMEP domain. To keep new model results consistent and comparable with the previous ones, we have kept these ISO2 country codes and use them to define the same areas as before in the old EMEP domain. Additional codes are used to identify parts of these countries' territories outside the old EMEP grid.

For Kazakhstan, the area of the country in the extension of the EMEP domain is denoted by 'KZE', as shown in Figure 1.1 (a). The total territory of Kazakhstan in the extended EMEP domain is then the sum of 'KZ' and 'KZE', and is denoted as 'KZT' in this report (see Figure 1.1 (b)).

For the Russian Federation, the territory in the extension of the domain is divided into two parts, 'RUX' and 'RFE', as shown in Figure 1.1 (a). The reason for this division is that the area called 'RUX' ('EMEP external part of Russian Federation') has been used in the modelling domain previously, although it was not included in the old EMEP domain. The combined territory of the Russian Federation inside the extended EMEP domain is denoted by 'RUE', which stands for 'Russian Federation in the extended EMEP domain' and is presented

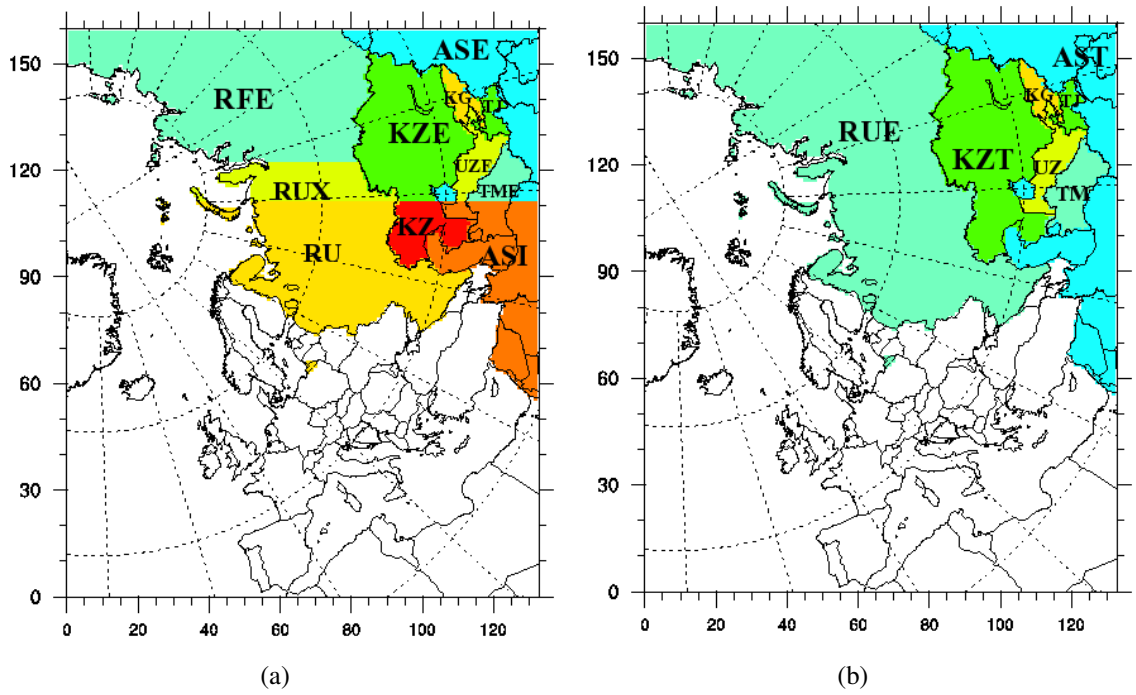

(a) (b)

Figure 1.1: Overview of the country/area codes in the extended EMEP domain. Panel (a) shows the previously defined areas in the old EMEP grid ('RU', 'KZ', 'ASI') together with the areas in the grid extension ('RUX', 'RFE', 'KZE', 'UZE', 'TME', 'TJ', 'KG', 'ASE'). Panel (b) shows the countries/areas with their codes in the extended EMEP grid ('RUE', 'KZT', 'UZ', 'TM', 'TJ', 'KG', 'AST').

in Figure 1.1 (b).

Until 2008 Turkmenistan and Uzbekistan were not included in the old EMEP domain as individual countries. However, parts of their territories were inside the old EMEP domain and included in the region called 'Remaining Asian Areas', denoted by country code 'ASI'. As indicated in Figure 1.1 (a), 'ASI' also includes Syria, Lebanon, Israel, parts of Iran, Iraq and Jordan. In the extended EMEP domain, the 'ASI' area has been redefined, and the areas of Turkmenistan and Uzbekistan inside the old 'ASI' have been extracted.

The territories of Turkmenistan and Uzbekistan in the domain extension are denoted by 'TME' and 'UZE', respectively, as in Figure 1.1 (a). The whole territories of Turkmenistan and Uzbekistan in the extended EMEP domain are the sum of the 'extended' and 'old' parts of the countries, namely the sum of 'TME' and 'TMO', and 'UZE' and 'UZO'. The respective ISO2 codes are 'TM' for Turkmenistan and 'UZ' for Uzbekistan.

The region code 'ASE' in Figure 1.1 (a) denotes Asian countries in the extension of the EMEP domain and includes parts of Afghanistan, India, Pakistan, China and Mongolia. The 'ASE' area together with those parts of 'ASI' which are left after the exclusion of the Turkmenistan and Uzbekistan territories forms 'AST' in Figure 1.1 (b) referring to all Asian areas in the extended EMEP domain.

Code	Country/Region
AL	Albania
AM	Armenia
ASI	Remaining Asian areas (old)
AST	Remaining Asian areas (extended)
AT	Austria
ATL	Remaining N.-E. Atlantic Ocean
AZ	Azerbaijan
BA	Bosnia and Herzegovina
BAS	Baltic Sea
BLS	Black Sea
BE	Belgium
BG	Bulgaria
BIC	Boundary and Initial Conditions
BY	Belarus
CH	Switzerland
CY	Cyprus
CZ	Czech Republic
DE	Germany
DK	Denmark
EE	Estonia
EMC	EMEP land areas (old)
EXC	EMEP land areas (extended)
ES	Spain
EU	European Union (EU28)
FI	Finland
FR	France
GB	United Kingdom
GE	Georgia
GL	Greenland
GR	Greece
HR	Croatia
HU	Hungary

Code	Country/Region
IE	Ireland
IS	Iceland
IT	Italy
KG	Kyrgyzstan
KZ	Kazakhstan (old)
KZT	Kazakhstan (extended)
LT	Lithuania
LU	Luxembourg
LV	Latvia
MD	Republic of Moldova
ME	Montenegro
MED	Mediterranean Sea
MK	The FYR of Macedonia
MT	Malta
NL	Netherlands
NO	Norway
NOA	North Africa
NOS	North Sea
PL	Poland
PT	Portugal
RO	Romania
RS	Serbia
RU	Russian Federation (old)
RUE	Russian Federation (extended)
SE	Sweden
SI	Slovenia
SK	Slovakia
TJ	Tajikistan
TM	Turkmenistan
TR	Turkey
UA	Ukraine
UZ	Uzbekistan

Table 1.2: Country/region codes used throughout this report:'old' refers to the area of the country/region which is inside the old EMEP grid domain, while 'extended' refers to the area of the country/region inside the extended EMEP grid domain.

1.4 Country codes

Many tables and graphs in this report make use of codes to denote countries and regions in the EMEP area. Table 1.2 provides an overview of these codes and lists the countries and regions included, with explicit mention whether the code refers to the official or the extended EMEP domain.

All 51 Parties to the LRTAP Convention, except four, are included in the analysis presented in this report. The Parties that are excluded of the analysis are: Canada and the United States of America, Monaco and Liechtenstein. Canada and USA are excluded because they lie

outside the EMEP domains, both the official and the extended domains. Monaco and Liechtenstein are excluded because their emissions and geographical extents are below the accuracy of the present source-receptor calculations in 50×50km^2.

Malta is introduced as a receptor country. However, the estimated emissions from Malta are below the accuracy limit of the source-receptor calculations and do not justify a separate study of Malta as an emitter country.

1.5 Other publications

This report is complemented by the country specific reports on the 2014 status of transboundary acidification, eutrophication, ground level ozone and PM (see Apendix D). Both English and Russian versions of the country reports are available to the twelve EECCA countries.

As noted above, time series plots of acidifying and eutrophying components (Gauss et al. 2016c), and ozone and NO_2 (Gauss et al. 2016a) have been made available online, at `www.emep.int` along with much other material.

A list of all associated technical reports and notes by the EMEP centres in 2015 (relevant for transboundary acidification, eutrophication, ozone and particulate matter) follows at the end of this section.

Peer-reviewed publications

The following scientific papers of relevance to transboundary acidification, eutrophication, ground level ozone and particulate matter, involving EMEP/MSC-W and EMEP/CCC staff, have become available in 2015:

Baker, L. H. , Collins, W. J., Olivié, D. J. L. , Cherian, R. , Hodnebrog, Ø., Myhre, G. , Quaas, J.: Climate responses to anthropogenic emissions of short-lived climate pollutants. Atmos. Chem. Phys.,15, 14, 8201-8216, 2015

Beekmann, M., Prévôt, A. S. H., Drewnick, F., Sciare, J., Pandis, S. N., Denier van der Gon, H. A. C., Crippa, M., Freutel, F., Poulain, L., Ghersi, V., Rodriguez, E., Beirle, S., Zotter, P., von der Weiden-Reinmüller, S.-L., Bressi, M., Fountoukis, C., Petetin, H., Szidat, S., Schneider, J., Rosso, A., El Haddad, I., Megaritis, A., Zhang, Q. J., Michoud, V., Slowik, J. G., Moukhtar, S., Kolmonen, P., Stohl, A., Eckhardt, S., Borbon, A., Gros, V., Marchand, N., Jaffrezo, J. L., Schwarzenboeck, A., Colomb, A., Wiedensohler, A., Borrmann, S., Lawrence, M., Baklanov, A., Baltensperger, U.: In-situ, satellite measurement and model evidence for the dominant regional contribution to fine particulate matter levels in the Paris Megacity. Atmos. Chem. Phys., 15, 9577-9591. DOI 10.5194/acp-15-9577, 2015.

Crenn, V., Sciare, J., Croteau, P. L., Verlhac, S., Fröhlich, R., Belis, C. A., Aas, W., Äijälä, M., Alastuey, A., Artiñano, B., Baisn ee, D., Bonnaire, N., Bressi, M., Canagaratna, M., Canonaco, F., Carbone, C., Cavalli, F., Coz, E., Cubison, M. J., Esser-Gietl, J. K., Green, D. C., Gros, V., Heikkinen, L., Herrmann, H., Lunder, C., Minguillón, M. C., Mocnik, G., O'Dowd, C. D., Ovadnevaite, J., Petit, J.-E., Petralia, E., Poulain, L., Priestman, M., Riffault, V., Ripoll, A., Sarda-Estève, R., Slowik, J. G., Setyan, A., Wiedensohler, A., Baltensperger, U., Prévôt, A. S. H., Jayne, J. T., Favez, O.: ACTRIS ACSM intercomparison - Part 1: Reproducibility of concentration and fragment results from 13 individual Quadrupole Aerosol Chemical Speciation Monitors (Q-ACSM) and consistency with co-located instruments. Atmos. Meas. Tech., 8, 5063-5087. DOI 10.5194/amt-8-5063, 2015.

Cuevas, E., Camino, C., Benedetti, A. , Basart, S. , Terradellas, E. , Baldasano, J. M. , Morcrette, J. J., Marticorena, B. , Goloub, P, Mortier, A., Berjon, A. , Hernandez, Y. , Gil-Ojeda, M. , Schulz, M.: The MACC-II 2007-2008 reanalysis: atmospheric dust evaluation and characterization over northern Africa and the Middle East. Atmos. Chem. Phys.,15, 8, 3991-4024, 2015

Dore, A. J., Carslaw, D. C., Braban, C., Cain, M., Chemel, C., Conolly, C., Derwent, R. G., Griffiths, S. J., Hall, J., Hayman, G., Lawrence, S., Metcalfe, S. E., Redington, A., Simpson, D., Sutton, M. A., Sutton, P., Tang, Y. S., Vieno, M., Werner, M., Whyatt, J. D.: Evaluation of the performance of different atmospheric chemical transport models and inter-comparison of nitrogen and sulphur deposition estimates for the UK. Atmos. Environ,119, 131-143, 2015

Eckhardt, S., Quennehen, B., Olivié, D. J. L., Berntsen, T. K., Cherian, R., Christensen, J. H., Collins, W., Crepinsek, S., Daskalakis, N., Flanner, M., Herber, A., Heyes, C., Hodnebrog, Ø., Huang, L., Kanakidou, M., Klimont, Z., Langner, J., Law, K. S., Lund, M. T., Mahmood, R., Massling, A., Myriokefalitakis, S., Nielsen, I. E., Nøjgaard, J. K., Quaas, J., Quinn, P. K., Raut, J.-C., Rumbold, S. T., Schulz, M., Sharma, S., Skeie, R. B., Skov, H., Uttal, T., von Salzen, K., and Stohl, A.: Current model capabilities for simulating black carbon and sulfate concentrations in the Arctic atmosphere: a multi-model evaluation using a comprehensive measurement data set. Atmos. Chem. Phys., 15, 16, 9413-9433, 2015, doi:10.5194/acp-15-9413-2015

Eskes, H., Huijnen, V., Arola, A., Benedictow, A., Blechschmidt, A.-M., Botek, E., Boucher, O., Bouarar, I., Chabrillat, S., Cuevas, E., Engelen, R., Flentje, H., Gaudel, A., Griesfeller, J., Jones, L., Kapsomenakis, J., Katragkou, E., Kinne, S., Langerock, B., Razinger, M., Richter, A., Schultz, M., Schulz, M., Sudarchikova, N., Thouret, V., Vrekoussis, M., Wagner, A., and Zerefos, C.: Validation of reactive gases and aerosols in the MACC global analysis and forecast system. Geosci. Model Dev., 8, 3523-3543, doi:10.5194/gmd-8-3523-2015, 2015.

Fowler, D., Steadman, C. E., Stevenson, D., Coyle, M., Rees, R. M., Skiba, U. M., Sutton, M. A., Cape, J. N., Dore, A. J., Vieno, M., Simpson, D. Zaehle, S., Stocker, B. D., Rinaldi, M., Facchini, M. C., Flechard, C. R., Nemitz, E., Twigg, M., Erisman, J. W., Butterbach-Bah, K. and Galloway, J. N.: Effects of global change during the 21st century on the nitrogen cycle. Atmos. Chem. Phys.,, 15, 13849-13893, 2015

Fröhlich, R., Crenn, V., Setyan, A., Belis, C. A., Canonaco, F., Favez, O., Riffault, V., Slowik, J. G., Aas, W., Äijälä, M., Alastuey, A., Artiñano, B., Bonnaire, N., Bozzetti, C., Bressi, M., Carbone, C., Coz, E., Croteau, P. L., Cubison, M. J., Esser-Gietl, J. K., Green, D. C., Gros, V., Heikkinen, L., Herrmann, H., Jayne, J. T., Lunder, C. R., Minguillón, M. C., Mocnik, G., O'Dowd, C. D., Ovadnevaite, J., Petralia, E., Poulain, L., Priestman, M., Ripoll, A., Sarda-Estève, R., Wiedensohler, A., Baltensperger, U., Sciare, J., Prévôt, A. S. H.: ACTRIS ACSM intercomparison - Part 2: Intercomparison of ME-2 organic source apportionment results from 15 individual, co-located aerosol mass spectrometers. Atmos. Meas. Tech., 8, 2555-2576. DOI 10.5194/amt-8-2555, 2015.

Garcia-Gomez, H., Garrido, J. L., (Vivanco, M. G., Lassaletta, L., Rabago, I.), Avila, A., Tsyro, S., Sanchez, G., Gonzalez Ortiz, A., Gonzalez-Fernandez, I. , Alonso, R.: Nitrogen deposition in Spain: Modeled patterns and threatened habitats within the Natura 2000 network (vol 485, pg 450, 2014). Science of the Total Env. ,505, 1234-1234, 2015

Gauss, M., V. K. Arora, C. D. Koven, D. J. K. Olivié, O. A. Søvde, L. Höglund-Isaksson, T. R. Christensen, F.-J. Parmentier, and D. A. Plummer; Chapter 8: Modeling the climate response to methane, in AMAP Assessment 2015: Methane as an Arctic climate forcer. Arctic Monitoring and Assessment Programme (AMAP), Oslo, Norway, viii+139pp, 2015

van der Gon, H. A. C. D., Bergström, R. , Fountoukis, C. , Johansson, C. , Pandis, S. N. , Simpson, D., Visschedijk, A. J. H.: Particulate emissions from residential wood combustion in Europe revised estimates and an evaluation. Atmos. Chem. Phys.,15, 11, 6503-6519, 2015

Healy, R.M., Wang, J.M., Jeong, C.-H., Lee, A.K.Y., Willis, M.D., Jaroudi, E., Zimmerman, N., Hilker, N., Murphy, M.S., Eckhardt, S., Stohl, A., Abbatt, J.P.D., Wenger, J.C., Evans, G.J.: Light-absorbing properties of ambient black carbon and brown carbon from fossil fuel and biomass burning sources. J. Geophys. Res. Atmos., 120, 6619-6633. DOI 10.1002/2015JD023382, 2015

Jonson, J. E., Jalkanen, J. P., Johansson, L., Gauss, M., Denier van der Gon, H. A. C.: Model calculations of the effects of present and future emissions of air pollutants from shipping in the Baltic Sea and the North Sea. Atmos. Chem. Phys., 15, 783-798. DOI 10.5194/acp-15-783, 2015

Karl, M., Svendby, T., Walker, S.-E., Velken, A.S., Castell, N., Solberg, S.: Modelling atmospheric oxidation of 2-aminoethanol (MEA) emitted from post-combustion capture using WRF-Chem. Sci. Total Environ., 527-528, 185-202. DOI 10.1016/j.scitotenv.2015.04.108, 2015

Kiesewetter, G., Borken-Kleefeld, J. , Schopp, W., Heyes, C., Thunis, P., Bessagnet, B., Terrenoire, E., Fagerli, H., Nyiri, A., Amann, M.: Modelling street level PM10 concentrations across Europe: source apportionment and possible futures. Atmos. Chem. Phys.,15, 3, 1539-1553, 2015

Kong, X., Forkel, R., Sokhi, R.S., Suppan, P. Baklanov, A. Gauss, M. Brunner, D., Baro, R., Balzarini, A., Chemel, C., Curci, G., Jimenez-Guerrero, P., Hirtl, M., Honzak, L., Im, U.,Perez, J.L., Pirovano, G.,San Jose, R.,Schlunzen, K,H.,Tsegas, G.,Tuccella, P.,Werhahn, J., Zabkar, R., Galmarini , S.: Analysis of meteorology-chemistry interactions during air pollution episodes using online coupled models within AQMEII phase-2. Atmospheric Environment, 115, 527-540, DOI: 10.1016/j.atmosenv.2014.09.020 , 2015

Lacagnina, C., O. P. Hasekamp, H. Bian, G. Curci, G. Myhre, T. van Noije, M. Schulz, R. B. Skeie, T. Takemura, and K. Zhang: Aerosol single-scattering albedo over the global oceans: Comparing PARASOL retrievals with AERONET, OMI, and AeroCom models estimates. J. Geophys. Res. Atmos., 120, 9814-9836, 2015, doi:10.1002/2015JD023501.

Leip, A., Billen, G., Garnier, J., Grizzetti, B., Lassaletta, L., Reis, S., Simpson, D. , Sutton, M. A., de Vries, W., Weiss, F., and Westhoek, H.: Impacts of European livestock production: nitrogen, sulphur, phosphorus and greenhouse gas emissions, land-use, water eutrophication and biodiversity. Env. Research Letters, 2015, 10, 115004

de Leeuw, G. , Holzer-Popp, T., Bevan, S., Davies, W.H., Descloitres, J., Grainger, R.G. , Griesfeller, J. , Heckel, A., Kinne, S., Kluser, L. , Kolmonen, P., Litvinov, P., Martynenko, D. , North, P., Ovigneur, B., Pascal, N. , Poulsen, C. , Ramon, D. , Schulz, M., , Siddans, R., Sogacheva, L., Tanre, D. , Thomas, G.E. , Virtanen, T.H., Huene, W.V., Vountas, M , Pinnock, S.: Evaluation of seven European aerosol optical depth retrieval algorithms for climate analysis. Remote Sensing of Env. ,162, 295-315, 2015

Marécal, V., V.-H. Peuch, C. Andersson, S. Andersson, J. Arteta, M. Beekmann, A. Benedictow, R. Bergström, B. Bessagnet, A. Cansado, F. Chéroux, A. Colette, A. Coman, R. L. Curier, H. A. C. Denier van der Gon, A. Drouin, H. Elbern, E. Emili, R. J. Engelen, H. J. Eskes, G. Foret, E. Friese, M. Gauss, C. Giannaros, J. Guth, M. Joly, E. Jaumouillé, B. Josse, N. Kadygrov, J. W. Kaiser, K. Krajsek, J. Kuenen, U. Kumar, N. Liora, E. Lopez, L. Malherbe, I. Martinez, D. Melas, F. Meleux, L. Menut, P. Moinat, T. Morales, J. Parmentier, A. Piacentini, M. Plu, A. Poupkou, S. Queguiner, L. Robertson, L. Rouïl, M. Schaap, A. Segers, M. Sofiev, L. Tarasson, M. Thomas, R. Timmermans, Á. Valdebenito, P. van Velthoven, R. van Versendaal, J. Vira, and A. Ung: A regional air quality

forecasting system over Europe: the MACC-II daily ensemble production. Geosci. Model Dev., 8, 2777-2813, doi:10.5194/gmd-8-2777-2015, 2015.

Outten, S., P. Thorne, I. Bethke, Ø. Seland: Investigating the recent apparent hiatus in surface temperature increases: Part 1. Construction of two 30-member Earth System Model ensembles. JGR - Atmospheres, 120 , 8575-8596, 2015, DOI:10.1002/2015JD023859

Pausata, F.S.R., Grini, A., Caballero, R., Hannachi, A., Seland, Ø.: High-latitude volcanic eruptions in the Norwegian Earth System Model: the effect of different initial conditions and of the ensemble size. Tellus Series B-Chemical And Physical Meteorology, 67, 26728, 2015, DOI: 10.3402/tellusb.v67.26728

Salter, M. E., P. Zieger, J. C. Acosta Navarro, H. Grythe, A. Kirkevåg, B. Rosati, I. Riipinen, and E. Nilsson: An empirically derived inorganic sea spray source function incorporating sea surface temperature. Atmos. Chem. Phys., 15, 11047-11066, 2015, www.atmos-chem-phys.net/15/11047/2015/doi:10.5194/acp-15-11047-2015.

Sand, M. , Iversen, T. , Bohlinger, P. , Kirkevåg, A., Seierstad, I., Seland, Ø. , Sorteberg, A.: A Standardized Global Climate Model Study Showing Unique Properties for the Climate Response to Black Carbon Aerosols. Climatic Change,28, 6, 2512-2526, 2015

Schaap, M., Cuvelier, C., Hendriks, C., Bessagnet, B., Baldasano, J.M., Colette, A. , Thunis, P., Karam, D., Fagerli, H., Graff, A., Kranenburg, R., Nyiri, A., Pay, M.T., Rouïl, L, Schulz, M., Simpson, D., Stern, R., Terrenoire, E., Wind, P.: Performance of European chemistry transport models as function of horizontal resolution. Atm. Env. ,112, 90-105, 2015

Schultz, M.G., Akimoto, H., Bottenheim, J., Buchmann, B., Galbally, I.E., Gilge, S., Helmig, D., Koide, H., Lewis, A.C., Novelli, P.C., Plass-Dülmer, C., Ryerson, T.B., Steinbacher, M., Steinbrecher, R., Tarasova, O., Tørseth, K., Thouret, V., Zellweger, C.: The Global Atmosphere Watch reactive gases measurement network. Elem. Sci. Anth., 3, 000067, DOI 10.12952/journal.elementa .000067, 2015

Simpson, D., Bartnicki, J., Jalkanen, J.-P., Hansson, H.C. , Hertel, H.C, Langner, J., Pryor, S.C., Environmental Impacts - Atmospheric Chemistry, Ch. 15 (pp 267-289) in Second Assessment of Climate Change for the Baltic Sea Basin, Eds: the BACC II author team, Springer, Germany, ISSN 1862-0248 ISBN 978-3-319-16005-4 (eBook ISBN 978-3-319-16006-1), doe:10.1007/978-3-319-16006-1, 2015.

Stohl, A., Aamaas, B., Amann, M., Baker, L.H., Bellouin, N., Berntsen, T.K., Boucher, O., Cherian, R., Collins, W., Daskalakis, N., Dusinska, M., Eckhardt, S., Fuglestvedt, J.S., Harju, M., Heyes, C., Hodnebrog, Ø., Hao, J., Im, U., Kanakidou, M., Klimont, Z., Kupiainen, K., Law, K.S., Lund, M.T., Maas, R., MacIntosh, C.R., Myhre, G., Myriokefalitakis, S., Olivié, D., Quaas, J., Quennehen, B., Raut, J.-C., Rumbold, S.T., Samset, B.H., Schulz, M., Seland, Ø., Shine, K.P., Skeie, R.B., Wang, S., Yttri, K.E., Zhu, T.: Evaluating the climate and air quality impacts of short-lived pollutants. Atmos. Chem. Phys., 15, 10529-10566. DOI 10.5194/acp-15-10529, 2015

Sofiev, M., Berger, U., Prank, M., Vira, J., Arteta, J., Belmonte, J., Bergmann, K.-C., Chéroux, F., Elbern, H., Friese, E., Galan, C., Gehrig, R., Khvorostyanov, D., Kranenburg, R., Kumar, U., Marécal, V., Meleux, F., Menut, L., Pessi, A.-M., Robertson, L., Ritenberga, O., Rodinkova, V., Saarto, A., Segers, A., Severova, E., Sauliene, I., Siljamo, P., Steensen, B. M., Teinemaa, E., Thibaudon, M., and Peuch, V.-H.: MACC regional multi-model ensemble simulations of birch pollen dispersion in Europe. Atmos. Chem. Phys., 15, 8115-8130, doi:10.5194/acp-15-8115-2015, 2015.

Thorne, P., S. Outten, I. Bethke, Ø. Seland: Investigating the recent apparent hiatus in surface temperature increases: Part 2. Comparison of model ensembles to observational estimates: Investigating Recent Hiatus. JGR - Atmospheres, 120(17), 8597-8620. 2015, DOI:10.1002/2014JD022805

Tomasi, C., Kokhanovsky, A. A., Lupi, A., Ritter, C., Smirnov, A., O'Neill, N. T., Stone, R. S., Holben, B. N., Nyeki, S., Wehrli, C., Stohl, A., Mazzola, M., Lanconelli, C., Vitale, V., Stebel, K., Aaltonen, V., de Leeuw, G., Rodriguez, E., Herber, A. B., Radionov, V. F., Zielinski, T., Petelski, T., Sakerin, S. M., Kabanov, D. M., Xue, Y., Mei, L., Istomina, L., Wagener, R., McArthur, B., Sobolewski, P. S., Kivi, R., Courcoux, Y., Larouche, P., Broccardo, S., Piketh, S. J.: Aerosol remote sensing in polar regions. Earth Sci. Rev., 140, 108-157. DOI 10.1016/j.earscirev.2014.11.001, 2015

Watson, L., G. Lacressonnière, M. Gauss , M. Engardt, C. Andersson, B. Josse, V. Marécal, A. Nyiri , S. Sobolowski, G. Siour, R. Vautard: The impact of meteorological forcings on gas phase air pollutants over Europe. Atmospheric Environment, 119, 240-257, 2015.

Winiger, P., Andersson, A., Yttri, K.E., Tunved, P., Gustafsson, Ö.: Isotope-based source apportionment of EC aerosol particles during winter high-pollution events at the Zeppelin Observatory, Svalbard. Environ. Sci. Technol., 49, 11959-11966. DOI 10.1021/acs.est.5b02644, 2015.

Yttri, K. E., Schnelle-Kreis, J., Maenhaut, W., Abbaszade, G., Alves, C., Bjerke, A., Bonnier, N., Bossi, R., Claeys, M., Dye, C., Evtyugina, M., García-Gacio, D., Hillamo, R., Hoffer, A., Hyder, M., Iinuma, Y., Jaffrezo, J.-L., Kasper-Giebl, A., Kiss, G., López-Mahia, P. L., Pio, C., Piot, C., Ramirez-Santa-Cruz, C., Sciare, J., Teinilä, K., Vermeylen, R., Vicente, A., Zimmermann, R.: An intercomparison study of analytical methods used for quantification of levoglucosan in ambient aerosol filter samples. Atmos. Meas. Tech., 8, 125-147. DOI 10.5194/amt-8-125, 2015.

Associated EMEP reports and notes in 2016

Joint reports

Transboundary particulate matter, photo-oxidants, acidification and eutrophication components. Joint MSC-W & CCC & CEIP Report. EMEP Status Report 1/2016

EMEP/MSC-W model performance for acidifying and eutrophying components, photo-oxidants and particulate matter in 2014. Supplementary material to EMEP Status Report 1/2016

Joint TFMM & CCC & MSC-W & MSC-E report

Colette, A., Aas, W., Banin, L., Braban, C.F., Ferm, M., González Ortiz, A., Ilyin, I., Mar, K., Pandolfi, M., Putaud, J.-P., Shatalov, V., Solberg, S., Spindler, G., Tarasova, O., Vana, M., Adani, M., Almodovar, P., Berton, E., Bessagnet, B., Bohlin-Nizzetto, P., Boruvkova, J., Breivik, K., Briganti, G., Cappelletti, A., Cuvelier, K., Derwent, R., D'Isidoro, M., Fagerli, H., Funk, C., Garcia Vivanco, M., González Ortiz, A., Haeuber, R., Hueglin, C., Jenkins, S., Kerr, J., de Leeuw, F., Lynch, J., Manders, A., Mircea, M., Pay, M.T., Pritula, D., Putaud, J.-P., Querol, X., Raffort,V., Reiss, I., Roustan, Y., Sauvage, S., Scavo, K., Simpson, D., Smith, R.I., Tang, Y.S., Theobald, M., Tørseth, K., Tsyro, S., van Pul, A., Vidic, S., Wallasch, M., Wind, P., Air pollution trends in the EMEP region between 1990 and 2012, Joint Report of the EMEP Task Force on Measurements and Modelling (TFMM), Chemical Co-ordinating Centre (CCC), Meteorological Synthesizing Centre-East (MSC-E), Meteorological Synthesizing Centre-West (MSC-W), EMEP/CCC-Report 1/2016.

CCC Technical and Data reports

Anne-Gunn Hjellbrekke. Data Report 2014 Acidifying and eutrophying compounds and particulate matter, EMEP/CCC-Report 2/2016

Anne-Gunn Hjellbrekke and Sverre Solberg, Ozone measurements 2014, EMEP/CCC-Report 3/2016

Sverre Solberg, VOC measurements 2014, EMEP/CCC-Report 5/2016

Fabrizia Cavalli, Jean-Philippe Putaud, Karl Espen Yttri, Availability and quality of the EC and OC measurements within EMEP, including results of the sixth interlaboratory comparison of analytical methods for carbonaceous particulate matter within EMEP,EMEP/CCC-Report 6/2016

CEIP Technical and Data reports

Mareckova, K., Pinterits, M., Tista, M, Wankmüller, R. Inventory review 2016. Review of emission data reported under the LRTAP Convention and NEC Directive. Stage 1 and 2 review. Status of gridded and LPS data. EEA/CEIP Vienna. EMEP/CEIP Technical Report 1/2016

MSC-W Technical and Data reports

Gauss, M., Nyíri, Á., Benedictow, A. C., Klein, H. Transboundary air pollution by main pollutants (S, N, O_3) and PM in 2014, Country Reports. EMEP/MSC-W Data Note 1/2016

References

Gauss, M., Hjellbrekke, A.-G., and Solberg, S.: Ozone, Supplementary material to EMEP Status Report 1/2016, available online at www.emep.int, The Norwegian Meteorological Institute, Oslo, Norway, 2016a.

Gauss, M., Tsyro, S., Benedictow, A., Fagerli, H., Hjellbrekke, A.-G., Aas, W., and Solberg, S.: EMEP/MSC-W model performance for acidifying and eutrophying components, photo-oxidants and particulate matter in 2014., Supplementary material to EMEP Status Report 1/2016, available online at www.emep.int, The Norwegian Meteorological Institute, Oslo, Norway, 2016b.

Gauss, M., Tsyro, S., Fagerli, H., Benedictow, A. C., Hjellbrekke, A.-G., and Aas, W.: Acidifying and eutrophying components, Supplementary material to EMEP Status Report 1/2016, available online at www.emep.int, The Norwegian Meteorological Institute, Oslo, Norway, 2016c.

LRTAP: Mapping critical levels for vegetation, in: Manual on Methodologies and Criteria for Mapping Critical Loads and Levels and Air Pollution Effects, Risks and Trends. Revision of 2009, edited by Mills, G., UNECE Convention on Long-range Transboundary Air Pollution. International Cooperative Programme on Effects of Air Pollution on Natural Vegetation and Crops, updated version available at www.icpmapping.com/, 2009.

Matthias-Maser, S.: Primary biological aerosol particles: Their significance, sources, sampling methods and size distribution in the atmosphere, in: Atmospheric particles, edited by Harrison, R. M. and van Grieken, R., pp. 349–368, John Wiley & Sons, Chichester, 1998.

Mills, G. and Simpson, D.: The Mediterranean region, in: Transboundary acidification, eutrophication and ground level ozone in Europe. EMEP Status Report 1/2010, pp. 37–48, The Norwegian Meteorological Institute, Oslo, Norway, 2010.

Mills, G., Hayes, F., Simpson, D., Emberson, L., Norris, D., Harmens, H., and Büker, P.: Evidence of widespread effects of ozone on crops and (semi-)natural vegetation in Europe (1990-2006) in relation to AOT40- and flux-based risk maps, Global Change Biology, 17, 592–613, doi:10.1111/j.1365-2486.2010.02217.x, 2011a.

Mills, G., Pleijel, H., Braun, S., Büker, P., Bermejo, V., Calvo, E., Danielsson, H., Emberson, L., Grünhage, L., Fernández, I. G., Harmens, H., Hayes, F., Karlsson, P.-E., and Simpson, D.: New stomatal flux-based critical levels for ozone effects on vegetation, Atmos. Environ., 45, 5064 – 5068, doi:10.1016/j.atmosenv.2011.06.009, 2011b.

Tsyro, S., Gauss, M., and Hjellbrekke, A.-G.: PM10, PM2.5 and individual aerosol components, Supplementary material to EMEP Status Report 1/2016, available online at www.emep.int, The Norwegian Meteorological Institute, Oslo, Norway, 2016.

UNECE: 2016-2017 workplan for the implementation of the Convention., Tech. Rep. ECE/EB.AIR/133.Add.1, UNECE, URL https://www.unece.org/fileadmin/DAM/env/lrtap/ExecutiveBody/E_ECE_EB_AIR_133.Add.1.pdf, 2016.

Willmott, C. J.: On the validation of models, Physical Geography, 2, 184–194, 1981.

Willmott, C. J.: Some Comments on the Evaluation of Model Performance, Bulletin American Meteorological Society, 63, 1309–1313, doi:10.1175/1520-0477(1982)063<1309:SCOTEO>2.0.CO;2, 1982.

Part I

Status of air pollution

CHAPTER 2

Status of transboundary pollution in 2014

Hilde Fagerli, Sverre Solberg, Svetlana Tsyro, Ágnes Nyíri, Anna Benedictow, Wenche Aas, Anne-Gunn Hjellbrekke and Maximilian Posch

This chapter describes the status of transboundary air pollution in 2014. A short summary of the meteorological conditions for 2014 is presented and the EMEP network of measurements in 2014 is briefly described. Thereafter, the status of air pollution and exceedances in 2014, as well as changes with respect to previous years, is discussed. In the end, preliminary model calculations for 2015 are presented.

2.1 Meteorological conditions in 2014

The meteorological data to drive the EMEP/MSC-W air quality model have been generated by the Integrated Forecast System model (IFS) of the European Centre for Medium-Range Weather forecasts (ECMWF), hereafter referred to as the ECMWF-IFS model. In the meteorological community the ECMWF-IFS model is considered as state-of-the-art, and MSC-W have been using this model in hindcast mode to generate accurate meteorological reanalyses for the year to be studied (Cycle 40r1 is the modelversion used for the year 2014 model run. For other years see 2.2).

2.1.1 Temperature

The year 2014 was unusually warm in Europe, and globally it was reported as the warmest year on record by the World Meteorological Organisation (WMO 2015). Especially in winter, NOAA reported (Overland et al. 2014) that extremely high Arctic air temperatures was linked to a strong jet stream that sent warm air into northern Europe and at the same time kept temperatures low over large parts of Russia. Temperatures above normal have been reported for almost all months in winter, spring and autumn across northern, central and southeastern

Europe, which is the most characteristic of that year. Only Portugal reported close to normal temperatures throughout the year except for a few months.

A persistent weather pattern, dominated by a strong Icelandic low in the beginning of 2014, directed a southwesterly flow of subtropical air into Europe. Germany, France, Austria, Switzerland, Croatia, Portugal and Spain reported record warm temperatures in January and February. The flow of warm air reached Scandinavia and the European part of Russia in February, with unusually high temperatures in Norway, continuing into spring with the highest temperatures for March on record in parts of Sweden.

The high temperature anomalies throughout much of Europe and Russia in spring can be explained by blocking anticyclones over the UK and Scandinavia and a high pressure ridge over Europe. A north-south gradient was observed in spring with Denmark, Germany, Slovakia and Spain reported above average temperatures in March, while France, Italy, Austria, Hungary and Greece reported below average temperatures in May.

June started unusually cold in Sweden, Finland and in the European part of Russia, however temperatures gradually gradually rose through the summer resulting in a record warm July in Scandinavia and the second warmest August on record since 1939 in the European part of Russia. In the UK the temperatures were higher than normal in June and July, whereas August was colder than average. July was very warm in Germany, but cold in Italy, Spain and Portugal. Temperatures were also low in France and Portugal in August.

In Autumn temperature anomalies were divided along an east-west transect, with southwesterly flows bringing warm air into western Europe and a northwesterly flow of polar air masses bringing cold air to the European part of Russia. Higher than normal temperatures were reported in UK, Germany, France, Italy and Spain. October was the warmest on record since 1931 in Portugal.

Italy reported above average temperatures in November and record high temperatures in December, whereas Portugal and Spain reported low temperatures. In most of Europe 2014 ended warmer than normal in Europe, exept for the Iberian peninsula and Iceland.

2.1.2 Precipitation

WMO reported that the global precipitation in 2014 was close to average according to NOAA (WMO 2015), but with both regional and sesonal rainfall anomalies. The annual precipitation amount over Europe in 2014 was close to normal, except for dryer conditions in parts of northern and eastern Europe, eastern Spain and northwestern European Russia. Northwestern Europe, Portugal, northern Italy and the southeastern Europe had rainfall above normal. In Serbia, 2014 was the wettest on record since 1951 and in May excessive rain led to flooding in Serbia and in Bosnia and Herzegovina. In June, large parts of Bulgaria and Romania was experiencing heavy rainfall leading to severe floods in the eastern parts of these countries.

UK experienced the most stormy period in 20 years, with persistent heavy rainfall in January and February resulting in the wettest winter since 1910. The south-westerly flow led to foehn conditions in the Mediterranean area and above average precipitation was reported in Portugal, France, Croatia and Italy. On the other hand, Germany and eastern Europe experienced dry conditions in winter and spring, while Greece had rainfalls higher than normal in February, but less in January and March.

The previously dry, sunny months in the beginning of the year came to an end in May with low pressure systems over Germany. In the European part of Russia the summer was drier than normal. June and July was relatively dry in UK, but August was wet, and in northern Scotland

it was the wettest month on record since 1910. The Azores high in July allowed low pressure systems moving into the Mediterranean and central Europe, leading to frequent rainfall and above average precipitation reported over Italy, Germany and Greece. France reported the wettest July since 1959.August was close to normal, but with less than average precipitation over Italy. Germany, Greece and France was wetter than normal.

September was recorded as the driest month in UK since 1910 due to high pressure over northern Europe, but Turkey reported much above average precipitation. In October and November the Icelandic low was noticeable again and southwesterly flow brought rainstorms to western and southern Europe. Above average precipitation was registered across Serbia. France, UK, Portugal and Italy reported above normal rainfall in November. The year ended with little precipitation over most of Europe.

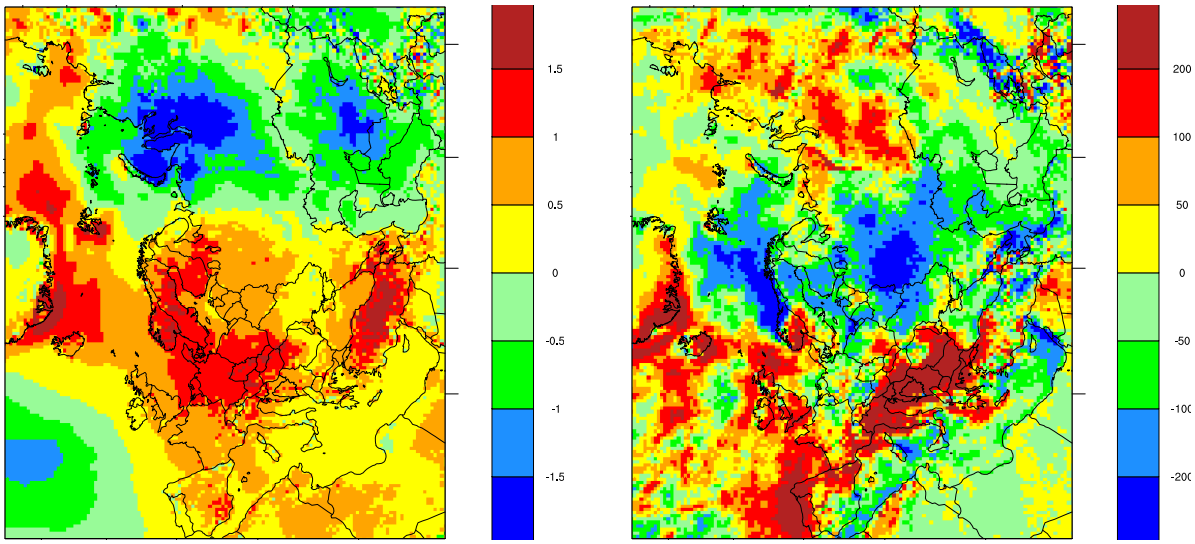

(a) Δtemperature at 2m (2014-climavg) (b) Δprecipitation (2014-climavg)

Figure 2.1: Meteorological conditions in 2014 compared to the 2000-2013 average (climavg) for: (a) Annual mean temperature at 2m [K] and (b) Annual precipitation [mm]

2.1.3 2014 compared to the 2000-2013 average

Particularities of the year 2014 appear clearer when compared to a multi-annual average. Here, the period 2000-2013 is the available climatological dataset (climavg) which is generated in a similar way as for the generation of 2014, using almost the same ECMWF-IFS model setup. Higher temperatures over northern, central and southeastern Europe in 2014 compared to the 2000-2013 average is clearly visible in Figure 2.1 (a). The 2014 summer months (April-September) compared to the 2000-2013 average in Figure 2.2 (a) show a cooler south and warmer north and east. Figure 2.2 (c) is showing that the 2014 winter months (January-March and October-December) divergence from the 2000-2013 average were very much influenced by the exceptionally warm weather pattern over Europe in March, but also the relatively warm winter and autumn had a large effect on the annual temperature. In Figure 2.1 (b) it is visible that southern and western Europe received larger amounts of precipitation compared to the 2000-2013 average. The 2014 summer months (April-September) compared to the 2000-2013 average in Figure 2.2 (b) show that southeastern Europe was very wet. Figure 2.2 (d)

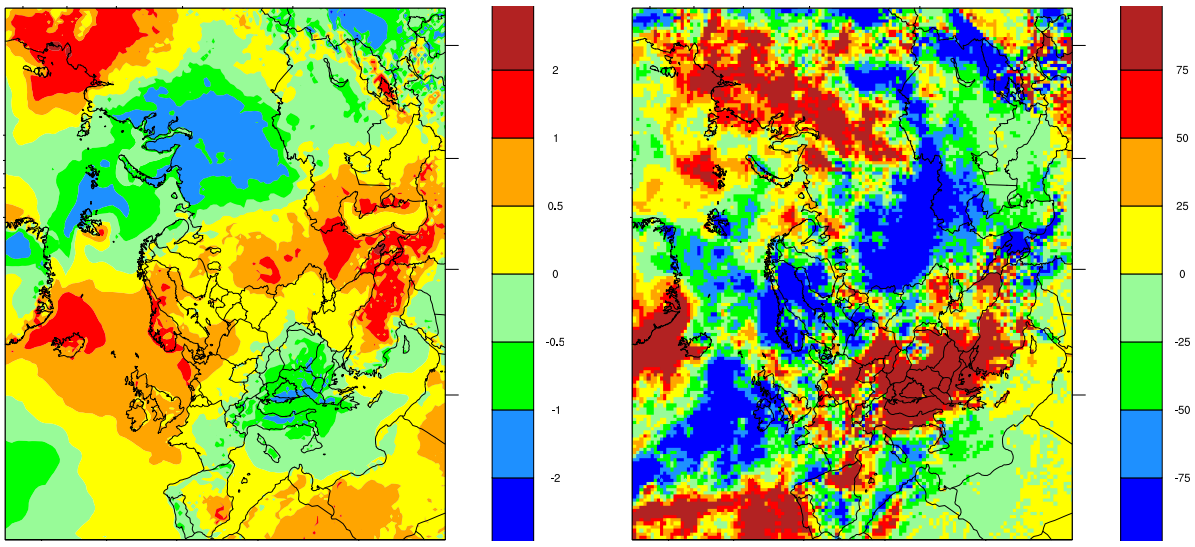

(a) Δtemperature at 2m (AprSep 2014-climavg) (b) Δprecipitation (AprSep 2014-climavg)

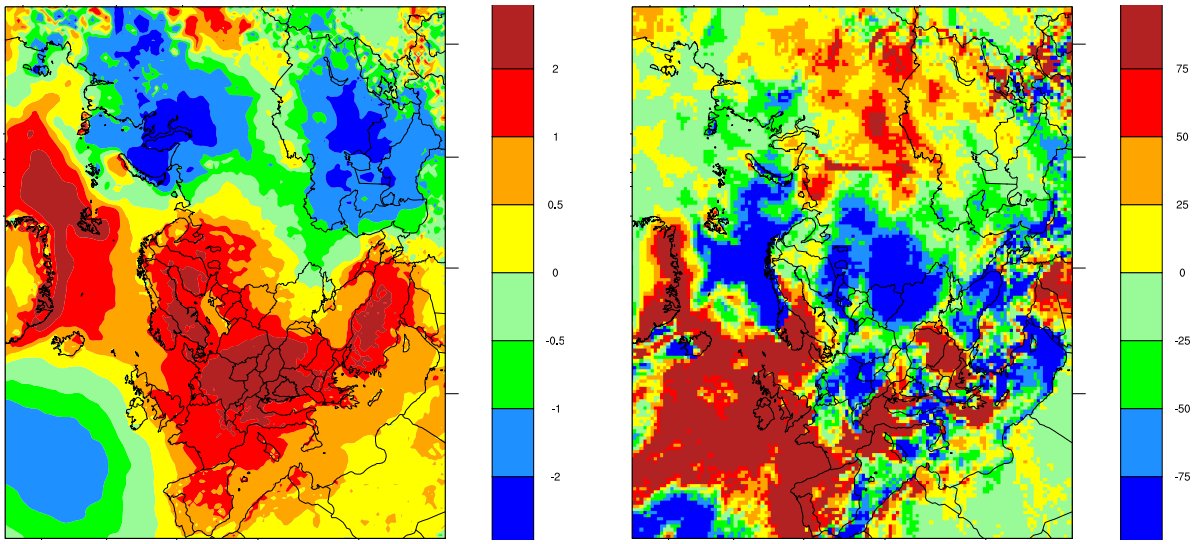

(c) Δtemperature at 2m (OctMar 2014-climavg) (d) Δprecipitation (OctMar 2014-climavg)

Figure 2.2: Meteorological conditions in 2014 compared to the 2000-2013 average (climavg) for: (a) Summer (April-September) temperature [K], (b) Summer (April-September) precipitation [mm], (c) Winter (January-March and October-December) temperature [K], (d) Winter (January-March and October-December) precipitation [mm]

is showing that the 2014 winter months (January-March and October-December) divergence from the 2000-2013 average precipitation was higher in western Europe, in the south of the European Alps and Bulgaria.

2.2 Measurement network 2014

In 2014, totally 36 Parties reported measurement data of inorganic components, particulate matter and/or ozone to EMEP, which is the relevant components for level 1 sites (UNECE

2009). In total 164 sites. All the data are available from the EBAS database (`http://ebas.nilu.no/`) and are also reported separately in technical reports by EMEP/CCC (Hjellbrekke 2016, Hjellbrekke and Solberg 2016). Figure 2.3 shows an overview of the spatial distribution of the sites reporting data for inorganic ions in air and precipitation, particulate matter and ozone in 2014. 129 sites reported measurements of inorganic ions in precipitation and/or main components in air; however not all of these sites were co-located as illustrated in Figure 2.3. 72 sites with measurements in both air and precipitation. The network of ozone measurements in EMEP included 138 sites.

There were 69 sites measuring either PM_{10} or $PM_{2.5}$ mass, 43 of these sites had measurements of both size fractions, which is recommended according to the EMEP Monitoring strategy (UNECE 2009). The stations measuring EMEP level 2 variables are shown in Figure 10.2. Compliance with the monitoring obligations, and the development of the programme the last decade discussed in Chapter 10.1.

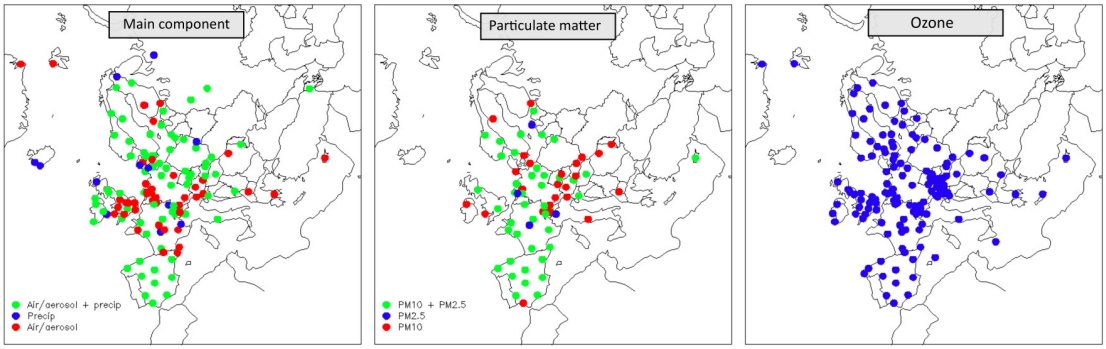

Figure 2.3: EMEP measurement network for main components (left), particulate matter (middle) and ozone (right) in 2014

2.3 Model setup for 2014 and overview of model runs

The EMEP/MSC-W model version rv4.9 has been used for the 2014 model runs and source receptor calculations presented in this report. The model is run in 50 km $\times$ 50 km resolution (from next year onwards, countries are requested to report emissions in the $0.1^\circ \times 0.1^\circ$ resolution, and the resolution of the standard status runs will change accordingly). Meteorology, emissions, boundary conditions and forest fires for 2014 have been used as input (for a description of these input data see Simpson et al. 2012). In addition, the SO_2 emissions from the Holuhraun eruption in 2014 are included (see section 3.6). For the first time, DMS emissions are created 'on-the-fly', e.g. they are meteorology dependent (see chapter 9). TNO/MACC ship emissions are available for 2000-2011, and for the years after 2011 (i.e. 2014) we apply 2011 ship emissions (see chapter 6 for a discussion about the ship emissions).

Whilst the 2014 run represents the best estimate for the year 2014 (Status2014), we have in addition performed a series of calculations that gives a 'climatological average' of 2014 (Clim2014). In these runs, we applied emissions, boundary conditions and forest fires for 2014, but meteorology was varied (14 different annual runs, representing meteorological conditions for 2000-2013). Also DMS is varying according to meteorology. The mean of these runs give an estimate of how the air pollution situation in 2014 would have been with

Acronym	Explanation
Status2014	Model run for 2014
Clim2014	Mean of 14 runs with meteorology for 2000-2013 All runs have emissions, boundary conditions and forest fires for 2014
Avg00-13	Mean of 14 runs with meteorology, emissions, boundary conditions and forest fires for respective years, 2000-2013.

Table 2.1: Overview of model runs.

Year	Version
2000–2007	IFS36r1
2012, 2013	IFS38r2
2008–2011, 2014	IFS40r1

Table 2.2: Overview of ECMWF model versions used for the different meteorological years

2000-2013 average meteorological conditions. The difference between the Status2014 and the Clim2014 results show how the specific 2014 meteorological situation affects the air pollution situation.

In addition, a set of runs for the years 2000-2013 were performed, using emissions, meteorology, boundary conditions and forest fires for the respective years. The mean of these 2000-2013 runs represent the average air pollution situation for the years 2000-2013 (Avg00-13). Comparing the Status2014 run with the Avg00-13 illustrates how different the air pollution situation is in 2014 compared to the average of the 14 years before. See table 2.1 for an overview of the model runs that are discussed in the following sections. Slightly different versions of the ECMWF meteorological has been used to create metetorology for the different years (Table 2.2).

2.4 Air pollution in 2014

2.4.1 Ozone

The ozone observed at a surface station is the net result of various physio-chemical processes; surface dry deposition and uptake in vegetation, titration by nearby NO_x emissions, regional photochemical ozone formation and atmospheric transport of baseline ozone levels, each of which may have seasonal and diurnal systematic variations. Episodes with elevated levels of ozone are observed during the summer half year when certain meteorological situations (dry, sunny, cyclonic stable weather) promote the formation of ozone over the European continent.

In Figure 2.4 (a) modelled and observed daily ozone max (averaged over the April- September period) is compared. Measurements from EMEP sites are put on top of the model fields as triangles. In general, the model reproduces the observed maximum ozone concentrations fairly well. A more detailed comparison between model and measurements for ozone for the year 2014 can be found in Gauss et al. (2016).

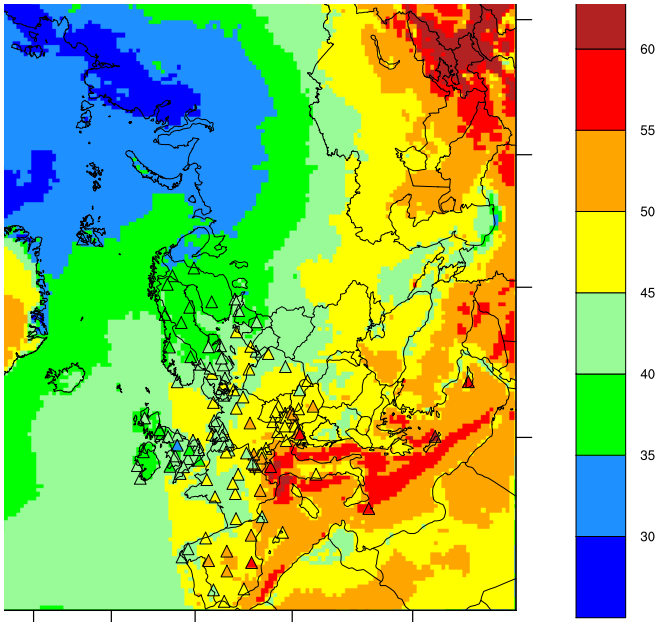

(a) Status2014

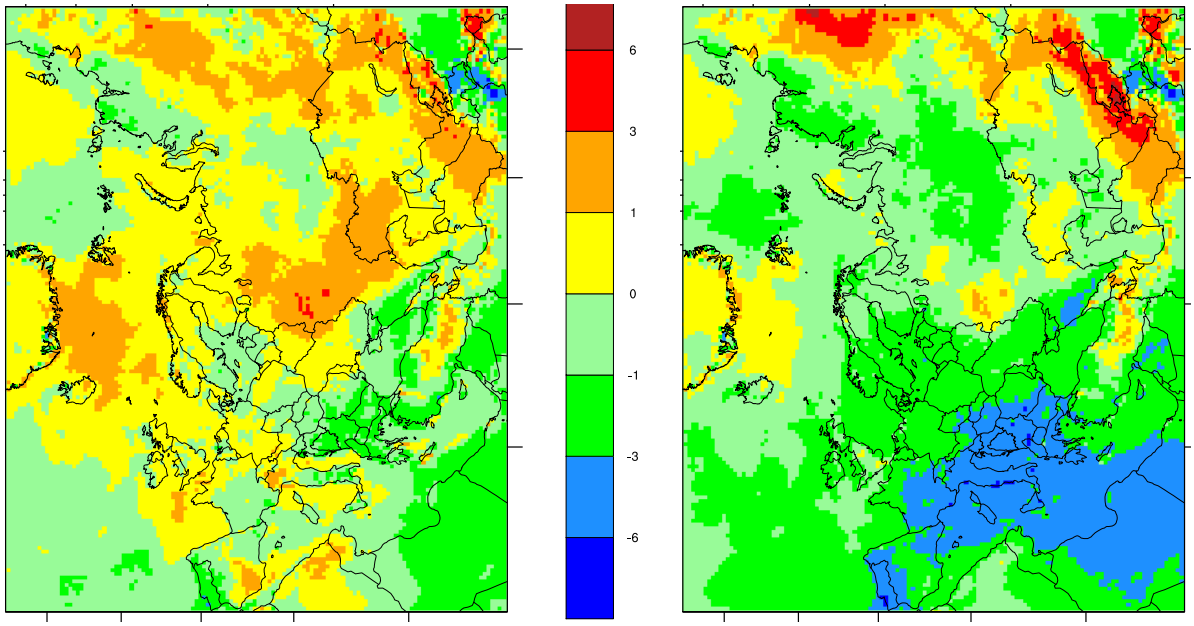

(b) Anomaly met

(c) Anomaly

Figure 2.4: Mean of daily maximum ozone concentrations for the period April-September. Status2014 = calculations for 2014 with observations on top (triangles), Anomaly met = Status2014 minus Clim2014, Anomaly = 2014 minus Avg00-13. [Unit: ppb]. Only data from sites situated below 1500 meter above sea level are shown. (Note that this map includes mountain sites which experience high O3 compared to the EMEP model's surface concentrations; underprediction is expected at such sites.)

Ozone in 2014 compared to the 2000-2013 climatology

The climatic conditions for the summer half year of 2014 described in section 2.1 are reflected in the anomaly of modelled ozone maximum concentrations due to different meteorological conditions in Figure 2.4 (b). Compared to the mean of the Clim2014 runs (see Table 2.1

for definition), the modelled ozone maximum concentrations in 2014 were higher by 1-3 ppb in parts of Russia, Norway and Spain. For Portugal and the south-eastern part of Europe, unusually low modelled ozone levels were modelled, coinciding with lower spring/summer temperatures. However, for most of Europe, the modelled ozone concentrations were only slightly different (ca 1 ppb) from the mean of the Clim2014 levels.

The seasonal mean of the daily maximum values as discussed above, will be strongly influenced by the ozone hemispheric baseline level. The metric consists of approximately 180 daily values, and the surplus of ozone stemming from photochemical reactions of European precursors varies substantially from day to day. Marked photochemical episodes leading to highly elevated ozone levels will typically occur on less than 10 % of these days. Thus, as a proxy for the year's episodicity and photochemical activity we calculated the 98 percentile of the maximum daily running 8h average ozone value (8h MDA) through the summer half year (April-September) for each year, separately. This metric corresponds approximately to the 4th highest 8h MDA which is a metric also used by the US-EPA.

These calculations were based on the Clim2014 scenario, i.e. using the same emissions each year with real varying meteorology. The purpose of this exercise was to single out the effect of the meteorology on ozone, i.e. to evaluate to what extent the ozone levels observed in 2014 could be attributed to a meteorology favourable or unfavourable for ozone formation.

We investigated the results for the ozone monitoring sites located below 1000 m asl and having data for at least 75 % of the years in the period 2000-2014. Figure 2.5 shows the results for each year in the period 2000-2014. The box and whiskers mark the spread in station data grouped into four regions for each year, separately. The overall mean value for the years 2000-2013, a proxy for the climatology prior to 2014, is shown by the red line for comparison. The following definition of areas were used in the station grouping:

NE : Norway, Sweden, Denmark, Finland, Estonia, Latvia, Lithuania

NW : UK, Ireland, Netherlands and Belgium

Central : Austria, Switzerland, Poland, Germany, Czech Rep., Slovakia, Hungary and France

South : Spain, Italy, Malta, Slovenia and Bulgaria

Figure 2.5 indicates that for the NE and NW sites, the meteorology of 2014 was a year where ozone levels were rather typical, although somewhat above normal for the NE sites and somewhat below normal for the NW sites. The spread and peaks in levels for the NW sites were particularly low in 2014. For the Central and South sites, however, the meteorology of 2014 was clearly unfavourable for ozone formation as compared to the climatology (2000-2013). For the Southern sites, the levels in 2014 were the lowest during the whole period 2000-2014. Based on this, we expect that the 2014 meteorology likely leads to lower ozone levels than normal in large parts of Europe, most pronounced in the southern and central areas. In the northwest (UK, BeNeLux etc) the meteorology would lead to somewhat lower peak values whereas slightly elevated levels would be expected in Scandinavia/Baltics. This refers to the effect of the meteorology alone. However, the effect of reduced anthropogenic emissions during the 2000-2014 period on ozone is expected to be larger than these meteorological effects.

When compared to the 2000-2013 average based on the standard runs with varying emissions (Figure 2.4 (c)), modelled mean ozone maximum concentrations for 2014 were 1-3 ppb

lower for most of Western Europe, and 3-6 ppb lower for the southernmost part of Europe. This is a much larger difference than given by the Clim2014 scenario (only meteorological variability), showing that the effect of reduced precursor emission is significantly stronger than the effect of the meteorology alone. During 2000 to 2014, NO_x and VOC emissions were reduced by 22% and 22% for the EMEP domain, although there are significant geographical differences (see Chapter 3).

It should be noted that the results for the most eastern areas are very uncertain, as information about emissions is limited (most countries do not report) and there are few measurements. The lack of informations about emissions and measurements makes it impossible to do a proper evaluation of the model results for these parts of the EMEP model, and the results should be interpreted with care.

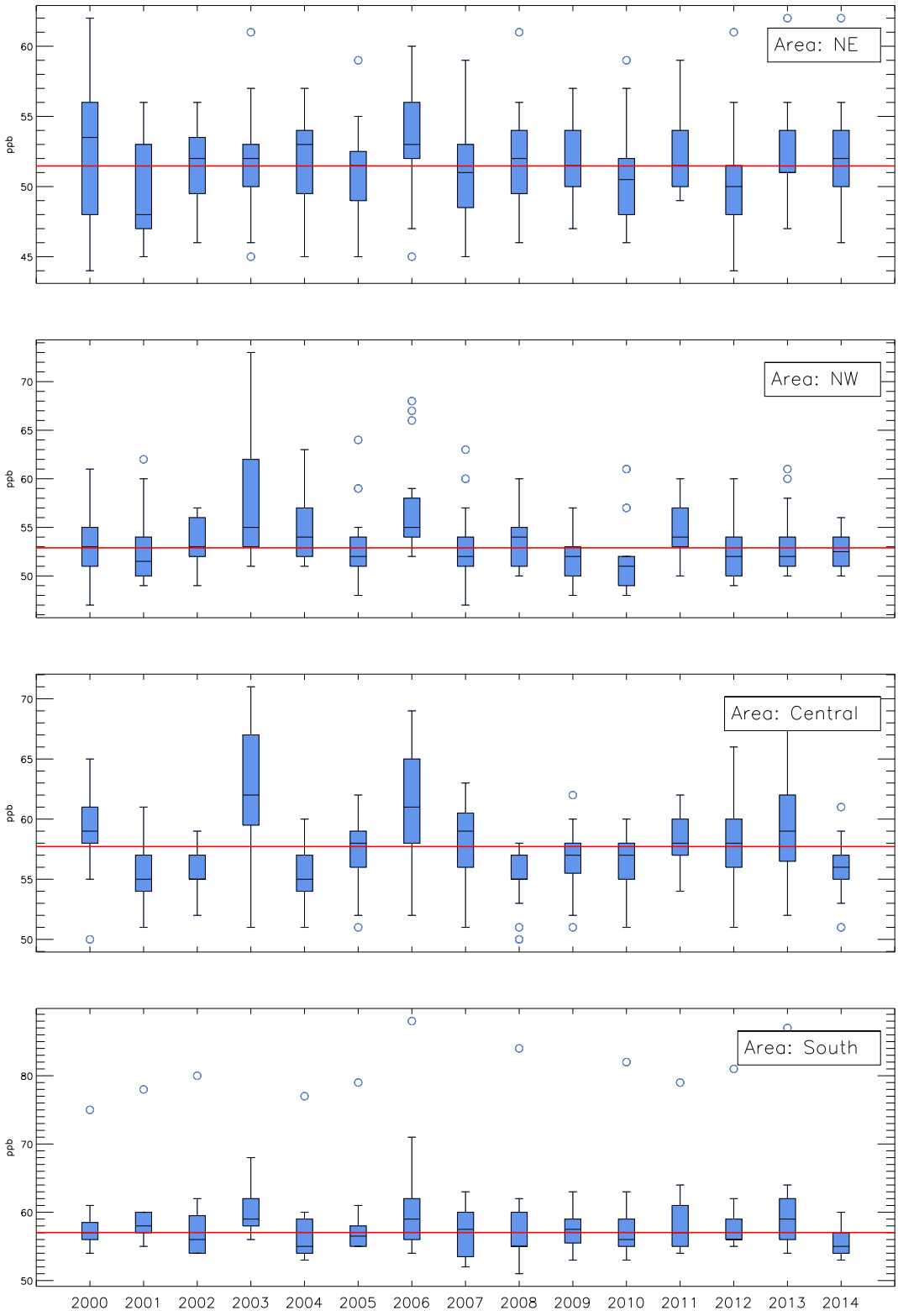

Figure 2.5: Box and whisker plots of the station-wise spread in the 98th percentile of the modelled 8h MDA based on the Clim2014 scenario. The boxes mark the 25th and 75th percentiles and the whiskers extend to the min and max or to 1.5 times the p25 and p75 if there are outliers. Outliers are marked with circles. The red line shows the mean of the annual medians for all years 2000-2013. The stations were grouped into four regions (see text for definition).

Ozone episodes in 2014

For this report, we performed a subjective identification of ozone episodes based on two criteria: Elevated ozone levels should be seen at a sufficient number of stations and, secondly, the episode should last for at least two consecutive days. More specifically, for each day of the year we calculated the daytime mean ozone value (based on the 9 hourly values from 09:00-18:00 UTC) for every monitoring site located below 1000 m asl. We neglected the mountain sites to reduce any bias due to vertical ozone gradients and to avoid problems relating these sites to model layers. We also neglected stations with less than 75% data capture the respective days. We then ended up with around 110 sites each day compared to a total of 138 ozone monitoring sites in 2014.

Then, for each day, we computed the 90th percentile of these approximately 110 values and if that percentile exceeded 65 ppb the day was classified as an episode day. When two or more consecutive days were classified as episode days, that period was defined as an ozone episode.

Based on this procedure, we identified only two episodes in 2014: 10-11 June and 18-19 July. Elevated ozone levels were also seen at many North European sites on 4 July and at a few Nordic sites 21-23 April, but none of these fulfilled the criteria stated above.

10-11 June

The observed and modelled daily max ozone levels for June 10-11 are shown in Figure 2.6. A high-pressure ridge was building up over central Europe from 8 June leading to warm southwesterly winds over the continent. This situation initiated an early heat wave with temperatures up to 35°C in several countries. Peak temperatures were observed on 10 June in most areas. A cold front was slowly approaching from the northwest and on 12-13 June colder air masses were replacing the heat wave in central Europe.

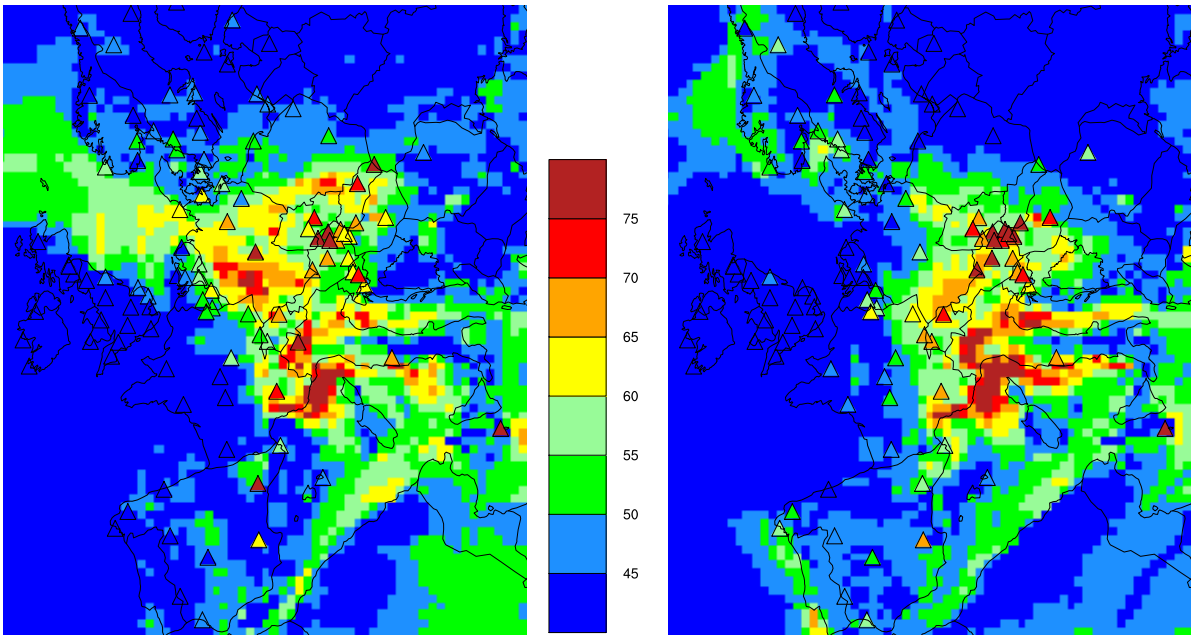

(a) 10/6 (b) 11/6

Figure 2.6: Modelled daily max ozone with measured values on top (triangles) for the episode 10-11 June 2014. [Unit: ppb].

Associated with this heat wave, surface ozone levels peaked in many areas. Illmitz (AT02) observed 97 ppb and Rigi (CH05) 94 ppb on 11 June as the highest values. Figure 2.6 shows the modelled daily maximum values for 10-11 June with the observed values on top. The model shows a band of high ozone stretching from SE France to N Germany on 10 June. On the following days the high ozone area was displaced to the south and located mostly over the Mediterranean area on the 13. When compared to the observations the model is seen to underestimate the ozone levels in the eastern part (Austria, Slovakia and Slovenia). Also for Malta, the observed levels were significantly higher than modelled.

18-19 July

The observed and modelled daily max ozone levels for July 18-19 are shown in Figure 2.7. An anticyclone over Scandinavia was gradually extending to the south during the middle of July. In southeast UK peak temperatures around 30°C were observed during 17-19 July and in Central Europe the temperature reached 30-35°C on 18-20 July. Peak ozone levels were observed on 18 July with 97 ppb at Sibton (GB39) and 85 ppb at De Zilt (NL91) as the highest values. On 19-20 July the ozone levels gradually dropped as the high pressure system weakened and colder air masses were transported in from west. The model results show a band of elevated ozone streching N-S from southern England to northern Italy on 18-19 July. Compared to the observations, a marked underestimation of the ozone levels in eastern parts of the continent (Czech Republic, Austria, Slovenia) is seen (Figure 2.7).

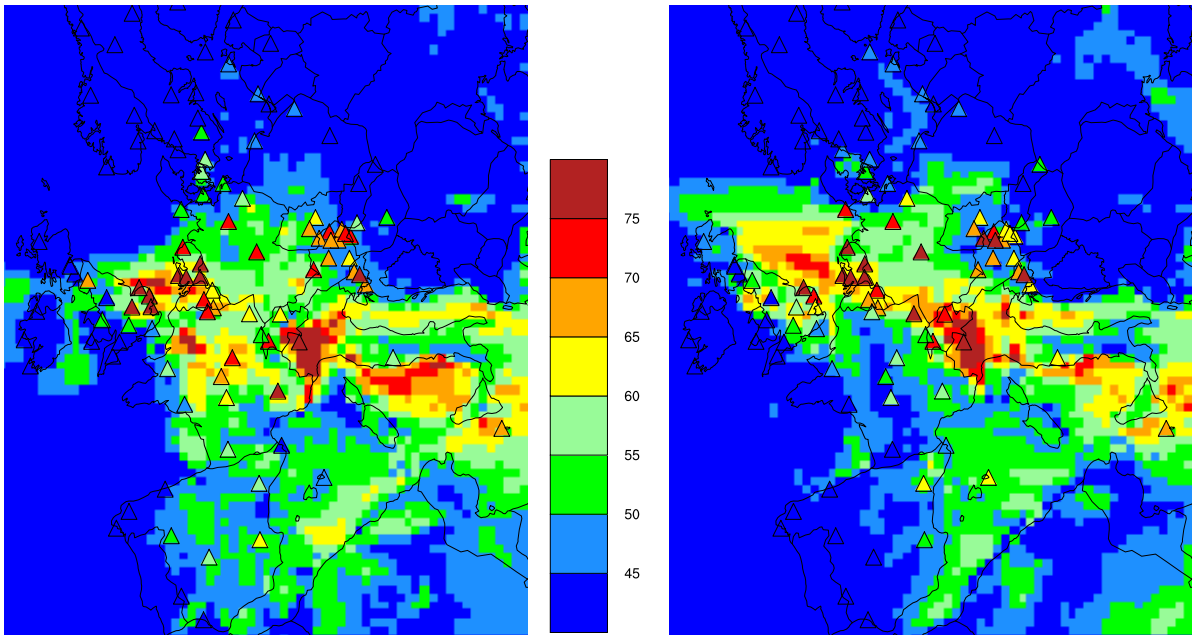

(a) 18/7 (b) 19/7

Figure 2.7: Modelled daily max ozone with measured values on top (triangles) for selected days for the episode 18-19 July 2014. [Unit: ppb].

Ozone Indicators

A number of ozone statistics (indicators) are used as a measure of the possible adverse effects on vegetation and humans. Guidelines set by WHO, EEA and UN-ECE are based on the peak

hourly concentrations, the daily max 8-hours running means, the Sum of Ozone Means Over 35 ppb (SOMO35), accumulation of hourly mean concentrations above a threshold of 40 ppb (AOT40) and the Phyto-toxic Ozone Dose above a threshold of Y (POD_Y) (see Chapter 1 for more information about the indicators). The two latter indicators are discussed further below.

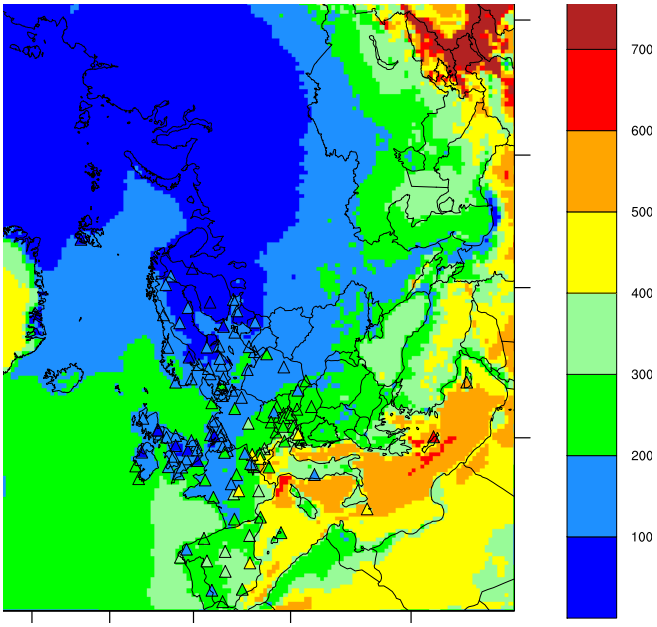

(a) Status2014

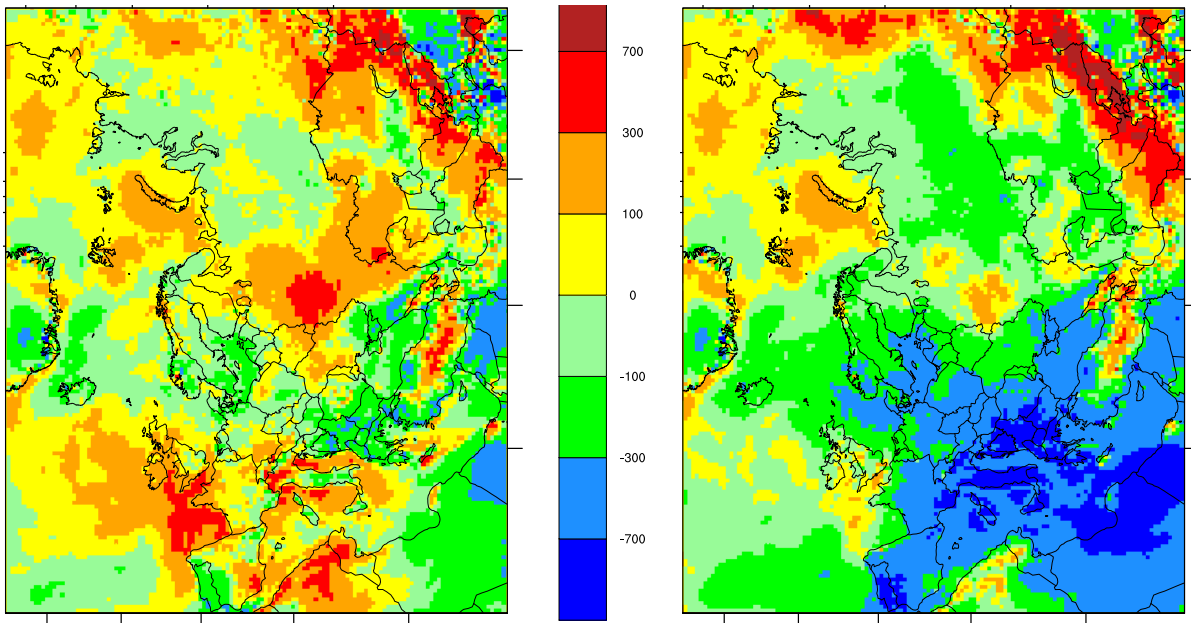

(b) Anomaly met

(c) Anomaly

Figure 2.8: SOMO35 [ppb.days]. Status2014 = calculations for 2014 with observations on top (triangles), Anomaly met = 2014 minus Clim2014, Anomaly = 2014 minus Avg00-13.Only data from sites situated below 1500 meter above sea level are shown. (As with Fig. 2.4, underpredictions are expected at some mountain sites.)

The SOMO35 map in Figure 2.8 shows a similar pattern as the maps of mean ozone maximum (Figure 2.4). Compared to the Clim2014 runs, most of Europe have SOMO35

close to the Clim2014 results, indicating that the meteorological conditions in 2014 did not lead to very large changes in this ozone metric. The exception is Portugal, parts of Spain and south-estern Europe (e.g. Greece and surronding countries), where the modelled SOMO35 was lower than Clim2014 by 100-300 ppb.days. Furthermore, Parts of Russia, Norway and Spain had SOMO35 100-300 ppb.days higher than the climatological average.

When the 2014 results are compared to SOMO35 results averaged over the years 2000-2013 (Figure 2.8), only the most easterly part of the EMEP domain show higher SOMO35 values. For most parts of Central and Southern Europe, SOMO35 is around 300-700 ppb.days lower in 2014 than the mean of the 2000-2013 period. These results reflect that overall high spring/summer ozone concentrations have been decreasing in the model calculations in this period due to emission reductions (except in the most eastern areas). As a consequence, the model predicts health impacts of ozone to be decreasing in Europe over the years 2000-2014.

Critical levels derived for the development of the Gothenburg Protocol were based on AOT40. Although AOT40 provided a simple first approach to mapping the risks of ozone damage to vegetation, newer approaches calculate the accumulated ozone flux via the stomatal pores of leaves; this uptake into the plant is considered to provide a more biologically sound method for describing observed effects. This parameter is the POD_Y (Mills et al. 2011b), which is calculated from modelling the effects of climate (temperature, humidity, light, soil mositure), plant development (growth stage), and in some cases ozone itself, on the extent of opening of the stomatal pores, and like AOT40 is accumulated over a threshold Y, in this case a stomatal flux with units of nmol m^{-2} s^{-1}.

In Figures 2.9-2.10 we present the indicators AOT40 and POD_1 for forest (see Chapter 1 for more information about the indicators). For deciduous forest trees (based upon beech, birch), a critical level of POD_1 of 4 mmol m^{-2} has been proposed Mills et al. (2011b). From Figure 2.10 it can be seen that the critical level of 4 mmol m^{-2} is exceeded in essentially all of Europe, indicating a clear risk of ozone damage to forests across the continent. As noted in previous work (Emberson et al. 2000, Simpson et al. 2007, Karlsson et al. 2009, Mills et al. 2011a) the geographical gradients of these flux-based ozone metrics are generally smaller than found for concentration based metrics such as AOT40.

Furthermore, whilst AOT40 basically just responds to changes in ozone (if ozone goes up, AOT40 goes up), POD_1 responds also to meteorology. Increasing ozone tends to increase POD_1, but changes in temperature, relative humidity or soil moisture might easily reduce POD_1. For instance, the hot and dry conditions that often promote high ozone concentrations are just those conditions where plants close their stomata to prevent water loss - thereby decreasing POD_1.

In addition to the maps of AOT40 and POD_1 for forests in Figures 2.9-2.10 we show the difference between the year 2014 and a 'climatological 2014'. AOT40 show a pattern that is very similar to the ozone maximum differences, with increase in the areas were the temperatures were particularly high during 2014. In contrast, POD_1 show a decrease for some of the same areas.

Both indicators are lower for 2014 compared to the mean of the 2000-2013 period for most of Europe. However, whilst the anomaly for AOT40 resembles the one for ozone maximum (Figure 2.4), the anomaly for POD_1 is more determined by the anomaly caused by different meteorological conditions.

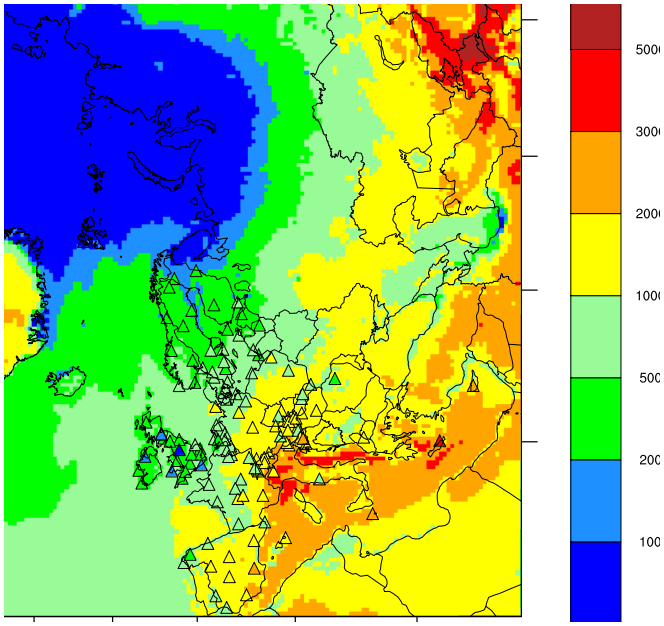

(a) Status2014

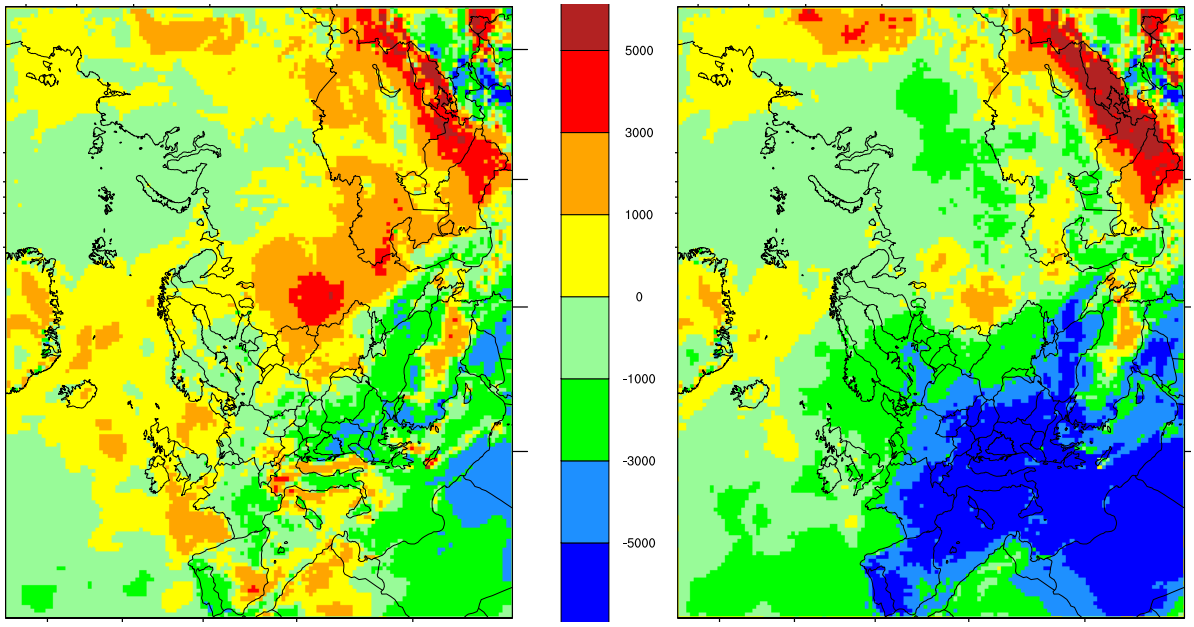

(b) Anomaly met

(c) Anomaly

Figure 2.9: AOT40 [ppb.hours] for forest. Status2014 = calculations for 2014, Anomaly met = 2014 minus Clim2014, Anomaly = 2014 minus Avg00-13. Only data from sites situated below 1500 meter above sea level are shown. (As with Fig. 2.4, underpredictions are expected at some mountain sites. Further, the modelled and observed AOT use somewhat different convenctions for daytime (08:00-20:00 UTC vs zenith angle criteria), but for most sites this difference is moderate.)

2.4.2 Particulate matter

Maps of annual mean concentrations of PM_{10} and $PM_{2.5}$ in 2014, based on concentrations calculated by the EMEP/MSC-W model and observed at EMEP monitoring network, are presented in Figure 2.11. The measured values are represented by colour triangles overlaying the

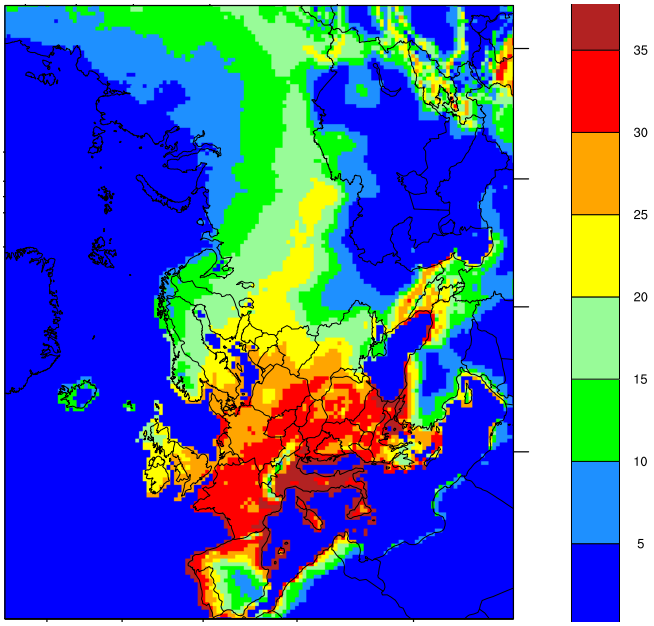

(a) Status2014

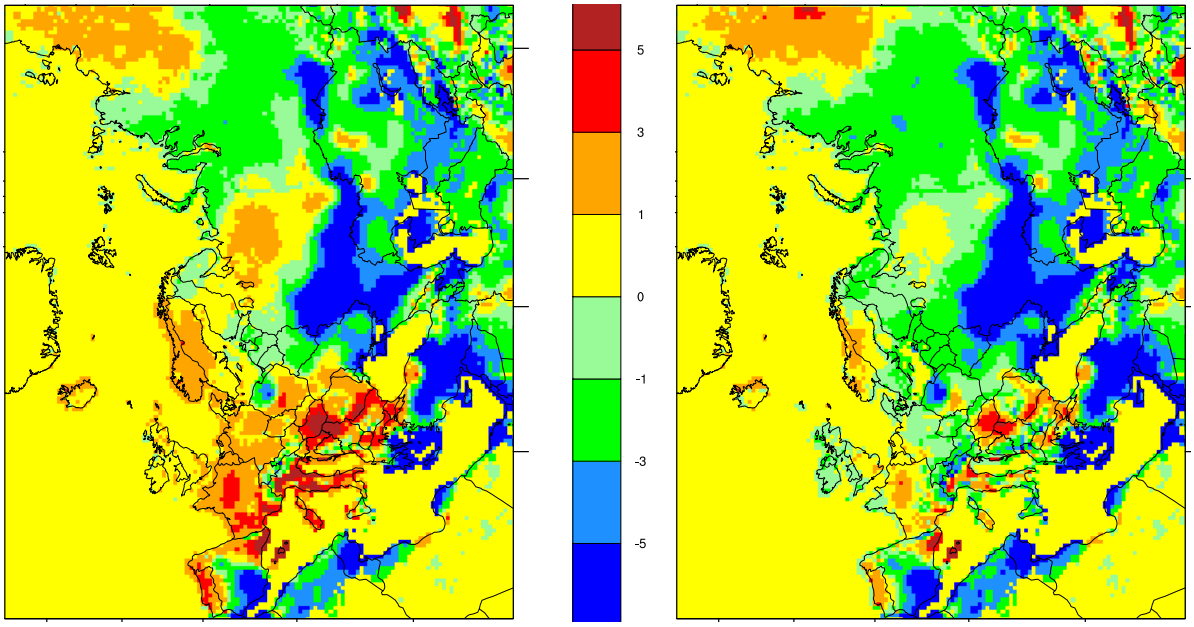

(b) Anomaly met

(c) Anomaly

Figure 2.10: POD_1 forest [mmol m^{-2}]. Status2014 = calculations for 2014, Anomaly met = 2014 minus Clim2014, Anomaly = 2014 minus Avg00-13.

modelled concentration fields.

There is a distinct north to south/south-east gradient in the annual mean levels of $PM_{2.5}$ and PM_{10} calculated with the model, which is also seen in the observational data. The modelled concentrations increase from 2-3 μg m^{-3} in the north of Europe to 10-15μg m^{-3} in the south. There are areas experiencing elevated PM_{10} and $PM_{2.5}$ levels (13-17μg m^{-3}), such as the Benelux countries, Germany and Poland, and a hotspot with calculated PM_{10} and $PM_{2.5}$ of 20-30μg m^{-3} is seen in the Po Valley. In the eastern parts of the EMEP domain and in the south,

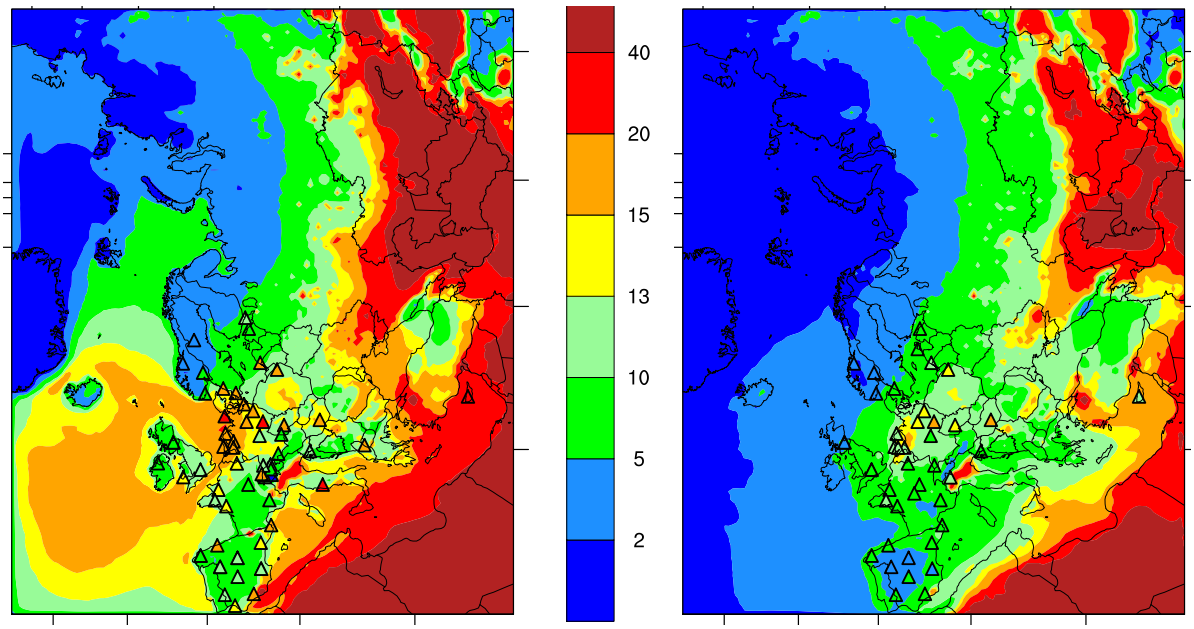

(a) PM_{10} [μg m^{-3}] (b) $PM_{2.5}$ [μg m^{-3}]

Figure 2.11: Annual mean concentrations of PM_{10} and $PM_{2.5}$ in 2014: calculated with the EMEP/MSC-W model (colour contours) and observed at EMEP monitoring network (colour triangles)

close to the African continent, the model calculates annual mean PM levels far in excess of 40μg m^{-3}. These values cannot be verified by observations, as there are no measurements available in these regions. There is a relatively good agreement between the modelled and observed distribution of mean PM_{10} and $PM_{2.5}$, with an annual mean correlation of 0.74, as documented in Gauss et al. 2016). The observations also show smaller scale PM gradients (e.g. within individual countries), which the model underestimates. The model underestimates the observed annual mean PM_{10} levels by 24% on average, whereas $PM_{2.5}$ the under-prediction is smaller, namely 13% (for comprehensive model evaluation see Gauss et al. 2016).

With the intention of characterizing the year 2014 in terms of the air pollution situation, two additional series of model runs have been performed for meteorological years from 2000 through 2013. As described in Table 2.1 in "Trend" runs, the emission data corresponding to each of the meteorological year are applied, whereas in the "Climatology" runs the 2014 emission data is used, the same as in the status run. The mean of the Trend runs (Avg00-13) characterizes the average pollution situation in the period 2000-2013, whereas the mean of the Climatology runs (Clim2014) indicates what the level of pollution in 2014 could have been under 14-years (2000-2013) average meteorological conditions. Thus, the comparison of calculated PM concentrations for 2014 (Stat2014) with Avg00-13 points to special features of PM pollution, resulting from the actual emissions and weather conditions in 2014, whereas the comparison of Stat2014 with Clim2014 gives an estimate of the effect of meteorological situation on PM air pollution in 2014.

The 2014 anomaly fields are quite similar for PM_{10} and $PM_{2.5}$ (upper and lower panels in Figure 2.12) and indicate cleaner than average conditions in the west/south-west and more polluted conditions in the east/south-east. The annual mean PM_{10} and $PM_{2.5}$ were in general lower by 2-5 μg m^{-3} in 2014 compared to Avg00-13 over France, Italy, the Balkan countries, Greece and parts of Germany and Spain (Figure 2.12 (a),(c)). The mean PM_{10} and $PM_{2.5}$

levels were quite close to Avg00-13 in the Nordic and Baltic countries, Poland and northern Germany, and also in most of Russia. In Ukraine, parts of Turkey and the remaining EECCA territory, 2014 PM_{10} and $PM_{2.5}$ levels exceeded the 2000-2013 average by 1-5 μg m^{-3}. Model results indicate that SIA was the main cause for the PM anomalies in 2014. The spatial distribution of Primary PM anomalies is similar to the total PM concentrations, except from higher than average levels in Scandinavia and Italy, but their contribution to PM_{10} and $PM_{2.5}$

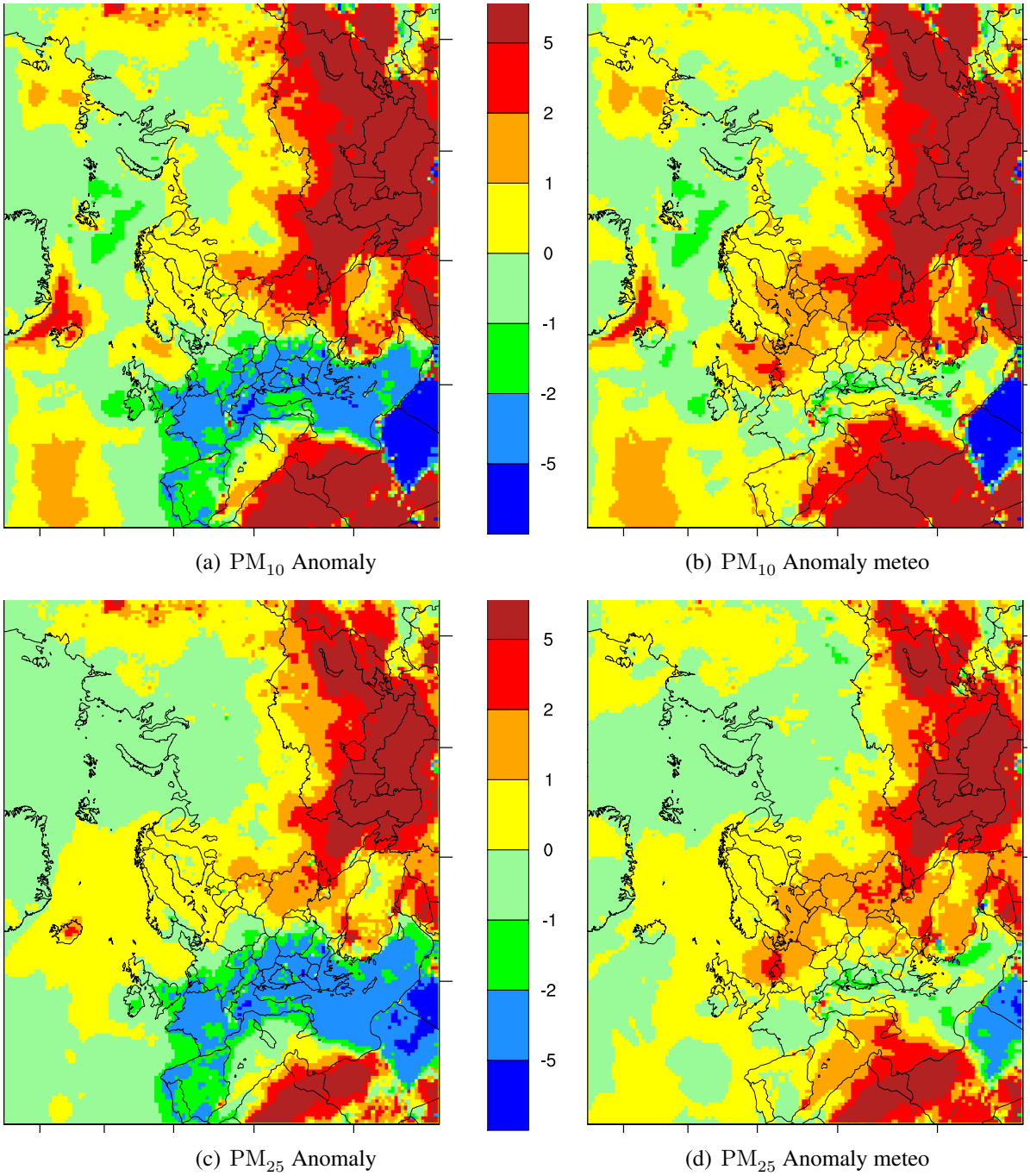

(a) PM_{10} Anomaly

(b) PM_{10} Anomaly meteo

(c) PM_{25} Anomaly

(d) PM_{25} Anomaly meteo

Figure 2.12: Model calculated inter-annual variability of PM_{10} (upper panel) and $PM_{2.5}$ (lower panel): Anomaly = 2014 minus mean of Avg00-13 (left panel), Anomaly meteo = 2014 minus mean of Clim2014 (right panel). Units: μg m^{-3}. *See Table 2.1 for explanations.*

is less important compared to the secondary aerosols. More natural mineral dust explains the elevated PM_{10} and $PM_{2.5}$ in 2014 compared to Avg00-13 in the south/south-east of Russia and Central Asia. More details regarding trends in modelled and measured PM concentrations in Europe can be found in the EMEP TFMM assessment report published this spring Colette et al. (2016))

Figures 2.12 (b),(d) compare the annual mean PM_{10} and PM_{25} from the Status 2014 run with the Clim2014 runs. The most pronounced feature of the meteorological effect on PM pollution in 2014 is an area with decreased (by 1-2 μg m^{-3}) annual concentrations, which stretches from the Eastern Mediterranean, over the Balkan countries (except Romania and Bulgaria), Austria, northern Italy, Switzerland, France and parts of Spain. This decrease in PM levels was apparently due to the enhanced precipitation over these regions in 2014 (Figure 2.1 (b)), causing efficient scavenging of aerosols from the air. Further, cloudy weather have likely reduced the intensity of photo-chemical and oxidation processes, causing less efficient formation of sulphate aerosol and secondary organics (SOA). In addition, positive temperature anomalies in the cold period (Figure 2.2 (c)) imply less emissions from residential heating sector in 2014. The other area where increased precipitation amounts led to less (up to 1 μg m^{-3}) PM pollution in 2014 is Russia east of Moscow.

For the rest of Europe, including EECCA, the meteorological conditions were more unfavourable in terms of PM pollution. In particular, the annual PM levels exceeded the "climatological mean" by 2-3 μg m^{-3} in Belgium and Ukraine, by 1-2 μg m^{-3} over the northern parts of Germany and Poland, in the Baltic countries and Belarus; and by 0.5-1 μg m^{-3} in the rest of Europe. Elevated levels of PM_{10} and $PM_{2.5}$ are also seen in southern Russia. The meteorological map (Figure 2.1 in Chapter 2) indicates relatively dry conditions, which inhibited wet removal of aerosols and thus cleaning of the air. Arid conditions also favoured dust uplifting from bare lands and deserts in the south of Russia and in Central Asia.

Exceedances of EU limit values and WHO Air Quality Guidelines in the regional background environment in 2014

This section compares PM_{10} and $PM_{2.5}$ concentrations calculated with the EMEP/MSC-W model and measured at EMEP sites to EU critical limits and WHO recommended Air Quality Guidelines WHO (2005). The EU limit values for PM_{10}, entered into force 01.01.2005 (Council Directive 1999/30/EC) are 40 μg m^{-3} for the annual mean and 50 μg m^{-3} for the daily mean, with the daily limit not to be exceeded more than 35 times per calendar year (EU 2008). For $PM_{2.5}$, there is an annual mean target value of 25 μg m^{-3}, which entered into force 01.01.2010 (whereas the limit value entered into force 01.01.2015). The Air Quality Guidelines (AQG) recommended by WHO WHO (2005) are:

- for PM_{10}: 20 μg m^{-3} annual mean, 50 μg m^{-3} 24-hourly (99th perc. or 3 days per year)
- for $PM_{2.5}$: 10 μg m^{-3} annual mean, 25 μg m^{-3} 24-hourly (99th perc. or 3 days per year)

The EU PM limit values for protection of human health and the WHO AQG for PM should apply to concentrations for so-called zones, or agglomerations, in rural and urban areas, which are representative for exposure of the general population. The EMEP/MSC-W model calculations on 50×50km^2 grid provide regional background PM concentrations, which still can be compared with the limit values and AQG. Clearly, the rural and urban PM levels are higher than those in the background environment due to the influence of local sources. However,

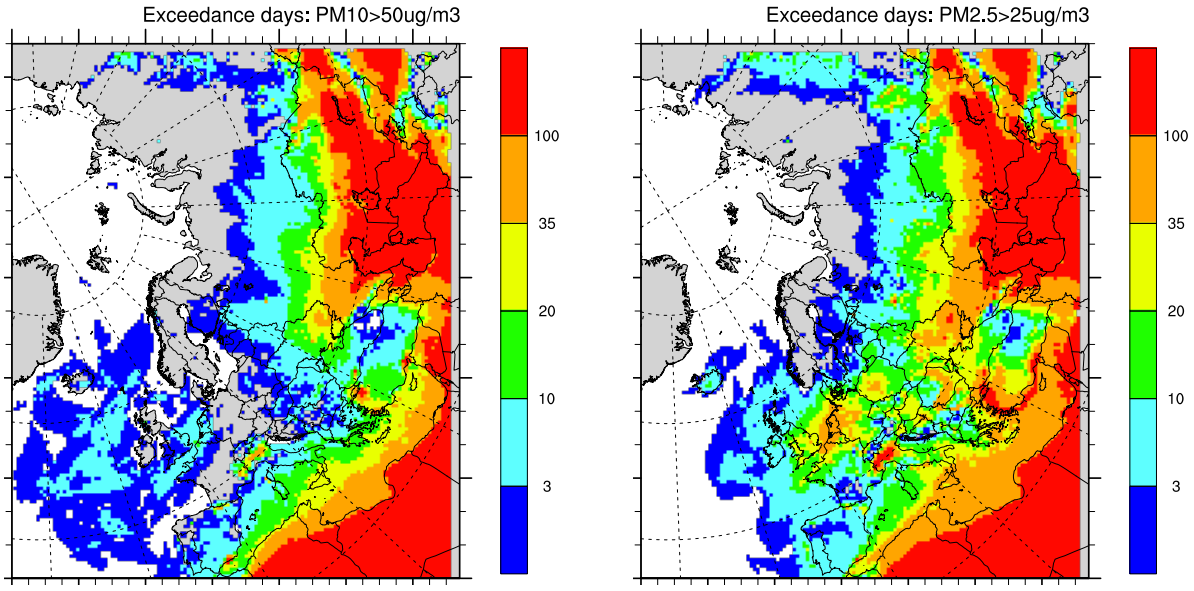

(a) PM_{10} (b) PM_{25}

Figure 2.13: Calculated number of days with exceedances in 2014: PM_{10} exceeding 50 μg m^{-3} (left) and $PM_{2.5}$ exceeding 25 μg m^{-3} (right). *Note: EU Directive requires no more than 35 days with exceedances for PM_{10}, whereas WHO recommends no more than 3 days with exceedances PM_{10} and $PM_{2.5}$ per a calendar year.*

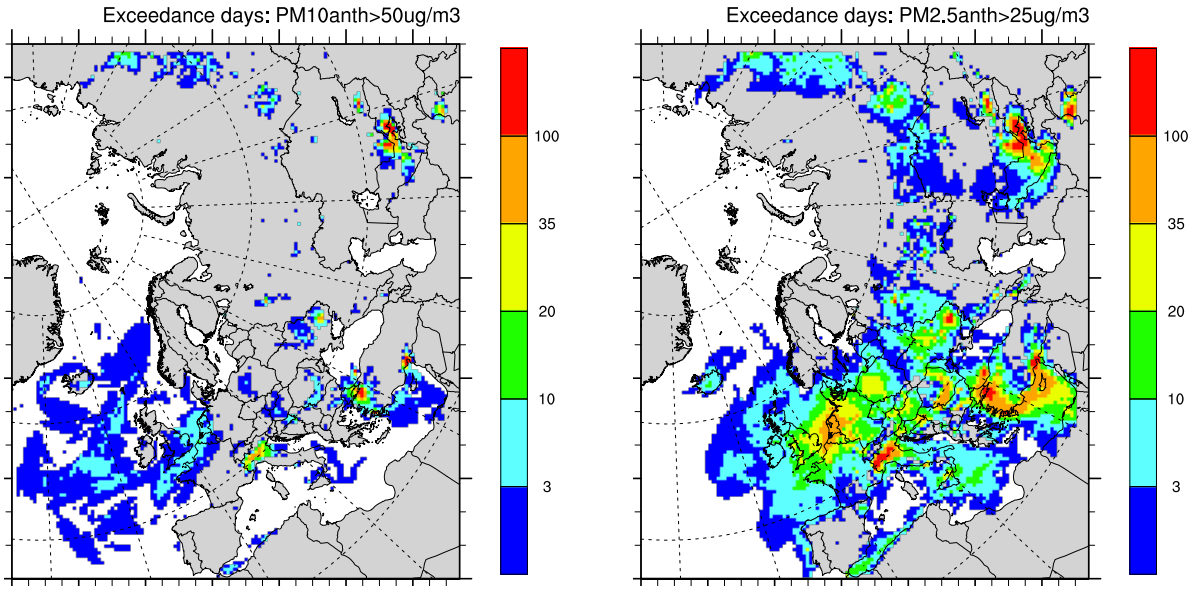

(a) PM_{10} (b) PM_{25}

Figure 2.14: Calculated number of days with exceedances of the WHO AQG in 2014: same as Figure 2.13, but for anthropogenic PM_{10} (left) and $PM_{2.5}$ (right).

comparison of model calculated PM_{10} and $PM_{2.5}$ with EU limit values and WHO AQG can provide an initial assessment of air quality with respect to PM pollution, flagging the regions where already the regional background PM is in excess of the critical values.

Model and observational data in Figure 2.11 (a) show that the annual mean regional background PM_{10} concentrations were below the EU limit value of 40 μg m^{-3} for all of Europe in 2014. Similar to what was reported in previous years, the annual mean PM_{10} from the model exceeds 40 μg m^{-3} over southern parts of Russia, the south of Siberia and in vast areas in Central Asia due to strong influence of desert dust. The observational data reveal that the WHO recommended AQG of 20 μg m^{-3} was exceeded by annual mean PM_{10} at two German (DE0001 and DE0044), one Italian (IT0001) and one Austrian (AT0002) site in 2014, marked as red triangles in Figure 2.11 (a). Observed PM_{10} concentrations in Moldova are also rather high, but are not plotted here due to too low data capture (66%). The model calculates annual mean PM_{10} above 20 μg m^{-3} in the Po Valley, the western parts of Turkey, Moldova, Eastern Ukraine and southern parts of Russia.

Model calculations show that the regional background $PM_{2.5}$ pollution did not exceed the annual mean EU target of 25 μg m^{-3} in 2014, except in the Po Valley. However, the observed annual mean $PM_{2.5}$ was above the WHO AQG value of 10 μg m^{-3} at fifteen sites, with the highest values observed in Germany, Hungary and Austria. This pattern is largerly reproduced by the model.

The maps in Figure 2.13 show the model calculated number of days with exceedances of 50 μg m^{-3} for PM_{10} and 25 μg m^{-3} for $PM_{2.5}$ in 2014. To distinguish between the effects of anthropogenic and natural contribution to the deterioration of air quality, Figure 2.14 shows the correspondent exceedance maps for anthropogenic sources of PM_{10} and $PM_{2.5}$, i.e. excluding sea salt, windblown dust and biogenic SOA.

From the model results and measurement data, the number of days with exceedances of the EU limit value and WHO AQG at EMEP sites have been calculated for 2014. The observed and calculated numbers of exceedance days, as well as the number of common exceedance days, i.e. the days for which observed PM exceedances are also predicted by the model, are presented in Table 2.3.

Exceedances of the PM_{10} EU limit value (50 μg m^{-3}) were observed at 27 of 41 sites with a daily sampling frequency (Table 2.3). At none of these background sites the EU requirement (not more than 35 days with exceedances) was breached, but at 10 sites PM_{10} exceeded 50 μg m^{-3} on more than 3 days (upper limit recommended by the WHO AQG). The sites with the highest number of observed exceedance days in 2014 were DE0044 (15 days), IT0001 and CY0002 (18 days) and MD0013 (33 days). Most of the PM_{10} exceedances at CY0002 occurred in the spring-summer, while at IT0001 and DE0044 in the winter-early spring, as well as in the autumn. The model tends to exaggerate the occurrence of exceedances at the sites in Southern Europe (due to dust episodes), otherwise it calculates fewer days with PM_{10} exceedances of the EU limit value and for fewer sites than observed.

The WHO AQG for $PM_{2.5}$ concentrations were more frequently exceeded than that for PM_{10}. Violations of the WHO AQG recommendation were observed at 17 and calculated at 19 out of 31 sites. The most frequent violations of the WHO AQG for $PM_{2.5}$ were observed at sites in Germany, Hungary, Poland and Italy. The model tends to calculate less $PM_{2.5}$ exceedance days than observed, except for CY0002 (due to both SIA+OM and periodic dust advection). The model overestimates the number of exceedances at Spanish sites due to Saharan dust advection.

Compared to the last five years, 2014 appears to be a moderately polluted year in terms of number of days with PM exceedances at the individual sites. This finding is valid for sites predominantly influenced by anthropogenic sources, such as for Central European, and also for Maditteranean sites, which often experience elevated levels due to mineral dust from nat-

ural sources. For German sites, an increased occurrence of $PM_{2.5}$ exceedances was observed, whereas the number of days with PM_{10} exceedances was only moderate.

Table 2.3: Number of calculated and observed days with exceedances of the EU limit value and the WHO AQG for PM_{10} (50 μg m^{-3}) and for $PM_{2.5}$ (25 μg m^{-3}) in 2014. Only sites with daily measurement frequency are included. *Hit ratio shows the percentage of observed exceedance days correctly predicted by the model (Common-days/Obs-days⋆100%). "v" means no exceedance days in both calculations and observations. *Only 8 months of data*

	PM_{10}				$PM_{2.5}$			
	Obs	Mod	Common	Hit Ratio(%)	Obs	Mod	Common	Hit Ratio (%)
AT0002	12	0	0	0	59	12	10	16
AT0005	0	0	0	v				
AT0048	0	0	0	v				
CH0001	0	0	0	v				
CH0002	2	0	0	0	3	1	1	33
CH0003	2	1	1	50				
CH0004	0	0	0	v				
CH0005	0	0	0	v	1	0	0	0
CY0002	18	19	8	44	7	76	4	57
CZ0001	2	0	0	0				
CZ0003	0	0	0	v	20	5	3	15
CZ0005	1	0	0	0				
DE0001	3	1	0	0				
DE0002	8	0	0	0	53	29	14	26
DE0003	2	0	0	0	14	6	1	7
DE0007	7	0	0	0	58	19	5	8
DE0008	2	0	0	0	23	15	5	21
DE0009	6	0	0	0				
DE0044	15	0	0	0	80	35	23	28
EE0009					2	2	0	0
EE0011					6	0	0	0
ES0001	2	3	0	0	1	3	0	0
ES0007	5	5	1	20	1	5	0	0
ES0008	1	2	0	0	4	5	1	25
ES0009	2	4	1	50	0	2	0	
ES0010	1	2	0	0	0	5	0	
ES0011	0	2	0		1	4	0	0
ES0012	1	3	0	0	0	5	0	
ES0013	0	1	0		0	2	0	
ES0014	1	2	0	0	1	5	0	0
ES0016	0	0	0	v	2	1	0	0
ES0017	0	3	0					
GB0036	2	1	0	0	11	15	6	54
GB0048	0	0	0	v	2	7	2	100
HU0002					72	24	13	18
IT0001	18	6	3	16				
IT0004					38	65	20	52
LV0010	3	0	0	0	28	1	1	3
MD0013	33	4	2	6				
PL0005	8	0	0	0	40	8	2	5
RO0008	0	1	0					
SE0005	0	0	0	v				
SE0012	0	0	0	v	0	0	0	
SE0014	2	0	0	0	10	6	1	10
SI0008	1	0	0	0	13	1	0	0

PM pollution episodes in 2014

Among the most noticeable features of PM pollution in 2014 was a series of PM pollution episodes in Central and Western Europe in the winter-early spring period, as illustrated for Melpitz (DE44) in Figure 2.15. Interestingly, the winter and spring pollution events appear to be caused by different factors. Figure 2.15 shows observed and modelled chemical composition of $PM_{2.5}$ from January to April revealing considerable differences between the three periods with high $PM_{2.5}$ concentrations.

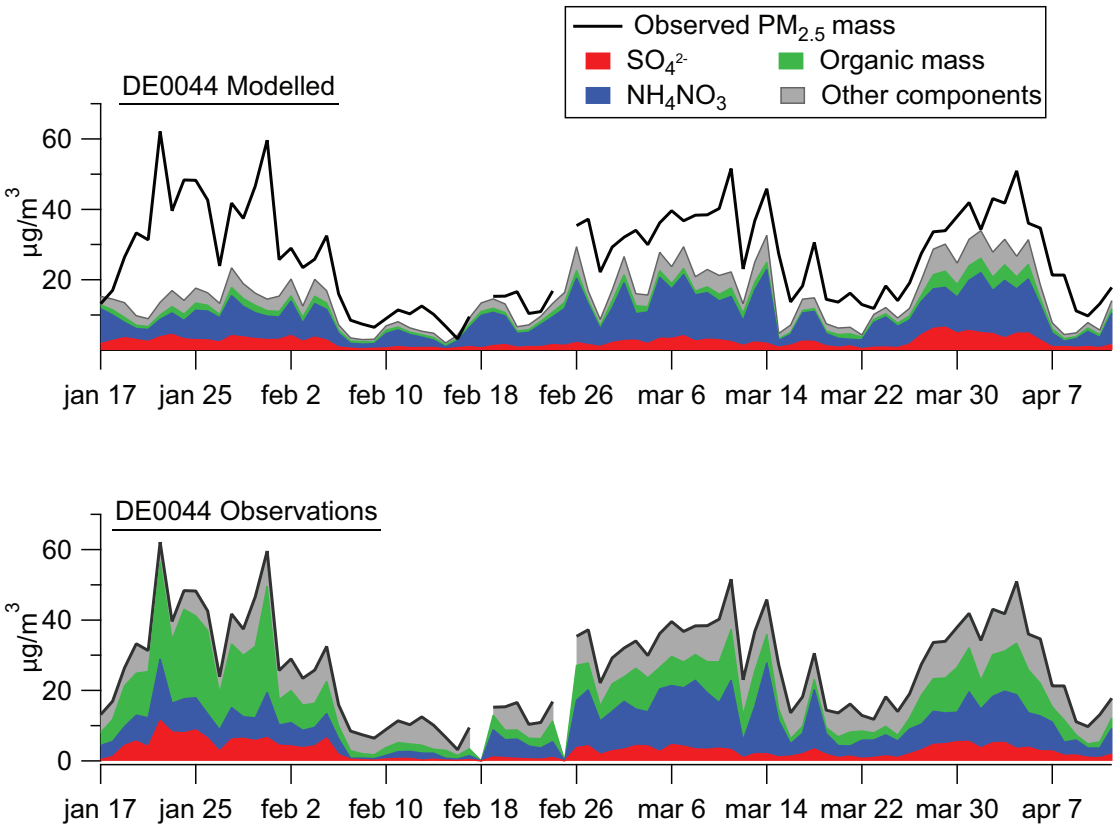

Figure 2.15: Modelled and observed chemical composition of the PM episodes in the winter and spring of 2014 at Melpitz (DE44). Unit: μg m^{-3}. Organic mass in observations is OC$*$1.4.

Typically, the most serious episodes of high PM pollution in Central, Western and Northern Europe prevailingly occur in winter, under cold waves, and are caused by enhanced emissions from wood burning for residential heating in a combination with stagnant air conditions. Such events have been presented in previous EMEP Status Reports (i.e. 4/2013 and 1/2014). In 2014, such a winter time PM pollution episode, being particularly pronounced at Melpitz (Figure 2.15), took place in the second half of January-beginning of February and was observed at German, Austrian, Czech and Polish sites. As seen in Figure 2.15, the observations show high levels of organic mass during the winter time episode, suggesting influence from residential wood burning, which was at least partly due to long range transport from the east (as suggested by FLEXPART trajectories). The elevated levels of organic aerosol are not well captured by the model. The main reason for that may well be problems with the emission inventories for primary organic aerosol. As concluded in Denier van der Gon et al. (2015), the current emission inventories have major issues, especially with regard to the inclusion or exclusion of condensible organics (see also Simpson and Denier van der Gon 2015). Addi-

tional uncertainties in the emission data for Eastern Europe and Russia makes it difficult for the EMEP/MSC-W model to reproduce long-range pollution from those parts.

At Melpitz, hourly measurements of chemical composition is performed with an aerosol mass spectrometer (ACSM), which allows for source identification of the organic mass. Initial evaluation of these data show that the January period is indeed more influenced by wood burning than the spring time episode. There are currently several EMEP sites equipped with ACSM instrumentation, and more detailed studies on sources and temporal variations of the aerosol mass are now possible Bressi et al. (2016).

The second pollution episode which took place in the first half of March 2014 shows less influence by organics aerosols and instead, $PM_{2.5}$ is dominated by ammonium nitrate. This large scale episode was observed in parts of France, Belgium and Germany in the period 7-17 March in 2014. EEA reported on March 14 (http://www.eea.europa.eu/highlights/very-high-air-pollution-levels) that PM concentrations were unusually high across a wide region of Western Europe, and that almost three quarters of France experienced PM_{10} concentrations above the limit of 50 μg m^{-3}, with some areas reporting concentrations more than twice as high as the limit. The pollution episode was severe in Paris with big public attention in the media. The French authorities tried some measures to reduce emissions from traffic and agriculture, but effectiveness was limited since it was a Europe-wide event. It was caused by stable weather conditions persistent over several days, which prevented the dispersion of air pollution from near-ground sources, and pollutants were emitted by a variety of sources from all over the region. Sources included road traffic, wood-burning stoves, and emissions from spring-time fertilizer spreading. Analyses, for example presented in Bessagnet and Rouïl (2014), showed a dramatic increase in ammonium nitrate concentrations with a contribution to PM_{10} mass exceeding 50%. That study pointed to NH_3 emissions from application of agricultural fertilisers, both domestic and abroad, and the NO_x from local traffic to be the main sources of the ammonium nitrate. Furthermore, the contribution of transboundary pollution was estimated to be 20-30% in the middle and south of France, and even larger close to the eastern borders.

In 2014, in addition to continuous PM measurements with TEOM FDMS monitors, chemical composition of PM_{25} for one 24-hour sample was measured every sixth day at several French sites. In Figure 2.16 (a-d), the measurement data (triangles) are plotted together with EMEP/MSC-W model results for a period from 1st of March to mid-April. The episode starts developing from 4-5th of March and peaks between the 9-th and 15-th depending on site. The model and measurements are largely in good agreement regarding the evolution of the pollution event, in particular at FR24 and FR25 (center parts of France), whereas at FR09 (north-east of France, close to the Belgian border), where the episode was shown to commence (Bessagnet and Rouïl 2014), and at FR13 (south-west), there are some time shifts between the modelled and the observed PM peaks. At FR09, the model and observations agree very well concerning the peak on the 13 March, but the first observed peak (11 March) is not calculated by the model. At FR13, the model overestimates the peak on the 11 March, whereas the second calculated peak on 14 March is lower and occurs a couple of days earlier than observed.

Both observations and model show a clear dominance of ammonium nitrate during this period, in accordance with the French study (Bessagnet and Rouïl (2014)).

The third episode, identifiable at both German and French sites (Figures 2.15 and 2.16), took place in late March - beginning of April of 2014. This event is part of a larger European PM pollution episode, but was particularly prominent in the UK, where hourly PM_{10} rose to 100 μg m^{-3} between 26 March and 8 April (Vieno et al. 2016). Similar to the early-March

PM event, this episode was also dominated by ammonium nitrate, as seen in Figure 2.16 (e, f). Vieno et al. (2016) showed that the agricultural NH_3 emissions in continental Europe was a major driver. An interesting aspect with the spring 2014 PM episode in the UK was that one initially thought Saharan dust was an important contributor to the event, as frequently reported in the media, but in retrospect the Saharan dust was shown to be regionally important only to a smaller area in southern UK (Vieno et al. 2016).

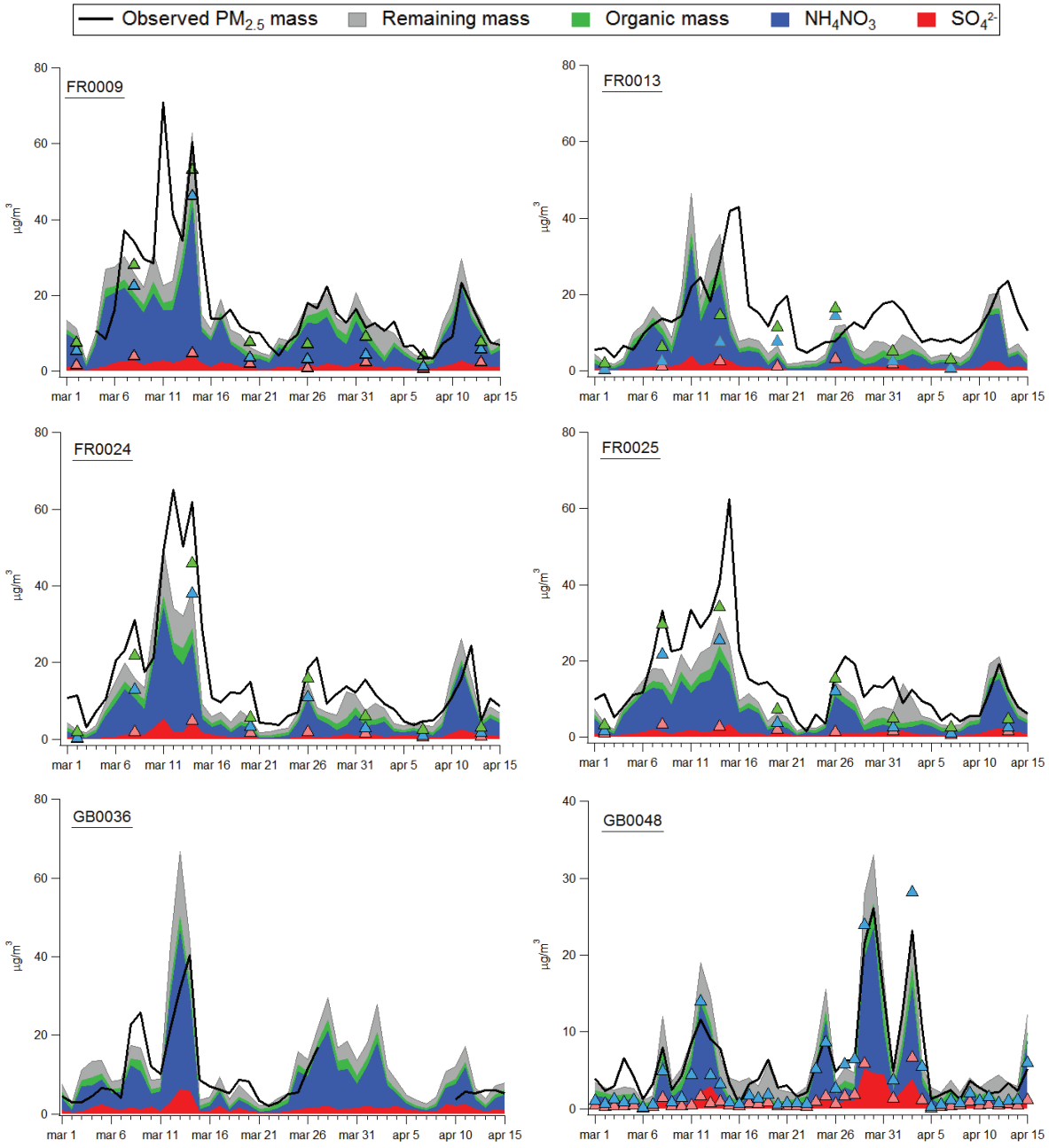

Figure 2.16: PM episodes in the spring of 2015: $PM_{2.5}$ timeseries for selected French sites (upper and middle rows) and PM_{10} timeseries for GB sites (lower row). Unit: μg m^{-3} . Modell results are shown with filled colours while measurements with superimposed triangles. Note that at the GB sites not all components are measured. Organic mass in observations is OC$*$1.4.

2.4.3 Deposition of sulphur and nitrogen

Modelled depositions for sulphur and oxidized and reduced nitrogen for 2014 are presented in Figure 2.17. In the same figure, the difference between 2014 and the mean of the period 2000-2013 is shown in Figure 2.17 (g)-(i). Furthermore, the difference to the mean of the Clim2014 is presented in Figure 2.17 (d)-(f).

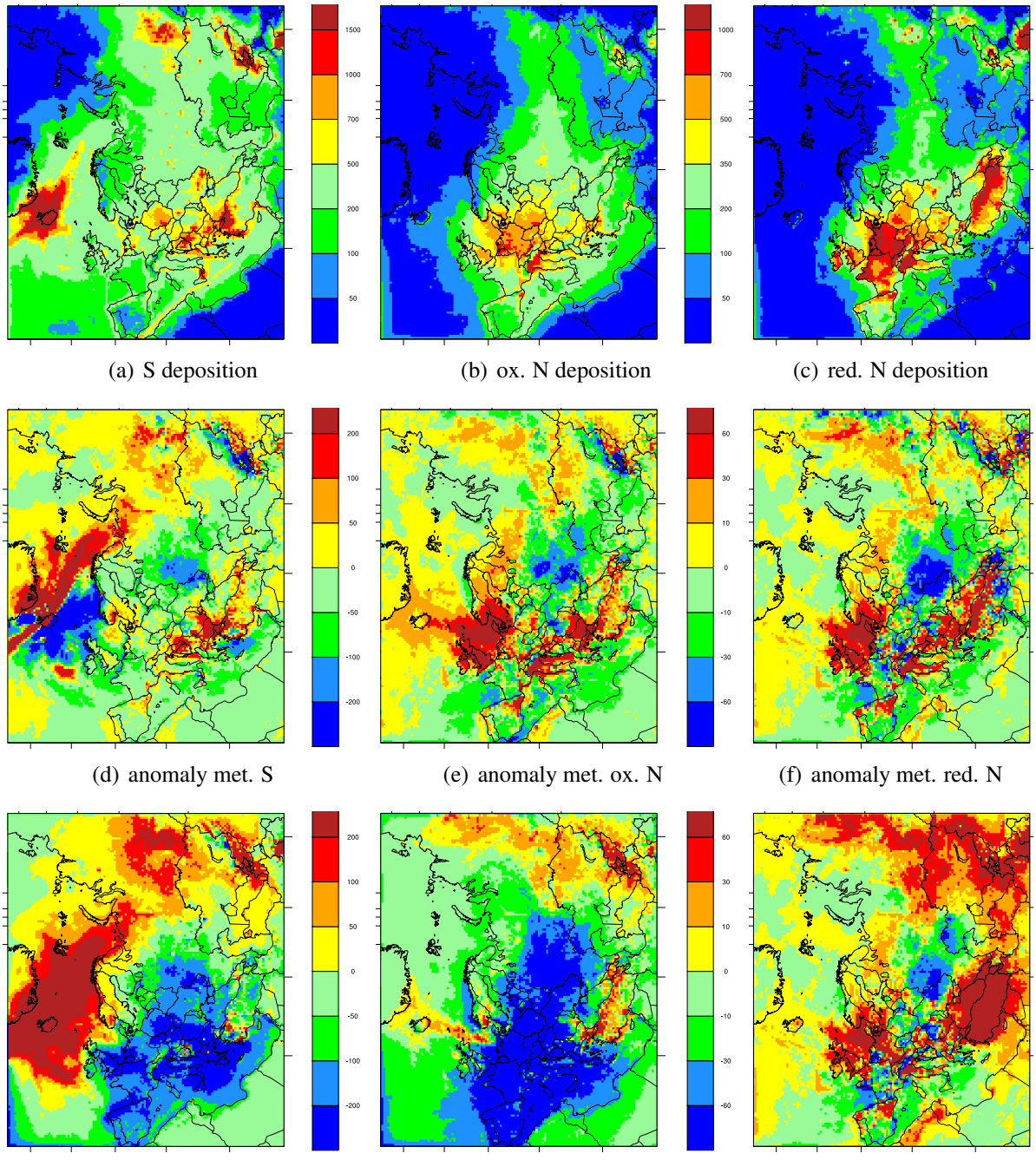

(a) S deposition (b) ox. N deposition (c) red. N deposition

(d) anomaly met. S (e) anomaly met. ox. N (f) anomaly met. red. N

(g) anomaly S (h) anomaly ox. N (i) anomaly red. N

Figure 2.17: Deposition of sulphur and nitrogen [mg(S/N)m^{-2}] in 2014 and anomalies. Anomaly = 2014 minus Avg00-13. Anomaly met = 2014 minus Clim2014. Oxidized and reduced nitrogen (ox. N and red. N) have the same scale.

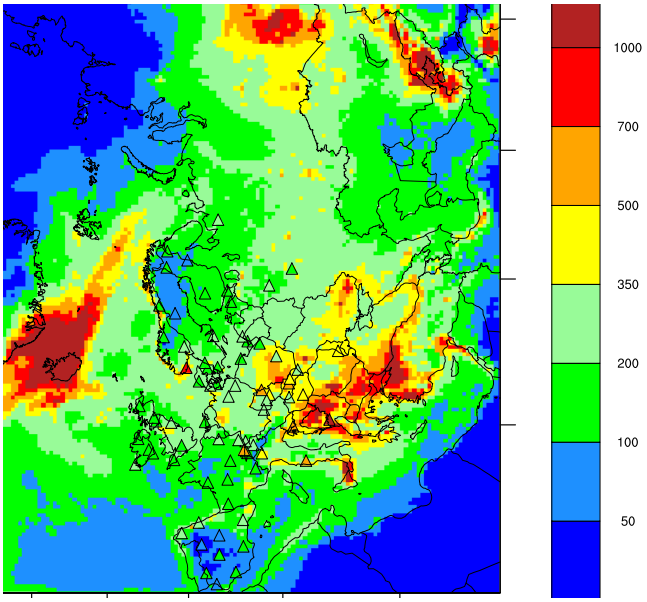

(a) S deposition

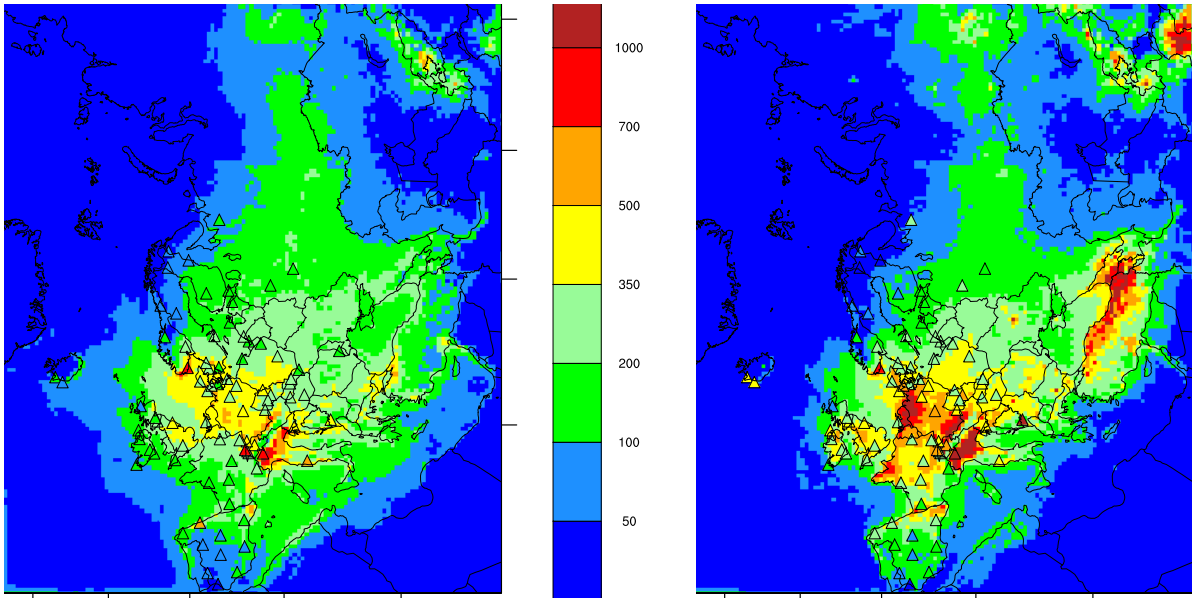

(b) ox. N deposition

(c) red. N deposition

Figure 2.18: Wet deposition of sulphur and nitrogen [mg(S/N)m^{-2}] in 2014. Observations on top (triangles).

As described in section 2.1, 2014 was unusually wet in north-western Europe and the Mediterrenean area compared to an average year. More precipitation leads to more wet deposition. Although partly compensated by less dry deposition, the overall effect of increased precipitation is higher total depositions. Thus, due to the weather pattern in 2014, parts of south Europe and north western Europe received more depositions than an average climatological year (Figure 2.17 (d)-(f)), but other parts less (largely following the precipitation pattern). Compared to the mean of the 2000-2013 period, however, most of Europe received less deposition of sulphur and oxidized nitrogen. The reason is the decrease of emissions of SO_x and NO_x in these areas. For the EMEP area as a whole, emissions of SO_x decreased

by 23% and NO_x by 22% from 2000 to 2014. This is reflected in the depositions of sulphur and oxidized nitrogen which in 2014 are lower than the 2000-2013 mean for the whole EMEP area, with the exception of the easternmost part of the EMEP domain, and northern Europe for deposition of SO_x. For SO_x, the large emissions of SO_2 from the Holuhraun eruption at Iceland in the autumn of 2014 lead to an increased deposition of SO_x in areas downwind of Iceland (see section2.5).

For NH_3, the change in the sum of national total emissions from 2000 to 2014 amounted to +18% for the EMEP domain. Many countries increased their emissions, with the strongest increases in Kazakhstan (+176%) and Turkey (+125%). These increases in emissions lead to an increase in modelled reduced nitrogen depositions in areas close to these countries. Higher depositions are also seen in the UK, Germany, parts of Spain and Italy and the Nordic countries, where emission changes during this period have been relatively small (except for Denmark, with a decrease of 25%), and the meteorological conditions favours higher deposition. In general, the smaller emission changes of NH_3 compared to SO_x and NO_x makes the meteorological 'signal' much more evident for reduced nitrogen deposition, and there is no consistent picture of a Europe with lower depositions.

In Figure 2.18, wet depositions of nitrogen and sulphur compounds are compared to measurements at EMEP sites for 2014. Overall, the bias between model and measurements are around +/- 10%, but higher for individual sites. A more detailed comparison between model and measurements for the year 2014 can be found in Gauss et al. (2016).

Exceedances of critical loads of acidification and eutrophication

The exceedances of European critical loads (CLs) under the 2014 N and S depositions are presented in Figure 2.19. The calculations are based on the official critical load data, described in Slootweg et al. (2015), which are also used by TFIAM in integrated assessment modelling. The exceedance in a grid cell is the so-called 'average accumulated exceedance (AAE)', computed as the area-weighted mean of the exceedances of the critical loads of all ecosystems in that grid cell.

The critical loads (for about 2.3 million ecosystems in Europe covering an area of about 3.8 million km^2) are attributed to a $0.250^\circ \times 0.125^\circ$longitude-latitude grid. In the Figure, the exceedances are shown for acidity critical loads, caused by both N and S deposition (maps on the left), and the exceedances of eutrophication critical loads, caused by excess N deposition (maps on the right), both on the $1.0^\circ \times 0.5^\circ$grid (comparable in size to the 50×50 km^2 EMEP grid) and the $0.250^\circ \times 0.125^\circ$grid.

In terms of acidification, hotspots of exceedances can be found in the Netherlands and its border areas to Germany and Belgium as well as in southern Germany and north-western Turkey. More generally, exceedances of acidity CLs in the north-western Europe are higher under 2014 depositions in comparison to 2013, most likely an effect of the increased S deposition due to the eruption of the Bardarbunga volcano on Iceland. Overall, acidity exceedances occur in about 7% of the ecosystem area, and the European average AAE is about 27 eq ha^{-1}yr^{-1}. In contrast, critical loads for eutrophication are exceeded in virtually all countries (in about 70% of the ecosystem area) and the European average AAE is about 286 eq ha^{-1}yr^{-1}. The highest exceedances are found in the Po valley in Italy, the Dutch-German border, and the Caucasus region. These results confirm that acidification, dominant in the 1980s, has diminished over the last decades, whereas nitrogen remains a threat to ecosystem health in terms of eutrophication and biodiversity.

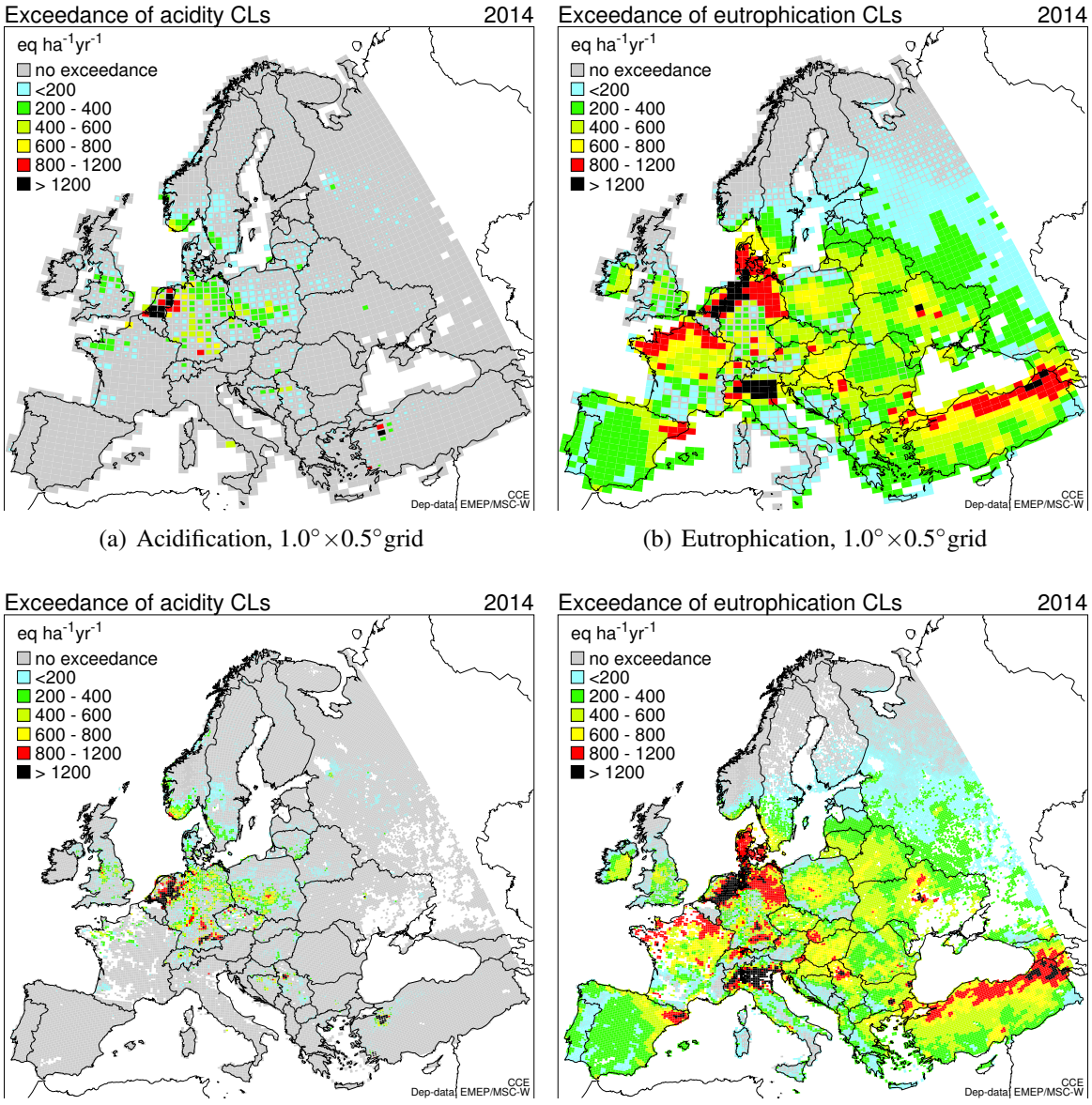

(a) Acidification, 1.0°×0.5°grid

(b) Eutrophication, 1.0°×0.5°grid

(c) Acidification, 0.250°×0.125°grid

(d) Eutrophication, 0.250°×0.125°grid

Figure 2.19: Exceedance of critical loads of acidification (left) and eutrophication (right), mapped on the 1.0°×0.5°(top) and 0.250°×0.125°(bottom) longitude-latitude grid under 2014 EMEP S and N depositions (given on the 50×50 km^2 EMEP grid).

2.5 Influence of the SO_2 emissions from the Holuhraun eruption in 2014

A volcanic fissure at Holuhraun, Iceland, started at the end of August 2014 and continued for 6 months until end of February 2015. There was little ash in the eruption, but large amounts of SO_2 were emitted into the atmosphere. The source has been estimated to be around 10,880 kt of SO_2 2014 (in total 12,006 kt, including January and February 2015) which is more than 3 times the amount of anthropogenic SO_2 emissions from all the European Union countries for the year 2014.

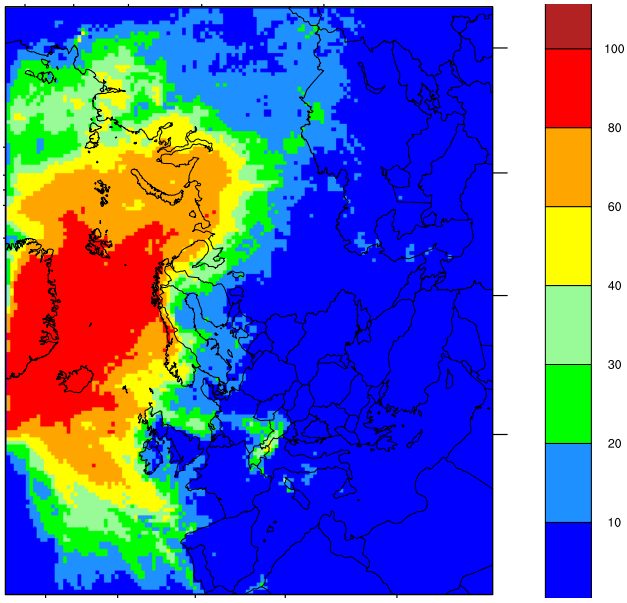

(a) S wet deposition

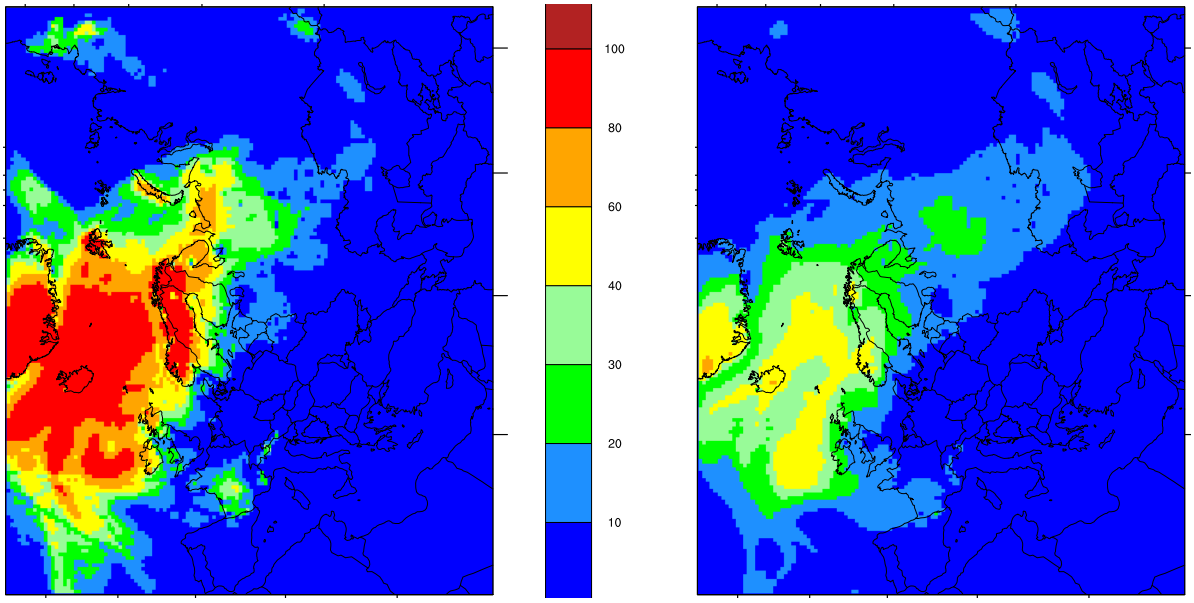

(b) SO_2 (c) SO_4^{2-}

Figure 2.20: Percent increase due to the Holuhraun eruption in (a) sulfur wet deposition, (b) SO_2 in air and (c) SO_4^{2-} in air.

A detailed EMEP/MSC-W model study of the air pollution effect of the Holuhraun volcanic fissure is recently published (Steensen et al. 2016), and we refer to that paper for a more through description of the event and the effects. The influence of the sulfur dioxide emissions from the Holuhraun eruption was also discussed in EMEP Status Report 1/2015 (2015). Here, we briefly present the effect of the Holuhraun emissions on the levels of air pollution in 2014, based on the status runs and an additional model simulations where Holuhraun emissions have been excluded.

In Figure 2.20, the effect of the volcanic eruption on SO_2 and SO_4^{2-} in air, as well as sulfur wet deposition, is shown.

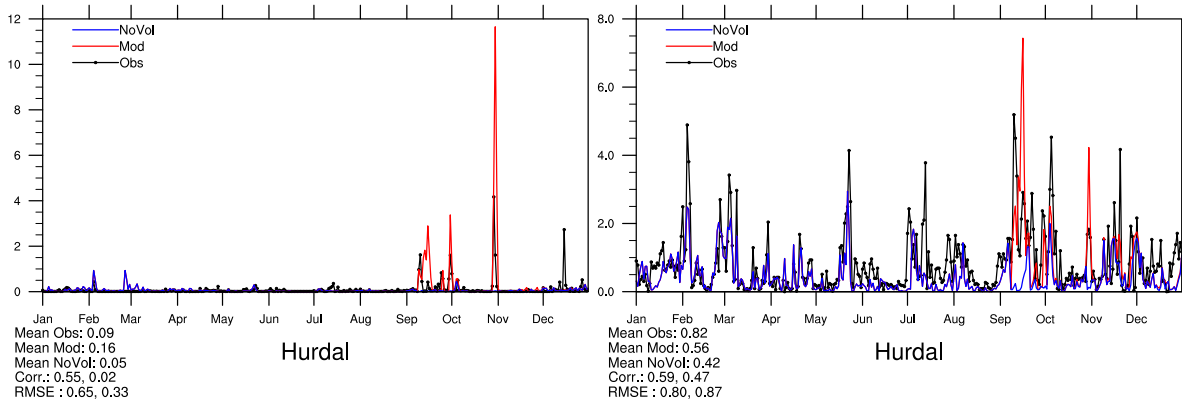

(a) SO_2 (b) SO_4^{2-}

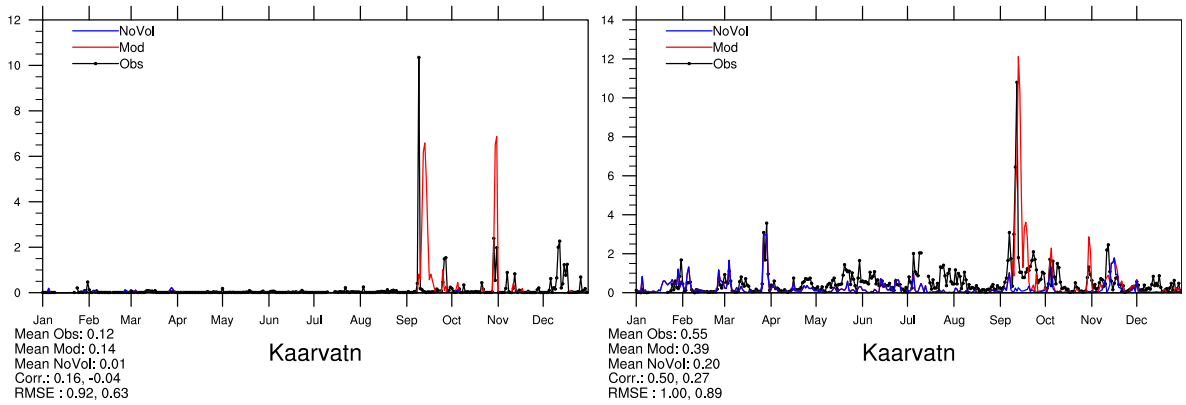

(c) SO_2 (d) SO_4^{2-}

Figure 2.21: Timeseries for model versus observations for Hurdal and Kaarvatn, Norway, with (Mod) and without (NoVol) Holuraun emissions included, for SO_2 in air and SO_4^{2-} in air.

The largest increases in deposition, apart from Iceland, are found on the coast of Northern Norway, a region with frequent precipitation during westerly winds. The total deposition levels in this region become equal to the most polluted regions over Europe and the average model deposition for Norway is at the same level it was back in 1990 for the yearly total.

For SO_2 and SO_4^{2-} in air, the largest increases are found over the Scandinavian countries, Scotland and Ireland. As can be seen from Figure 2.21, the increases occur as short peaks in concentration levels from a few hours to some days.

2.6 Model calculations for 2015

Preliminary model calculations for 2015 has been performed. The meteorology has been prepared the same way as for 2014, described in subchapter 2.3. For emissions, the 2014 data is used. Data for forest fires are from 2015. DMS is varying with the meteorological conditions and reflects 2015 conditions. For boundary conditions, climatological means are used. The EMEP/MSC-W model version is the same as used for 2014 (rv4.9).

As an example, 2015 results for the mean of daily ozone maximum (April-September) is shown in Figure 2.22 together with the difference from the mean of the 2000-2013 series (see

Chapter 2.3). The data can also be downloaded from the EMEP webpage.

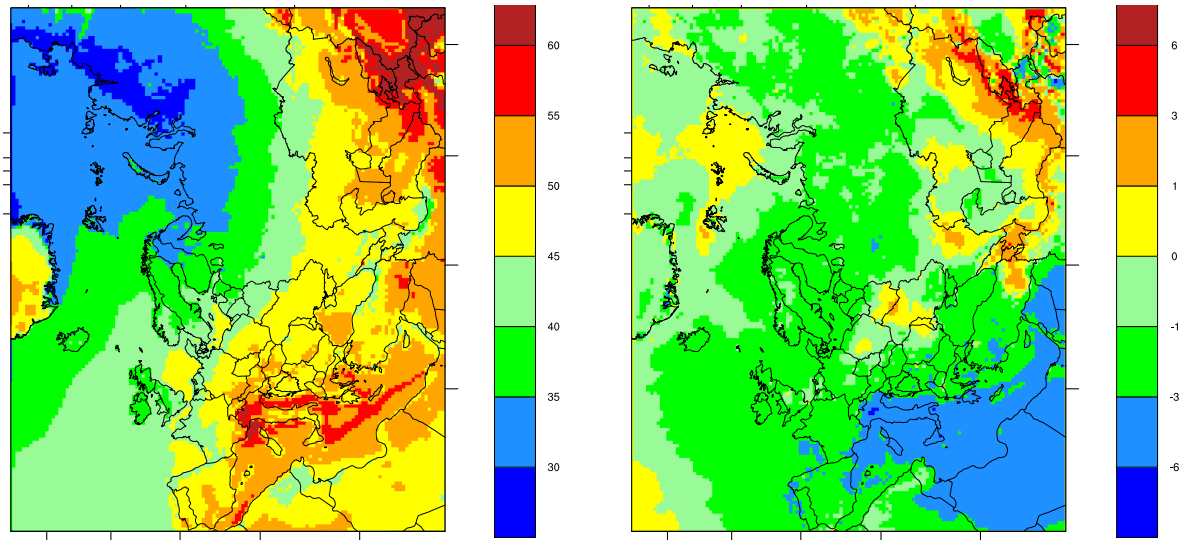

(a) Status2015 (b) Anomaly

Figure 2.22: Mean of daily maximum ozone concentrations for the period April-September for 2015. [Unit: ppb]. Status2015 = calculations for 2015, Anomaly = 2015 minus Trend2000-2013

No analysis of the 2015 results has been attempted here, as the EMEP measurement data are not available until spring 2017.

References

Bessagnet, B. and Rouïl, L.: Feedback on and analysis of the PM pollution episode in March 2014, presentation at 19-th EIONET Workshop on Air Quality Assessment and Management Berne, Switzerland, 30 September and 1 October 2014, 2014.

Bressi, M., Cavalli, F., Putaud, J. P., Prevot, A. S. H., et al.: A European aerosol phenomenology - 6: high-time resolution chemical characteristics of submicron particulate matter across Europe, In preparation, 2016.

Colette, A., Aas, W., Banin, L., Braban, C., Ferm, M., González Ortiz, A., Ilyin, I., Mar, K., Pandolfi, M., Putaud, J.-P., Shatalov, V., Solberg, S., Spindler, G., Tarasova, O., Vana, M., Adani, M., Almodovar, P., Berton, E., Bessagnet, B., Bohlin-Nizzetto, P., Boruvkova, J., Breivik, K., Briganti, G., Cappelletti, A., Cuvelier, K., Derwent, R., D'Isidoro, M., Fagerli, H., Funk, C., Garcia Vivanco, M., González Ortiz, A., Haeuber, R., Hueglin, C., Jenkins, S., Kerr, J., de Leeuw, F., Lynch, J., Manders, A., Mircea, M., Pay, M., Pritula, D., Putaud, J.-P., Querol, X., Raffort, V., Reiss, I., Roustan, Y., Sauvage, S., Scavo, K., Simpson, D., Smith, R., Tang, Y., Theobald, M., Tørseth, K., Tsyro, S., van Pul, A., Vidic, S., Wallasch, M., and Wind, P.: Air Pollution trends in the EMEP region between 1990 and 2012., Tech. Rep. Joint Report of the EMEP Task Force on Measurements and Modelling (TFMM), Chemical Co-ordinating Centre (CCC), Meteorological Synthesizing Centre-East (MSC-E), Meteorological Synthesizing Centre-West (MSC-W) EMEP/CCC Report 1/2016, Norwegian Institute for Air Research, Kjeller, Norway, URL http://www.unece.org/fileadmin/DAM/env/documents/2016/AIR/Publications/Air_pollution_trends_in_the_EMEP_region.pdf, 2016.

Denier van der Gon, H. A. C., Bergström, R., Fountoukis, C., Johansson, C., Pandis, S. N., Simpson, D., and Visschedijk, A. J. H.: Particulate emissions from residential wood combustion in Europe - revised estimates and an evaluation, Atmos. Chem. Physics, pp. 6503–6519, doi:doi:10.5194/acp-15-6503-2015, URL http://www.atmos-chem-phys.net/15/6503/2015/, 2015.

Emberson, L., Ashmore, M., Cambridge, H., Simpson, D., and Tuovinen, J.: Modelling stomatal ozone flux across Europe, Environ. Poll., 109, 403–413, 2000.

EMEP Status Report 1/2015: Transboundary particulate matter, photo-oxidants, acidifying and eutrophying components, EMEP MSC-W & CCC & CEIP, Norwegian Meteorological Institute (EMEP/MSC-W), Oslo, Norway, 2015.

EU: Directive 2008/50/EC of the European Parliament and of the Council on ambient air quality and cleaner air for Europe., Official Journal of the European Union L 152, 11 June 2008, pp. 1-44., L 152, 1–44, URL http://faolex.fao.org/docs/pdf/eur80016.pdf, 2008.

Gauss, M., Tsyro, S., Benedictow, A., Fagerli, H., Hjellbrekke, A.-G., Aas, W., and Solberg, S.: EMEP/MSC-W model performance for acidifying and eutrophying components, photo-oxidants and particulate matter in 2014., Supplementary material to EMEP Status Report 1/2016, available online at www.emep.int, The Norwegian Meteorological Institute, Oslo, Norway, 2016.

Hjellbrekke, A.-G.: Data Report 2014 Acidifying and eutrophying compounds and particulate matter, Tech. Rep. EMEP/CCC Report 2/2016, Norwegian Institute for Air Research, Kjeller, Norway, 2016.

Hjellbrekke, A.-G. and Solberg, S.: Ozone measurements 2014, Tech. Rep. EMEP/CCC Report 3/2016, Norwegian Institute for Air Research, Kjeller, Norway, 2016.

Karlsson, P. E., Pleijel, H., and Simpson, D.: Ozone Exposure and Impacts on Vegetation in the Nordic and Baltic Countries, Ambio: A Journal of the Human Environment, 38, 402–405, URL http://dx.doi.org/10.1579%2F0044-7447-38.8.402, 2009.

Mills, G., Hayes, F., Simpson, D., Emberson, L., Norris, D., Harmens, H., and Büker, P.: Evidence of widespread effects of ozone on crops and (semi-)natural vegetation in Europe (1990-2006) in relation to AOT40- and flux-based risk maps, Global Change Biology, 17, 592–613, doi:10.1111/j.1365-2486.2010.02217.x, 2011a.

Mills, G., Pleijel, H., Braun, S., Büker, P., Bermejo, V., Calvo, E., Danielsson, H., Emberson, L., Grünhage, L., Fernández, I. G., Harmens, H., Hayes, F., Karlsson, P.-E., and Simpson, D.: New stomatal flux-based critical levels for ozone effects on vegetation, Atmos. Environ., 45, 5064 – 5068, doi:10.1016/j.atmosenv.2011.06.009, 2011b.

Overland, J., Hanna, E., Hanssen-Bauer, I., Kim, B.-M., Kim, S.-J., Walsh, J., Wang, M., and Bhatt, U. S.: Air Temperature, in Arctic Report Card 2014, NOAA, http://http://www.arctic.noaa.gov/report14/air_temperature.html, 2014.

Simpson, D. and Denier van der Gon, H.: Problematic emissions - particles or gases?, in: Transboundary particulate matter, photo-oxidants, acidifying and eutrophying components. EMEP Status Report 1/2015, pp. 87–96, The Norwegian Meteorological Institute, Oslo, Norway, 2015.

Simpson, D., Emberson, L., Ashmore, M., and Tuovinen, J.: A comparison of two different approaches for mapping potential ozone damage to vegetation. A model study, Environ. Poll., 146, 715–725, doi:10.1016/j.envpol.2006.04.013, 2007.

Simpson, D., Benedictow, A., Berge, H., Bergström, R., Emberson, L. D., Fagerli, H., Hayman, G. D., Gauss, M., Jonson, J. E., Jenkin, M. E., Nyíri, A., Richter, C., Semeena, V. S., Tsyro, S., Tuovinen, J.-P., Valdebenito, A., and Wind, P.: The EMEP MSC-W chemical transport model – technical description, Atmos. Chem. Physics, 12, 7825–7865, doi:10.5194/acp-12-7825-2012, 2012.

Slootweg, J., Posch, M., , and Hettelingh, J.-P.: Modelling and mapping the impacts of atmospheric deposition of nitrogen and sulphur, in: CCE Status report 2015, RIVM Report 2015-0193, p. 141 pp, Coordination Centre for Effects, RIVM, Bilthoven, The Netherlands, URL http://www.wge-cce.org, 2015.

Steensen, B. M., Schulz, M., Theys, N., and Fagerli, H.: A model study of the pollution effects of the first three months of the Holuhraun volcanic fissure, Atmospheric Chemistry and Physics, 16, 9745–9760, doi:doi:10.5194/acp-16-9745-2016, URL http://www.atmos-chem-phys.net/16/9745/2016/, 2016.

UNECE: Progress in activities in 2009 and future work. Measurements and modelling (acidification, eutrophication, photooxidants, heavy metals, particulate matter and persistent organic pollutants). Draft revised monitoring strategy., Tech. Rep. ECE/EB.AIR/GE.1/2009/15, UNECE, URL http://www.unece.org/env/documents/2009/EB/ge1/ece.eb.air.ge.1.2009.15.e.pdf, 2009.

Vieno, M., Heal, M. R., Twigg, M. M., MacKenzie, I. A., Braban, C. F., Lingard, j. j. N. Ritchie, S., Beck, R. C., A., M., Ots, R., DiMarco, C. F., Nemitz, E., Sutton, M. A., and Reis, S.: The UK particulate matter air pollution episode of March-April 2014: more than Saharan dust., Environ. Res. Lett., doi:10.1088/1748-9326/11/4/044004, 2016.

WHO: Air quality guidelines. Global update 2005. Particulate matter, ozone, nitrogen dioxide and sulfur dioxide, URL http://www.who.int/phe/health_topics/outdoorair/outdoorair_aqg/en/, World Health Organisation, European Centre for Environment and Health Bonn Office, ISBN 92 890 2192, 2005.

WMO: WMO statement on the status of the global climate in 2014, WMO-No. 1152, http://library.wmo.int/opac/, ISBN 978-92-63-11152-2, 2015.

CHAPTER 3

Emissions for 2014

Christine Brendle, Katarina Mareckova, Marion Pinterits, Sabine Schindlbacher, Melanie Tista, Bernhard Ullrich and Robert Wankmüller
with contribution to the volcano emissions by
Ágnes Nyíri

In addition to meteorological variability, changes in the emissions affect the inter-annual variability and trends of air pollution, deposition and trans-boundary transport. The main changes in emissions in 2014 with respect to previous years are documented in the following sections.

3.1 Emissions for 2014

The EMEP Reporting guidelines (UNECE 2014) requests all Parties to the LRTAP Convention to report annually emissions of air pollutants (SO_x[1], NO_2[2], NMVOCs [3], NH_3, CO, HMs, POPs, PM [4] and voluntary BC), activity data, projections, gridded data and information on large point sources (LPS) to the EMEP Centre on Emission Inventories and Projections (CEIP).

[1]"Sulphur oxides (SO_x)" means all sulphur compounds, expressed as sulphur dioxide (SO_2), including sulphur trioxide (SO_3), sulphuric acid (H_2SO_4), and reduced sulphur compounds, such as hydrogen sulphide (H_2S), mercaptans and dimethyl sulphides, etc.

[2]"Nitrogen oxides (NO_x)" means nitric oxide and nitrogen dioxide, expressed as nitrogen dioxide (NO_2).

[3]"Non-methane volatile organic compounds" (NMVOCs) means all organic compounds of an anthropogenic nature, other than methane, that are capable of producing photochemical oxidants by reaction with nitrogen oxides in the presence of sunlight.

[4]"Particulate matter" (PM) is an air pollutant consisting of a mixture of particles suspended in the air. These particles differ in their physical properties (such as size and shape) and chemical composition. Particulate matter refers to:
(i) "$PM_{2.5}$", or particles with an aerodynamic diameter equal to or less than 2.5 micrometers (μm);
(ii) "PM_{10}", or particles with an aerodynamic diameter equal to or less than 10 (μm).

3.1.1 Reporting of emission inventories in 2016

Completeness and consistency of submitted data have improved significantly since EMEP started collecting information on emissions. About 40 to 48 Parties report regularly data since 2010. Slight improvement of reporting by EECCA countries have been observed in the last two years. 45 Parties (88%) submitted inventories[5] in 2016; six Parties[6] did not submit any data; and 33 countries reported black carbon (BC) emissions. Same number of countries reported since 2012 information on large point sources (LPS) for 2010 (Mareckova et al. 2016).

The quality of submitted data across countries differs quite significantly. Uncertainty of reported data (national totals, sectoral data) is considered relatively high, the completeness of reported data has not turned out satisfactory for all pollutants and sectors neither. Detailed information on recalculations, completeness and key categories, plus additional review findings can be found in the annual EEA & CEIP technical inventory review reports (Mareckova et al. 2015) and its Annexes[7].

3.1.2 Reporting of gridded data

In total, only 29 of the 48 countries which are considered to be part of the extended EMEP area reported sectoral gridded emissions for the main pollutants and PM for the year 2010, 16 countries for the year 2005 and 14 countries for the year 2000. Reported gridded data can be downloaded from the CEIP website[8].

Reported gridded sectoral data cover less than 50% of the geographic EMEP area. For remaining areas missing emissions are gap-filled and spatially distributed by expert estimates.

3.1.3 Gap filling in 2016

In order to create emission datasets which can be used for the spatial distribution, reported sectoral (NFR14) emissions were aggregated to 10 SNAP sectors and gap filled afterward as needed (if countries do not report complete sectoral time series). The gap-filled data have been imported to WebDab and can be accessed from the CEIP website[9]. Historical emissions from 1990-2013 were recalculated in 2015 to reflect revised reported data and new information obtained in diverse studies. In the course of this, also emissions from international shipping have been recalculated (detailed information can be found in the EMEP Status Report 2015). For 2014 in case of non-reported data or underestimated emissions, some data was completely replaced by different gap-filling methods.

The most frequently used method was extrapolation or interpolation of emission estimates provided by the IIASA (Laxenburg, Austria) from the Greenhouse Gas and Air Pollution

[5]The original submissions from the Parties can be accessed via the CEIP homepage on `http://www.ceip.at/status_reporting/2016_submissions`.

[6]Albania, Belarus, Bosnia and Herzegovina, Greece, Monaco and Montenegro

[7]`http://www.ceip.at/review_proces_intro/review_reports`

[8]`http://www.ceip.at/status_reporting/2016_submissions`.
In 2016 gridded sectoral emissions of the main pollutants and PM were available from Finland (2014), Poland (2014), Switzerland (for the whole timeline from 1980 to 2014) and the United Kingdom (2010).

[9]WebDab: "Emissions as used in EMEP models"
`http://www.ceip.at/webdab_emepdatabase/emissions_emepmodels`

Interactions and Synergies (GAINS)-Model[10]. Two data sets were provided by IIASA: One was generated in spring 2014 and covers the years from 1990 to 2010 (i.e. 1990, 1995, 2000, 2005 and 2010) and the other data set was generated in October 2014 and covers the years from 2005 to 2030 (i.e. 2005, 2010, 2015, 2020, 2025 and 2030). Not for all Parties the second data set was available. If both data sets were available for the overlapping years (2005 and 2010) the data set from October 2014 was used. The data was converted to SNAP level by CEIP. Interpolation between 2010 and 2015 was done if data for the respective Party was available for the year 2015. The data was extrapolated using the trend between 2005 and 2010, if 2010 was the last available year for the respective Party. In cases where extrapolation led to negative values either 2010 data was used as a surrogate for 2014 or the last plausible extrapolated year was used as surrogate for 2014.

Emission data on the "extended EMEP area" are in general not reported to CEIP (e.g. the Asian part of Russia, Kyrgyzstan, Uzbekistan, Tajikistan and North Africa). As a consequence, emissions are estimated by experts using the GDP trend[11] to extrapolate the emission trends, or expert estimates from previous gap-filling were copied for the year 2014.

3.1.4 Contribution of individual SNAP sectors to total EMEP emissions

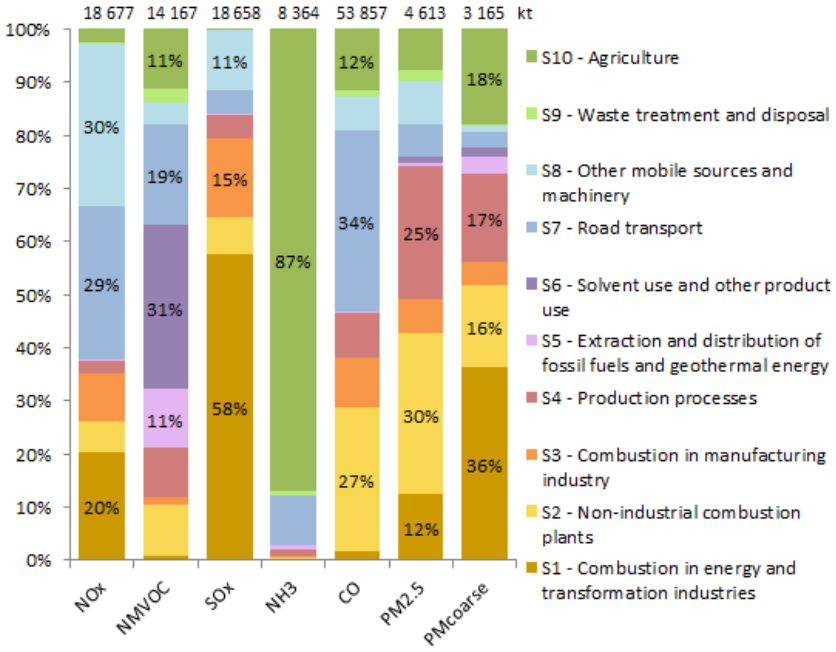

Figure 3.1: SNAP sector contribution to national total emissions in 2014 for the EMEP extended area (only percentages above 10% are visible).

[10] http://www.iiasa.ac.at/web/home/research/researchPrograms/air/GAINS.en.html

[11] Worldbank 2015, GDP PPP (constant 2011 international $, NY.GDP.MKTP.PP.KD). PPP GDP is gross domestic product converted to international dollars using purchasing power parity rates. An international dollar has the same purchasing power over GDP as the U.S. dollar has in the United States. GDP is the sum of gross value added by all resident producers in the economy plus any product taxes and minus any subsidies not included in the value of the products. It is calculated without making deductions for depreciation of fabricated assets or for depletion and degradation of natural resources. Data are in constant 2011 international dollars.

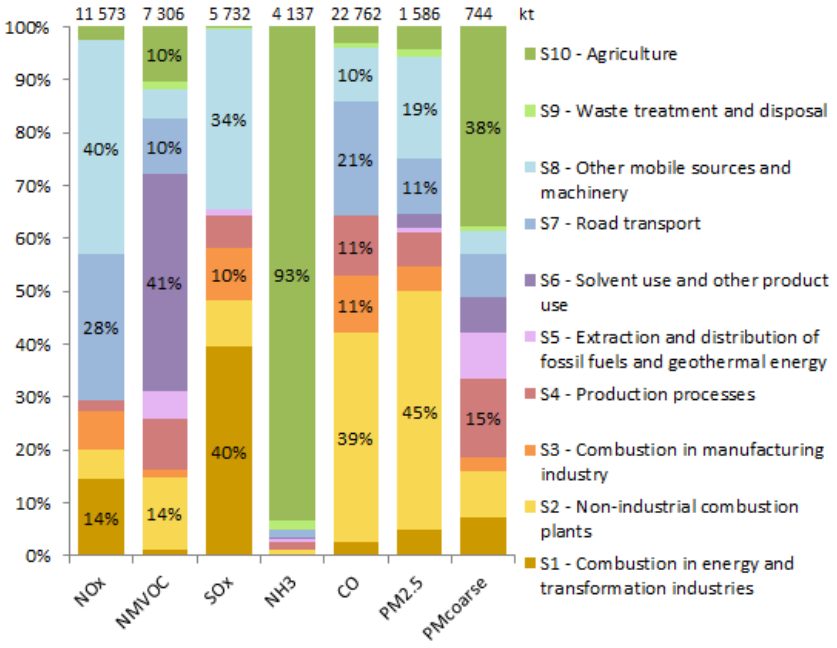

Figure 3.2: SNAP sector contribution to national total emissions in 2014 for the EMEP West region (only percentages above 10% are visible).

Figure 3.1 shows the contribution of each sector to the total emissions of individual air pollutants (SO_x, NO_x, CO, NMVOC, NH_3, $PM_{2.5}$ and PM_{coarse}). The share of individual sectors typically does not change significantly over years, the changes between 2013 and 2014 were minor.

The values above the graphs in Figure 3.1 are emission totals shown in thousand tons (kt). Only percentages above 10% are shown (percentages below are not included in the graphs).

It is evident that the combustion of fossil fuels is responsible for a significant part of all emissions. 59% of NO_x emissions are produced by transport (S7, S8) but 20% of NO_x also comes from large power plants. In 2012 the emissions from road transport formed 30%; in 2013 they slightly fell to 29% and showed no further reductions in 2014.

NMVOC sources are distributed more evenly among the different sectors, such as 'Solvent use' (31%), 'Road transport' (19%), 'Agriculture' (11%) as well as 'Non-industrial combustion plants' (11%).

The main source of SO_x emissions are large point sources from combustion in energy and transformation industries (58%).

Ammonia arises mainly from agricultural activities, about 87% across all years, while CO emissions originate primarily from road transport (34%) and residential heating (27%).

The main sources of primary PM emissions (up to 52%) are residential heating and combustion in energy and transformation industries but also production processes, which contribute 17 to 25 percent and agriculture with a share of 8 to 18 percent.

Figure 3.2 and Figure 3.3 illustrate the sector contribution for the sum of total emissions in the EMEP West region and the EMEP East region respectively. The split between EMEP West and EMEP East regions is according to `http://www.ceip.at/emep_countries`. 'Remaining Asian Areas' are included in the EMEP East region (in Figure 3.3). The comparison of both graphs highlights some significant differences between west and east.

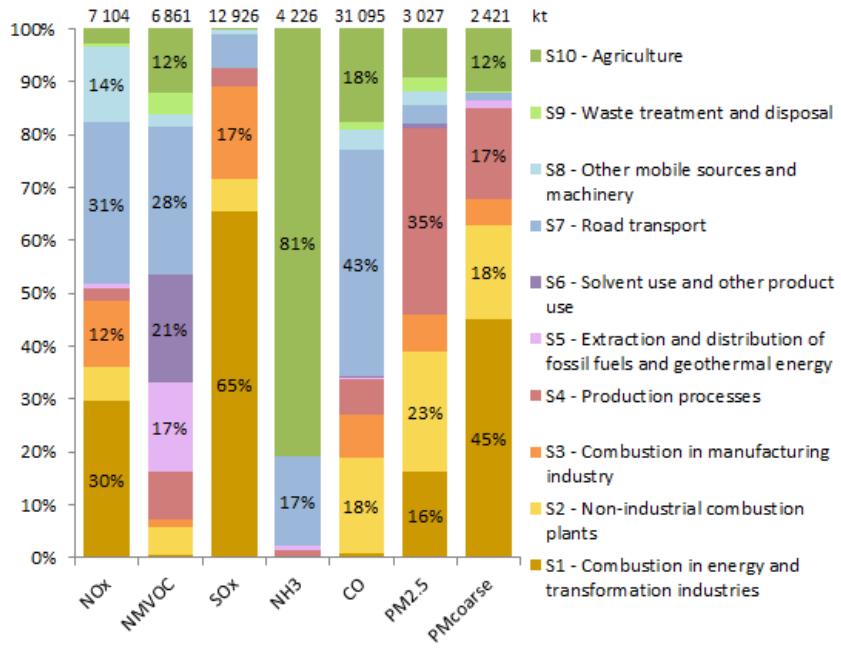

Figure 3.3: SNAP sector contribution to national total emissions in 2014 for the EMEP East region (only percentages above 10% are visible). 'Remaining Asian Areas' are included in the EMEP East region.

Whilst 'Other mobile sources and machinery' (S8) have a quite high share (up to 40%) for the pollutants NO_x, SO_x, CO and $PM_{2.5}$ in EMEP West area, the same sector is not really relevant for EMEP East area, for example 14% of NO_x.

For NMVOC in the EMEP West region the most relevant sector is 'Solvent use and other product use' (S6) with a share of 41%. In the EMEP East region the sector 'Road Transport' (28%) has a higher share than sector 6 (21%).

The main source of SO_x is 'Combustion in energy and transformation industries' (S1) with 40% in the EMEP West area, but in the EMEP East region this sector contributes even 65% of the SO_x emissions.

The main source of NH_3 emissions for EMEP West and EMEP East is the agricultural sector (S10) with 93% and 81% respectively. For the EMEP East region, 'Road transport' (S7) is important as well (17%).

CO emissions arise mainly from 'Road transport', 'Non-industrial combustion plants' and 'Agriculture' in EMEP East, which together account to a share of about 79%. In the EMEP West region, several sectors play an important role (S2, S7, S4, S3 and S8) - with the sector 'Non-industrial combustion plants' as the most significant sector (39%).

For $PM_{2.5}$ 'Non Industrial combustion plants' (S2) holds a quite significant share (45%) of the total in the EMEP West area. For the EMEP East area the sector 'Production processes' (S4) has the highest share, 35% of total emissions. Whilst for PM_{coarse} emissions 'Agriculture' (S2) is quite important in the west, yielding about 38%, for the eastern region 'Combustion in energy and transformation industries' (S1) is the key sector (45%).

3.2 Emission trends in the EMEP extended area

The emission trend in Figure 3.4 indicates that in the EMEP area total emissions (excluding shipping, natural and volcanic emissions and the North African area) of reported pollutants have decreased overall since 1990. Presented emission trends are partly based on reported data and partly on expert estimates, therefore there is a certain uncertainty in the magnitude of this development. The observed decrease is rather significant for SO_x, NO_x, CO and NMVOC. NH_3, $PM_{2.5}$ and PM_{coarse} emissions show a slight increase.

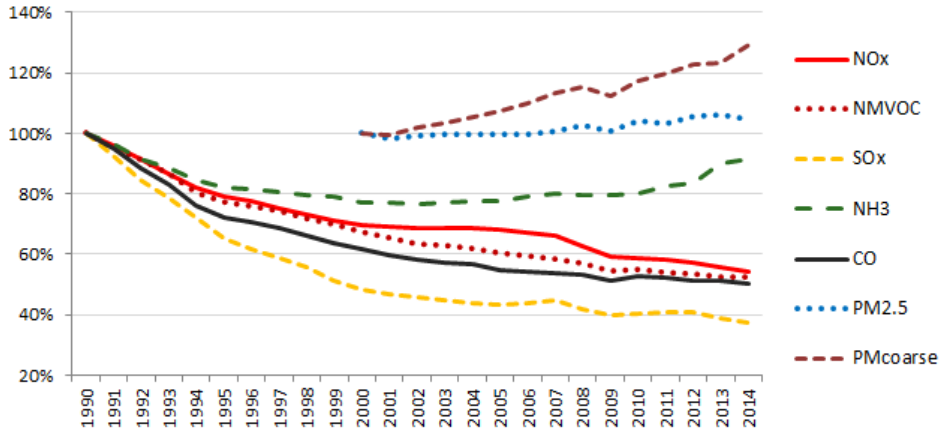

Figure 3.4: Emission trends for 1990-2014 in the EMEP area based on data reported by countries and gap-filled with expert estimates. (Shipping emissions are not included.)

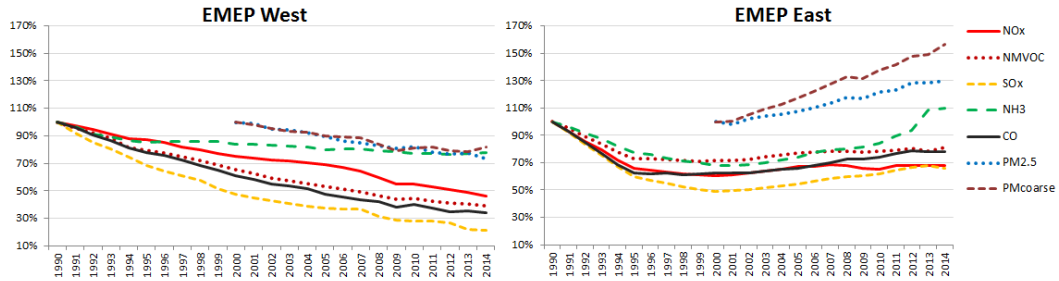

Figure 3.5: Emission trends for 1990-2014 in the EMEP area based on data reported by countries (gap-filled with expert estimates) divided in 2 areas "EMEP West" (left), "EMEP East" (right).

A more detailed assessment shows that emission developments in the eastern and western part of EMEP area seem to follow different patterns (see Figure 3.5)[12]. While emissions of most of the pollutants in the western part of EMEP area are slowly decreasing, emissions in the east seem to fluctuate around the same level or even increase. The emissions in western parts of EMEP area are almost 100% based on reported data, the emissions in eastern parts are rather often expert estimates so the uncertainty is rather high. The significant increase in NH_3 emissions in "eastern area" is mainly influenced by emissions reported by Turkey caused by revisions of the emission factors in agriculture.

[12]The split between EMEP West and EMEP East regions is according to `http://www.ceip.at/emep_countries`. 'North Africa' is not included and 'Remaining Asian Areas' are included in the EMEP East region.

A major reason for divergences in the trends is the implementation of various energy- and pollution-related EU directives into national law, which led to substantial increases in energy efficiency especially in the former communist new EU member states. A further reason is the economic recovery in the East region following the collapse of the Soviet Union. As a result, emissions in EMEP East began to stabilise or even increase slightly between 1995 and 2000. In the early 2000s, strong economic growth took place in this region. More information on socioeconomic drivers can be found in Colette et al. (2016).

3.3 Comparison of emission levels from the current year, the year 2000 and emission commitments

Emission levels for 2014 of individual countries[13] are compared to 2000 emission levels for SO_x, NO_x, NMVOC, CO, NH_3 and PMs (see Figures 3.6 - 3.8). Overview tables with reported emission trends for individual countries have been published on the CEIP website[14] and detailed information on the sectoral level can be accessed in WebDab[15].

The 1999 Gothenburg Protocol (GP) lists emission reduction commitments of SO_x, NO_x, NMVOC and NH_3 for thirty-three Parties[16] to the LRTAP Convention for the year 2010. These commitments should not be exceeded in subsequent years either. However, Figure 3.6 and Figure 3.7 indicate that a number of countries could not reduce their emissions[17] regarding the GP requirements.

3.3.1 Trend analysis

The assessment of emission levels in individual countries show an increase of emissions compared to 2000 emission levels in several countries. In the case of NH_3 even 20 countries have emissions in 2014 higher than the year 2000 level. In the case of PM_{coarse} these are 17 countries, for $PM_{2.5}$ 12 countries, NO_x and NMVOC 10 countries and SO_x and CO eight countries. Further, a comparison with last year's submissions showed, that for NO_x (+1 country), NMVOC (+3 countries), NH_3 (+3 countries) and PM_{coarse} (+2 countries) the number of countries with emissions above the year 2000 level increases. This indicates that after the year 2000 the emission reductions slowed down and trends did reverse in a certain number of countries. Detailed explanatory information on emission trends should be provided in the informative inventory reports (IIRs).

[13] Emissions from Tajikistan, Turkmenistan, Uzbekistan and Remaining Asian Areas are not included in this assessment because data are 100% expert estimates. Also shipping, natural and volcanic emissions and the North African area are excluded.

[14] http://www.ceip.at/status_reporting/2016_submissions

[15] http://www.ceip.at/webdab_emepdatabase/reported_emissiondata and/or http://www.ceip.at/webdab_emepdatabase/emissions_emepmodels

[16] 34 Parties with 2010 targets listed in 1999 GP: Armenia, Austria, Belgium, Bulgaria, Belarus, Croatia, Cyprus, Czech Republic, Denmark, EU15, Finland, France, Germany, Greece, Hungary, Ireland, Italy, Liechtenstein, Lithuania, Luxembourg, Latvia, the Republic of Moldova, the Netherlands, Norway, Poland, Portugal, Romania, Slovakia, Slovenia, Spain, Sweden, Switzerland, the United Kingdom and Ukraine. Of these 10 (Armenia, Austria, Belarus, Greece, Ireland, Italy, Liechtenstein, the Republic of Moldova, Poland and Ukraine) have not signed/ratified the 1999 GP yet.

[17] Based on 'fuel sold' data.

3.3.2 NO_x emissions

On the basis of reported data, the total reduction of NO_x emissions in the EMEP area for the period 2000 - 2014 was estimated at -22%. Emissions decreased in 37 countries and increased in 10 countries (see Figure 3.6). The strongest increase was reported by Kyrgyzstan (+161%). Six countries still exceed their NO_x ceilings stipulated in the GP, e.g. Luxembourg (by 156%) and Austria (by 41%). In comparison with last year, the emissions of one country

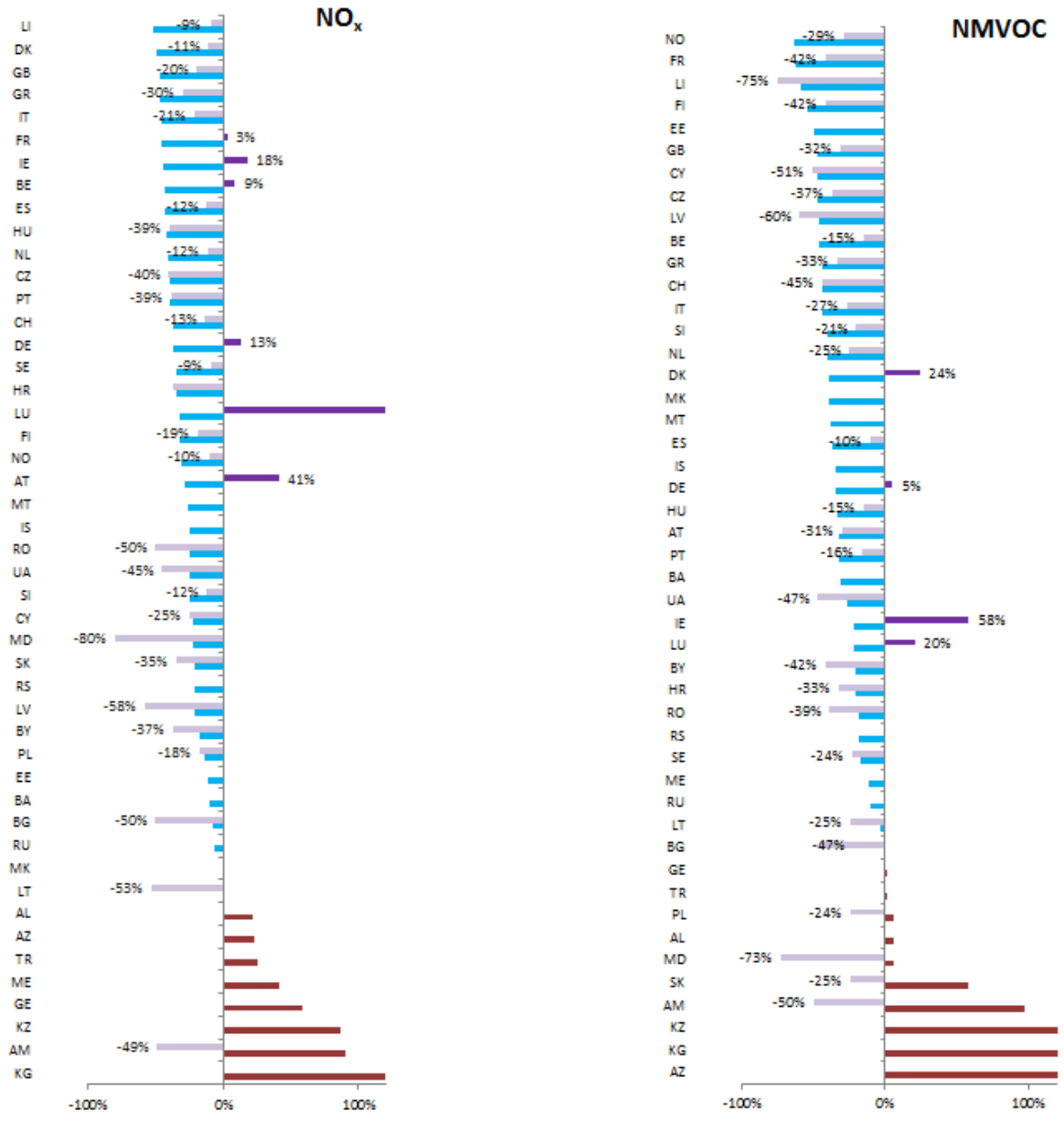

Figure 3.6: NO_x and NMVOC emissions - differences 2000-2014 and distance of 2014 emissions to the Gothenburg Protocol targets. *Blue and red bars: Differences between emissions reported for 2000 and 2014. Blue means that 2014 emissions were lower than 2000 emissions. Red means that 2014 emissions were higher than 2000 emissions. Purple bars: Distance of 2014 emissions to the GP targets. Light purple means that the reported 2014 emission value was below the GP target. Dark purple means that the 2014 emission value was above the GP target.*

(Liechtenstein) are now below the GP ceilings.

3.3.3 NMVOC emissions

Emissions in the EMEP area have decreased by -22% compared with 2000 levels. Compared with 2000, NMVOC emissions have decreased in 37 countries and increased in 10 countries

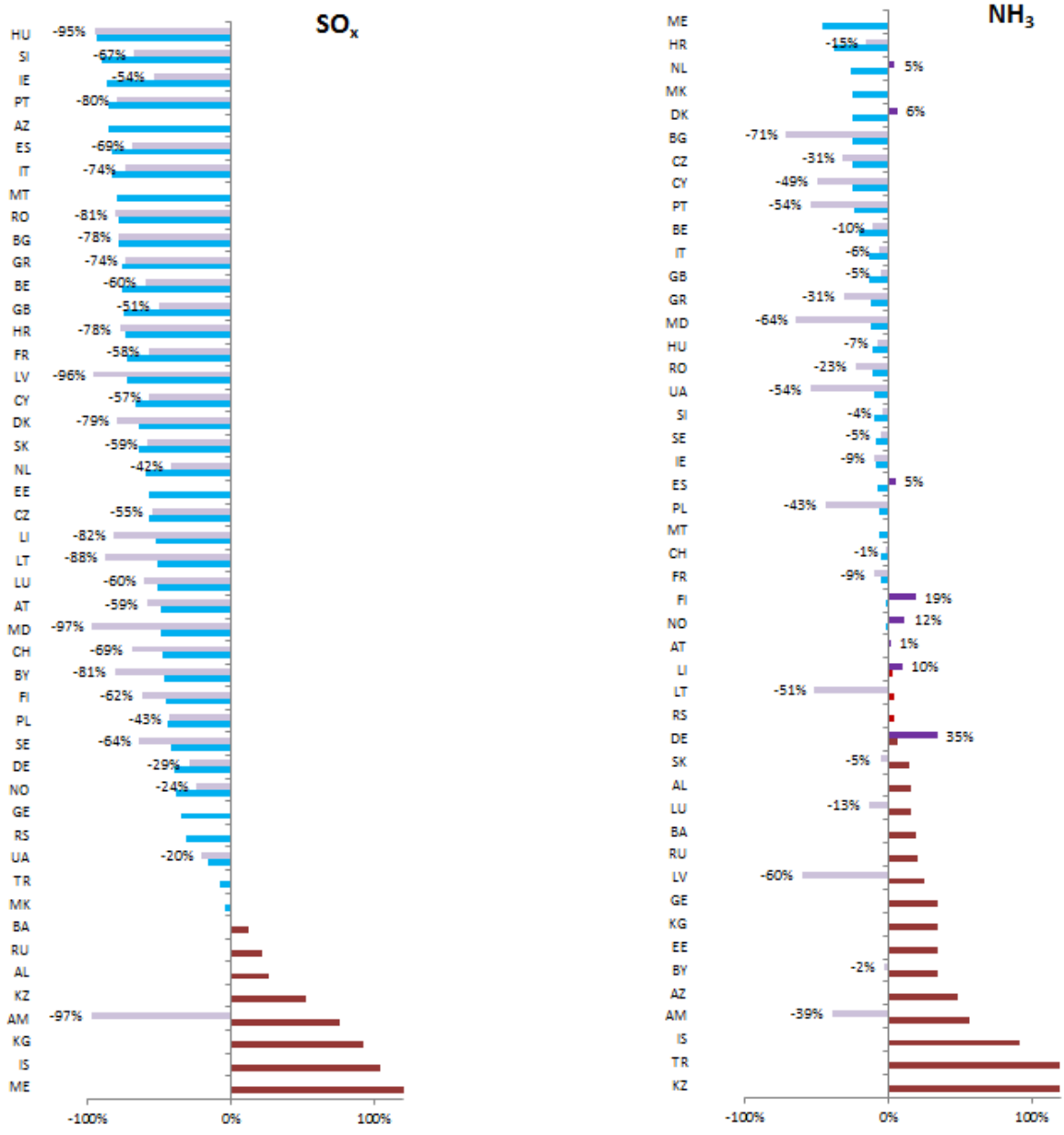

Figure 3.7: SO_x and NH_3 emissions - differences 2000-2014 and distance of 2014 emissions to the Gothenburg Protocol targets. *Blue and red bars: Differences between emissions reported for 2000 and 2014. Blue means that 2014 emissions were lower than 2000 emissions. Red means that 2014 emissions were higher than 2000 emissions. Purple bars: Distance of 2014 emissions to the GP targets. Light purple means that the reported 2014 emission value was below the GP target. Dark purple means that the 2014 emission value was above the GP target.*

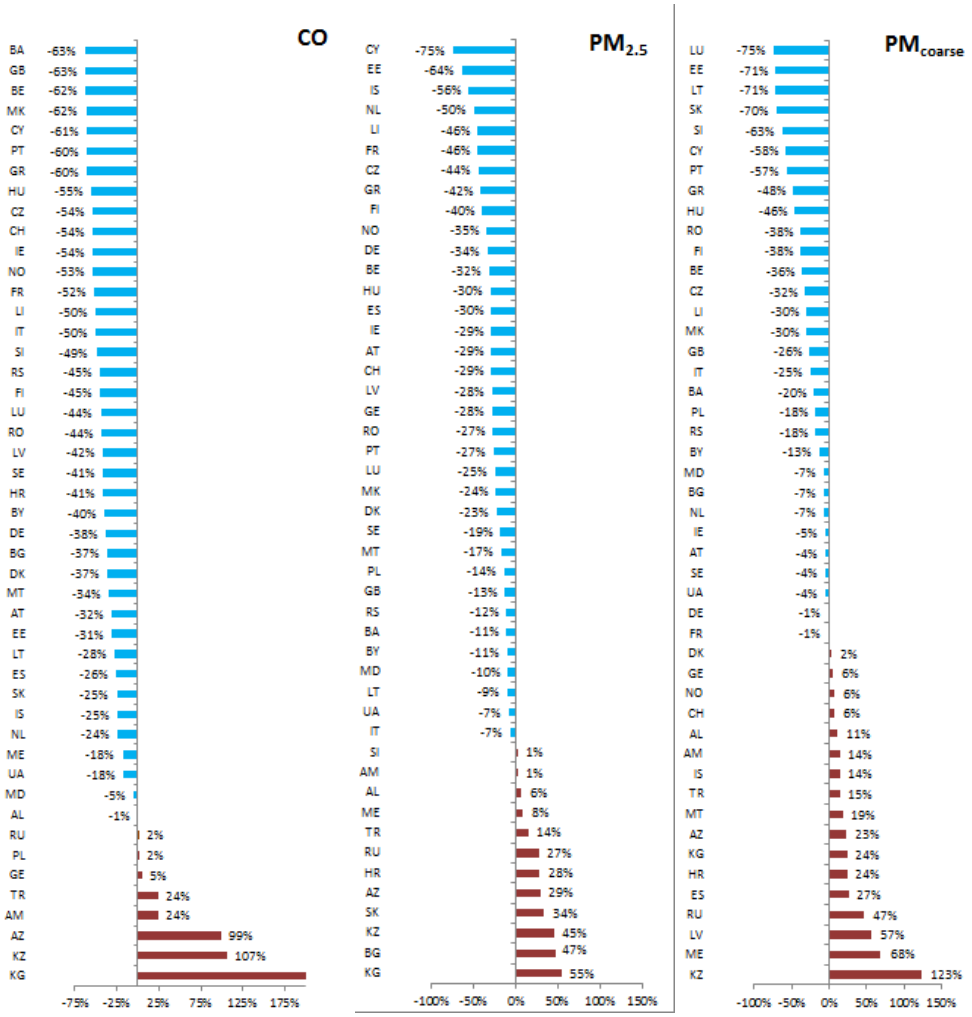

Figure 3.8: CO, $PM_{2.5}$ and PM_{coarse} emissions - differences 2000-2014. *Blue and red bars: Differences between emissions reported for 2000 and 2014. Blue means that 2014 emissions were lower than 2000 emissions. Red means that 2014 emissions were higher than 2000 emissions.*

(see Figure 3.6). The strongest NMVOC increase can be observed in Azerbaijan and Kyrgyzstan (+283% and +214%, respectively). Emissions of Ireland, Denmark, Luxembourg and Germany are above the GP ceilings (+58%, +24%, +20% and +5%, respectively). Last year, Luxembourg has reached the GP emission target (-15% in 2015).

3.3.4 SO_x emissions

Of all reported pollutants, SO_x emissions decreased by -23% between 2000 and 2014. Compared with 2000, SO_x emissions have decreased in 40 countries and increased in 7 countries - among them Macedonia (+194%) and Iceland (+104%). No country exceeded its SO_x GP target, neither in 2010, 2011, 2012 and 2013 nor in 2014 (see Figure 3.7).

3.3.5 NH_3 emissions

Emissions in the EMEP area have increased by +18% compared with 2000 levels. NH_3 emissions have decreased in 28 countries and increased in 19 countries (see Figure 3.7). The strongest increases were observed in Kazakhstan (+176%) and Turkey (+125%). Eight countries exceeded their GP targets also in 2014. In comparison with last year, the emissions of one country (Croatia) are now below the GP ceilings.

3.3.6 CO emissions

The total decrease in CO emissions from 2000 to 2014 amounted to -25%. Compared with 2000 CO emissions have decreased in 40 countries and increased in seven countries (see Figure 3.8), particularly in Kyrgyzstan (+217%), Kazakhstan (+107%) and Azerbaijan (+99%).

3.3.7 $PM_{2.5}$ emissions

$PM_{2.5}$ emissions in the EMEP area have increased by +5% compared with 2000 levels. Compared with the year 2000, $PM_{2.5}$ emissions have decreased in 35 countries and increased in 12 countries (see Figure 3.8). The highest increases are reported by Kyrgyzstan (+55%), Bulgaria (+47%) and Kazakhstan (+45%).

3.3.8 PM_{coarse} emissions

The total increase in PM_{coarse} emissions from 2000 to 2014 amounted to +29%. Compared with 2000, PM_{coarse} emissions have decreased in 30 countries and increased in 17 countries (see Figure 3.8). The strongest increases can be observed in Kazakhstan (+123%), Montenegro (+68%), Latvia (+57%) and the Russian Federation (+47%).

3.4 Comparison of 2013 data (reported in 2015) and 2014 data (reported in 2016)

The comparison of 2013 emissions (reported in 2015) and 2014 emissions (reported in 2016) showed, that for 30 countries data changed by more than 15% for one or several pollutants (see Figure 3.9). These changes can be caused either during the gap-filling procedure or due to emission reductions or increases and recalculations made by the respective country.

In two countries, NO_x emissions changed more than 15%: Liechtenstein and Serbia (see Figure 3.9).

For NMVOC, emissions changed more than 15% in Slovakia, Liechtenstein, Luxembourg, Latvia, Estonia, Croatia, Iceland, Finland, Kazakhstan and France.

SO_x emissions changed more than 15% for 16 countries: Azerbaijan, Latvia, Romania, Liechtenstein, Ireland, Serbia, France, Switzerland, Cyprus, Slovenia, the United Kingdom, Kazakhstan, Iceland, Greece, Portugal and Denmark.

For NH_3, emissions changed more than 15% in seven countries: Iceland, Slovakia, Luxembourg, Croatia, Latvia, Serbia and Estonia.

CO emissions changed more than 15% for nine countries: Malta, Belgium, Croatia, Slovenia, Liechtenstein, the FYR of Macedonia, Romania, Estonia and Spain. For this pollutant, the highest changes occurred (see Figure 3.10).

In 11 countries, $PM_{2.5}$ emissions changed more than 15%: Iceland, Estonia, Liechtenstein, Finland, the United Kingdom, Latvia, Kazakhstan, France, Lithuania, Bulgaria and Belgium.

For PM_{coarse}, emissions more than 15% changed in 16 countries: Spain, Slovakia, Lithuania, Kazakhstan, Iceland, Luxembourg, Croatia, Slovenia, Portugal, Serbia, France, Estonia, Montenegro, Liechtenstein, Finland and Denmark.

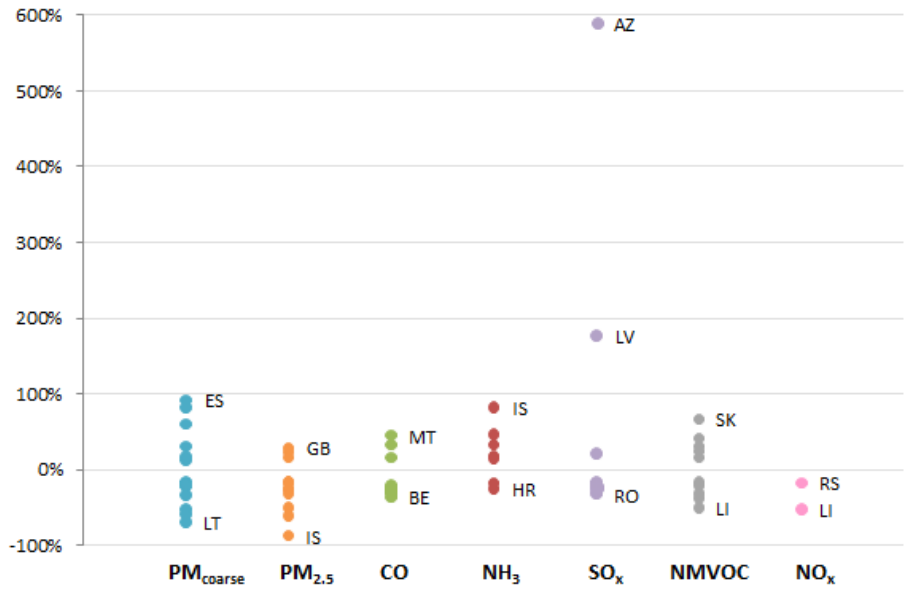

Figure 3.9: Changes between 2013 and 2014 (only changes larger than 15% are shown).

3.4.1 Changes due to the gap-filling

In Azerbaijan, the large change between 2013 and 2014 SO_x emissions (+589%) is caused by a change of the gap-filling methodology. In 2015 data was extrapolated until 2012 and then for the year 2013 the value of 2012 was copied. However, closer examination of the data suggested that steep decrease observed between 2005 and 2010 should not be linearly extrapolated. Instead it was decided to use 2010 data as a surrogate for 2014. This decision was justified as 2010 data in the case of Azerbaijan is the last available data that is supported by the scientific approach used for the models run by IIASA.

SO_x emissions in Greece changed by -18% compared to last year. Greece has provided national totals and sectoral data up to 2012. As emission estimates for a few sector/pollutant combinations where emissions were expected missing, and as there was a discrepancy for several sectors and the national totals between the reported data and the GAINS data, it was decided that for this year the GAINS data is to be used to fill missing values for 2014. For Greece GAINS data for the years 2010 and 2015 was available. The data for 2014 was interpolated between these two years. The GAINS model estimates a step decrease between 2010 and 2015. Interpolation of the data between 2010 and 2015 therefore resulted in a decrease of 30.7 Gg between 2013 and 2014.

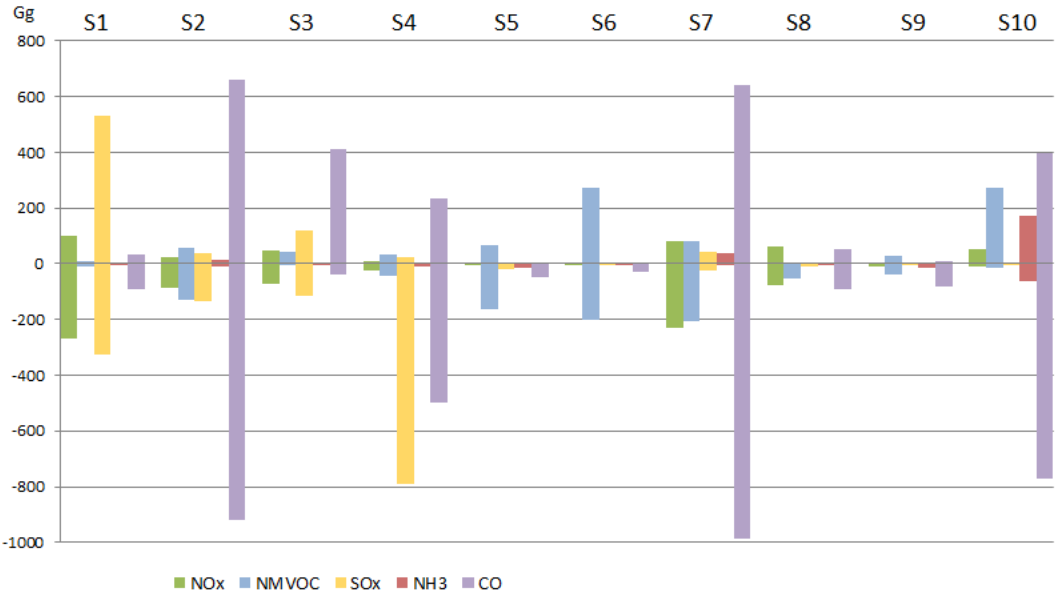

Figure 3.10: Total emission changes between 2013 and 2014 in the EMEP area, located in the individual SNAP sectors.

In Kazakhstan, large changes in SO_x emissions (-20%) and $PM_{2.5}$ emissions (-25%) between 2013 and 2014 occurred. For the EMEP inventory, the National Totals and sectoral data for the year 2013 and 2014 submitted by Kazakhstan were partly used. For a few sectors the discrepancy between reported data and the GAINS data seemed very high and comparison with other Parties showed exceptional emission estimates for these sectors. Kazakhstan and IIASA have been consulted. For the gap-filling in 2016 it was decided that a part of the sectors GAINS data is to be used as not all open questions could be clarified with Kazakhstan and IIASA before the submission of the gap-filled data. In the last gap-filling round, only extrapolated data GAINS data has been used. This explains the substantial difference between 2013 data gap-filled in 2015 and 2014 data gap-filled in 2016.

The emission changes of Macedonia for CO (-25%) can be explained as for the gap-filling in 2016 converted and interpolated GAINS data was used. In 2015 data was not gap-filled.

Emission data of Malta for CO showed high changes (+46%) between 2013 and 2014. For the gap-filling in 2015 converted and interpolated GAINS data was used. In 2016 data was not gap-filled as the submission of Malta seemed complete and plausible. This explains the substantial difference between 2013 data gap-filled in 2015 and 2014 data gap-filled in 2016.

SO_x emissions in Romania changed by -84%, and CO emissions by -23% compared to last year. For the gap-filling in 2015 converted and interpolated GAINS data was used. In 2016 data was not gap-filled as the submission of Romania seemed complete and plausible. This explains the substantial difference between 2013 data gap-filled in 2015 and 2014 data gap-filled in 2016.

3.4.2 Changes in reported data

High changes in country emissions between 2013 and 2014 are due to emission reductions or increases, and - more often - due to recalculations of the time series, mostly because of changes in emission factors or activity data, methodology updates or additional reporting.

Some explanations were given in the Informative Inventory Reports (IIRs) of the countries:

In Croatia, high changes of NH_3 emissions (-24%) occurred. Croatia reported in its IIR[18] an NH_3 emission decrease between 2013 and 2014 and recalculations were made in the agriculture sector due to improved methodology (Tier 2, EMEP/EEA (2013)) and updates in emission factors and activity data.

Between 2013 and 2014, a strong $PM_{2.5}$ emission increase (+29%) was detected in the United Kingdom. The United Kingdom explained in its IIR[19] that the main change between the 2015 submission and the 2016 submission is due to a significant revision in the consumption of wood fuel by the domestic sector in DUKES (much higher wood use now reported across the time series, and now showing a large increasing trend in wood use). In addition, the emission factor has been revised as part of the 2014 AQPI Improvement program - the new approach involves the use Tier 2 factors from the EMEP/EEA Guidebook (EMEP/EEA 2013).

In Latvia, high changes of SO_x emissions (+177%) occurred. Latvia stated in its IIR[20], that in the submission 2016 recalculations have been done. SO_2 emission factors have been updated for several fuel types for the whole time series. For the first time, SO_2 emissions for wood and natural gas for the whole time series (1990-2014) have been calculated and SO_2 and NO_x emissions from 1A1a sector have been recalculated, using country-specific or emission factors from the EMEP/EEA Guidebook (EMEP/EEA 2013).

In Serbia, large reductions in NOx emissions (-17%) were detected between 2013 and 2014. In the IIR of Serbia[21], large NOx reductions in the road transport sector were specified.

In Slovakia, large changes of NMVOC emissions (+67%) were given between 2013 and 2014. Slovakia stated in its IIR[22], that recalculations of NMVOC and reporting of categories, which were not reported before, are responsible for an increase in data compared to the previous reporting in 2015. In the agriculture sector, corrections of activity data, emission factors and notation keys have been done.

Large changes of PM_{coarse} emissions (+92%) in Spain were detected between 2013 and 2014. Spain reported in its IIR[23], that new emission estimates of particulate matter have been included in the subsectors Quarrying and mining (2A5a) and Construction and demolition (2A5b).

3.5 Spatial distribution of emissions

For this year it was agreed with the modellers to perform gap-filling and gridding for the year 2014 in 50×50 km^2 (PS) resolution on SNAP 10 sector level and in addition in $0.1^\circ\times0.1^\circ$longitude/latitude resolution on GNFR sector level.

[18] http://cdr.eionet.europa.eu/hr/un/UNECE_CLRTAP_HR/envvuipeq/IIR_CROATIA_2016_v2.pdf

[19] http://cdr.eionet.europa.eu/gb/un/cols3f2jg/envvuaj0w/GB_IIR_2016_Final.pdf

[20] http://cdr.eionet.europa.eu/lv/un/copy_of_colqhgwdg/envvugxfw/LV_IIR_15032016.pdf

[21] http://cdr.eionet.europa.eu/rs/un/UNECE_CLRTAP_CS/envvua4ia/CLRTAP_Serbia_IIR_2014_final.pdf

[22] http://cdr.eionet.europa.eu/sk/un/UNECE_CLRTAP_SK/envvzcncq/SK_IIR__2016_V2.pdf

[23] http://cdr.eionet.europa.eu/es/un/UNECE_CLRTAP_ES/envvubzaw/SPAIN_2016-CLRTAP_Informative_Inventory_Report-IIR.pdf

For the distribution of the 50×50 km^2 SNAP grid of NO_x, SO_x, NMVOC, NH_3, CO, $PM_{2.5}$, PM_{10} and PM_{coarse} for 2014 base grid data, which was calculated last year based on new reported gridded data, was used.

The 0.1°×0.1°GNFR grid of NO_x, SO_x, NMVOC, NH_3, CO, $PM_{2.5}$, PM_{10} and PM_{coarse} for 2014 were gridded based on the gridding system developed by CEIP, which is using EDGAR data[24], upgraded by point source information available under E-PRTR, for the distribution in areas where no reported gridded data in the 0.1°×0.1°resolution is available. This was the case for all areas, except Switzerland (where reported gridded data in the 0.1°×0.1°resolution is available for the whole time series from 1980 to 2014), United Kingdom (where reported gridded data in 0.1°×0.1°resolution is available for 2010) as well as Finland and Poland (where reported gridded data in 0.1°×0.1°resolution is available for 2014).

Comparisons between gridded emissions in 50×50 km^2 and 0.1°×0.1°resolutions are available on the CEIP website[25].

3.6 Volcanic emissions in 2014

3.6.1 Holuhraun fissure

On 16 August 2014 an intense seismic swarm started at the Barðarbunga volcanic system in Iceland (Sigmundsson et al. 2015), which eventually led to a non-explosive fissure eruption in the Holuhraun lava field (64.85°N, 16.83°W). A minor eruption was first observed in Holuhraun for about 4 hours on 29 August. This was followed by a long lasting fissure eruption on 31 August, which took six months with large gas emissions from the Icelandic volcanic system. There was little ash released in the eruption, but large amounts of SO_2 were emitted into the atmosphere. The eruption ended on 27 February 2015.

The 2014 Icelandic eruptions stands out from earlier ones in Iceland, e.g. the explosive volcanic eruptions of Eyjafjallajökull and Grímsvötn, in April-May 2010 and May 2011, respectively. These affected air traffic due to large amounts of ash emitted from Eyjafjallajökull, and ash and SO_2 in the case of Grímsvötn (see e.g. Moxnes et al. (2014), Stohl et al. (2011)). The explosive eruptions led to emissions in the middle and upper troposphere, while gas emissions from Holuhraun mainly affected lower altitudes and the transport of SO_2 influenced air quality in Iceland, Scandinavia and central Europe.

Preliminary results from a simulation with the EMEP model that included the emissions from the Holuhraun plain have been shown in last year's EMEP Status Report (Steensen et al. 2015). In that simulation the emissions were set to 400 kg/s (according to early estimates from Iceland Met Office) from August 31 to the rest of the year (Barsotti 2014), and the emissions were injected equally from the ground up to 3 km.

In 2016 Iceland included SO_2 emissions from this eruption in the emission data reported under the LRTAP Convention. According to the IIR of Iceland[26] the total SO_2 emission from the Holuhraun eruption was estimated to be 12,006 kt. Divided on calender years 10,880 kt of SO_2 was emitted in the year 2014 and 1,126 kt of SO_2 in the year 2015. To put these numbers in perspective it can be said that the total SO_2 emission from all the European Union countries

[24] http://edgar.jrc.ec.europa.eu/methodology.php

[25] http://www.ceip.at/new_emep-grid/grid_comparisons

[26] http://cdr.eionet.europa.eu/is/un/UNECE_CLRTAP_IS/envvuhkya/Infomative_Inventory_Report_Iceland_2016.pdf

for the year 2014 was 3,077 kt. So the emission from the eruption in the year 2014 i.e. from August 29th 2014 to December 31st 2014 was more than three times the total SO_2 emission from all the European Union countries for the whole year. Also, this emission represents a third part of all SO_2 emission within the EMEP domain in 2014, included both land-based anthropogenic, international shipping and natural emission sources.

For transport modelling, however, more detailed information about the source term of the eruption, that is, the source strength as a function of altitude and time is needed.

Time series of plume height observations/measurements and the time series of the SO_2 emission rate measurements have been kindly provided by Melissa Anne Pfeffer from the volcanic hazard team at the Icelandic Met Office with permission to use the information for input data in the EMEP/MSC-W model simulation.

For the days with no measurements we assumed persistence (i.e. kept the previous or next measured value) for plume height, while for the emission strength we assumed persistence only at the beginning and end of the eruption, and interpolated linearly elsewhere.

This gap-filling method resulted in a SO_2 emission total for 2014 that was 467 kt (4%) higher than the total SO_2 emission reported by Iceland. Therefore, we adjusted the source strength of eruption in order to reproduce the officially reported data for 2014. This was achieved by slightly reducing the emission rates during the first 11 days of eruption, which were significantly higher than the emission rates during later stages of the eruption. The relative effect of reduction was smallest for these days, and the adjusted emission rates are still significantly higher than those from day 12, the emission pattern over time has changed marginally.

3.6.2 Passive degassing of SO_2 from Italian volcanoes

SO_x emissions from passive degassing of Italian volcanoes (Etna, Stromboli and Vulcano) are included in the emission data reported by Italy. According to the reported data, SO_x emissions from the Italian volcanoes shows a generally down-going trend for the last two decades and decreased from 8326 Gg/year in 1990 to 943 Gg/year in 2010, then remained on the same level between 2010 and 2014.

For several years the reported emission data has been replaced by a default value of 2500 Gg/year in the EMEP/MSC-W model simulations as the reported trend seems to be questionable. In lack of more scientifically sound expert estimates, however, the reported SO_x emission from Italian volcanoes has been used in all model simulations presented in this report.

References

Barsotti: 100 Days of Continuous Eruptive Activity in Holuhtaun (Icelandic Met Office), URL en.vedur.is/media/jar/bb100days_ens.pdf, 2014.

Colette, A., Aas, W., Banin, L., Braban, C., Ferm, M., González Ortiz, A., Ilyin, I., Mar, K., Pandolfi, M., Putaud, J.-P., Shatalov, V., Solberg, S., Spindler, G., Tarasova, O., Vana, M., Adani, M., Almodovar, P., Berton, E., Bessagnet, B., Bohlin-Nizzetto, P., Boruvkova, J., Breivik, K., Briganti, G., Cappelletti, A., Cuvelier, K., Derwent, R., D'Isidoro, M., Fagerli, H., Funk, C., Garcia Vivanco, M., González Ortiz, A., Haeuber, R., Hueglin, C., Jenkins, S., Kerr, J., de Leeuw, F., Lynch, J., Manders, A., Mircea, M., Pay, M., Pritula, D., Putaud, J.-P., Querol, X., Raffort, V., Reiss, I., Roustan, Y., Sauvage, S., Scavo, K., Simpson, D., Smith, R., Tang, Y., Theobald, M., Tørseth, K., Tsyro, S., van Pul, A., Vidic, S., Wallasch, M., and Wind, P.: Air Pollution trends in the EMEP region between 1990 and 2012., Tech. Rep. Joint Report of the EMEP Task Force on Measurements and Modelling (TFMM), Chemical Co-ordinating Centre (CCC), Meteorological Synthesizing Centre-East (MSC-E), Meteorological Synthesizing Centre-West (MSC-W) EMEP/CCC Report 1/2016, Norwegian Institute for Air Research, Kjeller, Norway, URL http://www.unece.org/fileadmin/DAM/env/documents/2016/AIR/Publications/Air_pollution_trends_in_the_EMEP_region.pdf, 2016.

EMEP/EEA: EMEP/EEA air pollutant emission inventory guidebook - 2013, 12/2013, European Environment Agency, EEA, URL http://www.eea.europa.eu/publications/emep-eea-guidebook-2013, 2013.

Mareckova, K., Wankmüller, R., Pinterits, M., and Ullrich, B.: Inventory review 2015. Review of emission data reported under the LRTAP Convention and NEC Directive. Stage 1 and 2 review. Status of gridded and LPS data, EMEP/CEIP 1/2015, EEA/CEIP Vienna, 2015.

Mareckova, K., Pinterits, M., Tista, M., and Wankmüller, R.: Inventory review 2016. Review of emission data reported under the LRTAP Convention and NEC Directive. Stage 1 and 2 review. Status of gridded and LPS data, EMEP/CEIP 1/2016, EEA/CEIP Vienna, 2016.

Moxnes, E. D., Kristiansen, N. I., Stohl, A., Clarisse, L., Durant, A., Weber, K., and Vogel, A.: Separation of ash and sulfur dioxide during the 2011 Grímsvötn eruption, Journal of Geophysical Research: Atmospheres, 119, 7477–7501, doi:10.1002/2013JD021129, URL http://dx.doi.org/10.1002/2013JD021129, 2013JD021129, 2014.

Sigmundsson, F., Hooper, A., Hreinsdöttir, S., Vogfjörd, K., Ófeigsson, B., Heimisson, E. R., Dumont, S., Parks, M., Spaans, K., Gudmundsson, G. B., Drouin, V., Árnadöottir, T., Jónsdöttir, K., Gudmundsson, M. T., Högnadöottir, T., Fridriksdöottir, H., Hensch, M., Einarsson, P., Magnöusson, E., Samsonov, S., Brandsdöttir, B., White, R. S., Ágústsdöttir, T., Greenfield, T., Green, R., Hjartardöttir, A. R., Pedersen, R., Bennett, R. A., Geirsson, H., Femina, P. L., Björnsson, H., Pálsson, F., Sturkell, E., Bean, C. J., Möllhoff, M., Braiden, A., and Eibl, E.: Segmented lateral dyke growth in a rifting event at Bárðarbunga volcanic system, Iceland, Nature, 517, 191–195, doi:doi:10.1038/nature14111, 2015.

Steensen, B. M., Schulz, M., Stebel, K., Theys, N., Fagerli, H., and Aas, W.: Influence of the sulfur dioxide emissions from the Holuhraun eruption in 2014., in: Transboundary acid-

ification, eutrophication and ground level ozone in Europe in 2013. EMEP Status Report 1/2015, The Norwegian Meteorological Institute, Oslo, Norway, 2015.

Stohl, A., Prata, A. J., Eckhardt, S., Clarisse, L., Durant, A., Henne, S., Kristiansen, N. I., Minikin, A., Schumann, U., Seibert, P., Stebel, K., Thomas, H. E., Thorsteinsson, T., Tørseth, K., and Weinzierl, B.: Determination of time- and height-resolved volcanic ash emissions and their use for quantitative ash dispersion modeling: the 2010 Eyjafjallajökull eruption, Atmospheric Chemistry and Physics, 11, 4333–4351, doi:10.5194/acp-11-4333-2011, URL http://www.atmos-chem-phys.net/11/4333/2011/, 2011.

UNECE: Guidelines for reporting emission data under the Convention on Long-range Transboundary Air Pollution, Tech. Rep. ECE/EB.AIR/130, UNECE, URL http://www.ceip.at/fileadmin/inhalte/emep/2014_Guidelines/ece.eb.air.125_ADVANCE_VERSION_reporting_guidelines_2013.pdf, 2014.

Part II

Research Activities

CHAPTER 4

Development of a downscaling methodology for urban applications (uEMEP)

Bruce Rolstad Denby, Peter Wind

4.1 Introduction

In recent years, policy attention to air pollution has mostly been driven by health impact concerns. Urban areas receive most attention, both because this is where most people live and because these areas are most polluted. Air pollution in cities is often considered to be a local phenomenon - caused by emissions sources in the city itself. However, a substantial part of the concentrations in cities can originate from sources outside the city, often from neighbouring countries or even further away.

For many years the EMEP/MSC-W model has been used to study a range of policy and emission scenarios and to assess the impact of emission reduction schemes on a Europe wide basis. At present, official EMEP calculations are performed at a spatial resolution of ca. 50 x 50 km^2. From 2017 onwards, the standard resolution of the EMEP/MSC-W model and its application for EMEP and the LRTAP Convention will be performed at a spatial resolution of 0.1 x 0.1^o. Even so, the model only spatially resolves the largest cities and its application for heath assessment is limited to urban background exposure estimates.

In order to capture the high concentration gradients associated with urban emissions, there is a need to increase the resolution of the model. In particular road traffic presents a challenge since concentrations decrease rapidly from the kerbside. One method for improving the urban background levels is to increase the spatial resolution of the model itself, with a minimum feasible resolution of around 1 x 1 km^2. However, gridded models will never be able to capture the near road gradients so its use would still be limited. Another method is to nest sub-grid models, usually Gaussian dispersion models, into the modelling system. This method can be problematic due to the differences between the two dispersion descriptions and the problem with double counting within the grid.

An alternative approach to this is described in this chapter. This involves the spatial redistribution of the EMEP grid cell concentrations onto high resolution sub-grids (down to 50 x 50 m^2), using a redistribution scheme based on Gaussian dispersion. Such methods have shown great promise in previous studies (Denby 2014, 2015, Theobald et al. 2016), producing rather realistic estimates of sub-grid concentrations where emission inventories or good proxies for emissions are available. The method presented here preserves the EMEP grid concentrations, avoiding any problems with double counting of emissions, and provides a similar result to sub-grid modelling.

The method is applied to a test case in Oslo for NO_2 where the required sub-grid data is readily available for traffic sources. The resulting sub-grid fields resolve the near road gradients and, when compared to observations, show a remarkable improvement in results. The method has significant potential for improving exposure estimates for policy scenarios. Furthermore, it will allow much better estimates of the local versus transboundary contributions in urban areas.

4.1.1 Background

Enhanced resolution of the EMEP model has been obtained in a number of parallel applications including EMEP4UK and EMEP4HR. In these cases the model has been coupled to high resolution meteorological models and emission fields to provide resolutions down to 1 x 1 km^2. Such applications are very useful in estimating the impact of enhanced resolution on both the physical processes in the model and the resulting exposure and concentration fields. However, they are computationally expensive and require high resolution emission data that is not generally available.

An alternative to increased model resolution (dynamic downscaling) is the use of sub-grid downscaling methods. There are basically two sub-grid downscaling methods. The first implements additional high resolution models, such as Gaussian dispersion models, within the model grid and the second redistributes existing model concentrates at high resolutions within the model grid. The first method is applied in many urban and local scale models used to assess city wide concentration fields. The second method makes use of additional high resolution spatial information available within a model grid that can be used to redistribute model concentrations or provide an alternative statistical interpretation of the model results. An example of such a sub-grid application can be found in Denby et al. (2011) where high resolution emission and population data were used to assess the impact of sub-grid variability on population exposure.

In previous studies concerning traffic related emissions and regression modelling, (Denby 2015, 2014), it was found that a single traffic proxy could be used to spatially distribute concentrations. For an application in Bergen (Denby 2015) this proxy was used for regression modelling, creating maps of NO_2 concentrations at 25 m resolution based on measurements from 32 passive samplers. These high resolution fields were used to assess the population exposure and to map air quality zones. The spatial proxy for traffic used as starting point in these studies was the parameter 'vehicle kilometres driven', based on road network data. This parameter, when multiplied by an emission factor, provides actual emissions so it is highly representative of the emissions themselves. To distribute this parameter in space a pseudo dispersion algorithm was used, in order to mimic the spatial distribution of the near surface emissions. This algorithm had the form of an inverse power relationship, with parameters determined by a fit to the Gaussian dispersion model URBIS (Denby 2014). The method

proved very successful in reproducing the spatial distribution of pollutants from traffic and from shipping.

This pseudo dispersion methodology can also be applied as a redistribution method for gridded concentrations. Since it is based on a single parameter (regression coefficient) it is also possible to use the gridded concentrations and redistribute these using the same methodology. To do this for the EMEP/MSC-W model a number of developments are required. In this chapter we describe the development of a more robust physically based redistribution scheme and provide some initial tests of the methodology to ascertain its feasibility.

When implemented the redistribution methodology, named 'uEMEP' to represent 'urban EMEP', will provide enhanced spatial resolution of pollutant concentrations in urban areas (~50m), where appropriate data is available, that can be used for the following applications

- High resolution population exposure assessments
- Direct validation of the model against urban background and traffic stations
- Ability to assess the impact of European wide policy scenarios on limit value exceedances
- A methodology for validating EMEP emissions in urban environments
- A consistent approach for urban and rural areas in European air quality policies

4.1.2 Concept

Within each EMEP grid, particularly in urban areas, are a number of emission sources. Major sources here include traffic, domestic heating and shipping. Additionally other industrial sources may be included. Determination of emissions within each grid is a complex task and is based on actual known emissions as well as distributed emissions based on proxies such as shipping activities, road network density and population density. These proxies are used to disaggregate national emission totals. Some proxy data is actually very well defined at high resolution. Road network data (positioning) is available through a range of European wide GIS systems used for route planning. Unfortunately there is currently no European wide data source for traffic volumes. Population density is also available at 100 m resolution for all of Europe. Home address positions are also available in many countries.

The concept behind the redistribution method to be employed in uEMEP is based on the use of these proxy data. Sub-grids of aggregated proxy data, e.g. vehicle kilometres or population density, can be defined at high resolution (~50 m) and these treated as pseudo emission sources. These are then redistributed in space according to Gaussian plume dispersion theory. This redistribution occurs not just at the surface but throughout the lowest layer grid volume. By averaging the Gaussian distribution in the EMEP grid volume and calculating the Gaussian distribution at each sub-grid then the fraction of the grid concentration at each surface sub-grid can be determined. This fraction is then used to directly redistribute the EMEP grid volume concentration on the surface. This approach requires knowledge of the contribution of each specific source to the total concentration in each EMEP grid.

The method can be used as a post processing tool, applied to annual concentrations or can be applied on an hourly basis online in the model. The first of these requires a redistribution representative of the entire meteorological year which, for many applications with uniform

wind distributions, can be approximated as a rotationally symmetric plume. For the hourly application information on wind speeds and atmospheric stability are required each hour and the redistribution must occur online. This is more demanding on computations and on the temporal profiles used to describe emissions in the EMEP model. For the time being we focus on the post processing of annual mean data but the concepts are the same.

In order to implement and test this concept a number of steps must be carried out. These include:

1. Specification of suitable Gaussian dispersion schemes for the redistribution
2. Assessment of the compatibility of EMEP model K theory diffusion with Gaussian dispersion theory
3. Assessment of the availability of required data sources in Europe
4. Implementation and testing of a scheme in the EMEP model to determine the local grid source contribution to concentrations
5. Development of a scheme suitable for implementing chemistry in the redistribution
6. Verification and validation of the methodology against a subset of measurement data

In this first preliminary study we will describe points 1 and 4 and provide an example validation, point 6, for Oslo where suitable data is already available.

4.2 Redistribution scheme

In order to implement a Gaussian dispersion redistribution scheme the following steps are taken:

- Derive a rotationally symmetric Gaussian dispersion kernel, based on 'standard' Gaussian dispersion formulations, for the redistribution scheme
- Derive an integrated form of the dispersion kernel for determining volume average concentrations
- Develop and describe a methodology for its implementation

4.2.1 Gaussian dispersion modelling

The Gaussian slender plume model intensity (I) can be written, in Cartesian co-ordinates (x,y,z), by normalising the concentration (C) with the wind speed U and the emission Q at height h with total reflection from the surface (Seinfeld and Pandis 2006) as

$$I(x,y,z,h) = C\frac{U}{Q} = \frac{1}{2\pi\sigma_y\sigma_z}\exp\frac{-y^2}{2\sigma_y^2}\left\{\exp\frac{-(z-h)^2}{2\sigma_z^2} + \frac{-(z+h)^2}{2\sigma_z^2}\right\} \qquad (4.1)$$

This normalised form has units m^{-2} and represents the intensity of the plume in the y, z plane at a position x. The plume size in the y, z plane is defined by the standard deviation of the

Table 4.1: Examples of Gaussian plume dispersion parameters in neutral conditions

Source	Description	a_y	b_y	a_z	b_z
Smith (1973)	60 minute averages, elevated release	0.32	0.78	0.22	0.78
Klug (1969)	10 minute averages, elevated release	0.22	0.76	0.14	0.73
Liu et al. (2015)	Optimised for ground level release	0.64	0.46	0.088	0.72

plume $\sigma(y, z)$ which in turn is often parametrised in terms of distance *x* from the source. There are various forms of these parametrisations available but we use a common simple form given by

$$\sigma_{(y,z)} = \sigma_{0(y,z)} + a_{(y,z)} x^{b_{(y,z)}} \tag{4.2}$$

Here $\sigma_{0(y,z)}$ is the initial plume size in the y or z direction that may be the result of plume turbulence from stacks, from traffic turbulence or may also represent the initial size of the plume if it is emitted from area sources. For an area source of dimensions dx x dy then $\sigma_{0(y,z)}$ can be approximated as

$$\begin{aligned} \sigma_{0y} &= \sigma_{init,y} + \frac{dy}{2} \\ \sigma_{0z} &= \sigma_{init,z} + a_z \left(\frac{dx}{2} \right)^{b_z} \end{aligned} \tag{4.3}$$

Here $\sigma_{init(y,z)}$ are initial dispersions from the specific sources within an area. For traffic this would be due to traffic induced turbulence.

The factors $a_{(y,z)}$ and $b_{(y,z)}$ have been derived empirically by a number of authors and some typical values, under neutral conditions, for a and b are shown in Table 4.1. There is a wide range of parameters available in the literature.

4.2.2 Derivation of a rotationally symmetric Gaussian dispersion model

In order to determine a rotationally symmetric version of the Gaussian plume model, which will be used as a redistribution kernel, it is necessary to rewrite Equation 4.1 in terms of polar coordinates (r, θ, z) and integrate in θ to represent a homogeneous wind direction distribution. Unfortunately there is no direct analytical solution to this transformation and integration. Attempts to rewrite the plume model in polar or spherical co-ordinates (Green 1980) have relied on simplifications of the geometry in order to derive a set of useful equations. These simplifications depend upon assumptions concerning the width of the plume compared to the angle θ. When the plume width in the y direction is small then good approximations can be made but when the plume is large compared to the distance travelled, i.e. near source, then these assumptions are less valid.

Making a number of the necessary assumptions we derive the rotationally symmetric Gaussian plume equation, as a function of r and z, to be

$$I(r,z,h) = \frac{1}{\sqrt[3/2]{2\pi}\sqrt{1+B}r\epsilon_z} erf\left(\frac{\pi\sqrt{1+B}}{\sqrt[3/2]{2}\epsilon_\theta}\right)\left\{\exp\frac{-(z-h)^2}{2\epsilon_z^2} + \frac{-(z+h)^2}{2\epsilon_z^2}\right\} \quad (4.4)$$

where

$$\begin{aligned}\epsilon_z &= \sigma_{0z} + a_z r^{b_z}\\ \epsilon_\theta &= \frac{1}{r}\left(\sigma_{0y} + a_y r^{b_y}\right)\\ B &= -\epsilon_\theta^2\left(\frac{b_z(\epsilon_z - \sigma_{0z})}{r\epsilon_\theta} + \frac{b_y(r\epsilon_\theta - \sigma_{0y})}{\epsilon_z}\right)\end{aligned} \quad (4.5)$$

Equation 4.4 has been assessed against an 'exact' numerical integration of Equation 4.1. For $r \gg \sigma_{0y}$ Equation 4.4 is very accurate. In the region where $r \approx \sigma_{0y}$ then we find an error of around 10% in the solution.

4.2.3 Volume integration of the Gaussian dispersion model

In order to apply the redistribution method then we need to calculate the volume average intensity of the Gaussian plume (Equation 4.4) within an EMEP grid. Analytical solutions to this integration are only possible in the vertical direction so numerical methods are applied in the horizontal. The mean concentration of the plume between two heights H_1 and H_2 can be calculated by vertically integrating Equation 4.4, which involves only the terms within the $\{\}$ brackets, and can be written as

$$\begin{aligned}&I_H(r,h) = \frac{1}{(H_2-H_1)4\pi\sqrt{1+B}r} erf\left(\frac{\pi\sqrt{1+B}}{\sqrt[3/2]{2}\epsilon_\theta}\right)\\ &\left\{erf\left(\frac{(H_2-h)}{\sqrt{2}\epsilon_z}\right) - erf\left(\frac{(H_1-h)}{\sqrt{2}\epsilon_z}\right) + erf\left(\frac{(H_2+h)}{\sqrt{2}\epsilon_z}\right) - erf\left(\frac{(H_1+h)}{\sqrt{2}\epsilon_z}\right)\right\}\end{aligned} \quad (4.6)$$

In general H_1 will be at the surface and H_2 will be at the height of the lowest grid. However, it is also possible to carry out this integration over a number of vertical grid layers if necessary.

4.2.4 Numerical implementation and integration for multiple sources

The above radial plume model description will be used to redistribute the EMEP grid concentrations at any specified height z. Since there is no direct analytical solution to the radial integral in Equations 4.4 and 4.6 we must integrate this equations numerically in the r coordinate. In practise this simply involves applying Equations 4.4 and 4.6 at each sub-grid for each sub-grid source and numerically integrating over the EMEP grid area to determine the grid average intensity. Generally this integration is intended to give surface values but any height can be chosen.

The Gaussian dispersion functions described here are for single sources. In general we will have multiple sources that will require addition of all sources at all sub-grid points. We

describe below its implementation for the traffic contribution but the method is generally applicable.

To implement the method for traffic then the pseudo emission parameter *ADT.L* (Annual Daily Traffic x road link Length) is summed in sub-grid cells of the required resolution, in this case the maps are to be made on a 50 x 50 m^2. This is done by aggregating all road links, and their *ADT.L*, into this fine grid. This aggregated proxy emission source at height h, $S_h(i,j)$, is then dispersed to the proxy sub-grid $P_z(i,j)$ at height z using Equation 4.4 and summing over all sub-grid sources in the following way.

$$P_z(i,j) = \sum_{i'=1}^{n_x} \sum_{j'=1}^{n_y} S_h(i',j') I\left(r(i,j,i',j'), z(i,j), h(i',j')\right) \tag{4.7}$$

In addition to the surface proxy sub-grid $P_z(i,j)$ it is also necessary to determine the column average proxy sub-grid $P_H(i,j)$ using Equation 4.6 in order to redistribute the volume average concentrations from the EMEP model.

$$P_H(i,j) = \sum_{i'=1}^{n_x} \sum_{j'=1}^{n_y} S_h(i',j') I_H\left(r(i,j,i',j'), h(i',j')\right) \tag{4.8}$$

To convert the grid concentrations from the EMEP model to the sub-grid distribution then the mean of the column proxy sub-grid values $P_G(I,J)$ must be determined within the large scale grid, indexed with (I,J), by averaging all the sub-grid elements

$$P_G(I,J) = \frac{1}{n_x n_y} \sum_{i=1}^{n_x} \sum_{j=1}^{n_y} P_H(i,j) \tag{4.9}$$

The final sub-grid concentration field $C_{SG}(I,J,i,j)$ within the EMEP model grid (I,J), with local and non-local contributions to the model concentration given by $C_{G,local}(I,J)$ and $C_{G,nonlocal}(I,J)$, is then calculated as

$$C_{SG}(I,J,i,j) = F_{SG}(I,J,i,j).C_{G,local}(I,J) + C_{G,nonlocal}(I,J) \tag{4.10}$$

where the term $F_{SG}(I,J,i,j)$ is the 'redistribution scaling factor' that converts a large scale grid concentration to a sub-grid concentration and is derived as

$$F_{SG}(I,J,i,j) = \frac{P_z(i,j)}{P_G(I,J)} \tag{4.11}$$

and where the total concentration in the lowest layer EMEP grid is given by

$$C_G(I,J) = C_{G,local}(I,J) + C_{G,nonlocal}(I,J) \tag{4.12}$$

The large scale model grids are step wise in nature. Applying the above method directly to each grid will lead to significant edge effects because the sudden change in C_G from grid to grid will lead to non-continuous distributions of the sub-grid elements. We wish to apply Equation 4.10 continuously over the entire domain we are interested in (usually one city) without these discrete steps. We apply a 'moving window' concept where we estimate the concentration at each sub-grid point by moving window interpolation of the $C_G(I,J)$ fields.

4.3 Determination of local grid emission contributions in the EMEP model

In order to implement the redistribution methodology (Equation 4.10) then it is necessary to develop an efficient method for calculating the contribution of local grid emissions in each EMEP grid. There is currently a methodology already in place for doing this based on the Source Receptor (SR) calculations regularly made by EMEP. Using this it is possible, one grid at a time, to remove or reduce a particular emission from a particular grid and calculate the difference. This, however, is a tedious and time consuming solution if the redistribution methodology is to be applied over large regions, since it requires a new model calculation for every grid point. A first version of an efficient method for achieving this has been developed. In this Section we describe this new method briefly and present preliminary results that show the validity of the approach. The results from this development are tested in the example case for Oslo given in Section 4.4.

4.3.1 Overview of the local contribution methodology

The aim of this development is to provide the required information for the application of the redistribution methodology described in Section 4.2. This is specified as being the local grid contribution, from a particular emission source and pollutant, to the total concentration in that grid. Several processes affect the flux of concentrations within a grid including emissions, advection, vertical dispersion, chemical transformations and deposition.

The developed method traces the fluxes of the various source specific chemical compounds through these processes within a single grid column. Because the method does not rely on information outside each grid column, applying a simplified description of advection, then it is possible to assess the local grid emission contributions for all grids using, essentially, just one extra calculation. This is in contrast to the SR methodology that requires a new model calculation for every grid.

A local fraction, $F_{local}(I, J, K)$, is defined in the model at all grids which specifies the ratio of the local source contribution $C_{G,local}(I, J, K)$ to the total concentration within a grid $C_G(I, J, K)$.

$$F_{G,local}(I, J, K) = \frac{C_{G,local}(I, J, K)}{C_G(I, J, K)} \tag{4.13}$$

The routine for calculating the local fraction has been implemented at the various time splitting steps within the model, with the exception of deposition and chemistry, and provides hourly calculations of the local contribution. This can be aggregated to provide average values for an entire year.

4.3.2 Example results for Oslo

The local contribution scheme has been implemented in the EMEP model at 0.1^o resolution in the region around Oslo and we show results for the month of February 2012. At the same time the SR methodology, considered to be more 'exact' (ignoring numerical problems with the advection scheme), has also been applied to the highest emission grid cell in the Oslo region. Calculations for NO_x have been carried out for road traffic (SNAP sector 7) and

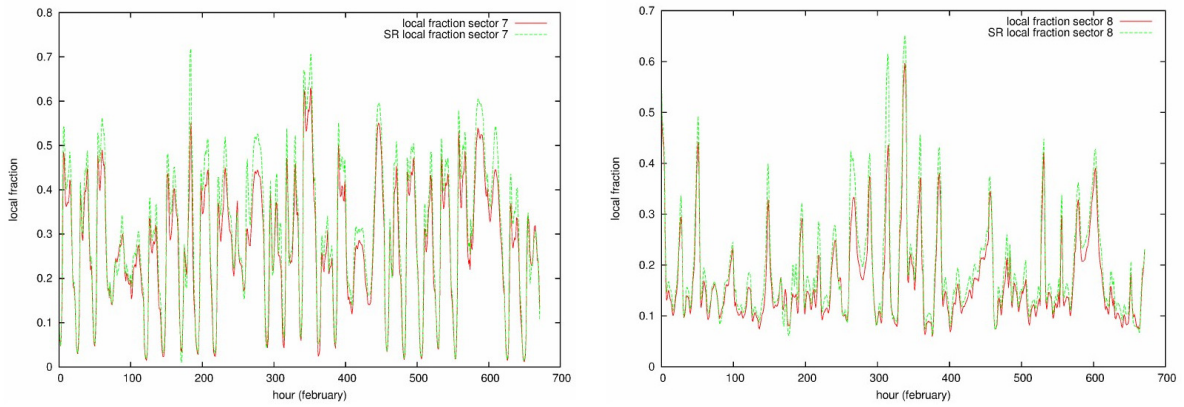

Figure 4.1: Local fractions for NO_x from sector 7 road traffic (left) and sector 8 shipping (right), in the Oslo grid cell obtained by two methods: In red the local fraction method presented above and in green the 'exact' Source Receptor (SR) method. Sector 7 and sector 8 account for 61.6% and 28.1% respectively of all NO_x emissions for this grid cell.

shipping (sector 8). A comparison of hourly local fractions of the two methods is shown in Figure 4.1.

For the traffic sector the local grid contribution (local fraction) varies with a daily cycle, due to the temporal variability of traffic. The local fraction is lowest during the early morning, corresponding to low traffic loads, and highest during the day, corresponding to high traffic loads. The local contribution scheme tends to give slightly lower fractions than the SR scheme. Both have peaks for local fractions of around 0.6 to 0.7. The average local fraction for this grid cell is around 0.26. In this grid cell road traffic accounts for 61% of the total emissions. This indicates that a significant fraction of the grid concentrations are from other neighbouring grid cells.

For the shipping sector the local fraction peaks during the early morning. This is mainly due to the lack of road traffic at this time, making the shipping contribution more important. The local contribution scheme, as with the traffic, is also slightly lower than the SR scheme. The average local fraction for this grid cell is around 0.15. In this grid cell shipping accounts for 28% of the total emissions.

The results show a very good performance of the new local contribution scheme. Further work is required to assess why there is a small difference between the two methods and to make the methodology more robust and applicable to a wider range of pollutants.

4.4 Example application Oslo

The redistribution methodology is applied to Oslo for road traffic. We produce sub-grid concentrations for NO_2 in Oslo in 2013 and compare with fixed monitoring (2013) and passive sampler campaigns (2009). The following steps are undertaken in order to produce sub-grid concentration fields for Oslo, Figures 4.2 and 4.3.

1. The EMEP model is run for the year 2013, to determine the annual mean local and non-local grid contributions and local scaling factor for the traffic contribution to NO_2 as presented in Section 4.3. The model calculation is carried out at 0.1^o

2. Traffic data for Oslo are aggregated on sub-grids of 50 x 50 m^2 and these are distributed in space using the pseudo dispersion routines described in Section 4.2.

3. Sub-grid concentrations for NO_2 are determined for all of Oslo using the annual mean EMEP NO_2 concentrations and the redistribution scaling factor derived for NO_x (Equation 4.10). NO_x is used to determine the scaling factor as it is a better conserved compound than NO_2. This aspect of the methodology is still under development.

4. The results are compared to passive sampling measurements made in 2009 and fixed monitoring data from 2013.

We compare EMEP and uEMEP calculated NO_2 concentrations with observations. Two sets of data are available. A passive sampling campaign carried out in 2009 for the ESCAPE project (6 week averages over the year) with around 40 stations, and fixed monitoring site annual mean concentrations for 2013 from 7 stations.

In Figure 4.3 scatter plots show the effect that redistribution has on the concentrations. This is particularly clear for the spatially distributed passive samplers. For the fixed site samplers, many of which are kerb side traffic sites, we see that the redistribution methodology provides much improved concentration estimates.

4.5 Discussion and conclusions

In the example provided in Section 4.4 a number of points should be made. Firstly in the EMEP emissions inventory roughly 60% of the total NO_x emissions in the Oslo region are from the SNAP sector 7, corresponding to traffic emissions. Conversely the maximum local grid contribution from traffic in this region is calculated to be 26%. This means that roughly 2/3 of the local grid emissions are removed from the lowest layer through vertical diffusion and advection, and replaced from neighbouring grids in the city. Regional background levels for NO_x are low, at around 10% of the city average concentrations. This local grid contribution is perhaps lower than expected and warrants further investigation in regard to the vertical diffusion in EMEP and the emission inventory. Bottom up emission inventories are available for Oslo (and many other cities) so some effort should be made, when further testing the methodology, to determine differences between these two types of emission inventories.

In this calculation the local grid contribution from traffic has been calculated for NO_x and this has been used to represent the contribution from NO_2. This aspect of the methodology requires further exploration to see if this is a reasonable approximation or not. Including chemistry in the scheme is not straight forward but in urban areas reasonable assumptions can be made to implement a simplified chemistry scheme. In regard to chemistry it should also be noted that the oxidation of NO to NO_2 through ozone occurs on time scales of minutes. Since the majority of NO_x from traffic is emitted as NO then conversion of NO to NO_2 will occur within the first few hundred metres from the source. The effect of this is that NO_2 concentrations reduce at a slower rate than NO_x as they are dispersed from the source, due to the production of NO_2 in the plume. For dispersion modelling there are some parametrisations available for dealing with this but this aspect should be assessed in further developing the redistribution method.

In Map 5 (Figure 4.2) a significant non-local contribution to the NO_2 concentrations is seen to the south-west of Oslo. This has been identified to be the result of shipping emissions.

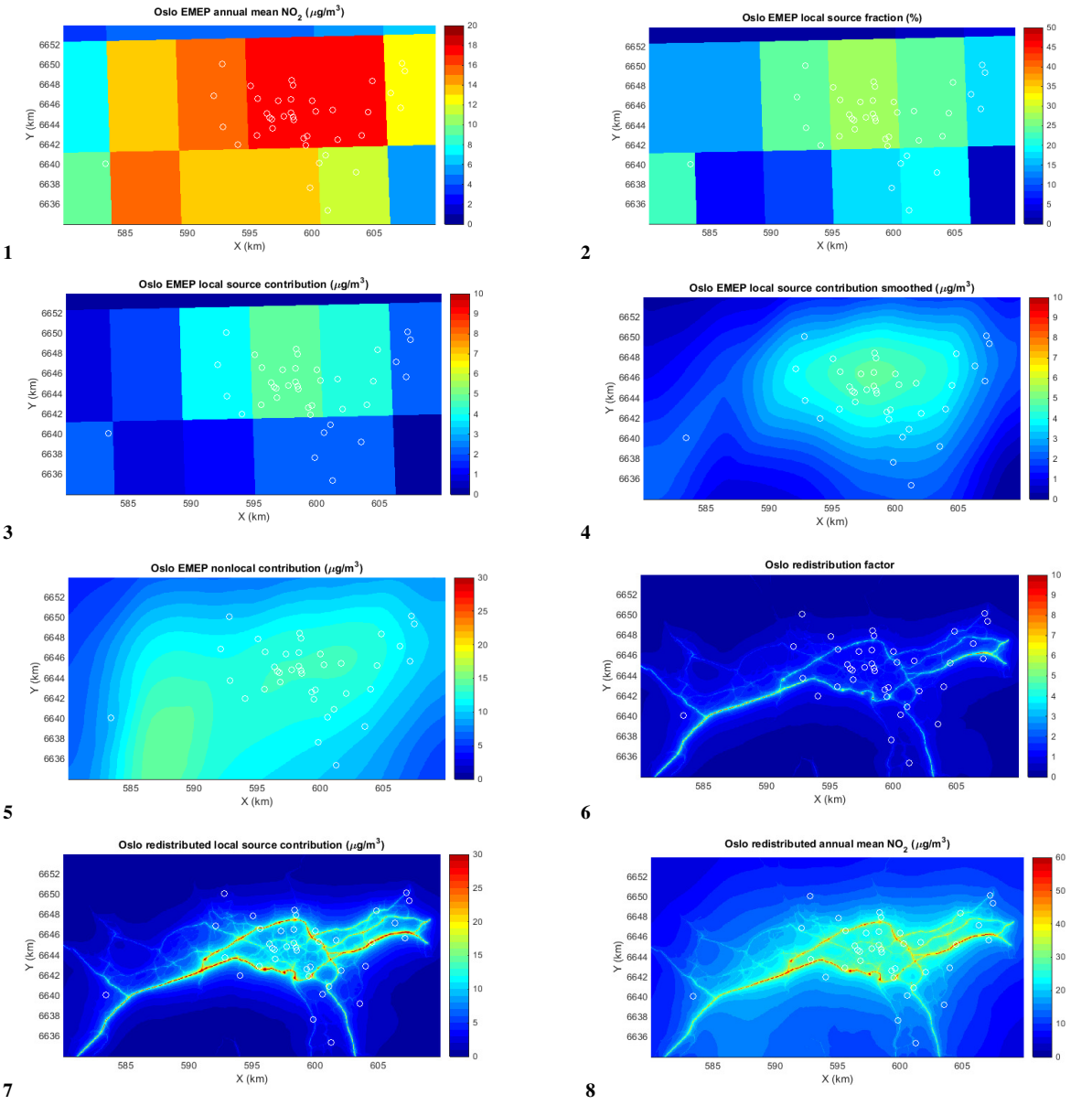

Figure 4.2: Step by step presentation of the methodology for redistributing local traffic contributions to NO_2. The EMEP model calculation is carried out at 0.1°, approximately 10 km, and the sub-grid resolution is 50 m. In all plots the white circles indicate the positions of passive sampler sites from 2009 that are used for comparison. **Map 1**: EMEP model calculated 2013 annual mean concentrations for NO_2 in the Oslo region. Maximum concentration of 17 $\mu g/m^3$. **Map 2**: EMEP model calculated annual mean (2013) local grid contribution in % from traffic emissions to NO_x concentrations in the Oslo region. Maximum contribution is 26%. **Map 3**: EMEP model calculated 2013 annual mean local grid traffic contribution to NO_2 concentrations in the Oslo region, made by combining maps 1 and 2. Maximum contribution is 5 $\mu g/m^3$. **Map 4**: As in map 3 but with the EMEP grids interpolated to the 50 m sub-grids using a moving window interpolation. **Map 5**: Similar to map 4 but showing the non-local interpolated grid contribution. **Map 6**: Redistribution scaling factor on the 50 m sub-grids. Major roads have a factor of 5, indicating that the sub-grid concentrations are 5 times larger than the EMEP gridded concentrations. **Map 7**: Maps 4 and 6 are combined at all sub-grids to produce the redistributed NO_2 concentration from the local grid sources only. Maximum values are around 30 $\mu g/m^3$. **Map 8**: Maps 5 and 7 are combined at all sub-grids to produce the total redistributed NO_2 concentrations. Maximum values are around 55 $\mu g/m^3$.

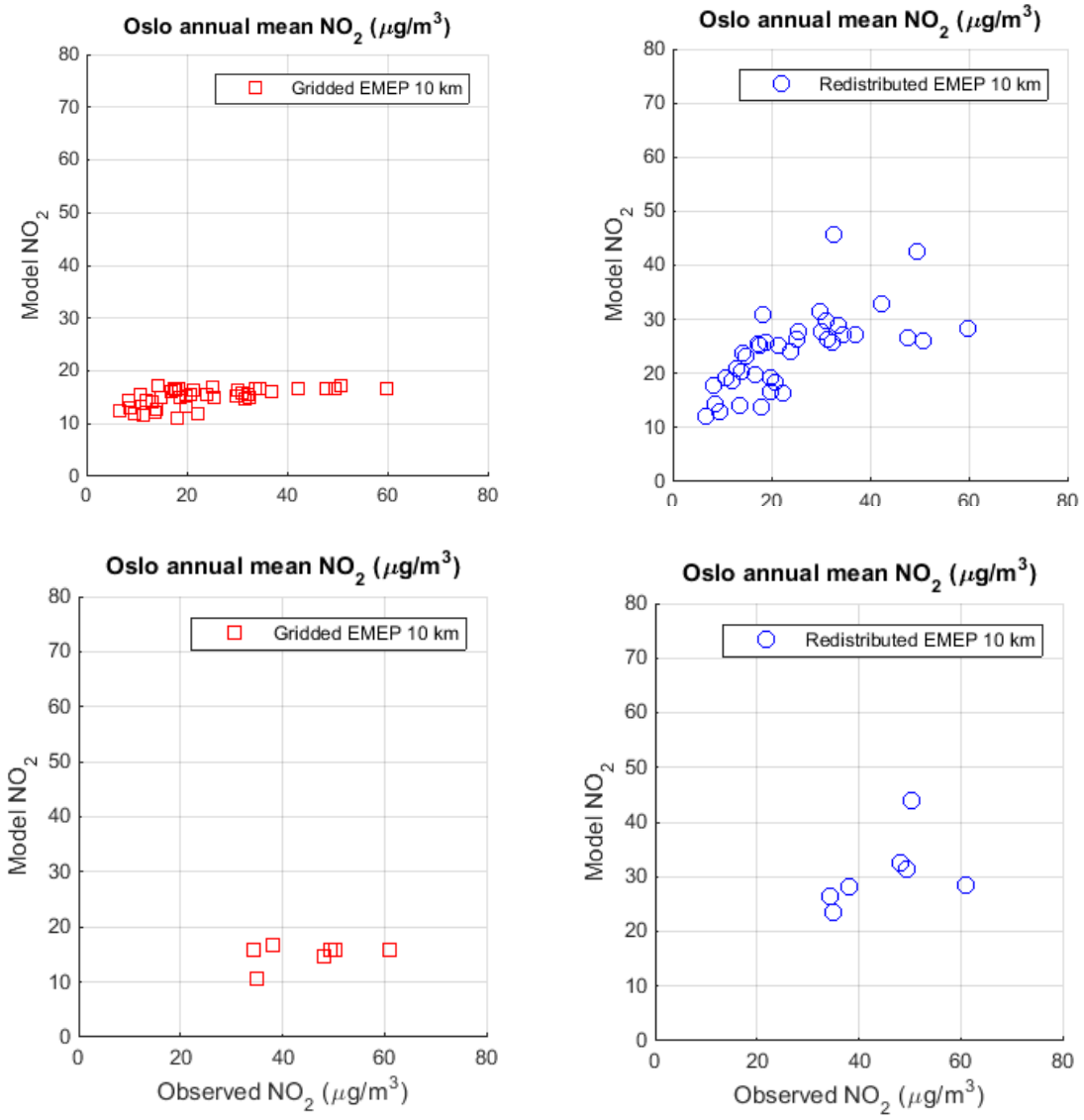

Figure 4.3: Scatter plots of model verses measured concentrations. Top plots show passive sampler measurements (2009) and bottom plots fixed monitoring site measurements of NO_2 (2013). Left plots show the comparison with the normal gridded EMEP model and right the uEMEP results, after redistribution of the concentrations.

These emissions appear misplaced but further assessment is required of the actual emissions to determine if this is the case. This represents a potential problem with the methodology. If the spatial distribution of emission sources in EMEP do not correspond to the proxy data distribution then the redistribution methodology will fail. This requires that the proxy data used in building the emissions inventory and used for the redistribution methodology be based on the same, or similar, information to ensure coherence.

Despite the discrepancies in data sources the methodology shows a clear improvement in the spatial distribution of the concentrations for traffic, allowing a direct comparison of EMEP concentrations with both urban and traffic sites. As a result of this preliminary work

we conclude the following:

- A redistribution method, based in Gaussian dispersion theory, has been developed and implemented
- Changes to the EMEP/MSC-W model have been tested that will allow more efficient local source contribution calculations
- The application of the method to a test case in Oslo shows the workability of the methodology allowing, for the first time, a direct comparison between urban and traffic stations with EMEP calculations
- Mismatches between EMEP emission data and proxy emission data sets can lead to poor results if they are not spatially distributed in a similar way
- The method shows significant potential for further development and can provide new information for applications in policy and health studies

There are a large number of aspects of the methodology that require further attention and include the following activities

- Collection of compatible datasets for a number of Norwegian and European cities to further demonstrate and test the methodology.
- An assessment of the availability of relevant datasets. An important dataset is the traffic load on the roads for which there is no uniform European dataset available. Other relevant datasets include AIS data from coastal shipping and population data for distribution of residential heating
- Collection of measurement datasets with good spatial coverage. Such datasets exist for a number of European cities through the ESCAPE project, particularly for NO_2, but also for PM.
- There are a range of available dispersion parameters cited in the literature. A set of parameters must be defined for further use.
- The relation between the Gaussian dispersion and K theory dispersion (used in the EMEP model) needs to be assessed to ensure compatibility between the two methods.
- A direct comparison with local scale modelling will provide insight into the quality of the results
- The methodology for generating EMEP emissions should be compared to bottom up methods to assess potential errors related to the emissions.
- NO_2 chemistry and its implementation in the methodology should be addressed. If necessary simplified schemes will be introduced

References

Denby, B.: Spatially distributed source contributions for health studies: comparison of dispersion and land use regression models., Tech. Rep. Transphorm Deliverable D2.2.4., URL http://www.transphorm.eu/Portals/51/Documents/Deliverables/New%20Deliverables/D2.2.4_v6.pdf, 2014.

Denby, B.: Mapping of NO2 concentrations in Bergen (2012-2014), Tech. Rep. METreport No. 12/15, URL http://www.met.no/Forskning/Publikasjoner/MET_report/, 2015.

Denby, B., Cassiani, M., de Smet, P., de Leeuw, F., and Horalek, J.: Sub-grid variability and its impact on European wide air quality exposure assessment, Atmospheric Environment, 45, 4220 – 4229, doi:http://dx.doi.org/10.1016/j.atmosenv.2011.05.007, URL http://www.sciencedirect.com/science/article/pii/S1352231011004791, 2011.

Green, A. E.S., S. R. V. R.: Analytic Extensions of the Gaussian Plume Model, Journal of the Air Pollution Control Association, 30, 773–776, doi:10.1080/00022470.1980.10465108, 1980.

Klug: Staub, Reinhaltung der Luft, v. 29, Hauptverband der Gewerblichen Berufsgenossenschaften. Staubforschungsinstitut and VDI-Kommission Reinhaltung der Luft, VDI-Verlag, 1969.

Liu, X., Godbole, A., Lu, C., Michal, G., and Venton, P.: Optimisation of dispersion parameters of Gaussian plume model for CO2 dispersion, Environmental Science and Pollution Research, 22, 18 288–18 299, doi:10.1007/s11356-015-5404-8, URL http://dx.doi.org/10.1007/s11356-015-5404-8, 2015.

Seinfeld, J. H. and Pandis, S. N.: Atmospheric chemistry and physics : from air pollution to climate change. Second edition., Hoboken, N.J. J. Wiley, 2006.

Smith, M.: Recommended Guide for the Prediction of the Dispersion of Airborne Effluents. Vol. 2, Amer. Soc.Mech. Eng., New York, 1973.

Theobald, M. R., Simpson, D., and Vieno, M.: A sub-grid model for improving the spatial resolution of air quality modelling at a European scale, Geoscientific Model Development Discussions, 2016, 1–22, doi:10.5194/gmd-2016-160, URL http://www.geosci-model-dev-discuss.net/gmd-2016-160/, 2016.

CHAPTER 5

Modelled versus EARLINET aerosol extinction/backscatter profiles

Svetlana Tsyro, Augustin Mortier, Lucia Mona and Michael Schulz

Providing valuable information on aerosol profiles, lidar measurements offer new possibilities to model evaluation. In a close collaboration between EMEP and EARLINET scientists, within the framework of EU ACTRIS-1 and ACTRIS-2 projects, as well as the Norwegian Research Council project AeroCom-P3, comparison between EMEP/MSC-W model calculated and lidar measured aerosol extinction and backscatter profiles has been performed for the year 2012 with a specific focus on the period of EMEP/ACTRIS campaign in June-July 2012. The main findings are outlined in the chapter.

5.1 Tools and Methodology

5.1.1 Measurements

EARLINET

Established in 2000, the European Aerosol Research lidar Network (EARLINET), is dedicated to observations of the vertical distribution of aerosols (Bösenberg et al. (2001), Pappalardo et al. (2014)). At present, it is composed of 27 active stations distributed over Europe. Most of them operate Raman (non-elastic) lidars, which make direct measurements of aerosol extinction profiles (typically during nighttime) together with independent aerosol backscatter profiles. Elastic lidars and also Raman ones, when signal-to-noise ratio (SNR) is too low, provide backscatter profiles, from which extinction profiles can be calculated making assuptions about the lidar ratio (extinction-to-backscatter ratio), i.e. assumption on the aerosol type and composition.

A common schedule has been established at network level as minimum basic schedule for the EARLINET climatological aim: one daytime measurement per week (Monday) around

noon and two night-time measurements per week (Monday and Thursday). Additional observations are made to monitor the occurrence of pollution events, such as Saharan dust outbreaks and forest fires. Besides the operational activities, EARLINET stations also participate in research measurement/validation campaigns (Pappalardo et al. (2010), Pappalardo et al. (2013), Sicard et al. (2015)). The quality of the measurements is insured by the well-known qualification of each instrument and of used algorithms. This is made possible by the standardized check-up procedures recommended through ACTRIS dedicated tasks and by intercomparison campaigns with reference instruments (Pappalardo et al. (2014), Wandinger et al. (2016), Freudenthaler (2016), D'Amico et al. (2015), Matthais et al. (2004)). Data uploaded on EARLINET database passed then thrpugh a quality check procedure. A first manual quality check resulted in the removal of some low cloud-contaminated profiles and to the publication of the screened datasets in dedicated volumes of the World Data Center for Climate (WDCC)(EARLINET 2014).

Datasets

The operational lidar data for 2012 were retrieved from the EARLINET database in February 2016 (www.earlinet.org). The data were available for the stations Evora (Portugal), Madrid, Granada and Barcelona (Spain), Potenza (Italy), Athens (Greece), Sofia (Bulgaria), Palaiseau (France) and Maisach (Germany). The dataset used for comparison with the model included: extinction at 355 nm (46 profiles at 4 sites) and at 532 nm (38 profiles at 5 sites); backscatter at 355 nm (135 profiles at 8 sites) and 532 nm (91 profiles at 6 sites).

For the extended analysis, data obtained during the EMEP/ACTRIS measurement campaign have been made use of. The campaign took place in the period of 8 June-17 July 2012 and was dedicated to Saharan dust studies (Sicard et al. (2015), Alastuey et al. (2016), EU (2013)). The lidar measurements were performed at eleven stations in the Mediterranean area with the observation frequency higher than operationally required. In order to capture particular interesting pollution cases, the weather prediction and air quality models were consulted (Sicard et al. 2015). In addition, continuous 72-hour measurements were performed during 9-12 July. In this study, the measurements from the following six stations have been used: Athens (Greece), Barcelona (Spain), Evora (Portugal), Granada (Spain), L'Aquila (Italy) and Potenza (Italy). Whenever available, measurements of backscatter and extinction profiles at a wavelength of 355 nm and/or 532 nm have been included.

5.1.2 Model

The EMEP/MSC-W model calculates aerosol extinction applying prescribed Mass Extinction Coefficients (MEC) to the concentrations of aerosol components at 20 model layers. The effect of aerosol hygroscopic growth is accounted for through the tabulated dependency of the aerosol effective cross-section on relative humidity (EMEP Report 1/2014). For this study, hourly 3D fields of aerosol extinction have been calculated for the year 2012. In addition, the aerosol backscatter profiles have been derived from the extinction profiles.

5.1.3 Data pre-processing

In order to assure a consistent comparison, the model results and lidar data needed to be co-located in space and time. Firstly, model calculated hourly extinction profiles have been

extracted for the grid-cells corresponding to each of the six considered stations and averaged between the start-time and the end-time of the lidar data acquisition provided for each observation. Then, using the information about station elevations, the profiles have been re-calculated to heights above sea level.

The model calculated extinction coefficients are the layer-mean values for 20 model layers (from the surface up to 15-16 km). The vertical resolution of the observed profiles is instrument-dependent, but in general much finer compared to the model resolution. To harmonize the observation data and make them consistent with model results, calculated and measured profiles have been vertically aggregated. We have tested three ways of data aggregation, averaging within:

- 100 m thick layers (the measurement mean for each 100 m layer is compared with the calculated value from the model layer containing the considered 100 m layer)
- 1 km thick layers (the measurement mean for each 1 km layer is compared with the calculated value averaged over the model layers which are included fully or partially in the considered 1 km layer)
- model layers

The first option allows for a better description of the vertical structure while the second one provides a statistically more robust average since more measurements are present in these thicker layers.

Only common layers, i.e. those for which both model and lidar extinction values are available, are included in the comparison.

More lidar measurements of aerosol backscatter are available compared to extinction data, because the Raman signal is characterized by a lower SNR with respect to the elastic ones, which typically limits the extinction profile retrieval to nighttime conditions and not extremely low aerosol load layers. The extinction coefficient (α) and the backscatter coefficient (β) are related through the so-called lidar ratio (extinction to backscatter ratio). In order to make use of aerosol backscatter measurements, backscatter profiles have been derived from model calculated extinction profiles applying a constant lidar ratio. In reality, the lidar ratio strongly depends on the size, morphology and chemical composition of the particles and is highly variable with respect to height. For instance for 532 nm wave length, it can vary from about 20 sr for the coarsest (sea salt) particles to 70 sr for the smallest particles (Omar et al. 2009). However even for a certain aerosol type an high variability in lidar ratio values is observed as reported in many papers (e.g. Groß et al. (2013)). Climatologies in urban areas show a large variability in the lidar ratio: 49 to 70 sr as derived from Sun-photometer observations (Cattrall et al. 2005), 53 $\pm$11 sr in Central Europe and 45 $\pm$9 sr in Southwestern Europe from Raman lidars (Müller et al. 2007). For Saharan dust, the lidar ratio can widely vary in relation to aging and mixing processes wityh marine particles as can happens for Saharan dust plumes tarvelling on Mediterranean before reaching Europe. This leads to an high varibaility in desert dust lidar ratio values observed over Europe around the typical value of about 50 sr at 532nm observed over different location around Europe (Müller et al. (2007), Mona et al. (2014)).

Climatologies in urban areas show a large variability in the lidar ratio: 49 to 70 sr as derived from Sun-photometer observations (Cattrall et al. 2005), 53 $\pm$11 sr in Central Europe and 45 $\pm$9 sr in Southwestern Europe from Raman lidars (Muller et al., 2007). For pure dust, the lidar ratio can be as low as 30 sr (Omar et al. 2009), but for the aged Saharan dust

in the plumes over Europe, the lidar ratio values may be larger (59 $\pm$11 sr) as reported in Müller et al. (2007). As a first approach, the lidar ratio of 50 sr has been used in this work.

5.2 Results

5.2.1 The whole year of 2012

Examples of monthly average backscatter profiles at 355 nm for the sites with more data available are shown in Figure 5.1. There is a generally reasonable agreement between the model and the observations in terms of backscatter values and vertical structure, though some aerosol events are not well reproduced by the model (e.g. in July at Barcelona site). Figure 5.1 also reveals considerable gaps in the observation datasets.

Further, we try to provide a quantitative comparison between model calculated and lidar measured profiles. Figure 5.2 displays the scatter-plots for calculated and measured monthly mean extinction and backscatter coefficients values for all the sites and all layers. Figures 5.2 (a, c) show the comparison based on 100 m aggregated layers and Figures 5.2 (b, d) are based on 1 km aggregated layer. The dots for individual data points are colored corresponding to the altitude above sea level they correspond to (see the color bar).

The correlation coefficients between model and lidar are 0.58 for α and 0.36 β for 100 m aggregated layers, increasing respectively to 0.62 and 0.43 for 1 km aggregated layers. The model tends to underestimate measured extinction and even more backscatter. The underestimation gets slightly reduced when comparison is made for the thicker (1 km) layers.

The colored dots indicate that the underestimation is more significant at the most elevated layers (above 5-6 km), whereas below 5 km the model results are closer to the measured data, and even some overestimations can be found for backscatter in the lowest 2-3 km. Similar comparison results are obtained for extinction and backscatter profiles at 532 nm.

The worse correlation between the calculations and observations for backscatter compared to extinction could partly be explained by a the variability of lidar ratio, which was unaccounted for in the model results.

Correlation can also be investigated for each layer separately across all sites and times. Figure 5.3 shows the vertical profiles of correlation coefficients attained from the model results and lidar measurements at each aggregated height layer. There is a considerable variability in correlation with altitude. The correlation of extinction profiles has a maximum of 0.6 at 1 km height (which is the lowest available layer) and decreases to 0.1 at 7 km altitude. For backscatter profiles, the correlation is also the poorest at higher altitudes, while the best correlation of 0.65 is found at around 3 km.

The occurrence of best correlation at mid-altitude is even more pronounced for extinction and backscatter at 532 nm, for which correlation coefficients exceed 0.7 at the layers between 3 km and 6 km. The correlation between the model and lidar drops below 0.1 at the lower (1 km) and upper (7 km) altitudes.

5.2.2 EMEP/ACTRIS campaign in June-July 2012

Applying the same methodology, model comparison has been performed with the dust campaign dataset (8 June - 17 July 2012). Although the time period of the campaign was just a bit over one month, an appreciable amount of observational data was collected due to more

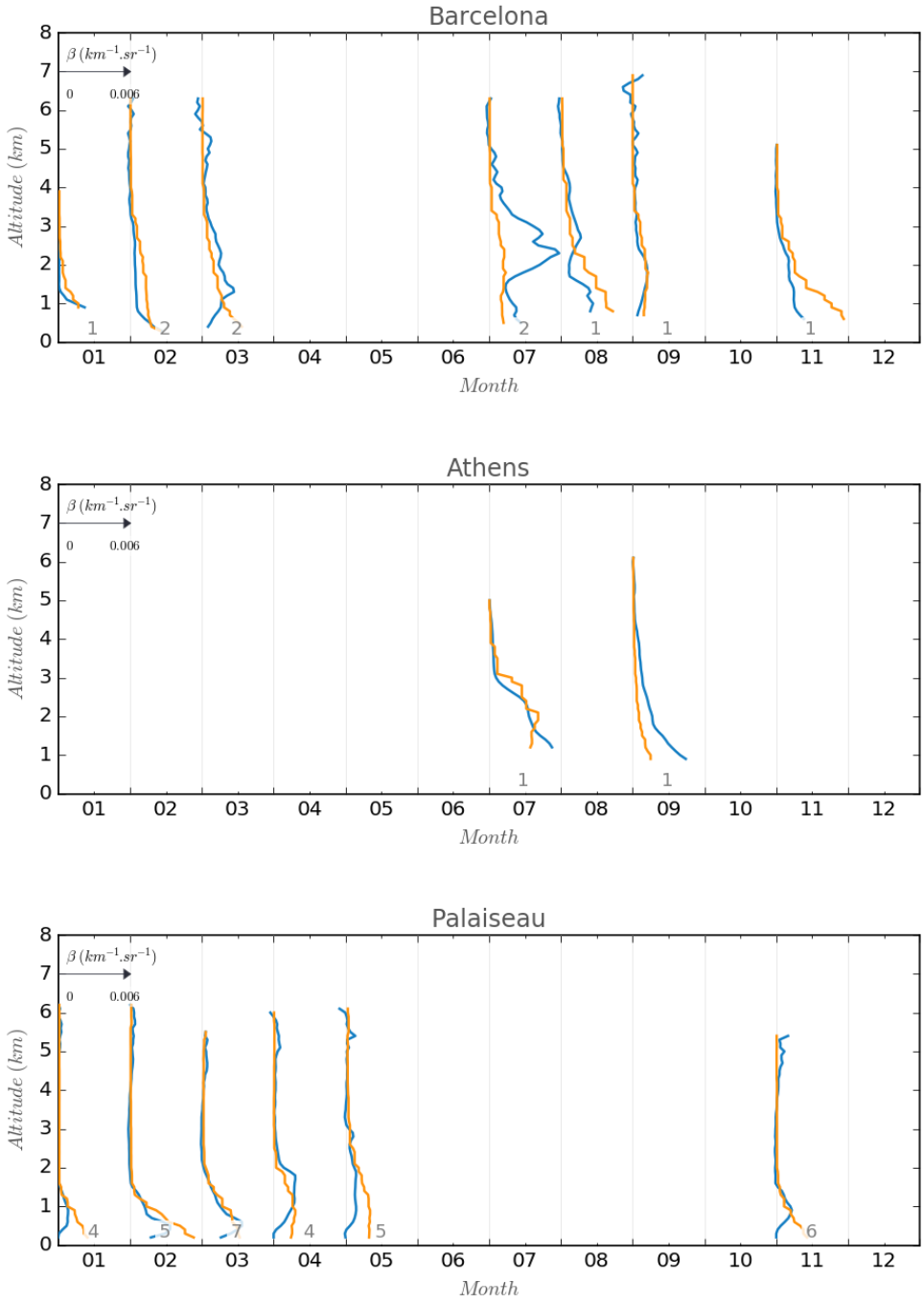

Figure 5.1: Monthly averaged backscatter profiles at 355 nm for EARLINET observations (blue) and EMEP model (orange) for 2012. The bottom numbers refer to the number of averaged profiles during the respective month

frequent measurements performed. The observational data made available to us include: extinction at 355 nm (45 profiles at 4 sites) and at 532 nm (30 profiles at 5 sites); backscatter at 355 nm (84 profiles at 8 sites) and 532 nm (88 profiles at 6 sites).

Table 5.1 summarizes the correlation coefficients and regression slopes for model versus lidar comparison for extinction and backscatter at the two wavelengths. Similar to the whole year results, the correlation between the model and lidar is better for 1 km aggregated layers

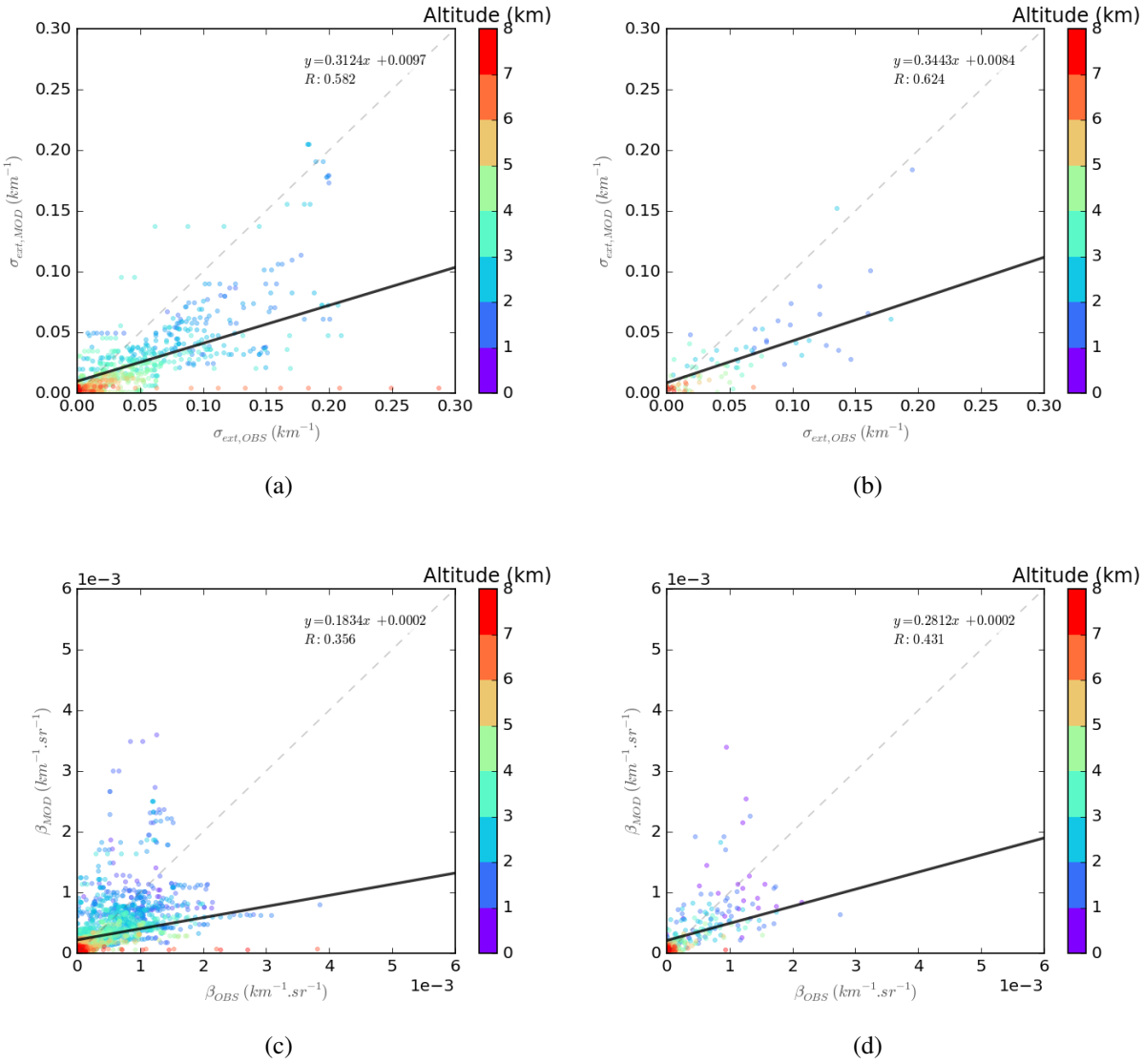

Figure 5.2: Scatter-plots of extinction (a, b) and backscatter (c, d) coefficients measured (x-axis) and modeled (y-axis) at 355 nm at all the stations and all vertical layers, using 100 m (a, c) and 1 km (b, d) aggregated vertical layers.

than for 100 m layers, i.e. for more smoothed vertically profiles. But on the contrary to the whole 2012, the correlation is better for extinction profiles than for backscatter profiles for the campaign period. Partly this can be explained by the larger measurement dataset for backscatter, which contains about twice as many profiles compared to the extinction measurements. The other reason is that the assumption of a constant lidar ratio is certainly a better approximation for the shorter (about 40 days) period than for the whole year, so that the associated inaccuracy in model derived backscatter profiles should be smaller. In addition, the value of lidar ratio used for the modle profiles conversion (50sr) is a good proxy for the Saharan dust particles while it is less effective for different aerosol types like local pollution or fires.

The vertical profiles of correlation coefficients are similar to the results for the whole 2012 dataset. Namely, the lowest correlation coefficients are found close to the ground and at the

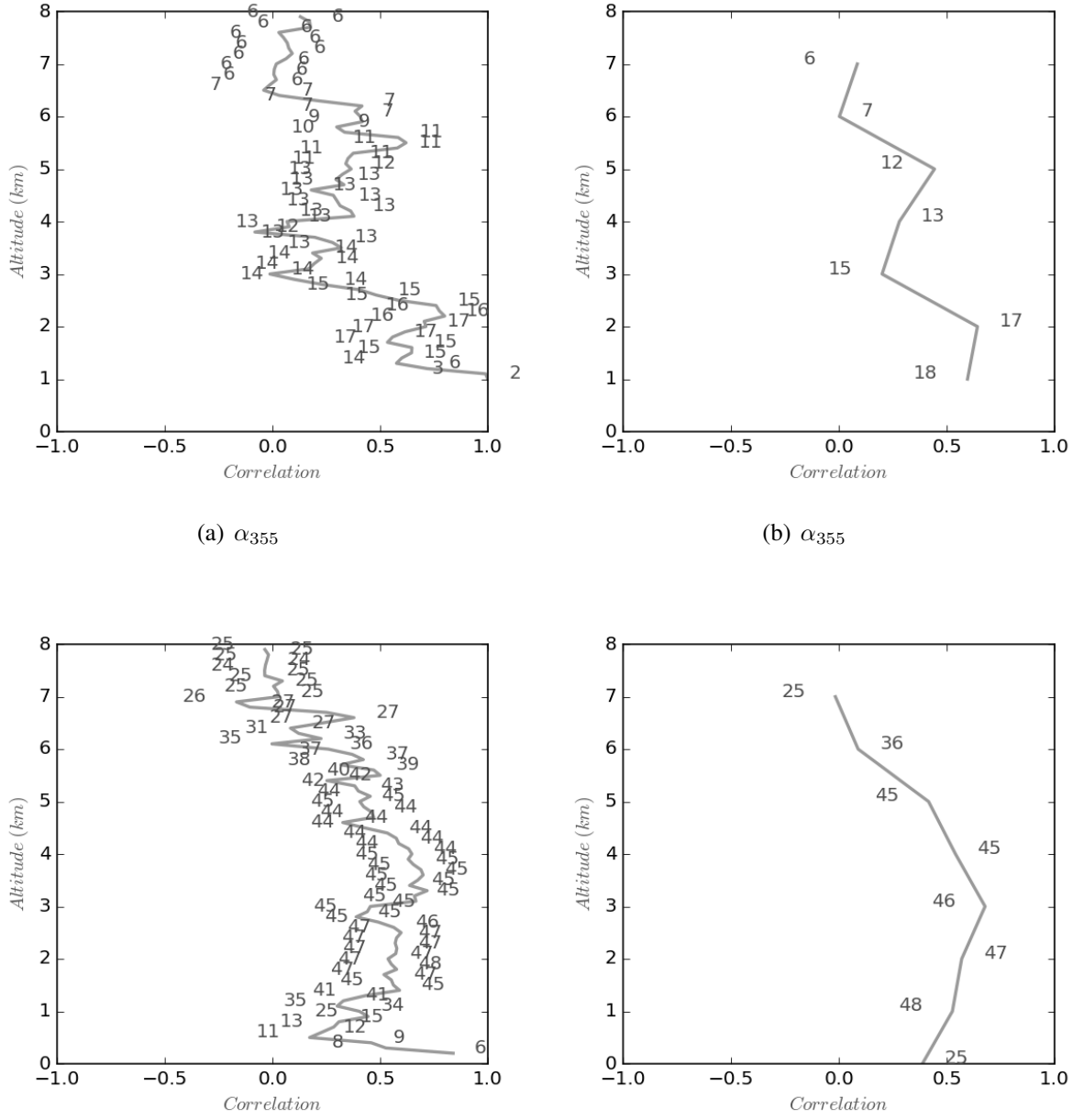

(a) α_{355} (b) α_{355}

(c) β_{355} (d) β_{355}

Figure 5.3: Correlation coefficients between the model and observations as function of altitude for extinction (a, b) and backscatter (c, d) coefficients at 355 nm for all the stations, using 100 m (a, c) and 1 km (b, d) aggregated vertical layers. The numbers refer to the number of data points available at each level.

upper layers, whereas the correlation considerably improves at mid-altitude layers.

The model calculates smaller than measured values of extinction and backscatter (Table 5.1), doing a somewhat better job for the latter (especially for β_{532}).

We have looked separately at the days with identified Saharan dust events and the days without Saharan dust influence, exemplified in Figure 5.4 for backscatter and extinction at

Table 5.1: Correlation and regression slope between model results and lidar measurements

Parameter	Aggregation	Npoints	R	Regr.slope	Npoints	R	Regr.slope
		June-July 2012			Whole 2012		
α_{532}	100 m	889	0.22	0.09	421	0.49	0.20
	1 km	115	0.25	0.10	52	0.55	0.24
β_{532}	100 m	5646	0.65	0.58	1735	0.36	0.18
	1 km	624	0.65	0.59	190	0.43	0.28
α_{355}	100 m	1859	0.48	0.32	639	0.58	0.31
	1 km	224	0.49	0.33	75	0.62	0.34
β_{355}	100 m	4779	0.57	0.32	1377	0.54	0.38
	1 km	527	0.61	0.36	152	0.62	0.50

355 nm.

For extinction, better agreement between the model and lidar profiles is found for Dust cases. This is partly driven by relatively good agreements at mid-altitude layers, where the extinction values are rather high. In addition, no data below 1 km, where the model tends to overestimate the lidar observations, were available for those cases. For the backscatter profiles we find quite similar results, with the agreement between the calculations and observations in no-dust cases being somewhat better than for the extinction. Overall, the model calculations of both α and β correspond with the lidar data better at the layers below 3-4 km in no-dust cases, but at the mid-altitudes (4-6 km) during Saharan dust episodes.

Continuous 72-hour measurements 9-12 July 2012

Continuous 72-h evolutions of extinction profiles were available for seven EARLINET sites thanks to the controlled exercise of near-real time operativity of the research network (Sicard et al. 2015), which made use of a automatic evalutaion of lidar data from raw signals to final products through a common and centralized calculous chain, the Single Calculus Chain algorithm (D'Amico et al. 2015).

Table 5.2 summarizes the correlation between model calculated and lidar measured hourly extinction profiles at the individual stations. The correlation is highly variable, from 0.0 to 0.97. The best results are obtained for Athens, Potenza and Granada, with correlations between 0.77 and 0.97. At Potenza and Granada, Saharan dust episodes were identified for those days, so the results indicate that the model captures those quite well. At Evora, which is a relatively clean site, periodically influenced by marine aerosol, the correlation between the model and lidar is very poor. Overall, the correlation is better for extinction at 355 nm (for which more data was available).

Table 5.2: Correlation between model calculated and measured extinction profiles for the 72-hour period 9-12 July 2014

Wave length	Athens	Barcelona	Budapest	Evora	Granada	L'Aquila	Limassol	Potenza
355	0.97	0.62	0.49	0.0	0.87	0.92		0.90
532	0.86	0.33	0.31	0.05	0.77		0.67	0.89

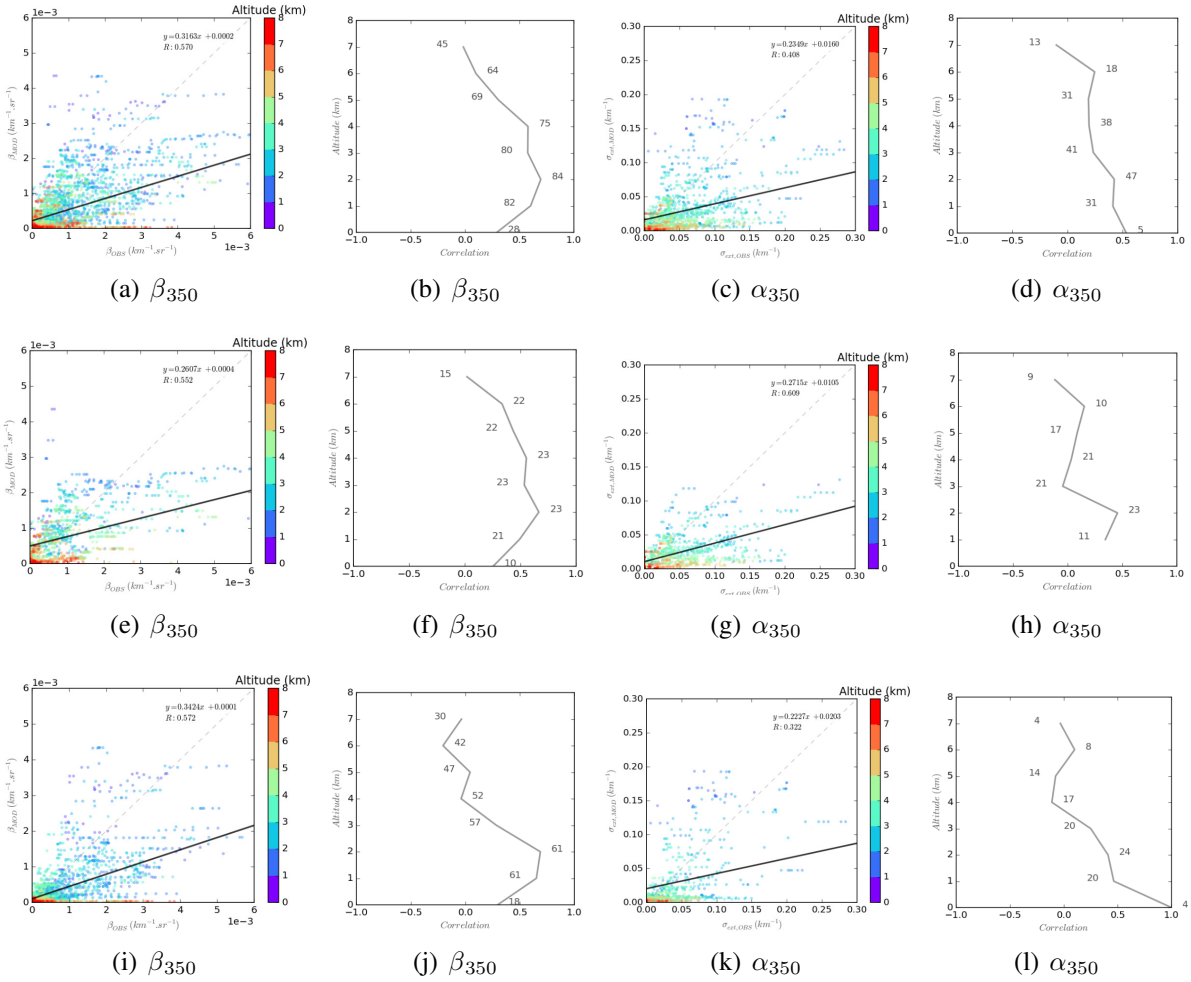

(a) β_{350} (b) β_{350} (c) α_{350} (d) α_{350}

(e) β_{350} (f) β_{350} (g) α_{350} (h) α_{350}

(i) β_{350} (j) β_{350} (k) α_{350} (l) α_{350}

Figure 5.4: Scatter-plots (100 m aggregation) and correlation profiles (1 km aggregation) between modelled and lidar backscatter and extinction at 355 nm for the entire July-July 2012 period (upper row), for days with (middle row) and without (bottom row) dust events.

Figure 5.5 displays the correlation coefficients between calculated and observed hourly extinction profiles against measured AOD during the 72-hour period 9-12 July for all the seven stations (Evora is plotted separately because of rather different type of pollution). Though there is a considerable spread of correlation values, it appears to be fewer cases of poor correlation towards higher AOD. This suggests a model tendency to reproduce the observed profiles somewhat better as AOD increases. At Evora, the degree of agreement between the modelled and observed extinction profiles is even more variable (with the correlation coefficients ranging between -0.6 and 0.8). As pointed out earlier, Evora is located in a clean environment and can alternately be influenced by both continental and marine aerosol plumes. Thus, to accurately reproduce the evolution of hourly aerosol profiles is indeed a big challenge for the regional model with relatively coarse resolution.

In general, when comparing the individual hourly extinction profiles from the model and observations, considerable differences can be expected due to even quite small shifts in space and time. Therefore, statistical distributions may give a better characterization of the general ability of the model to reproduce lidar data. Figure 5.6 shows the frequency distribution of observed and modelled aerosol extinction values for the seven sites and two altitude ranges,

i.e. within 1-3 km and 3-5 km layers. Both the model and observations indicate more aerosols in the 1-3 km layer. The correspondence appears to be somewhat better within the free tropospheric layer, except for the cases of especialy large aerosol loads. For the both height intervals, the over-presentation in the model results of the smallest extinction values (below 0.01-0.02 km^{-1}) is obvious, whereas the occurrence of extinction coefficients of 0.02-0.12 km^{-1} is too seldom. For larger extinction coefficiens, the model is in a better agreement with lidar in the lower 1-3 km layer.

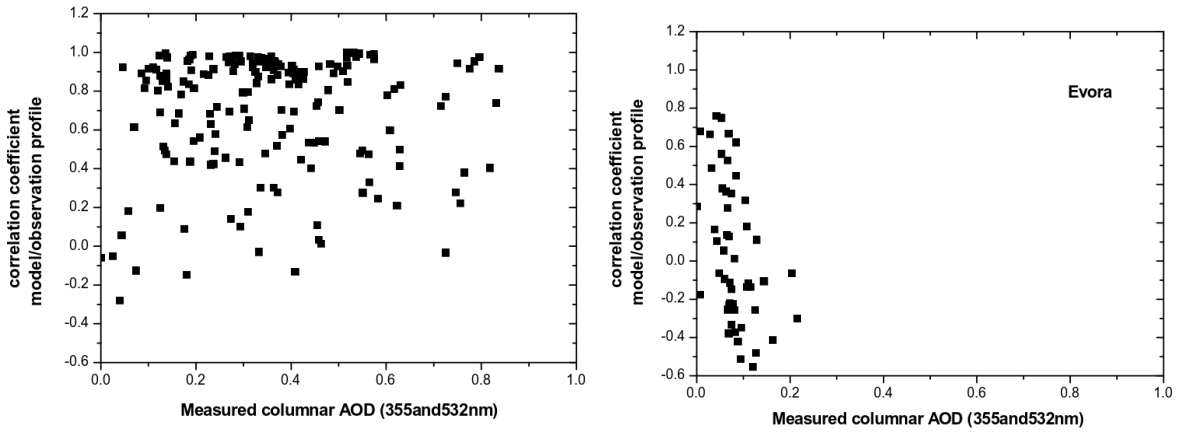

(a) All except Evora (b) Evora

Figure 5.5: Correlation between modelled vs measured extinction as function of AOD.

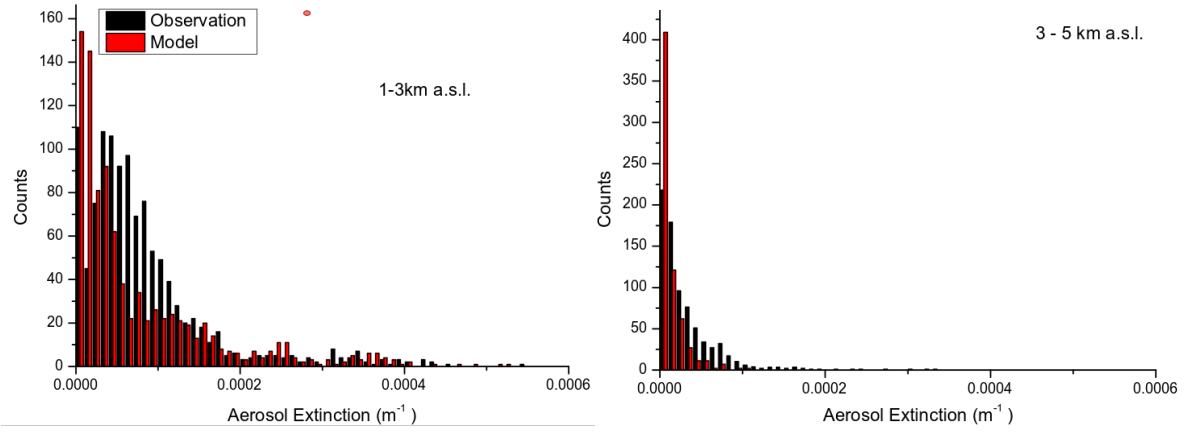

(a) Frequency (1-3km) (b) Frequency (3-5km)

Figure 5.6: Frequency distribution of modelled and measured extinction at different altitudes: (a) 1-3 and (b) 3-5 km.

5.3 Summary

- For the whole 2012 and for June-July 2012 campaign the agreement between the model and lidar measurements was better:

  - for backscatter than for extinction (partly due to the larger β dataset with better vertical resolution)
  - for 355 nm than for 532 nm (more data for 355 nm were available)
  - in mid-troposphere (between 3 and 6 km) than at the layers below and above (for both β than α values and temporal correlation)

- The model tends to overestimate below 2 km and to underestimate above 7-8 km (probably due to vertical variability of lidar ratio unaccounted in this work)

- Comparison methodology: using smoother measured profiles (i.e. vertical aggregation to 1 km compared to 100 m) gives better agreement between the model and observations

- Closing remarks:

  The comparison results suggest that we should revise the model calculations of aerosol vertical distrubution in the boundary layer and also in the upper troposphere. As at the moment the model does not perform online calculation of aerosol backscatter, using lidar extinction data is preferable as they allow a direct comparison. Unfortunately less extinction than backscatter data are available, which makes the comparison results less robust. On the other hand, more backscatter measurements are available for model evaluation and there should be made broader use of them for model evaluations. At the same time, model derived backscatter coefficients should be improved by using more sound assumptions on lidar ratio as it strongly depends on the size, morphology and chemical composition of the particles and is highly variable with respect to height. The accuracy of modelled backscatter coefficients could be made more sound by using climatological vertical profiles of lidar ratios.

  To understand why the model results are better for 355 nm, calculated Ångström exponents should be looked at closer.

  Finally, in addition to vertical smoothing (layer aggregations), temporal smoothing can be considered used for hourly profiles (e.g. averaging model profiles over $\pm$ 3-6 h intervals around the measurement time could be advantegeous).

References

Alastuey, A., Querol, X., Aas, W., Lucarelli, F., Pérez, N., Moreno, T., Cavalli, F., Areskoug, H., Balan, V., Catrambone, M., et al.: Geochemistry of PM 10 over Europe during the EMEP intensive measurement periods in summer 2012 and winter 2013, Atmos. Chem. Physics, 16, 6107–6129, 2016.

Bösenberg, J., Ansmann, A., Baldasano, J. M., Balis, D., Böckmann, C., Calpini, B., and Chaikovsky, A.: EARLINET: A European Aerosol Research Lidar Network, in Advances in Laser Remote Sensing, École Polytechnique, Palaiseau, France, 2001.

Cattrall, C., Reagan, J., Thome, K., and Dubovik, O.: Variability of aerosol and spectral lidar and backscatter and extinction ratios of key aerosol types derived from selected Aerosol Robotic Network locations, Journal of Geophysical Research: Atmospheres, 110, 2005.

D'Amico, G., Amodeo, A., Baars, H., Binietoglou, I., Freudenthaler, V., Mattis, I., Wandinger, U., and Pappalardo, G.: EARLINET Single Calculus Chain–overview on methodology and strategy, Atmospheric Measurement Techniques, 8, 4891–4916, 2015.

EARLINET: The EARLINET publishing group 2000–2010. EARLINET all observations (2000–2010), World Data Center for Climate (WDCC), doi:10.1594/WDCC/EN_all_measurements_2000-2010, 2014.

EU: EU public servicereview, URL `http://www.actris.net/Portals/97/documentation/dissemination/other/Public_service_review_Issue_25.pdf`, 2013.

Freudenthaler, V.: About the effects of polarising optics on lidar signals and the ÎŤ90-calibration, Atmos. Meas. Tech. Discuss., doi:doi:10.5194/amt-2015-338, in review, 2016, 2016.

Groß, S., Esselborn, M., Weinzierl, B., Wirth, M., Fix, A., and Petzold, A.: Aerosol classification by airborne high spectral resolution lidar observations, Atmospheric chemistry and physics, 13, 2487–2505, 2013.

Matthais, V., Freudenthaler, V., Amodeo, A., Balin, I., Balis, D., Bösenberg, J., Chaikovsky, A., Chourdakis, G., Comeron, A., Delaval, A., et al.: Aerosol lidar intercomparison in the framework of the EARLINET project. 1. Instruments, Applied Optics, 43, 961–976, 2004.

Mona, L., Papagiannopoulos, N., Basart Alpuente, S., Baldasano Recio, J. M., Binietoglou, I., Cornacchia, C., and Pappalardo, G.: EARLINET dust observations vs. BSC-DREAM8b modeled profiles: 12-year-long systematic comparison at Potenza, Italy, Atmospheric chemistry and physics, 14, 8781–8793, 2014.

Müller, D., Ansmann, A., Mattis, I., Tesche, M., Wandinger, U., Althausen, D., and Pisani, G.: Aerosol-type-dependent lidar ratios observed with Raman lidar, Journal of Geophysical Research: Atmospheres, 112, 2007.

Omar, A. H., Winker, D. M., Vaughan, M. A., Hu, Y., Trepte, C. R., Ferrare, R. A., Lee, K.-P., Hostetler, C. A., Kittaka, C., Rogers, R. R., et al.: The CALIPSO automated aerosol classification and lidar ratio selection algorithm, Journal of Atmospheric and Oceanic Technology, 26, 1994–2014, 2009.

Pappalardo, G., Wandinger, U., Mona, L., Hiebsch, A., Mattis, I., Amodeo, A., Ansmann, A., Seifert, P., Linné, H., Apituley, A., et al.: EARLINET correlative measurements for CALIPSO: First intercomparison results, Journal of Geophysical Research: Atmospheres, 115, 2010.

Pappalardo, G., Mona, L., D'Amico, G., Wandinger, U., Adam, M., Amodeo, A., Ansmann, A., Apituley, A., Alados Arboledas, L., Balis, D., et al.: Four-dimensional distribution of the 2010 Eyjafjallajökull volcanic cloud over Europe observed by EARLINET, Atmospheric Chemistry and Physics, 13, 4429–4450, 2013.

Pappalardo, G., Amodeo, A., Apituley, A., Comeron, A., Freudenthaler, V., Linné, H., Ansmann, A., Bösenberg, J., D'Amico, G., Mattis, I., et al.: EARLINET: towards an advanced sustainable European aerosol lidar network, Atmospheric Measurement Techniques, 7, 2389–2409, 2014.

Sicard, M., D' Amico, G., Comerón, A., Mona, L., Alados-Arboledas, L., Amodeo, A., Baars, H., Baldasano, J. M., Belegante, L., Binietoglou, I., Bravo-Aranda, J. A., Fernández, A. J., Fréville, P., García-Vizcaíno, D., Giunta, A., Granados-Muñoz, M. J., Guerrero-Rascado, J. L., Hadjimitsis, D., Haefele, A., Hervo, M., Iarlori, M., Kokkalis, P., D. Lange, D., Mamouri, R. E., Mattis, I., Molero, F., Montoux, N., Muñoz, A., Muñoz Porcar, C., Navas-Guzmán, F., Nicolae, D., Nisantzi, A., Papagiannopoulos, N., Papayannis, A., Pereira, S., Preißler, J., Pujadas, M., Rizi, V., Rocadenbosch, F., Sellegri, K., Simeonov, V., Tsaknakis, G., Wagner, F., and Pappalardo, G.: EARLINET: potential operationality of a research network, Atmos. Meas. Tech, pp. 4587–4613, 2015.

Wandinger, U., Freudenthaler, V., Baars, H., Amodeo, A., Engelmann, R., Mattis, I., Gross, S., Pappalardo, G., Giunta, G., D'Amico, G., et al.: EARLINET instrument intercomparison campaigns: overview on strategy and results, Atmospheric Measurement Techniques, 9 (3) 2016, 2016.

CHAPTER 6

Emissions from international shipping

Michael Gauss and Jan Eiof Jonson

Obtaining reliable data on emissions from international shipping has always been challenging. However, in view of the decrease in land-based emissions during the last two to three decades and the non-monotonic trends in ship emissions especially during the last ten years, the use of accurate ship emissions data for air quality modelling appears increasingly important. This chapter gives an overview of the different data sets being considered for modelling at EMEP/MSC-W.

6.1 Introduction

Emissions from shipping activities are a relevant source to air pollution and depositions in Europe (Jonson et al. 2015). While land-based emissions of SO_x and NO_x have been signficantly reduced since 1990 as a result of air quality legislation, emissions from international shipping have decreased less for SO_x emissions and even increased for NO_x over the same period, related to enhanced ship traffic. This has led to a general increase in the relative importance of emissions from shipping, as illustrated in Figure 6.1, which shows the percentage contribution of international shipping emissions to total emissions integrated over marine areas and adjacent countries for 1990, 2000, and for the recent past (2011). For example for NO_x emissions in the Mediterranean area this contribution has increased from 16% in 1990 to almost 25% in 2011. Only in the case of SO_x emissions in the North Sea and Baltic Sea this trend could be reversed during the last ten years or so, most likely due to the new IMO (International Maritime Organization) regulations for fuel oil in SECAs (Sulphur Emission Control Areas) and the EU Sulphur Directive.

Although emissions from international shipping mainly impact marine ecosystems they also affect air quality on land, through atmospheric transport of air pollutants, leading to increased population exposure especially in coastal areas. Figure 6.2 (from Jonson et al. (2015)) shows the percentage contribution of shipping on $\mathrm{PM}_{2.5}$ concentrations and nitrogen deposi-

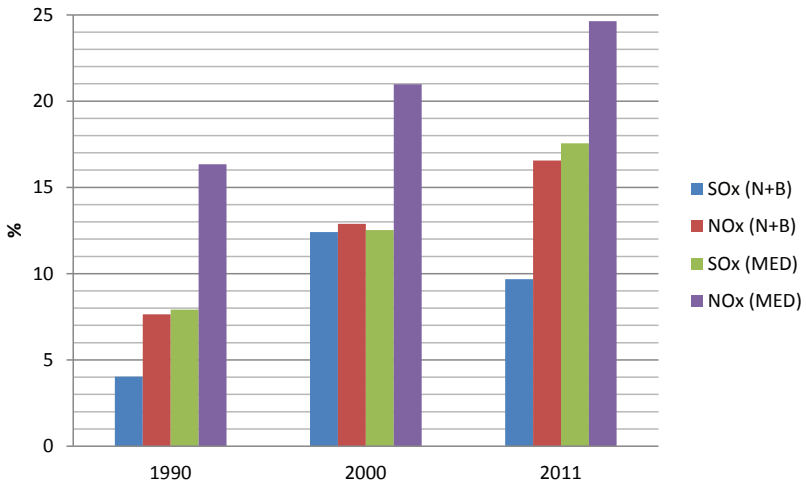

Figure 6.1: Percentage contribution of international shipping emissions to total emissions integrated over marine areas and adjacent countries, for SO_x and NO_x in 1990, 2000 and 2011. Emission data have been downloaded from the CEIP data base (www.ceip.at) in June 2016. 'N+B' means North Sea and Baltic Sea; 'MED' means Mediterranean Sea. Adjacent countries for 'N+B': *BE, DE (=FGD+FFR), DK, EE, FI, GB, LT, LV, NL, NO, PL, RU (=RUA+RUO+RUP), SE*; and for 'MED': *AL, BA, CY, ES, FR, GR, HR, IT, ME, MT, NOA, SI, TR*.

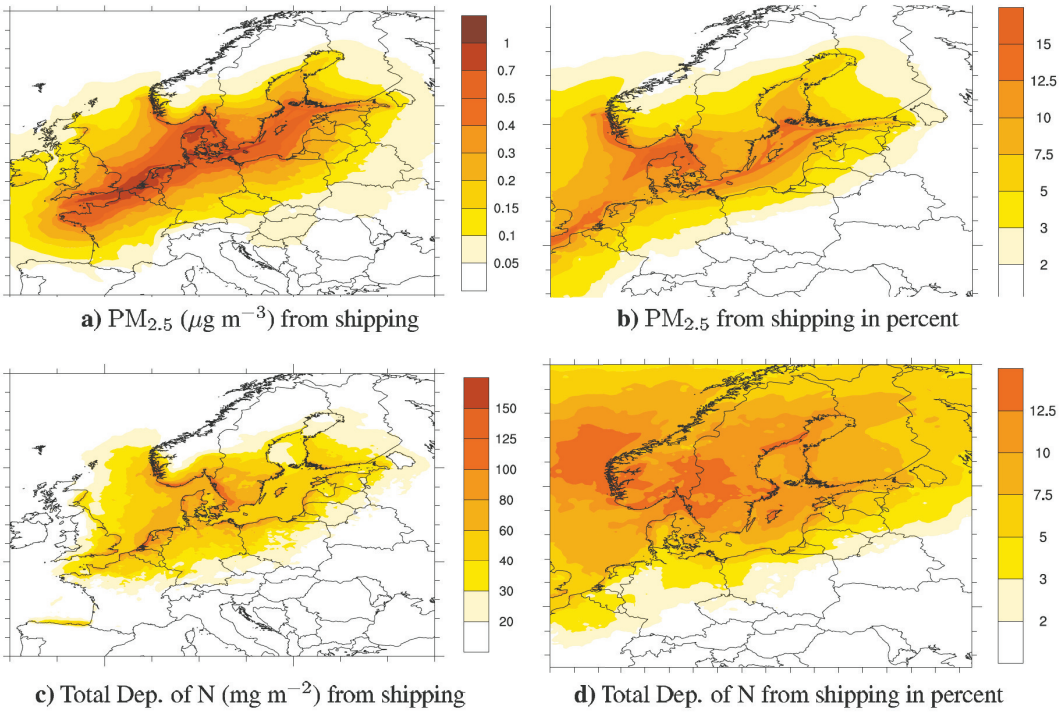

a) $PM_{2.5}$ (μg m^{-3}) from shipping

b) $PM_{2.5}$ from shipping in percent

c) Total Dep. of N (mg m^{-2}) from shipping

d) Total Dep. of N from shipping in percent

Figure 6.2: Contributions from year 2009 ship emissions in the Baltic Sea and the North Sea to a) $PM_{2.5}$ concentrations and c) total deposition of nitrogen. The right panels (b and d) show the same contributions in percent.

tions in Europe, according to EMEP/MSC-W model calculations. Percentage contributions are particularly large in areas where the natural background and/or other anthropogenic impacts are small, as for example in Scandinavia.

6.2 Trends and Regulations

Trends in ship emissions are mainly determined by ship traffic and emission regulations. The most notable change in ship traffic was caused by the economic crisis in 2008 and 2009, while the most significant changes in SO_x emission regulations have been due to IMO, with new rules on fuel oil sulphur content, and the EU Directives 1999/32/EC and 2005/33/EC:

- Since 2010, the limit for sulphur content in ship fuel used at EU ports has been 0.1%, following the EU Directives;
- Within all SECAs, the sulphur content in ship fuel had to be reduced from 1.5% to 1% in 2010, and then further from 1% to 0.1% in 2015, following the IMO regulation (SECAs in Europe are the Baltic Sea, the North Sea and the English Channel);
- Outside SECAs, the limit was reduced from 4.5% to 3.5% in 2012, and a further reduction to 0.5% is planned for the early 2020s (IMO).

As NO_x emissions do not derive from the fuel itself, regulations on NO_x are implemented on engine technology. So-called tier standards were introduced in several steps for new ship engines. For example, ships built after the year 2000 had to comply with Tier I, while ships built after 2010 and after 2016 have to comply with the Tier II and Tier III standards, respectively. Tier III represents a reduction in NO_x emissions by 80% compared to Tier I. However, Tier III applies only to NO_x emission control areas (NECAs), which so far are declared only in North America, and only to new ships built in 2016 or later. But also among the states surrounding the North Sea and Baltic Sea there is now political will to submit a propsoal for a North Sea and Baltic Sea NECA, in time for the IMO MEPC 70 meeting in autumn 2016.

These regulations, in addition to changes in activity, are likely to lead to distinct trends in ship emissions, differing between the various marine areas of Europe. Thus, for air pollution modelling and policy-relevant assessments (e.g. within OSPAR and HELCOM) it is important to have access to up-to-date and accurate ship emission data, and to use best available knowledge on past trends.

6.3 Ship emissions for EMEP/MSC-W

For modelling air concentrations and depositions EMEP/MSC-W uses emission data for international shipping provided by CEIP. Until 2014, CEIP provided international shipping emissions data based on ENTEC and IIASA estimates. Since 2015 (EMEP status report for 2013) CEIP have used the TNO-MACC-III inventory, which was developed within the EU H2020 project MACC-III and includes ship emissions in European Seas (European part of the North Atlantic, Baltic Sea, Black Sea, Mediterranean Sea, North Sea and Caspian Sea).

The TNO-MACC-III data set extends until the year 2011. Therefore, CEIP and EMEP/MSC-W have used the same ship emissions in their reports for the years 2011, 2012 and 2013. Also this year's reporting (for 2014) is based on TNO-MACC-III data for 2011, as this is assumed to be the most accurate data on ship emissions currently available to EMEP/MSC-W modelling.

Independently, the Finnish Meteorological Institute (FMI) has developed a ship emission data set based on real ship movements obtained through the Automatic Identification System

(AIS), which is mandatory worldwide for all ships with a gross tonnage of 300 tonnes or more, and for all passenger ships (regardless of size). For the Baltic Sea, the FMI data set extends until 2014. EMEP/MSC-W has already applied FMI data sets in various research projects (BSR Innoship, EnviSuM, North Sea NECA assessment), but not yet for their status reports to the LRTAP Convention.

6.3.1 TNO-MACC-III

Data on emissions and trends for international sea shipping have been developed by TNO based on reviews of existing information and expert knowledge on activity levels and emission factors. One of the underlying assumptions is that, at sea, mainly HFO (heavy fuel oil) is used, while MDO (marine diesel oil) is used in and around ports. In-port emissions are included based on TNO expert judgement. The TNO-MACC-III data set takes into account different influences on ship emission trends:

- Economic growth of the sector per year;
- SECA – Sulphur emission control areas (North Sea and Baltic Sea);
- Economic crisis: slow steaming to save fuel (costs); less emission per mile;
- Trend towards bigger ships – economics of size.

According to this data set, international shipping emissions were increasing after 2000 until a trend change occurred in 2006. Related to the stepwise reductions in marine fuel sulphur content by IMO regulations and the EU Directives there has been a significant drop in SO_x emissions from 2006 to 2010, and then again from 2010 to 2011.

The TNO-MACC-III data for international shipping are, in general, lower than the ones that were used by CEIP until 2014 (see Wankmüller et al. (2015), their Figure 3.5).

6.3.2 FMI

The FMI data set is a bottom-up inventory based on real ship movements (AIS) and the STEAM model (Jalkanen et al. 2016). FMI combines ship movements with vessel specific technical data and predicts the fuel usage and emissions based on modeling of individual ships. As a result, the emission data sets fully reflect the changes of ship activity and the variability of ship building and powering options. The benefits of this approach include:

- A realistic description of ship traffic and ship emissions;
- The possibility to validate ship specific emission data with ship stack measurements;
- Conservation of geographical and temporal variability of emissions instead of reporting flat annual emission totals and static emission maps;
- Classification of emissions according to various criteria (vessel type, age, flag state).

However, there are also some drawbacks:

- The earliest possible year for FMI emission inventory is year 2006 in the Baltic Sea area, because the AIS system became mandatory only during 2005;
- Limited availability of AIS data from the relevant organizations collecting these data.

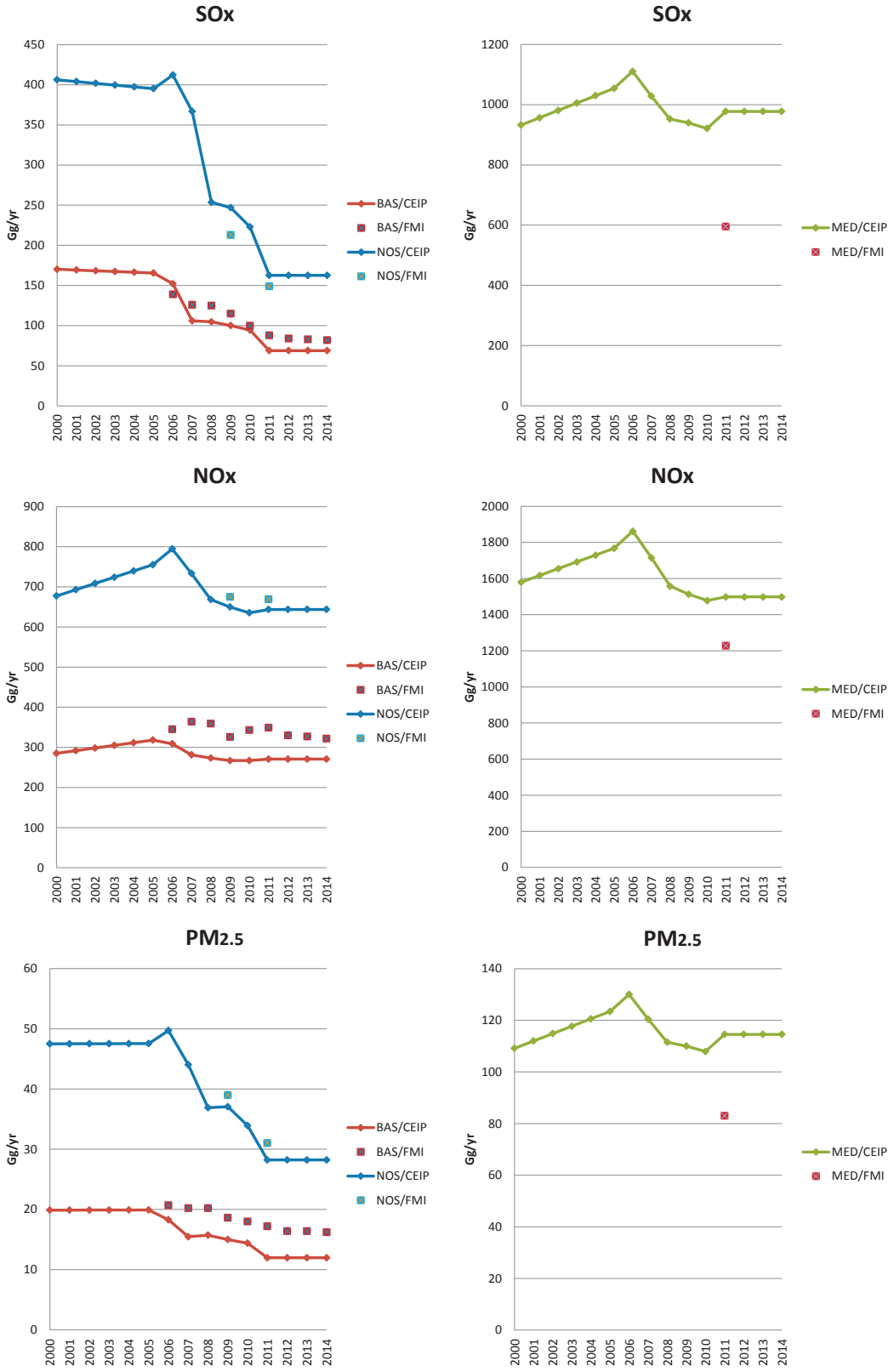

Figure 6.3: Total annual ship emissions of SO_x, NO_x and $PM_{2.5}$ for years since 2000, according to the CEIP and FMI data sets. Unit: Gg/yr. Left panels show data for the North Sea ('NOS') and the Baltic Sea (BAS); right panels: Mediterranean Sea ('MED'). Note that trends after 2011 in the CEIP data set are set to zero because the underlying TNO-MACC-III data set extends to 2011 only.

6.3.3 Comparison of data sets

Figure 6.3 compares emission data from CEIP (TNO-MACC-III) and FMI for the period since 2000. Possible reasons for differences in 2011 have been discussed in detail by Jalkanen et al. (2016). While differences between the two data sets for the North Sea region are relatively small, they are larger for the Baltic Sea region, in particular for NO_x and $PM_{2.5}$, probably related to different assumptions on activity growth and emission factors, but also on slow steaming (as pointed out by Jalkanen et al. (2016) – see their Table – significant differences can be observed between the average design speed and the average speed over ground during cruising). As mentioned above, emissions in the CEIP data have been kept constant since 2011, while the FMI data (based on AIS) suggest slightly decreasing emissions in the Baltic Sea, probably resulting from economic downturn.

For the Mediterranean Sea, the absolute differences between the CEIP and FMI data sets are largest. In this region the FMI data suggest much lower emissions than CEIP (TNO-MACC-III), especially for SO_x. Different assumptions on slow steaming in the Mediterranean and the uncertainties in emission factors may contribute to this disagreement. Given the relative importance of shipping emissions in this region (see Figure 6.1), this is a rather critical uncertainty, which deserves further attention.

6.4 The way forward

For EMEP/MSC-W modelling, access to accurate emission data is of crucial importance. However, the judgement on which emission data set in regard to shipping is fittest for purpose is not a straightforward task because measurements to constrain the estimates are sparse. Uncertainties remain in the estimates of total fuel use, the spatial distribution of emissions, and in the emission factors (exhaust per kg of burnt fuel).

The fact that the FMI data are based on real ship movements and extend to 2014 in the Baltic Sea, with 2015 data becoming available soon, makes them interesting for EMEP/MSC-W trend modelling. However, the availability of data until year 2014/15 only applies to the Baltic Sea. Data for other seas in the EMEP domain are only available until 2011 (e.g. North Sea and Mediterranean), or not at all (North Atlantic, Caspian Sea). From a technical point of view, annual updates of global ship emissions are fully feasible using the FMI approach, but global (and European-wide) emission calculations require access to AIS data that are currently only available from commercial data providers, i.e. require funding. For European sea areas, AIS data is collected by EU maritime authorities, but the question whether these data can be made available for ship emission research is still open. For these reasons, the use of FMI data is, at present, not an option for EMEP/MSC-W modelling. Also, and quite importantly, further investigation is needed on emission factors, which differ between the FMI and TNO-MACC-III data sets.

In conclusion, we note that for this year's EMEP/MSC-W modelling (for 2014 and trends), the trend in international ship emissions is assumed to be zero after 2011. Trends after 2011 in the FMI data for the Baltic Sea are rather small, suggesting that the error introduced by assuming a zero trend is not large, and probably well within the uncertainties in other input data and the modelling. Nevertheless, negotiations with AIS data providers have to continue, as well as the search for funding to support further research on emission factors. The question of ship emission data for EMEP/MSC-W modelling will be revisited before next year's reporting (for 2015).

References

Jalkanen, J.-P., Johansson, L., and Kukkonen, J.: A comprehensive inventory of ship traffic exhaust emissions in the European sea areas in 2011, Atmos. Chem. Physics, 16, 71–84, doi:10.5194/acp-16-71-2016, URL http://www.atmos-chem-phys.net/16/71/2016/acp-16-71-2016.pdf, 2016.

Jonson, J. E., Jalkanen, J. P., Johansson, L., Gauss, M., and Denier van der Gon, H. A. C.: Model calculations of the effects of present and future emissions of air pollutants from shipping in the Baltic Sea and the North Sea, Atmospheric Chemistry and Physics, 15, 783–798, doi:10.5194/acp-15-783-2015, URL http://www.atmos-chem-phys.net/15/783/2015/, 2015.

Wankmüller, R., Mareckova, K., Pinterits, M., Ullrich, B., Denier van der Gon, H., Gauss, M., and Nyíri, A.: Emissions for 2013, in: Transboundary particulate matter, photo-oxidants, acidifying and eutrophying components. EMEP Status Report 1/2015, pp. 45–62, The Norwegian Meteorological Institute, Oslo, Norway, 2015.

CHAPTER 7

Reduced European sulfur emissions unleashes the Arctic greenhouse warming

A. Kirkevåg, J. C. Acosta Navarro, A. M. L. Ekman, H.-C. Hansson, T. Iversen, I. Riipinen, Ø. Seland, H. Struthers, and V. Varma

In a time with an increasing greenhouse effect, the Arctic warms even faster than the rest of the world. This is usually referred to as Arctic amplification, meaning that local feedback mechanisms enhance the Arctic warming relative to the global. The best known example of such a mechanism is probably the ice-albedo feedback, where a warmer climate leads to less sea-ice and thereby a lower surface albedo, which again enhances absorption of sun-light, giving further warming.

The sharp reduction of pollutants in the air over Europe since the 1980s, at the time when important international agreements to reduce acid rain in Europe were concluded, has now been found to explain a significant part of the recent observed rapid warming trend in the Arctic. This is shown in a recent study by Acosta Navarro and Varma et al. (2016) published in Nature Geoscience. The authors of this paper here present a summary of the main results, which emphasize the importance of rapidly reducing greenhouse gas emissions to mitigate further the climate change that now has become evident in the Arctic. The study also demonstrates that our actions in Europe to improve air quality and other environmental aspects may have profound climate effects in other regions of the world.

Small liquid or solid particles, known as aerosol particles, are emitted into air from industry, automobiles, energy production, wood burning and other human as well as natural activities, and can be transported far away from their sources. High concentrations in air near major sources have immediate negative impacts on health and environment, contributing to increased mortality and reduced visibility, while those transported farther away may cause acid rain. Emissions of sulfur dioxide, which becomes sulfate in air, peaked around 1980 in Europe and North America, and the acidifying effect on freshwater and soils led to strict international agreements to reduce the emissions.

Aerosol particles vary in size, composition and other physical characteristics which to-

(a)

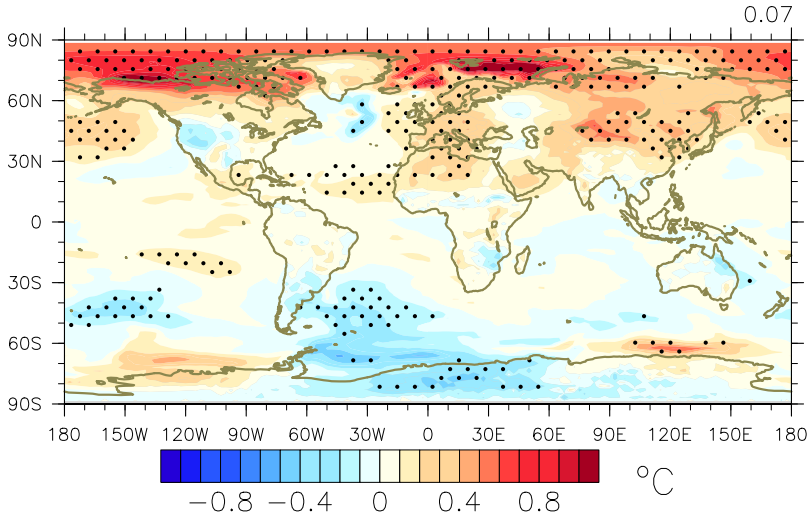

(b)

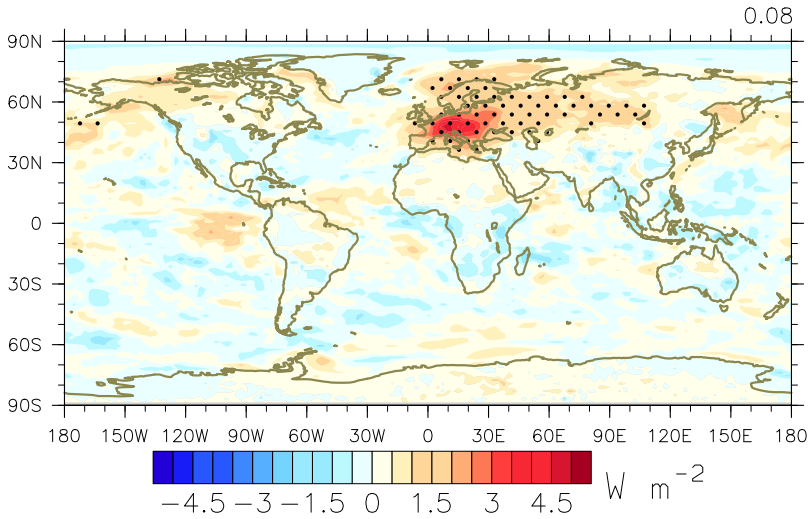

Figure 7.1: Effect of reduced sulfur dioxide and sulfate emissions on surface temperatures (a, top panel) and net incoming short-wave plus long-wave radiative flux at top of the atmosphere (b, bottom panel), annually averaged for the years 1996–2005. Black dots indicate statistically significant results.

gether determine their effect on climate. Soot particles, which consist of black and organic carbon, heat the air when they absorb solar radiation. Sulfate aerosols, on the other hand, reflect solar radiation and contribute to more but smaller droplets in clouds, also enhancing the reflection of sun-light and therefore having an overall cooling effect on the climate system. Aerosols from human activities contributed to a cooling of climate during the first decades after World War II and have thus muted, or masked, the warming caused by increased emissions of greenhouse gases.

Using the advanced climate model NorESM1-M, the Norwegian Earth System Model (for more information, see Bentsen et al. (2013), Iversen et al. (2013), Kirkevåg et al. (2013)), Acosta Navarro and Varma et al. (2016) find that the reduction of sulfate in Europe between 1980 and 2005 can explain a large part of the warming observed in the Arctic during the same period. In other words, as a result of regulations on emissions in Europe to improve air quality

and acidification of water and soils, a substantial portion of the dampening effect of aerosol particles has been removed, and consequently more of the actual warming of the Arctic due to increased (manmade) greenhouse gas levels has emerged.

Natural climate variability is large at high latitudes. To statistically distinguish the signal from the noise in Europe and the Arctic, the climate model had to be run multiple times, branching off three times, in 1980, from each of the three member ensemble of the historical transient simulations (Iversen et al. 2013), using different initial meteorological conditions. Thus, in total nine simulations were run using the (same) current best estimates of emissions (IPCC, see Kirkevåg et al. (2013)) of aerosol and their gas precursors world-wide, and another nine where the European emissions of sulfate and sulfur dioxide, for a EMEP-defined domain, were kept constant (high) at 1980 levels from year 1980 onwards, but elsewhere being the same as in the former reference simulations. Greenhouse gas concentrations (also from the IPCC) increase with time in the same way in all simulations.

The modeled impact of the reduction in European sulfur emissions on near surface temperatures since 1980 is shown in Fig. 7.1a. The largest areas with substantial and significant increases in temperatures are found at high northern latitudes. Over continental Europe itself the warming amounts to 0.13 °C, which is about a fifth of the 0.59 °C increase found in the reference simulations over the same area, i.e. in the simulations where sulfate emissions have declined according to historical records. In the Arctic, here defined as 70–90°N, the temperature increase due to reduced sulfur emissions alone is estimated to be 0.54 °C. Compared to the 1.0 °C warming found over the same area in the reference simulations this is about half of the total temperature increase since 1980.

The corresponding annual anomalies in net incoming radiative flux at top of the atmosphere (Fig. 7.1b), originating from enhanced reflection of sun-light either directly by sulfate aerosols or by associated changes in cloud parameters such as droplet number and size, are geographically much more constrained to Europe and other downstream areas. Based on this information only, one would not expect the Arctic to warm as the regional masking effect of the European sulfur emissions is removed. So what are the mechanisms present in the model, and most likely also in nature, which allow reductions in European sulfur emissions to warm the Arctic? The short answer is that a redistribution of the energy input to the Arctic over the year appears to be a critical factor. This mechanism is discussed in detail by Acosta Navarro and Varma et al. (2016), see also the review paper by Mauritsen (2016), and is only briefly summarized here.

Comparing the results for the period 1996–2005 in the historical simulations with those using fixed 1980 sulfur emissions, i.e. looking at the effect of the regulations on sulfur emissions in Europe, the study finds the following:

During summer, as insolation peaks and the extent of highly reflective and insulating sea-ice has started to shrink, there is a considerable increase in net input of solar radiation in the Arctic. Local background aerosols are here relatively pristine, so that even a small decrease in aerosol concentrations is effective in warming the region in summer. This summertime energy surplus is mainly used to melt sea ice, however, resulting in a relatively small surface temperature increase compared to other seasons. In contrast, the increase in surface temperatures over Europe is largest in summer, leading to a strengthened poleward atmospheric heat transport. Together with the ocean transport, which is enhanced during the whole year when sulfur emissions are reduced, this increases the amount of available energy in the Arctic in summer, which again boosts the melting of sea ice and delays the onset of freezing in autumn. The delayed freezing is reflected in a larger heat transfer from the ocean to the atmosphere

during fall and winter. As the atmosphere warms, additional feedback mechanisms associated with e.g. relative humidity, clouds, temperature lapse rate and long-wave radiation are also initiated, which further amplifies the Arctic warming.

It is expected that the Arctic will continue to warm, since the concentration of greenhouse gases in the atmosphere continue to rise while emissions of aerosol particles most likely will decline in response to the need to combat local and regional air pollution also in other parts of the world. In light of this, the presented study emphasizes the importance and urgency of rapidly reducing greenhouse gas emissions in order to mitigate further climate change in the Arctic, as well as globally.

References

Acosta Navarro, J. C., Varma, V., Riipinen, I., Seland, Ø., Kirkevåg, A., Struthers, H., Iversen, T., Hansson, H.-C., and Ekman, A. M. L.: Amplification of Arctic warming by past air pollution reductions in Europe, Nature Geoscience, 9, 277–281, doi:10.1038/ngeo2673, 2016.

Bentsen, M., Bethke, I., Debernard, J. B., Iversen, T., Kirkevåg, A., Seland, Ø., Drange, H., Roelandt, C., Seierstad, I. A., Hoose, C., and Kristjánsson, J. E.: The Norwegian Earth System Model, NorESM1-M – Part 1: Description and basic evaluation of the physical climate, Geoscientific Model Dev., 6, 687–720, doi:10.5194/gmd-6-687-2013, 2013.

Iversen, T., Bentsen, M., Bethke, I., Debernard, J. B., Kirkevåg, A., Seland, Ø., Drange, H., Kristjansson, J. E., Medhaug, I., Sand, M., and Seierstad, I. A.: The Norwegian Earth System Model, NorESM1-M – Part 2: Climate response and scenario projections, Geoscientific Model Dev., 6, 389–415, doi:10.5194/gmd-6-389-2013, 2013.

Kirkevåg, A., Iversen, T., Seland, Ø., Hoose, C., Kristjánsson, J. E., Struthers, H., Ekman, A. M. L., Ghan, S., Griesfeller, J., Nilsson, E. D., and Schulz, M.: Aerosol-climate interactions in the Norwegian Earth System Model – NorESM1-M, Geoscientific Model Dev., 6, 207–244, doi:10.5194/gmd-6-207-2013, 2013.

Mauritsen, T.: Arctic climate change: Greenhouse warming unleashed, Nature Geoscience, 9, 271–272, doi:10.1038/ngeo2677, 2016.

CHAPTER 8

Climate impact of the 2012 revision of the Gothenborg Protocol

Dirk Olivié, Hilde Fagerli, Ágnes Nyíri and Michael Schulz

8.1 Introduction

By the emission of gases and particles through various anthropogenic activities, mankind alters the composition of the atmosphere, leading to lower air quality, ecosystem degradation, and changes in climate. Climate can be influenced through impacts on the radiation balance in the atmosphere: this is done by greenhouse gases like CO_2, methane, ozone and others, but also by small solid or liquid particles which can reflect or absorb (mainly) solar radiation (sulfate, nitrate, black carbon, organic matter, etc.) or act as cloud condensation nuclei. Air quality at the Earth surface is mainly degraded by the presence of ozone, NO_x, and fine particulate matter.

Emissions of a single species can have impacts on both air quality and climate. E.g., the emission of carbon monoxide (CO) enhances tropospheric ozone formation leading to a warming effect for climate and a lowering of the air quality. One should be aware of this when considering emission mitigation: measures to limit air quality deterioration might impact climate, and, vice-versa, measures to protect climate can possibly impact air-quality. E.g., the reduction of SO_2 in Europe and the US over the period 1960–1990 initiated to improve air quality, has lead to extra warming in the northern hemisphere (see Chapter 7).

Here we analyze the climate impact of the 2012 amendments to the Convention's 1999 Gothenborg Protocol to Abate Acidification, Eutrophication and Ground-level Ozone (Gothenborg Protocol). The aims of the Gothenborg Protocol and its amendments have been primarily abating acidification, eutrophication and ground-level ozone. In May 2012, Parties to the Convention on Long-range Transboundary Air pollution have reached agreement on a revision of its Gothenborg Protocol. The revised protocol includes quantitative emission reduction commitments for the year 2020 for the main air pollutants, and thus, for the first time,

incorporates emission reduction commitments for fine particulate matter. Whereas the expected improvements from the amendments for human health and ecosystem protection have been described elsewhere (Amann et al. 2012), we will here describe their impact on climate.

The reduction commitments affect the emission of so-called short-lived climate forcers (SLCFs) or their precursors. These are substances which affect climate, but have a relatively short lifetime (on the order of days to weeks for black carbon, to several years for methane). As we look at the climate impact of short-lived species, location of the emissions plays a considerable role (as opposed to long-lived species as CO_2, N_2O, and most CFCs and HFCs). Therefore, we use results from a study which among other topics looked at how the emission location influences the radiative forcing, and use their Europe-specific results (Bellouin et al. 2016). To estimate the impacts on surface air temperature, we use results from a study which investigated how regional forcing impacts surface temperature in the same or different regions (Shindell and Faluvegi 2009). In the analysis performed here, we limit ourselves to the impact on radiative forcing and surface temperature. We will discuss impacts globally averaged, but also distinguish 4 different latitude bands, i.e., 90°S–28°S, 28°S–28°N, 28°N–60°N, and 60°N–90°N.

In Section 8.2 we present the emission scenarios and describe the method followed to estimate the radiative forcing and temperature impact, in Section 8.3 we present our results, and in Section 8.4 we present our conclusions.

8.2 Method

In this section, we explain the methodology followed to estimate the climate impact of the Gothenborg Protocol amendments. We present first the different emission scenarios we compare, then we describe the radiative forcing efficiency estimates our analysis is based upon, and, finally, how the surface temperature impacts are estimated.

8.2.1 Emission scenarios

The new text of the protocol includes emissions reduction commitments to be achieved in 2020 and beyond. These commitments are expressed with respect to the emissions in 2005.

In preparation of the revision of the Gothenborg Protocol, different scenarios for emission estimates have been made for the year 2020. Firstly, one based on coherent projections of economic activities and baseline activity data (energy use, transport and agricultural activities), reflecting the continued implementation of already agreed emission control legislation, which we will call the CLE scenario.

Secondly, the future emission levels in 2020 are collected based on the emission reduction commitments that have actually been agreed upon by the Parties to the Convention, and which are specified in relation to the respective 2005 emission levels. This scenario will be called GP here.

To evaluate the impact of the 2012 amendments, we compare three emission data sets for the European Parties to the Gothenborg Protocol[1]. The reference emission data set contains

[1]Parties included in the comparison and in Table 8.1: Albania, Armenia, Austria, Belarus, Belgium, Bulgaria, Croatia, Cyprus, Czech Republic, Denmark, Finland, France, Germany, Greece, Hungary, Ireland, Italy, Latvia, Liechtenstein, Lithuania, Luxembourg, TFYR of Macedonia,| the Republic of Moldova, Montenegro, the Netherlands, Norway, Poland, Portugal, Romania, Serbia, Slovakia, Slovenia, Spain, Sweden, Switzerland,

Table 8.1: European emissions [Tg yr^{-1}] in three different scenarios: 2005 as reference scenario, 2020 (GP) takes into account the measures from the 2012 Gothenborg Protocol amendments, and 2020 (CLE) takes into account all current legislation. Emission amounts for VOC, BC, and OC are expressed in Tg[C] yr^{-1}.

	2005	2020 (GP)	2020 (CLE)
NO_2	12.6	7.7	6.6
SO_2	9.7	5.0	3.4
NH_3	4.43	4.19	4.36
VOC	10.5	7.8	7.0
CO	36.2	24.0	25.7
BC	0.44	0.30	0.27
OC	0.51	0.39	0.45

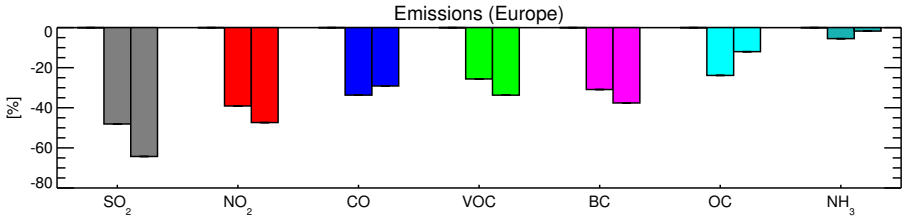

Figure 8.1: Change in emission amounts in the scenarios 2020 (GP) (left bars) and 2020 (CLE) (right bars) compared to the 2005 emission amounts.

the emission amounts as have been estimated for the year 2005 (see left column in Table 8.1). The second data set contains the emissions for year 2020 taking into account the measures from the Gothenborg Protocol amendments (GP). The third data set contains emission data for the year 2020, as they would emerge for 2020 from the progressive implementation of current emission control legislation (CLE). The emission scenarios were provided by CIAM/IIASA and described in Amann et al. (2012).

The data sets presented here contain emissions for 7 different species, and the total annual values for emissions from European Parties to the Gothenborg Protocol are are given in Table 8.1. For most of the 7 species, European emissions are reduced considerably in the year 2020 compared to 2005, both in the GP and the CLE scenario. Figure 8.1 indicates how large the emissions amounts in the scenarios 2020 (GP) and 2020 (CLE) are reduced as compared to 2005. Strongest emission reductions are expected for SO_2 and NO_2 being around 40–60 %, followed by reduction amounts of 25–35% for CO, VOCs, and BC. Reduction amounts are smaller for particulate organic carbon (OC) and smallest for NH_3, being around 0–5 %. One can see that the reduction in CLE is stronger than in GP for SO_2, NO_2, VOCs and BC. Note, as the agreed GP commitments for some of the species are smaller than under a CLE scenario, the GP agreed reductions are also much weaker than some other scenarios suggested during the preparation of the revised protocol (Amann et al. 2011a,b) – scenarios aimed at reaching an even higher level of environmental protection where the additional measures were based

Ukraine and the United Kingdom.

on a cost-effectiveness optimization. Amann et al. (2012) mention possible explications for a commitment level which is less stringent than CLE, i.e., (i) disagreement about underlying projections of energy use and economic development, (ii) different assumptions about the implementation success and effectiveness of recent emission control legislation, (iii) uncertainties in emission inventories, and (iv) Parties introducing some uncertainty margin to safeguard against unexpected developments.

8.2.2 Radiative forcing

Radiative forcing expresses how strongly radiative fluxes (at the tropopause or top of the atmosphere (TOA)) are modified by changing the atmospheric composition, and gives an indication of how the energy budget of the Earth is perturbed. It is a theoretical concept, as any imbalance on a global scale in the net radiative flux at the tropopause (or TOA) will induce responses counteracting the initial perturbation in the long term. Despite its shortcomings, radiative forcing has been proven to be a useful concept to estimate induced surface temperature change (Andrews et al. 2012, Boucher et al. 2013, Myhre et al. 2013). However, it has taken a while to arrive at a robust determination (Sherwood et al. 2015): for ozone (and CO_2) one has to allow for stratospheric temperature adjustments to be taken into account, or, for aerosols the cloud-mediated (or indirect) impact has to be considered, and for BC the semi-direct effect caused by the uneven distribution of atmospheric heating by BC needs to be included.

Bellouin et al. (2016) have made an extensive study on the RF caused by anthropogenic emissions, and we will base our analysis on their results. The emission of one single species, can impact several different radiatively active species. E.g., emissions of NO_2 affect directly O_3 and nitrate, but through their impact on OH indirectly also the lifetime of CH_4 and the formation rate of SO_4. Bellouin et al. (2016) have tried to obtain an accurate picture, evaluating the effect of single emitted species on all relevant radiatively active gases (ozone and methane) and aerosols (black carbon, organic matter, sulfate, and nitrate), using 4 different global atmospheric models (ECHAM6, HadGEM2, NorESM1, and Oslo-CTM2). The radiative forcing mechanisms taken into account by Bellouin et al. (2016) are: aerosols (both aerosol-radiation and aerosol-cloud interactions), BC deposition on snow, BC rapid adjustments to semi-direct effects, short-lived changes in ozone concentrations, methane, and primary-mode ozone (their forcing estimates for ozone take into account stratospheric adjustments). Although the scenarios we study do not differ in the amount of CH_4 emissions, we take into account the fact that the emissions of other species (mainly NO_x) can change the atmospheric methane concentration and so have an extra impact on radiative forcing. Bellouin et al. (2016) have further split their analysis into origin and season of the emissions. They studied separately the impact from emissions in Europe, South-East Asia, shipping, and the so-called "rest of the world", and distinguished between emissions done in the period May–October or in the period November–April.

The lifetime of the perturbation induced on the radiatively active species, varies among species. Perturbations in aerosol species have life times in the order of one week, direct impact on O_3 on the order of 1–4 weeks, but methane perturbations persist on the order of 9–12 years. The radiative forcing values we present here are calculated under the assumption of steady state, i.e., it represents the induced radiative forcing for a constant emission rate (of, e.g., $1\,\mathrm{Tg\,yr^{-1}}$). Table 8.2 gives the net equilibrium forcing efficiency (summed over all forcing mechanisms) induced by SO_2, NO_2, CO, VOC, BC, OC, and NH_3 emissions from Europe, South-East Asia, and rest of the world, and separately for emissions in

Table 8.2: Radiative forcing efficiencies for SO_2, NO_2, CO, VOC, BC, OC, and NH_3 emissions [mW m^{-2} (Tg yr^{-1})$^{-1}$]. Distinction is made between emissions from Europe, South-East Asia (China, Taiwan, South-Korea, North-Korean, and Japan), and the rest of the world, and between emissions in summer (May–October) and winter (November–April). Values are taken from Bellouin et al. (2016, Supplementary Material).

	Europe		South-East Asia		Rest of the world	
	Summer	Winter	Summer	Winter	Summer	Winter
SO_2	-10.8	-3.1	-2.7	-12.5	-12.5	-8.1
NO_2	-1.0	-0.5	-0.6	-1.2	-1.2	-1.7
CO	0.2	0.2	0.2	0.2	0.2	0.2
VOC	1.1	0.7	1.1	0.3	1.0	1.1
BC	52.9	45.7	52.8	28.7	77.1	65.6
OC	-19.0	-9.8	-12.2	-4.4	-25.7	-22.4
NH_3	-1.4	-0.9	-0.7	-1.3	-0.5	-0.8

the period May–October and November–April (data taken from Bellouin et al. (2016, Supplementary Material)). These radiative forcing efficiency values have been recently used, e.g., by Aamaas et al. (2016). In the rest of the analysis, we will only use the European values, and as we only focus on annual-mean impacts, we use the average of the summer and winter values of Table 8.2.

8.2.3 Temperature response

To quantify the impact of the three different emission scenarios, we try to estimate their impact on the Earths surface temperature. We look both at the global averaged temperature response, and at the response in various latitude bands, i.e., 90°S–28°S, 28°S–28°N, 28°N–60°N, and 60°N–90°N.

Once a species is emitted, through affecting the radiative fluxes (expressed as a radiative forcing) it can finally impact climate (surface temperature, precipitation, circulation patterns, etc). Due to natural climate variability on annual and decadal time scales, estimating the climate impact caused by relatively small radiative forcings is very demanding. If one bases impact analysis on observations one would need very long observational time series, and if one bases it on climate models one would need very long simulations. Quantifying the climate impact of any possible specific emission location is impossible.

On the global scale, however, one expects that the ultimate mean temperature impact is proportional to the globally averaged radiative forcing, which is expressed by the climate sensitivity: the surface temperature change when imposing a radiative forcing of 1 W m^{-2} globally averaged. Andrews et al. (2012) estimated the climate sensitivity for a group of 15 global climate models and found values varying between 0.66 and 1.58 K (W m^{-2})$^{-1}$, with a model-mean of 1.0 K (W m^{-2})$^{-1}$. Others have tried to estimate the Earth's climate sensitivity based on observed temperature changes in the atmosphere and upper part of the ocean, combined with estimates for radiative forcing evolution over the 20th and 21st century. For a doubling of CO_2, Skeie et al. (2014) found an equilibrium temperature change of 1.8 K as a best estimate (with a 90 % credible interval from 0.9 to 3.2 K). Assuming the standard expression for

CO_2 forcing, this corresponds to a climate sensitivity of 0.49 K $(W m^{-2})^{-1}$, with a 90 % credible interval from 0.24 to 0.86 K $(W m^{-2})^{-1}$. These estimates are considerably lower than the model-derived estimates. Here we have chosen to adopt the model-mean climate sensitivity of Andrews et al. (2012), i.e., 1.0 K $(W m^{-2})^{-1}$.

Once a radiative forcing has been imposed, it might take hundreds and possibly thousands of years before the Earth finds a new equilibrium. This long response time is caused by the large thermal capacity of the world oceans and the slow mixing of heat into the deep ocean. E.g., Caldeira and Myhrvold (2013) estimated that after 10 years only half (range 38–61 %) of the warming is realised, and one quarter (14–40 %) of the warming occurs more than one century after the start of the forcing – the range comes from the spread among different climate models. Specific approaches (e.g., Global Temperature change Potential, Shine et al. (2005)) exist where one concentrates on the climate impact of emissions on much shorter time horizons, i.e., often 20, 50 or 100 yrs, and takes explicitly into account the time scales present in the climate system influencing the rate of warming (Olivié et al. 2012, Olivié and Peters 2013). Here we limit the analysis to the equilibrium temperature impact.

It is known that climate change is not uniform, and that geographical location of temperature is not collocated with the forcing. Therefore, although the forcing of European emissions is mainly located at the northern mid-latitudes and in the Arctic, the temperature response can be found also in other regions of the world. To estimate the impact on regional temperature, we use results from Shindell and Faluvegi (2009), and use an approach comparable with Shindell (2012), Collins et al. (2013) and Sand et al. (2016). Shindell and Faluvegi (2009) have made an extensive study where they perturbed the concentrations of radiatively active species in 4 different latitude bands – they did this for CO_2, SO_4, BC, and OM. They have tried to estimate how forcing in a specific latitude band results in temperature changes in the same as well as in other latitude bands. Their simulations had a length of 120 year, and they looked at the impact on the temperature over the last 80 years.

Table 8.3 is taken from Shindell (2012) and gives the expected temperature change in a specific region from forcing in the same or a different region. The values in the table are dimensionless and should be multiplied with the global climate sensitivity to obtain the temperature change cause by 1 W m^{-2} of forcing in the forcing region. It shows that regional forcing often causes the strongest temperature impact in its own region: the diagonal elements are in most cases larger than the off-diagonal elements (compare values within the same column). However, the off-diagonal elements can still be considerable as meridional heat-transport (via the atmosphere or the ocean) can impact neigbouring regions. One should also be aware that the surface area of these 4 regions are very different: the southern extra-tropics, the tropics, the northern mid-latitudes and the Arctic cover 26.5, 46.9, 19.8, and 6.7 % of the Earths surface, respectively. This is, e.g., the reason why the off-diagonal elements in the last column are relatively small. These latitude bands have been chosen by Shindell and Faluvegi (2009) because of the clear horizontal mixing barriers between them. As a result, forcings from anthropogenic SLCFs show large gradients between those bands (Shindell 2012).

Originally, Shindell and Faluvegi (2009) derived results for the forcing-temperature relationship separately for BC, ozone, CO_2 and sulfate. However, Shindell (2012) mention that in their experiments the response to different forcing agents were typically statistically indistinguishable for sulfate, BC, and O_3. They therefore suggest to use only one set of coefficients which are the ones for sulfate (those experiments had the largest forcing and hence the smallest uncertainty). Some studies (Collins et al. 2013, Sand et al. 2016) use coefficients specific for each agent.

Table 8.3: Regional response coefficients (see Table 1 in Shindell 2012).

Forcing region	90°S–28°S	28°S–28°N	28°N–60°N	60°N–90°N
Response region				
90°S–28°S	**0.38**	0.02	0.05	0.00
28°S–28°N	0.19	**0.51**	0.15	0.08
28°N–60°N	0.11	0.55	**0.49**	0.16
60°N–90°N	0.14	0.36	0.43	**0.77**

As the coefficients in Table 8.3 have been derived using only one coupled atmosphere-ocean climate model, i.e. GISS-ER (Schmidt et al. 2006), they reflect only the characteristics of that single climate model. So far, no other equally thorough analysis has been made with other climate models, the robustness of the regional patterns of the forcing-response relations is largely unknown. There are some specific results available for BC (Sand et al. 2013, Flanner 2013), and Shindell (2012) did a comparison with results from 4 different coupled atmosphere-ocean models, and concluded that differences are in the order of $\pm 20\,\%$, but larger in the Arctic (Sand et al. 2016).

8.3 Results

Here we present the impact of the 3 scenarios of European emissions on radiative forcing and surface temperature. First, we focus on the globally averaged impact. Later, we distinguish between the 4 different zonal bands.

8.3.1 Globally averaged impact

Figure 8.2 shows the emission amount (for each species) and the impact on globally averaged radiative forcing and surface temperature for each of the three scenarios. Emissions of SO_2, NO_2, OC and NH_3 lead to negative radiative forcing and a reduction in temperature, whereas emissions of CO, VOC, and BC generally lead to a positive radiative forcing and an increase in temperature. The negative impact from SO_2 and OC emissions results from the formation of sulfate and OM aerosols, whereas the emissions of NO_2 and NH_3 lead to the formation of nitrate aerosol. All these aerosols scatter solar radiation, and therefore have a cooling effect. Emissions of NO_2 in addition lead to a decrease in methane concentrations (cooling effect) and an increase in tropospheric ozone (warming effect). CO and VOC emissions lead to a warming impact, via an increase in methane concentration due to lower OH concentrations. Atmospheric BC aerosol as well as BC deposited on snow and sea ice lead to a positive radiative forcing and temperature increase.

The uncertainty estimates on the radiative forcing and surface temperature indicated in Fig. 8.2 represent the impact of uncertainties on the radiative forcing efficiencies. In addition to a best estimate, Bellouin et al. (2016) published also a lower and upper estimate, based on the spread among the results from the different atmospheric models.

Figure 8.3 shows the impact on global-mean radiative forcing and temperature, summed over the impact from all individual emission species (total impact is indicated in yellow). It

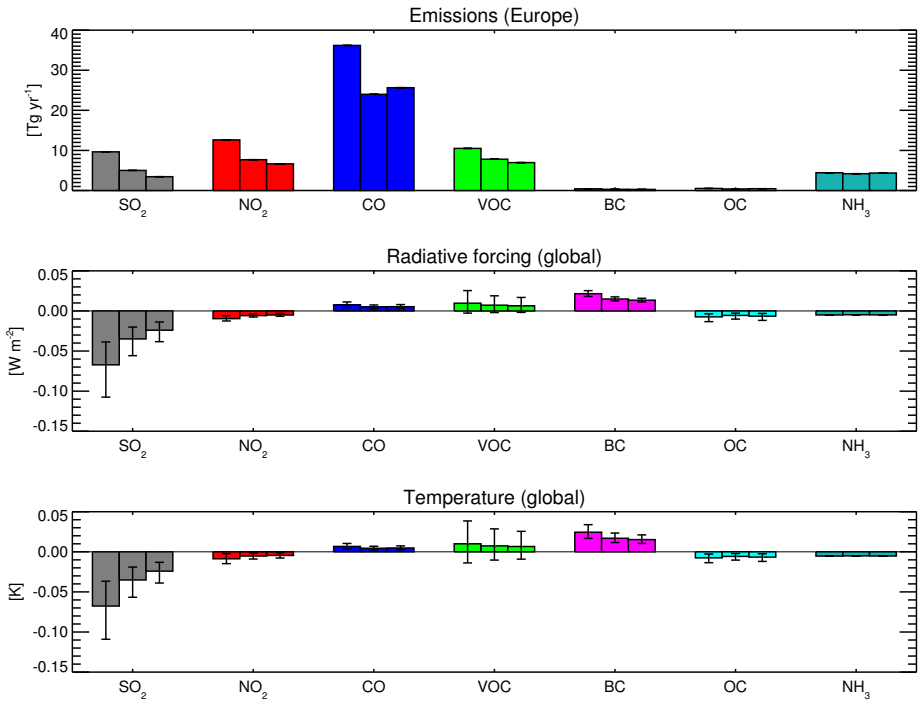

Figure 8.2: Emissions (top panel), RF (middle panel), and temperature response (bottom panel) for individual species in three scenarios: 2005 (left bars), 2020 (GP) (middle bars), and 2020 (CLE) (right bars).

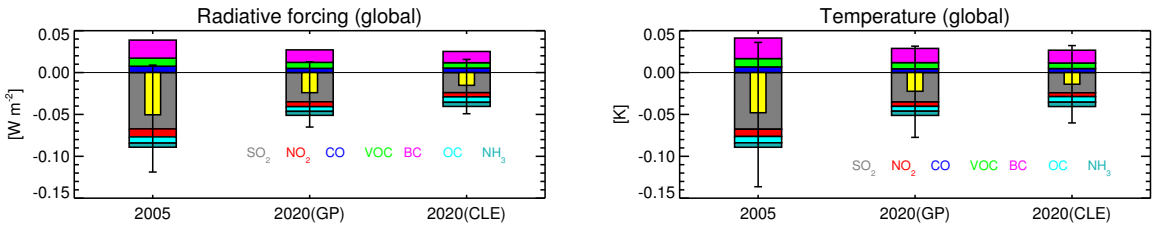

Figure 8.3: Globally averaged radiative forcing (left) and temperature response (right) from European emissions for the 3 scenarios: 2005, 2020 (GP), and 2020 (CLE). The yellow bar indicates the total impact.

indicates that the globally averaged total impact on both radiative forcing and temperature in all three scenarios is negative. The impact is strongest in the 2005 scenario with a radiative forcing of around –0.05 W m^{-2} and a temperature impact of around –0.045 K. The impacts in the 2020 (GP) scenario are half of those in 2005, whereas the impact in 2020 (CLE) is around one third of the 2005 impact. The indicated uncertainty is again based on the the uncertainty in the radiative forcing efficiencies. However, as it is derived by just combining all lower estimates or all upper estimates (and not taking into account possible anti-correlations), we probably overestimate the uncertainty.

8.3.2 Regional impact

Figure 8.4 shows the radiative forcing and temperature impact in four different latitude bands, i.e., 90°S–28°S (southern extra-tropics), 28°S–28°N (tropics), 28°N–60°N (northern mid-latitudes), and 60°S–90°N (the Arctic). The impacts of European emissions on radiative forcing are strongest in the Arctic and northern mid-latitudes, considerably smaller in the tropics, and very small in the southern extra-tropics (notice the different scales on the vertical axis in Fig. 8.4). In the Arctic, the RF consists of a strong positive contribution caused by BC emissions and a negative contribution from SO_2 emissions: the total forcing is relatively small but positive. In the northern mid-latitudes, the forcing is negative and dominated by the impact of SO_2 emissions.

In the tropics and southern extra-tropics, the net forcing from European emissions is small, i.e., between –0.02 and –0.005 W m^{-2} in the tropics and between -0.006 and -0.001 W m^{-2} in the southern extra-tropics. The role of CO emissions and mainly NO_x emissions becomes (relatively) more important in these regions, whereas the impact of BC becomes smaller. This is due to the fact that CO (and NO_x) emissions impact the CH_4 concentration by increasing (decreasing) the OH concentration. As CH_4 has a long lifetime, European emissions of NO_x and CO will finally impact also the CH_4 concentrations in the tropics and southern extra-tropics. On the other hand, due to the relatively short lifetime of BC and SO_4, European emissions of BC ad SO_2 have almost no impact on radiative forcing in the southern hemisphere.

In general the impact from all scenarios is negative, strongest for 2005 and weakest for 2020 (CLE). The Arctic is an exception where the forcing is positive in all three scenarios (weakest for 2005 and strongest for 2020(CLE)). Net forcing in 2005 in the northern mid-latitudes, tropics, and southern extra-tropics is around –0.2, –0.02, and –0.005 W m^{-2}, respectively – in 2020 (GP) and 2020 (CLE) the values are around one half and one third of the 2005 values, respectively.

The right panels in Fig. 8.4 show the impact on the surface temperature in the four latitude bands. The general patterns visible in the RF, are reflected in the temperature impact: stronger impacts in the northern mid-latitudes than in the the tropics and southern extra-tropics; temperature impact reduced by half in 2020 (GP) compared to 2005, and even more reduced in 2020 (CLE). However, there are also clear differences compared to the results for radiative forcing. The difference between the two most northern and two most southern bands is much less pronounced. The role of SO_2 in the two southern bands remains the prevailing contribution (in contrast to the radiative forcing), and the impact from CO and NO_2 remains relatively minor. This is caused by the fact that the response is not only the consequence of local forcing, but also induced by remote forcing (warming induced by meridional heat transport), represented by the off-diagonal elements in the matrix in Table 8.3.

Another large difference between the radiative forcing and the temperature pattern impact, is the general cooling in the Arctic due to the local positive radiative forcing. It is the consequence of the negative RF in the northern mid-latitudes, which overwhelms the impact from local radiative forcing. Uncertainties in Fig. 8.4 again represent the spread resulting from uncertainties in the radiative forcing efficiencies.

8.4 Discussion and conclusions

This chapter describes the expected climate impact of the 2012 amendments to the Gothenborg Protocol. Three different scenarios have been compared: the reference scenario 2005, a

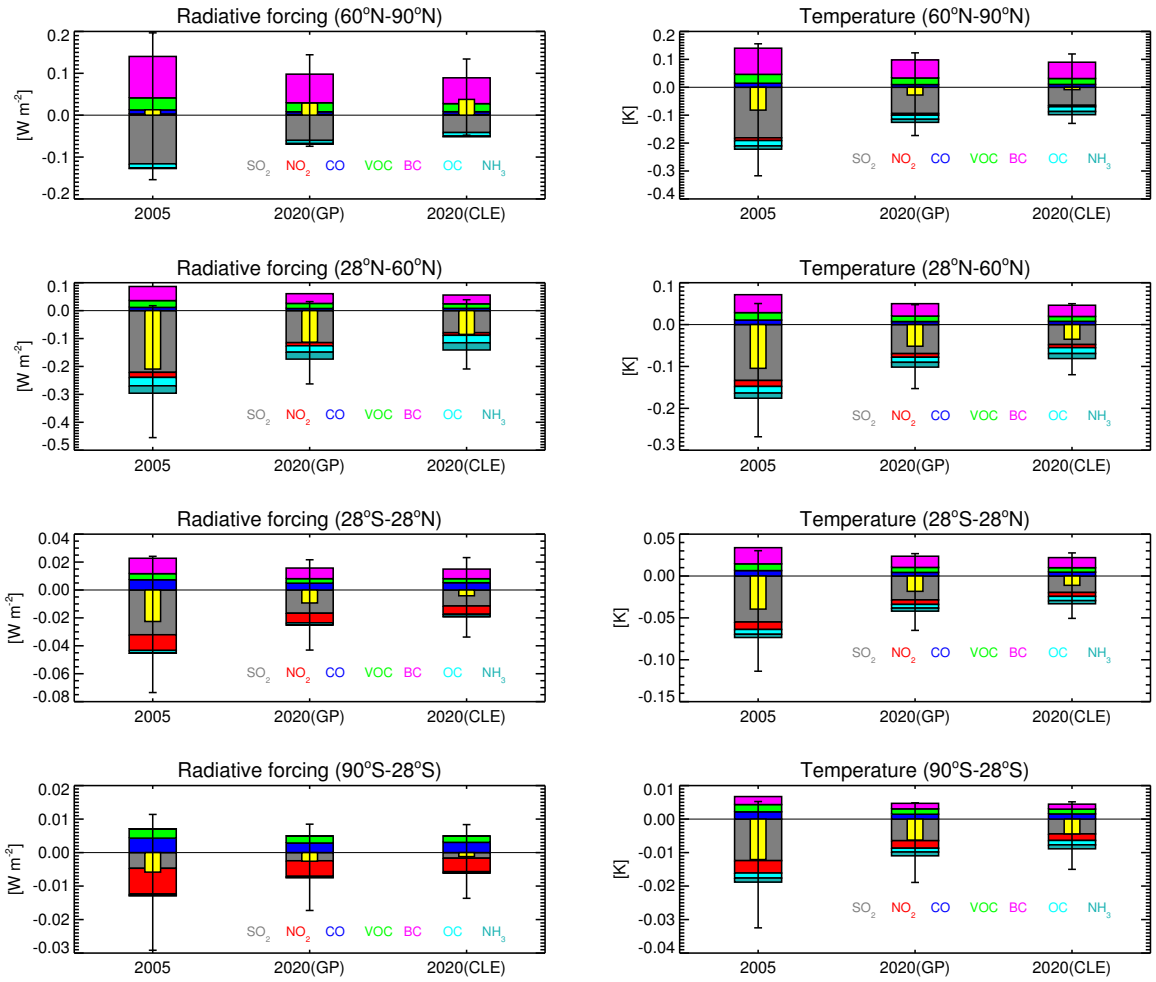

Figure 8.4: Regional response in radiative forcing (left) and temperature (right) to European emissions in four latitude bands, i.e., 60°N–90°N (first row, the Arctic), 28°N–60°N (second row, northern mid-latitudes), 28°S–28°N (third row, tropics), and 90°S–28°S (last row, southern extra-tropics).

scenario for the year 2020 with all measures from the Gothenborg Protocol amendments in place, and a scenario for 2020 taking into account all current legislations. European emissions in the reference scenario for 2005 lead to a cooling of around –0.05 K globally averaged. On the regional scale, the cooling is around –0.1 K both in the Arctic and northern mid-latitudes, while it is only -0.04 K in the tropics and –0.013 K in the southern extra-tropics. The net cooling comes from the prevailing impact from SO_2 emissions, but additional cooling is also caused by emissions of NO_2, OC and NH_3. The cooling is partially compensated by emissions of BC, CO, and VOCs.

Due to the 2012 amendments, the net impact in 2020 (GP scenario) is estimated to be still a cooling, but only of half the value caused by European emissions in 2005. All 4 regions we studied showed a similar reduction rate (in cooling), except for the Arctic were the reduction was stronger. The cooling in 2005 of –0.08, –0.1,–0.04, and –0.012 K in the Arctic, northern mid-latitudes, tropics and southern extra-tropics, respectively, is reduced to a cooling of around –0.03, –0.06, –0.02, and –0.006 K. The impact of the current legislation in 2020 (CLE scenario) is even stronger (due to in general even stronger emission reductions), resulting in

a net cooling which is only one third of the value in 2005. This is due to the fact that the agreed emission reduction commitments (GP scenario) are clearly lower than reduction estimations based on the implementation of existing emission control legislation (CLE scenario, Amann et al. 2012).

The results obtained here are in line with the results of the study described in Chap. 7, i.e., the mitigation of SLCF emissions in Europe leads to a reduction of the SLCF related cooling component in the Arctic (and also in the northern mid-latitudes), illustrating that future SLCF emission mitigation will make CO_2 emission reduction even more necessary. A recent study by Stohl et al. (2015) has investigated the possibility to select SLCF emission mitigation measures in such a way that they lead to beneficial impacts simultaneously on both air quality and climate. They found that the introduction of a stringent (but technically feasible) mitigation scenario introduced over the period 2015–2030 could cut warming in 2050 globally by 0.22 K and in the Arctic even by 0.44 K. The strongest temperature impact was caused by reducing CH_4 emissions, whereas the resulting impact of strong BC mitigation (leading to a cooling) was however strongly counteracted by the mitigation in co-emitted OC (leading to a warming). The fact, however, that measures for reducing SO_2 and NO_2 were largely postponed in that scenario, makes it an improbable option when one is concerned about air quality.

Another recent study (Sand et al. 2016) has focused on the impact of regional emissions of BC, SO_2, NO_x, VOCs, and OC on Arctic surface temperature change. They found that the largest Arctic warming source is primarily from emissions in Asia due to the large amount of emissions, but that it is most sensitive to emissions from Canada, Russia, and northern Europe. For the same scenario as in Stohl et al. (2015), but without considering changes in CH_4 from either direct emissions or the impact of NO_2 emissions, they suggest that the introduction of the stringent mitigation scenario could cut warming in the Arctic by 0.2 K in 2050.

To estimate the climate impact of the Gothenborg Protocol amendments in 2012, we have built our analysis mainly on the emission-radiative forcing relations of Bellouin et al. (2016) and on the radiative forcing-temperature change relationships of Shindell and Faluvegi (2009, 2010), and Shindell (2012). As Bellouin et al. (2016) was only based on 4 models, and Shindell and Faluvegi (2009, 2010), Shindell (2012) on only 1 model, still strong uncertainties exist.

Several studies looking at the climate impact of regional emissions have used similar methodologies (Collins et al. 2013, Sand et al. 2016, Aamaas et al. 2016). Our study differs from Collins et al. (2013) and Sand et al. (2016) in that we have used just one matrix (see Table 8.3) to express the relation between regional radiative forcing and regional temperature change, where they used 3 or 4 different matrices depending on the forcing agent (ozone, scattering aerosols, atmospheric BC, and BC deposited on snow or sea ice – for BC deposited on snow and ice they assume a three times as effective radiative forcing-temperature relation). Also, for BC Sand et al. (2016) used a direct forcing estimate combined with specific BC sensitivities in the Arctic which depend on the altitude (Flanner 2013), whereas we explicitly have used both direct and semi-direct BC forcing estimates (Hodnebrog et al. 2014) combined with the standard radiative forcing-temperature relationships.

References

Aamaas, B., Berntsen, T. K., Fuglestvedt, J. S., Shine, K. P., and Bellouin, N.: Regional emission metrics for short-lived climate forcers from multiple models, Atmos. Chem. Physics, 16, 7451–7468, doi:10.5194/acp-16-7451-2016, 2016.

Amann, M., Bertok, I., Borken-Kleefeld, J., Cofala, J., Heyes, C., Höglund-Isaksson, L., Klimont, Z., Rafaj, P., Schöpp, W., and Wagner, F.: Cost-effective emission reductions to improve air quality in Europe in 2020, Tech. Rep. 1/2011, Centre for Integrated Assessment Modelling (CIAM), International Institute for Applied Systems Analysis (IIASA), Schlossplatz 1, A-2361 Laxenburg, Austria, http://www.iiasa.ac.at/web/home/research/researchPrograms/air/MAG-CIAM1.pdf, 2011a.

Amann, M., Bertok, I., Borken-Kleefeld, J., Cofala, J., Heyes, C., Höglund-Isaksson, L., Klimont, Z., Rafaj, P., Schöpp, W., and Wagner, F.: An updated set of scenarios of cost-effective emission reductions for the revision of the Gothenburg protocol, Tech. Rep. 4/2011, Centre for Integrated Assessment Modelling (CIAM), International Institute for Applied Systems Analysis (IIASA), Schlossplatz 1, A-2361 Laxenburg, Austria, http://www.iiasa.ac.at/web/home/research/researchPrograms/air/MAG-CIAM4.pdf, 2011b.

Amann, M., Bertok, I., Borken-Kleefeld, J., Cofala, J., Heyes, C., Höglund-Isaksson, L., Klimont, Z., Rafaj, P., Schöpp, W., and Wagner, F.: Environmental improvements of the 2012 revision of the Gothenburg protocol, Tech. Rep. 1/2012, Centre for Integrated Assessment Modelling (CIAM), International Institute for Applied Systems Analysis (IIASA), Schlossplatz 1, A-2361 Laxenburg, Austria, http://www.iiasa.ac.at/web/home/research/researchPrograms/air/CIAM1-2012-v11.pdf, 2012.

Andrews, T., Gregory, J. M., Webb, M. J., and Taylor, K. E.: Forcing, feedbacks and climate sensitivity in CMIP5 coupled atmosphere-ocean climate models, Geophys. Res. Lett., 39, L09 712, doi:10.1029/2012GL051607, 2012.

Bellouin, N., Baker, L., Hodnebrog, Ø., Olivié, D., Cherian, R., Macintosh, C., Samset, B., Esteve, A., Aamaas, B., Quaas, J., and Myhre, G.: Regional and seasonal radiative forcing by perturbations to aerosol and ozone precursor emissions, Atmos. Chem. Phys. Discuss., 16, 1–76, doi:10.5194/acp-2016-310, 2016.

Boucher, O., Randall, D., Artaxo, P., Bretherton, C., Feingold, G., Forster, P., Kerminen, V.-M., Kondo, Y., Liao, H., Lohmann, U., Rasch, P., Satheesh, S. K., Sherwood, S., Stevens, B., and Zhang, X.: Climate Change 2013: The Physical Science Basis. Contribution of Working Group I to the Fifth Assessment Report of the Intergovernmental Panel on Climate Change, chap. Clouds and aerosols, Cambridge University Press, Cambridge, United Kingdom and New York, NY, USA, 2013.

Caldeira, K. and Myhrvold, N. P.: Projections of the pace of warming following an abrupt increase in atmospheric carbon dioxide concentration, Environ. Res. Lett., 8, 034 039, 2013.

Collins, W. J., Fry, M. M., Yu, H., Fuglestvedt, J. S., Shindell, D. T., and West, J. J.: Global and regional temperature-change potentials for near-term climate forcers, Atmos. Chem. Physics, 13, 2471–2485, doi:10.5194/acp-13-2471-2013, 2013.

Flanner, M. G.: Arctic climate sensitivity to local black carbon, J. Geophys. Res., 118, 1840–1851, doi:10.1002/jgrd.50176, 2013.

Hodnebrog, Ø., Myhre, G., and Samset, B. H.: How shorter black carbon lifetime alters its climate effect, Nature Communications, 5, 5065, doi:10.1038/ncomms6065, 2014.

Myhre, G., Shindell, D., Bréon, F.-M., Collins, W., Fuglestvedt, J., Huang, J., Koch, D., Lamarque, J.-F., Lee, D., Mendoza, B., Nakajima, T., Robock, A., Stephens, G., Takemura, T., and Zhang, H.: Climate Change 2013: The Physical Science Basis. Contribution of Working Group I to the Fifth Assessment Report of the Intergovernmental Panel on Climate Change, chap. Anthropogenic and natural radiative forcing, Cambridge University Press, Cambridge, United Kingdom and New York, NY, USA, 2013.

Olivié, D. J. L. and Peters, G. P.: Variation in emission metrics due to variation in CO_2 and temperature impulse response functions, Earth Syst. Dynam., 4, 267–286, doi:10.5194/esd-4-267-2013, 2013.

Olivié, D. J. L., Peters, G. P., and Saint-Martin, D.: Atmospheric response time scales estimated from AOGCM experiments, J. Climate, 25, 7956–7972, doi:10.1175/JCLI-D-11-00475.1, 2012.

Sand, M., Berntsen, T. K., Kay, J. E., Lamarque, J. F., Seland, Ø., and Kirkevåg, A.: The Arctic response to remote and local forcing of black carbon, Atmos. Chem. Physics, 13, 211–224, doi:10.5194/acp-13-211-2013, 2013.

Sand, M., Berntsen, T. K., von Salzen, K., Flanner, M. G., Langner, J., and Victor, D. G.: Response of Arctic temperature to changes in emissions of short-lived climate forcers, Nat. Clim. Change, 6, 286–290, doi:10.1038/nclimate2880, 2016.

Schmidt, G. A., Ruedy, R., Hansen, J. E., Aleinov, I., Bell, N., Bauer, M., Bauer, S., Cairns, B., Canuto, V., Cheng, Y., Genio, A. D., Faluvegi, G., Friend, A. D., Hall, T. M., Hu, Y., Kelley, M., Kiang, N. Y., Koch, D., Lacis, A. A., Lerner, J., Lo, K. K., Miller, R. L., Nazarenko, L., Oinas, V., Perlwitz, J., Perlwitz, J., Rind, D., Romanou, A., Russell, G. L., Sato, M., Shindell, D. T., Stone, P. H., Sun, S., Tausnev, N., Threshera, D., and Yao, M.-S.: Present-day atmospheric simulations using GISS modelE: Comparison to in situ, satellite, and reanalysis data, J. Climate, 19, 153–192, doi:10.1175/JCLI3612.1, 2006.

Sherwood, S. C., Bony, S., Boucher, O., Bretherton, C., Forster, P. M., Gregory, J. M., and Stevens, B.: Adjustments in the forcing-feedback framework for understanding climate change, Bulletin American Meteorological Society, 96, 217–228, doi:10.1175/BAMS-D-13-00167.1, 2015.

Shindell, D. and Faluvegi, G.: Climate response to regional radiative forcing during the twentieth century, Nature Geoscience, 2, 294–300, doi:10.1038/ngeo473, 2009.

Shindell, D. and Faluvegi, G.: The net climate impact of coal-fired power plant emissions, Atmos. Chem. Physics, 10, 3247–3260, doi:10.5194/acp-10-3247-2010, 2010.

Shindell, D. T.: Evaluation of the absolute regional temperature potential, Atmos. Chem. Physics, 12, 7955–7960, doi:10.5194/acp-12-7955-2012, 2012.

Shine, K. P., Fuglestvedt, J., Hailemariam, K., and Stuber, N.: Alternatives to the global warming potential for comparing climate impacts of emissions of greenhouse gases, Climatic Change, 68, 281–302, doi:10.1007/s10584-005-1146-9, 2005.

Skeie, R. B., Berntsen, T., Aldrin, M., Holden, M., and Myhre, G.: A lower and more constrained estimate of climate sensitivity using updated observations and detailed radiative forcing time series, Earth Syst. Dynam., 5, 139–175, doi:10.5194/esd-5-139-2014, 2014.

Stohl, A., Aamaas, B., Amann, M., Baker, L. H., Bellouin, N., Berntsen, T. K., Boucher, O., Cherian, R., Collins, W., Daskalakis, N., Dusinska, M., Eckhardt, S., Fuglestvedt, J. S., Harju, M., Heyes, C., Hodnebrog, Ø., Hao, J., Im, U., Kanakidou, M., Klimont, Z., Kupiainen, K., Law, K. S., Lund, M. T., Maas, R., MacIntosh, C. R., Myhre, G., Myriokefalitakis, S., Olivié, D., Quaas, J., Quennehen, B., Raut, J.-C., Rumbold, S. T., Samset, B. H., Schulz, M., Seland, Ø., Shine, K. P., Skeie, R. B., Wang, S., Yttri, K. E., and Zhu, T.: Evaluating the climate and air quality impacts of short-lived pollutants, Atmos. Chem. Physics, 15, 10 529–10 566, doi:10.5194/acp-15-10529-2015, 2015.

Part III

Technical EMEP Developments

CHAPTER 9

Updates to the EMEP/MSC-W model, 2015-2016

David Simpson, Ágnes Nyíri, Svetlana Tsyro, Álvaro Valdebenito and Peter Wind

This chapter summarises the changes made to the EMEP MSC-W model since Simpson et al. (2015), and along with changes discussed in Simpson et al. (2013) and Tsyro et al. (2014), updates the standard description given in Simpson et al. (2012). The model version used for reporting this year is denoted rv4.9. Table 9.2 summarises the changes made in the EMEP model since the version documented in Simpson et al. (2012)

9.1 GNFR sectors

Anthropogenic emissions have previously been categorized into 11 SNAP sectors. This year emissions defined using 13 GNFR sectors have been tested. Such emission sectors are characterised in the model by release heights, timefactors and species-splits (e.g. NOx to NO and NO_2, or NMVOC to individual VOC surrogates) for each sector, and Simpson et al. (2012) describes how these were obtained for the 11 SNAP sectors.

In order to implement GNFR sectors, and to generally allow for more flexibility, a new interface defining the mapping between sector and classes has been implemented. The new mapping approach assigns release heights, timefactors and splits for each sector. For now, we have used the factors designed for SNAP sectors as the base, and mapped any new sectors to these. The mapping for the 11 SNAP sectors (which becomes trivially 1:1) and 13 GNFR sectors is given in table 9.1

So far only a crude mapping of the GNFR to the 11 SNAP sectors is defined, but now it is possible to define new classes for release height, timefactors and splits, that can be assigned to specific sectors.

Table 9.1: Mapping of the SNAP and GNFR sectors into classes for release heights, timefactors and species-splits currently defined

Sector	Name	release height class	timefactor class	split class
SNAP 1	Combustion in energy and transformation industries	1	1	1
SNAP 2	Non-industrial combustion plants	2	2	2
SNAP 3	Combustion in manufacturing industry	3	3	3
SNAP 4	Production processes	4	4	4
SNAP 5	Extraction and distribution of fossil fuels and geothermal energy	5	5	5
SNAP 6	Solvent use and other product use	6	6	6
SNAP 7	Road transport	7	7	7
SNAP 8	Other mobile sources and machinery	8	8	8
SNAP 9	Waste treatment and disposal	9	9	9
SNAP 10	Agriculture	10	10	10
SNAP 11	Other sources and sinks	11	11	11
GNFR 1	Public Power	1	1	1
GNFR 2	Industry	3	3	3
GNFR 3	Other Stationary Combustion	2	2	2
GNFR 4	Fugitive	4	4	4
GNFR 5	Solvents	6	6	6
GNFR 6	Road Transport	7	7	7
GNFR 7	Shipping	8	8	8
GNFR 8	Aviation	8	8	8
GNFR 9	Offroad	8	8	8
GNFR 10	Waste	9	9	9
GNFR 11	Agriculture Live stock	10	10	10
GNFR 12	Agriculture Other	10	10	10
GNFR 13	Other	5	5	5

9.2 DMS

Biogenic emissions of dimethyl sulphide (DMS) have been updated using sea surface DMS concentrations from the database by Kettle et al. (1999). Monthly DMS concentration maps are available from the website http://dss.ucar.edu/datasets/ds289.2/. Using the sea surface DMS concentrations, the fluxes of DMS from the water into the air, are calculated using the parameterisations from Liss and Merlivat (1986) and Saltzman et al. (1993):

$$Sc = 2674 - 147.12\ SST + 3.726\ SST^2 - 0.038\ SST^3$$

$$K_w = 0.17\ u_{10}(\tfrac{600}{Sc})^{\frac{2}{3}} \quad \text{for } u_{10} \leq 3.6$$

$$K_w = 0.17\ u_{10}(\tfrac{600}{Sc})^{\frac{2}{3}} + 2.68\ (u_{10} - 3.6)\sqrt{\tfrac{600}{Sc}} \quad \text{for } 3.6 < u_{10} \leq 13.0$$

$$K_w = 0.17\ u_{10}(\tfrac{600}{Sc})^{\frac{2}{3}} + 2.68\ (u_{10} - 3.6)\sqrt{\tfrac{600}{Sc}} + 3.05\ (u_{10} - 13)\sqrt{\tfrac{600}{Sc}} \quad \text{for } u_{10} < 13.0$$

Where SST is the Sea Surface Temperature in °C, u_{10} is the 10 meter wind speed, Sc is the Schmidt number and K_w is the transfer velocity.

Finally the DMS in air is converted into SO_2, assumming an effective conversion rate of 66%.

9.3 Sea-salt

The source function for sea salt production is represented in the model as a product of the whitecap area fraction (the fraction of water area covered by whitecap due to wind forcing) and the shape function (describing the dependence of sea spray flux per unit whitecap area), as documented in Tsyro et al. (2011). Earlier, the whitecap area was calculated based on Monahan and O'Muircheartaigh (1980). This year, the paramaterisation has been updated based on the results from more recent measurements in North Atlantic, published in Norris et al. (2013) and Callaghan et al. (2008). Thus, two more alternative schemes to calculate whitecap coverage have been implemented. Compared to the earlier results based on Monahan and O'Muircheartaigh (1980), both of the new schemes give somewhat smaller whitecap area. In the present report, the scheme by Callaghan et al. (2008) have been used, which gives the best fit between modelled and measured sodium concentrations.

9.4 Aerosol surface area and uptake rates

As discussed in Simpson et al. (2015), aerosol surface is now estimated using the empirical relations of Gerber (1985). A mis-interpretation of the units used in the equations resulted in somewhat erroneous surface area estimates however. After correction of this, the model seems to give a little better results with the so-called 'Smix' rates for N_2O_5 hydrolysis rather than with the simpler $\gamma = 0.002$ version used in 2015 (c.f. Simpson et al. 2015). Thus, the results from version rv4.9 used in this report use Smix, but further work is clearly required to understand the importance and impacts of the model's gas-aerosol update scheme.

9.5 Dust

For this year reporting, boundary conditions (BCs) for mineral dust in 2014 are based on 3D fields of dust concentration from a 2014 global run of the EMEP/MSC-W model. Two sets of the BCs have been constructed and tested, namely 3-hourly and monthly mean.

The largest effect of using 3-hourly versus monthly dust BCs are seen for PM_{10} and $PM_{2.5}$ at the Mediterranean sites in Spain and Cyprus (Figure 9.1). In general, the model reproduces better the occurrance of dust episodes when the 3-hourly dust BCs are used, but tends to overestimate the highest peaks. The results with monthly dust BCs produce sometimes PM peaks which are not observed. All in all, PM calculated with 3-hourly dust BCs correlates better with the measured concentrations. Also NO_3^- gets affected (though rather slightly) by the choice of dust BCs due to coarse nitrate formed on the dust particles. As seen in Figure 9.1, using the 3-hourly BCs results in a small improvement of the correlation between modelled and observed NO_3^- in PM_{10} at the same sites.

Given that the effect of using 3-hourly BCs for mineral dust is relatively small and mostly limited to PM and NO_3^- in very southern regions, while it does not appear important for other

components, and that using 3-hourly BCs leads to some increase of the computation time, the monthly dust BCs have been used in status and source-receptor runs.

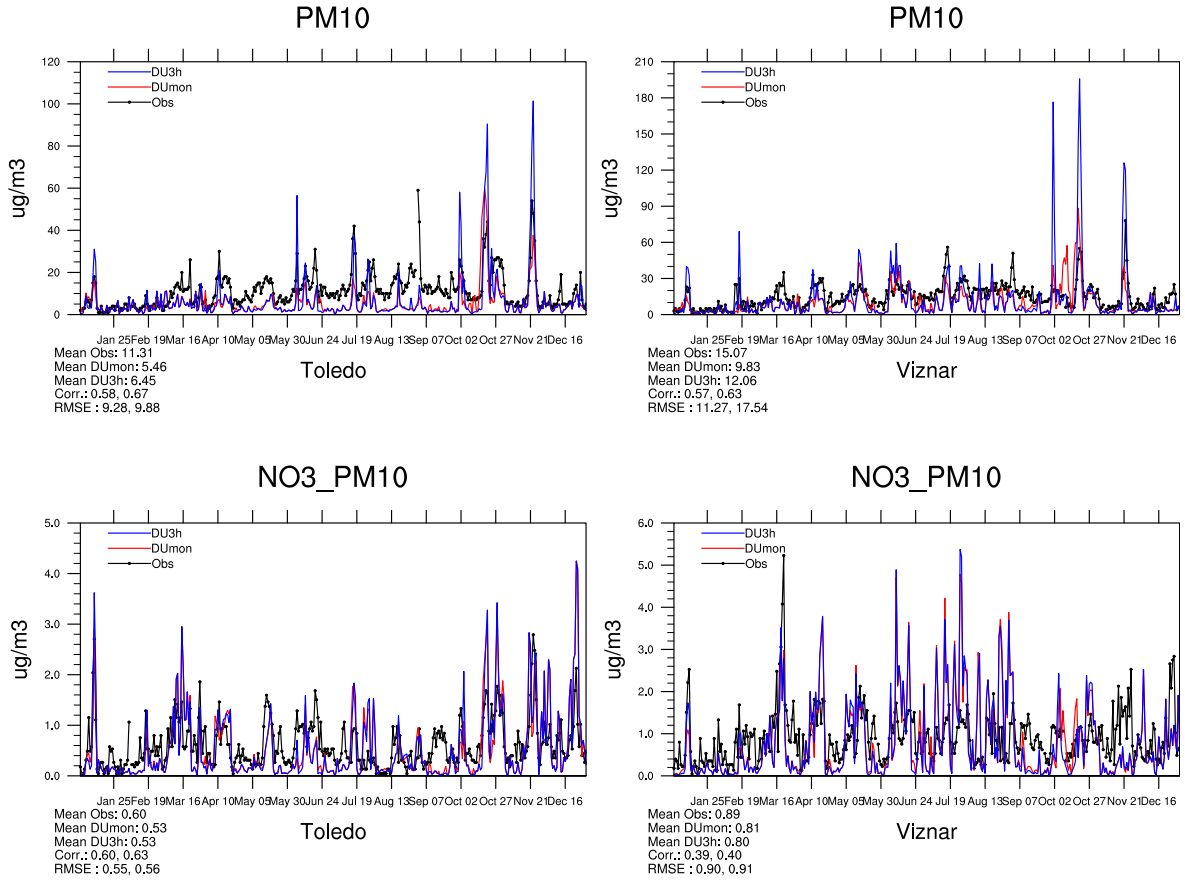

Figure 9.1: Timeseries of PM_{10} and NO_3^- in PM_{10} calculated using 3-hourly (blue) and monthly (red) boundary conditions for mineral dust, and observed (black) at two Spanish sites.

9.6 EC/OC/Rem splits

The gridded emissions of particulate matter (PM) provided to the model for standard runs are for fine and coarse PM, rather than for the constituent compounds of that PM. For modelling purposes we split these PM emissions into elemental carbon (EC), organic matter (OM) and the remainder (Rem). These divisions, done separately for both fine and coarse matter, are based upon data provided by EMEP-CIAM (C. Heyes, International Institute for Applied Systems Analysis, pers. comm., 2016).

The OM emissions are further divided into fossil-fuel and wood-burning compounds, based upon the country-specific SNAP sector OM/OC ratio and the assumption that the OM/OC ratios for fossil-fuel and wood-burning emissions are 1.3 and 1.8, respectively.

Table 9.2: Summary of major EMEP MSC-W model versions from 2012–2016. Extends Table S1 of Simpson et al. 2012

Version	Update	Ref[(a)]
rv4.9	Updates for GNFR sectors, DMS, sea-salt, dust, S_A and γ, N_2O_5, see Sect.9.1–9.6	This report
rv4.8	Public domain (Oct. 2015) ShipNOx introduced	R2015
rv4.7	Used for reporting, summer 2015 New calculations of aerosol surface area New gas-aerosol uptake and N2O5 hydrolysis rates (Used $\gamma = 0.002$, N_2O_5 hydrolysis, for reporting.) Added 3-D calculations of aerosol extinction and AODs Emissions - new flexible mechanisms for interpolation and merging sources Revised boundary condition treatments Global - monthly emissions from ECLIPSE project Global - LAI changes from LPJ-GUESS model WRF meteorology (Skamarock and Klemp 2008) can now be used directly in EMEP model.	R2015
rv4.5	Sixth open-source (Sep 2014) Improved dust, sea-salt, SOA modelling AOD and extinction coefficient calculations updated Data assimilition system added Hybrid vertical coordinates replace earlier sigma Flexibility of grid projection increased.	R2014
rv4.4	Fifth open-source (Sep 2013) (small changes from 4.4 tp 4.5) Improved dust and sea-salt modelling AOD and extinction coefficient calculations added. gfortran compatibility improved	R2014, R2013
rv4.3	Fourth public domain (Mar. 2013) Initial use of namelists Smooothing of MARS results Emergency module for volcanic ash and other events Dust and road-dust options added as defaults Advection algorithm changed	R2013
rv4.0	Third public domain (Sep. 2012) As documented in Simpson et al. (2012)	R2013
v2011-06	Second public domain (Aug. 2011)	
rv3	First public domain (Sep. 2008)	

Notes: (a) R2015 refers to EMEP Status report 1/2015, etc.

References

Callaghan, A., de Leeuw, G., Cohen, L., and O'Dowd, C. D.: Relationship of oceanic whitecap coverage to wind speed and wind history, Geophys. Res. Lett., 35, L23 609, doi:0.1029/2008GL036165, 2008.

Gerber, H. E.: Relative-Humidity Parameterization of the Navy Aerosol Model (NAM), NRL Report 8956, Naval Research Laboratory, Washington, DC, 1985.

Kettle, A. J., Andreae, M. O., et al., et al., and et al.: A global data base of sea surface dimethylsulfide (DMS)measurements and a procedure to predict sea surface DMS as a function of latitude, longitude, and month, Global Biogeochem. Cycles, 13, 399–444, 1999.

Liss, P. S. and Merlivat, L.: Air-sea gas exchange rates:Introduction and synthes, in: The Role of Air-Sea Exchange in Geochemical Cycling, pp. 113–127, D. Reidel, Norwell, Mass., 1986.

Monahan, E. C. and O'Muircheartaigh, I.: Optimal power-law description of oceanic whitecap coverage dependence on wind speed, J. Phys. Oceanogr., 10, 2094–2099, URL http://dx.doi.org/10.1029/JC087iC11p08898, 1980.

Norris, S. J., Brooks, I. M.and Moat, B. I., Yelland, M. J., de Leeuw, G., Pascal, R. W., and Brooks, B.: Near-surface measurements of sea spray aerosol production over whitecaps in the open ocean, Ocean Sci., 9, 133–145, doi:10.5194/os-9-133-2013, URL www.ocean-sci.net/9/133/2013/, 2013.

Saltzman, E. S., King, D. B., Holmen, K., and Leck, C.: Experimental determination of the diffusion coefficient of dimethylsulfide in water, J. Geophys. Res., 98, 16,481–16,486, 1993.

Simpson, D., Benedictow, A., Berge, H., Bergström, R., Emberson, L. D., Fagerli, H., Hayman, G. D., Gauss, M., Jonson, J. E., Jenkin, M. E., Nyíri, A., Richter, C., Semeena, V. S., Tsyro, S., Tuovinen, J.-P., Valdebenito, A., and Wind, P.: The EMEP MSC-W chemical transport model – technical description, Atmos. Chem. Physics, 12, 7825–7865, doi:10.5194/acp-12-7825-2012, 2012.

Simpson, D., Tsyro, S., Wind, P., and Steensen, B. M.: EMEP model development, in: Transboundary acidification, eutrophication and ground level ozone in Europe in 2011. EMEP Status Report 1/2013, The Norwegian Meteorological Institute, Oslo, Norway, 2013.

Simpson, D., Tsyro, S., and Wind, P.: Updates to the EMEP/MSC-W model, in: Transboundary particulate matter, photo-oxidants, acidifying and eutrophying components. EMEP Status Report 1/2015, pp. 129–138, The Norwegian Meteorological Institute, Oslo, Norway, 2015.

Skamarock, W. C. and Klemp, J. B.: A time-split nonhydrostatic atmospheric model for weather research and forecasting applications, J. Comp. Phys., 227, 3465–3485, doi:10.1016/j.jcp.2007.01.037, 2008.

Tsyro, S., Aas, W., Soares, J., Sofiev, M., Berge, H., and Spindler, G.: Modelling of sea salt concentrations over Europe: key uncertainties and comparison with observations, Atmos. Chem. Physics, 11, 10 367–10 388, doi:10.5194/acp-11-10367-2011, URL http://www.atmos-chem-phys.net/11/10367/2011/, 2011.

Tsyro, S., Karl, M., Simpson, D., Valdebenito, A., and Wind, P.: Updates to the EMEP/MSC-W model, in: Transboundary particulate matter, photo-oxidants, acidifying and eutrophying components. EMEP Status Report 1/2014, pp. 143–146, The Norwegian Meteorological Institute, Oslo, Norway, 2014.

CHAPTER 10

Development in the monitoring network

Wenche Aas, Anne Hjellbrekke, Richard Olav Rud, Sverre Solberg, Kjetil Tørseth and Karl Espen Yttri

10.1 Compliance with the EMEP monitoring strategy

The monitoring obligations in EMEP is described in the Monitoring Strategy for 2010-2019 (UNECE (2009); Tørseth et al. (2012)). The complexity in the monitoring program, with respect to the number of variables and sites, whether it is a level 1 or level 2 parameter, and the required time resolution (hourly, daily, weekly), makes it challenging to assess whether a country is in compliance or not. CCC has developed an index to illustrate to what extent the Parties comply.

For the level 1 parameters, an index is defined, calculated based on what has been reported compared to what is expected. It is recommended to have one EMEP site pr 50.000 km^2, but this target number is adjusted for very large countries (i.e. KZ, RU, TR and UA). The components and number of variables to be measured in accordance to the strategy is as follows: major inorganic ions in precipitation (10 variables), major inorganic components in air (13 variables), ozone (1 variable), PM mass (2 variables) and heavy metals in precipitation (7 variables). For heavy metals, the sampling frequency is weekly, and for the other components it is daily or hourly (ozone). Based on the relative implementation of the different variables, the index has been given the following relative weights: Inorganics in precipitation: 30%, inorganics in air: 30%, ozone: 20%, PM mass: 10%, heavy metals: 10%.

Figure 10.1 summarises the compliance in 2014 compared to 2000, 2005 and 2010. The countries are sorted from left to right with increasing index for 2014. Slovenia and Slovakia have almost full score as they measure all the required parameters with satisfactory sampling frequency. Some countries have improved their network during this period, i.e. the Czech Republic, Sweden, Slovenia; and some new Parties have begun monitoring, such as

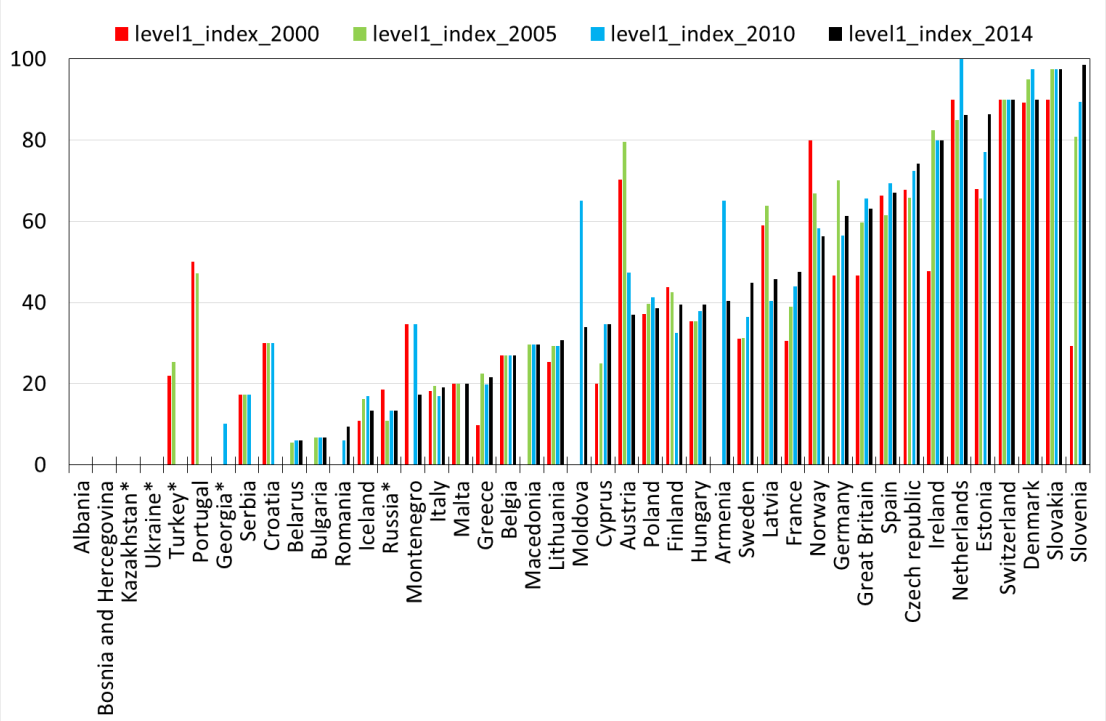

Figure 10.1: Index for implementation of the EMEP monitoring strategy, level 1 based on what has been reported for 2000, 2005, 2010 and 2014. * means adjusted land area

Moldova, Bulgaria, Romania and Armenia. There are also countries which have less monitoring now than previously, e.g. Austria, Norway and Russia, and some have stopped reporting/measuring, e.g. Portugal, Croatia, Serbia and Turkey. In Figure 2.3 in Chapter 2.2, the geographical distribution of level 1 sites is mapped for 2014. In large parts of Europe implementation of the EMEP monitoring strategy is far from beeing satisfactory.

For the Level 2 parameters, an index based system has not been defined, but mapping the site distribution illustrate the compliance to the monitoring strategy. 53 sites reported at least one of the required EMEP level 2 parameters. In Figure 10.2, the sites with measurements of the three level 2 topics relevant to this report: aerosols, photo-oxidants and trace gases are plotted. POPs and heavy metals are covered in the EMEP status reports 2 and 3. Figure 10.2 shows that level 2 measurements of aerosols have better spatial coverage than oxidant precursors (VOC + methane) and trace gases. Few sites have a complete measurement program, and only 6 sites have a complete aerosol program. Nevertheless, regarding the aerosol monitoring, there have been large improvements in the spatial coverage and the data quality over the last decade. Standardization and reference methodologies have been developed, and the reporting has improved significantly with much more metadata information available. For oxidant precursors and trace gases, there are ongoing improvement in the measurement capabilities resulting from recent development in research projects such as ICOS (Integrated Carbon Observation System), InGOS (Integrated non-CO_2 Greenhouse gas Observation System) and ACTRIS (Aerosols, Clouds, and Trace gases Research InfraStructure Network) in cooperation with the WMO Global Atmospheric Watch Programme (GAW).

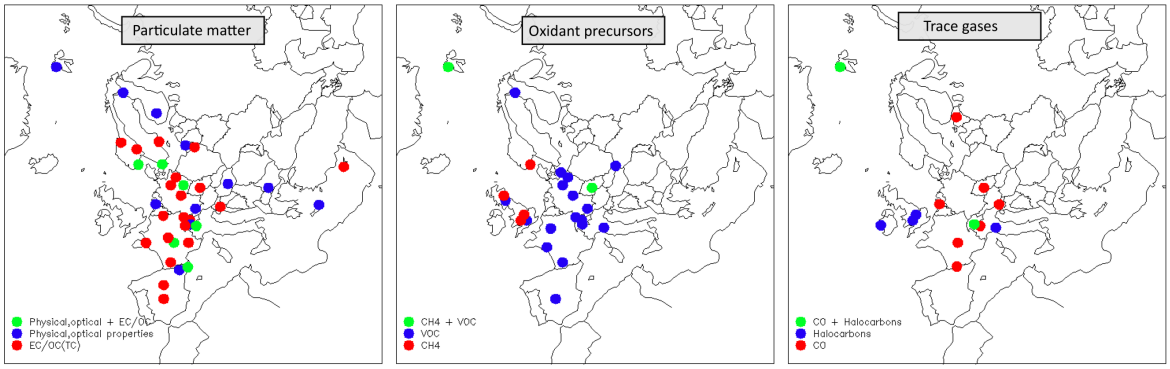

Figure 10.2: Sites measuring and reporting EMEP level 2 parameters for the year 2014

10.2 Reporting of data and new submission tool

In addition to the requirements of variables to be measured as defined in the EMEP monitoring strategy discussed above, it is important that the data are reported in time to ensure that they can be quality assured and included in the database. This allows them to be included in the annual model validation, interpretations for the EMEP status reports as well as other regional assessments and studies carried out beyond EMEP.

Figure 10.3 shows the status of the submission of data for 2014 and to what extent the data were reported in time. From Figure 10.3, it is obvious that large volumes of data are reported late and some not at all. The reporting deadline has been set to allow time for interaction between the data submitter and EMEP/CCC. By experience, such interaction is often needed to ensure correct format and proper data quality. The deadline is set so that the quality checked data can be used for model verification and status reporting. Late reporting of monitoring data causes problems at all stages of this processing.

In 2014, the new EBAS database (http://ebas.nilu.no) was launched with increased possibilities and demands for metadata reporting, including more harmonized and detailed information on methodology and quality. With the increased complexity in the number of parameters and metadata information required, data submission has become more extensive for the Parties as well as for CCC. It has therefore been a strong need to improve the data reporting system with tools doing automatic checks of file consistency and feedback to data originators.

In spring 2016, a new online data submission and validation tool was launched (http://ebas-submit-tool.nilu.no) to give data submitters a possibility to check and correct their files before submitting them. The tool gives information on how to best troubleshoot errors in the file, including information on how to format the data files, as well as offering the user a way to plot data. The tool is designed to give the data submitters direct feedback with respect to the file format and aid on how to submit the files. The portal also provides a page with common errors/warnings, suggesting possible solutions for file specific errors. In addition, an issue tracker is hosted on GitHub (https://github.com/ebas-submission-tool/troubleshooting/issues). The idea is to gather feedback regarding the tool itself as well as helping the user to debug file specific errors/warnings.

Along with the submission tool, new templates for the NASA Ames files to be used for reporting of surface ozone, NOx, VOC and aerosols have been developed. These includes detailed information on all kinds of metadata. The metadata contain both freetext variables for descriptive elements as well as fixed options for various types of metadata elements, such

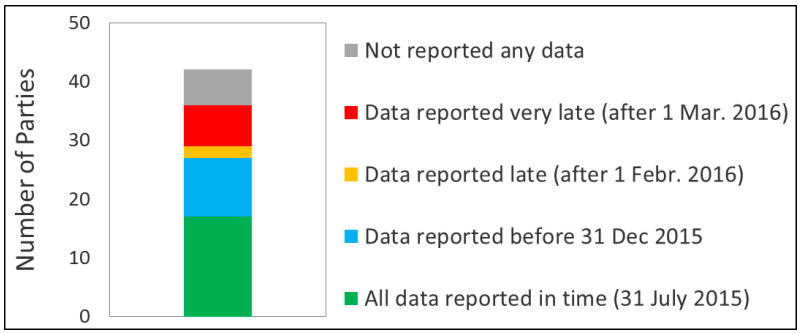

Figure 10.3: Submission of 2014 data to EMEP/CCC.

as instrument type, unit etc. Files not following the specifications defined in these templates will not be accepted by the submission tool.

The EBAS submission tool had it's first official release in May 2016. From 6th of May until 1th of August the traffic shows 1155 sessions by 399 different users from 39 different countries with an average session duration of 13 minutes. This is indicating relatively high activity across countries.

To further improve the reporting, EMEP/CCC will arrange a Technical workshop on data format, quality assurance and data submission 26-28 October 2016 for all data providers interested.

At 1st January 2016, the responsibility related to archiving of reactive gases measurement data was transferred from WMO/GAW WDCGG (World Data Centre for Greenhouse Gases) to the newly established WMO/GAW World Data Centre for Reactive Gases (WDCRG) hosted by NILU. WDCRG will be utilizing the EBAS data infrastructure at NILU, and the procedures and formats etc will follow the same approach as for GAW-WDCA, EMEP and ACTRIS.

The gases to be hosted by WDCRG are SO_2, oxidized nitrogen species, tropospheric ozone and VOCs (but not CO). Thus, from 2016, EMEP data of these species will be reported only once to EBAS, with no need for a second submission to WDCGG as was the case before. In EBAS, the data will be affiliated with both the GAW and EMEP programmes. The new metadata requirements differ significantly from the previous requirements of the WDCGG, and thus the data providers are asked to resubmit their full historic time series to WDCRG at NILU to provide the most updated and fully documented dataset possible.

Despite large improvements in the database infrastructure, continued development of the observational database is still necessary, including e.g. statistical tools, plotting and provision of tools for data interpretation, such as e.g. trajectories. The ACTRIS project continues to support the QA/QC work within EMEP as described in previous annual reports, and provides a very valuable contribution to the EMEP monitoring programme.

References

Tørseth, K., Aas, W., Breivik, K., Fjæraa, A. M., Fiebig, M., Hjellbrekke, A. G., Lund Myhre, C., Solberg, S., and Yttri, K. E.: Introduction to the European Monitoring and Evaluation Programme (EMEP) and observed atmospheric composition change during 1972–2009, Atmos. Chem. Physics, 12, 5447–5481, doi:10.5194/acp-12-5447-2012, URL http://www.atmos-chem-phys.net/12/5447/2012/, 2012.

UNECE: Progress in activities in 2009 and future work. Measurements and modelling (acidification, eutrophication, photooxidants, heavy metals, particulate matter and persistent organic pollutants). Draft revised monitoring strategy., Tech. Rep. ECE/EB.AIR/GE.1/2009/15, UNECE, URL http://www.unece.org/env/documents/2009/EB/ge1/ece.eb.air.ge.1.2009.15.e.pdf, 2009.

Part IV

Appendices

APPENDIX A

National emissions for 2014 in the extended EMEP domain

This appendix contains the national emission data for 2014 used throughout this report for main pollutants and primary particle emissions in the extended EMEP domain. These are the emissions that are used as basis for the 2014 source-receptor calculations. Results of these source-receptor calculations are presented in Appendix C.

The land-based emissions for 2014 have been derived from the 2016 official data submissions to UNECE CLRTAP (Mareckova et al. 2016). Emissions from international shipping are based on emissions data developed within the EU Horizon2020 project MACC-III (MACC-III 2015) by TNO.

Note that emissions in this appendix are given in different units than used elsewhere in this report in order to keep consistency with the reported data.

References

MACC-III: Report on the update of global and European anthropogenic emissions., Tech. Rep. COPERNICUS Grant agreement 633080, MACC-III (Monitoring Atmospheric Composition and Climate, 2015.

Mareckova, K., Pinterits, M., Tista, M., and Wankmüller, R.: Inventory review 2016. Review of emission data reported under the LRTAP Convention and NEC Directive. Stage 1 and 2 review. Status of gridded and LPS data, EMEP/CEIP 1/2016, EEA/CEIP Vienna, 2016.

Table A:1: National total emissions for 2014 in the extended EMEP domain. Unit: Gg. (Emissions of SO_x and NO_x are given as Gg(SO_2) and Gg(NO_2), respectively.)

Area/Pollutant	SO_x	NO_x	NH_3	NMVOC	CO	$PM_{2.5}$	PM_{co}	PM_{10}
Albania	13	19	21	30	65	9	2	11
Armenia	2	24	15	40	101	4	2	6
Austria	16	151	67	110	537	17	15	31
Azerbaijan	31	101	57	428	539	20	5	24
Belarus	91	161	155	180	405	51	18	70
Belgium	42	197	66	122	353	28	10	38
Bosnia and Herzegovina	214	31	20	35	66	14	12	26
Bulgaria	189	133	31	99	291	34	12	46
Croatia	16	55	26	60	203	19	7	26
Cyprus	17	17	5	7	14	1	1	2
Czech Republic	127	170	69	138	462	23	12	35
Denmark	11	113	73	106	312	18	13	31
Estonia	41	33	13	23	127	8	5	12
Finland	44	137	37	75	339	24	10	34
France	169	886	708	639	3090	169	107	276
Georgia	8	36	51	65	227	20	3	24
Germany	388	1224	740	1041	2964	104	117	221
Greece	144	242	51	174	525	38	15	53
Hungary	27	120	84	116	289	26	19	45
Iceland	71	21	5	5	16	0	0	1
Ireland	19	77	105	87	115	15	10	24
Italy	131	790	393	849	2340	152	25	177
Kazakhstan (KZT)	2275	688	270	836	2346	156	134	290
Kyrgyzstan	48	55	34	62	285	11	4	16
Latvia	4	35	17	54	136	18	6	24
Lithuania	18	51	41	69	144	17	2	19
Luxembourg	2	28	6	11	31	2	1	3
Malta	5	6	2	3	5	1	1	1
Montenegro	40	13	3	9	33	5	7	12
Netherlands	29	235	134	143	571	13	14	26
Norway	17	140	26	138	241	27	8	35
Poland	800	723	265	606	2704	135	98	232
Portugal	35	160	49	169	263	44	10	55
Republic of Moldova	4	18	15	27	74	10	4	14
Romania	176	218	162	319	774	116	38	154
Russian Federation (RUE)	3698	3105	934	2803	13178	1242	993	2235
Serbia	327	113	86	118	236	34	14	48
Serbia and Montenegro	0	0	0	0	0	0	0	0
Slovakia	45	85	37	106	225	30	7	37
Slovenia	9	39	19	32	108	12	2	14
Spain	243	745	371	599	1995	67	53	120
Sweden	24	135	54	184	497	21	14	34
Switzerland	8	69	63	80	196	8	11	18
Tajikistan	57	90	54	42	1046	34	34	67
TFYR of Macedonia	101	33	8	18	45	11	8	19
Turkey	2147	1055	1085	967	2469	539	263	802
Turkmenistan	329	134	91	70	758	92	112	204
Ukraine	1161	667	271	421	2770	360	182	541
United Kingdom	308	949	281	819	2072	105	43	148
Uzbekistan	1361	399	143	140	2147	272	414	685
North Africa	529	123	301	123	430	77	113	190
Asian areas (AST)	1689	505	1050	791	4773	216	259	475
Baltic Sea	69	271	0	7	28	11	1	12
Black Sea	53	79	0	2	8	6	0	6
Mediterranean Sea	976	1497	0	45	151	109	6	114
North Sea	163	644	0	17	67	27	1	28
Remaining N-E Atlantic Ocean	452	695	0	21	71	50	3	53
Natural marine emissions	2218	0	0	0	0	0	0	0
Volcanic emissions	11823	0	0	0	0	0	0	0
TOTAL	33052	18541	8664	14281	54262	4671	3277	7948

APPENDIX B

National emission trends

This appendix contains trends of national emission data for main pollutants and primary particle emissions in the extended EMEP domain for the years 2000–2014.

The land-based emissions for 2014 have been derived from the 2016 official data submissions to UNECE CLRTAP (Mareckova et al. 2016), while for the period of 2000–2013 the land-based emissions are the same as in EMEP Status Report 1/2015 (2015) and have been derived from the data submissions to UNECE CLRTAP as of May 2015. Re-submissions of emission data in 2016 are not included since the gridded emissions for 2000–2013 have not been updated by CEIP this year. Emissions from international shipping are based on emissions data developed within the EU Horizon2020 project MACC-III (MACC-III 2015) by TNO.

Natural marine emissions of dimethyl sulphid (DMS) have been updated in the model. Rather than being prescribed, DMS emissions are now calculated dynamically during the model calculation and vary with current meteorological conditions. The new method yields DMS emissions about three times higher than in previous years.

SO_x emissions from passive degassing of Italian volcanoes (Etna, Stromboli and Vulcano) are those reported by Italy.

Note that emissions in this appendix are given in different units than used elsewhere in this report in order to keep consistency with the reported data.

References

EMEP Status Report 1/2015: Transboundary particulate matter, photo-oxidants, acidifying and eutrophying components, EMEP MSC-W & CCC & CEIP, Norwegian Meteorological Institute (EMEP/MSC-W), Oslo, Norway, 2015.

MACC-III: Report on the update of global and European anthropogenic emissions., Tech. Rep. COPERNICUS Grant agreement 633080, MACC-III (Monitoring Atmospheric Composition and Climate, 2015.

Mareckova, K., Pinterits, M., Tista, M., and Wankmüller, R.: Inventory review 2016. Review of emission data reported under the LRTAP Convention and NEC Directive. Stage 1 and 2 review. Status of gridded and LPS data, EMEP/CEIP 1/2016, EEA/CEIP Vienna, 2016.

Table B:1: National total emission trends of sulphur (2000-2006), as used for modelling at the MSC-W (Gg of SO_2 per year).

Area/Year	2000	2001	2002	2003	2004	2005	2006
Albania	10	12	14	15	17	19	18
Armenia	1	1	1	1	1	2	2
Austria	32	33	32	32	27	27	28
Azerbaijan	214	194	173	153	132	112	95
Belarus	170	153	136	119	102	85	84
Belgium	174	167	158	154	158	143	134
Bosnia and Herzegovina	192	199	205	212	218	225	225
Bulgaria	861	827	756	824	789	776	763
Croatia	59	58	63	63	51	58	54
Cyprus	50	47	47	49	42	38	32
Czech Republic	301	283	265	247	229	211	204
Denmark	32	30	28	35	29	26	30
Estonia	97	91	87	100	88	76	70
Finland	79	86	80	100	84	69	84
France	628	557	518	507	482	461	435
Georgia	12	10	9	8	6	5	5
Germany	645	625	562	534	496	472	478
Greece	591	578	566	554	541	529	477
Hungary	428	347	273	246	149	41	39
Iceland	35	39	41	38	33	38	44
Ireland	142	137	104	81	74	74	63
Italy	754	701	621	524	486	407	384
Kazakhstan (KZT)	1499	1565	1630	1696	1762	1827	1955
Kyrgyzstan	25	25	25	25	25	25	27
Latvia	15	12	10	8	6	6	6
Lithuania	37	41	35	27	28	31	30
Luxembourg	3	4	3	3	2	2	3
Malta	23	21	18	16	14	11	10
Montenegro	14	11	15	15	14	13	14
Netherlands	73	75	68	64	67	65	64
Norway	27	25	23	23	25	24	21
Poland	1451	1436	1331	1287	1249	1217	1292
Portugal	250	236	235	176	176	177	152
Republic of Moldova	8	8	8	8	8	7	7
Romania	818	783	747	712	677	642	586
Russian Federation (RUE)	3044	3124	3202	3340	3461	3577	3635
Serbia	474	469	494	519	521	436	454
Serbia and Montenegro	0	0	0	0	0	0	0
Slovakia	127	131	103	105	96	89	88
Slovenia	93	63	63	62	51	41	17
Spain	1464	1415	1541	1273	1305	1255	1134
Sweden	42	41	41	41	37	36	36
Switzerland	15	18	16	15	15	16	15
Tajikistan	20	22	24	27	29	31	34
TFYR of Macedonia	106	106	105	105	105	104	107
Turkey	2335	2075	1965	1888	1881	2106	2270
Turkmenistan	101	106	106	109	115	130	144
Ukraine	1390	1327	1263	1200	1137	1073	1083
United Kingdom	1217	1132	1011	989	833	710	670
Uzbekistan	507	528	549	573	617	660	708
North Africa	303	314	322	332	346	361	386
Asian areas (AST)	1004	1033	1089	1155	1227	1302	1381
Baltic Sea	170	169	168	167	166	166	152
Black Sea	50	51	52	53	55	56	59
Mediterranean Sea	931	955	980	1004	1028	1053	1109
North Sea	406	404	402	400	397	395	412
Remaining N-E Atlantic Ocean	433	444	456	467	478	490	516
Natural marine emissions	2338	2283	2343	2197	2250	2271	2351
Volcanic emissions	5746	4278	5300	3556	2701	1204	1308
TOTAL	32064	29900	30482	28232	27138	25502	25982

Table B:2: National total emission trends of sulphur (2007-2014), as used for modelling at the MSC-W (Gg of SO_2 per year).

Area/Year	2007	2008	2009	2010	2011	2012	2013	2014
Albania	18	17	16	16	15	14	13	13
Armenia	2	2	2	2	2	2	2	2
Austria	25	22	17	19	18	17	17	16
Azerbaijan	79	63	47	31	18	5	5	31
Belarus	83	82	82	81	83	86	89	91
Belgium	125	97	76	61	53	47	46	42
Bosnia and Herzegovina	224	224	224	224	221	219	217	214
Bulgaria	819	569	440	387	515	329	194	189
Croatia	59	53	56	35	29	25	16	16
Cyprus	29	22	18	22	21	16	14	17
Czech Republic	196	189	182	174	162	150	138	127
Denmark	28	21	15	15	15	13	14	11
Estonia	88	69	55	83	73	41	36	41
Finland	83	70	59	67	61	51	47	44
France	422	357	305	285	249	235	219	169
Georgia	6	6	6	6	7	7	7	8
Germany	461	462	412	434	431	417	416	388
Greece	424	371	319	266	236	205	174	144
Hungary	35	35	30	31	34	31	29	27
Iceland	58	74	69	73	80	84	86	71
Ireland	57	47	34	28	27	25	25	19
Italy	341	286	233	215	194	175	145	131
Kazakhstan (KZT)	2083	2210	2338	2466	2593	2721	2849	2275
Kyrgyzstan	30	33	35	38	40	42	44	48
Latvia	5	4	4	3	2	2	2	4
Lithuania	26	22	21	21	23	20	19	18
Luxembourg	2	2	2	2	1	1	2	2
Malta	9	7	6	5	5	5	5	5
Montenegro	12	15	8	28	40	40	40	40
Netherlands	61	51	38	34	34	34	30	29
Norway	20	20	15	20	19	17	17	17
Poland	1229	1007	868	937	885	859	847	800
Portugal	145	96	61	53	48	43	42	35
Republic of Moldova	6	6	5	4	4	4	4	4
Romania	531	475	420	364	329	294	259	176
Russian Federation (RUE)	3711	3736	3497	3504	3588	3658	3685	3698
Serbia	463	479	435	422	470	433	429	327
Serbia and Montenegro	0	0	0	0	0	0	0	0
Slovakia	71	69	64	69	68	58	53	45
Slovenia	15	13	11	10	12	11	11	9
Spain	1096	477	427	401	436	385	272	243
Sweden	32	30	30	32	29	28	27	24
Switzerland	13	13	12	12	10	10	10	8
Tajikistan	36	39	41	43	47	50	54	57
TFYR of Macedonia	109	112	114	117	113	109	105	101
Turkey	2648	2561	2665	2561	2641	2716	1939	2147
Turkmenistan	160	183	195	213	244	271	298	329
Ukraine	1093	1103	1113	1123	1132	1142	1151	1161
United Kingdom	589	492	399	428	391	440	393	308
Uzbekistan	775	845	913	991	1073	1161	1254	1361
North Africa	413	443	463	487	496	507	517	529
Asian areas (AST)	1470	1488	1535	1595	1642	1695	1680	1689
Baltic Sea	106	105	100	95	69	69	69	69
Black Sea	55	51	50	50	53	53	53	53
Mediterranean Sea	1027	951	938	920	976	976	976	976
North Sea	367	254	247	223	163	163	163	163
Remaining N-E Atlantic Ocean	478	443	437	426	452	452	452	452
Natural marine emissions	2313	2367	2327	2259	2388	2332	2409	2218
Volcanic emissions	840	973	950	1070	1943	943	943	11823
TOTAL	25702	24316	23480	23579	25002	23939	23054	33052

Table B:3: National total emission trends of nitrogen oxides (2000-2006), as used for modelling at the MSC-W (Gg of NO_2 per year).

Area/Year	2000	2001	2002	2003	2004	2005	2006
Albania	15	16	17	18	19	19	19
Armenia	12	13	13	14	14	14	15
Austria	210	220	226	235	233	235	221
Azerbaijan	82	86	89	93	96	100	100
Belarus	194	190	187	184	180	177	174
Belgium	347	307	296	294	300	320	277
Bosnia and Herzegovina	35	35	34	34	34	33	33
Bulgaria	145	147	168	170	170	179	176
Croatia	84	83	86	85	83	82	81
Cyprus	22	22	22	22	22	21	21
Czech Republic	283	280	277	274	271	268	256
Denmark	224	221	217	226	210	202	201
Estonia	37	40	41	42	39	36	35
Finland	201	211	201	215	195	169	188
France	1610	1568	1538	1503	1472	1430	1359
Georgia	23	23	24	24	25	25	26
Germany	1925	1848	1770	1715	1648	1573	1557
Greece	450	441	431	421	411	402	379
Hungary	206	209	216	207	204	169	172
Iceland	28	26	28	27	28	26	26
Ireland	137	138	131	131	134	136	132
Italy	1456	1423	1371	1348	1305	1244	1179
Kazakhstan (KZT)	369	390	411	432	453	474	503
Kyrgyzstan	21	22	23	24	25	26	30
Latvia	44	47	45	47	46	44	44
Lithuania	51	52	52	52	53	54	57
Luxembourg	42	43	44	47	56	59	54
Malta	9	9	9	9	9	10	9
Montenegro	9	7	7	7	8	8	8
Netherlands	395	388	375	369	354	341	327
Norway	202	200	195	195	196	196	194
Poland	844	839	806	828	855	851	856
Portugal	262	261	267	245	249	255	234
Republic of Moldova	23	24	25	26	27	28	26
Romania	291	294	298	302	305	309	293
Russian Federation (RUE)	3315	3379	3441	3543	3625	3704	3645
Serbia	144	151	161	167	182	169	171
Serbia and Montenegro	0	0	0	0	0	0	0
Slovakia	107	108	100	98	99	102	96
Slovenia	52	53	54	52	51	50	50
Spain	1300	1267	1309	1300	1336	1322	1270
Sweden	207	197	190	186	180	176	172
Switzerland	108	104	98	96	94	93	90
Tajikistan	31	34	38	42	46	49	53
TFYR of Macedonia	32	33	34	34	35	35	36
Turkey	840	812	795	818	829	879	921
Turkmenistan	41	43	43	45	47	53	59
Ukraine	888	886	883	880	878	875	838
United Kingdom	1798	1758	1679	1661	1607	1586	1542
Uzbekistan	149	155	161	168	181	193	207
North Africa	71	73	75	77	80	84	90
Asian areas (AST)	296	304	318	337	359	383	406
Baltic Sea	285	292	298	305	312	318	309
Black Sea	83	85	87	89	91	93	98
Mediterranean Sea	1578	1615	1653	1690	1728	1765	1860
North Sea	677	693	709	724	740	755	795
Remaining N-E Atlantic Ocean	733	750	768	785	803	820	864
Natural marine emissions	0	0	0	0	0	0	0
Volcanic emissions	0	0	0	0	0	0	0
TOTAL	23026	22916	22833	22960	23028	23020	22836

Table B:4: National total emission trends of nitrogen oxides (2007-2014), as used for modelling at the MSC-W (Gg of NO_2 per year).

Area/Year	2007	2008	2009	2010	2011	2012	2013	2014
Albania	19	19	18	18	18	18	18	19
Armenia	16	17	18	19	20	21	22	24
Austria	212	195	179	180	170	165	162	151
Azerbaijan	100	100	101	101	101	101	101	101
Belarus	172	169	166	164	163	162	161	161
Belgium	267	236	210	252	235	216	208	197
Bosnia and Herzegovina	33	33	33	32	32	32	32	31
Bulgaria	166	161	139	139	154	140	123	133
Croatia	83	80	73	64	60	56	56	55
Cyprus	22	20	20	19	21	21	16	17
Czech Republic	244	232	220	208	199	190	181	170
Denmark	187	170	150	145	138	128	124	113
Estonia	38	36	30	36	36	32	30	33
Finland	187	168	155	167	154	147	145	137
France	1297	1198	1116	1096	1036	1008	990	886
Georgia	27	29	30	31	32	33	34	36
Germany	1484	1411	1310	1334	1311	1270	1269	1224
Greece	357	335	312	290	278	266	254	242
Hungary	167	164	157	154	140	124	121	120
Iceland	27	25	25	23	21	21	20	21
Ireland	129	116	93	85	76	78	79	77
Italy	1129	1056	982	969	950	863	821	790
Kazakhstan (KZT)	532	561	591	620	649	679	708	688
Kyrgyzstan	33	36	39	43	45	48	51	55
Latvia	45	40	38	38	33	34	34	35
Lithuania	54	55	48	50	46	48	46	51
Luxembourg	49	45	39	39	39	35	31	28
Malta	9	9	9	9	9	8	8	6
Montenegro	8	9	7	10	13	13	14	13
Netherlands	310	299	275	274	258	248	240	235
Norway	196	185	175	177	170	163	154	140
Poland	861	829	809	861	843	819	798	723
Portugal	229	203	191	177	169	162	161	160
Republic of Moldova	24	22	21	19	19	18	18	18
Romania	277	262	246	230	224	217	210	218
Russian Federation (RUE)	3595	3522	3334	3253	3231	3204	3158	3105
Serbia	183	180	171	172	184	188	137	113
Serbia and Montenegro	0	0	0	0	0	0	0	0
Slovakia	96	94	84	89	85	81	80	85
Slovenia	51	56	48	47	47	46	43	39
Spain	1265	1077	949	891	885	854	743	745
Sweden	166	157	148	150	139	131	126	135
Switzerland	87	85	80	78	73	73	72	69
Tajikistan	57	62	64	68	73	79	84	90
TFYR of Macedonia	36	36	37	37	36	35	34	33
Turkey	1031	984	961	945	1120	1090	1047	1055
Turkmenistan	65	75	79	87	99	110	121	134
Ukraine	801	764	727	690	684	678	673	667
United Kingdom	1471	1325	1149	1123	1051	1073	1020	949
Uzbekistan	227	248	268	290	314	340	367	399
North Africa	96	103	108	113	115	118	120	123
Asian areas (AST)	430	437	449	463	477	493	497	505
Baltic Sea	281	273	267	267	271	271	271	271
Black Sea	91	82	80	78	79	79	79	79
Mediterranean Sea	1713	1556	1511	1476	1497	1497	1497	1497
North Sea	733	668	650	635	644	644	644	644
Remaining N-E Atlantic Ocean	796	723	702	686	695	695	695	695
Natural marine emissions	0	0	0	0	0	0	0	0
Volcanic emissions	0	0	0	0	0	0	0	0
TOTAL	22260	21032	19889	19711	19662	19362	18948	18541

Table B:5: National total emission trends of ammonia (2000-2006), as used for modelling at the MSC-W (Gg of NH_3 per year).

Area/Year	2000	2001	2002	2003	2004	2005	2006
Albania	18	18	18	18	17	17	18
Armenia	10	10	10	11	11	11	12
Austria	67	67	66	66	66	66	66
Azerbaijan	39	40	42	44	45	47	48
Belarus	115	115	116	116	117	117	125
Belgium	83	84	82	79	74	69	72
Bosnia and Herzegovina	17	17	17	18	18	18	18
Bulgaria	41	42	46	47	47	47	50
Croatia	41	43	42	43	45	42	42
Cyprus	6	6	6	6	6	6	6
Czech Republic	92	89	86	82	79	76	74
Denmark	98	95	94	93	93	89	85
Estonia	10	10	9	10	11	10	10
Finland	38	37	38	39	39	39	38
France	748	747	732	725	716	714	710
Georgia	38	39	40	41	41	42	43
Germany	696	703	688	688	680	668	668
Greece	57	57	57	58	58	58	57
Hungary	94	93	96	96	94	89	90
Iceland	3	3	3	3	3	3	3
Ireland	115	115	114	114	113	113	112
Italy	453	459	446	442	434	421	419
Kazakhstan (KZT)	98	103	108	113	118	123	125
Kyrgyzstan	26	26	27	27	27	28	29
Latvia	14	15	15	15	15	15	15
Lithuania	39	41	43	44	44	45	47
Luxembourg	5	5	5	5	5	5	5
Malta	2	2	2	2	2	2	2
Montenegro	6	5	6	6	5	4	3
Netherlands	182	175	168	164	162	160	162
Norway	26	26	26	28	27	28	28
Poland	284	280	278	271	266	272	287
Portugal	65	61	59	53	52	49	49
Republic of Moldova	17	17	17	17	17	16	16
Romania	183	183	184	185	185	186	181
Russian Federation (RUE)	774	774	773	780	787	793	825
Serbia	82	81	89	84	97	94	96
Serbia and Montenegro	0	0	0	0	0	0	0
Slovakia	32	32	33	32	29	29	27
Slovenia	21	21	22	21	19	20	20
Spain	397	398	392	410	398	376	394
Sweden	59	56	55	56	56	55	55
Switzerland	66	66	65	64	63	64	64
Tajikistan	19	21	23	25	28	30	32
TFYR of Macedonia	10	10	10	9	9	9	8
Turkey	482	452	447	465	478	496	513
Turkmenistan	28	29	29	30	32	36	40
Ukraine	302	292	282	273	263	253	253
United Kingdom	322	321	314	304	310	304	301
Uzbekistan	53	56	58	60	65	69	75
North Africa	173	179	183	189	197	205	219
Asian areas (AST)	611	626	654	690	736	786	834
Baltic Sea	0	0	0	0	0	0	0
Black Sea	0	0	0	0	0	0	0
Mediterranean Sea	0	0	0	0	0	0	0
North Sea	0	0	0	0	0	0	0
Remaining N-E Atlantic Ocean	0	0	0	0	0	0	0
Natural marine emissions	0	0	0	0	0	0	0
Volcanic emissions	0	0	0	0	0	0	0
TOTAL	7254	7243	7213	7257	7298	7313	7469

Table B:6: National total emission trends of ammonia (2007-2014), as used for modelling at the MSC-W (Gg of NH_3 per year).

Area/Year	2007	2008	2009	2010	2011	2012	2013	2014
Albania	18	19	19	20	20	20	20	21
Armenia	12	12	13	13	14	14	15	15
Austria	68	67	68	68	67	67	66	67
Azerbaijan	49	50	52	53	54	55	56	57
Belarus	132	139	146	153	154	154	154	155
Belgium	69	69	69	65	64	63	62	66
Bosnia and Herzegovina	19	19	19	19	19	19	20	20
Bulgaria	52	51	42	41	40	38	30	31
Croatia	42	39	38	39	39	39	34	26
Cyprus	6	6	5	6	5	5	5	5
Czech Republic	72	71	69	67	67	68	69	69
Denmark	85	83	80	80	79	77	74	73
Estonia	10	11	10	11	11	11	11	13
Finland	38	37	38	38	37	37	37	37
France	719	731	722	729	721	722	718	708
Georgia	44	45	46	47	48	49	50	51
Germany	663	669	680	643	675	655	671	740
Greece	57	57	56	56	55	53	52	51
Hungary	90	81	77	77	77	77	81	84
Iceland	3	3	3	3	3	3	3	5
Ireland	108	110	111	109	105	106	108	105
Italy	427	417	401	388	402	415	402	393
Kazakhstan (KZT)	127	129	131	133	269	273	276	270
Kyrgyzstan	29	30	31	31	32	33	33	34
Latvia	14	15	15	14	14	15	15	17
Lithuania	45	42	43	43	42	42	40	41
Luxembourg	5	5	5	5	5	5	5	6
Malta	2	2	2	2	2	2	2	2
Montenegro	3	3	3	3	3	3	3	3
Netherlands	160	149	146	144	140	136	134	134
Norway	28	28	27	27	27	27	27	26
Poland	291	286	274	271	271	263	263	265
Portugal	50	50	50	46	48	49	49	49
Republic of Moldova	16	15	15	15	15	15	15	15
Romania	177	172	168	163	165	167	169	162
Russian Federation (RUE)	860	886	865	888	906	921	929	934
Serbia	100	88	100	85	87	91	104	86
Serbia and Montenegro	0	0	0	0	0	0	0	0
Slovakia	27	25	25	25	24	25	25	37
Slovenia	20	19	20	19	18	18	17	19
Spain	398	367	376	388	378	365	377	371
Sweden	53	52	50	52	52	51	52	54
Switzerland	65	65	64	64	63	62	62	63
Tajikistan	34	37	39	41	44	47	51	54
TFYR of Macedonia	8	8	8	8	8	8	8	8
Turkey	489	460	467	485	506	562	1090	1085
Turkmenistan	44	51	54	59	67	75	82	91
Ukraine	252	252	252	251	256	261	266	271
United Kingdom	292	278	278	279	279	275	271	281
Uzbekistan	82	89	96	104	113	122	132	143
North Africa	235	252	264	277	282	288	294	301
Asian areas (AST)	881	893	922	948	975	1008	1021	1050
Baltic Sea	0	0	0	0	0	0	0	0
Black Sea	0	0	0	0	0	0	0	0
Mediterranean Sea	0	0	0	0	0	0	0	0
North Sea	0	0	0	0	0	0	0	0
Remaining N-E Atlantic Ocean	0	0	0	0	0	0	0	0
Natural marine emissions	0	0	0	0	0	0	0	0
Volcanic emissions	0	0	0	0	0	0	0	0
TOTAL	7572	7534	7549	7592	7844	7954	8552	8664

Table B:7: National total emission trends of non-methane volatile organic compounds (2000-2006), as used for modelling at the MSC-W (Gg of NMVOC per year).

Area/Year	2000	2001	2002	2003	2004	2005	2006
Albania	29	30	31	32	33	34	34
Armenia	20	21	22	23	23	24	26
Austria	164	165	168	167	150	159	169
Azerbaijan	112	123	134	145	156	167	196
Belarus	228	222	217	212	207	202	201
Belgium	227	175	164	157	149	186	142
Bosnia and Herzegovina	52	50	49	48	46	45	44
Bulgaria	99	96	101	103	97	99	103
Croatia	76	72	73	73	72	69	69
Cyprus	13	13	13	13	13	12	12
Czech Republic	261	243	226	208	190	172	167
Denmark	174	166	162	156	153	149	145
Estonia	45	45	44	43	43	40	38
Finland	166	164	158	153	149	136	131
France	1681	1611	1484	1406	1333	1239	1134
Georgia	65	64	63	61	60	59	60
Germany	1600	1500	1430	1361	1369	1340	1326
Greece	312	302	292	283	273	263	250
Hungary	176	178	176	178	176	146	143
Iceland	8	8	8	7	7	7	6
Ireland	112	113	110	107	106	106	106
Italy	1524	1462	1394	1349	1280	1242	1193
Kazakhstan (KZT)	373	394	416	438	459	481	512
Kyrgyzstan	20	21	23	25	26	28	32
Latvia	102	105	103	102	101	100	99
Lithuania	72	75	76	74	76	76	76
Luxembourg	14	13	13	12	13	12	12
Malta	5	5	5	4	4	4	4
Montenegro	10	9	8	9	10	8	9
Netherlands	239	212	200	185	174	178	171
Norway	379	389	344	300	267	218	188
Poland	575	571	567	562	586	575	628
Portugal	248	239	236	224	218	209	203
Republic of Moldova	25	26	28	29	30	31	31
Romania	393	394	394	394	394	394	383
Russian Federation (RUE)	3148	3152	3156	3259	3280	3299	3261
Serbia	145	146	147	151	154	149	148
Serbia and Montenegro	0	0	0	0	0	0	0
Slovakia	67	71	70	71	72	75	72
Slovenia	53	52	52	50	47	45	45
Spain	960	931	866	869	845	802	773
Sweden	224	214	208	209	205	202	199
Switzerland	143	135	125	116	107	102	99
Tajikistan	14	16	18	19	21	23	25
TFYR of Macedonia	29	28	27	25	24	23	23
Turkey	955	875	897	923	931	919	917
Turkmenistan	21	22	22	23	24	28	31
Ukraine	574	579	583	587	591	595	572
United Kingdom	1567	1485	1401	1292	1211	1136	1090
Uzbekistan	52	54	57	59	64	68	73
North Africa	71	73	75	77	80	84	90
Asian areas (AST)	460	472	492	519	554	592	629
Baltic Sea	9	9	9	9	9	9	9
Black Sea	3	3	3	3	3	3	3
Mediterranean Sea	47	48	49	50	51	53	55
North Sea	20	21	21	21	22	22	23
Remaining N-E Atlantic Ocean	22	22	23	23	24	24	26
Natural marine emissions	0	0	0	0	0	0	0
Volcanic emissions	0	0	0	0	0	0	0
TOTAL	18183	17683	17228	16998	16765	16466	16201

Table B:8: National total emission trends of non-methane volatile organic compounds (2007-2014), as used for modelling at the MSC-W (Gg of NMVOC per year).

Area/Year	2007	2008	2009	2010	2011	2012	2013	2014
Albania	33	33	33	32	32	31	31	30
Armenia	28	30	31	33	35	36	38	40
Austria	157	148	119	131	126	133	126	110
Azerbaijan	225	254	283	312	337	361	385	428
Belarus	200	199	198	197	193	188	184	180
Belgium	133	127	115	155	143	141	137	122
Bosnia and Herzegovina	42	41	40	39	38	37	36	35
Bulgaria	98	96	104	103	101	92	89	99
Croatia	66	64	57	55	53	49	46	60
Cyprus	12	11	10	10	8	8	7	7
Czech Republic	161	155	150	144	141	139	136	138
Denmark	141	136	129	125	119	116	114	106
Estonia	38	37	35	35	34	34	33	23
Finland	129	118	111	116	106	105	95	75
France	1026	943	861	874	807	772	758	639
Georgia	60	61	62	63	63	64	64	65
Germany	1266	1216	1130	1239	1169	1136	1138	1041
Greece	237	225	212	199	193	186	180	174
Hungary	135	130	128	125	118	117	120	116
Iceland	6	6	5	5	5	5	4	5
Ireland	106	100	97	91	89	88	90	87
Italy	1127	1069	1003	942	919	862	906	849
Kazakhstan (KZT)	544	575	607	639	665	691	718	836
Kyrgyzstan	36	39	43	47	50	53	56	62
Latvia	94	93	91	89	88	89	87	54
Lithuania	73	75	72	71	69	68	63	69
Luxembourg	12	10	9	8	8	8	8	11
Malta	4	4	3	3	3	3	3	3
Montenegro	10	10	10	8	9	8	8	9
Netherlands	169	167	157	158	156	154	150	143
Norway	185	152	137	140	133	135	134	138
Poland	614	637	617	653	638	630	636	606
Portugal	200	191	180	180	174	168	170	169
Republic of Moldova	30	30	29	29	28	28	27	27
Romania	371	360	349	337	323	310	296	319
Russian Federation (RUE)	3230	3180	3033	2977	2947	2911	2860	2803
Serbia	153	148	145	147	147	143	124	118
Serbia and Montenegro	0	0	0	0	0	0	0	0
Slovakia	69	69	66	64	70	61	63	106
Slovenia	43	41	39	38	37	35	33	32
Spain	755	691	635	633	602	555	534	599
Sweden	196	191	191	192	187	179	174	184
Switzerland	95	94	92	90	87	85	84	80
Tajikistan	26	29	30	32	34	36	39	42
TFYR of Macedonia	22	22	21	20	20	19	18	18
Turkey	927	928	963	977	985	1034	868	967
Turkmenistan	34	39	41	45	52	57	63	70
Ukraine	550	527	504	481	466	451	436	421
United Kingdom	1054	975	883	855	835	824	803	819
Uzbekistan	80	87	94	102	111	120	129	140
North Africa	96	103	108	113	115	118	120	123
Asian areas (AST)	665	675	694	713	734	758	771	791
Baltic Sea	8	8	7	7	7	7	7	7
Black Sea	3	2	2	2	2	2	2	2
Mediterranean Sea	51	46	45	44	45	45	45	45
North Sea	21	19	19	17	17	17	17	17
Remaining N-E Atlantic Ocean	24	22	21	20	21	21	21	21
Natural marine emissions	0	0	0	0	0	0	0	0
Volcanic emissions	0	0	0	0	0	0	0	0
TOTAL	15867	15436	14852	14961	14692	14526	14286	14281

Table B:9: National total emission trends of carbon monoxide (2000-2006), as used for modelling at the MSC-W (Gg of CO per year).

Area/Year	2000	2001	2002	2003	2004	2005	2006
Albania	66	69	72	75	78	81	79
Armenia	82	82	83	83	84	84	86
Austria	785	760	727	730	710	699	673
Azerbaijan	270	285	300	315	330	345	367
Belarus	671	631	590	550	510	470	463
Belgium	942	854	844	821	796	766	663
Bosnia and Herzegovina	181	167	153	139	125	111	104
Bulgaria	461	410	430	453	405	414	428
Croatia	345	301	291	299	279	266	263
Cyprus	36	35	34	33	30	27	25
Czech Republic	1009	926	844	762	680	597	586
Denmark	491	484	465	472	461	465	454
Estonia	183	189	182	174	171	158	144
Finland	611	603	598	578	566	530	507
France	6392	6043	5815	5560	5667	5164	4637
Georgia	217	214	212	210	208	205	208
Germany	4787	4600	4328	4146	3910	3705	3639
Greece	1321	1226	1131	1036	941	846	798
Hungary	649	657	638	666	594	447	466
Iceland	21	21	21	22	23	18	20
Ireland	247	243	232	223	219	217	201
Italy	4672	4395	4045	3831	3655	3239	2943
Kazakhstan (KZT)	1133	1149	1164	1180	1195	1211	1394
Kyrgyzstan	90	97	105	113	120	128	146
Latvia	236	240	229	229	222	204	198
Lithuania	199	204	201	205	188	197	193
Luxembourg	55	55	49	48	50	45	41
Malta	8	7	7	7	6	6	6
Montenegro	40	37	34	40	40	37	36
Netherlands	755	748	738	732	751	727	729
Norway	516	496	487	444	398	392	365
Poland	2647	2713	2791	2758	2836	2754	2905
Portugal	665	585	567	533	504	466	433
Republic of Moldova	77	80	82	85	87	90	88
Romania	1375	1366	1356	1346	1336	1326	1273
Russian Federation (RUE)	12949	12903	12853	13005	13068	13118	13367
Serbia	429	439	445	473	476	457	419
Serbia and Montenegro	0	0	0	0	0	0	0
Slovakia	300	305	290	292	292	272	273
Slovenia	213	207	201	198	185	181	171
Spain	2705	2638	2386	2450	2317	2142	2121
Sweden	849	810	767	753	707	700	666
Switzerland	426	405	377	365	347	330	307
Tajikistan	360	397	440	488	539	575	615
TFYR of Macedonia	117	76	81	139	95	96	96
Turkey	1996	1732	1804	1884	1907	1897	1959
Turkmenistan	233	243	244	252	264	299	331
Ukraine	3363	3380	3396	3413	3430	3447	3335
United Kingdom	5553	5209	4656	4249	3878	3493	3282
Uzbekistan	800	834	867	903	973	1041	1117
North Africa	247	256	262	270	281	294	314
Asian areas (AST)	2750	2811	2914	3063	3282	3524	3742
Baltic Sea	30	30	31	32	32	33	32
Black Sea	9	9	9	9	9	10	10
Mediterranean Sea	160	163	167	171	175	178	188
North Sea	71	72	74	75	77	79	83
Remaining N-E Atlantic Ocean	74	76	78	80	81	83	87
Natural marine emissions	0	0	0	0	0	0	0
Volcanic emissions	0	0	0	0	0	0	0
TOTAL	65868	63966	62188	61462	60590	58684	58073

Table B:10: National total emission trends of carbon monoxide (2007-2014), as used for modelling at the MSC-W (Gg of CO per year).

Area/Year	2007	2008	2009	2010	2011	2012	2013	2014
Albania	76	74	72	70	69	68	67	65
Armenia	88	90	92	94	95	97	99	101
Austria	638	620	582	596	575	582	582	537
Azerbaijan	388	410	431	453	471	489	507	539
Belarus	456	448	441	434	427	420	413	405
Belgium	664	669	441	526	423	374	553	353
Bosnia and Herzegovina	96	89	82	75	72	70	68	66
Bulgaria	370	343	308	332	332	326	302	291
Croatia	252	207	200	185	179	172	153	203
Cyprus	24	22	20	19	17	16	15	14
Czech Republic	575	563	552	541	534	526	519	462
Denmark	460	439	413	407	370	355	339	312
Estonia	163	167	168	172	148	162	158	127
Finland	501	486	465	485	455	453	369	339
France	4429	4273	3824	4239	3508	3133	3196	3090
Georgia	210	212	215	217	219	221	223	227
Germany	3558	3482	3082	3529	3450	3063	3089	2964
Greece	751	704	656	609	588	567	546	525
Hungary	427	388	392	383	366	350	326	289
Iceland	21	20	20	19	18	18	17	16
Ireland	189	179	159	146	135	129	123	115
Italy	2684	2567	2290	2283	2229	2062	2571	2340
Kazakhstan (KZT)	1577	1760	1942	2125	2278	2430	2583	2346
Kyrgyzstan	163	180	198	215	230	244	259	285
Latvia	187	174	186	154	158	165	149	136
Lithuania	179	182	177	182	167	168	146	144
Luxembourg	44	37	33	32	29	30	30	31
Malta	5	5	5	4	4	4	4	5
Montenegro	37	35	29	30	33	32	32	33
Netherlands	720	719	673	679	656	636	621	571
Norway	352	337	318	331	303	294	259	241
Poland	2831	2834	2788	3019	2933	2791	2876	2704
Portugal	408	387	361	350	327	298	288	263
Republic of Moldova	86	84	82	79	78	77	75	74
Romania	1220	1167	1114	1061	1044	1027	1010	774
Russian Federation (RUE)	13665	13822	13252	13362	13413	13427	13322	13178
Serbia	455	417	403	421	410	381	273	236
Serbia and Montenegro	0	0	0	0	0	0	0	0
Slovakia	249	245	208	221	227	221	218	225
Slovenia	163	160	156	153	160	159	155	108
Spain	2106	1991	1924	2002	1990	1753	1709	1995
Sweden	665	652	642	632	588	580	562	497
Switzerland	289	279	262	251	231	224	216	196
Tajikistan	663	715	742	791	849	913	980	1046
TFYR of Macedonia	98	98	90	70	72	66	59	45
Turkey	2039	2394	2529	2546	3041	3304	2541	2469
Turkmenistan	368	422	448	489	561	623	687	758
Ukraine	3223	3111	2999	2887	2858	2829	2800	2770
United Kingdom	2972	2783	2303	2182	2005	1942	1971	2072
Uzbekistan	1223	1333	1441	1564	1693	1832	1979	2147
North Africa	336	360	377	396	403	412	421	430
Asian areas (AST)	3935	3999	4112	4198	4316	4465	4616	4773
Baltic Sea	29	28	28	28	28	28	28	28
Black Sea	9	8	8	8	8	8	8	8
Mediterranean Sea	173	157	153	149	151	151	151	151
North Sea	76	70	68	67	67	67	67	67
Remaining N-E Atlantic Ocean	81	73	71	70	71	71	71	71
Natural marine emissions	0	0	0	0	0	0	0	0
Volcanic emissions	0	0	0	0	0	0	0	0
TOTAL	57647	57470	55032	56564	56064	55308	55402	54262

Table B:11: National total emission trends of fine Particulate Matter (2000-2006), as used for modelling at the MSC-W (Gg of $PM_{2.5}$ per year).

Area/Year	2000	2001	2002	2003	2004	2005	2006
Albania	8	8	9	9	9	9	9
Armenia	4	4	4	4	4	4	4
Austria	24	24	23	23	23	23	22
Azerbaijan	15	16	16	16	17	17	17
Belarus	58	57	56	56	55	55	54
Belgium	41	38	37	38	38	36	36
Bosnia and Herzegovina	16	17	18	19	20	20	19
Bulgaria	23	21	26	29	28	28	30
Croatia	15	13	13	16	16	15	15
Cyprus	4	4	3	3	3	3	2
Czech Republic	41	38	36	33	30	28	28
Denmark	24	24	24	25	26	27	28
Estonia	22	23	23	21	23	20	16
Finland	41	42	43	42	40	39	40
France	311	300	276	278	265	245	228
Georgia	28	26	25	23	21	19	19
Germany	158	154	148	144	140	133	130
Greece	66	65	64	63	62	61	57
Hungary	37	42	40	40	36	27	29
Iceland	1	1	1	1	1	1	1
Ireland	21	20	19	19	19	19	19
Italy	163	161	148	146	151	140	136
Kazakhstan (KZT)	107	109	110	111	112	114	126
Kyrgyzstan	7	8	8	8	8	8	9
Latvia	25	28	27	29	30	29	29
Lithuania	19	20	20	21	21	22	22
Luxembourg	3	3	3	3	3	3	3
Malta	1	1	1	1	1	1	1
Montenegro	4	4	5	5	5	5	5
Netherlands	25	24	23	22	21	20	19
Norway	42	41	43	40	38	39	37
Poland	157	160	166	165	162	167	165
Portugal	61	59	58	56	58	56	52
Republic of Moldova	11	11	11	11	11	10	10
Romania	159	150	141	133	124	115	112
Russian Federation (RUE)	977	994	1011	1051	1076	1101	1131
Serbia	39	39	40	40	41	40	37
Serbia and Montenegro	0	0	0	0	0	0	0
Slovakia	23	33	29	28	28	37	32
Slovenia	12	12	12	12	12	13	13
Spain	95	93	93	94	92	91	88
Sweden	25	25	25	26	26	26	26
Switzerland	11	10	10	10	10	9	9
Tajikistan	12	13	14	16	17	19	20
TFYR of Macedonia	14	14	13	13	13	12	12
Turkey	471	394	463	455	441	443	448
Turkmenistan	28	29	30	31	32	36	40
Ukraine	388	389	390	390	391	392	385
United Kingdom	121	118	103	101	98	96	95
Uzbekistan	101	105	110	114	123	132	141
North Africa	44	46	47	48	50	53	56
Asian areas (AST)	129	133	140	149	158	168	178
Baltic Sea	19	19	19	19	19	19	17
Black Sea	6	6	6	6	6	6	7
Mediterranean Sea	104	106	109	112	114	117	123
North Sea	45	45	45	45	45	45	47
Remaining N-E Atlantic Ocean	48	49	51	52	53	54	57
Natural marine emissions	0	0	0	0	0	0	0
Volcanic emissions	0	0	0	0	0	0	0
TOTAL	4452	4387	4425	4462	4466	4466	4491

Table B:12: National total emission trends of fine Particulate Matter (2007-2014), as used for modelling at the MSC-W (Gg of $PM_{2.5}$ per year).

Area/Year	2007	2008	2009	2010	2011	2012	2013	2014
Albania	9	9	9	9	9	9	9	9
Armenia	4	4	4	4	4	4	4	4
Austria	21	20	19	20	19	19	18	17
Azerbaijan	17	18	18	18	19	19	20	20
Belarus	53	52	52	51	51	51	51	51
Belgium	34	35	32	37	30	32	33	28
Bosnia and Herzegovina	18	17	16	15	15	15	15	14
Bulgaria	29	28	26	29	31	31	29	34
Croatia	14	14	14	15	16	16	15	19
Cyprus	2	2	2	2	1	1	1	1
Czech Republic	28	27	27	27	27	26	26	23
Denmark	31	29	27	27	24	22	21	18
Estonia	21	20	19	24	27	17	20	8
Finland	34	36	38	40	37	37	35	24
France	213	208	199	206	179	181	181	169
Georgia	19	19	20	20	20	20	20	20
Germany	126	121	116	125	120	114	113	104
Greece	54	51	48	45	43	42	40	38
Hungary	28	26	28	29	31	30	30	26
Iceland	1	1	2	2	2	2	2	0
Ireland	18	18	18	17	16	15	16	15
Italy	136	133	127	126	123	121	168	152
Kazakhstan (KZT)	137	149	161	173	185	197	208	156
Kyrgyzstan	9	9	10	10	10	11	11	11
Latvia	28	28	30	24	25	26	24	18
Lithuania	21	21	21	21	21	21	21	17
Luxembourg	3	2	2	2	2	2	2	2
Malta	1	1	1	1	1	1	1	1
Montenegro	5	6	4	4	5	5	5	5
Netherlands	19	17	16	15	14	13	13	13
Norway	37	36	34	38	35	35	30	27
Poland	161	155	149	160	151	145	145	135
Portugal	51	49	47	46	47	46	44	44
Republic of Moldova	10	10	10	10	10	10	10	10
Romania	114	135	129	129	117	122	116	116
Russian Federation (RUE)	1165	1189	1158	1178	1201	1222	1233	1242
Serbia	41	36	44	43	41	43	36	34
Serbia and Montenegro	0	0	0	0	0	0	0	0
Slovakia	28	28	27	27	29	29	29	30
Slovenia	13	12	12	12	12	12	12	12
Spain	88	79	78	75	73	70	65	67
Sweden	26	25	24	25	23	23	22	21
Switzerland	9	9	9	8	8	8	8	8
Tajikistan	21	23	24	26	27	30	32	34
TFYR of Macedonia	12	12	12	12	11	11	11	11
Turkey	454	499	480	541	503	559	508	539
Turkmenistan	45	51	54	59	68	76	83	92
Ukraine	378	371	364	357	358	358	359	360
United Kingdom	93	90	84	87	81	82	82	105
Uzbekistan	155	169	182	198	214	232	250	272
North Africa	60	64	67	71	72	74	75	77
Asian areas (AST)	189	192	198	206	212	219	216	216
Baltic Sea	15	15	14	14	11	11	11	11
Black Sea	6	6	6	6	6	6	6	6
Mediterranean Sea	114	106	104	102	109	109	109	109
North Sea	42	35	35	32	27	27	27	27
Remaining N-E Atlantic Ocean	53	49	49	47	50	50	50	50
Natural marine emissions	0	0	0	0	0	0	0	0
Volcanic emissions	0	0	0	0	0	0	0	0
TOTAL	4514	4568	4500	4643	4604	4708	4721	4671

Table B:13: National total emission trends of coarse Particulate Matter (2000-2006), as used for modelling at the MSC-W (Gg of PM_{coarse} per year).

Area/Year	2000	2001	2002	2003	2004	2005	2006
Albania	2	2	2	2	2	2	2
Armenia	1	1	1	1	1	1	1
Austria	15	15	15	15	15	15	15
Azerbaijan	4	4	4	4	4	4	4
Belarus	21	21	20	19	19	18	18
Belgium	15	12	12	12	12	12	10
Bosnia and Herzegovina	15	15	16	16	16	17	16
Bulgaria	13	13	11	14	15	18	19
Croatia	5	5	6	7	8	7	7
Cyprus	2	2	2	2	2	2	2
Czech Republic	18	17	17	16	16	15	15
Denmark	12	13	11	12	11	12	12
Estonia	16	15	11	9	8	7	5
Finland	16	15	16	16	17	16	17
France	108	106	102	105	104	99	98
Georgia	3	3	3	3	3	3	3
Germany	118	114	111	109	108	105	106
Greece	29	28	27	26	24	23	22
Hungary	35	31	31	30	30	22	22
Iceland	0	0	0	0	0	0	0
Ireland	10	10	10	10	10	10	10
Italy	33	34	34	33	33	31	30
Kazakhstan (KZT)	60	61	61	61	61	62	65
Kyrgyzstan	4	4	3	3	3	3	4
Latvia	4	4	4	4	12	6	6
Lithuania	6	6	6	6	6	6	6
Luxembourg	3	2	2	4	2	2	2
Malta	0	1	1	1	1	1	1
Montenegro	4	3	5	5	4	3	4
Netherlands	15	14	15	13	14	14	14
Norway	8	8	8	8	8	8	8
Poland	120	123	133	128	122	128	131
Portugal	24	31	28	23	26	30	24
Republic of Moldova	5	5	5	5	5	5	5
Romania	61	56	51	46	41	36	37
Russian Federation (RUE)	678	705	731	772	808	842	881
Serbia	17	17	17	17	18	17	18
Serbia and Montenegro	0	0	0	0	0	0	0
Slovakia	22	14	11	8	4	5	5
Slovenia	5	5	5	4	5	5	5
Spain	42	41	43	42	41	40	38
Sweden	14	14	14	15	15	15	15
Switzerland	10	10	10	10	10	10	10
Tajikistan	12	13	14	16	17	18	20
TFYR of Macedonia	12	12	11	11	10	10	10
Turkey	230	192	226	222	215	216	218
Turkmenistan	34	36	36	37	39	44	49
Ukraine	190	191	192	193	194	194	193
United Kingdom	59	59	52	52	53	51	52
Uzbekistan	154	161	167	174	187	201	215
North Africa	88	88	88	88	88	88	88
Asian areas (AST)	156	161	171	182	193	204	216
Baltic Sea	1	1	1	1	1	1	1
Black Sea	0	0	0	0	0	0	0
Mediterranean Sea	5	6	6	6	6	6	6
North Sea	3	3	3	3	3	3	3
Remaining N-E Atlantic Ocean	3	3	3	3	3	3	3
Natural marine emissions	0	0	0	0	0	0	0
Volcanic emissions	0	0	0	0	0	0	0
TOTAL	2541	2526	2586	2624	2674	2719	2788

Table B:14: National total emission trends of coarse Particulate Matter (2007-2014), as used for modelling at the MSC-W (Gg of PM_{coarse} per year).

Area/Year	2007	2008	2009	2010	2011	2012	2013	2014
Albania	2	2	2	2	2	2	2	2
Armenia	1	1	1	1	1	1	2	2
Austria	15	15	15	15	15	15	15	15
Azerbaijan	4	4	4	4	4	4	5	5
Belarus	18	18	18	18	18	18	18	18
Belgium	9	8	7	10	9	9	10	10
Bosnia and Herzegovina	15	14	13	12	12	12	12	12
Bulgaria	23	19	14	14	15	14	13	12
Croatia	7	7	7	6	6	6	5	7
Cyprus	2	2	2	2	1	1	1	1
Czech Republic	15	14	14	14	14	14	14	12
Denmark	12	12	11	12	11	11	11	13
Estonia	9	6	5	9	16	4	6	5
Finland	14	13	13	14	14	13	12	10
France	96	93	88	88	89	90	90	107
Georgia	3	3	3	3	3	3	3	3
Germany	106	105	100	109	114	114	116	117
Greece	21	20	18	17	17	16	15	15
Hungary	21	21	20	19	19	18	18	19
Iceland	0	1	1	1	1	1	1	0
Ireland	10	10	10	10	10	10	10	10
Italy	30	29	27	27	27	26	25	25
Kazakhstan (KZT)	67	70	73	76	78	81	84	134
Kyrgyzstan	4	4	4	4	4	4	4	4
Latvia	7	7	5	5	7	7	6	6
Lithuania	6	6	6	6	6	6	6	2
Luxembourg	2	2	2	2	2	2	1	1
Malta	1	1	1	1	1	1	1	1
Montenegro	3	4	3	4	7	8	8	7
Netherlands	14	14	14	14	14	14	14	14
Norway	9	8	8	7	8	9	8	8
Poland	125	118	111	116	107	100	102	98
Portugal	22	23	23	19	18	16	13	10
Republic of Moldova	4	4	4	4	4	4	4	4
Romania	41	37	35	37	37	38	37	38
Russian Federation (RUE)	923	952	902	926	953	976	987	993
Serbia	18	17	18	18	18	18	18	14
Serbia and Montenegro	0	0	0	0	0	0	0	0
Slovakia	4	4	3	3	4	4	4	7
Slovenia	4	3	3	3	3	3	3	2
Spain	38	32	30	30	31	29	28	53
Sweden	15	15	14	15	14	14	14	14
Switzerland	10	10	10	10	10	10	10	11
Tajikistan	21	23	24	25	27	29	32	34
TFYR of Macedonia	10	10	9	9	9	9	9	8
Turkey	221	243	234	264	245	272	248	263
Turkmenistan	54	62	66	72	83	92	102	112
Ukraine	192	191	190	188	187	185	184	182
United Kingdom	50	47	43	43	42	43	42	43
Uzbekistan	236	257	278	301	326	353	381	414
North Africa	88	95	99	104	106	109	111	113
Asian areas (AST)	231	234	241	252	260	268	262	259
Baltic Sea	1	1	1	1	1	1	1	1
Black Sea	0	0	0	0	0	0	0	0
Mediterranean Sea	6	6	5	5	6	6	6	6
North Sea	2	2	2	2	1	1	1	1
Remaining N-E Atlantic Ocean	3	3	3	2	3	3	3	3
Natural marine emissions	0	0	0	0	0	0	0	0
Volcanic emissions	0	0	0	0	0	0	0	0
TOTAL	2868	2921	2860	2976	3040	3118	3134	3277

Table B:15: National total emission trends of Particulate Matter (2000-2006), as used for modelling at the MSC-W (Gg of PM_{10} per year).

Area/Year	2000	2001	2002	2003	2004	2005	2006
Albania	10	10	11	11	11	11	11
Armenia	5	5	5	5	5	5	5
Austria	39	39	38	38	38	38	36
Azerbaijan	19	19	20	20	21	21	21
Belarus	79	78	76	75	74	73	72
Belgium	56	50	48	50	50	49	46
Bosnia and Herzegovina	31	32	34	35	36	37	35
Bulgaria	36	34	37	43	43	46	49
Croatia	20	18	20	23	23	22	22
Cyprus	6	6	5	5	5	4	4
Czech Republic	59	56	53	49	46	43	42
Denmark	36	37	35	37	37	39	40
Estonia	38	38	34	31	31	28	21
Finland	57	57	59	58	57	54	57
France	419	406	378	383	369	345	326
Georgia	31	30	28	26	24	22	22
Germany	276	267	259	253	248	238	236
Greece	95	93	90	88	86	84	80
Hungary	72	73	71	70	66	50	51
Iceland	1	1	1	1	1	1	1
Ireland	31	31	30	29	29	30	29
Italy	196	195	183	179	184	171	166
Kazakhstan (KZT)	168	169	171	172	174	176	190
Kyrgyzstan	11	11	11	11	12	12	12
Latvia	29	32	31	33	42	35	35
Lithuania	25	26	26	27	27	28	28
Luxembourg	5	5	5	7	5	5	5
Malta	1	2	2	2	2	2	2
Montenegro	8	7	9	10	10	8	9
Netherlands	40	39	38	36	35	34	33
Norway	49	49	50	47	46	47	45
Poland	276	283	299	293	284	295	297
Portugal	85	90	86	79	84	86	77
Republic of Moldova	15	15	15	15	15	15	15
Romania	221	207	193	179	165	151	149
Russian Federation (RUE)	1655	1699	1742	1823	1885	1943	2012
Serbia	56	55	56	57	58	57	55
Serbia and Montenegro	0	0	0	0	0	0	0
Slovakia	45	47	40	36	31	42	37
Slovenia	17	17	17	17	17	17	17
Spain	137	134	137	136	133	131	127
Sweden	40	39	39	40	41	41	41
Switzerland	21	20	20	19	19	19	19
Tajikistan	23	26	28	31	35	37	40
TFYR of Macedonia	26	25	24	24	23	22	22
Turkey	701	587	689	677	656	659	667
Turkmenistan	63	65	66	68	71	80	89
Ukraine	578	580	581	583	584	586	578
United Kingdom	179	177	155	154	151	147	147
Uzbekistan	255	266	277	288	311	332	357
North Africa	133	134	135	137	139	141	145
Asian areas (AST)	285	294	311	331	351	371	394
Baltic Sea	20	20	20	20	20	20	18
Black Sea	6	6	6	6	6	7	7
Mediterranean Sea	109	112	115	118	120	123	130
North Sea	47	47	48	48	48	48	50
Remaining N-E Atlantic Ocean	51	52	53	55	56	57	60
Natural marine emissions	0	0	0	0	0	0	0
Volcanic emissions	0	0	0	0	0	0	0
TOTAL	6993	6913	7011	7086	7140	7184	7279

Table B:16: National total emission trends of Particulate Matter (2007-2014), as used for modelling at the MSC-W (Gg of PM_{10} per year).

Area/Year	2007	2008	2009	2010	2011	2012	2013	2014
Albania	11	11	11	11	11	11	11	11
Armenia	5	5	5	5	5	5	6	6
Austria	35	36	34	34	34	33	33	31
Azerbaijan	22	22	22	23	23	24	24	24
Belarus	71	71	70	69	69	70	70	70
Belgium	43	43	39	47	39	41	43	38
Bosnia and Herzegovina	33	31	29	27	27	27	26	26
Bulgaria	51	48	41	43	46	45	42	46
Croatia	21	21	21	21	22	22	20	26
Cyprus	4	4	3	3	3	2	2	2
Czech Republic	42	42	42	41	41	40	39	35
Denmark	43	41	38	39	36	34	32	31
Estonia	30	26	24	32	42	21	25	12
Finland	49	49	52	54	51	50	47	34
France	308	300	287	294	268	271	272	276
Georgia	22	23	23	23	23	23	23	24
Germany	233	226	216	233	234	228	228	221
Greece	75	71	67	62	60	58	55	53
Hungary	49	47	48	49	50	48	47	45
Iceland	2	2	2	2	3	3	3	1
Ireland	28	28	28	27	25	25	26	24
Italy	166	162	154	153	150	147	194	177
Kazakhstan (KZT)	205	219	234	249	263	278	292	290
Kyrgyzstan	13	13	14	14	14	15	15	16
Latvia	35	35	35	30	31	33	30	24
Lithuania	27	27	27	27	27	26	26	19
Luxembourg	5	4	4	4	4	4	4	3
Malta	2	2	2	1	1	1	1	1
Montenegro	8	10	7	8	12	12	13	12
Netherlands	33	31	30	29	28	27	27	26
Norway	46	44	42	45	42	45	38	35
Poland	286	273	261	276	258	245	246	232
Portugal	73	72	70	65	64	61	57	55
Republic of Moldova	15	14	14	14	14	14	14	14
Romania	155	172	164	165	154	160	153	154
Russian Federation (RUE)	2088	2140	2060	2104	2154	2198	2220	2235
Serbia	59	53	62	61	59	61	53	48
Serbia and Montenegro	0	0	0	0	0	0	0	0
Slovakia	32	31	31	30	32	32	33	37
Slovenia	17	15	15	15	16	16	15	14
Spain	126	112	109	105	104	99	93	120
Sweden	41	40	38	40	38	36	36	34
Switzerland	19	19	19	19	18	18	18	18
Tajikistan	43	46	48	51	55	59	63	67
TFYR of Macedonia	22	21	21	21	20	20	19	19
Turkey	676	742	714	805	748	831	756	802
Turkmenistan	99	114	121	132	151	168	185	204
Ukraine	570	562	554	546	545	544	542	541
United Kingdom	143	138	127	129	123	125	123	148
Uzbekistan	390	426	460	499	541	585	632	685
North Africa	149	159	167	175	178	182	186	190
Asian areas (AST)	421	426	439	458	472	487	478	475
Baltic Sea	15	16	15	14	12	12	12	12
Black Sea	6	6	6	6	6	6	6	6
Mediterranean Sea	120	111	110	108	114	114	114	114
North Sea	44	37	37	34	28	28	28	28
Remaining N-E Atlantic Ocean	56	52	51	50	53	53	53	53
Natural marine emissions	0	0	0	0	0	0	0	0
Volcanic emissions	0	0	0	0	0	0	0	0
TOTAL	7382	7489	7361	7620	7643	7826	7855	7948

APPENDIX C

Source-receptor tables for 2014

The source-receptor tables in this appendix are calculated for the meteorological and chemical conditions of 2014.

The tables are calculated for the extended EMEP domain and are based on model runs driven by ECMWF-IFS meteorology.

The source-receptor (SR) relationships give the change in air concentrations or depositions resulting from a change in emissions from each emitter country.

For each country, reductions in five different pollutants have been calculated separately, with an emission reduction of 15% for SO_x, NO_x, NH_3, NMVOC or PPM, respectively. Here reduction in PPM means that PPM_{fine} and PPM_{coarse} are reduced together in one simulation. For year 2014, reductions in volcanic emissions are done both for passive SO_2 degassing of Italian volcanoes (Etna, Stromboli and Vulcano) and for SO_2 emissions from the Holuhraun eruption.

The deposition tables show the contribution from one country to another. They have been calculated adding the differences obtained by a 15% reduction for all emissions in one country multiplied by a factor of 100/15, in order to arrive at total estimates.

For the concentrations and indicator tables, the differences obtained by the 15% emission reduction of the relevant pollutants are given directly. Thus, the tables should be interpreted as estimates of this reduction scenario from the chemical conditions in 2014.

The SR tables in the following aim to respond to two fundamental questions about transboundary air pollution:

1. Where do the pollutants emitted by a country or region end up?

2. Where do the pollutants in a given country or region come from?

Each column answers the first question. The numbers within a column give the change in the value of each pollutant (or indicator) for each receiver country caused by the emissions in the country given at the top of the column.

Each row answers the second question. The numbers given in each row show which emitter countries were responsible for the change in pollutants in the country given at the beginning of each row.

Note that more information on aerosol components and SR tables in electronic format are available from the EMEP website `www.emep.int`.

Acidification and eutrophication

- Deposition of OXS (oxidised sulphur). The contribution from SO_x, NO_x, NH_3, PPM and VOC emissions have been summed up and scaled to a 100% reduction. Units: 100 Mg of S.
- Deposition of OXN (oxidised nitrogen). The contribution from SO_x, NO_x, NH_3, PPM and VOC emissions have been summed up and scaled to a 100% reduction. Units: 100 Mg of N.
- Deposition of RDN (reduced nitrogen). The contribution from SO_x, NO_x, NH_3, PPM and VOC emissions have been summed up and scaled to a 100% reduction. Units: 100 Mg of N.

Ground Level Ozone

- $AOT40_f^{uc}$. Effect of a 15% reduction in NO_x emissions. Units: ppb.h
- $AOT40_f^{uc}$. Effect of a 15% reduction in VOC emissions. Units: ppb.h
- SOMO35. Effect of a 15% reduction in NO_x emissions. Units: ppb.d
- SOMO35. Effect of a 15% reduction in VOC emissions. Units: ppb.d

Particulate Matter

- $PM_{2.5}$. Effect of a 15% reduction in PPM emissions. Units: ng/m^3
- $PM_{2.5}$. Effect of a 15% reduction in SO_x emissions. Units: ng/m^3
- $PM_{2.5}$. Effect of a 15% reduction in NO_x emissions. Units: ng/m^3
- $PM_{2.5}$. Effect of a 15% reduction in NH_3 emissions. Units: ng/m^3
- $PM_{2.5}$. Effect of a 15% reduction in VOC emissions. Units: ng/m^3
- $PM_{2.5}$. Effect of a 15% reduction in all emissions. The contribution from a 15% reduction in PPM, SO_x, NO_x, NH_3 and VOC emissions have been summed up. Units: ng/m^3

Fine Elemental Carbon

- Fine EC. Effect of a 15% reduction in PPM emissions. Units: 0.1 ng/m^3

Coarse Elemental Carbon

- Coarse EC. Effect of a 15% reduction in PPM emissions. Units: 0.1 ng/m^3

Table C.1: 2014 country-to-country blame matrices for **oxidised sulphur** deposition.
Units: 100 Mg of S. **Emitters →, Receptors ↓.**

	AL	AM	AT	AZ	BA	BE	BG	BY	CH	CY	CZ	DE	DK	EE	ES	FI	FR	GB	GE	GR	HR	HU	IE	IS	IT	KG	KZT	LT	LU	LV	MD	ME	
AL	24	-0	0	-0	5	0	2	0	0	0	0	0	0	0	2	0	0	0	-0	12	0	0	0	0	4	0	0	0	0	0	-0	5	AL
AM	0	3	0	4	0	0	0	0	0	0	0	0	0	0	0	0	0	0	1	0	0	0	0	0	0	0	3	0	0	-0	0	0	AM
AT	0	-0	29	0	9	1	2	0	2	0	20	41	0	0	1	0	3	2	-0	0	1	3	0	0	6	0	0	0	0	0	-0	1	AT
AZ	0	1	0	46	0	0	0	0	0	0	0	0	-0	0	0	0	0	0	2	0	0	0	-0	0	0	0	18	0	0	-0	0	0	AZ
BA	1	0	1	0	311	0	3	0	0	0	4	3	0	0	2	0	1	0	0	2	6	3	0	0	6	0	0	0	0	0	0	17	BA
BE	0	0	0	0	0	49	0	0	0	-0	1	17	0	0	1	0	18	9	-0	0	0	0	0	0	0	-0	0	0	1	0	-0	0	BE
BG	1	0	0	0	9	0	352	1	0	0	2	1	0	0	2	0	1	0	0	27	0	1	0	0	2	0	9	0	0	0	0	4	BG
BY	0	0	1	0	16	1	7	162	0	0	12	14	0	2	1	1	2	3	0	2	1	2	0	0	2	0	13	4	0	1	1	2	BY
CH	0	-0	1	0	0	0	0	0	15	-0	1	11	0	0	2	0	8	1	-0	0	0	0	0	0	5	-0	0	0	0	-0	-0	0	CH
CY	0	0	0	0	0	0	0	0	0	4	0	0	0	0	0	0	0	0	0	0	0	0	0	0	0	0	0	0	0	0	0	0	CY
CZ	0	0	5	0	11	1	2	1	0	0	147	43	0	0	1	0	3	3	0	0	1	4	0	0	2	-0	1	0	0	0	0	1	CZ
DE	0	-0	9	-0	5	28	2	2	8	0	83	876	2	0	10	0	67	49	-0	0	0	1	1	0	4	0	2	1	2	0	-0	0	DE
DK	0	0	0	0	1	2	1	1	0	0	4	26	13	0	1	0	4	12	0	0	0	0	0	0	0	0	0	0	0	0	0	0	DK
EE	0	0	0	0	2	0	1	3	0	0	2	4	0	16	0	3	1	1	0	0	0	0	0	0	0	0	2	2	0	1	0	0	EE
ES	0	-0	0	0	1	1	0	0	0	0	1	4	0	0	411	0	8	4	-0	0	0	0	0	0	2	0	0	0	0	0	-0	0	ES
FI	0	0	0	0	3	1	1	8	0	0	5	14	1	21	1	72	2	8	0	0	0	0	0	0	0	0	6	4	0	1	0	0	FI
FR	0	-0	1	-0	1	16	0	0	4	0	7	72	0	0	128	0	337	51	-0	0	0	0	2	0	14	0	0	0	1	0	0	0	FR
GB	0	-0	0	0	0	7	0	0	0	0	3	28	1	0	9	0	24	436	-0	0	0	0	11	0	0	-0	0	0	0	0	-0	0	GB
GE	0	1	0	10	1	0	2	0	0	0	0	0	-0	0	0	0	0	0	17	1	0	0	0	0	0	0	9	0	0	-0	0	0	GE
GL	0	0	0	0	0	0	0	0	0	0	0	0	-0	0	0	0	0	1	0	0	0	-0	0	3	0	0	0	0	0	0	-0	0	GL
GR	3	0	0	0	6	0	49	0	0	0	1	1	0	0	3	0	1	0	0	169	0	0	0	0	5	0	3	0	0	0	0	2	GR
HR	1	0	2	0	72	0	4	0	0	0	5	4	0	0	3	0	2	0	0	2	26	5	0	0	11	0	0	0	0	0	0	4	HR
HU	1	-0	4	0	63	0	13	1	0	0	10	7	0	0	2	0	2	1	-0	3	6	62	0	0	5	0	2	0	0	0	0	6	HU
IE	0	0	0	0	0	0	0	0	0	0	0	2	0	0	1	0	2	23	-0	0	0	0	31	0	0	-0	0	0	0	0	-0	0	IE
IS	0	0	0	0	0	0	0	0	0	0	0	1	0	0	0	0	0	3	0	0	0	0	0	103	0	0	0	0	-0	0	0	0	IS
IT	1	0	3	0	33	0	2	0	2	0	6	7	0	0	26	0	23	2	-0	2	5	1	0	0	268	0	1	0	0	0	-0	3	IT
KG	0	0	0	1	0	0	0	0	0	0	0	0	0	0	0	0	0	0	0	0	0	0	0	0	0	98	263	0	0	0	0	0	KG
KZT	0	1	0	16	8	0	8	5	0	1	3	5	0	2	1	1	1	1	2	3	0	0	0	0	1	54	4249	0	0	0	0	1	KZT
LT	0	-0	0	0	4	0	1	12	0	0	6	9	0	1	0	1	1	2	0	0	0	0	0	0	0	0	2	27	0	1	0	0	LT
LU	0	0	0	0	0	1	0	0	0	0	0	3	0	0	0	0	2	0	0	0	0	0	0	0	0	0	0	0	1	0	0	0	LU
LV	0	0	0	0	3	0	1	10	0	0	4	8	0	3	0	1	1	2	0	0	0	0	0	0	0	0	3	8	0	7	0	0	LV
MD	0	0	0	0	2	0	5	1	0	0	1	1	0	0	0	0	0	0	0	1	0	0	0	0	0	0	3	0	0	0	6	0	MD
ME	2	-0	0	0	6	0	1	0	0	-0	0	0	0	0	1	0	0	0	-0	1	0	0	0	0	2	-0	0	0	0	0	-0	36	ME
MK	2	0	0	0	2	0	12	0	0	0	0	0	0	0	1	0	0	0	0	27	0	0	0	0	1	-0	0	0	0	0	0	1	MK
MT	0	0	0	-0	0	0	0	0	0	0	0	0	0	0	0	0	0	0	-0	0	0	0	0	0	0	0	0	0	0	0	0	0	MT
NL	0	-0	0	0	0	21	0	0	0	0	2	35	0	0	1	0	12	19	-0	0	-0	0	0	0	0	0	0	0	0	0	0	0	NL
NO	0	0	0	0	3	2	1	3	0	0	6	22	2	2	2	3	4	27	0	0	0	0	1	1	0	0	1	1	0	0	0	0	NO
PL	0	0	3	0	33	3	5	20	1	0	84	109	2	1	3	1	8	13	0	2	2	6	0	0	4	-0	6	3	0	0	1	3	PL
PT	0	0	0	0	0	0	0	0	0	0	0	0	0	0	11	0	1	0	0	0	0	0	0	0	0	0	0	0	0	0	-0	0	PT
RO	1	0	1	0	48	0	94	2	0	0	7	7	0	0	3	0	2	2	0	16	2	7	0	0	5	0	14	0	0	0	4	11	RO
RS	3	0	1	0	65	0	38	0	0	0	4	3	0	0	2	0	1	0	0	12	2	5	0	0	4	0	2	0	0	0	0	29	RS
RUE	1	1	4	28	74	5	69	134	1	1	46	70	2	103	8	60	13	25	7	18	2	4	1	2	7	8	3869	15	0	4	2	11	RUE
SE	0	0	1	0	6	4	2	10	0	0	13	41	6	7	2	15	7	22	0	0	0	1	1	0	1	0	5	4	0	1	0	1	SE
SI	0	-0	2	0	9	0	1	0	0	0	2	2	0	0	1	0	1	0	-0	0	4	1	0	0	7	-0	0	0	0	0	-0	0	SI
SK	0	0	2	0	21	0	4	0	0	0	12	5	0	0	1	0	1	1	0	1	1	12	0	0	2	0	1	0	0	0	0	2	SK
TJ	0	0	0	0	0	0	0	0	0	0	0	0	-0	0	0	0	0	0	0	0	-0	0	-0	0	0	4	42	0	-0	-0	-0	0	TJ
TM	0	0	0	5	0	0	1	0	0	0	0	0	0	0	0	0	0	0	1	0	0	0	0	0	0	1	85	0	0	0	0	0	TM
TR	1	1	0	2	8	0	35	1	0	13	1	1	0	0	4	0	1	0	1	42	0	0	0	0	4	0	13	0	0	0	0	2	TR
UA	1	0	2	2	36	1	47	29	0	0	19	20	0	1	3	1	3	4	1	13	1	6	0	0	4	0	63	2	0	0	6	6	UA
UZ	0	0	0	3	1	0	1	0	0	0	0	0	-0	0	0	0	0	0	0	1	0	0	-0	0	0	11	197	0	0	0	0	0	UZ
ATL	0	0	1	0	9	15	6	13	1	0	21	85	2	15	154	23	55	347	-0	2	0	1	38	249	1	0	38	3	0	1	0	1	ATL
BAS	0	0	2	0	13	6	6	17	1	0	31	101	12	25	4	31	11	26	-0	1	0	1	1	0	1	0	6	10	0	3	0	1	BAS
BLS	1	0	1	3	23	0	74	4	0	2	4	4	0	0	2	0	1	1	5	24	1	1	0	0	3	0	38	0	0	0	1	6	BLS
MED	13	0	3	0	137	2	86	2	1	31	14	19	0	0	232	0	92	8	0	201	10	2	0	0	251	0	7	0	0	0	0	27	MED
NOS	0	0	2	0	10	39	5	8	1	0	38	203	12	2	19	1	95	411	0	1	0	2	8	3	1	0	3	2	1	0	0	1	NOS
AST	0	1	0	52	3	0	6	1	0	6	1	1	-0	0	1	0	0	0	2	6	0	0	-0	0	1	27	804	0	0	-0	0	1	AST
NOA	1	0	0	0	9	0	7	0	0	1	1	3	0	0	39	0	9	1	0	15	1	0	0	0	13	0	1	0	0	0	0	2	NOA
SUM	60	10	82	175	1083	209	958	454	40	60	634	1933	57	203	1104	217	833	1526	40	612	77	136	96	363	655	203	9787	89	8	21	22	191	SUM
EXC	45	8	73	120	880	146	769	409	36	21	526	1519	31	161	652	161	570	731	33	363	65	128	50	111	382	176	8888	73	6	16	20	151	EXC
EU	9	0	63	1	340	137	538	73	19	4	427	1367	26	50	623	94	533	663	0	226	51	106	48	2	341	0	58	50	6	11	5	38	EU
emis	63	9	80	156	1072	211	945	457	40	84	635	1940	57	204	1214	218	847	1538	38	718	78	136	97	353	653	238	11373	89	8	21	22	199	emis
	AL	AM	AT	AZ	BA	BE	BG	BY	CH	CY	CZ	DE	DK	EE	ES	FI	FR	GB	GE	GR	HR	HU	IE	IS	IT	KG	KZT	LT	LU	LV	MD	ME	

Table C.1 Cont.: 2014 country-to-country blame matrices for **oxidised sulphur** deposition.
Units: 100 Mg of S. **Emitters →, Receptors ↓.**

	MK	MT	NL	NO	PL	PT	RO	RS	RUE	SE	SI	SK	TJ	TM	TR	UA	UZ	ATL	BAS	BLS	MED	NOS	AST	NOA	BIC	DMS	VOL	SUM	EXC	EU	
AL	15	0	0	0	2	0	1	10	0	0	0	0	0	0	2	1	0	0	0	0	21	0	0	4	6	3	56	178	87	24	AL
AM	0	0	0	0	0	0	0	0	2	0	0	0	0	3	29	1	2	0	0	0	1	0	33	1	8	0	5	98	50	1	AM
AT	1	0	0	0	29	0	3	16	2	0	5	4	0	0	2	10	0	0	0	0	5	2	0	1	9	1	47	262	197	153	AT
AZ	0	0	0	0	0	0	0	0	16	0	0	0	0	12	19	5	9	0	0	0	1	0	50	1	7	0	13	203	130	2	AZ
BA	3	0	0	0	17	0	6	83	2	0	0	3	0	0	3	9	0	0	0	0	15	0	0	4	8	3	32	550	488	59	BA
BE	0	0	5	0	2	0	0	0	1	0	0	0	-0	0	0	1	0	2	0	0	1	11	0	0	4	2	5	132	106	104	BE
BG	43	0	0	0	10	0	39	39	29	0	0	2	0	2	156	67	3	0	0	12	22	0	1	7	14	3	70	933	803	441	BG
BY	4	0	0	0	147	0	14	25	94	0	0	6	0	2	20	175	3	1	3	1	4	2	1	2	15	3	32	803	741	223	BY
CH	0	0	0	0	1	0	0	0	0	0	0	0	-0	0	0	0	0	1	0	0	3	1	0	1	8	1	17	77	47	31	CH
CY	0	0	0	0	0	0	0	0	0	0	0	0	-0	0	15	0	0	0	0	0	4	0	2	1	1	1	3	32	20	4	CY
CZ	1	0	0	0	82	0	5	21	3	0	1	14	0	0	2	12	0	1	1	0	2	2	0	1	7	1	21	404	368	315	CZ
DE	1	0	22	0	164	0	4	14	14	1	1	5	0	0	5	33	0	9	18	0	8	46	0	4	41	17	140	1701	1418	1332	DE
DK	0	0	2	0	28	0	1	3	4	1	0	1	0	0	2	8	0	2	15	0	1	14	0	0	5	7	18	177	117	96	DK
EE	1	0	0	0	24	0	1	2	17	1	0	1	0	0	1	11	0	0	6	0	0	1	0	0	3	2	14	125	98	59	EE
ES	0	0	0	0	2	21	0	1	0	0	0	0	0	0	0	2	0	61	0	0	97	2	0	20	130	22	21	812	459	455	ES
FI	1	0	1	1	59	0	3	6	68	9	0	2	0	0	3	34	1	2	17	0	1	6	0	0	21	15	120	523	340	208	FI
FR	0	0	6	0	15	4	1	2	3	0	0	1	-0	0	1	4	0	66	1	0	100	38	0	26	104	51	60	1119	674	658	FR
GB	0	0	6	0	14	1	0	1	3	0	0	0	-0	0	2	6	0	56	2	0	3	48	0	1	39	39	79	823	556	542	GB
GE	2	0	0	0	1	0	1	2	10	0	0	0	0	7	72	10	5	0	0	2	3	0	26	2	12	1	15	213	153	8	GE
GL	0	0	-0	0	2	0	0	0	1	0	0	0	0	0	1	1	0	1	0	0	0	0	0	0	141	8	2051	2213	11	5	GL
GR	71	0	0	0	5	0	6	19	11	0	0	1	0	0	89	21	1	0	0	3	79	0	1	14	20	10	109	705	469	241	GR
HR	3	0	0	0	22	0	7	72	2	0	3	5	0	0	3	10	0	0	0	0	29	0	0	6	9	4	37	355	268	101	HR
HU	10	0	0	0	46	0	47	139	7	0	2	20	0	0	9	37	0	0	0	1	9	1	0	3	9	1	24	552	504	228	HU
IE	0	0	0	0	1	0	0	0	1	0	0	0	-0	0	0	1	0	21	0	0	0	3	0	0	13	20	27	149	64	62	IE
IS	0	0	0	0	2	0	0	0	0	0	0	0	0	0	0	1	0	5	0	0	0	1	0	0	18	17	8599	8753	113	8	IS
IT	3	1	0	0	20	1	3	25	2	0	5	3	0	0	4	10	0	3	0	0	202	1	0	47	58	26	384	1183	463	379	IT
KG	0	0	0	0	0	0	0	0	11	0	0	0	36	16	6	1	1068	0	0	0	0	0	64	0	31	0	16	1611	1499	0	KG
KZT	5	0	0	0	27	0	8	9	1029	0	0	2	27	292	129	236	1384	1	1	3	6	1	287	3	154	3	619	8596	7519	68	KZT
LT	1	0	0	0	76	0	2	7	19	1	0	2	0	0	6	25	1	0	4	0	1	2	0	0	5	2	16	239	209	132	LT
LU	0	0	0	-0	0	0	0	0	0	0	0	0	0	0	0	0	0	0	0	0	0	0	0	0	0	0	0	9	8	8	LU
LV	1	0	0	0	50	0	2	5	20	1	0	1	0	0	3	20	1	0	5	0	1	2	0	0	5	3	21	195	158	94	LV
MD	1	0	0	0	6	0	8	4	12	0	0	0	0	1	26	64	1	0	0	2	2	0	0	1	2	0	6	161	147	25	MD
ME	2	0	0	0	1	0	1	10	0	0	0	0	-0	0	0	1	0	0	0	0	8	0	0	2	3	1	18	99	66	8	ME
MK	120	0	0	0	1	0	1	13	1	0	0	0	0	0	4	3	0	0	0	0	4	0	0	2	3	1	19	221	191	44	MK
MT	0	0	0	-0	0	0	0	0	0	0	0	0	0	0	0	0	0	0	0	0	2	0	0	0	0	0	0	3	1	1	MT
NL	0	0	26	0	7	0	0	0	1	0	0	0	-0	0	0	1	0	2	1	0	1	32	0	0	5	4	18	190	128	124	NL
NO	1	0	2	25	45	0	2	5	20	5	0	1	0	0	6	17	0	13	10	0	1	26	0	0	41	52	563	920	214	131	NO
PL	5	0	2	0	1339	0	19	58	49	1	2	24	0	1	19	167	2	2	9	1	6	8	1	2	25	9	62	2127	2001	1638	PL
PT	0	0	0	0	0	57	0	0	0	0	0	0	0	0	0	0	0	40	0	0	2	0	0	1	37	7	4	162	69	69	PT
RO	29	0	0	0	46	0	372	115	57	0	1	7	0	3	167	218	4	0	0	15	20	1	2	6	23	3	74	1392	1247	572	RO
RS	54	0	0	0	16	0	39	464	7	0	0	4	0	0	13	26	1	0	0	1	11	0	0	4	10	2	43	868	797	131	RS
RUE	30	0	4	3	442	0	75	98	13538	13	2	19	7	176	541	1817	488	14	32	26	29	17	170	13	1041	160	4211	27562	21848	1011	RUE
SE	1	0	4	5	130	0	5	12	50	48	0	4	0	0	8	51	1	5	38	0	1	26	0	1	33	23	197	796	472	320	SE
SI	1	0	0	0	7	0	2	12	1	0	14	1	0	0	1	4	0	0	0	0	9	0	0	2	3	1	9	98	74	46	SI
SK	3	0	0	0	57	0	14	42	4	0	1	48	0	0	3	20	0	0	0	0	3	0	0	1	5	1	13	285	261	163	SK
TJ	0	0	0	0	0	-0	0	0	4	0	0	0	102	26	5	0	349	0	0	0	0	0	38	0	33	0	6	610	532	0	TJ
TM	1	0	0	0	1	0	0	0	28	0	0	0	5	239	27	11	211	0	0	0	1	0	139	1	41	0	25	822	615	3	TM
TR	17	0	0	0	7	0	12	18	44	0	0	1	0	5	4417	76	5	0	0	24	125	0	258	58	135	21	235	5594	4738	126	TR
UA	17	0	1	0	193	0	78	67	319	0	1	12	0	12	294	1694	18	1	2	23	19	2	11	9	44	4	96	3191	2979	415	UA
UZ	1	0	0	-0	1	-0	0	1	28	0	0	0	35	120	26	11	1170	0	0	0	1	0	96	1	38	0	31	1776	1608	4	UZ
ATL	5	0	12	33	141	25	7	13	329	13	0	5	0	1	27	71	4	1372	20	1	14	87	2	5	3792	3598	31944	42604	1769	973	ATL
BAS	3	0	5	2	346	0	9	23	97	22	1	8	0	1	13	100	2	4	126	1	3	27	1	1	29	33	163	1329	941	663	BAS
BLS	21	0	0	0	27	0	48	37	200	0	0	2	0	8	1189	393	11	0	1	123	41	1	32	18	45	5	160	2561	2136	197	BLS
MED	52	14	1	-0	67	5	24	94	29	0	4	7	0	1	1313	93	2	17	1	14	2965	4	128	578	400	449	1616	9017	2845	1073	MED
NOS	3	0	39	12	236	1	10	21	33	4	0	7	0	0	19	65	1	68	31	0	8	393	0	3	99	167	718	2808	1321	1140	NOS
AST	3	0	0	-0	5	0	2	3	193	0	0	0	28	252	289	71	590	0	0	2	36	0	3287	25	778	7	189	6676	2351	31	AST
NOA	6	1	0	0	7	2	3	10	3	0	0	1	0	0	50	9	0	6	0	1	211	1	6	374	289	30	135	1250	198	106	NOA
SUM	540	20	143	84	3980	120	891	1626	16417	121	45	225	240	1182	9041	5736	5338	1780	344	258	4141	808	4641	1256	7858	4847	53225	146845			SUM
EXC	448	4	86	37	3151	86	787	1423	15533	82	39	194	212	918	6142	4934	4729	313	166	118	862	295	1186	252	2426	558	18298		56126	10872	EXC
EU	175	3	78	8	2237	84	538	613	366	63	34	144	0	9	502	774	15	275	118	34	608	244	9	145	628	277	1590		11554	8546	EU
emis	507	23	145	83	4001	174	879	1636	18491	120	44	226	286	1646	10737	5804	6806	2262	345	263	4881	813	8445	2644	0	11090	59116	165260	75401	15385	emis
	MK	MT	NL	NO	PL	PT	RO	RS	RUE	SE	SI	SK	TJ	TM	TR	UA	UZ	ATL	BAS	BLS	MED	NOS	AST	NOA	BIC	DMS	VOL	SUM	EXC	EU	

Table C.2: 2014 country-to-country blame matrices for **oxidised nitrogen** deposition.
Units: 100 Mg of N. **Emitters →, Receptors ↓.**

	AL	AM	AT	AZ	BA	BE	BG	BY	CH	CY	CZ	DE	DK	EE	ES	FI	FR	GB	GE	GR	HR	HU	IE	IS	IT	KG	KZT	LT	LU	LV	MD	ME	
AL	10	0	1	-0	1	0	1	0	0	-0	0	1	0	0	3	0	2	0	0	18	1	1	0	0	13	0	0	0	0	0	0	1	AL
AM	0	14	0	12	0	0	0	0	0	0	0	0	0	0	0	0	0	0	2	0	0	0	0	0	0	0	1	0	0	0	0	0	AM
AT	0	0	87	0	1	3	1	1	10	0	19	103	1	0	3	0	15	5	0	0	5	7	0	0	37	0	0	0	1	0	0	0	AT
AZ	0	4	0	62	0	0	0	0	0	0	0	0	0	0	0	0	0	0	5	0	0	0	0	0	0	0	3	0	0	0	0	0	AZ
BA	1	0	7	-0	21	1	1	0	1	0	5	11	0	0	3	0	4	1	0	2	11	11	0	0	23	-0	0	0	0	0	0	3	BA
BE	0	0	1	0	0	27	0	0	1	0	1	21	1	0	3	0	37	21	0	0	0	0	1	0	1	0	0	0	2	0	0	0	BE
BG	2	0	2	0	1	0	116	1	0	0	2	6	0	0	3	0	3	1	0	34	1	5	0	0	8	0	1	0	0	0	2	1	BG
BY	0	0	5	0	1	3	3	62	1	0	11	41	4	1	2	3	8	9	0	2	2	8	0	0	9	0	2	10	0	3	2	0	BY
CH	0	0	3	0	0	2	0	0	41	0	1	25	0	-0	4	0	32	3	0	0	0	0	0	0	34	0	0	0	1	-0	0	0	CH
CY	0	0	0	0	0	0	0	0	0	3	0	0	0	0	0	0	0	0	0	0	0	0	0	0	0	0	0	0	0	0	0	0	CY
CZ	0	0	26	0	1	5	1	1	4	0	62	105	1	0	2	0	16	7	0	1	4	14	0	0	11	0	0	0	1	0	0	0	CZ
DE	0	0	49	0	0	81	1	3	38	0	58	850	13	0	23	1	219	115	0	1	2	8	5	0	37	0	0	1	20	1	0	0	DE
DK	0	0	2	0	0	7	0	1	1	0	3	45	8	0	2	0	14	28	0	0	0	1	1	0	1	0	0	1	1	0	0	0	DK
EE	0	0	1	0	0	2	0	5	0	0	2	14	2	5	1	6	3	4	0	0	0	1	0	0	1	0	0	4	0	4	0	0	EE
ES	0	0	1	-0	0	4	0	0	1	0	1	9	0	0	595	0	44	12	0	0	0	0	1	0	7	0	0	0	0	0	0	0	ES
FI	0	0	2	0	0	7	0	14	1	0	5	51	10	13	2	94	12	25	0	0	0	2	1	0	1	0	1	9	1	8	0	0	FI
FR	0	0	6	0	0	54	0	1	21	0	6	148	2	0	233	0	737	128	0	0	1	1	7	0	67	0	0	0	11	0	0	0	FR
GB	0	0	2	0	0	21	0	1	1	0	3	63	7	0	16	0	76	383	0	0	0	1	25	0	3	0	0	0	2	0	0	0	GB
GE	0	5	0	21	0	0	1	0	0	0	0	1	0	0	0	0	0	0	28	1	0	0	0	0	1	0	1	0	0	0	0	0	GE
GL	-0	-0	0	-0	-0	1	-0	0	0	-0	0	6	1	0	0	0	2	6	-0	-0	-0	0	0	1	-0	-0	-0	0	0	0	0	-0	GL
GR	3	0	1	0	1	0	23	0	0	0	1	3	0	0	5	0	3	1	0	154	1	2	0	0	15	0	0	0	0	0	0	1	GR
HR	1	0	14	-0	7	1	2	0	1	0	7	15	0	0	5	0	6	1	0	2	22	15	0	0	52	-0	0	0	0	0	0	1	HR
HU	1	0	20	0	6	2	6	1	2	0	13	30	0	0	3	0	7	3	0	4	10	54	0	0	26	0	0	0	0	0	1	1	HU
IE	0	0	0	-0	0	2	0	0	0	-0	0	6	1	0	2	0	9	42	0	0	0	0	18	0	0	-0	0	0	0	0	0	0	IE
IS	-0	-0	0	-0	-0	1	-0	0	0	-0	0	5	1	0	0	0	2	10	-0	-0	0	0	1	8	-0	-0	-0	0	0	0	0	-0	IS
IT	1	0	26	-0	3	2	1	0	13	0	7	34	0	0	51	0	76	5	0	3	14	7	0	0	899	0	0	0	1	0	0	1	IT
KG	0	0	0	1	0	0	0	0	0	0	0	0	0	0	0	0	0	0	0	0	0	0	0	0	0	52	48	0	0	0	0	0	KG
KZT	0	7	3	33	0	2	3	9	1	0	3	18	2	1	4	4	7	8	7	3	1	3	0	0	10	42	732	2	0	1	1	0	KZT
LT	0	0	2	0	0	2	1	12	1	0	5	27	4	1	1	2	5	6	0	0	1	3	0	0	2	0	0	9	0	3	0	0	LT
LU	0	0	0	0	0	1	0	0	0	0	0	3	0	0	0	0	5	1	0	0	0	0	0	0	0	-0	0	0	2	0	0	0	LU
LV	0	0	1	0	0	2	0	11	0	0	3	22	4	2	1	3	4	6	0	0	0	2	0	0	1	0	0	8	0	6	0	0	LV
MD	0	0	1	0	0	0	3	1	0	0	1	3	0	0	0	0	1	0	0	1	0	1	0	0	1	0	1	0	0	0	2	0	MD
ME	2	0	0	-0	1	0	0	0	0	0	0	1	0	0	1	0	1	0	0	2	0	1	0	0	6	0	0	0	0	0	0	6	ME
MK	2	0	0	0	0	0	4	0	0	0	0	1	0	0	1	0	1	0	0	30	0	1	0	0	3	-0	0	0	0	0	0	0	MK
MT	0	0	0	0	0	0	0	0	0	0	0	0	0	0	0	0	0	0	0	0	0	0	0	0	0	0	0	0	0	0	0	0	MT
NL	0	0	1	0	0	20	0	0	1	-0	1	35	1	0	3	0	29	36	0	0	0	0	1	0	1	-0	0	0	1	0	0	0	NL
NO	0	0	2	0	0	10	0	5	1	0	5	56	18	1	3	7	21	64	0	0	0	1	4	0	1	-0	0	2	1	2	0	0	NO
PL	0	0	26	0	4	19	3	22	6	0	73	282	15	1	7	3	43	40	0	2	7	30	2	0	22	0	1	7	3	2	2	1	PL
PT	0	0	0	-0	0	0	0	0	0	0	0	1	0	0	31	0	3	1	0	0	0	0	0	0	1	-0	0	0	0	0	0	0	PT
RO	2	0	9	1	4	2	47	3	2	0	9	27	1	0	5	0	8	5	1	17	4	21	0	0	23	0	2	1	0	0	8	2	RO
RS	3	0	5	0	7	1	18	0	1	0	6	13	0	0	3	0	4	2	0	19	4	15	0	0	15	0	0	0	0	0	1	5	RS
RUE	1	7	23	49	3	28	22	184	7	0	38	244	33	43	19	135	65	87	21	15	7	27	4	2	45	5	608	43	4	33	8	1	RUE
SE	0	0	5	0	0	19	1	15	2	0	11	117	36	6	5	32	32	61	0	0	1	5	3	0	3	0	1	9	2	7	0	0	SE
SI	0	0	13	-0	1	0	0	0	1	0	3	8	0	0	1	0	3	0	0	0	6	3	0	0	26	0	0	0	0	0	0	0	SI
SK	0	0	8	0	3	1	2	1	1	0	11	20	0	0	2	0	4	2	0	1	4	21	0	0	10	0	0	0	0	0	0	0	SK
TJ	0	0	0	1	0	0	0	0	0	0	0	0	0	0	0	0	0	0	0	0	0	0	0	0	0	2	8	0	0	0	0	0	TJ
TM	0	2	0	12	0	0	0	0	0	0	0	1	0	0	0	0	0	0	2	0	0	0	0	0	1	1	21	0	0	0	0	0	TM
TR	1	7	3	5	1	1	18	2	1	8	2	7	0	0	10	0	6	2	4	40	1	3	0	0	16	0	2	0	0	0	1	0	TR
UA	1	1	13	4	3	5	23	32	2	0	19	66	4	1	6	2	14	13	3	12	4	23	1	0	21	0	12	5	1	2	11	1	UA
UZ	0	2	0	8	0	0	0	0	0	0	0	1	0	0	0	0	0	1	2	1	0	0	0	0	1	8	45	0	0	0	0	0	UZ
ATL	-0	0	9	-1	-0	88	1	19	5	-0	19	294	58	8	216	53	280	773	-0	1	0	5	102	42	5	0	2	9	9	7	0	0	ATL
BAS	0	0	11	0	1	25	2	23	4	0	24	222	36	12	8	40	45	65	0	1	2	9	3	0	7	0	1	17	3	14	1	0	BAS
BLS	1	2	5	6	2	1	35	6	1	1	4	16	1	0	5	1	6	4	17	22	2	6	0	0	15	0	5	1	0	0	4	1	BLS
MED	14	0	38	-0	16	15	45	3	15	20	20	100	1	0	480	1	318	34	0	219	32	22	2	0	832	0	1	1	3	0	2	6	MED
NOS	0	0	14	0	0	89	2	12	6	0	30	371	60	1	38	3	236	664	0	1	1	10	33	1	10	0	0	5	8	2	1	0	NOS
AST	0	7	1	74	0	1	2	1	0	6	1	4	0	0	4	1	3	2	7	7	0	1	0	0	7	18	129	0	0	0	0	0	AST
NOA	1	0	5	0	1	3	5	1	3	1	2	15	0	0	111	0	43	7	0	26	2	3	0	0	60	0	0	0	0	0	0	1	NOA
SUM	48	60	454	287	92	565	392	456	197	40	499	3569	329	98	1929	394	2516	2693	99	645	157	353	220	56	2393	128	1630	146	83	98	49	35	SUM
EXC	31	51	372	207	72	343	302	390	163	12	399	2546	172	77	1067	296	1584	1144	75	368	117	299	80	12	1457	110	1492	114	59	74	40	27	EXC
EU	10	1	306	2	34	288	205	93	106	3	307	2045	109	28	1004	144	1415	938	2	222	85	204	68	1	1258	0	8	51	51	32	15	8	EU
emis	57	72	460	308	95	600	406	489	209	52	519	3726	345	101	2267	418	2695	2889	109	738	168	365	234	63	2405	169	2093	156	86	107	54	38	emis
	AL	AM	AT	AZ	BA	BE	BG	BY	CH	CY	CZ	DE	DK	EE	ES	FI	FR	GB	GE	GR	HR	HU	IE	IS	IT	KG	KZT	LT	LU	LV	MD	ME	

Table C.2 Cont.: 2014 country-to-country blame matrices for **oxidised nitrogen** deposition.
Units: 100 Mg of N. **Emitters →, Receptors ↓.**

	MK	MT	NL	NO	PL	PT	RO	RS	RUE	SE	SI	SK	TJ	TM	TR	UA	UZ	ATL	BAS	BLS	MED	NOS	AST	NOA	BIC	DMS	VOL	SUM	EXC	EU	
AL	4	0	0	0	1	0	1	4	0	0	0	0	0	0	1	0	0	0	0	0	22	0	0	0	3	-0	0	89	63	42	AL
AM	0	0	0	0	0	0	0	0	1	0	0	0	0	0	15	0	0	0	0	0	1	0	4	0	4	-0	0	55	46	1	AM
AT	0	0	3	0	17	0	3	3	1	0	10	4	0	0	0	3	0	1	1	0	6	5	0	0	1	-0	-0	360	346	326	AT
AZ	0	0	0	0	0	0	0	0	13	0	0	0	0	3	9	1	2	0	0	0	1	0	9	0	5	-0	0	120	105	2	AZ
BA	1	0	1	0	10	0	4	14	1	0	1	5	0	0	1	3	0	0	0	0	16	1	0	0	2	-0	-0	166	146	101	BA
BE	0	0	12	0	2	0	0	0	0	0	0	0	0	0	0	0	0	4	1	0	1	20	0	0	4	0	0	163	133	131	BE
BG	8	0	1	0	7	0	33	15	21	0	0	2	0	0	73	28	0	0	0	12	23	1	0	1	7	-0	0	426	381	227	BG
BY	1	0	5	2	91	0	14	5	92	4	1	8	0	0	6	79	0	2	11	1	4	10	0	0	6	-0	0	538	504	249	BY
CH	0	0	2	0	0	0	0	0	0	0	0	0	0	0	0	0	0	1	0	0	3	2	0	0	2	-0	0	157	149	107	CH
CY	0	0	0	0	0	0	0	0	0	0	0	0	0	0	5	0	0	0	0	0	4	0	0	0	1	-0	-0	15	10	4	CY
CZ	0	0	5	0	52	0	4	5	2	1	4	11	0	0	1	4	0	1	3	0	3	7	0	0	3	-0	0	374	356	336	CZ
DE	0	0	91	4	93	2	4	3	9	4	3	6	0	0	1	9	0	18	31	0	11	123	0	0	27	0	1	1969	1757	1689	DE
DK	0	0	11	2	16	0	1	0	4	3	0	1	0	0	0	3	0	3	17	0	1	33	0	0	3	0	0	217	160	148	DK
EE	0	0	2	1	16	0	1	0	17	4	0	1	0	0	0	4	0	1	14	0	0	5	0	0	1	-0	0	123	102	73	EE
ES	0	0	4	0	1	76	0	0	0	0	0	0	0	0	0	1	0	65	0	0	119	8	0	2	65	0	0	1017	759	757	ES
FI	0	0	11	8	39	0	2	1	65	31	0	2	0	0	1	11	0	5	52	0	1	29	0	0	10	-0	0	527	430	329	FI
FR	0	0	37	1	9	16	1	0	1	1	1	1	0	0	0	1	0	81	3	0	107	106	0	2	49	0	1	1846	1496	1470	FR
GB	0	0	31	3	10	3	1	0	2	2	0	1	0	0	0	2	0	55	8	0	3	107	0	0	24	1	1	861	662	651	GB
GE	0	0	0	0	1	0	1	0	8	0	0	0	0	1	32	2	1	0	0	2	2	0	3	0	6	-0	0	121	107	7	GE
GL	0	-0	2	2	2	0	-0	0	1	1	0	0	-0	-0	0	0	-0	2	2	0	0	5	-0	-0	90	-0	0	126	27	22	GL
GR	13	0	0	0	3	0	6	6	7	0	0	1	0	0	50	8	0	1	0	4	88	0	0	2	10	-0	0	415	311	220	GR
HR	1	0	1	0	14	0	5	12	1	0	7	6	-0	0	1	3	0	0	0	0	30	1	0	0	3	-0	0	240	204	176	HR
HU	2	0	2	0	36	0	30	29	4	0	6	22	0	0	3	16	0	1	1	1	10	3	0	0	3	-0	-0	359	341	275	HU
IE	0	0	3	0	1	0	0	0	0	0	0	0	-0	0	0	0	0	16	1	0	0	10	0	0	7	0	0	121	86	85	IE
IS	0	-0	2	2	1	0	-0	0	0	1	0	0	-0	-0	0	0	-0	5	1	0	0	6	-0	-0	8	0	0	57	36	25	IS
IT	1	1	2	0	11	3	3	4	1	0	17	4	0	0	1	3	0	4	1	0	212	3	0	4	30	0	1	1453	1198	1169	IT
KG	0	0	0	0	0	0	0	0	4	0	0	0	32	3	2	0	191	0	0	0	0	0	12	0	14	-0	0	363	337	2	KG
KZT	1	0	3	3	17	0	6	2	825	2	1	2	29	61	48	67	244	4	5	3	6	7	58	0	86	-0	1	2384	2214	103	KZT
LT	0	0	3	1	46	0	2	1	20	3	1	3	0	0	2	11	0	1	12	0	1	8	0	0	1	-0	0	204	180	132	LT
LU	0	0	1	0	0	0	0	0	0	0	0	0	-0	0	0	0	0	0	0	0	0	1	0	0	0	0	0	16	14	14	LU
LV	0	0	3	1	32	0	2	1	22	5	0	2	0	0	1	8	0	1	15	0	1	8	0	0	1	-0	0	185	158	112	LV
MD	0	0	0	0	5	0	8	1	11	0	0	1	0	0	7	28	0	0	0	3	2	0	0	0	1	-0	0	84	77	26	MD
ME	0	0	0	0	1	0	0	2	0	0	0	0	0	0	0	0	0	0	0	0	8	0	0	0	1	-0	0	36	26	14	ME
MK	19	0	0	0	1	0	1	5	1	0	0	0	0	0	3	1	0	0	0	0	5	0	0	0	2	-0	0	84	76	44	MK
MT	0	0	0	0	0	0	0	0	0	0	0	0	0	0	0	0	0	0	0	0	1	0	0	0	0	0	0	2	1	1	MT
NL	0	0	25	0	3	0	0	0	1	0	0	0	-0	0	0	0	0	5	2	0	1	33	0	0	5	0	0	209	163	160	NL
NO	0	0	15	51	26	1	1	1	13	27	0	1	0	0	1	5	0	15	28	0	1	70	0	0	19	0	0	482	348	270	NO
PL	1	0	26	3	487	1	19	13	43	7	6	34	0	0	5	73	0	6	35	1	8	44	0	0	11	-0	1	1448	1341	1166	PL
PT	0	0	0	0	0	79	0	0	0	0	0	0	0	0	0	0	0	41	0	0	4	1	0	0	19	0	-0	182	116	116	PT
RO	5	0	2	0	34	0	198	32	42	1	2	10	0	0	54	95	1	1	1	15	20	4	0	0	9	-0	0	731	680	426	RO
RS	12	0	1	0	12	0	27	72	4	0	1	6	0	0	5	9	0	0	0	1	11	1	0	0	4	-0	-0	292	273	153	RS
RUE	4	0	41	33	263	2	57	16	6102	57	6	23	6	31	161	563	64	35	124	26	30	98	31	1	611	-2	5	10199	9239	1364	RUE
SE	0	0	28	25	88	1	4	2	43	85	1	5	0	0	2	17	0	10	100	0	2	97	0	0	16	-0	1	900	674	566	SE
SI	0	0	0	0	4	0	1	2	0	0	17	1	0	0	0	1	0	0	0	0	9	0	0	0	1	-0	0	106	96	90	SI
SK	1	0	1	0	38	0	11	10	2	0	3	24	0	0	1	9	0	0	1	0	4	2	0	0	2	-0	0	203	194	165	SK
TJ	0	0	0	0	0	0	0	0	2	0	0	0	83	7	2	0	64	0	0	0	0	0	18	0	15	-0	0	204	170	1	TJ
TM	0	0	0	0	1	0	0	0	24	0	0	0	6	61	12	3	53	0	0	0	1	0	41	0	27	-0	-0	272	202	6	TM
TR	3	0	1	0	6	1	11	5	36	0	1	1	0	1	1086	30	1	2	0	29	133	1	23	8	78	-0	0	1597	1323	138	TR
UA	3	0	7	2	143	0	75	14	283	3	3	18	0	2	96	551	3	3	8	25	20	12	2	1	23	-0	1	1601	1507	482	UA
UZ	0	0	0	0	1	0	0	0	27	0	0	0	37	33	11	3	216	0	0	0	1	0	31	0	24	-0	-0	456	399	7	UZ
ATL	0	-0	113	173	91	67	2	2	183	64	1	5	0	0	3	23	0	842	97	0	17	408	0	0	2032	12	5	6144	2731	2280	ATL
BAS	0	0	37	11	165	1	8	4	73	46	2	9	0	0	3	32	0	9	138	1	4	95	0	0	10	0	1	1223	966	811	BAS
BLS	3	0	2	1	18	0	40	10	178	1	1	3	0	1	390	142	1	1	2	77	42	3	3	2	17	-0	0	1108	960	189	BLS
MED	12	13	13	2	40	22	25	24	21	1	18	11	0	0	414	36	0	36	3	19	2312	23	14	57	194	1	5	5555	2890	2324	MED
NOS	0	0	116	38	122	6	7	4	23	24	1	8	0	0	4	21	0	97	78	0	10	454	0	0	54	3	1	2673	1976	1864	NOS
AST	1	0	1	1	4	0	2	1	130	0	0	1	29	56	137	18	99	1	1	2	51	1	453	5	465	-0	-0	1738	758	48	AST
NOA	2	2	2	0	5	8	4	3	4	0	1	2	0	0	27	5	0	10	0	1	360	4	1	49	235	-0	-0	1017	358	310	NOA
SUM	98	17	668	374	2086	293	626	328	8370	382	119	245	222	264	2680	1937	941	1388	800	230	3732	1863	704	136	4353	14	28	53608			SUM
EXC	79	3	384	149	1641	189	537	281	7759	245	95	206	193	206	1703	1658	840	393	482	128	937	875	232	23	1346	-2	15		29721	14183	EXC
EU	32	2	305	53	1060	184	331	140	311	149	80	140	0	1	203	311	2	322	300	36	670	659	1	12	315	1	7		12347	11014	EU
emis	99	20	715	426	2201	486	664	345	9450	411	120	258	274	408	3212	2029	1214	2117	824	241	4555	1959	1536	374	0	0	0	56429	44823	23611	emis
	MK	MT	NL	NO	PL	PT	RO	RS	RUE	SE	SI	SK	TJ	TM	TR	UA	UZ	ATL	BAS	BLS	MED	NOS	AST	NOA	BIC	DMS	VOL	SUM	EXC	EU	

Table C.3: 2014 country-to-country blame matrices for **reduced nitrogen** deposition.
Units: 100 Mg of N. **Emitters →, Receptors ↓.**

	AL	AM	AT	AZ	BA	BE	BG	BY	CH	CY	CZ	DE	DK	EE	ES	FI	FR	GB	GE	GR	HR	HU	IE	IS	IT	KG	KZT	LT	LU	LV	MD	ME	
AL	71	0	1	0	1	0	0	0	0	-0	0	1	0	0	3	0	2	0	0	7	0	1	0	0	10	0	0	0	0	0	0	1	AL
AM	0	56	0	37	0	0	0	0	0	0	0	0	0	0	0	0	0	0	9	0	0	0	0	0	0	0	1	0	0	0	0	0	AM
AT	0	0	212	0	1	2	0	1	19	0	27	183	1	0	2	0	16	3	0	0	4	15	0	0	58	0	0	0	0	0	0	0	AT
AZ	0	14	0	194	0	0	0	0	0	0	0	0	0	0	0	0	0	0	17	0	0	0	0	0	0	0	2	0	0	0	0	0	AZ
BA	1	0	7	0	75	0	1	0	1	0	5	9	0	0	4	0	3	0	0	1	21	17	0	0	22	0	0	0	0	0	0	1	BA
BE	-0	-0	1	-0	-0	131	-0	0	1	0	1	33	1	0	2	0	89	10	0	0	0	0	1	-0	1	0	0	0	6	0	0	-0	BE
BG	4	0	2	0	1	0	130	2	0	0	2	4	0	0	5	0	2	0	1	35	1	7	0	0	8	0	2	0	0	0	3	0	BG
BY	1	0	4	0	2	1	2	481	1	0	8	34	4	1	2	1	6	3	1	1	2	10	0	0	7	0	2	22	0	5	4	0	BY
CH	0	0	3	0	0	1	0	0	273	0	1	44	0	0	4	0	47	1	0	0	0	0	0	0	36	0	0	0	0	0	0	0	CH
CY	0	0	0	0	0	0	0	0	0	5	0	0	0	0	0	0	0	0	0	0	0	0	0	0	0	0	0	0	0	0	0	0	CY
CZ	0	0	37	0	1	3	0	2	5	0	210	148	1	0	2	0	14	4	0	0	4	20	1	0	11	0	0	1	0	0	0	0	CZ
DE	0	0	54	0	0	69	0	7	82	0	50	2971	19	0	17	0	279	53	0	0	2	9	9	0	34	0	0	3	15	1	1	0	DE
DK	0	0	1	0	0	4	0	3	1	0	2	91	138	0	1	0	14	12	0	0	0	1	2	0	1	0	0	1	0	0	0	0	DK
EE	0	0	1	0	0	1	0	9	0	0	1	11	2	33	1	2	2	1	0	0	0	1	0	0	1	0	0	7	0	7	0	0	EE
ES	0	0	1	0	0	3	0	0	1	-0	0	8	0	0	1434	0	80	5	0	-0	0	0	2	0	9	-0	0	0	0	0	0	-0	ES
FI	0	0	1	0	0	3	0	19	1	0	3	37	8	9	2	144	10	9	0	0	0	2	1	0	1	0	2	11	0	6	1	0	FI
FR	0	0	5	0	0	46	0	1	47	0	4	149	2	0	247	0	3101	56	0	0	0	1	13	0	75	0	0	1	6	0	0	-0	FR
GB	0	0	2	0	0	18	0	2	2	0	2	80	8	0	16	0	158	851	0	0	0	1	93	0	2	0	0	1	1	0	0	0	GB
GE	0	12	0	43	0	0	0	0	0	0	0	0	0	0	0	0	0	0	207	1	0	0	0	0	1	0	2	0	0	0	0	0	GE
GL	0	0	0	0	0	0	0	0	0	0	0	1	0	0	0	0	1	1	0	0	0	0	0	0	0	-0	0	0	0	0	0	0	GL
GR	10	0	1	0	1	0	10	1	0	0	1	2	0	0	6	0	3	0	0	180	1	3	0	0	11	0	1	0	0	0	1	0	GR
HR	1	0	15	0	12	0	1	1	1	0	7	12	0	0	5	0	5	0	0	1	68	29	0	0	48	-0	0	0	0	0	0	0	HR
HU	1	0	27	0	6	1	2	2	2	0	11	24	0	0	4	0	6	1	0	1	21	254	0	0	26	-0	0	0	0	0	1	0	HU
IE	0	-0	0	0	0	1	0	0	0	-0	0	7	1	0	2	0	18	42	0	0	0	0	328	-0	0	-0	0	0	0	0	0	0	IE
IS	0	0	0	0	0	0	0	0	0	0	0	2	0	0	0	0	2	4	0	0	0	0	1	15	0	-0	0	0	0	0	0	0	IS
IT	1	0	20	0	2	1	0	1	19	0	6	24	0	0	47	0	57	2	0	1	7	9	0	0	2050	0	0	0	0	0	0	0	IT
KG	0	0	0	2	0	0	0	0	0	0	0	0	0	0	0	0	0	0	0	0	0	0	0	0	0	136	51	0	0	0	0	0	KG
KZT	0	10	1	51	1	1	1	12	1	0	1	9	1	1	2	1	4	1	19	1	1	2	0	0	7	63	993	2	0	1	1	0	KZT
LT	0	0	2	0	1	1	0	43	1	0	4	23	4	0	1	0	5	2	0	1	1	4	0	0	2	0	0	97	0	6	1	0	LT
LU	0	0	0	0	-0	4	0	0	0	-0	0	7	0	0	0	0	12	0	0	0	0	0	0	-0	0	-0	0	0	5	0	0	0	LU
LV	0	0	1	0	0	1	0	30	0	0	2	18	4	3	1	1	5	3	0	0	0	2	0	0	2	0	1	30	0	44	0	0	LV
MD	0	0	1	0	0	0	1	1	0	0	0	2	0	0	1	0	0	0	0	1	0	1	0	0	1	0	1	0	0	0	24	0	MD
ME	5	0	0	0	2	0	0	0	0	0	0	1	0	0	1	0	1	0	0	1	0	1	0	0	5	0	0	0	0	0	0	8	ME
MK	8	0	0	0	0	0	0	0	0	0	0	1	0	0	2	0	1	0	0	14	0	1	0	0	2	-0	0	0	0	0	0	0	MK
MT	0	-0	0	0	0	0	0	0	0	-0	0	0	0	0	0	0	0	0	0	0	0	0	0	-0	0	-0	-0	0	0	0	0	0	MT
NL	-0	-0	0	-0	-0	47	-0	1	1	-0	1	112	2	0	2	0	44	18	0	-0	0	0	2	-0	1	0	-0	0	1	0	0	-0	NL
NO	0	0	2	0	0	5	0	7	1	0	4	55	21	1	3	3	22	33	0	0	0	2	6	0	1	0	0	3	0	1	0	0	NO
PL	0	0	20	0	3	8	1	61	6	0	71	306	18	1	6	1	37	16	0	1	7	38	3	0	18	0	1	15	1	2	4	0	PL
PT	0	0	0	0	-0	0	-0	0	0	0	0	1	0	0	52	0	4	0	0	-0	0	0	0	-0	1	0	0	0	0	0	0	-0	PT
RO	4	0	9	1	5	1	19	7	2	0	7	23	1	0	6	0	7	2	1	11	5	40	0	0	23	0	3	1	0	0	21	1	RO
RS	12	0	6	0	10	0	4	1	1	0	4	9	0	0	4	0	3	1	0	8	11	31	0	0	15	0	1	0	0	0	1	2	RS
RUE	3	10	14	75	6	10	13	320	7	1	23	165	22	28	17	64	52	27	89	7	6	29	4	0	37	8	685	59	1	32	13	1	RUE
SE	0	0	3	0	1	9	0	23	2	0	8	115	48	4	4	18	29	24	0	0	1	6	4	0	4	0	1	12	1	6	1	0	SE
SI	0	0	18	0	1	0	0	0	0	0	3	7	0	0	1	0	2	0	0	0	7	6	0	0	32	0	0	0	0	0	0	0	SI
SK	0	0	12	0	2	1	1	2	1	0	13	18	0	0	2	0	3	1	0	0	4	47	0	0	11	0	0	0	0	0	1	0	SK
TJ	0	0	0	1	0	-0	0	0	0	0	0	0	0	0	0	0	0	-0	0	0	0	0	-0	-0	0	4	7	0	-0	0	0	0	TJ
TM	0	3	0	14	0	0	0	0	0	0	0	0	0	0	0	0	0	0	4	0	0	0	0	-0	0	1	13	0	0	0	0	0	TM
TR	2	11	3	8	1	0	8	4	1	5	1	4	0	0	11	0	5	1	12	18	1	3	0	-0	14	0	3	0	0	0	2	0	TR
UA	2	1	11	4	3	2	12	78	2	0	13	53	3	0	7	1	10	5	6	6	4	30	1	0	18	0	11	7	0	2	28	1	UA
UZ	0	3	0	11	0	0	0	0	0	0	0	0	0	0	0	0	0	0	4	0	0	0	0	-0	0	16	35	0	0	0	0	0	UZ
ATL	0	0	6	0	1	42	1	24	5	0	10	193	38	4	238	20	618	534	0	1	1	4	318	29	9	0	5	9	3	4	1	0	ATL
BAS	0	0	6	0	1	11	1	43	4	0	16	304	102	16	7	36	40	23	0	1	2	10	4	0	7	0	1	33	1	18	1	0	BAS
BLS	2	2	3	8	2	0	22	12	1	1	2	10	0	0	6	0	4	1	45	11	2	6	0	0	14	0	7	1	0	0	7	1	BLS
MED	24	0	22	1	14	5	16	6	14	13	10	47	1	0	409	0	296	10	1	66	15	17	2	0	654	0	2	1	1	0	3	3	MED
NOS	0	0	9	0	1	91	1	22	7	0	20	586	140	1	32	1	505	473	0	1	1	9	59	0	6	0	1	7	3	2	1	0	NOS
AST	0	10	0	87	0	0	1	1	0	3	0	1	0	0	3	0	1	0	17	2	0	0	0	0	3	28	104	0	0	0	0	0	AST
NOA	2	0	2	0	1	1	2	1	2	0	1	6	0	0	86	0	37	2	0	6	1	2	0	0	37	0	0	0	0	0	0	0	NOA
SUM	159	132	547	542	159	523	252	1234	517	28	556	5949	595	105	2711	296	5662	2239	437	385	205	674	858	45	3338	255	1940	327	48	140	121	23	SUM
EXC	130	120	498	446	139	373	208	1124	483	12	496	4801	313	83	1930	238	4160	1195	372	298	183	626	475	16	2607	228	1819	275	40	114	107	18	EXC
EU	23	0	446	3	37	352	166	218	195	5	434	4411	261	51	1867	168	4002	1118	4	232	136	496	462	0	2430	0	14	181	38	74	34	3	EU
emis	171	125	552	472	166	546	256	1273	516	38	570	6092	604	107	3052	304	5827	2316	422	416	210	688	867	44	3240	283	2224	337	50	144	125	25	emis
	AL	AM	AT	AZ	BA	BE	BG	BY	CH	CY	CZ	DE	DK	EE	ES	FI	FR	GB	GE	GR	HR	HU	IE	IS	IT	KG	KZT	LT	LU	LV	MD	ME	

Table C.3 Cont.: 2014 country-to-country blame matrices for **reduced nitrogen** deposition.
Units: 100 Mg of N. **Emitters →, Receptors ↓.**

	MK	MT	NL	NO	PL	PT	RO	RS	RUE	SE	SI	SK	TJ	TM	TR	UA	UZ	ATL	BAS	BLS	MED	NOS	AST	NOA	BIC	DMS	VOL	SUM	EXC	EU	
AL	1	0	0	0	1	0	1	11	0	0	0	0	0	0	0	0	0	0	0	-0	-0	0	0	3	2	0	-0	119	114	28	AL
AM	0	0	0	0	0	0	0	0	1	0	0	0	0	1	116	0	0	0	0	0	0	0	39	1	3	0	0	266	223	1	AM
AT	0	0	3	0	9	0	3	4	1	0	19	8	0	0	1	3	0	0	0	0	0	0	0	0	3	0	0	601	596	567	AT
AZ	0	0	0	0	0	0	0	0	12	0	0	0	0	5	47	1	1	-0	0	0	0	0	28	1	3	0	-0	325	294	1	AZ
BA	0	0	0	0	6	0	6	19	1	0	1	5	0	0	1	3	0	0	0	0	1	0	0	2	3	0	0	218	211	108	BA
BE	-0	0	34	0	1	0	0	0	0	0	0	0	0	0	0	0	0	-0	0	0	0	-1	0	0	1	-0	-0	315	315	313	BE
BG	6	0	0	0	4	0	58	27	17	0	0	2	0	1	58	23	1	0	0	0	1	0	0	6	5	0	1	424	410	263	BG
BY	0	0	3	1	78	0	24	7	53	3	1	6	0	1	12	92	0	0	-0	0	0	0	0	1	5	0	-1	893	886	226	BY
CH	0	0	1	0	0	0	0	0	0	0	0	0	0	0	0	0	0	0	0	0	0	0	0	0	3	0	-0	417	413	139	CH
CY	0	0	0	0	0	0	0	0	0	0	0	0	0	0	5	0	0	0	0	0	-0	0	2	1	0	-0	-0	14	11	5	CY
CZ	0	0	4	0	32	0	5	6	2	1	4	19	0	0	1	3	0	0	0	0	0	0	0	0	2	0	0	546	542	522	CZ
DE	0	0	198	1	78	1	5	3	7	4	3	5	0	0	1	10	0	1	-3	0	1	-10	0	2	11	-0	-1	3994	3992	3879	DE
DK	0	0	14	1	12	0	1	1	2	5	0	1	0	0	1	3	0	0	-2	0	0	-3	0	0	2	-0	-0	313	316	305	DK
EE	0	0	1	0	13	0	1	1	7	3	0	1	0	0	1	4	0	0	-0	0	0	0	0	0	1	0	0	116	115	92	EE
ES	0	0	3	0	0	64	0	0	0	0	0	0	0	0	0	0	0	-5	0	-0	-7	1	0	10	43	-1	-1	1653	1614	1612	ES
FI	0	0	6	3	28	0	3	2	25	19	0	1	0	0	1	13	0	0	0	0	0	1	0	0	8	-0	1	384	373	306	FI
FR	-0	0	33	0	6	10	1	0	1	0	1	1	0	0	0	1	0	-7	0	0	2	-8	0	14	35	-3	-4	3840	3811	3759	FR
GB	0	0	31	0	9	2	0	0	2	2	0	1	0	0	1	3	0	-5	1	0	1	-3	0	1	12	-2	-1	1290	1287	1277	GB
GE	0	0	0	0	0	0	1	1	17	0	0	0	0	3	207	2	1	0	0	0	0	0	15	1	4	0	0	521	500	6	GE
GL	0	-0	0	0	1	0	0	0	0	0	0	0	-0	0	0	0	0	0	0	0	0	0	0	0	70	0	0	78	7	5	GL
GR	4	0	0	0	2	0	7	10	6	0	0	1	0	0	32	7	0	0	0	0	-1	0	0	15	7	0	-0	322	301	227	GR
HR	0	0	0	0	6	0	7	18	1	0	13	7	-0	0	1	3	0	0	0	0	1	0	0	3	3	0	0	273	264	225	HR
HU	1	0	1	0	11	0	48	45	4	0	8	30	0	0	3	8	0	0	0	0	0	0	0	1	3	0	-0	556	551	478	HU
IE	0	0	2	0	1	0	0	0	0	0	0	0	-0	0	0	0	0	-3	0	0	0	0	0	0	5	-3	-1	403	405	403	IE
IS	0	0	1	0	1	0	0	0	0	0	0	0	-0	0	0	0	0	0	0	0	0	0	0	0	6	0	0	34	27	11	IS
IT	0	1	1	0	6	2	3	4	1	0	12	4	0	0	1	2	0	1	0	0	-5	1	0	25	21	0	-2	2326	2286	2254	IT
KG	0	0	0	0	0	0	0	0	4	0	0	0	46	6	11	0	168	0	0	0	0	0	38	0	11	0	0	476	426	0	KG
KZT	0	0	1	0	10	0	6	3	410	1	0	1	35	114	169	41	212	0	0	0	1	0	247	2	52	0	2	2497	2192	58	KZT
LT	0	0	2	0	49	0	3	2	10	3	1	2	0	0	3	9	0	0	-0	0	0	0	0	0	2	0	-1	285	283	213	LT
LU	0	0	1	0	0	0	0	0	0	0	0	0	-0	0	0	0	0	-0	0	0	0	-0	0	0	0	0	-0	30	30	30	LU
LV	0	0	2	0	28	0	3	1	10	4	0	1	0	0	2	7	0	0	-0	0	0	0	0	0	2	0	-0	210	208	156	LV
MD	0	0	0	0	2	0	20	1	7	0	0	1	0	0	8	20	0	0	0	-0	0	0	0	0	1	0	0	98	96	33	MD
ME	0	0	0	0	1	0	1	7	0	0	0	0	0	0	0	0	0	0	0	0	0	0	0	1	1	0	0	39	36	12	ME
MK	23	0	0	0	1	0	1	14	1	0	0	0	0	0	1	1	0	0	0	0	0	0	0	1	1	0	0	76	73	24	MK
MT	-0	1	0	-0	0	0	0	0	0	0	0	0	-0	0	0	0	-0	0	-0	-0	-0	0	0	0	0	-0	-0	1	1	1	MT
NL	-0	0	307	0	2	0	0	0	0	0	0	0	-0	0	0	0	-0	-0	-0	-0	0	-4	-0	0	1	-0	-0	540	543	541	NL
NO	0	0	12	93	19	0	2	2	6	21	0	1	0	0	3	7	0	1	1	0	0	1	0	0	15	0	1	359	340	220	NO
PL	0	0	19	1	989	0	28	15	27	7	5	29	0	1	8	51	0	1	-0	0	1	2	0	1	8	1	-1	1840	1827	1647	PL
PT	-0	0	0	0	0	131	0	-0	0	0	0	0	0	0	0	0	0	-3	0	0	-0	0	0	0	14	-1	-0	201	190	190	PT
RO	2	0	1	0	17	0	675	43	31	0	2	9	0	1	55	61	1	0	0	-0	2	0	1	4	8	0	-0	1112	1097	858	RO
RS	5	0	0	0	6	0	38	308	4	0	1	5	0	0	4	7	0	0	0	0	1	0	0	3	3	0	-0	511	503	147	RS
RUE	3	0	20	9	180	1	83	26	5865	33	4	16	8	67	416	489	65	2	3	2	4	5	149	9	453	3	10	9753	9114	948	RUE
SE	0	0	22	15	66	0	7	4	23	196	1	4	0	0	4	20	0	1	-2	0	0	1	0	0	12	0	1	701	687	592	SE
SI	0	0	0	0	2	0	2	3	0	0	54	2	0	0	0	1	0	0	0	0	0	0	0	1	1	0	0	145	143	136	SI
SK	0	0	1	0	17	0	17	13	2	0	2	91	0	0	1	5	0	0	0	0	0	0	0	1	2	0	0	271	268	241	SK
TJ	0	0	-0	-0	0	-0	0	0	2	0	0	0	209	10	9	0	56	-0	0	0	0	-0	60	0	11	0	-0	370	299	0	TJ
TM	0	0	0	0	0	0	0	0	13	0	0	0	7	171	48	1	41	-0	0	0	0	0	51	1	14	0	-1	383	318	2	TM
TR	1	0	0	0	3	1	13	7	25	0	1	1	0	2	5002	25	1	0	0	-2	-5	0	151	56	47	-1	-11	5438	5202	95	TR
UA	2	0	4	0	88	0	132	20	160	2	2	15	0	5	151	923	3	0	0	-0	2	1	5	6	15	1	-2	1857	1830	428	UA
UZ	0	0	0	0	0	0	0	0	13	0	0	0	55	56	48	2	331	-0	0	0	0	0	46	0	13	0	-0	636	576	2	UZ
ATL	0	0	66	53	47	49	5	3	79	28	1	3	0	0	10	23	0	-16	5	0	2	8	1	3	1686	-6	8	4178	2488	2252	ATL
BAS	0	0	32	4	147	0	11	6	34	73	1	6	0	0	6	30	0	1	-8	0	1	-3	0	0	10	-2	-1	1043	1044	911	BAS
BLS	2	0	1	0	11	0	50	15	115	0	1	2	0	3	800	167	2	0	0	-5	3	0	16	15	15	0	1	1389	1342	151	BLS
MED	4	8	6	0	14	15	29	27	15	0	12	7	0	1	339	28	0	2	0	0	-38	2	81	356	141	-4	-1	2699	2159	1676	MED
NOS	0	0	235	26	81	3	9	5	14	26	1	5	0	0	7	23	0	-1	-2	0	2	-19	0	2	33	-3	3	2429	2415	2307	NOS
AST	0	0	0	0	2	0	2	1	80	0	0	0	41	107	319	9	73	-0	0	0	-3	0	4096	18	318	-1	-5	5322	897	20	AST
NOA	1	1	1	0	2	6	3	4	2	0	1	1	0	0	14	4	0	1	0	0	-7	0	2	490	113	-0	-3	830	232	200	NOA
SUM	60	11	1072	211	2088	290	1317	688	7116	435	157	295	401	558	7928	2139	959	-26	-7	-4	-35	-24	5032	1062	3262	-18	-9	65957			SUM
EXC	51	2	732	127	1783	216	1207	627	6776	307	140	271	360	446	6432	1855	883	-13	-2	1	4	-12	835	179	945	-3	-11		46146	23585	EXC
EU	15	2	689	23	1387	213	878	201	180	246	127	218	0	4	179	239	3	-17	-6	0	-2	-21	5	88	211	-8	-9		22466	21091	EU
emis	64	13	1102	212	2183	407	1337	708	7693	444	158	304	447	747	8935	2233	1180	0	0	0	0	0	8646	2478	0	0	0	71353	60229	32165	emis
	MK	MT	NL	NO	PL	PT	RO	RS	RUE	SE	SI	SK	TJ	TM	TR	UA	UZ	ATL	BAS	BLS	MED	NOS	AST	NOA	BIC	DMS	VOL	SUM	EXC	EU	

Table C.4: 2014 country-to-country blame matrices for $\mathbf{AOT40}_f^{\mathbf{uc}}$.
Units: ppb.h per 15% emis. red. of NO_x. **Emitters →, Receptors ↓.**

	AL	AM	AT	AZ	BA	BE	BG	BY	CH	CY	CZ	DE	DK	EE	ES	FI	FR	GB	GE	GR	HR	HU	IE	IS	IT	KG	KZT	LT	LU	LV	MD	
AL	451	0	34	1	38	1	45	5	5	0	22	45	2	0	73	3	75	9	0	116	45	44	2	0	293	0	3	2	1	1	2	AL
AM	1	293	2	467	1	0	4	2	1	2	1	4	0	0	16	1	8	1	74	6	1	2	0	0	12	1	34	0	0	0	1	AM
AT	1	0	323	0	4	1	7	9	35	0	84	285	4	1	42	6	140	15	0	4	29	38	4	1	202	0	2	3	2	1	1	AT
AZ	0	30	2	717	1	0	3	4	1	1	2	6	1	0	13	3	8	3	71	4	1	2	0	0	10	1	86	1	0	1	1	AZ
BA	8	0	69	0	340	1	20	9	6	0	49	85	3	1	49	5	66	8	0	16	195	117	2	1	206	0	2	3	1	2	1	BA
BE	0	0	1	0	0	-412	1	6	5	0	3	-40	7	1	39	5	206	18	0	1	0	1	9	2	10	0	1	4	-5	2	0	BE
BG	11	0	16	3	11	0	656	13	2	0	17	37	2	1	23	4	26	6	3	128	11	41	2	1	51	0	9	3	0	2	13	BG
BY	0	0	4	1	1	1	1	105	1	0	9	37	4	3	5	10	13	12	0	1	2	9	2	1	6	0	13	20	1	8	3	BY
CH	0	0	40	0	2	2	3	4	272	0	14	157	2	0	78	4	376	20	0	2	5	5	5	1	274	0	1	2	2	1	0	CH
CY	6	1	12	3	6	1	40	5	3	313	8	20	1	0	58	2	46	7	3	169	9	9	1	0	108	0	6	1	0	1	4	CY
CZ	1	0	91	1	6	-8	11	15	8	0	198	229	8	1	25	9	96	19	0	5	24	64	5	1	42	0	3	6	0	2	2	CZ
DE	0	0	23	0	1	-22	2	10	11	0	23	108	7	1	30	8	133	22	0	2	2	7	8	2	26	0	1	5	1	2	1	DE
DK	0	0	3	0	0	-3	1	13	1	0	4	32	-45	3	10	14	26	58	0	0	1	3	13	2	5	0	1	7	1	4	0	DK
EE	0	0	1	0	0	0	0	18	0	0	4	29	6	26	3	22	11	16	0	0	1	1	3	1	2	0	5	16	1	21	1	EE
ES	0	0	2	0	0	3	0	0	1	0	1	14	1	0	1067	1	128	15	0	0	1	1	5	1	14	0	0	0	1	0	0	ES
FI	0	0	1	0	0	-0	0	6	0	0	2	14	2	6	1	34	4	7	0	1	1	1	1	1	2	0	3	5	0	4	0	FI
FR	0	0	5	0	0	-4	1	3	14	0	4	67	3	1	137	3	657	41	0	1	1	2	13	2	46	0	0	2	3	1	0	FR
GB	0	0	1	0	0	-13	0	2	1	0	1	-4	7	1	17	7	40	-202	0	0	0	1	20	2	1	0	1	2	0	1	0	GB
GE	1	50	3	305	1	0	6	3	1	1	2	7	0	0	16	2	10	2	427	9	1	3	0	0	15	1	38	1	0	0	1	GE
GL	0	0	0	0	0	0	0	0	0	0	0	0	0	0	0	0	0	0	0	0	0	0	0	0	0	0	0	0	0	0	0	GL
GR	44	0	24	1	16	1	211	8	4	0	17	40	2	0	58	3	62	9	1	700	20	31	2	1	194	0	6	2	0	1	6	GR
HR	5	0	124	0	94	1	17	10	9	0	65	124	4	1	46	6	91	12	0	11	372	154	3	1	252	0	2	3	1	2	2	HR
HU	2	0	83	1	26	-1	31	16	7	0	68	126	5	1	25	7	59	13	1	9	74	364	3	1	73	0	4	4	1	2	4	HU
IE	0	0	0	0	0	-5	0	2	0	0	1	-1	4	1	8	4	39	39	0	0	0	0	38	1	1	0	0	1	0	1	0	IE
IS	0	0	0	0	0	0	0	0	0	0	0	1	1	0	2	6	7	21	0	0	0	0	4	26	0	0	0	0	0	0	0	IS
IT	2	0	80	0	13	2	7	4	28	0	26	90	2	0	128	3	268	19	0	9	45	28	3	1	860	0	1	2	1	1	1	IT
KG	0	4	3	19	1	0	3	2	1	0	2	7	0	0	20	1	11	3	5	4	1	2	0	0	13	364	305	1	0	0	0	KG
KZT	0	1	2	9	1	1	2	7	1	0	2	10	1	1	12	7	10	7	3	2	1	2	1	1	8	10	378	2	0	1	1	KZT
LT	0	0	4	0	1	1	1	59	1	0	11	52	10	4	6	14	19	19	0	1	2	8	4	1	5	0	5	67	1	16	2	LT
LU	0	0	2	0	0	-24	2	7	9	0	3	16	5	1	49	4	203	38	0	1	0	2	10	2	14	0	1	4	-359	2	1	LU
LV	0	0	3	0	0	1	1	39	1	0	7	40	8	9	5	17	15	21	0	1	1	4	3	1	4	0	5	37	1	38	1	LV
MD	1	0	7	4	4	1	24	23	1	0	13	36	4	1	12	5	21	10	2	14	6	18	2	1	23	0	17	7	0	2	96	MD
ME	76	0	40	0	94	1	32	7	5	0	27	57	3	1	67	4	66	7	1	39	61	65	2	0	253	0	3	2	1	2	1	ME
MK	90	0	26	1	18	0	152	7	3	0	24	46	2	0	52	4	44	6	1	125	20	55	2	1	121	0	4	2	1	1	4	MK
MT	5	0	26	0	10	3	13	3	7	0	12	55	2	0	197	3	241	25	0	36	16	13	4	1	397	0	1	2	1	1	1	MT
NL	0	0	2	0	0	-96	1	6	2	0	3	-70	12	1	21	8	77	13	0	1	0	2	9	2	5	0	1	4	0	2	0	NL
NO	0	0	1	0	0	1	0	3	0	0	2	16	5	2	6	9	11	23	0	0	0	1	4	1	2	0	1	2	0	2	0	NO
PL	1	0	16	1	4	-2	5	27	3	0	42	118	10	2	13	13	41	19	0	3	10	32	4	1	19	0	4	11	2	5	4	PL
PT	0	0	0	0	0	2	0	0	0	0	0	6	1	0	439	0	43	12	0	0	0	0	5	1	2	0	0	0	0	0	0	PT
RO	3	0	16	3	13	0	88	14	2	0	19	43	3	1	21	4	29	6	2	19	14	57	2	1	41	0	10	4	0	2	23	RO
RS	28	0	36	1	55	-0	106	10	4	0	36	65	3	1	36	4	41	6	1	42	49	122	2	1	94	0	5	2	1	1	4	RS
RUE	0	0	1	3	0	0	1	5	0	0	1	4	1	1	2	4	3	3	2	1	0	1	0	0	2	0	26	1	0	1	0	RUE
SE	0	0	1	0	0	0	0	6	0	0	3	20	7	3	4	15	8	25	0	1	1	3	4	1	3	0	1	4	0	3	0	SE
SI	1	0	244	0	10	1	10	9	13	0	73	177	4	1	44	6	108	14	0	6	173	63	3	1	300	0	2	3	1	2	1	SI
SK	1	0	41	1	15	-1	19	18	6	0	95	122	5	1	20	8	49	12	1	7	35	207	3	1	49	0	4	6	1	3	5	SK
TJ	0	4	2	17	1	0	2	1	1	0	1	4	0	0	15	1	7	1	4	3	1	1	0	0	10	39	112	0	0	0	0	TJ
TM	0	5	3	34	1	1	3	5	1	0	2	11	1	1	17	4	12	5	8	3	1	2	1	1	11	4	269	1	0	1	1	TM
TR	3	15	7	21	3	1	30	6	2	10	6	16	1	0	41	2	24	4	15	57	4	9	1	0	48	0	10	1	0	1	4	TR
UA	1	1	5	4	2	1	12	33	1	0	9	29	3	1	9	7	16	10	3	7	3	14	2	1	14	0	29	7	0	3	11	UA
UZ	0	3	3	18	1	1	2	5	1	0	2	9	1	1	15	4	11	5	5	3	1	2	1	1	10	14	347	1	0	1	1	UZ
ATL	0	0	0	0	0	-0	0	0	0	0	0	0	0	0	1	0	2	0	0	0	0	0	0	0	0	0	0	0	0	0	0	ATL
BAS	0	0	1	0	0	-1	0	9	0	0	3	20	3	4	3	12	9	20	0	0	1	2	4	1	2	0	1	8	0	7	0	BAS
BLS	0	1	1	4	1	0	10	5	0	0	2	4	0	0	3	1	4	2	11	6	1	2	0	0	6	0	6	1	0	1	3	BLS
MED	3	0	9	0	5	1	19	2	2	2	5	13	1	0	50	1	55	5	0	42	11	6	1	0	85	0	1	1	0	0	1	MED
NOS	0	0	0	0	0	-6	0	1	0	0	0	-0	2	0	4	2	11	-4	0	0	0	0	4	1	1	0	0	1	0	1	0	NOS
AST	1	3	2	22	1	0	4	2	1	6	1	5	0	0	14	1	8	2	3	10	1	1	0	0	13	16	102	0	0	0	0	AST
NOA	1	0	4	0	2	1	6	1	2	0	2	8	0	0	77	0	33	3	0	20	3	3	1	0	43	0	1	0	0	0	0	NOA
EXC	1	2	6	9	2	-1	8	7	2	1	5	18	1	1	38	5	34	5	4	9	4	7	2	1	24	5	74	2	0	1	1	EXC
EU	2	0	25	0	5	-7	30	9	7	1	19	58	4	2	171	9	150	8	0	26	14	25	7	1	93	0	2	5	1	3	3	EU
	AL	AM	AT	AZ	BA	BE	BG	BY	CH	CY	CZ	DE	DK	EE	ES	FI	FR	GB	GE	GR	HR	HU	IE	IS	IT	KG	KZT	LT	LU	LV	MD	

Table C.4 Cont.: 2014 country-to-country blame matrices for $\mathbf{AOT40}_f^{\mathbf{uc}}$.
Units: ppb.h per 15% emis. red. of NO_x. **Emitters →, Receptors ↓.**

	ME	MK	MT	NL	NO	PL	PT	RO	RS	RUE	SE	SI	SK	TJ	TM	TR	UA	UZ	ATL	BAS	BLS	MED	NOS	AST	NOA	BIC	DMS	VOL	EXC	EU	
AL	59	81	2	1	7	54	5	52	172	32	5	9	20	0	0	23	36	1	23	5	6	362	8	0	9	195	0	0	1876	960	AL
AM	1	1	0	0	1	5	1	7	2	102	1	0	1	0	28	311	22	18	5	1	10	29	1	154	6	245	0	0	1438	79	AM
AT	1	1	0	-1	13	86	3	22	11	36	11	54	23	0	0	9	28	0	39	9	2	42	13	0	2	181	0	0	1543	1391	AT
AZ	0	1	0	0	3	8	1	7	2	296	2	1	1	0	64	81	32	44	8	2	9	13	2	115	2	200	0	0	1515	80	AZ
BA	48	5	1	0	10	108	3	46	90	34	8	16	53	0	0	13	41	0	22	7	4	114	9	0	5	162	0	0	1743	1133	BA
BE	0	0	0	-134	22	23	3	4	1	25	9	0	2	0	0	2	10	0	66	6	0	14	-108	0	1	152	0	0	-169	-243	BE
BG	7	44	0	0	7	63	2	222	90	162	6	3	20	0	1	69	176	2	16	6	68	76	7	1	3	162	0	0	1969	1345	BG
BY	0	0	0	1	10	104	1	13	3	205	12	1	8	0	1	6	112	1	16	15	2	3	10	1	0	116	0	0	753	287	BY
CH	1	1	0	-5	9	27	6	6	3	14	7	4	3	0	0	4	9	0	51	5	1	47	7	0	2	202	0	0	1361	1041	CH
CY	3	9	1	1	4	17	4	31	14	73	3	4	5	0	1	701	62	1	19	3	34	866	5	15	21	271	0	0	1778	874	CY
CZ	1	2	0	-4	20	163	2	36	20	55	16	15	65	0	1	9	41	1	42	13	3	21	22	0	1	173	0	0	1305	1119	CZ
DE	0	0	0	-34	22	68	3	8	3	39	16	2	6	0	0	4	22	0	53	2	1	13	-3	0	1	164	0	0	575	457	DE
DK	0	0	0	-8	52	41	2	3	2	44	26	1	2	0	0	1	14	0	64	-67	0	3	-1	0	0	149	0	0	336	206	DK
EE	0	0	0	-1	11	43	0	3	0	62	28	0	2	0	0	1	19	0	18	32	0	1	12	0	0	73	0	0	359	239	EE
ES	0	0	0	1	3	3	178	1	0	2	1	0	0	0	0	0	1	0	132	1	0	113	6	0	4	326	0	0	1450	1440	ES
FI	0	0	0	-0	6	24	0	2	0	38	16	0	2	0	0	1	9	0	10	19	0	1	5	0	0	44	0	0	197	130	FI
FR	0	0	0	-13	12	19	10	3	1	13	6	1	1	0	0	1	6	0	107	6	0	59	-0	0	2	206	0	0	1068	1013	FR
GB	0	0	0	-23	21	9	4	1	0	15	9	0	1	0	0	1	5	0	90	6	0	2	-55	0	0	124	0	0	-70	-118	GB
GE	1	2	0	0	2	9	2	10	3	171	2	1	2	0	30	226	36	21	7	2	39	26	2	57	4	202	0	0	1421	103	GE
GL	0	0	0	0	0	0	0	0	0	0	0	0	0	0	0	0	0	0	1	0	0	0	0	0	0	19	0	0	2	1	GL
GR	10	84	2	1	7	43	4	79	72	81	5	6	15	0	1	101	90	1	24	5	31	428	8	1	10	213	0	0	2068	1535	GR
HR	7	3	0	-0	13	125	3	44	67	39	10	63	58	0	0	10	42	1	29	9	4	162	12	0	4	164	0	0	1896	1592	HR
HU	5	5	0	1	14	217	2	164	88	73	11	20	148	0	1	14	108	1	27	11	7	34	16	0	2	161	0	0	1880	1510	HU
IE	0	0	0	-6	15	5	1	1	0	8	6	0	0	0	0	1	3	0	113	6	0	1	6	0	0	117	0	0	170	138	IE
IS	0	0	0	-0	12	1	1	0	0	3	6	0	0	0	0	0	0	0	45	3	0	0	9	0	0	79	0	0	93	52	IS
IT	3	2	2	1	8	45	8	18	12	15	6	34	15	0	0	7	17	0	43	5	2	318	10	0	8	203	0	0	1818	1703	IT
KG	0	1	0	0	2	6	2	5	2	108	1	1	1	155	31	43	10	425	7	1	2	11	2	124	2	345	0	0	1566	88	KG
KZT	0	1	0	1	7	11	2	6	2	477	5	1	2	2	13	17	25	27	13	4	2	6	4	16	1	274	0	0	1082	100	KZT
LT	0	0	0	0	16	119	1	7	2	114	26	1	7	0	0	4	52	0	22	34	1	3	16	0	0	107	0	0	664	407	LT
LU	0	0	0	-56	21	35	4	7	1	28	10	0	2	0	0	2	13	0	62	7	0	16	-22	0	1	171	0	0	64	-23	LU
LV	0	0	0	0	15	71	1	4	1	76	28	1	4	0	0	2	33	0	21	37	1	2	15	0	0	88	0	0	497	322	LV
MD	2	2	0	1	10	113	1	136	10	244	9	2	12	0	2	45	415	3	18	10	32	28	10	1	1	171	0	0	1359	476	MD
ME	412	17	1	1	8	80	5	50	164	32	7	8	30	0	0	19	39	1	21	6	6	241	8	0	8	194	0	0	1791	911	ME
MK	15	568	1	1	6	60	4	80	242	53	5	5	24	0	1	39	58	1	17	5	13	123	7	1	7	175	0	0	1973	863	MK
MT	4	4	-239	2	6	28	11	18	10	12	4	10	7	0	0	12	15	0	58	4	3	542	11	0	19	242	0	0	979	887	MT
NL	0	0	0	-352	31	24	3	3	1	27	12	0	1	0	0	2	10	0	55	7	0	7	-146	0	0	132	0	0	-230	-313	NL
NO	0	0	0	1	64	17	1	1	0	16	19	0	1	0	0	1	5	0	27	8	0	2	17	0	0	76	0	0	220	129	NO
PL	1	1	0	-2	21	338	1	33	12	95	22	5	34	0	1	7	98	1	31	26	2	11	21	0	1	143	0	0	1076	795	PL
PT	0	0	0	1	2	1	616	0	0	1	1	0	0	0	0	0	0	0	241	1	0	20	4	0	1	298	0	0	1139	1132	PT
RO	5	6	0	0	8	94	2	582	54	154	7	3	28	0	1	36	227	2	17	7	34	36	8	1	1	155	0	0	1649	1084	RO
RS	38	60	0	-1	8	103	3	160	408	69	7	6	45	0	1	19	77	1	20	6	11	62	8	0	4	156	0	0	1759	969	RS
RUE	0	0	0	0	3	6	0	2	0	190	3	0	1	0	1	5	14	2	5	3	1	2	2	1	0	65	0	0	291	39	RUE
SE	0	0	0	-0	27	39	1	2	1	27	41	0	3	0	0	1	14	0	23	22	0	2	13	0	0	74	0	0	275	194	SE
SI	1	1	0	0	13	102	3	29	21	36	12	264	33	0	0	8	32	1	32	9	3	125	12	0	3	166	0	0	1828	1676	SI
SK	2	3	0	2	16	313	2	110	40	73	14	13	323	0	1	15	106	1	26	14	6	25	19	1	1	160	0	0	1767	1457	SK
TJ	0	1	0	0	1	3	2	3	1	65	1	0	1	641	64	44	6	356	4	1	1	10	1	251	2	351	0	0	1416	57	TJ
TM	0	1	0	1	5	11	2	6	2	301	3	1	2	16	201	34	27	223	12	3	3	8	3	78	1	363	0	0	1246	106	TM
TR	2	6	1	1	3	17	3	32	11	134	3	2	5	0	3	1090	86	3	12	2	58	160	3	47	14	321	0	0	1746	328	TR
UA	1	1	0	1	10	90	1	50	7	356	10	1	10	0	3	33	358	4	15	10	20	15	9	2	1	168	0	0	1174	315	UA
UZ	0	1	0	1	5	10	2	6	2	292	3	1	2	62	54	26	21	267	11	3	2	7	3	45	1	323	0	0	1218	96	UZ
ATL	0	0	0	-0	1	0	0	0	0	0	0	0	0	0	0	0	0	0	4	0	0	0	0	0	0	4	0	0	7	5	ATL
BAS	0	0	0	-3	14	42	1	2	1	31	25	0	2	0	0	1	13	0	20	-3	0	1	10	0	0	59	0	0	242	170	BAS
BLS	0	1	0	0	2	9	0	16	3	108	2	0	2	0	1	46	77	1	3	2	52	10	1	1	1	39	0	0	345	75	BLS
MED	2	3	1	0	2	10	4	12	7	17	1	4	3	0	0	41	18	0	14	1	8	202	3	2	6	68	0	0	445	342	MED
NOS	0	0	0	-10	14	4	1	0	0	6	5	0	0	0	0	0	1	0	24	0	0	1	-38	0	0	37	0	0	42	18	NOS
AST	0	1	0	0	1	4	1	4	2	92	1	0	1	19	33	123	12	56	5	1	3	51	1	365	4	276	0	0	574	83	AST
NOA	1	2	1	0	1	4	7	5	3	5	1	1	1	0	0	16	6	0	12	1	2	142	1	1	37	137	0	0	264	223	NOA
EXC	1	2	0	-1	7	23	8	15	6	186	5	2	5	7	9	48	33	20	18	4	5	22	3	10	1	136	0	0	656	229	EXC
EU	1	4	0	-10	14	69	37	52	14	44	14	8	17	0	0	11	40	0	61	10	5	68	2	0	2	169	0	0	990	831	EU
	ME	MK	MT	NL	NO	PL	PT	RO	RS	RUE	SE	SI	SK	TJ	TM	TR	UA	UZ	ATL	BAS	BLS	MED	NOS	AST	NOA	BIC	DMS	VOL	EXC	EU	

Table C.5: 2014 country-to-country blame matrices for $\mathbf{AOT40}_f^{\mathbf{uc}}$.
Units: ppb.h per 15% emis. red. of VOC. **Emitters →, Receptors ↓.**

	AL	AM	AT	AZ	BA	BE	BG	BY	CH	CY	CZ	DE	DK	EE	ES	FI	FR	GB	GE	GR	HR	HU	IE	IS	IT	KG	KZT	LT	LU	LV	MD	
AL	37	0	14	2	7	4	6	6	6	0	16	63	4	0	20	1	36	28	0	41	9	15	1	0	144	0	1	2	0	1	1	AL
AM	0	129	1	136	0	1	1	2	1	0	2	8	1	0	4	1	5	4	15	2	0	1	0	0	12	0	9	1	0	0	0	AM
AT	0	0	121	2	1	12	2	7	44	0	41	289	6	0	11	2	70	51	0	2	7	10	2	0	136	0	1	2	2	1	1	AT
AZ	0	8	2	330	0	1	1	4	1	0	2	12	1	0	4	1	7	7	18	2	1	1	0	0	12	0	18	1	0	1	0	AZ
BA	2	0	18	1	17	7	3	7	7	0	22	84	4	0	14	1	35	32	0	5	13	17	1	0	93	0	1	2	1	1	1	BA
BE	0	0	3	2	0	108	0	6	7	0	7	181	9	1	11	2	120	113	0	1	0	1	3	0	12	0	1	3	4	3	0	BE
BG	2	0	7	5	2	4	45	8	4	0	12	52	3	0	7	2	20	22	1	20	3	11	1	0	32	0	3	2	0	2	2	BG
BY	0	0	2	4	0	3	0	31	1	0	7	33	3	1	2	2	10	22	0	1	1	3	1	0	6	0	5	4	0	2	1	BY
CH	0	0	22	1	0	14	1	5	248	0	14	234	4	0	17	1	126	55	0	1	3	3	2	0	302	0	0	2	2	1	0	CH
CY	3	1	9	9	3	4	11	8	5	21	11	45	2	0	20	2	33	24	2	50	5	8	1	0	91	0	4	2	0	2	2	CY
CZ	1	0	32	3	2	15	2	9	11	0	106	221	9	0	7	2	52	52	0	2	5	16	2	0	40	0	1	3	2	2	1	CZ
DE	0	0	20	2	0	28	1	8	23	0	28	385	11	1	8	2	81	74	0	1	1	4	3	0	35	0	1	3	3	2	1	DE
DK	0	0	3	0	0	11	0	7	1	0	7	96	51	1	2	3	24	125	0	0	1	2	5	0	6	0	0	4	0	3	0	DK
EE	0	0	1	1	0	4	0	7	1	0	4	29	4	4	1	5	9	31	0	0	0	1	1	0	3	0	2	4	0	4	0	EE
ES	0	0	1	0	0	5	0	1	1	0	1	21	1	0	151	0	40	28	0	0	1	1	1	0	15	0	0	0	0	0	0	ES
FI	0	0	1	0	0	2	0	4	0	0	2	14	2	1	0	5	4	13	0	0	0	1	1	0	2	0	1	2	0	2	0	FI
FR	0	0	4	0	0	22	0	4	14	0	5	115	5	0	32	1	151	102	0	0	1	1	3	0	49	0	0	2	2	2	0	FR
GB	0	0	1	1	0	14	0	3	1	0	3	59	7	0	4	2	39	248	0	0	0	1	5	0	2	0	1	2	1	2	0	GB
GE	0	11	2	133	0	1	1	3	1	0	2	11	1	0	4	1	6	6	60	3	1	2	0	0	13	0	9	1	0	1	0	GE
GL	0	0	0	0	0	0	0	0	0	0	0	0	0	0	0	0	0	0	0	0	0	0	0	-0	0	0	0	0	0	0	0	GL
GR	10	0	12	4	4	5	17	7	5	0	15	63	4	0	18	2	35	29	1	130	6	13	1	0	103	0	3	2	1	2	2	GR
HR	2	0	36	2	7	9	3	8	11	0	32	130	5	0	14	2	50	43	0	4	30	22	2	0	151	0	1	2	1	2	1	HR
HU	1	0	26	3	3	9	4	10	9	0	31	114	6	0	8	2	36	39	0	3	8	54	2	0	53	0	2	3	1	2	1	HU
IE	0	0	1	1	0	7	0	2	0	0	2	29	4	0	2	1	22	116	0	0	0	0	12	0	1	0	0	1	0	1	0	IE
IS	0	0	0	0	0	1	0	0	0	0	0	5	1	0	1	0	5	16	0	0	0	0	1	0	0	0	0	0	0	0	0	IS
IT	1	0	37	1	3	10	2	5	27	0	24	139	4	0	37	1	96	49	0	4	12	11	2	0	853	0	1	2	1	1	1	IT
KG	0	1	1	13	0	1	0	2	1	0	1	8	0	0	3	1	5	4	1	1	0	1	0	0	9	80	109	1	0	0	0	KG
KZT	0	0	2	8	0	1	0	4	1	0	2	14	1	0	3	2	7	10	1	1	0	1	1	0	8	4	50	1	0	1	0	KZT
LT	0	0	3	1	0	5	0	15	1	0	9	44	8	1	2	2	13	40	0	0	1	4	2	0	5	0	2	14	0	4	0	LT
LU	0	0	5	1	0	65	1	7	10	0	11	283	8	1	12	2	123	89	0	1	0	1	2	0	18	0	1	4	35	3	0	LU
LV	0	0	2	1	0	4	0	11	1	0	7	35	7	1	1	3	11	36	0	0	1	2	1	0	4	0	2	6	0	8	0	LV
MD	0	0	5	5	1	3	3	9	2	0	9	43	4	0	4	2	15	24	1	3	2	6	1	0	17	0	5	3	0	1	7	MD
ME	10	0	12	1	8	5	4	5	6	0	16	65	4	0	18	1	33	26	0	12	8	13	1	0	114	0	1	2	1	1	1	ME
MK	13	0	9	3	3	5	13	6	4	0	14	57	3	0	13	1	25	23	0	89	4	13	1	0	59	0	2	2	0	1	1	MK
MT	3	0	15	1	3	9	5	5	11	0	14	99	4	0	55	2	88	52	0	15	6	8	2	0	297	0	1	2	1	1	1	MT
NL	0	0	4	2	0	56	0	6	3	0	8	207	10	1	7	2	74	119	0	1	0	2	3	0	7	0	1	3	2	2	0	NL
NO	0	0	1	0	0	2	0	1	0	0	2	17	4	0	1	1	6	24	0	0	0	1	1	0	2	0	0	1	0	1	0	NO
PL	0	0	10	3	1	8	1	11	4	0	30	108	10	1	4	2	27	43	0	1	3	11	2	0	18	0	2	4	1	2	1	PL
PT	0	0	0	0	0	3	0	0	0	0	0	9	1	0	73	0	20	22	0	0	0	0	1	0	4	0	0	0	0	0	0	PT
RO	1	0	7	4	2	4	7	7	3	0	12	53	4	0	6	2	19	24	1	5	3	10	1	0	27	0	3	2	0	1	3	RO
RS	3	0	12	3	6	6	8	7	5	0	18	74	4	0	10	1	27	30	0	11	7	22	2	0	49	0	2	2	1	2	1	RS
RUE	0	0	0	3	0	0	0	2	0	0	1	5	1	0	1	1	2	4	0	0	0	0	0	0	2	0	4	1	0	1	0	RUE
SE	0	0	1	0	0	3	0	3	0	0	3	22	6	1	1	2	7	31	0	0	0	1	1	0	3	0	1	2	0	2	0	SE
SI	1	0	83	2	2	11	2	8	16	0	39	187	6	0	13	2	61	49	0	3	22	15	2	0	226	0	1	2	1	1	1	SI
SK	1	0	18	3	3	8	3	10	7	0	36	103	6	0	6	2	31	36	0	3	5	31	2	0	36	0	2	3	1	2	2	SK
TJ	0	1	1	13	0	0	0	1	1	0	1	6	0	0	3	0	3	3	1	1	0	1	0	0	7	11	43	0	0	0	0	TJ
TM	0	1	2	27	0	1	1	4	1	0	3	16	1	0	4	2	8	10	2	1	1	1	0	0	12	2	46	1	0	1	0	TM
TR	1	5	4	17	1	2	5	5	2	1	6	26	1	0	11	1	15	12	4	14	2	4	1	0	35	0	4	2	0	1	1	TR
UA	0	0	3	9	1	3	2	10	2	0	8	34	3	1	3	2	12	20	1	2	1	4	1	0	12	0	8	3	0	2	1	UA
UZ	0	1	2	16	0	1	1	3	1	0	2	13	1	0	4	1	7	8	1	1	0	1	0	0	10	14	75	1	0	1	0	UZ
ATL	0	0	0	0	0	0	0	0	0	0	0	1	0	0	0	0	1	2	0	0	0	0	0	0	0	0	0	0	0	0	0	ATL
BAS	0	0	1	0	0	4	0	5	0	0	4	37	12	1	1	4	9	38	0	0	1	2	2	0	3	0	1	3	0	3	0	BAS
BLS	0	0	1	5	0	1	2	2	0	0	2	8	1	0	1	1	3	5	2	2	0	1	0	0	5	0	2	1	0	1	1	BLS
MED	1	0	5	1	1	2	3	2	3	0	5	24	1	0	15	0	22	12	0	16	3	3	1	0	67	0	1	1	0	0	0	MED
NOS	0	0	0	0	0	5	0	1	0	0	1	21	4	0	1	1	14	46	0	0	0	0	1	0	1	0	0	1	0	1	0	NOS
AST	0	1	1	14	0	1	1	2	1	0	2	8	0	0	4	0	5	4	1	4	1	1	0	0	11	3	17	0	0	0	0	AST
NOA	1	0	3	1	1	2	1	1	2	0	3	15	1	0	15	0	14	8	0	5	1	2	0	0	30	0	0	0	0	0	0	NOA
EXC	0	1	3	6	0	3	1	3	3	0	4	27	2	0	7	1	14	17	1	2	1	2	1	0	22	2	12	1	0	1	0	EXC
EU	1	0	11	1	1	11	3	5	8	0	14	101	6	1	29	2	52	60	0	5	3	6	2	0	86	0	1	2	1	2	1	EU
	AL	AM	AT	AZ	BA	BE	BG	BY	CH	CY	CZ	DE	DK	EE	ES	FI	FR	GB	GE	GR	HR	HU	IE	IS	IT	KG	KZT	LT	LU	LV	MD	

Table C.5 Cont.: 2014 country-to-country blame matrices for $\mathbf{AOT40}_f^{\mathbf{uc}}$.
Units: ppb.h per 15% emis. red. of VOC. **Emitters →, Receptors ↓.**

	ME	MK	MT	NL	NO	PL	PT	RO	RS	RUE	SE	SI	SK	TJ	TM	TR	UA	UZ	ATL	BAS	BLS	MED	NOS	AST	NOA	BIC	DMS	VOL	EXC	EU	
AL	6	11	0	7	4	53	2	19	33	25	5	3	11	0	0	13	13	0	0	0	0	7	1	0	1	168	0	0	675	509	AL
AM	0	0	0	1	1	7	1	3	1	44	1	0	1	0	2	28	6	1	0	0	0	1	0	8	0	71	0	0	435	58	AM
AT	0	0	0	21	5	78	1	9	4	27	6	13	11	0	0	5	12	0	0	1	0	1	2	0	0	156	0	0	1015	906	AT
AZ	0	0	0	2	2	12	1	3	1	100	2	0	1	0	4	14	12	3	0	0	0	0	0	16	0	134	0	0	594	78	AZ
BA	2	1	0	10	4	80	1	16	18	25	6	4	14	0	0	6	12	0	0	0	0	2	1	0	0	136	0	0	588	484	BA
BE	0	0	0	94	6	29	1	3	1	25	7	0	2	0	0	1	7	0	1	1	0	1	8	0	0	150	0	0	776	720	BE
BG	1	2	0	8	4	51	1	38	16	64	6	1	8	0	0	45	29	0	0	0	0	2	1	0	0	153	0	0	548	360	BG
BY	0	0	0	6	3	44	0	4	2	82	5	0	4	0	0	2	21	0	0	0	0	0	1	0	0	103	0	0	319	166	BY
CH	0	0	0	25	4	35	2	4	2	15	5	4	3	0	0	2	5	0	0	0	0	1	2	0	0	137	0	0	1164	881	CH
CY	1	2	0	6	3	36	3	24	10	59	4	3	7	0	0	233	30	0	0	0	1	11	1	3	2	265	0	0	799	425	CY
CZ	0	0	0	22	6	146	1	14	7	37	8	5	19	0	0	5	17	0	0	1	0	1	2	0	0	162	0	0	888	786	CZ
DE	0	0	0	51	6	72	1	5	2	31	9	1	5	0	0	3	13	0	1	1	0	1	4	0	0	164	0	0	929	837	DE
DK	0	0	0	30	14	50	1	2	2	30	23	1	3	0	0	0	7	0	1	4	0	0	7	0	0	137	0	0	517	454	DK
EE	0	0	0	7	2	27	0	1	1	38	8	0	2	0	0	1	5	0	0	1	0	0	1	0	0	69	0	0	209	152	EE
ES	0	0	0	8	1	5	22	1	0	4	2	0	1	0	0	0	1	0	1	0	0	5	1	0	1	113	0	0	316	306	ES
FI	0	0	0	3	1	17	0	1	1	23	4	0	2	0	0	1	4	0	0	0	0	0	0	0	0	36	0	0	113	78	FI
FR	0	0	0	34	5	23	2	2	1	14	5	1	1	0	0	1	4	0	1	1	0	2	4	0	0	127	0	0	611	568	FR
GB	0	0	0	32	4	17	1	1	0	12	7	0	1	0	0	1	5	0	1	1	0	0	6	0	0	101	0	0	477	449	GB
GE	0	0	0	1	1	11	1	3	1	62	2	0	1	0	2	23	10	1	0	0	0	1	0	6	0	85	0	0	396	75	GE
GL	0	0	0	0	0	0	0	0	0	0	0	0	0	0	0	0	0	0	0	0	0	0	0	0	0	-7	0	0	1	1	GL
GR	1	8	0	8	4	50	2	27	23	47	5	3	10	0	0	46	24	0	0	0	0	8	1	0	1	198	0	0	750	561	GR
HR	1	1	0	16	6	100	1	17	16	30	7	14	18	0	0	5	14	0	0	1	0	3	2	0	0	172	0	0	817	713	HR
HU	1	1	0	16	6	125	1	36	19	43	8	5	30	0	0	7	25	0	0	1	0	1	2	0	0	164	0	0	752	621	HU
IE	0	0	0	14	3	11	0	1	0	7	4	0	1	0	0	1	3	0	1	0	0	0	3	0	0	50	0	0	250	232	IE
IS	0	0	0	3	1	1	0	0	0	1	1	0	0	0	0	0	0	0	0	0	0	0	1	0	0	-12	0	0	39	36	IS
IT	0	1	1	16	5	58	3	11	7	19	5	15	9	0	0	5	10	0	1	0	0	8	2	0	1	215	0	0	1491	1405	IT
KG	0	0	0	1	1	6	1	2	1	42	1	0	1	21	2	5	4	93	0	0	0	0	0	4	0	35	0	0	424	49	KG
KZT	0	0	0	2	2	12	1	3	1	92	3	0	1	1	1	5	8	4	0	0	0	0	0	2	0	83	0	0	261	78	KZT
LT	0	0	0	9	4	61	0	3	1	46	9	1	5	0	0	2	11	0	0	1	0	0	1	0	0	98	0	0	331	245	LT
LU	0	0	0	78	7	37	1	4	1	27	8	0	2	0	0	1	9	0	1	1	0	1	6	0	0	158	0	0	859	793	LU
LV	0	0	0	9	4	42	0	2	1	36	9	0	3	0	0	1	7	0	0	1	0	0	1	0	0	81	0	0	260	196	LV
MD	0	0	0	7	5	60	1	20	4	80	6	1	5	0	0	18	46	0	0	0	0	1	1	0	0	138	0	0	427	243	MD
ME	21	2	0	8	4	58	2	16	24	23	5	3	10	0	0	9	12	0	0	0	0	4	1	0	1	142	0	0	565	437	ME
MK	1	35	0	8	4	48	1	22	38	32	5	2	10	0	0	23	17	0	0	0	0	3	1	0	0	146	0	0	608	429	MK
MT	1	2	117	14	4	47	5	16	8	22	5	5	7	0	0	8	12	0	1	0	0	34	2	0	2	298	0	0	978	894	MT
NL	0	0	0	140	7	35	1	3	1	25	8	0	2	0	0	2	8	0	1	1	0	0	9	0	0	147	0	0	754	698	NL
NO	0	0	0	5	7	10	0	0	0	8	5	0	1	0	0	0	1	0	0	0	0	0	1	0	0	18	0	0	105	85	NO
PL	0	0	0	13	6	206	1	13	5	52	10	2	14	0	0	4	25	0	0	1	0	0	2	0	0	144	0	0	660	545	PL
PT	0	0	0	5	1	3	146	0	0	2	1	0	0	0	0	0	0	0	4	0	0	1	1	0	0	88	0	0	295	290	PT
RO	0	1	0	8	4	60	1	70	12	58	6	1	8	0	0	21	31	0	0	0	0	1	1	0	0	137	0	0	493	341	RO
RS	2	4	0	11	5	74	1	35	70	38	6	2	15	0	0	12	19	0	0	0	0	1	1	0	0	147	0	0	604	427	RS
RUE	0	0	0	1	1	5	0	1	0	44	1	0	0	0	0	1	4	0	0	0	0	0	0	0	0	29	0	0	88	28	RUE
SE	0	0	0	8	3	23	0	2	1	16	10	0	2	0	0	1	5	0	0	1	0	0	1	0	0	39	0	0	160	130	SE
SI	0	0	0	18	5	91	1	12	8	28	7	70	13	0	0	5	13	0	0	1	0	3	2	0	0	181	0	0	1029	937	SI
SK	0	1	0	12	6	181	1	29	12	42	9	3	47	0	0	8	24	0	0	1	0	1	2	0	0	151	0	0	734	613	SK
TJ	0	0	0	1	1	4	0	1	1	31	1	0	1	75	3	5	3	50	0	0	0	0	0	10	0	23	0	0	275	36	TJ
TM	0	0	0	2	2	13	1	3	1	96	2	0	2	4	7	8	10	16	0	0	0	0	0	5	0	152	0	0	319	90	TM
TR	0	1	0	3	2	23	1	12	5	55	3	1	4	0	0	197	20	0	0	0	1	3	0	2	1	123	0	0	512	192	TR
UA	0	0	0	5	4	47	0	11	3	115	5	1	4	0	0	15	62	0	0	0	0	0	1	1	0	137	0	0	419	188	UA
UZ	0	0	0	2	2	11	1	3	1	83	2	0	1	16	3	5	7	57	0	0	0	0	0	4	0	126	0	0	363	76	UZ
ATL	0	0	0	0	0	0	0	0	0	0	0	0	0	0	0	0	0	0	0	0	0	0	0	0	0	1	0	0	6	6	ATL
BAS	0	0	0	11	4	34	0	2	1	24	13	0	2	0	0	1	5	0	0	2	0	0	2	0	0	66	0	0	228	187	BAS
BLS	0	0	0	1	1	9	0	5	1	33	1	0	1	0	0	27	13	0	0	0	0	0	0	0	0	42	0	0	142	53	BLS
MED	0	1	0	3	1	15	2	6	3	12	2	2	3	0	0	21	6	0	0	0	0	6	0	0	1	78	0	0	266	211	MED
NOS	0	0	0	11	4	6	0	0	0	4	3	0	0	0	0	0	1	0	0	0	0	0	2	0	0	30	0	0	128	116	NOS
AST	0	0	0	1	1	6	1	3	1	29	1	0	1	2	1	21	5	6	0	0	0	1	0	44	0	46	0	0	163	58	AST
NOA	0	0	0	3	1	8	2	4	2	6	1	1	2	0	0	6	3	0	0	0	0	3	0	0	2	65	0	0	146	121	NOA
EXC	0	0	0	5	2	18	2	4	2	47	3	1	2	1	0	10	8	3	0	0	0	1	1	1	0	64	0	0	244	143	EXC
EU	0	0	0	19	4	52	7	10	4	26	6	3	6	0	0	6	11	0	1	1	0	2	2	0	0	122	0	0	571	501	EU
	ME	MK	MT	NL	NO	PL	PT	RO	RS	RUE	SE	SI	SK	TJ	TM	TR	UA	UZ	ATL	BAS	BLS	MED	NOS	AST	NOA	BIC	DMS	VOL	EXC	EU	

Table C.6: 2014 country-to-country blame matrices for **SOMO35**.
Units: ppb.d per 15% emis. red. of NO_x. **Emitters →, Receptors ↓.**

	AL	AM	AT	AZ	BA	BE	BG	BY	CH	CY	CZ	DE	DK	EE	ES	FI	FR	GB	GE	GR	HR	HU	IE	IS	IT	KG	KZT	LT	LU	LV	MD	
AL	44	0	3	0	4	0	5	0	0	0	2	4	0	0	10	0	8	1	0	11	4	4	0	0	31	0	0	0	0	0	0	AL
AM	0	20	0	53	0	0	0	0	0	0	0	0	0	0	2	0	1	0	9	1	0	0	0	0	2	0	4	0	0	0	0	AM
AT	0	0	20	0	0	-1	1	1	2	0	7	17	0	0	6	1	11	1	0	1	3	4	0	0	14	0	0	0	0	0	0	AT
AZ	0	4	0	90	0	0	0	0	0	0	0	1	0	0	2	0	1	0	9	1	0	0	0	0	1	0	10	0	0	0	0	AZ
BA	1	0	7	0	36	0	3	1	1	0	4	7	0	0	8	0	7	1	0	3	21	12	0	0	25	0	0	0	0	0	0	BA
BE	0	0	0	0	0	-65	0	1	0	0	0	-11	1	0	5	1	16	-2	0	0	0	0	1	0	2	0	0	0	-2	0	0	BE
BG	1	0	2	0	1	-0	63	1	0	0	2	3	0	0	3	0	3	0	0	14	1	4	0	0	6	0	1	0	0	0	1	BG
BY	0	0	0	0	0	-0	0	11	0	0	1	3	0	0	1	1	1	1	0	0	0	1	0	0	1	0	1	2	0	1	0	BY
CH	0	0	2	0	0	-0	0	0	7	0	1	7	0	0	9	0	31	1	0	0	1	1	0	0	12	0	0	0	0	0	0	CH
CY	0	0	1	1	1	0	4	0	0	30	1	2	0	0	6	0	5	1	0	15	1	1	0	0	11	0	1	0	0	0	0	CY
CZ	0	0	7	0	1	-1	1	2	0	0	15	12	1	0	3	1	8	1	0	1	2	5	1	0	4	0	0	1	-0	0	0	CZ
DE	0	0	1	0	0	-4	0	1	0	0	1	-12	0	0	4	1	11	0	0	0	0	1	1	0	2	0	0	1	-0	0	0	DE
DK	0	0	0	0	0	-1	0	2	0	0	0	-0	-10	0	1	1	1	2	0	0	0	0	1	0	0	0	0	1	-0	1	0	DK
EE	0	0	0	0	0	-0	0	3	0	0	0	2	1	3	1	4	1	2	0	0	0	0	0	0	0	0	1	2	0	3	0	EE
ES	0	0	0	0	0	0	0	0	0	0	0	1	0	0	104	0	11	1	0	0	0	0	0	0	2	0	0	0	0	0	0	ES
FI	0	0	0	0	0	-0	0	1	0	0	0	1	0	1	0	5	0	1	0	0	0	0	0	0	0	0	0	1	0	0	0	FI
FR	0	0	0	0	0	-1	0	0	1	0	0	2	0	0	16	0	56	3	0	0	0	0	1	0	4	0	0	0	0	0	0	FR
GB	0	0	0	0	0	-2	0	0	0	0	0	-2	1	0	3	1	4	-44	0	0	0	0	2	0	1	0	0	0	-0	0	0	GB
GE	0	6	0	35	0	0	1	0	0	0	0	1	0	0	3	0	1	0	51	1	0	0	0	0	2	0	5	0	0	0	0	GE
GL	0	0	-0	0	0	-0	0	-0	-0	0	-0	-1	-0	-0	0	-0	-0	-0	0	0	0	-0	0	0	0	0	0	-0	-0	-0	0	GL
GR	4	0	2	0	1	0	19	1	0	0	1	3	0	0	7	0	6	1	0	66	2	3	0	0	20	0	1	0	0	0	1	GR
HR	1	0	11	0	10	-0	2	1	1	0	6	9	0	0	6	0	8	1	0	2	35	16	0	0	25	0	0	0	0	0	0	HR
HU	0	0	7	0	3	-0	3	2	0	0	6	8	0	0	3	1	5	1	0	1	8	35	0	0	8	0	1	0	0	0	0	HU
IE	0	0	0	0	0	-1	0	0	0	0	0	-1	0	0	2	0	5	1	0	0	0	0	-2	0	0	0	0	0	-0	0	0	IE
IS	0	0	-0	0	0	-0	0	0	-0	0	-0	-1	-0	0	1	0	1	2	0	0	0	-0	1	4	0	0	0	0	-0	0	0	IS
IT	0	0	6	0	1	0	1	0	2	0	2	6	0	0	15	0	23	1	0	1	4	3	0	0	59	0	0	0	0	0	0	IT
KG	0	0	0	2	0	0	0	0	0	0	0	1	0	0	2	0	1	0	1	0	0	0	0	0	2	27	26	0	0	0	0	KG
KZT	0	0	0	1	0	0	0	1	0	0	0	1	0	0	1	1	1	1	0	0	0	0	0	0	1	1	41	0	0	0	0	KZT
LT	0	0	0	0	0	-0	0	7	0	0	1	4	1	1	1	2	2	1	0	0	0	1	0	0	1	0	1	7	0	2	0	LT
LU	0	0	0	0	0	-6	0	1	1	0	-1	-13	0	0	6	0	16	2	0	0	0	0	1	0	2	0	0	0	-53	0	0	LU
LV	0	0	0	0	0	-0	0	5	0	0	1	3	1	1	1	3	2	2	0	0	0	0	0	0	0	0	1	4	0	4	0	LV
MD	0	0	1	1	0	-0	2	3	0	0	1	2	0	0	2	1	2	1	0	2	1	2	0	0	2	0	2	1	0	0	10	MD
ME	9	0	4	0	9	0	4	1	1	0	2	5	0	0	9	0	7	1	0	6	6	7	0	0	29	0	0	0	0	0	0	ME
MK	9	0	2	0	2	0	15	1	0	0	2	4	0	0	7	0	5	1	0	4	2	5	0	0	14	0	0	0	0	0	0	MK
MT	1	0	2	0	1	0	2	0	1	0	1	5	0	0	25	0	24	2	0	5	2	1	0	0	42	0	0	0	0	0	0	MT
NL	0	0	0	0	0	-16	0	1	0	0	0	-14	1	0	3	1	6	-6	0	0	0	0	1	0	1	0	0	0	-0	0	0	NL
NO	0	0	0	0	0	-0	0	0	0	0	0	1	0	0	1	1	1	1	0	0	0	0	1	0	0	0	0	0	0	0	0	NO
PL	0	0	1	0	0	-1	1	3	0	0	3	7	1	0	2	1	4	1	0	0	1	3	0	0	2	0	1	1	0	1	0	PL
PT	0	0	0	0	0	0	0	0	0	0	0	0	0	0	46	0	4	1	0	0	0	0	0	0	1	0	0	0	0	0	0	PT
RO	0	0	1	0	1	-0	9	2	0	0	2	3	0	0	3	0	3	0	0	2	2	6	0	0	4	0	1	0	0	0	3	RO
RS	3	0	3	0	6	-0	11	1	0	0	3	5	0	0	5	0	4	0	0	4	5	12	0	0	11	0	1	0	0	0	0	RS
RUE	0	0	0	0	0	-0	0	1	0	0	0	0	0	0	0	1	0	0	0	0	0	0	0	0	0	0	4	0	0	0	0	RUE
SE	0	0	0	0	0	-0	0	1	0	0	0	1	0	0	1	3	1	2	0	0	0	0	1	0	0	0	0	1	-0	0	0	SE
SI	0	0	21	0	1	-0	1	1	1	0	6	11	0	0	6	0	9	1	0	1	16	7	0	0	23	0	0	0	0	0	0	SI
SK	0	0	3	0	2	-1	2	2	0	0	8	7	0	0	3	1	4	0	0	1	4	20	0	0	6	0	1	1	-0	0	1	SK
TJ	0	0	0	2	0	0	0	0	0	0	0	0	0	0	2	0	1	0	0	0	0	0	0	0	1	2	9	0	0	0	0	TJ
TM	0	1	0	5	0	0	0	1	0	0	0	1	0	0	2	0	1	1	1	0	0	0	0	0	1	0	27	0	0	0	0	TM
TR	0	1	1	2	0	0	3	1	0	1	0	1	0	0	5	0	2	0	2	6	0	1	0	0	5	0	1	0	0	0	0	TR
UA	0	0	0	1	0	-0	1	4	0	0	1	2	0	0	1	1	1	1	0	1	0	1	0	0	2	0	3	1	0	0	1	UA
UZ	0	0	0	3	0	0	0	1	0	0	0	1	0	0	2	0	1	1	1	0	0	0	0	0	1	1	36	0	0	0	0	UZ
ATL	0	0	0	0	0	-0	0	0	0	0	-0	-0	0	0	2	0	2	2	0	0	0	0	1	0	0	0	0	0	0	0	0	ATL
BAS	0	0	0	0	0	-1	0	2	0	0	0	-1	-0	1	1	4	1	2	0	0	0	0	1	0	0	0	0	2	0	2	0	BAS
BLS	0	1	1	3	0	-0	5	2	0	0	1	1	0	0	2	1	2	0	8	3	0	1	0	0	3	0	3	1	0	0	2	BLS
MED	1	0	2	0	2	0	4	0	1	1	1	4	0	0	22	0	22	2	0	12	3	2	0	0	35	0	0	0	0	0	0	MED
NOS	0	0	0	0	0	-3	0	1	0	0	0	-3	0	0	2	1	2	-9	0	0	0	0	2	1	0	0	0	1	-0	0	0	NOS
AST	0	0	0	5	0	0	0	0	0	1	0	0	0	0	2	0	1	0	1	1	0	0	0	0	1	2	12	0	0	0	0	AST
NOA	1	0	1	0	1	0	2	0	0	0	0	2	0	0	18	0	7	1	0	7	1	1	0	0	13	0	0	0	0	0	0	NOA
EXC	0	0	1	1	0	-0	1	1	0	0	0	1	0	0	4	1	3	0	0	1	0	1	0	0	2	0	8	0	-0	0	0	EXC
EU	0	0	2	0	1	-1	3	1	0	0	1	2	0	0	18	1	13	-1	0	3	1	2	1	0	7	0	0	1	-0	0	0	EU
	AL	AM	AT	AZ	BA	BE	BG	BY	CH	CY	CZ	DE	DK	EE	ES	FI	FR	GB	GE	GR	HR	HU	IE	IS	IT	KG	KZT	LT	LU	LV	MD	

Table C.6 Cont.: 2014 country-to-country blame matrices for **SOMO35**.
Units: ppb.d per 15% emis. red. of NO_x. **Emitters →, Receptors ↓.**

	ME	MK	MT	NL	NO	PL	PT	RO	RS	RUE	SE	SI	SK	TJ	TM	TR	UA	UZ	ATL	BAS	BLS	MED	NOS	AST	NOA	BIC	DMS	VOL	EXC	EU	
AL	6	8	0	0	1	4	1	6	18	3	0	1	2	0	0	3	4	0	3	0	1	46	1	0	2	28	0	0	190	97	AL
AM	0	0	0	0	0	1	0	1	0	12	0	0	0	0	3	38	2	2	1	0	1	5	0	19	1	35	0	0	155	10	AM
AT	0	0	0	-1	1	5	0	3	1	3	1	4	2	0	0	2	3	0	5	1	0	6	1	0	0	23	0	0	115	101	AT
AZ	0	0	0	0	0	1	0	1	0	33	0	0	0	0	7	12	4	5	1	0	1	2	0	15	0	27	0	0	184	9	AZ
BA	6	1	0	-0	1	10	1	6	11	4	1	2	5	0	0	3	6	0	3	1	1	20	1	0	1	25	0	0	194	124	BA
BE	0	0	0	-18	2	2	1	1	0	3	1	0	0	0	0	0	1	0	10	1	0	2	-15	0	0	22	0	0	-58	-66	BE
BG	1	4	0	-0	1	6	0	23	10	16	1	0	2	0	0	6	18	0	2	1	7	12	1	0	1	22	0	0	196	134	BG
BY	0	0	0	-0	1	9	0	1	0	23	1	0	1	0	0	1	11	0	2	1	0	1	1	0	0	15	0	0	79	28	BY
CH	0	0	0	-1	1	2	1	1	0	1	1	0	0	0	0	1	1	0	6	0	0	6	0	0	0	26	0	0	82	70	CH
CY	0	1	0	0	0	1	1	3	1	7	0	0	0	0	0	77	5	0	2	0	3	94	0	4	3	33	0	0	180	84	CY
CZ	0	0	0	-1	2	11	0	3	1	6	1	1	5	0	0	1	5	0	5	1	0	3	1	0	0	21	0	0	100	81	CZ
DE	0	0	0	-5	2	5	0	1	0	4	2	0	1	0	0	1	3	0	7	-0	0	2	-2	0	0	22	0	0	24	12	DE
DK	0	0	0	-2	6	3	0	0	0	6	3	0	0	0	0	0	2	0	9	-10	0	0	-3	0	0	21	0	0	22	5	DK
EE	0	0	0	-0	2	5	0	0	0	8	4	0	0	0	0	0	2	0	3	3	0	0	1	0	0	14	0	0	45	28	EE
ES	0	0	0	0	0	0	18	0	0	0	0	0	0	0	0	0	0	0	15	0	0	10	0	0	0	37	0	0	141	139	ES
FI	0	0	0	-0	2	3	0	0	0	6	3	0	0	0	0	0	1	0	3	2	0	0	1	0	0	12	0	0	27	16	FI
FR	0	0	0	-1	1	1	1	1	0	1	1	0	0	0	0	0	1	0	14	0	0	7	-1	0	0	27	0	0	91	86	FR
GB	0	0	0	-3	2	1	1	0	0	2	1	0	0	0	0	0	1	0	13	0	0	1	-9	0	0	22	0	0	-30	-36	GB
GE	0	0	0	0	0	1	0	1	0	23	0	0	0	0	3	31	5	2	1	0	6	5	0	7	1	31	0	0	177	13	GE
GL	0	0	0	-0	0	-0	0	0	0	-0	-0	-0	-0	0	0	0	-0	0	1	-0	0	0	-0	0	0	12	0	0	-2	-2	GL
GR	1	8	0	0	1	3	1	7	6	7	0	1	1	0	0	11	8	0	3	0	3	51	1	0	2	27	0	0	195	145	GR
HR	1	0	0	-0	1	10	1	6	8	4	1	6	6	0	0	2	5	0	4	1	1	21	1	0	1	22	0	0	187	152	HR
HU	1	0	0	-0	1	18	0	17	8	7	1	2	14	0	0	2	12	0	3	1	1	5	1	0	0	20	0	0	177	138	HU
IE	0	0	0	-1	2	0	1	0	0	1	1	0	0	0	0	0	0	0	16	0	0	0	-0	0	0	23	0	0	10	7	IE
IS	0	0	0	-0	2	-1	0	0	0	-0	1	0	-0	0	0	0	0	0	10	-0	0	0	1	0	0	22	0	0	9	4	IS
IT	0	0	0	0	1	3	1	2	1	1	0	3	1	0	0	1	2	0	5	0	0	34	1	0	1	26	0	0	146	134	IT
KG	0	0	0	0	0	0	0	0	0	9	0	0	0	14	3	5	1	28	1	0	0	2	0	17	0	39	0	0	125	9	KG
KZT	0	0	0	0	1	1	0	1	0	50	1	0	0	0	2	2	3	3	2	0	0	1	0	3	0	31	0	0	116	10	KZT
LT	0	0	0	-0	2	11	0	1	0	13	3	0	1	0	0	1	5	0	3	3	0	1	1	0	0	15	0	0	68	39	LT
LU	0	0	0	-6	2	1	1	1	0	3	1	0	0	0	0	0	1	0	9	1	0	2	-3	0	0	23	0	0	-36	-45	LU
LV	0	0	0	-0	2	6	0	0	0	10	3	0	0	0	0	0	3	0	3	4	0	0	1	0	0	14	0	0	56	33	LV
MD	0	0	0	-0	1	9	0	13	1	23	1	0	1	0	0	4	42	0	2	1	3	3	1	0	0	20	0	0	130	42	MD
ME	41	2	0	0	1	7	1	6	18	3	1	1	3	0	0	3	5	0	3	0	1	34	1	0	2	29	0	0	193	99	ME
MK	2	54	0	0	1	5	1	8	24	5	0	0	2	0	0	4	6	0	3	0	2	18	1	0	1	25	0	0	187	78	MK
MT	0	1	-35	0	0	2	1	2	1	1	0	1	1	0	0	2	2	0	7	0	0	65	1	0	3	33	0	0	95	84	MT
NL	0	0	0	-55	3	2	0	1	0	3	1	0	0	0	0	0	1	0	8	0	0	1	-27	0	0	19	0	0	-61	-71	NL
NO	0	0	0	-0	9	1	0	0	0	2	3	0	0	0	0	0	1	0	5	1	0	0	1	0	0	18	0	0	25	12	NO
PL	0	0	0	-1	2	24	0	3	1	11	2	0	3	0	0	1	10	0	4	2	0	2	1	0	0	18	0	0	93	61	PL
PT	0	0	0	-0	0	0	62	0	0	0	0	0	0	0	0	0	0	0	29	0	0	2	0	0	0	37	0	0	117	116	PT
RO	1	1	0	-0	1	9	0	58	5	15	1	0	3	0	0	4	25	0	2	1	4	6	1	0	0	22	0	0	169	109	RO
RS	4	6	0	-0	1	9	0	17	41	7	1	1	4	0	0	3	9	0	3	1	1	11	1	0	1	22	0	0	183	99	RS
RUE	0	0	0	-0	1	1	0	0	0	24	0	0	0	0	0	1	2	0	1	0	0	0	0	0	0	11	0	0	38	5	RUE
SE	0	0	0	-1	5	4	0	0	0	4	6	0	0	0	0	0	2	0	5	2	0	0	0	0	0	17	0	0	32	19	SE
SI	0	0	0	-0	1	6	0	4	2	3	1	19	3	0	0	2	4	0	4	1	0	15	1	0	1	21	0	0	155	138	SI
SK	0	0	0	-0	2	27	0	10	4	8	1	1	25	0	0	2	12	0	3	1	1	5	1	0	0	21	0	0	158	124	SK
TJ	0	0	0	0	0	0	0	0	0	6	0	0	0	46	6	4	1	25	1	0	0	1	0	27	0	39	0	0	108	6	TJ
TM	0	0	0	0	1	1	0	1	0	32	0	0	0	1	29	5	3	24	2	0	0	2	0	12	0	42	0	0	142	11	TM
TR	0	1	0	0	0	1	0	3	1	12	0	0	0	0	0	102	7	0	2	0	5	20	0	6	2	38	0	0	164	32	TR
UA	0	0	0	-0	1	8	0	5	1	34	1	0	1	0	0	3	33	1	2	1	2	2	1	0	0	20	0	0	112	29	UA
UZ	0	0	0	0	1	1	0	1	0	33	0	0	0	5	8	4	3	21	2	0	0	1	0	6	0	38	0	0	125	10	UZ
ATL	0	0	0	-0	1	-0	0	0	0	0	0	0	0	0	0	0	0	0	12	0	0	0	1	0	0	18	0	0	9	6	ATL
BAS	0	0	0	-1	4	7	0	1	0	9	6	0	0	0	0	0	3	0	6	-2	0	0	1	0	0	20	0	0	47	27	BAS
BLS	0	0	0	-0	1	4	0	9	1	56	1	0	1	0	1	14	37	1	2	1	35	7	1	1	1	26	0	0	166	36	BLS
MED	1	1	1	0	1	2	2	3	2	4	0	1	1	0	0	15	4	0	7	0	2	93	1	1	3	35	0	0	153	122	MED
NOS	0	0	0	-5	9	2	0	0	0	4	3	0	0	0	0	0	1	0	17	-0	0	1	-25	0	0	30	0	0	12	-4	NOS
AST	0	0	0	0	0	0	0	1	0	15	0	0	0	2	5	13	2	6	1	0	0	6	0	44	0	36	0	0	72	9	AST
NOA	0	1	0	0	0	1	2	2	1	1	0	0	0	0	0	5	2	0	3	0	0	40	0	0	12	56	0	0	71	59	NOA
EXC	0	0	0	-0	1	2	1	2	1	21	1	0	0	1	1	5	3	2	3	0	1	3	0	1	0	19	0	0	68	21	EXC
EU	0	0	0	-2	2	5	4	5	1	5	2	1	1	0	0	1	4	0	8	1	1	8	-1	0	0	23	0	0	87	70	EU
	ME	MK	MT	NL	NO	PL	PT	RO	RS	RUE	SE	SI	SK	TJ	TM	TR	UA	UZ	ATL	BAS	BLS	MED	NOS	AST	NOA	BIC	DMS	VOL	EXC	EU	

Table C.7: 2014 country-to-country blame matrices for **SOMO35**.
Units: ppb.d per 15% emis. red. of VOC. **Emitters →, Receptors ↓.**

	AL	AM	AT	AZ	BA	BE	BG	BY	CH	CY	CZ	DE	DK	EE	ES	FI	FR	GB	GE	GR	HR	HU	IE	IS	IT	KG	KZT	LT	LU	LV	MD	
AL	6	0	2	0	1	1	1	1	1	0	2	7	0	0	3	0	5	3	0	7	1	2	0	0	21	0	0	0	0	0	0	AL
AM	0	26	0	21	0	0	0	0	0	0	0	1	0	0	1	0	1	1	3	0	0	0	0	0	2	0	1	0	0	0	0	AM
AT	0	0	15	0	0	1	0	1	5	0	5	32	1	0	2	0	9	6	0	1	1	2	0	0	26	0	0	0	0	0	0	AT
AZ	0	3	0	53	0	0	0	0	0	0	0	2	0	0	1	0	1	1	4	0	0	0	0	0	2	0	2	0	0	0	0	AZ
BA	1	0	2	0	3	1	1	1	1	0	2	9	0	0	2	0	5	4	0	2	2	2	0	0	18	0	0	0	0	0	0	BA
BE	0	0	1	0	0	14	0	1	1	0	1	23	1	0	2	0	16	15	0	0	0	0	0	0	2	0	0	0	1	0	0	BE
BG	0	0	1	1	0	1	8	1	0	0	1	6	0	0	1	0	3	3	0	4	0	1	0	0	5	0	1	0	0	0	0	BG
BY	0	0	0	0	0	0	0	4	0	0	1	4	0	0	0	0	1	3	0	0	0	0	0	0	1	0	1	1	0	0	0	BY
CH	0	0	4	0	0	2	0	0	34	0	2	26	0	0	3	0	18	6	0	0	1	1	0	0	56	0	0	0	0	0	0	CH
CY	0	0	1	1	0	0	1	1	0	3	1	5	0	0	2	0	4	3	0	5	1	1	0	0	10	0	1	0	0	0	0	CY
CZ	0	0	4	0	0	2	1	1	1	0	13	26	1	0	1	0	7	6	0	0	1	2	0	0	8	0	0	0	0	0	0	CZ
DE	0	0	3	0	0	3	0	1	3	0	4	46	1	0	1	0	11	9	0	0	0	1	0	0	6	0	0	0	0	0	0	DE
DK	0	0	0	0	0	1	0	1	0	0	1	11	6	0	0	0	3	13	0	0	0	0	1	0	1	0	0	1	0	1	0	DK
EE	0	0	0	0	0	0	0	1	0	0	1	4	1	1	0	1	2	4	0	0	0	0	0	0	0	0	0	1	0	1	0	EE
ES	0	0	0	0	0	0	0	0	0	0	0	2	0	0	18	0	4	3	0	0	0	0	0	0	2	0	0	0	0	0	0	ES
FI	0	0	0	0	0	0	0	0	0	0	0	2	0	0	0	1	1	3	0	0	0	0	0	0	0	0	0	0	0	0	0	FI
FR	0	0	1	0	0	2	0	0	2	0	1	14	0	0	5	0	21	11	0	0	0	0	0	0	8	0	0	0	0	0	0	FR
GB	0	0	0	0	0	2	0	0	0	0	1	8	1	0	1	0	6	32	0	0	0	0	1	0	1	0	0	0	0	0	0	GB
GE	0	3	0	20	0	0	0	0	0	0	0	2	0	0	1	0	1	1	18	1	0	0	0	0	2	0	1	0	0	0	0	GE
GL	0	0	0	0	0	0	0	0	0	0	0	1	0	0	0	0	0	0	0	0	0	0	0	-0	0	0	0	0	0	0	0	GL
GR	1	0	1	1	0	1	2	1	1	0	1	6	0	0	2	0	4	3	0	19	1	1	0	0	14	0	0	0	0	0	0	GR
HR	0	0	4	0	1	1	1	1	2	0	4	14	0	0	2	0	7	4	0	1	4	3	0	0	27	0	0	0	0	0	0	HR
HU	0	0	3	0	1	1	1	1	1	0	4	12	1	0	1	0	5	4	0	1	1	7	0	0	9	0	0	0	0	0	0	HU
IE	0	0	0	0	0	1	0	0	0	0	0	4	1	0	1	0	3	15	0	0	0	0	2	0	0	0	0	0	0	0	0	IE
IS	0	0	0	0	0	0	0	0	0	0	0	2	0	0	0	0	1	3	0	0	0	0	0	0	0	0	0	0	0	0	0	IS
IT	0	0	4	0	0	1	0	1	3	0	3	14	0	0	5	0	12	5	0	1	2	1	0	0	115	0	0	0	0	0	0	IT
KG	0	0	0	1	0	0	0	0	0	0	0	1	0	0	0	0	0	0	0	0	0	0	0	0	1	15	11	0	0	0	0	KG
KZT	0	0	0	1	0	0	0	0	0	0	0	2	0	0	0	0	1	1	0	0	0	0	0	0	1	1	8	0	0	0	0	KZT
LT	0	0	0	0	0	0	0	2	0	0	1	5	1	0	0	0	2	5	0	0	0	0	0	0	1	0	0	2	0	1	0	LT
LU	0	0	1	0	0	8	0	1	1	0	2	35	1	0	2	0	16	11	0	0	0	0	0	0	3	0	0	0	4	0	0	LU
LV	0	0	0	0	0	0	0	1	0	0	1	4	1	0	0	1	2	4	0	0	0	0	0	0	1	0	0	1	0	1	0	LV
MD	0	0	1	1	0	0	1	1	0	0	1	5	0	0	1	0	2	3	0	1	0	1	0	0	2	0	1	0	0	0	1	MD
ME	2	0	2	0	1	1	1	1	1	0	2	7	0	0	3	0	5	3	0	3	1	2	0	0	19	0	0	0	0	0	0	ME
MK	2	0	1	0	0	1	2	1	1	0	1	6	0	0	2	0	3	2	0	16	1	2	0	0	9	0	0	0	0	0	0	MK
MT	1	0	2	0	0	1	1	1	1	0	2	11	0	0	8	0	12	6	0	2	1	1	0	0	37	0	0	0	0	0	0	MT
NL	0	0	1	0	0	7	0	1	0	0	1	26	1	0	1	0	10	17	0	0	0	0	1	0	1	0	0	0	0	0	0	NL
NO	0	0	0	0	0	0	0	0	0	0	0	3	0	0	0	0	1	4	0	0	0	0	0	0	1	0	0	0	0	0	0	NO
PL	0	0	1	0	0	1	0	2	0	0	3	13	1	0	1	0	3	5	0	0	0	1	0	0	3	0	0	1	0	0	0	PL
PT	0	0	0	0	0	0	0	0	0	0	0	1	0	0	9	0	2	2	0	0	0	0	0	0	1	0	0	0	0	0	0	PT
RO	0	0	1	1	0	1	2	1	1	0	2	7	0	0	1	0	3	3	0	1	0	1	0	0	5	0	1	0	0	0	0	RO
RS	1	0	1	0	1	1	2	1	1	0	2	8	0	0	1	0	4	3	0	3	1	3	0	0	8	0	0	0	0	0	0	RS
RUE	0	0	0	0	0	0	0	0	0	0	0	1	0	0	0	0	0	1	0	0	0	0	0	0	0	0	1	0	0	0	0	RUE
SE	0	0	0	0	0	1	0	0	0	0	0	3	1	0	0	0	1	5	0	0	0	0	0	0	0	0	0	0	0	0	0	SE
SI	0	0	10	0	0	1	1	1	2	0	5	20	0	0	2	0	8	5	0	1	3	3	0	0	43	0	0	0	0	0	0	SI
SK	0	0	3	1	0	1	1	1	1	0	5	13	1	0	1	0	4	4	0	1	1	5	0	0	8	0	0	0	0	0	0	SK
TJ	0	0	0	1	0	0	0	0	0	0	0	1	0	0	0	0	0	0	0	0	0	0	0	0	1	2	4	0	0	0	0	TJ
TM	0	0	0	4	0	0	0	0	0	0	0	2	0	0	1	0	1	1	0	0	0	0	0	0	2	0	6	0	0	0	0	TM
TR	0	1	0	2	0	0	1	0	0	0	1	3	0	0	1	0	2	1	1	2	0	0	0	0	5	0	1	0	0	0	0	TR
UA	0	0	0	1	0	0	1	1	0	0	1	4	0	0	0	0	2	2	0	0	0	1	0	0	2	0	1	0	0	0	0	UA
UZ	0	0	0	2	0	0	0	0	0	0	0	2	0	0	0	0	1	1	0	0	0	0	0	0	1	2	10	0	0	0	0	UZ
ATL	0	0	0	0	0	0	0	0	0	0	0	2	0	0	1	0	1	4	0	0	0	0	0	0	0	0	0	0	0	0	0	ATL
BAS	0	0	0	0	0	1	0	1	0	0	1	8	3	0	0	2	3	8	0	0	0	0	0	0	1	0	0	1	0	1	0	BAS
BLS	0	1	1	4	0	0	2	1	0	0	1	5	0	0	1	0	2	3	3	2	0	1	0	0	4	0	1	0	0	0	0	BLS
MED	1	0	2	1	1	1	1	1	1	0	2	10	0	0	8	0	11	5	0	5	1	1	0	0	35	0	0	0	0	0	0	MED
NOS	0	0	0	0	0	2	0	1	0	0	1	11	2	0	1	0	7	24	0	0	0	0	1	0	1	0	0	0	0	0	0	NOS
AST	0	0	0	4	0	0	0	0	0	0	0	1	0	0	0	0	1	1	0	0	0	0	0	0	1	0	2	0	0	0	0	AST
NOA	0	0	1	0	0	0	1	0	1	0	1	4	0	0	4	0	4	2	0	2	0	1	0	0	10	0	0	0	0	0	0	NOA
EXC	0	0	0	1	0	0	0	0	0	0	1	3	0	0	1	0	2	2	0	0	0	0	0	0	3	0	2	0	0	0	0	EXC
EU	0	0	1	0	0	1	1	1	1	0	2	12	1	0	4	0	7	7	0	1	0	1	0	0	12	0	0	0	0	0	0	EU
	AL	AM	AT	AZ	BA	BE	BG	BY	CH	CY	CZ	DE	DK	EE	ES	FI	FR	GB	GE	GR	HR	HU	IE	IS	IT	KG	KZT	LT	LU	LV	MD	

Table C.7 Cont.: 2014 country-to-country blame matrices for **SOMO35**.
Units: ppb.d per 15% emis. red. of VOC. **Emitters →, Receptors ↓.**

	ME	MK	MT	NL	NO	PL	PT	RO	RS	RUE	SE	SI	SK	TJ	TM	TR	UA	UZ	ATL	BAS	BLS	MED	NOS	AST	NOA	BIC	DMS	VOL	EXC	EU	
AL	1	2	0	1	0	6	0	3	4	4	0	0	1	0	0	3	2	0	0	0	0	1	0	0	0	24	0	0	92	67	AL
AM	0	0	0	0	0	1	0	0	0	6	0	0	0	0	0	10	1	0	0	0	0	0	0	1	0	12	0	0	78	9	AM
AT	0	0	0	2	0	11	0	2	1	4	1	2	2	0	0	1	2	0	0	0	0	0	0	0	0	22	0	0	135	120	AT
AZ	0	0	0	0	0	2	0	1	0	14	0	0	0	0	1	4	2	0	0	0	0	0	0	2	0	18	0	0	96	12	AZ
BA	0	0	0	1	0	9	0	3	3	4	1	1	2	0	0	2	2	0	0	0	0	0	0	0	0	21	0	0	86	67	BA
BE	0	0	0	11	1	5	0	0	0	3	1	0	0	0	0	0	1	0	0	0	0	0	1	0	0	21	0	0	103	95	BE
BG	0	0	0	1	0	6	0	5	2	8	1	0	1	0	0	7	4	0	0	0	0	0	0	0	0	21	0	0	75	49	BG
BY	0	0	0	1	0	5	0	1	0	10	1	0	0	0	0	1	3	0	0	0	0	0	0	0	0	13	0	0	41	22	BY
CH	0	0	0	2	0	4	0	1	0	2	0	1	0	0	0	0	1	0	0	0	0	0	0	0	0	21	0	0	167	128	CH
CY	0	0	0	1	0	4	0	3	1	7	0	0	1	0	0	30	3	0	0	0	0	1	0	1	0	33	0	0	92	46	CY
CZ	0	0	0	3	1	21	0	2	1	5	1	1	3	0	0	1	2	0	0	0	0	0	0	0	0	23	0	0	117	103	CZ
DE	0	0	0	6	1	11	0	1	0	4	1	0	1	0	0	0	2	0	0	0	0	0	1	0	0	22	0	0	119	107	DE
DK	0	0	0	3	2	7	0	0	0	5	3	0	0	0	0	0	1	0	0	0	0	0	1	0	0	18	0	0	64	55	DK
EE	0	0	0	1	0	4	0	0	0	7	2	0	0	0	0	0	1	0	0	0	0	0	0	0	0	10	0	0	33	24	EE
ES	0	0	0	1	0	1	3	0	0	1	0	0	0	0	0	0	0	0	0	0	0	1	0	0	0	14	0	0	37	35	ES
FI	0	0	0	1	0	2	0	0	0	3	1	0	0	0	0	0	0	0	0	0	0	0	0	0	0	5	0	0	18	13	FI
FR	0	0	0	3	0	3	0	0	0	2	1	0	0	0	0	0	1	0	0	0	0	0	0	0	0	18	0	0	80	74	FR
GB	0	0	0	4	1	3	0	0	0	2	1	0	0	0	0	0	1	0	0	0	0	0	1	0	0	15	0	0	66	61	GB
GE	0	0	0	0	0	2	0	1	0	10	0	0	0	0	0	7	1	0	0	0	0	0	0	1	0	14	0	0	75	13	GE
GL	0	0	0	0	0	0	0	0	0	0	0	0	0	0	0	0	0	0	0	0	0	0	0	0	0	-2	0	0	4	3	GL
GR	0	1	0	1	0	5	0	3	2	6	0	0	1	0	0	7	3	0	0	0	0	1	0	0	0	25	0	0	91	67	GR
HR	0	0	0	2	1	12	0	3	2	5	1	2	2	0	0	2	2	0	0	0	0	1	0	0	0	24	0	0	113	96	HR
HU	0	0	0	2	1	14	0	5	2	6	1	1	4	0	0	1	3	0	0	0	0	0	0	0	0	21	0	0	96	78	HU
IE	0	0	0	2	0	2	0	0	0	1	1	0	0	0	0	0	0	0	0	0	0	0	0	0	0	7	0	0	36	33	IE
IS	0	0	0	1	0	1	0	0	0	1	0	0	0	0	0	0	0	0	0	0	0	0	0	0	0	0	0	0	14	11	IS
IT	0	0	0	1	0	7	1	2	1	3	0	2	1	0	0	1	2	0	0	0	0	1	0	0	0	29	0	0	189	177	IT
KG	0	0	0	0	0	1	0	0	0	4	0	0	0	3	0	1	0	11	0	0	0	0	0	1	0	6	0	0	53	5	KG
KZT	0	0	0	0	0	1	0	0	0	11	0	0	0	0	0	1	1	1	0	0	0	0	0	0	0	10	0	0	34	9	KZT
LT	0	0	0	1	1	7	0	1	0	7	1	0	0	0	0	0	1	0	0	0	0	0	0	0	0	12	0	0	42	30	LT
LU	0	0	0	8	1	7	0	1	0	3	1	0	0	0	0	0	1	0	0	0	0	0	1	0	0	22	0	0	111	103	LU
LV	0	0	0	1	1	6	0	0	0	6	1	0	0	0	0	0	1	0	0	0	0	0	0	0	0	11	0	0	36	26	LV
MD	0	0	0	1	1	7	0	5	1	9	1	0	1	0	0	3	5	0	0	0	0	0	0	0	0	17	0	0	56	34	MD
ME	3	1	0	1	0	6	0	3	3	4	0	0	1	0	0	2	2	0	0	0	0	1	0	0	0	22	0	0	82	61	ME
MK	0	6	0	1	0	5	0	3	5	5	0	0	1	0	0	4	2	0	0	0	0	0	0	0	0	20	0	0	84	57	MK
MT	0	0	11	2	0	5	1	2	1	3	0	1	1	0	0	2	2	0	0	0	0	4	0	0	0	39	0	0	118	107	MT
NL	0	0	0	17	1	6	0	1	0	4	1	0	0	0	0	0	1	0	0	0	0	0	1	0	0	21	0	0	100	92	NL
NO	0	0	0	1	1	2	0	0	0	2	1	0	0	0	0	0	0	0	0	0	0	0	0	0	0	3	0	0	19	15	NO
PL	0	0	0	2	1	27	0	2	1	7	1	0	2	0	0	1	3	0	0	0	0	0	0	0	0	19	0	0	84	69	PL
PT	0	0	0	0	0	0	20	0	0	0	0	0	0	0	0	0	0	1	0	0	0	0	0	0	0	13	0	0	39	38	PT
RO	0	0	0	1	0	7	0	13	2	8	1	0	1	0	0	3	4	0	0	0	0	0	0	0	0	19	0	0	72	51	RO
RS	0	1	0	1	0	8	0	5	9	6	1	0	2	0	0	2	3	0	0	0	0	0	0	0	0	20	0	0	82	55	RS
RUE	0	0	0	0	0	1	0	0	0	6	0	0	0	0	0	0	1	0	0	0	0	0	0	0	0	3	0	0	13	4	RUE
SE	0	0	0	1	1	3	0	0	0	3	2	0	0	0	0	0	1	0	0	0	0	0	0	0	0	6	0	0	24	19	SE
SI	0	0	0	2	0	12	0	2	1	4	1	8	2	0	0	1	2	0	0	0	0	0	0	0	0	26	0	0	144	130	SI
SK	0	0	0	2	1	22	0	5	2	6	1	0	7	0	0	1	3	0	0	0	0	0	0	0	0	21	0	0	101	84	SK
TJ	0	0	0	0	0	0	0	0	0	3	0	0	0	11	0	1	0	6	0	0	0	0	0	3	0	6	0	0	34	4	TJ
TM	0	0	0	0	0	2	0	1	0	12	0	0	0	1	1	1	1	2	0	0	0	0	0	1	0	20	0	0	44	12	TM
TR	0	0	0	0	0	2	0	1	1	6	0	0	0	0	0	32	2	0	0	0	0	0	0	0	0	17	0	0	68	22	TR
UA	0	0	0	1	0	6	0	2	0	13	1	0	1	0	0	2	7	0	0	0	0	0	0	0	0	17	0	0	54	26	UA
UZ	0	0	0	0	0	1	0	0	0	11	0	0	0	2	1	1	1	7	0	0	0	0	0	1	0	17	0	0	48	10	UZ
ATL	0	0	0	1	0	1	0	0	0	1	0	0	0	0	0	0	0	0	0	0	0	0	0	0	0	0	0	0	13	11	ATL
BAS	0	0	0	2	1	8	0	1	0	7	4	0	0	0	0	0	1	0	0	1	0	0	0	0	0	16	0	0	56	44	BAS
BLS	0	0	0	1	0	5	0	4	1	22	1	0	1	0	0	24	7	0	0	0	0	0	0	0	0	29	0	0	102	35	BLS
MED	0	0	0	1	0	6	1	3	1	5	1	1	1	0	0	8	2	0	0	0	0	3	0	0	1	40	0	0	120	98	MED
NOS	0	0	0	5	2	4	0	0	0	4	2	0	0	0	0	0	1	0	0	0	0	0	1	0	0	18	0	0	73	64	NOS
AST	0	0	0	0	0	1	0	0	0	5	0	0	0	0	0	3	1	1	0	0	0	0	0	9	0	8	0	0	25	8	AST
NOA	0	0	0	1	0	3	1	1	1	2	0	0	1	0	0	2	1	0	0	0	0	1	0	0	0	23	0	0	48	38	NOA
EXC	0	0	0	1	0	2	0	1	0	6	0	0	0	0	0	2	1	0	0	0	0	0	0	0	0	8	0	0	34	19	EXC
EU	0	0	0	2	0	7	1	2	1	4	1	0	1	0	0	1	1	0	0	0	0	0	0	0	0	17	0	0	75	65	EU
	ME	MK	MT	NL	NO	PL	PT	RO	RS	RUE	SE	SI	SK	TJ	TM	TR	UA	UZ	ATL	BAS	BLS	MED	NOS	AST	NOA	BIC	DMS	VOL	EXC	EU	

Table C.8: 2014 country-to-country blame matrices for **PM2.5**.
Units: ng/m^3 per 15% emis. red. of PPM. **Emitters →, Receptors ↓.**

	AL	AM	AT	AZ	BA	BE	BG	BY	CH	CY	CZ	DE	DK	EE	ES	FI	FR	GB	GE	GR	HR	HU	IE	IS	IT	KG	KZT	LT	LU	LV	MD	
AL	120	0	0	0	1	0	1	0	0	-0	0	0	0	0	0	0	1	0	0	22	1	1	0	0	7	0	0	0	0	0	0	AL
AM	0	49	0	25	0	0	0	0	0	0	0	0	0	0	0	0	0	0	14	0	0	0	0	-0	0	0	0	0	0	-0	0	AM
AT	0	-0	72	0	1	0	1	0	1	-0	7	13	0	0	0	0	2	0	0	0	6	9	0	0	16	0	0	0	0	0	0	AT
AZ	0	4	0	103	0	0	0	0	0	0	0	0	0	0	0	0	0	0	19	0	0	0	0	0	0	0	2	0	0	0	0	AZ
BA	1	0	1	0	81	0	1	0	0	0	1	1	0	0	0	0	1	0	0	1	23	4	0	0	7	0	0	0	0	0	0	BA
BE	-0	-0	1	-0	0	201	0	0	1	-0	1	29	0	0	1	0	80	14	-0	-0	0	0	1	0	1	-0	0	0	5	0	0	BE
BG	1	0	0	0	1	0	170	1	0	0	0	0	0	0	0	0	0	0	0	9	0	2	0	0	1	0	0	0	0	0	1	BG
BY	0	0	0	0	0	0	1	97	0	0	1	1	0	0	0	0	0	0	0	0	0	1	0	0	1	0	1	5	0	2	1	BY
CH	-0	-0	3	0	0	0	-0	0	84	0	0	13	0	0	0	0	20	1	-0	-0	0	0	0	0	27	0	0	0	0	0	0	CH
CY	0	0	0	0	0	0	1	0	0	13	0	0	0	0	0	0	0	0	0	3	0	0	0	0	1	0	0	0	0	0	0	CY
CZ	0	0	12	0	1	1	1	1	1	-0	96	22	0	0	0	0	5	1	0	0	4	12	0	0	3	-0	0	0	0	0	0	CZ
DE	0	-0	7	0	0	8	0	1	4	-0	8	134	1	0	0	0	18	4	0	0	0	1	0	0	2	-0	0	0	1	0	0	DE
DK	0	0	0	0	0	4	0	2	0	-0	1	16	71	0	0	0	6	7	0	0	0	0	0	0	0	-0	0	1	0	1	0	DK
EE	0	0	0	0	0	0	0	7	0	0	1	2	1	23	0	5	1	1	0	0	0	0	0	0	0	0	0	6	0	14	0	EE
ES	0	0	0	0	0	0	0	0	0	0	0	0	0	0	53	0	4	0	0	0	0	0	0	0	1	0	0	0	0	0	0	ES
FI	0	0	0	0	0	0	0	2	0	0	0	1	0	1	0	27	0	0	0	0	0	0	0	0	0	-0	0	1	0	2	0	FI
FR	-0	-0	0	0	0	5	0	0	2	0	0	8	0	0	3	0	143	5	-0	-0	0	0	0	0	4	0	0	0	1	0	0	FR
GB	-0	-0	0	0	0	2	0	0	0	0	0	3	1	0	0	0	7	115	0	-0	0	0	4	0	0	0	0	0	0	0	0	GB
GE	0	3	0	14	0	0	0	0	0	0	0	0	0	0	0	0	0	0	160	0	0	0	0	0	0	0	0	0	0	0	0	GE
GL	-0	-0	0	-0	-0	0	-0	0	0	0	-0	0	-0	-0	-0	-0	0	0	-0	0	-0	-0	0	0	-0	-0	-0	-0	0	-0	-0	GL
GR	4	0	0	0	0	0	9	0	0	0	0	0	0	0	0	0	0	0	0	101	0	1	0	0	4	0	0	0	0	0	0	GR
HR	1	0	4	0	19	0	2	0	0	0	3	2	0	0	0	0	1	0	0	0	124	12	0	0	18	0	0	0	0	0	0	HR
HU	0	0	7	0	4	0	3	1	0	0	5	3	0	0	0	0	1	0	0	1	18	125	0	0	6	0	0	0	0	0	1	HU
IE	0	-0	0	-0	0	0	0	0	0	0	0	1	0	0	0	0	2	14	-0	0	0	0	44	0	0	0	0	0	0	0	0	IE
IS	0	0	0	0	0	0	0	0	0	0	0	0	0	0	0	0	0	0	0	0	0	0	0	0	0	0	-0	0	0	0	0	IS
IT	0	-0	2	0	1	0	0	0	1	-0	0	1	0	0	1	0	5	0	-0	0	2	1	0	0	300	0	0	0	0	0	0	IT
KG	0	0	-0	0	-0	-0	0	0	-0	0	-0	-0	-0	0	-0	0	-0	-0	0	0	-0	-0	-0	0	-0	29	11	-0	-0	-0	-0	KG
KZT	0	0	0	0	0	0	0	0	0	0	0	0	0	0	0	0	0	0	0	0	0	0	0	0	0	1	39	0	0	0	0	KZT
LT	0	0	0	0	0	0	0	27	0	0	1	3	1	1	0	1	1	1	0	0	0	1	0	0	0	-0	0	78	0	9	1	LT
LU	-0	-0	1	0	0	42	0	0	1	0	2	52	0	0	1	0	100	6	-0	-0	0	0	0	0	1	0	0	0	64	0	0	LU
LV	0	0	0	0	0	0	0	16	0	0	1	3	1	2	0	1	1	1	0	0	0	1	0	0	0	0	0	21	0	59	0	LV
MD	0	0	0	0	0	0	10	3	0	0	1	1	0	0	0	0	0	0	0	1	0	1	0	0	1	0	1	0	0	0	65	MD
ME	13	0	0	0	8	0	1	0	0	0	0	0	0	0	0	0	0	0	0	1	2	1	0	0	5	0	0	0	0	0	0	ME
MK	14	0	0	0	1	0	10	0	0	0	0	0	0	0	0	0	0	0	0	57	1	2	0	0	2	0	0	0	0	0	0	MK
MT	0	0	0	0	0	0	0	0	0	0	0	1	0	0	2	0	5	0	0	1	0	0	0	0	20	0	0	0	0	0	0	MT
NL	-0	-0	1	-0	0	64	0	0	1	-0	2	54	1	0	0	0	34	17	-0	-0	0	1	1	0	0	-0	0	0	1	0	0	NL
NO	0	0	0	0	0	0	0	0	0	0	0	0	0	0	0	0	0	1	0	0	0	0	0	0	0	-0	0	0	0	0	0	NO
PL	0	0	1	0	1	1	1	8	0	0	9	10	1	0	0	0	2	1	0	0	1	5	0	0	1	-0	0	2	0	1	1	PL
PT	0	0	0	0	0	0	0	0	0	0	0	0	0	0	18	0	2	0	-0	0	0	0	0	0	0	0	0	0	0	0	0	PT
RO	0	0	1	0	1	0	15	1	0	0	1	1	0	0	0	0	0	0	0	1	1	4	0	0	2	0	0	0	0	0	5	RO
RS	4	0	1	0	6	0	12	0	0	0	1	1	0	0	0	0	1	0	0	4	5	8	0	0	3	0	0	0	0	0	1	RS
RUE	0	0	0	0	0	0	0	1	0	0	0	0	0	0	0	0	0	0	0	0	0	0	0	0	0	0	2	0	0	0	0	RUE
SE	0	0	0	0	0	1	0	1	0	0	0	2	2	0	0	2	1	1	0	0	0	0	0	0	0	-0	0	1	0	1	0	SE
SI	0	0	18	0	2	0	1	0	0	0	3	3	0	0	0	0	1	0	0	0	46	7	0	0	38	0	0	0	0	0	0	SI
SK	0	0	4	0	2	0	2	1	0	0	9	4	0	0	0	0	1	0	0	1	4	38	0	0	3	-0	0	0	0	0	0	SK
TJ	0	0	-0	0	-0	-0	0	0	-0	0	-0	-0	-0	0	-0	0	-0	-0	0	0	-0	-0	-0	0	-0	1	2	-0	-0	-0	-0	TJ
TM	0	0	0	1	0	0	0	0	0	0	0	0	0	0	0	0	0	0	0	0	0	0	0	0	0	0	6	0	0	0	0	TM
TR	0	1	0	0	0	0	1	0	0	0	0	0	0	0	0	0	0	0	1	1	0	0	0	-0	0	0	0	0	0	0	0	TR
UA	0	0	0	0	0	0	2	5	0	0	0	1	0	0	0	0	0	0	0	0	0	1	0	0	0	0	1	0	0	0	4	UA
UZ	0	0	0	0	0	0	0	0	0	0	0	0	0	0	0	0	0	0	0	0	0	0	0	0	0	3	16	0	0	0	0	UZ
ATL	0	0	0	0	0	0	0	0	0	0	0	0	0	0	0	0	1	1	0	0	0	0	0	0	0	0	0	0	0	0	0	ATL
BAS	0	0	0	0	0	1	0	4	0	0	1	8	8	2	0	7	2	2	0	0	0	1	0	0	0	-0	0	4	0	7	0	BAS
BLS	0	0	0	1	0	0	5	1	0	0	0	0	0	0	0	0	0	0	11	1	0	0	0	0	1	0	1	0	0	0	1	BLS
MED	1	0	0	0	1	0	1	0	0	0	0	1	0	0	3	0	6	0	0	5	1	0	0	0	21	0	0	0	0	0	0	MED
NOS	0	0	0	0	0	4	0	1	0	0	0	6	3	0	0	0	10	22	0	0	0	0	1	0	0	-0	0	0	0	0	0	NOS
AST	0	0	0	2	0	0	0	0	0	0	0	0	0	0	0	0	0	0	0	0	0	0	0	-0	0	0	2	0	0	0	0	AST
NOA	0	0	0	0	0	0	0	0	0	0	0	0	0	0	1	0	1	0	0	1	0	0	0	0	2	0	0	0	0	0	0	NOA
EXC	0	0	1	1	0	1	1	2	0	0	1	3	0	0	1	1	4	2	1	1	1	1	0	0	5	0	6	1	0	0	0	EXC
EU	0	0	3	0	1	4	6	2	1	0	4	15	1	0	7	2	22	8	0	3	3	5	1	0	23	0	0	2	0	1	0	EU
	AL	AM	AT	AZ	BA	BE	BG	BY	CH	CY	CZ	DE	DK	EE	ES	FI	FR	GB	GE	GR	HR	HU	IE	IS	IT	KG	KZT	LT	LU	LV	MD	

Table C.8 Cont.: 2014 country-to-country blame matrices for **PM2.5**.
Units: ng/m^3 per 15% emis. red. of PPM. **Emitters →, Receptors ↓.**

	ME	MK	MT	NL	NO	PL	PT	RO	RS	RUE	SE	SI	SK	TJ	TM	TR	UA	UZ	ATL	BAS	BLS	MED	NOS	AST	NOA	BIC	DMS	VOL	EXC	EU	
AL	6	13	0	0	0	1	0	3	25	1	0	0	1	0	0	1	2	0	0	0	0	5	0	0	0	0	0	0	207	38	AL
AM	0	0	0	0	-0	0	0	0	0	2	0	0	0	0	1	17	0	1	0	0	0	0	0	9	0	0	0	0	110	0	AM
AT	0	0	0	0	0	6	0	3	2	1	0	18	11	0	0	0	2	0	0	0	0	0	0	0	0	0	0	0	172	164	AT
AZ	0	0	0	0	0	0	0	0	0	17	0	0	0	0	5	3	2	3	0	0	0	0	0	16	0	0	0	0	157	1	AZ
BA	6	1	0	0	0	4	0	4	13	1	0	1	3	0	0	0	3	0	0	0	0	1	0	0	0	0	0	0	159	52	BA
BE	-0	-0	0	17	0	3	0	0	0	1	0	0	1	-0	0	-0	1	-0	1	0	0	0	11	-0	0	0	0	0	358	356	BE
BG	0	3	0	0	0	2	0	39	10	8	0	0	1	0	0	12	20	0	0	0	2	1	0	0	0	0	0	0	285	227	BG
BY	0	0	0	0	0	14	0	9	1	48	0	0	2	0	0	1	45	0	0	0	0	0	0	0	0	0	0	0	234	40	BY
CH	0	0	0	0	0	1	0	0	0	0	0	0	0	0	0	-0	0	0	0	0	-0	0	0	0	0	0	0	0	150	66	CH
CY	0	0	0	0	0	0	0	1	0	2	0	0	0	0	0	107	3	0	0	0	0	15	0	4	1	0	0	0	133	19	CY
CZ	0	0	0	0	0	33	0	7	3	2	0	3	29	-0	0	1	5	0	0	0	0	0	0	0	0	0	0	0	245	231	CZ
DE	0	0	-0	4	0	16	0	2	0	2	0	1	2	-0	0	0	3	0	0	2	0	0	3	0	0	0	0	0	222	210	DE
DK	0	0	-0	2	2	13	0	1	0	5	3	0	1	0	0	0	4	0	0	11	0	0	8	0	0	0	0	0	144	130	DK
EE	0	0	0	0	1	8	0	2	0	29	2	0	1	0	0	0	6	0	0	4	0	0	0	0	0	0	0	0	110	67	EE
ES	0	0	0	0	0	0	8	0	0	0	0	0	0	0	0	0	0	0	2	0	0	5	0	0	1	0	0	0	68	68	ES
FI	0	0	0	0	1	2	0	1	0	9	2	0	0	0	0	0	1	0	0	1	0	0	0	0	0	0	0	0	51	38	FI
FR	0	0	0	1	0	1	0	0	0	0	0	0	0	0	0	0	0	0	1	0	0	2	2	0	0	0	0	0	176	173	FR
GB	0	0	0	1	0	1	0	0	0	0	0	0	0	-0	0	0	0	0	3	0	0	0	6	0	0	0	0	0	137	136	GB
GE	0	0	0	0	-0	0	0	0	0	14	0	0	0	0	1	9	1	1	0	0	0	0	0	2	0	0	0	0	204	1	GE
GL	-0	0	-0	0	0	-0	-0	-0	-0	0	0	-0	-0	-0	0	0	0	0	0	-0	-0	-0	0	-0	-0	0	0	0	0	-0	GL
GR	0	6	0	0	0	1	0	4	4	3	0	0	0	0	0	8	6	0	0	0	0	11	0	0	1	0	0	0	153	122	GR
HR	1	0	0	0	0	6	0	7	16	2	0	15	5	0	0	0	5	0	0	0	0	4	0	0	0	0	0	0	245	200	HR
HU	1	1	0	0	0	14	0	60	23	4	0	6	36	0	0	1	12	0	0	0	0	1	0	0	0	0	0	0	335	287	HU
IE	0	0	-0	0	0	0	0	0	0	0	0	0	0	-0	0	0	0	0	4	0	0	0	1	0	0	0	0	0	62	62	IE
IS	0	0	0	0	0	0	0	0	0	0	0	0	0	-0	0	0	0	0	0	0	0	0	0	0	0	0	0	0	1	1	IS
IT	0	0	0	0	0	1	0	1	0	0	0	4	1	0	0	0	1	0	0	0	0	10	0	0	1	0	0	0	323	319	IT
KG	0	0	0	-0	-0	-0	-0	0	0	1	0	-0	-0	8	0	0	0	85	-0	-0	0	0	-0	2	0	0	0	0	134	-0	KG
KZT	0	0	0	0	0	0	0	0	0	29	0	0	0	0	2	0	2	12	0	0	0	0	0	1	0	0	0	0	86	0	KZT
LT	0	0	0	0	0	27	0	5	1	37	1	0	2	0	0	1	17	0	0	1	0	0	0	0	0	0	0	0	220	135	LT
LU	0	0	0	3	0	3	0	1	0	1	0	0	1	0	0	0	1	0	0	0	0	0	2	-0	0	0	0	0	281	278	LU
LV	0	0	0	0	0	13	0	3	0	32	1	0	1	0	0	0	12	0	0	2	0	0	0	0	0	0	0	0	174	112	LV
MD	0	0	0	0	0	6	0	87	1	24	0	0	1	0	0	9	121	0	0	0	1	0	0	0	0	0	0	0	335	109	MD
ME	84	2	0	0	0	2	0	2	21	1	0	0	1	0	0	0	1	0	0	0	0	2	0	0	0	0	0	0	148	18	ME
MK	1	104	0	0	0	1	0	5	35	1	0	0	1	0	0	1	3	0	0	0	0	2	0	0	0	0	0	0	242	81	MK
MT	0	0	28	0	0	0	0	1	0	0	0	0	0	0	0	0	1	0	0	0	0	61	0	0	3	0	0	0	63	60	MT
NL	-0	0	-0	77	0	7	0	1	0	1	0	0	1	-0	0	0	2	0	1	1	0	0	25	-0	0	0	0	0	267	262	NL
NO	0	0	0	0	22	1	0	0	0	1	1	0	0	0	0	0	0	0	0	0	0	0	1	0	0	0	0	0	30	6	NO
PL	0	0	0	0	0	180	0	11	2	11	0	1	13	0	0	1	20	0	0	1	0	0	1	0	0	0	0	0	286	241	PL
PT	0	0	0	0	0	0	140	0	0	0	0	0	0	0	0	0	0	0	9	0	-0	1	0	0	0	0	0	0	161	161	PT
RO	0	1	0	0	0	4	0	298	7	9	0	0	2	0	0	5	31	0	0	0	1	0	0	0	0	0	0	0	393	332	RO
RS	5	15	0	0	0	4	0	34	186	3	0	0	4	0	0	1	8	0	0	0	0	1	0	0	0	0	0	0	309	80	RS
RUE	0	0	0	0	0	0	0	0	0	66	0	0	0	0	0	0	4	0	0	0	0	0	0	0	0	0	0	0	77	2	RUE
SE	0	0	0	0	3	4	0	1	0	4	13	0	0	0	0	0	2	0	0	2	0	0	1	0	0	0	0	0	42	31	SE
SI	0	0	0	0	0	5	0	4	3	1	0	222	3	0	0	0	3	0	0	0	0	3	0	0	0	0	0	0	361	351	SI
SK	0	1	0	0	0	34	0	29	7	3	0	2	191	0	0	1	14	0	0	0	0	0	0	0	0	0	0	0	353	323	SK
TJ	0	0	0	-0	-0	-0	-0	-0	0	1	0	-0	-0	129	3	0	0	73	-0	-0	0	0	-0	16	0	0	0	0	211	-0	TJ
TM	0	0	0	0	0	0	0	0	0	7	0	0	0	3	88	1	1	55	0	0	0	0	0	16	0	0	0	0	163	0	TM
TR	0	0	0	0	0	0	0	1	0	3	0	0	0	0	0	372	4	0	0	0	1	2	0	2	0	0	0	0	386	4	TR
UA	0	0	0	0	0	7	0	22	1	54	0	0	1	0	1	6	284	1	0	0	1	0	0	0	0	0	0	0	395	38	UA
UZ	0	0	0	0	0	0	0	0	0	9	0	0	0	14	16	0	1	254	0	0	0	0	0	5	0	0	0	0	314	0	UZ
ATL	0	0	0	0	0	0	1	0	0	1	0	0	0	0	0	0	0	0	2	0	0	0	0	0	0	0	0	0	5	4	ATL
BAS	0	0	0	1	1	19	0	2	0	14	7	0	1	0	0	0	5	0	0	11	0	0	2	0	0	0	0	0	99	73	BAS
BLS	0	0	0	0	0	1	0	10	1	38	0	0	0	0	0	76	48	1	0	0	9	1	0	0	0	0	0	0	199	19	BLS
MED	0	0	0	0	0	1	0	1	1	1	0	1	0	0	0	24	2	0	0	0	0	36	0	1	4	0	0	0	74	43	MED
NOS	0	0	0	3	4	3	0	0	0	2	1	0	0	0	0	0	1	0	1	1	0	0	16	0	0	0	0	0	64	57	NOS
AST	0	0	0	0	0	0	0	0	0	4	0	0	0	1	4	19	1	5	0	0	0	0	0	32	0	0	0	0	39	0	AST
NOA	0	0	0	0	0	0	0	0	0	0	0	0	0	0	0	2	1	0	0	0	0	6	0	0	10	0	0	0	11	7	NOA
EXC	0	0	0	0	0	4	1	5	1	38	0	0	1	1	3	13	12	9	0	0	0	1	0	1	0	0	0	0	123	35	EXC
EU	0	0	0	1	1	18	4	21	2	5	2	2	5	0	0	1	6	0	1	1	0	2	1	0	0	0	0	0	182	164	EU
	ME	MK	MT	NL	NO	PL	PT	RO	RS	RUE	SE	SI	SK	TJ	TM	TR	UA	UZ	ATL	BAS	BLS	MED	NOS	AST	NOA	BIC	DMS	VOL	EXC	EU	

Table C.9: 2014 country-to-country blame matrices for **PM2.5**.
Units: ng/m^3 per 15% emis. red. of SO_x. **Emitters →, Receptors ↓.**

	AL	AM	AT	AZ	BA	BE	BG	BY	CH	CY	CZ	DE	DK	EE	ES	FI	FR	GB	GE	GR	HR	HU	IE	IS	IT	KG	KZT	LT	LU	LV	MD	
AL	49	0	0	0	23	0	7	0	0	0	2	2	0	0	2	0	1	0	0	30	1	1	0	0	11	0	1	0	0	0	0	AL
AM	0	15	0	25	0	0	1	0	0	0	0	0	0	0	0	0	0	0	4	0	0	0	-0	0	0	0	19	0	0	0	0	AM
AT	0	0	19	0	7	1	2	1	1	0	17	38	0	0	1	0	3	2	0	0	2	4	0	0	11	0	1	0	0	0	0	AT
AZ	0	1	0	84	0	0	1	0	0	0	0	0	0	0	0	0	0	0	4	0	0	0	-0	0	0	0	51	0	0	0	0	AZ
BA	1	0	1	0	208	0	5	1	0	0	7	6	0	0	1	0	2	1	0	2	6	3	0	0	8	0	1	0	0	0	0	BA
BE	0	-0	1	0	1	71	0	1	1	0	6	62	0	0	4	0	53	32	0	0	0	0	1	0	1	-0	0	0	1	0	0	BE
BG	1	0	0	0	7	0	174	2	0	0	3	3	0	0	1	0	1	1	0	14	0	2	0	0	1	0	5	0	0	0	0	BG
BY	0	0	0	0	3	0	3	44	0	0	2	6	0	3	0	1	1	2	0	1	0	1	0	0	0	0	10	3	0	0	0	BY
CH	0	-0	2	0	0	1	0	0	33	0	3	33	0	0	2	0	13	3	-0	0	0	0	0	0	12	0	0	0	0	0	0	CH
CY	1	0	0	0	3	0	12	0	0	31	0	0	0	0	2	0	1	0	0	26	0	0	0	0	4	0	3	0	0	0	0	CY
CZ	0	0	7	0	12	1	4	2	1	0	81	62	0	0	1	0	7	5	0	1	2	8	0	0	3	0	1	0	0	0	0	CZ
DE	0	0	4	0	2	7	1	1	2	0	21	165	1	0	2	0	20	14	0	0	0	1	1	0	1	0	1	0	1	0	0	DE
DK	0	0	0	0	1	4	1	3	0	0	3	30	11	2	1	1	6	20	0	0	0	0	1	0	0	0	1	1	0	0	0	DK
EE	0	0	0	0	1	0	1	9	0	0	2	5	1	19	0	7	1	3	0	0	0	0	0	0	0	0	4	3	0	2	0	EE
ES	0	0	0	0	1	1	0	0	0	0	0	3	0	0	96	0	6	3	0	0	0	0	0	0	1	0	0	0	0	0	0	ES
FI	0	0	0	0	0	0	0	3	0	0	1	2	0	5	0	17	0	2	0	0	0	0	0	0	0	0	2	1	0	0	0	FI
FR	0	-0	0	0	0	5	0	0	1	0	3	27	0	0	14	0	49	17	0	0	0	0	1	0	3	0	0	0	0	0	0	FR
GB	0	0	0	0	0	2	0	0	0	0	1	8	0	0	2	0	6	109	0	0	0	0	6	0	0	-0	0	0	0	0	0	GB
GE	0	2	0	24	1	0	1	0	0	0	0	0	0	0	0	0	0	0	29	1	0	0	-0	0	0	0	17	0	0	0	0	GE
GL	0	0	0	0	0	0	0	0	0	0	0	0	0	0	0	0	0	0	0	0	0	0	0	0	0	0	0	0	0	0	0	GL
GR	4	0	0	0	9	0	47	1	0	0	2	2	0	0	2	0	1	0	0	88	0	1	0	0	7	0	2	0	0	0	0	GR
HR	1	0	3	0	85	0	6	1	0	0	12	12	0	0	1	0	3	1	0	2	17	6	0	0	14	0	1	0	0	0	0	HR
HU	1	0	3	0	35	1	13	2	0	0	15	15	0	0	1	0	2	2	0	2	4	33	0	0	6	0	3	0	0	0	0	HU
IE	0	0	0	0	0	1	0	0	0	0	0	2	0	0	1	0	2	38	0	0	0	0	29	0	0	0	0	0	0	0	0	IE
IS	0	0	0	0	0	0	0	0	0	0	0	0	0	0	0	0	0	2	0	0	0	0	0	79	0	0	0	0	0	0	0	IS
IT	0	0	2	0	11	0	1	0	1	0	4	6	0	0	7	0	10	1	0	1	2	1	0	0	79	0	0	0	0	0	0	IT
KG	0	0	-0	0	0	-0	0	0	-0	0	0	-0	-0	0	-0	0	-0	-0	0	0	-0	0	-0	-0	-0	41	110	0	-0	0	0	KG
KZT	0	0	0	0	0	0	0	0	0	0	0	0	0	0	0	0	0	0	0	0	0	0	0	0	0	2	186	0	0	0	0	KZT
LT	0	0	0	0	3	0	2	23	0	0	3	9	1	4	0	3	1	3	0	0	0	1	0	0	0	0	5	20	0	1	0	LT
LU	0	-0	2	0	1	20	0	1	1	0	7	108	0	0	4	0	61	23	0	0	0	1	1	0	1	0	0	0	13	0	0	LU
LV	0	0	0	0	2	0	1	16	0	0	2	7	1	7	0	4	1	3	0	0	0	0	0	0	0	0	4	8	0	4	0	LV
MD	0	0	0	0	2	0	14	5	0	0	3	4	0	0	0	0	0	1	0	2	0	1	0	0	0	0	12	0	0	0	9	MD
ME	9	0	0	0	36	0	5	0	0	0	2	2	0	0	2	0	1	0	0	5	1	1	0	0	6	0	0	0	0	0	0	ME
MK	10	0	0	0	11	0	37	0	0	0	3	2	0	0	2	0	1	1	0	51	0	2	0	0	3	0	1	0	0	0	0	MK
MT	1	0	1	0	8	1	3	0	0	0	2	5	0	0	16	0	10	3	0	7	1	0	0	0	31	0	0	0	0	0	0	MT
NL	0	-0	1	0	1	33	0	1	0	-0	8	79	1	1	2	0	31	38	0	0	0	0	1	0	0	-0	0	0	0	0	0	NL
NO	0	0	0	0	0	0	0	1	0	0	1	2	0	1	0	2	0	3	0	0	0	0	0	0	0	0	0	0	0	0	0	NO
PL	0	0	1	0	8	1	3	8	0	0	15	28	1	1	0	1	3	4	0	1	1	3	0	0	1	0	4	1	0	0	0	PL
PT	0	0	0	0	0	0	0	0	0	0	0	1	0	0	44	0	3	2	0	0	0	0	0	0	0	0	0	0	0	0	0	PT
RO	0	0	1	0	9	0	27	2	0	0	4	4	0	0	0	0	1	1	0	3	0	3	0	0	1	0	6	0	0	0	1	RO
RS	3	0	1	0	39	0	31	1	0	0	7	6	0	0	1	0	1	1	0	10	1	5	0	0	3	0	2	0	0	0	0	RS
RUE	0	0	0	0	0	0	0	1	0	0	0	0	0	1	0	1	0	0	0	0	0	0	0	0	0	0	23	0	0	0	0	RUE
SE	0	0	0	0	1	1	0	2	0	0	1	5	1	2	0	4	1	5	0	0	0	0	0	0	0	0	1	1	0	0	0	SE
SI	0	0	8	0	17	0	4	1	0	0	13	15	0	0	1	0	2	1	0	1	12	4	0	0	26	0	1	0	0	0	0	SI
SK	0	0	2	0	21	1	7	2	0	0	20	16	0	0	1	0	2	2	0	1	2	17	0	0	3	0	2	0	0	0	0	SK
TJ	0	0	-0	0	0	-0	0	0	-0	0	0	-0	-0	0	-0	0	-0	-0	0	0	0	0	-0	-0	0	4	43	0	-0	0	0	TJ
TM	0	0	0	2	0	0	0	0	0	0	0	0	0	0	0	0	0	0	0	0	0	0	-0	0	0	1	95	0	0	0	0	TM
TR	0	0	0	1	1	0	6	0	0	2	0	0	0	0	1	0	0	0	0	7	0	0	0	0	1	0	3	0	0	0	0	TR
UA	0	0	0	1	2	0	6	7	0	0	2	4	0	1	0	0	0	1	0	1	0	1	0	0	0	0	18	1	0	0	1	UA
UZ	0	0	0	1	0	0	0	0	0	0	0	0	0	0	0	0	0	0	0	0	0	0	-0	0	0	5	154	0	0	0	0	UZ
ATL	0	0	0	0	0	0	0	0	0	0	0	1	0	0	1	0	1	4	0	0	0	0	0	1	0	0	1	0	0	0	0	ATL
BAS	0	0	0	0	1	1	1	5	0	0	2	14	2	5	0	7	2	7	0	0	0	0	0	0	0	0	2	2	0	1	0	BAS
BLS	0	0	0	2	2	0	11	2	0	0	1	1	0	0	0	0	0	0	3	3	0	0	0	0	0	0	15	0	0	0	0	BLS
MED	1	0	1	0	13	0	11	0	0	1	2	4	0	0	17	0	9	2	0	20	1	1	0	0	23	0	1	0	0	0	0	MED
NOS	0	0	0	0	0	2	0	1	0	0	1	12	1	1	1	1	6	34	0	0	0	0	2	0	0	0	0	0	0	0	0	NOS
AST	0	0	0	2	0	0	1	0	0	1	0	0	0	0	0	0	0	0	0	1	0	0	0	0	0	1	38	0	0	0	0	AST
NOA	0	0	0	0	4	0	4	0	0	0	1	1	0	0	9	0	2	0	0	10	0	0	0	0	5	0	0	0	0	0	0	NOA
EXC	0	0	0	1	2	1	2	2	0	0	2	5	0	1	3	1	2	3	0	1	0	0	0	0	2	1	40	0	0	0	0	EXC
EU	0	0	1	0	5	3	8	2	1	0	7	26	0	1	15	2	11	13	0	3	1	2	1	0	7	0	1	1	0	0	0	EU
	AL	AM	AT	AZ	BA	BE	BG	BY	CH	CY	CZ	DE	DK	EE	ES	FI	FR	GB	GE	GR	HR	HU	IE	IS	IT	KG	KZT	LT	LU	LV	MD	

Table C.9 Cont.: 2014 country-to-country blame matrices for **PM2.5**.
Units: ng/m^3 per 15% emis. red. of SO_x. **Emitters →, Receptors ↓.**

	ME	MK	MT	NL	NO	PL	PT	RO	RS	RUE	SE	SI	SK	TJ	TM	TR	UA	UZ	ATL	BAS	BLS	MED	NOS	AST	NOA	BIC	DMS	VOL	EXC	EU	
AL	26	46	0	0	0	13	0	7	69	2	0	0	2	0	0	5	10	0	0	0	0	57	0	0	5	6	5	53	315	82	AL
AM	0	0	0	0	0	1	0	0	0	14	0	0	0	0	15	67	4	13	0	0	0	2	0	71	1	10	0	10	180	3	AM
AT	0	1	0	0	0	33	0	5	17	4	0	5	4	0	0	2	13	0	0	0	0	6	1	0	1	5	1	10	197	148	AT
AZ	0	0	0	0	0	1	0	1	1	50	0	0	0	0	34	22	13	29	0	0	0	1	0	67	0	7	0	22	293	3	AZ
BA	21	5	0	0	0	27	0	6	86	4	0	1	4	0	0	4	18	0	0	0	0	16	0	0	2	5	2	17	429	80	BA
BE	0	0	0	10	0	17	0	1	2	3	0	0	1	0	0	0	6	0	11	2	0	3	34	0	1	6	15	16	278	264	BE
BG	2	16	0	0	0	14	0	33	40	32	0	0	2	0	1	47	68	1	0	0	11	12	0	0	2	6	1	23	472	249	BG
BY	0	1	0	0	0	42	0	5	5	82	1	0	1	0	1	10	76	2	0	2	1	1	2	1	0	6	2	33	307	73	BY
CH	0	0	0	1	0	5	0	0	1	0	0	0	0	0	0	0	1	0	1	0	0	3	2	0	1	6	1	10	113	76	CH
CY	1	7	0	0	0	2	0	3	5	12	0	0	0	0	0	874	26	1	0	0	5	135	0	32	13	10	29	66	1016	83	CY
CZ	1	2	0	1	0	86	0	10	26	10	0	2	11	0	0	5	24	0	1	1	0	3	4	0	1	5	3	15	376	292	CZ
DE	0	1	0	5	0	45	0	2	6	8	0	0	2	0	0	3	15	0	3	5	0	2	15	0	0	5	8	15	335	295	DE
DK	0	0	0	4	1	32	0	1	2	15	2	0	1	0	0	4	13	0	5	21	0	0	30	0	0	5	17	20	163	121	DK
EE	0	0	0	0	0	19	0	1	1	48	2	0	0	0	0	2	17	1	1	11	0	0	3	0	0	5	6	26	150	67	EE
ES	0	0	0	0	0	2	8	0	1	0	0	0	0	0	0	0	1	0	21	0	0	44	1	0	5	17	9	7	124	121	ES
FI	0	0	0	0	1	9	0	0	1	22	3	0	0	0	0	1	5	0	1	5	0	0	1	0	0	4	8	26	77	42	FI
FR	0	0	0	2	0	6	0	1	1	1	0	0	0	0	0	0	2	0	16	1	0	15	11	0	3	8	13	19	139	131	FR
GB	0	0	0	1	0	5	0	0	1	2	0	0	0	0	0	1	2	0	24	1	0	1	15	0	0	5	21	29	148	141	GB
GE	0	1	0	0	0	1	0	1	1	22	0	0	0	0	12	43	10	10	0	0	3	1	0	22	1	7	0	9	175	5	GE
GL	0	0	-0	0	0	0	-0	0	0	0	0	0	0	0	0	0	0	0	0	0	0	0	0	0	0	21	1	13	1	0	GL
GR	4	45	0	0	0	8	0	11	28	13	0	0	1	0	0	43	28	0	0	0	3	88	0	0	7	6	8	61	351	172	GR
HR	5	4	0	0	0	43	0	11	88	7	0	3	7	0	0	5	24	0	0	1	0	26	1	0	2	5	3	18	362	142	HR
HU	4	7	0	0	0	76	0	49	86	16	0	1	16	0	0	12	55	1	0	1	1	8	1	0	1	6	2	17	462	240	HU
IE	0	0	0	1	0	1	0	0	0	1	0	0	0	0	0	0	1	0	30	0	0	0	4	0	0	6	29	31	78	76	IE
IS	0	0	-0	0	0	1	0	0	0	0	0	0	0	0	0	1	1	0	3	0	0	0	0	0	0	4	13	79	85	3	IS
IT	1	1	1	0	0	13	0	3	11	1	0	2	2	0	0	1	6	0	1	0	0	77	1	0	7	6	8	54	168	134	IT
KG	0	0	0	-0	-0	0	-0	0	0	7	0	-0	0	11	3	1	0	319	-0	0	0	0	-0	24	0	9	0	9	492	0	KG
KZT	0	0	0	0	0	1	0	0	0	90	0	0	0	1	6	1	10	32	0	0	0	0	0	7	0	8	0	40	331	2	KZT
LT	0	1	0	1	0	53	0	4	4	56	1	0	1	0	1	8	45	1	1	6	0	1	3	0	0	6	5	30	256	109	LT
LU	0	0	0	6	0	17	0	1	2	3	0	0	1	0	0	1	6	0	7	1	0	4	15	0	1	6	9	13	282	268	LU
LV	0	0	0	1	0	29	0	2	2	52	1	0	1	0	0	4	30	1	1	7	0	0	3	0	0	5	5	26	187	74	LV
MD	0	2	0	0	0	35	0	29	6	64	0	0	2	0	2	37	173	3	0	1	7	3	1	1	1	7	1	25	411	95	MD
ME	125	11	0	0	0	14	0	5	76	2	0	0	2	0	0	3	10	0	0	0	0	23	0	0	3	6	3	24	322	49	ME
MK	6	194	0	0	0	12	0	11	84	6	0	0	2	0	0	12	18	0	0	0	1	17	0	0	4	6	2	26	472	128	MK
MT	2	4	20	0	0	6	0	2	8	1	0	1	1	0	0	2	4	0	2	0	0	279	1	0	27	10	26	99	140	109	MT
NL	0	0	0	20	0	31	0	1	2	7	0	0	1	0	0	1	10	0	9	3	0	1	56	0	0	5	16	17	274	251	NL
NO	0	0	0	0	5	6	0	0	0	6	2	0	0	0	0	2	3	0	3	1	0	0	4	0	0	6	15	28	37	19	NO
PL	1	1	0	1	0	192	0	8	15	30	1	0	6	0	0	7	56	1	1	4	1	2	4	0	0	5	5	22	406	273	PL
PT	0	0	0	0	0	1	37	0	0	0	0	0	0	0	0	0	1	0	65	0	0	7	1	0	2	17	15	4	93	91	PT
RO	2	6	0	0	0	31	0	113	31	34	0	0	3	0	1	28	101	2	0	0	6	4	0	1	1	7	1	23	418	194	RO
RS	18	36	0	0	0	31	0	37	232	12	0	0	5	0	0	11	39	0	0	0	2	10	1	0	2	6	1	21	539	143	RS
RUE	0	0	0	0	0	2	0	0	0	95	0	0	0	0	1	1	9	2	0	0	0	0	0	1	0	8	4	17	139	5	RUE
SE	0	0	0	1	2	13	0	1	2	12	7	0	0	0	0	1	8	0	2	7	0	0	5	0	0	4	7	28	73	44	SE
SI	1	2	0	0	0	38	0	9	39	5	0	29	5	0	0	3	17	0	0	0	0	24	1	0	1	4	2	14	254	169	SI
SK	2	4	0	0	0	111	0	26	46	15	0	1	34	0	0	11	49	1	0	1	1	4	1	0	1	5	2	15	402	247	SK
TJ	0	0	0	-0	-0	0	-0	0	0	5	0	-0	0	60	14	2	0	243	-0	0	0	0	-0	21	0	11	0	7	373	0	TJ
TM	0	0	0	0	0	1	0	0	0	38	0	0	0	4	76	5	8	139	0	0	0	0	0	27	0	11	0	38	369	2	TM
TR	0	3	0	0	0	3	0	3	4	16	0	0	0	0	1	519	26	1	0	0	6	21	0	25	5	10	4	29	601	24	TR
UA	0	1	0	0	0	32	0	10	4	94	0	0	1	0	3	26	195	5	0	1	5	2	1	1	0	7	1	26	417	61	UA
UZ	0	0	0	0	0	1	-0	0	0	45	0	0	0	11	26	3	7	322	0	0	0	0	0	11	0	10	0	33	574	1	UZ
ATL	0	0	0	0	0	1	0	0	0	5	0	0	0	0	0	0	1	0	12	0	0	0	1	0	0	14	34	16	19	10	ATL
BAS	0	0	0	1	1	29	0	2	3	27	4	0	1	0	0	2	16	0	2	20	0	0	8	0	0	5	9	27	141	83	BAS
BLS	0	2	0	0	0	10	0	12	6	79	0	0	1	0	4	142	111	5	0	0	33	6	0	4	1	7	1	24	413	41	BLS
MED	3	6	2	0	0	8	1	4	12	6	0	1	1	0	0	127	15	0	2	0	2	239	1	5	24	11	26	101	293	107	MED
NOS	0	0	0	2	2	11	0	0	1	6	1	0	0	0	0	2	5	0	12	4	0	1	26	0	0	5	24	34	94	76	NOS
AST	0	0	0	0	0	0	0	0	0	17	0	0	0	2	13	42	5	30	0	0	0	6	0	126	1	16	2	16	155	4	AST
NOA	1	4	1	0	0	3	0	2	6	2	0	0	0	0	0	25	4	0	1	0	0	63	0	1	43	21	11	60	86	39	NOA
EXC	0	1	0	0	0	9	0	3	4	64	0	0	1	1	4	21	17	18	2	1	1	4	1	4	1	9	4	22	213	36	EXC
EU	1	3	0	1	0	32	2	10	11	12	1	1	2	0	0	8	20	0	9	3	1	17	6	0	2	7	9	24	217	152	EU
	ME	MK	MT	NL	NO	PL	PT	RO	RS	RUE	SE	SI	SK	TJ	TM	TR	UA	UZ	ATL	BAS	BLS	MED	NOS	AST	NOA	BIC	DMS	VOL	EXC	EU	

Table C.10: 2014 country-to-country blame matrices for **PM2.5**.
Units: ng/m^3 per 15% emis. red. of NO_x. **Emitters →, Receptors ↓.**

	AL	AM	AT	AZ	BA	BE	BG	BY	CH	CY	CZ	DE	DK	EE	ES	FI	FR	GB	GE	GR	HR	HU	IE	IS	IT	KG	KZT	LT	LU	LV	MD	
AL	42	0	1	0	2	0	2	0	0	0	0	2	0	-0	1	-0	2	0	0	23	2	2	0	0	15	0	0	0	0	0	0	AL
AM	0	70	0	61	0	0	0	-0	0	0	0	0	0	-0	0	-0	0	0	10	0	0	0	0	0	0	0	1	-0	0	-0	0	AM
AT	0	0	90	0	1	2	1	0	8	0	18	76	0	0	1	0	10	3	0	0	7	12	0	0	52	0	0	0	1	0	0	AT
AZ	0	12	0	191	0	0	0	-0	0	0	0	0	0	-0	0	-0	0	0	17	0	0	0	0	0	0	0	5	-0	0	-0	0	AZ
BA	1	0	5	0	40	0	1	0	0	0	3	5	0	-0	1	0	2	1	0	1	14	8	0	0	14	0	0	0	0	0	0	BA
BE	0	0	5	0	0	50	0	1	6	0	5	135	3	0	7	0	185	68	0	0	0	1	3	0	5	0	0	0	11	0	0	BE
BG	0	0	0	0	0	0	40	0	0	0	0	0	0	-0	0	-0	0	0	0	7	0	1	0	0	1	0	0	0	0	0	1	BG
BY	0	0	1	0	0	1	1	37	0	0	1	8	1	1	0	1	1	2	0	0	0	2	0	0	1	0	1	5	0	2	1	BY
CH	0	0	15	0	0	3	0	0	165	0	3	84	0	-0	3	0	63	5	0	0	0	0	0	0	88	0	0	0	1	0	-0	CH
CY	0	0	0	0	0	0	2	-0	0	15	0	0	0	-0	1	-0	0	0	0	9	0	0	0	0	2	0	0	-0	0	-0	0	CY
CZ	0	0	46	0	2	3	1	1	5	0	73	116	1	0	2	0	18	5	0	1	6	25	0	0	12	0	0	0	1	0	0	CZ
DE	0	0	27	0	0	19	0	1	16	0	22	305	5	0	5	0	62	23	0	0	1	3	1	0	10	0	0	1	5	0	0	DE
DK	0	0	2	0	0	17	0	3	1	0	5	99	39	1	2	1	30	31	0	0	0	1	2	0	1	0	0	2	2	1	0	DK
EE	0	0	0	0	0	1	0	8	0	0	1	8	2	7	0	5	2	2	0	0	0	1	0	0	0	0	0	5	0	6	0	EE
ES	0	0	0	0	0	0	0	0	0	0	0	2	0	-0	85	-0	11	2	0	0	0	0	0	0	2	0	0	-0	0	-0	0	ES
FI	0	0	0	0	0	0	0	0	0	0	0	3	1	0	0	7	1	1	0	0	0	0	0	0	0	0	0	0	0	0	-0	FI
FR	0	0	3	0	0	16	0	0	10	0	2	52	1	0	12	0	182	29	0	0	0	0	2	0	13	0	0	0	3	0	0	FR
GB	0	0	1	0	0	6	0	0	1	0	1	20	2	0	3	0	27	105	0	0	0	0	9	0	1	0	0	0	1	0	0	GB
GE	0	13	0	52	0	0	0	0	0	0	0	0	0	-0	0	-0	0	0	69	0	0	0	0	0	1	0	1	-0	0	-0	0	GE
GL	0	0	0	0	0	-0	0	0	-0	0	-0	-0	-0	-0	0	0	-0	-0	0	0	-0	-0	0	0	0	-0	0	0	-0	0	-0	GL
GR	2	0	0	0	0	0	10	0	0	0	0	0	0	-0	1	-0	1	0	0	45	0	0	0	0	6	0	0	0	0	0	0	GR
HR	0	0	18	0	15	1	2	0	1	0	8	14	0	-0	1	0	3	1	0	1	37	20	0	0	32	0	0	0	0	0	0	HR
HU	1	0	27	0	8	2	5	1	2	0	16	27	0	-0	1	-0	6	3	0	3	18	91	0	0	20	0	0	0	0	0	1	HU
IE	0	0	0	0	0	2	0	0	0	0	0	5	1	0	1	0	8	65	0	0	0	0	38	0	0	0	0	0	0	0	0	IE
IS	0	0	-0	0	0	0	0	0	0	0	-0	-0	0	0	0	0	0	1	0	0	0	0	0	7	0	0	0	0	-0	0	0	IS
IT	0	0	12	0	1	0	0	0	4	0	2	10	0	-0	4	-0	13	1	0	0	5	3	0	0	332	0	0	0	0	0	0	IT
KG	0	0	0	0	0	0	0	0	0	0	0	0	0	-0	0	-0	0	0	0	0	0	0	0	0	0	27	12	-0	0	-0	0	KG
KZT	0	0	0	0	0	0	0	0	0	0	0	0	0	-0	0	-0	0	0	0	0	0	0	0	0	0	1	28	0	0	-0	0	KZT
LT	0	0	1	0	0	1	0	29	0	0	3	15	4	1	0	2	3	4	0	0	0	2	0	0	1	0	1	20	0	5	1	LT
LU	0	0	7	0	0	56	0	0	9	0	8	207	2	0	7	0	181	39	0	0	0	1	2	0	6	0	0	0	7	0	0	LU
LV	0	0	1	0	0	1	0	18	0	0	1	10	2	2	0	3	3	3	0	0	0	1	0	0	1	0	0	13	0	8	0	LV
MD	0	0	1	0	0	0	7	3	0	0	1	2	0	0	0	-0	1	1	0	1	0	2	0	0	2	0	1	0	0	0	11	MD
ME	6	0	1	0	5	0	1	0	0	0	0	1	0	-0	1	-0	1	0	0	3	3	1	0	0	9	0	0	0	0	-0	0	ME
MK	8	0	1	0	1	0	7	0	0	0	1	1	0	-0	1	-0	1	0	0	6	1	2	0	0	5	0	0	0	0	0	0	MK
MT	0	0	0	0	0	0	0	-0	0	0	0	1	0	-0	5	-0	8	1	-0	2	0	0	0	0	20	0	0	-0	0	-0	0	MT
NL	0	0	5	0	0	67	0	1	5	0	10	238	8	0	8	0	124	77	0	0	0	1	3	0	4	0	0	1	7	0	0	NL
NO	0	0	0	0	0	0	0	0	0	0	0	2	0	0	0	0	1	2	0	0	0	0	0	0	0	0	0	0	0	0	0	NO
PL	0	0	6	0	1	2	1	7	1	0	16	48	2	0	1	1	6	5	0	0	2	8	0	0	3	0	0	2	0	1	0	PL
PT	0	0	0	0	0	0	0	0	0	0	0	1	0	-0	37	-0	3	1	0	0	0	0	0	0	1	0	0	-0	0	-0	0	PT
RO	0	0	2	0	1	1	14	1	0	0	2	5	0	0	0	-0	2	1	0	2	1	8	0	0	5	0	1	0	0	0	3	RO
RS	4	0	6	0	8	1	13	0	1	0	5	10	0	0	1	0	3	2	0	10	5	19	0	0	9	0	0	0	0	0	0	RS
RUE	0	0	0	0	0	0	0	1	0	0	0	0	0	0	0	0	0	0	0	0	0	0	0	0	0	0	2	0	0	0	0	RUE
SE	0	0	0	0	0	1	0	1	0	0	0	10	3	0	0	1	3	3	0	0	0	0	0	0	0	0	0	1	0	0	0	SE
SI	0	0	55	0	2	1	1	0	2	0	10	24	0	0	1	0	5	1	0	1	31	14	0	0	91	0	0	0	0	0	0	SI
SK	0	0	15	0	3	1	3	1	1	0	17	21	0	-0	1	-0	5	2	0	1	6	53	0	0	8	0	0	0	0	0	0	SK
TJ	0	0	0	0	0	0	0	-0	0	0	0	0	0	-0	0	-0	0	0	0	0	0	0	0	0	0	2	5	-0	0	-0	0	TJ
TM	0	0	0	2	0	0	0	0	0	0	0	0	0	-0	0	-0	0	0	0	0	0	0	0	0	0	0	17	0	0	-0	0	TM
TR	0	2	0	1	0	0	2	0	0	1	0	1	0	0	1	-0	1	0	1	3	0	0	0	0	2	0	0	0	0	0	0	TR
UA	0	0	0	1	0	0	2	4	0	0	0	2	0	0	0	0	0	1	0	0	0	1	0	0	1	0	2	0	0	0	1	UA
UZ	0	0	0	1	0	0	0	0	0	0	0	0	0	-0	0	-0	0	0	0	0	0	0	0	0	0	4	26	0	0	-0	0	UZ
ATL	0	0	0	0	0	0	0	0	0	0	0	1	0	0	1	0	3	3	0	0	0	0	1	0	0	0	0	0	0	0	0	ATL
BAS	0	0	1	0	0	4	0	3	1	0	2	34	6	1	0	2	7	7	0	0	0	1	0	0	1	0	0	3	0	2	0	BAS
BLS	0	1	0	1	0	0	3	0	0	0	0	0	0	-0	0	-0	0	0	5	1	0	0	0	0	1	0	1	0	0	-0	0	BLS
MED	0	0	1	0	1	0	1	-0	0	0	0	1	0	-0	6	-0	7	0	0	5	1	0	0	0	23	0	0	-0	0	-0	0	MED
NOS	0	0	1	0	0	7	0	1	1	0	1	36	5	0	2	0	29	32	0	0	0	0	2	0	1	0	0	1	1	0	0	NOS
AST	0	0	0	3	0	0	0	-0	0	0	0	0	0	-0	0	-0	0	0	0	0	0	0	0	0	0	0	6	-0	0	-0	0	AST
NOA	0	0	0	0	0	0	0	-0	0	0	0	0	0	-0	4	-0	1	0	-0	2	0	0	0	0	4	0	-0	-0	0	-0	0	NOA
EXC	0	0	2	1	0	1	1	1	1	0	1	10	0	0	3	0	7	3	0	1	0	1	0	0	6	0	6	0	0	0	0	EXC
EU	0	0	8	0	1	6	2	2	4	0	6	48	2	0	13	1	36	15	0	2	2	5	2	0	30	0	0	1	1	0	0	EU
	AL	AM	AT	AZ	BA	BE	BG	BY	CH	CY	CZ	DE	DK	EE	ES	FI	FR	GB	GE	GR	HR	HU	IE	IS	IT	KG	KZT	LT	LU	LV	MD	

Table C.10 Cont.: 2014 country-to-country blame matrices for **PM2.5**.
Units: ng/m^3 per 15% emis. red. of NO_x. **Emitters →, Receptors ↓.**

	ME	MK	MT	NL	NO	PL	PT	RO	RS	RUE	SE	SI	SK	TJ	TM	TR	UA	UZ	ATL	BAS	BLS	MED	NOS	AST	NOA	BIC	DMS	VOL	EXC	EU	
AL	5	12	0	0	0	2	0	2	21	0	-0	0	1	0	0	1	2	0	0	0	0	21	0	0	0	6	0	0	142	56	AL
AM	0	0	0	0	-0	0	0	0	0	2	-0	0	0	0	2	46	0	1	0	0	0	1	0	9	0	7	0	0	196	2	AM
AT	0	0	0	1	0	17	0	3	3	0	0	14	6	0	0	0	3	0	1	1	0	4	2	0	0	7	0	0	333	316	AT
AZ	0	0	0	0	0	0	0	0	0	16	-0	0	0	0	5	9	1	4	0	0	0	0	0	13	0	8	0	0	263	2	AZ
BA	4	0	0	0	0	5	0	3	13	0	0	1	3	0	0	0	3	0	0	0	0	6	0	0	0	5	0	0	129	66	BA
BE	0	0	0	48	2	8	1	0	0	1	2	0	1	0	0	0	1	0	15	5	0	3	62	0	0	21	0	0	550	539	BE
BG	0	2	0	0	0	1	0	15	5	5	-0	0	0	0	0	12	11	0	0	0	5	4	0	0	0	6	0	0	108	69	BG
BY	0	0	0	1	0	25	0	5	1	45	1	0	2	0	0	2	39	0	1	4	1	1	2	0	0	6	0	0	190	62	BY
CH	0	0	0	3	0	3	0	0	0	-0	0	1	0	0	0	0	0	0	2	0	0	3	4	0	0	10	0	0	439	273	CH
CY	0	0	0	0	0	0	0	0	0	1	-0	0	0	0	0	68	2	0	0	0	2	58	0	2	1	10	0	0	101	30	CY
CZ	0	0	0	3	0	40	0	6	5	1	0	6	20	0	0	1	4	0	2	2	0	3	4	0	0	9	0	0	406	385	CZ
DE	0	0	0	26	1	31	1	1	1	2	2	1	2	0	0	1	2	0	6	11	0	3	32	0	0	16	0	0	578	553	DE
DK	0	0	0	26	5	26	0	1	0	5	10	0	1	0	0	1	3	0	6	44	0	1	64	0	0	12	0	0	317	299	DK
EE	0	0	0	1	1	7	0	1	0	9	3	0	1	0	0	0	4	0	1	9	0	0	4	0	0	4	0	0	78	54	EE
ES	0	0	0	0	0	0	8	0	0	-0	-0	0	0	0	0	0	0	0	7	0	0	9	1	0	0	7	0	0	112	112	ES
FI	0	0	0	1	1	1	0	0	0	2	3	0	0	0	0	0	0	0	1	3	0	0	2	0	0	3	0	0	24	20	FI
FR	0	0	0	10	0	3	1	0	0	-0	0	0	0	0	0	0	0	0	11	1	0	5	26	0	0	9	0	0	341	330	FR
GB	0	0	0	9	1	2	0	0	0	0	1	0	0	0	0	0	0	0	16	3	0	1	31	0	0	9	0	0	192	189	GB
GE	0	0	0	0	0	0	0	0	0	9	-0	0	0	0	1	22	1	1	0	0	2	1	0	3	0	5	0	0	171	3	GE
GL	0	0	0	-0	0	-0	0	-0	0	0	0	-0	-0	0	0	0	0	0	0	0	0	0	-0	0	0	3	0	0	-0	-0	GL
GR	0	7	0	0	0	0	0	2	3	1	-0	0	0	0	0	10	3	0	0	0	1	22	0	0	0	6	0	0	95	67	GR
HR	1	1	0	0	0	12	0	7	20	1	0	9	7	0	0	0	5	0	0	0	0	10	1	0	0	5	0	0	218	174	HR
HU	1	2	0	1	0	29	0	48	36	3	0	7	31	0	0	2	15	0	1	0	1	5	2	0	0	8	0	0	406	336	HU
IE	0	0	0	3	1	0	0	0	0	0	0	0	0	0	0	0	0	0	20	1	0	0	11	0	0	6	0	0	125	124	IE
IS	0	0	0	0	0	-0	0	0	0	0	0	0	0	0	0	0	0	0	2	0	0	0	0	0	0	3	0	0	8	1	IS
IT	0	0	0	0	0	3	0	1	1	0	0	8	2	0	0	0	1	0	1	0	0	36	1	0	1	10	0	0	407	398	IT
KG	0	0	0	0	0	0	0	0	0	0	-0	0	0	7	0	0	0	30	0	0	0	0	0	5	0	6	0	0	78	1	KG
KZT	0	0	0	0	0	-0	0	0	0	15	-0	0	0	0	1	0	0	3	0	0	0	0	0	2	0	7	0	0	51	0	KZT
LT	0	0	0	2	1	40	0	3	1	32	3	0	2	0	0	1	18	0	1	11	0	1	5	0	0	6	0	0	198	115	LT
LU	0	0	0	28	1	9	1	0	0	0	1	0	1	0	0	0	1	0	9	3	0	3	31	0	0	16	0	0	574	562	LU
LV	0	0	0	2	1	18	0	2	1	19	2	0	1	0	0	1	9	0	1	8	0	0	4	0	0	5	0	0	123	73	LV
MD	0	0	0	0	0	7	0	36	1	13	-0	0	1	0	0	7	55	0	0	0	5	2	0	0	0	6	0	0	156	63	MD
ME	30	2	0	0	0	1	0	1	13	0	-0	0	1	0	0	1	1	0	0	-0	0	8	0	0	0	4	0	0	82	24	ME
MK	1	41	0	0	0	1	0	3	22	0	-0	0	1	0	0	2	2	0	0	0	0	6	0	0	0	6	0	0	111	31	MK
MT	0	0	5	0	-0	-0	0	0	0	-0	-0	0	0	0	0	0	0	0	1	-0	0	52	1	0	1	7	0	0	44	43	MT
NL	0	0	0	67	2	23	1	1	0	2	2	0	1	0	0	1	2	0	17	13	0	3	94	0	0	26	0	0	665	650	NL
NO	0	0	0	0	6	0	0	0	0	0	1	0	0	0	0	0	0	0	1	1	0	0	2	0	0	3	0	0	15	9	NO
PL	0	0	0	3	1	111	0	5	2	8	1	1	9	0	0	1	17	0	2	6	0	1	5	0	0	8	0	0	275	234	PL
PT	0	0	0	0	-0	0	46	0	0	-0	-0	0	0	0	0	0	0	0	19	0	0	2	1	0	0	7	0	0	90	89	PT
RO	0	1	0	0	0	7	0	106	8	8	-0	1	3	0	0	6	27	0	0	0	4	2	1	0	0	6	0	0	217	160	RO
RS	5	14	0	1	0	11	0	24	79	2	0	1	6	0	0	2	8	0	1	0	1	5	1	0	0	7	0	0	248	126	RS
RUE	0	0	0	0	0	0	0	0	0	18	0	0	0	0	0	0	1	0	0	0	0	0	0	0	0	3	0	0	25	2	RUE
SE	0	0	0	2	3	3	0	0	0	0	6	0	0	0	0	0	1	0	1	6	0	0	5	0	0	4	0	0	41	36	SE
SI	0	0	0	1	0	16	0	5	7	0	0	83	6	0	0	0	4	0	1	0	0	15	1	0	0	7	0	0	364	347	SI
SK	1	1	0	1	0	34	0	23	13	2	0	3	63	0	0	1	12	0	1	0	1	3	1	0	0	7	0	0	294	258	SK
TJ	0	0	0	0	0	0	0	0	0	0	-0	0	0	64	4	0	0	34	0	-0	0	0	0	12	0	7	0	0	111	0	TJ
TM	0	0	0	0	0	0	0	0	0	9	-0	0	0	3	35	1	0	33	0	0	0	0	0	8	0	11	0	0	101	1	TM
TR	0	0	0	0	0	0	0	1	0	3	-0	0	0	0	0	182	3	0	0	0	3	10	0	3	0	10	0	0	207	13	TR
UA	0	0	0	0	0	7	0	9	0	28	0	0	1	0	1	5	55	1	0	1	3	1	1	0	0	6	0	0	125	26	UA
UZ	0	0	0	0	0	0	0	0	0	9	-0	0	0	10	10	1	0	58	0	0	0	0	0	4	0	11	0	0	121	1	UZ
ATL	0	0	0	0	0	0	0	0	0	0	0	0	0	0	0	0	0	0	3	0	0	0	2	0	0	3	0	0	10	9	ATL
BAS	0	0	0	5	1	15	0	1	0	3	5	0	1	0	0	0	3	0	2	13	0	0	11	0	0	5	0	0	111	100	BAS
BLS	0	0	0	0	-0	0	0	4	0	20	-0	0	0	0	0	42	18	0	0	-0	16	2	0	0	0	5	0	0	103	12	BLS
MED	0	0	0	0	-0	0	0	0	0	0	-0	0	0	0	0	10	1	0	1	-0	1	40	0	1	2	7	0	0	61	47	MED
NOS	0	0	0	10	3	6	0	0	0	1	2	0	0	0	0	0	1	0	7	8	0	1	25	0	0	7	0	0	144	137	NOS
AST	0	0	0	0	0	0	0	0	0	3	-0	0	0	1	3	8	0	4	0	0	0	2	0	35	0	8	0	0	29	1	AST
NOA	0	0	0	0	-0	-0	0	0	0	-0	-0	0	0	0	0	2	0	0	0	-0	0	17	0	0	3	10	0	0	16	13	NOA
EXC	0	0	0	1	0	4	0	2	1	12	0	0	1	1	1	7	4	3	1	1	0	2	2	1	0	5	0	0	86	46	EXC
EU	0	0	0	6	1	16	2	8	2	3	1	2	3	0	0	1	5	0	5	4	0	6	11	0	0	8	0	0	239	220	EU
	ME	MK	MT	NL	NO	PL	PT	RO	RS	RUE	SE	SI	SK	TJ	TM	TR	UA	UZ	ATL	BAS	BLS	MED	NOS	AST	NOA	BIC	DMS	VOL	EXC	EU	

Table C.11: 2014 country-to-country blame matrices for **PM2.5**.
Units: ng/m^3 per 15% emis. red. of NH_3. **Emitters →, Receptors ↓.**

	AL	AM	AT	AZ	BA	BE	BG	BY	CH	CY	CZ	DE	DK	EE	ES	FI	FR	GB	GE	GR	HR	HU	IE	IS	IT	KG	KZT	LT	LU	LV	MD	
AL	106	0	1	0	1	0	0	0	0	-0	1	1	0	0	0	-0	1	0	0	12	1	3	0	-0	6	0	-0	0	0	0	0	AL
AM	0	16	0	7	-0	-0	0	-0	0	-0	0	0	-0	-0	0	-0	0	-0	2	-0	0	0	-0	-0	0	-0	-0	-0	0	-0	-0	AM
AT	0	0	111	0	1	1	0	1	4	-0	18	57	0	0	0	0	5	1	0	0	5	15	0	-0	29	0	-0	0	0	0	0	AT
AZ	0	2	0	73	0	-0	0	-0	0	-0	-0	0	-0	-0	-0	-0	0	-0	5	0	0	0	-0	-0	0	-0	-0	-0	-0	-0	-0	AZ
BA	1	0	4	0	114	0	1	0	0	-0	4	6	0	0	0	0	1	0	0	0	24	11	0	-0	10	0	0	0	0	0	0	BA
BE	-0	-0	2	-0	-0	203	-0	1	2	-0	4	100	2	0	2	0	107	41	-0	-0	0	1	4	-0	2	-0	-0	0	8	0	0	BE
BG	1	0	1	0	0	0	85	1	0	0	1	2	0	0	0	0	0	0	0	13	1	6	0	-0	2	0	0	0	0	0	2	BG
BY	0	0	1	0	0	0	1	139	0	0	3	12	1	0	0	0	1	1	0	0	1	4	0	0	1	0	1	6	0	1	2	BY
CH	-0	0	2	-0	-0	1	-0	0	113	-0	0	32	0	0	1	0	21	1	-0	-0	0	0	0	-0	49	0	-0	0	0	0	-0	CH
CY	-0	0	0	-0	-0	-0	-1	-0	-0	9	-0	-0	-0	-0	-1	-0	-0	-0	-0	-3	-0	-0	-0	-0	-2	0	-0	-0	-0	-0	-0	CY
CZ	0	0	29	0	1	3	1	3	2	0	191	116	1	0	1	0	11	4	0	0	5	35	1	-0	7	-0	-0	1	0	0	0	CZ
DE	0	0	9	0	0	15	0	2	5	-0	20	346	4	0	1	0	36	13	0	0	1	5	2	-0	4	-0	0	0	2	0	0	DE
DK	0	0	1	0	0	8	0	8	1	0	4	101	161	0	0	0	17	24	0	0	0	2	3	0	0	-0	0	3	0	1	0	DK
EE	0	0	1	0	0	1	0	25	0	0	3	23	3	51	0	3	4	2	0	0	0	2	0	0	1	0	0	16	0	17	0	EE
ES	-0	0	0	0	0	0	-0	0	0	-0	0	1	0	-0	83	0	10	1	0	-0	0	0	0	-0	2	-0	-0	0	0	0	0	ES
FI	0	0	0	0	0	1	0	7	0	0	0	7	1	3	0	30	2	1	0	0	0	0	0	0	0	-0	0	3	0	2	0	FI
FR	-0	0	1	0	-0	11	-0	0	5	-0	1	31	0	0	7	0	166	15	0	-0	0	0	2	-0	9	-0	0	0	1	0	0	FR
GB	-0	-0	1	-0	-0	8	-0	0	0	-0	1	33	4	0	1	0	29	218	0	-0	0	0	8	0	0	-0	0	0	0	0	0	GB
GE	0	1	0	10	0	-0	0	-0	0	-0	-0	0	-0	-0	-0	-0	0	-0	31	0	0	0	-0	-0	0	-0	-0	-0	0	-0	0	GE
GL	-0	-0	-0	-0	-0	-0	-0	0	0	-0	-0	-0	-0	-0	-0	-0	-0	-0	-0	-0	-0	-0	-0	-0	-0	-0	-0	0	0	0	-0	GL
GR	4	0	1	0	0	0	8	0	0	-0	0	0	0	0	-0	0	0	0	0	74	0	2	0	-0	0	0	-0	0	0	0	0	GR
HR	0	0	12	0	23	0	1	1	1	-0	9	12	0	0	0	0	2	0	0	0	83	23	0	-0	38	0	0	0	0	0	0	HR
HU	0	0	14	0	3	1	2	2	1	0	15	20	0	0	0	0	3	1	0	1	15	149	0	-0	14	0	-0	1	0	0	0	HU
IE	0	-0	0	-0	-0	2	0	0	0	-0	0	7	1	0	1	0	10	53	-0	0	0	0	63	0	0	-0	-0	0	0	0	0	IE
IS	0	0	0	0	-0	0	-0	0	0	-0	0	1	0	0	0	0	0	1	0	0	-0	0	0	0	0	-0	-0	0	0	0	-0	IS
IT	0	0	4	0	1	0	-0	0	3	-0	1	3	0	0	1	0	6	0	0	0	1	2	0	-0	266	0	-0	0	0	0	0	IT
KG	-0	0	-0	0	-0	-0	-0	-0	0	-0	-0	-0	-0	-0	-0	-0	-0	-0	0	-0	-0	-0	-0	-0	-0	46	15	-0	-0	-0	-0	KG
KZT	0	0	0	0	0	0	0	0	0	-0	0	0	0	0	0	0	0	0	0	0	0	0	0	-0	0	2	57	0	0	0	0	KZT
LT	0	0	1	0	0	1	0	67	0	0	5	31	5	0	0	0	3	3	0	0	1	5	1	0	1	-0	0	96	0	6	1	LT
LU	-0	-0	3	-0	-0	68	-0	0	3	0	5	179	1	0	1	0	110	18	-0	-0	0	1	2	0	2	0	-0	0	57	0	0	LU
LV	0	0	1	0	0	1	0	49	0	0	4	26	3	3	0	1	4	2	0	0	0	3	0	0	1	0	0	44	0	53	1	LV
MD	0	0	1	0	0	0	12	6	0	0	2	7	0	0	0	0	1	1	1	1	0	3	0	-0	1	0	1	1	0	0	105	MD
ME	16	0	2	0	11	0	0	0	0	-0	1	2	0	0	0	0	1	0	0	1	3	5	0	-0	8	0	0	0	0	0	0	ME
MK	19	0	2	0	1	0	2	0	0	-0	1	1	0	0	0	0	0	0	0	47	1	6	0	-0	2	0	-0	0	0	0	0	MK
MT	0	0	1	0	0	0	0	0	0	0	0	1	0	0	3	-0	9	0	0	0	0	1	0	-0	21	0	0	0	0	0	0	MT
NL	-0	-0	2	-0	-0	52	-0	1	1	-0	7	144	5	-0	1	0	57	57	-0	-0	0	2	5	-0	1	-0	0	0	1	0	0	NL
NO	0	0	0	0	0	0	0	1	0	0	0	4	2	0	0	0	2	2	0	0	0	0	0	-0	0	-0	-0	0	0	0	0	NO
PL	0	0	4	0	1	2	1	17	1	0	27	74	3	0	0	0	7	4	0	0	2	17	1	0	4	-0	0	3	0	0	2	PL
PT	-0	-0	0	-0	-0	0	-0	0	0	-0	0	1	0	-0	27	-0	4	0	0	-0	0	0	0	-0	1	-0	-0	0	0	0	-0	PT
RO	1	0	1	0	1	0	10	2	0	0	2	6	0	0	0	0	1	0	0	1	1	11	0	-0	4	0	0	0	0	0	6	RO
RS	4	0	4	0	6	0	4	1	0	0	4	6	0	0	0	0	1	0	0	4	7	21	0	-0	4	0	0	0	0	0	1	RS
RUE	0	0	0	0	0	0	0	3	0	-0	0	1	0	0	0	0	0	0	0	0	0	0	0	-0	0	0	5	0	0	0	0	RUE
SE	0	0	0	0	0	1	0	5	0	0	1	21	9	0	0	2	4	3	0	0	0	1	0	-0	0	-0	0	3	0	1	0	SE
SI	0	0	36	0	2	0	1	1	1	-0	8	16	0	0	0	0	3	0	0	0	28	14	0	-0	90	0	-0	0	0	0	0	SI
SK	0	0	9	0	2	1	1	3	1	0	25	26	1	0	0	0	4	1	0	0	4	77	0	0	6	0	-0	1	0	0	0	SK
TJ	-0	0	-0	0	-0	-0	-0	-0	-0	-0	-0	-0	-0	-0	-0	-0	-0	-0	0	-0	-0	-0	-0	-0	-0	3	2	-0	-0	-0	-0	TJ
TM	0	0	0	2	-0	0	0	0	0	-0	-0	-0	-0	-0	0	-0	0	-0	0	-0	-0	-0	-0	-0	0	0	6	-0	-0	-0	0	TM
TR	0	0	0	0	-0	0	1	0	0	0	0	0	-0	-0	0	0	0	0	0	0	0	0	0	-0	0	-0	-0	0	0	0	0	TR
UA	0	0	1	1	0	0	3	10	0	0	2	7	0	0	0	0	1	1	1	0	0	4	0	-0	1	0	2	1	0	0	7	UA
UZ	0	0	-0	1	-0	0	0	0	0	-0	0	0	-0	-0	0	-0	0	-0	0	0	-0	-0	0	-0	0	5	15	-0	0	-0	0	UZ
ATL	0	0	0	-0	-0	0	-0	0	0	0	0	1	0	-0	1	-0	5	4	0	0	0	0	1	-0	0	-0	-0	0	0	0	0	ATL
BAS	0	0	1	0	0	3	0	16	0	0	5	75	26	4	0	6	8	7	0	0	0	3	1	0	1	-0	0	12	0	6	0	BAS
BLS	0	0	0	1	0	0	7	2	0	0	0	1	0	0	0	0	0	0	4	1	0	1	0	-0	1	0	0	0	0	0	1	BLS
MED	-0	0	1	0	-0	0	-0	-0	0	-0	0	1	-0	0	1	-0	5	0	0	-2	0	0	0	-0	9	-0	-0	-0	0	-0	-0	MED
NOS	0	0	1	0	0	13	0	2	0	0	2	63	23	0	1	0	41	79	0	0	0	1	5	-0	0	-0	0	1	0	0	0	NOS
AST	0	0	0	2	-0	0	0	0	0	0	0	0	0	-0	0	-0	0	-0	0	0	0	0	0	-0	0	0	1	0	0	0	0	AST
NOA	-0	0	0	-0	-0	-0	-0	-0	0	0	-0	-0	-0	0	1	-0	1	-0	-0	-0	-0	-0	0	-0	-1	-0	-0	-0	-0	-0	-0	NOA
EXC	0	0	1	1	0	1	1	4	1	0	2	11	1	0	2	1	6	4	0	1	1	2	0	-0	5	1	10	1	0	0	1	EXC
EU	0	0	5	0	1	6	3	5	2	0	9	51	4	1	11	2	30	18	0	3	2	8	2	-0	23	0	0	3	0	1	1	EU
	AL	AM	AT	AZ	BA	BE	BG	BY	CH	CY	CZ	DE	DK	EE	ES	FI	FR	GB	GE	GR	HR	HU	IE	IS	IT	KG	KZT	LT	LU	LV	MD	

Table C.11 Cont.: 2014 country-to-country blame matrices for **PM2.5**.
Units: ng/m^3 per 15% emis. red. of NH_3. **Emitters →, Receptors ↓.**

	ME	MK	MT	NL	NO	PL	PT	RO	RS	RUE	SE	SI	SK	TJ	TM	TR	UA	UZ	ATL	BAS	BLS	MED	NOS	AST	NOA	BIC	DMS	VOL	EXC	EU	
AL	3	8	-0	0	0	1	-0	3	23	0	0	0	0	0	-0	1	1	-0	0	0	0	0	0	-0	0	0	0	0	174	30	AL
AM	0	-0	-0	0	-0	-0	-0	0	0	-1	-0	0	0	-0	-0	18	-0	-0	0	0	0	0	0	6	0	0	0	0	40	0	AM
AT	0	0	0	1	0	8	0	3	5	0	0	18	5	0	0	0	1	-0	0	0	0	0	0	0	0	0	0	0	292	279	AT
AZ	0	0	-0	-0	-0	-0	-0	0	0	3	-0	0	-0	0	1	6	0	0	0	0	0	0	0	5	0	0	0	0	91	0	AZ
BA	3	0	0	0	0	5	-0	5	31	1	0	1	3	0	0	1	2	0	0	0	0	0	0	0	0	0	0	0	231	77	BA
BE	-0	-0	-0	64	0	5	0	0	0	0	0	0	1	-0	-0	-0	1	-0	0	0	0	0	0	-0	0	1	0	0	550	546	BE
BG	0	2	0	0	0	2	0	50	21	2	0	0	1	0	0	42	9	0	0	0	0	0	0	0	0	1	0	0	247	165	BG
BY	0	0	0	1	0	33	0	9	2	38	1	0	2	0	0	3	53	0	0	0	0	0	0	0	0	1	0	0	322	81	BY
CH	-0	-0	-0	1	0	1	0	-0	-0	-0	0	0	0	-0	-0	-0	0	-0	0	0	0	0	0	-0	0	0	0	0	223	110	CH
CY	-0	-0	-0	-0	-0	-0	-0	-1	-1	-3	-0	-0	-0	0	-0	-40	-3	-0	0	0	0	0	0	10	0	-0	0	0	-48	-0	CY
CZ	0	0	0	3	0	54	0	10	11	1	0	5	25	0	0	1	3	-0	0	0	0	0	0	0	0	1	0	0	524	501	CZ
DE	0	0	-0	24	0	28	0	3	2	1	1	1	2	-0	-0	0	3	-0	0	0	0	0	0	-0	0	0	0	0	529	515	DE
DK	0	0	-0	23	1	41	0	3	1	4	12	0	1	0	0	1	6	0	0	0	0	0	0	0	0	1	0	0	428	406	DK
EE	0	0	0	3	0	26	0	2	1	21	5	0	1	0	0	1	8	0	0	0	0	0	0	0	0	1	0	0	224	166	EE
ES	0	-0	0	0	0	0	3	0	0	0	0	0	0	-0	-0	-0	0	-0	0	0	0	0	0	-0	1	1	0	0	102	102	ES
FI	0	0	-0	1	0	5	0	1	0	6	4	0	0	0	0	0	2	0	0	0	0	0	0	0	0	0	0	0	77	62	FI
FR	-0	-0	-0	9	0	2	0	0	0	0	0	0	0	0	0	0	0	-0	0	0	0	0	0	0	0	1	0	0	261	255	FR
GB	-0	-0	-0	18	0	3	0	0	0	0	1	0	0	-0	-0	0	0	-0	0	0	0	0	0	-0	0	0	0	0	329	327	GB
GE	0	0	-0	-0	-0	-0	-0	0	0	1	-0	0	-0	0	-0	11	-0	-0	0	0	0	0	0	1	-0	0	0	0	55	1	GE
GL	-0	-0	-0	-0	-0	-0	-0	-0	-0	-0	-0	-0	-0	-0	-0	-0	-0	-0	0	0	0	0	0	-0	-0	8	0	0	-0	-0	GL
GR	0	3	-0	0	0	0	-0	4	7	0	0	0	0	0	0	14	2	0	0	0	0	0	0	0	0	0	0	0	121	89	GR
HR	0	0	0	0	0	8	-0	7	30	1	0	14	5	0	0	1	2	0	0	0	0	0	0	0	0	0	0	0	278	217	HR
HU	0	0	0	1	0	19	0	34	36	1	0	5	23	0	0	2	4	0	0	0	0	0	0	0	0	1	0	0	369	318	HU
IE	-0	-0	-0	4	0	0	0	0	0	0	0	0	0	-0	-0	0	0	-0	0	0	0	0	0	-0	0	0	0	0	142	141	IE
IS	-0	0	-0	0	0	0	0	0	-0	-0	0	0	0	-0	-0	0	0	-0	0	0	0	0	0	-0	0	0	0	0	2	2	IS
IT	0	0	0	0	0	1	0	1	1	0	0	3	1	0	0	-0	1	-0	0	0	0	0	0	0	1	0	0	0	297	291	IT
KG	-0	-0	-0	-0	-0	-0	-0	-0	-0	-0	-0	-0	-0	7	0	0	-0	18	0	0	0	0	0	9	0	1	0	0	86	-0	KG
KZT	0	0	-0	0	0	0	0	0	0	22	0	0	0	1	2	0	1	5	0	0	0	0	0	5	0	1	0	0	92	1	KZT
LT	0	0	0	4	0	89	0	6	2	26	3	0	3	0	0	2	19	0	0	0	0	0	0	0	0	1	0	0	385	265	LT
LU	-0	-0	-0	29	0	5	0	0	0	-0	0	0	1	-0	-0	-0	1	-0	0	0	0	0	0	-0	0	0	0	0	489	485	LU
LV	0	0	0	3	0	46	0	4	1	27	4	0	2	0	0	1	16	0	0	0	0	0	0	0	0	1	0	0	305	207	LV
MD	0	0	0	1	0	9	0	96	3	19	0	0	1	0	1	23	79	0	0	0	0	0	0	0	0	1	0	0	377	138	MD
ME	50	1	0	0	0	3	-0	3	35	0	0	0	1	0	0	1	1	0	0	0	0	0	0	0	0	1	0	0	147	31	ME
MK	0	99	0	0	0	2	-0	6	45	0	0	0	1	0	-0	3	1	0	0	0	0	0	0	0	0	1	0	0	242	73	MK
MT	0	0	105	0	-0	0	0	0	0	0	0	0	0	0	-0	0	0	-0	0	0	0	0	0	-0	2	0	0	0	144	142	MT
NL	-0	-0	-0	233	0	10	0	2	1	0	1	0	1	-0	-0	-0	2	-0	0	0	0	0	0	-0	0	1	0	0	589	583	NL
NO	0	0	-0	1	8	2	0	0	0	0	2	0	0	-0	-0	0	0	-0	0	0	0	0	0	0	0	-0	0	0	26	16	NO
PL	0	0	0	5	0	316	0	14	6	8	1	1	14	0	0	2	21	0	0	0	0	0	0	0	0	1	0	0	560	502	PL
PT	-0	-0	-0	0	-0	0	76	0	-0	-0	-0	0	0	-0	-0	-0	0	-0	0	0	0	0	0	-0	0	1	0	0	109	109	PT
RO	0	0	0	0	0	5	0	188	15	4	0	0	2	0	0	11	15	0	0	0	0	0	0	0	0	1	0	0	291	235	RO
RS	1	6	0	0	0	6	-0	39	172	1	0	1	4	0	0	2	4	0	0	0	0	0	0	0	0	1	0	0	305	107	RS
RUE	0	0	0	0	0	1	0	0	0	57	0	0	0	0	0	0	4	0	0	0	0	0	0	0	0	1	0	0	75	5	RUE
SE	0	0	-0	4	1	12	0	1	0	3	32	0	0	0	0	1	2	0	0	0	0	0	0	0	0	0	0	0	109	97	SE
SI	0	0	0	0	0	7	0	5	10	0	0	140	3	0	0	0	1	0	0	0	0	0	0	0	0	1	0	0	369	352	SI
SK	0	0	0	1	0	51	0	26	19	1	0	2	150	0	0	2	5	0	0	0	0	0	0	0	0	1	0	0	422	388	SK
TJ	-0	-0	-0	-0	-0	-0	-0	-0	-0	-0	-0	-0	-0	54	2	0	-0	30	0	0	0	0	0	7	-0	0	0	0	91	-0	TJ
TM	-0	-0	-0	0	-0	-0	0	0	-0	2	-0	0	-0	3	52	1	0	22	0	0	0	0	0	5	0	1	0	0	89	-0	TM
TR	0	0	0	0	-0	-0	-0	1	0	-1	0	0	0	0	-0	151	1	-0	0	0	0	0	0	2	0	0	0	0	156	3	TR
UA	0	0	0	1	0	15	0	23	2	42	0	0	2	0	1	12	140	0	0	0	0	0	0	0	0	1	0	0	282	62	UA
UZ	-0	0	-0	0	-0	0	-0	0	-0	1	-0	0	-0	13	14	1	0	99	0	0	0	0	0	3	0	1	0	0	149	0	UZ
ATL	-0	-0	-0	1	-0	0	0	0	-0	-1	0	0	0	-0	-0	0	0	-0	0	0	0	0	0	-0	0	-1	0	0	13	14	ATL
BAS	0	0	0	8	1	64	0	3	2	10	21	0	2	0	0	1	8	0	0	0	0	0	0	0	0	1	0	0	298	258	BAS
BLS	0	0	0	0	0	1	-0	14	2	18	0	0	0	0	0	74	26	0	0	0	0	0	0	0	0	1	0	0	158	29	BLS
MED	-0	-0	-0	-0	-0	-0	-0	-0	-1	-1	-0	0	0	0	-0	-6	-1	-0	0	0	0	0	0	1	-1	-0	0	0	5	14	MED
NOS	0	0	0	35	1	10	0	1	0	1	3	0	0	-0	0	0	2	0	0	0	0	0	0	0	0	0	0	0	288	280	NOS
AST	-0	-0	0	0	-0	-0	-0	0	0	1	-0	0	-0	0	3	4	0	1	0	0	0	0	0	25	0	2	0	0	13	0	AST
NOA	-0	-0	-0	-0	-0	-0	-0	-0	-0	-0	-0	0	-0	-0	-0	-1	-0	-0	0	0	0	0	0	0	5	1	0	0	-4	-1	NOA
EXC	0	0	0	2	0	7	0	4	2	32	1	0	1	1	2	6	7	3	0	0	0	0	0	1	0	1	0	0	124	54	EXC
EU	0	0	0	8	0	33	2	15	4	3	4	2	4	0	0	2	4	0	0	0	0	0	0	0	0	1	0	0	274	252	EU
	ME	MK	MT	NL	NO	PL	PT	RO	RS	RUE	SE	SI	SK	TJ	TM	TR	UA	UZ	ATL	BAS	BLS	MED	NOS	AST	NOA	BIC	DMS	VOL	EXC	EU	

Table C.12: 2014 country-to-country blame matrices for **PM2.5**.
Units: ng/m^3 per 15% emis. red. of VOC. **Emitters →, Receptors ↓.**

	AL	AM	AT	AZ	BA	BE	BG	BY	CH	CY	CZ	DE	DK	EE	ES	FI	FR	GB	GE	GR	HR	HU	IE	IS	IT	KG	KZT	LT	LU	LV	MD	
AL	1	0	1	0	0	0	1	0	0	0	1	2	0	0	1	0	2	1	0	3	0	1	0	0	8	0	0	0	0	0	0	AL
AM	0	9	0	1	0	0	0	0	0	0	0	0	0	0	0	0	0	0	1	0	0	0	0	0	0	0	1	0	0	0	0	AM
AT	0	0	7	0	0	0	0	0	1	0	1	7	0	0	1	0	3	1	0	0	1	1	0	0	8	0	0	0	0	0	0	AT
AZ	0	1	0	3	0	0	0	0	0	0	0	0	0	0	0	0	0	0	2	0	0	0	0	0	1	0	2	0	0	0	0	AZ
BA	0	0	1	0	-0	0	1	0	0	0	1	3	0	0	1	0	2	1	0	1	1	1	0	0	6	0	0	0	0	0	0	BA
BE	0	0	2	0	0	9	0	1	2	0	2	25	1	0	2	0	15	15	0	0	0	1	1	0	5	0	0	0	0	0	0	BE
BG	0	0	0	0	0	0	7	0	0	0	1	2	0	0	1	0	1	1	0	4	0	1	0	0	3	0	1	0	0	0	0	BG
BY	0	0	0	0	0	0	0	2	0	0	0	2	0	0	0	0	1	1	0	0	0	0	0	0	1	0	1	0	0	0	0	BY
CH	0	0	2	0	0	0	0	0	14	0	0	6	0	0	1	0	4	1	0	0	0	0	0	0	20	0	0	0	0	0	0	CH
CY	0	0	0	0	0	0	1	0	0	0	0	2	0	0	1	0	2	1	0	4	0	0	0	0	6	0	0	0	0	0	0	CY
CZ	0	0	3	0	0	0	1	1	1	0	6	11	0	0	1	0	4	2	0	1	1	2	0	0	6	0	0	0	0	0	0	CZ
DE	0	0	5	0	0	2	1	1	4	0	3	28	1	0	2	0	12	5	0	1	1	1	0	0	9	0	0	0	0	0	0	DE
DK	0	0	1	0	0	1	0	0	1	0	1	10	3	0	1	0	6	6	0	0	0	0	0	0	2	0	0	0	0	0	0	DK
EE	0	0	0	0	0	0	0	0	0	0	0	2	0	0	0	1	1	1	0	0	0	0	0	0	0	0	0	0	0	0	0	EE
ES	0	0	0	0	0	0	0	0	0	0	0	1	0	0	7	0	2	1	0	0	0	0	0	0	1	0	0	0	0	0	0	ES
FI	0	0	0	0	0	0	0	0	0	0	0	1	0	0	0	1	0	1	0	0	0	0	0	0	0	0	0	0	0	0	0	FI
FR	0	0	0	0	0	1	0	0	1	0	1	4	0	0	2	0	6	2	0	0	0	0	0	0	4	0	0	0	0	0	0	FR
GB	0	0	0	0	0	1	0	0	0	0	0	5	0	0	1	0	3	13	0	0	0	0	0	0	2	0	0	0	0	0	0	GB
GE	0	0	0	0	0	0	0	0	0	0	0	0	0	0	0	0	0	0	8	0	0	0	0	0	0	0	1	0	0	0	0	GE
GL	0	0	0	0	0	0	0	0	0	0	0	0	0	0	0	0	0	0	0	0	0	0	0	0	0	0	0	0	0	0	0	GL
GR	1	0	1	0	0	0	1	0	0	0	1	2	0	0	1	0	2	1	0	9	0	1	0	0	7	0	0	0	0	0	0	GR
HR	0	0	2	0	0	0	1	0	1	0	1	5	0	0	1	0	2	1	0	1	2	1	0	0	11	0	0	0	0	0	0	HR
HU	0	0	2	0	0	0	1	1	1	0	2	4	0	0	1	0	2	1	0	1	1	4	0	0	7	0	0	0	0	0	0	HU
IE	0	0	0	0	0	0	0	0	0	0	0	1	0	0	0	0	1	1	0	0	0	0	0	0	1	0	0	0	0	0	0	IE
IS	0	0	0	0	0	0	0	0	0	0	0	0	0	0	0	0	0	1	0	0	0	0	0	0	0	0	0	0	0	0	0	IS
IT	0	0	3	0	0	0	0	0	3	0	1	6	0	0	4	0	8	2	0	1	1	1	0	0	131	0	0	0	0	0	0	IT
KG	0	0	0	0	0	0	0	0	0	0	0	0	0	0	0	0	0	0	0	0	0	0	0	0	0	10	7	0	0	0	0	KG
KZT	0	0	0	0	0	0	0	0	0	0	0	1	0	0	0	0	0	0	0	0	0	0	0	0	0	1	8	0	0	0	0	KZT
LT	0	0	0	0	0	0	0	1	0	0	1	3	0	0	0	0	1	1	0	0	0	1	0	0	1	0	0	1	0	0	0	LT
LU	0	0	3	0	0	3	0	1	2	0	2	21	0	0	2	0	13	5	0	0	0	1	0	0	6	0	0	0	1	0	0	LU
LV	0	0	0	0	0	0	0	1	0	0	1	2	0	0	0	0	1	1	0	0	0	0	0	0	1	0	0	1	0	1	0	LV
MD	0	0	0	0	0	0	2	1	0	0	1	2	0	0	0	0	1	1	0	1	0	1	0	0	1	0	1	0	0	0	1	MD
ME	0	0	1	0	0	0	0	0	0	0	1	2	0	0	1	0	1	1	0	1	0	1	0	0	6	0	0	0	0	0	0	ME
MK	1	0	0	0	0	0	1	0	0	0	1	2	0	0	1	0	1	1	0	9	0	1	0	0	4	0	0	0	0	0	0	MK
MT	0	0	1	0	0	0	0	0	1	0	1	5	0	0	4	0	7	2	0	1	0	1	0	0	20	0	0	0	0	0	0	MT
NL	0	0	2	1	0	9	0	1	2	0	2	30	1	0	4	0	21	18	0	1	0	1	1	0	7	0	1	0	0	0	0	NL
NO	0	0	0	0	0	0	0	0	0	0	0	1	0	0	0	0	0	1	0	0	0	0	0	0	0	0	0	0	0	0	0	NO
PL	0	0	1	0	0	0	0	1	1	0	3	9	0	0	1	0	3	2	0	0	0	1	0	0	3	0	1	0	0	0	0	PL
PT	0	0	0	0	0	0	0	0	0	0	0	1	0	0	4	0	1	1	0	0	0	0	0	0	1	0	0	0	0	0	0	PT
RO	0	0	0	0	0	0	2	0	0	0	1	2	0	0	0	0	1	1	0	1	0	1	0	0	2	0	1	0	0	0	0	RO
RS	0	0	1	0	0	0	1	0	0	0	1	3	0	0	1	0	1	1	0	2	0	1	0	0	4	0	0	0	0	0	0	RS
RUE	0	0	0	0	0	0	0	0	0	0	0	0	0	0	0	0	0	0	0	0	0	0	0	0	0	0	1	0	0	0	0	RUE
SE	0	0	0	0	0	0	0	0	0	0	0	2	0	0	0	0	1	1	0	0	0	0	0	0	0	0	0	0	0	0	0	SE
SI	0	0	4	0	1	0	1	0	1	0	2	7	0	0	1	0	3	1	0	1	3	1	0	0	23	0	0	0	0	0	0	SI
SK	0	0	1	0	0	0	1	1	1	0	2	5	0	0	1	0	2	1	0	1	0	3	0	0	4	0	0	0	0	0	0	SK
TJ	0	0	0	0	0	0	0	0	0	0	0	0	0	0	0	0	0	0	0	0	0	0	0	0	0	3	3	0	0	0	0	TJ
TM	0	0	0	1	0	0	0	0	0	0	0	1	0	0	0	0	0	0	0	0	0	0	0	0	0	1	4	0	0	0	0	TM
TR	0	0	0	0	0	0	0	0	0	0	0	1	0	0	1	0	1	0	0	1	0	0	0	0	2	0	0	0	0	0	0	TR
UA	0	0	0	1	0	0	1	1	0	0	0	2	0	0	0	0	1	1	0	0	0	0	0	0	1	0	1	0	0	0	0	UA
UZ	0	0	0	1	0	0	0	0	0	0	0	1	0	0	0	0	0	0	0	0	0	0	0	0	1	7	11	0	0	0	0	UZ
ATL	0	0	0	0	0	0	0	0	0	0	0	0	0	0	0	0	0	1	0	0	0	0	0	0	0	0	0	0	0	0	0	ATL
BAS	0	0	0	0	0	0	0	0	0	0	1	5	1	0	0	1	2	2	0	0	0	0	0	0	1	0	0	0	0	0	0	BAS
BLS	0	0	0	1	0	0	1	1	0	0	0	1	0	0	0	0	1	1	1	1	0	0	0	0	1	0	1	0	0	0	0	BLS
MED	0	0	1	0	0	0	1	0	1	0	1	4	0	0	3	0	5	1	0	2	0	1	0	0	15	0	0	0	0	0	0	MED
NOS	0	0	0	0	0	1	0	0	0	0	0	5	1	0	1	0	3	6	0	0	0	0	0	0	1	0	0	0	0	0	0	NOS
AST	0	0	0	0	0	0	0	0	0	0	0	0	0	0	0	0	0	0	0	0	0	0	0	0	1	0	1	0	0	0	0	AST
NOA	0	0	0	0	0	0	0	0	0	0	0	2	0	0	2	0	2	1	0	1	0	0	0	0	5	0	0	0	0	0	0	NOA
EXC	0	0	0	0	0	0	0	0	0	0	0	2	0	0	0	0	1	1	0	0	0	0	0	0	3	0	2	0	0	0	0	EXC
EU	0	0	1	0	0	1	1	0	1	0	1	6	0	0	2	0	4	3	0	1	0	1	0	0	12	0	0	0	0	0	0	EU
	AL	AM	AT	AZ	BA	BE	BG	BY	CH	CY	CZ	DE	DK	EE	ES	FI	FR	GB	GE	GR	HR	HU	IE	IS	IT	KG	KZT	LT	LU	LV	MD	

Table C.12 Cont.: 2014 country-to-country blame matrices for **PM2.5**.
Units: ng/m^3 per 15% emis. red. of VOC. **Emitters →, Receptors ↓**.

	ME	MK	MT	NL	NO	PL	PT	RO	RS	RUE	SE	SI	SK	TJ	TM	TR	UA	UZ	ATL	BAS	BLS	MED	NOS	AST	NOA	BIC	DMS	VOL	EXC	EU	
AL	0	1	0	0	0	2	0	1	1	1	0	0	0	0	0	1	1	0	0	0	0	0	0	0	0	-2	0	0	32	25	AL
AM	0	0	0	0	0	0	0	0	0	3	0	0	0	0	0	2	0	0	0	0	0	0	0	1	0	-7	0	0	19	1	AM
AT	0	0	0	0	0	4	0	1	0	2	0	1	0	0	0	1	1	0	0	0	0	0	0	0	0	-2	0	0	46	39	AT
AZ	0	0	0	0	0	1	0	0	0	7	0	0	0	0	0	1	1	0	0	0	0	0	0	1	0	-4	0	0	22	4	AZ
BA	0	0	0	0	0	4	0	1	0	2	0	0	1	0	0	1	1	0	0	0	0	0	0	0	0	-2	0	0	29	23	BA
BE	0	0	0	11	1	10	0	2	0	5	1	0	1	0	0	1	2	0	0	0	0	0	1	0	0	12	0	0	118	105	BE
BG	0	0	0	0	0	3	0	4	1	7	0	0	1	0	0	6	3	0	0	0	0	0	0	0	0	0	0	0	50	30	BG
BY	0	0	0	0	0	3	0	1	0	7	1	0	0	0	0	1	2	0	0	0	0	0	0	0	0	-3	0	0	27	13	BY
CH	0	0	0	0	0	1	0	1	0	1	0	0	0	0	0	0	0	0	0	0	0	0	0	0	0	-2	0	0	56	40	CH
CY	0	0	0	0	0	2	0	1	0	4	0	0	0	0	0	9	2	0	0	0	0	1	0	0	0	-4	0	0	39	22	CY
CZ	0	0	0	1	0	10	0	2	0	4	0	0	1	0	0	1	2	0	0	0	0	0	0	0	0	1	0	0	64	52	CZ
DE	0	0	0	3	0	8	0	2	1	5	1	0	1	0	0	1	2	0	0	0	0	0	0	0	0	7	0	0	103	87	DE
DK	0	0	0	2	1	4	0	1	0	4	2	0	0	0	0	1	1	0	0	0	0	0	0	0	0	4	0	0	52	44	DK
EE	0	0	0	0	0	2	0	0	0	5	1	0	0	0	0	0	1	0	0	0	0	0	0	0	0	-1	0	0	19	11	EE
ES	0	0	0	0	0	0	1	0	0	0	0	0	0	0	0	0	0	0	0	0	0	0	0	0	0	-2	0	0	15	14	ES
FI	0	0	0	0	0	1	0	0	0	2	1	0	0	0	0	0	0	0	0	0	0	0	0	0	0	-1	0	0	10	7	FI
FR	0	0	0	1	0	2	0	1	0	1	0	0	0	0	0	0	1	0	0	0	0	0	0	0	0	-3	0	0	30	27	FR
GB	0	0	0	2	0	2	0	0	0	1	1	0	0	0	0	0	1	0	0	0	0	0	0	0	0	2	0	0	35	32	GB
GE	0	0	0	0	0	0	0	0	0	4	0	0	0	0	0	2	1	0	0	0	0	0	0	1	0	-3	0	0	19	2	GE
GL	0	0	0	0	0	0	0	0	0	0	0	0	0	0	0	0	0	0	0	0	0	0	0	0	0	0	0	0	0	0	GL
GR	0	1	0	0	0	2	0	2	1	3	0	0	0	0	0	3	2	0	0	0	0	1	0	0	0	-1	0	0	44	32	GR
HR	0	0	0	0	0	5	0	2	1	3	0	1	1	0	0	1	2	0	0	0	0	0	0	0	0	-1	0	0	47	38	HR
HU	0	0	0	0	0	7	0	5	1	5	0	0	2	0	0	2	3	0	0	0	0	0	0	0	0	-1	0	0	55	41	HU
IE	0	0	0	0	0	0	0	0	0	0	0	0	0	0	0	0	0	0	0	0	0	0	0	0	0	-2	0	0	6	5	IE
IS	0	0	0	0	0	0	0	0	0	0	0	0	0	0	0	0	0	0	0	0	0	0	0	0	0	-0	0	0	3	2	IS
IT	0	0	0	1	0	3	0	1	1	1	0	1	1	0	0	1	1	0	0	0	0	1	0	0	0	5	0	0	175	167	IT
KG	0	0	0	0	0	0	0	0	0	1	0	0	0	1	0	0	0	4	0	0	0	0	0	1	0	-2	0	0	25	1	KG
KZT	0	0	0	0	0	1	0	0	0	6	0	0	0	0	0	0	1	1	0	0	0	0	0	0	0	-3	0	0	21	3	KZT
LT	0	0	0	0	0	5	0	1	0	6	1	0	1	0	0	1	2	0	0	0	0	0	0	0	0	-2	0	0	29	18	LT
LU	0	0	0	3	0	7	0	2	0	3	0	0	1	0	0	1	2	0	0	0	0	0	0	0	0	4	0	0	82	73	LU
LV	0	0	0	0	0	3	0	1	0	5	1	0	0	0	0	0	1	0	0	0	0	0	0	0	0	-2	0	0	23	14	LV
MD	0	0	0	0	0	3	0	5	0	8	0	0	0	0	0	3	3	0	0	0	0	0	0	0	0	-2	0	0	38	19	MD
ME	-0	0	0	0	0	2	0	1	-0	1	0	0	0	0	0	1	1	0	0	0	0	0	0	0	0	-2	0	0	21	18	ME
MK	0	2	0	0	0	3	0	2	1	2	0	0	0	0	0	2	1	0	0	0	0	0	0	0	0	-1	0	0	39	27	MK
MT	0	0	2	1	0	2	0	1	0	1	0	0	0	0	0	0	1	0	0	0	0	2	0	0	0	1	0	0	56	51	MT
NL	0	0	0	19	1	9	1	2	1	7	1	0	1	0	0	1	3	0	0	0	0	0	1	0	0	18	0	0	148	131	NL
NO	0	0	0	0	1	1	0	0	0	1	0	0	0	0	0	0	0	0	0	0	0	0	0	0	0	-0	0	0	5	4	NO
PL	0	0	0	1	0	15	0	2	1	6	1	0	1	0	0	1	3	0	0	0	0	0	0	0	0	2	0	0	61	47	PL
PT	0	0	0	0	0	0	4	0	0	0	0	0	0	0	0	0	0	0	0	0	0	0	0	0	0	-1	0	0	14	13	PT
RO	0	0	0	0	0	4	0	8	1	6	0	0	1	0	0	3	3	0	0	0	0	0	0	0	0	-2	0	0	39	25	RO
RS	0	1	0	0	0	4	0	3	1	3	0	0	1	0	0	2	2	0	0	0	0	0	0	0	0	-2	0	0	37	26	RS
RUE	0	0	0	0	0	0	0	0	0	5	0	0	0	0	0	0	0	0	0	0	0	0	0	0	0	-0	0	0	10	3	RUE
SE	0	0	0	0	0	2	0	0	0	2	1	0	0	0	0	0	0	0	0	0	0	0	0	0	0	-0	0	0	13	10	SE
SI	0	0	0	0	0	6	0	2	1	3	0	5	1	0	0	1	2	0	0	0	0	0	0	0	0	0	0	0	72	62	SI
SK	0	0	0	0	0	8	0	4	1	4	0	0	3	0	0	2	2	0	0	0	0	0	0	0	0	-0	0	0	51	39	SK
TJ	0	0	0	0	0	0	0	0	0	2	0	0	0	6	0	0	0	3	0	0	0	0	0	1	0	-1	0	0	20	1	TJ
TM	0	0	0	0	0	1	0	0	0	5	0	0	0	1	0	1	1	1	0	0	0	0	0	1	0	-4	0	0	17	3	TM
TR	0	0	0	0	0	1	0	1	0	3	0	0	0	0	0	11	1	0	0	0	0	0	0	0	0	-6	0	0	25	8	TR
UA	0	0	0	0	0	3	0	2	0	10	0	0	0	0	0	2	4	0	0	0	0	0	0	0	0	-1	0	0	33	14	UA
UZ	0	0	0	0	0	1	0	0	0	6	0	0	0	2	0	1	1	8	0	0	0	0	0	1	0	-1	0	0	40	4	UZ
ATL	0	0	0	0	0	0	0	0	0	0	0	0	0	0	0	0	0	0	0	0	0	0	0	0	0	-0	0	0	2	2	ATL
BAS	0	0	0	1	0	4	0	1	0	4	1	0	0	0	0	0	1	0	0	0	0	0	0	0	0	1	0	0	29	22	BAS
BLS	0	0	0	0	0	2	0	2	0	10	0	0	0	0	0	10	3	0	0	0	0	0	0	0	0	-1	0	0	41	13	BLS
MED	0	0	0	0	0	2	0	1	0	2	0	0	0	0	0	2	1	0	0	0	0	1	0	0	0	-1	0	0	47	40	MED
NOS	0	0	0	2	1	2	0	0	0	2	1	0	0	0	0	0	1	0	0	0	0	0	0	0	0	2	0	0	30	25	NOS
AST	0	0	0	0	0	0	0	0	0	2	0	0	0	0	0	1	0	0	0	0	0	0	0	1	0	-4	0	0	8	3	AST
NOA	0	0	0	0	0	1	0	1	0	1	0	0	0	0	0	1	1	0	0	0	0	0	0	0	0	-0	0	0	21	17	NOA
EXC	0	0	0	0	0	1	0	1	0	4	0	0	0	0	0	1	1	0	0	0	0	0	0	0	0	-1	0	0	20	11	EXC
EU	0	0	0	1	0	4	0	2	0	3	0	0	0	0	0	1	1	0	0	0	0	0	0	0	0	1	0	0	48	41	EU
	ME	MK	MT	NL	NO	PL	PT	RO	RS	RUE	SE	SI	SK	TJ	TM	TR	UA	UZ	ATL	BAS	BLS	MED	NOS	AST	NOA	BIC	DMS	VOL	EXC	EU	

Table C.13: 2014 country-to-country blame matrices for **PM2.5**.
Units: ng/m^3 per 15% emis. red. of PPM, SO_x, NO_x, NH_3 and VOC. **Emitters →, Receptors ↓.**

	AL	AM	AT	AZ	BA	BE	BG	BY	CH	CY	CZ	DE	DK	EE	ES	FI	FR	GB	GE	GR	HR	HU	IE	IS	IT	KG	KZT	LT	LU	LV	MD	
AL	320	0	3	0	28	0	11	1	1	0	4	7	0	0	5	0	6	2	0	90	6	8	0	0	46	0	1	0	0	0	0	AL
AM	0	158	0	119	0	0	1	0	0	0	0	1	0	0	0	-0	0	0	31	1	0	0	0	0	1	0	21	0	0	0	0	AM
AT	0	0	299	0	9	4	5	3	17	0	61	191	1	0	3	0	23	8	0	1	22	41	1	0	116	0	1	1	1	0	0	AT
AZ	0	20	0	454	0	0	1	0	0	0	0	1	0	0	0	0	1	0	47	1	0	0	0	0	1	0	59	0	0	0	0	AZ
BA	4	0	12	0	443	1	9	2	1	0	16	20	0	0	3	0	7	2	0	5	68	26	0	0	45	0	1	0	0	0	1	BA
BE	0	0	10	1	1	533	1	3	11	0	18	351	7	0	16	1	441	171	0	0	1	3	10	0	13	0	1	1	25	1	0	BE
BG	3	0	3	1	9	0	477	4	1	0	6	8	0	0	2	0	3	2	1	48	2	11	0	0	9	0	7	1	0	0	5	BG
BY	0	0	2	1	4	2	6	318	1	0	7	29	3	4	1	3	4	7	1	1	2	8	1	0	4	0	13	19	0	5	5	BY
CH	0	0	24	0	0	5	0	0	409	0	8	167	0	0	6	0	121	11	0	0	1	1	1	0	196	0	0	0	1	0	0	CH
CY	1	0	1	0	4	0	14	1	0	68	1	2	0	0	4	0	2	1	0	39	1	1	0	0	11	0	3	0	0	0	0	CY
CZ	1	0	97	0	16	8	8	8	10	0	446	328	2	0	5	1	45	16	0	2	18	81	1	0	31	0	2	2	2	0	1	CZ
DE	0	0	52	0	2	51	2	6	32	0	74	978	12	0	10	1	147	59	0	1	2	11	4	0	27	0	1	2	9	1	1	DE
DK	0	0	5	0	1	34	1	16	3	0	14	256	286	3	4	3	65	88	0	1	1	3	6	0	3	0	1	7	3	3	1	DK
EE	0	0	1	0	1	3	1	49	1	0	6	40	7	100	0	20	8	9	0	0	1	3	1	0	2	0	5	30	0	39	1	EE
ES	0	0	1	0	1	2	0	0	1	0	1	7	0	0	324	0	33	7	0	0	0	0	1	0	7	0	0	0	0	0	0	ES
FI	0	0	0	0	0	1	0	12	0	0	1	14	3	10	0	82	4	6	0	0	0	1	0	0	0	0	2	5	0	5	0	FI
FR	0	0	6	0	1	37	0	1	20	0	7	122	2	0	37	0	545	69	0	0	1	1	5	0	33	0	0	0	5	0	0	FR
GB	0	0	2	0	0	19	0	1	1	0	4	68	7	0	7	1	72	560	0	0	0	1	28	0	4	0	0	1	1	0	0	GB
GE	0	19	0	101	1	0	2	0	0	0	0	1	0	0	0	0	0	0	296	1	0	0	0	0	2	0	19	0	0	0	0	GE
GL	0	0	0	0	0	0	0	0	0	0	0	0	0	0	0	0	0	0	0	0	0	0	0	0	0	0	0	0	0	0	0	GL
GR	16	0	2	0	10	0	75	2	0	0	3	5	0	0	4	0	4	1	0	317	2	4	0	0	24	0	3	0	0	0	1	GR
HR	3	0	39	0	142	2	12	3	3	0	33	45	1	0	3	0	12	4	0	4	264	62	0	0	114	0	1	1	0	0	1	HR
HU	2	0	52	1	50	3	24	6	4	0	53	70	1	0	3	0	14	8	0	7	55	401	1	0	53	0	3	2	1	0	2	HU
IE	0	0	0	0	0	6	0	0	1	0	1	15	2	0	3	0	22	171	0	0	0	0	174	1	1	0	0	0	0	0	0	IE
IS	0	0	0	0	0	0	0	0	0	0	0	1	0	0	0	0	1	4	0	0	0	0	0	87	0	0	0	0	0	0	0	IS
IT	1	0	21	0	14	1	1	1	12	0	8	26	0	0	17	0	43	4	0	2	11	7	0	0	1109	0	1	0	0	0	0	IT
KG	0	0	0	1	0	0	0	0	0	0	0	0	0	0	0	0	0	0	0	0	0	0	0	0	0	153	155	0	0	0	0	KG
KZT	0	0	0	1	0	0	0	1	0	0	0	1	0	0	0	0	0	1	0	0	0	0	0	0	1	8	318	0	0	0	0	KZT
LT	0	0	3	1	4	3	3	147	1	0	13	61	11	6	1	6	9	13	1	1	2	9	1	0	4	0	7	216	0	21	3	LT
LU	0	0	16	0	1	190	1	2	17	0	24	566	3	0	15	0	464	91	0	0	1	4	6	0	16	0	0	1	143	0	0	LU
LV	0	0	2	1	2	3	2	100	0	0	9	48	7	15	1	9	9	10	0	1	1	6	1	0	3	0	6	87	0	125	2	LV
MD	1	0	3	2	3	1	44	17	1	0	7	16	1	1	1	1	4	3	2	6	1	8	0	0	5	0	16	2	0	1	190	MD
ME	45	0	4	0	61	0	7	1	1	0	5	7	0	0	3	0	5	1	0	10	9	9	0	0	34	0	1	0	0	0	0	ME
MK	52	0	4	0	14	0	57	1	1	0	6	7	0	0	4	0	4	2	0	171	4	12	0	0	17	0	2	0	0	0	1	MK
MT	2	0	3	0	9	1	4	1	2	0	3	13	0	0	30	0	39	6	0	11	2	2	0	0	112	0	0	0	0	0	0	MT
NL	0	0	11	1	1	225	1	5	9	0	29	546	16	1	16	1	267	207	0	1	1	5	11	0	13	0	1	2	10	1	1	NL
NO	0	0	0	0	0	1	0	2	0	0	1	8	4	1	0	3	4	9	0	0	0	0	1	0	0	0	0	1	0	1	0	NO
PL	0	0	13	1	11	7	5	40	3	0	70	169	7	1	2	2	21	16	0	2	6	34	1	0	13	0	5	8	1	2	3	PL
PT	0	0	1	0	0	1	0	0	0	0	1	4	0	0	129	0	13	5	0	0	0	0	0	0	3	0	0	0	0	0	0	PT
RO	2	0	5	1	12	1	68	7	1	0	9	18	0	0	2	0	5	3	1	9	4	27	0	0	13	0	8	1	0	0	15	RO
RS	15	0	12	0	59	1	62	3	1	0	18	26	1	0	3	0	7	4	0	31	20	56	0	0	23	0	3	1	0	0	2	RS
RUE	0	0	0	1	0	0	0	5	0	0	0	2	0	1	0	2	1	1	1	0	0	0	0	0	0	0	34	1	0	1	0	RUE
SE	0	0	1	0	1	4	1	9	0	0	3	40	15	3	1	9	10	14	0	0	0	2	1	0	1	0	1	5	0	3	0	SE
SI	1	0	121	0	24	2	7	2	6	0	36	65	0	0	4	0	15	4	0	2	120	41	0	0	267	0	1	1	0	0	1	SI
SK	1	0	31	1	28	3	14	8	3	0	73	72	1	0	2	0	15	7	0	4	16	187	1	0	24	0	3	2	0	1	2	SK
TJ	0	0	0	1	0	0	0	0	0	0	0	0	0	0	0	0	0	0	0	0	0	0	0	0	0	13	56	0	0	0	0	TJ
TM	0	1	0	7	0	0	0	0	0	0	0	1	0	0	0	0	0	0	1	0	0	0	0	0	1	2	127	0	0	0	0	TM
TR	0	3	1	3	2	0	10	1	0	3	1	2	0	0	2	0	1	1	2	12	0	1	0	0	5	0	4	0	0	0	0	TR
UA	0	0	2	3	2	1	13	27	0	0	5	15	1	1	1	1	3	3	2	3	1	7	0	0	3	0	23	2	0	1	14	UA
UZ	0	0	0	3	0	0	0	0	0	0	0	1	0	0	0	0	0	1	1	0	0	0	0	0	1	24	222	0	0	0	0	UZ
ATL	0	0	0	0	0	1	0	0	0	0	0	4	0	0	4	0	9	12	0	0	0	0	2	2	0	0	1	0	0	0	0	ATL
BAS	0	0	3	0	2	9	1	29	1	0	11	135	43	13	1	23	21	25	0	0	1	5	2	0	3	0	2	21	1	16	1	BAS
BLS	0	1	1	6	2	0	28	6	0	0	2	5	0	0	1	0	2	1	23	7	1	2	0	0	5	0	17	1	0	0	4	BLS
MED	2	0	3	0	15	1	13	1	1	2	3	9	0	0	30	0	32	4	0	29	4	2	0	0	91	0	2	0	0	0	0	MED
NOS	0	0	2	0	0	28	0	5	1	0	5	123	33	1	6	1	89	172	0	0	0	1	11	1	2	0	0	2	1	1	0	NOS
AST	0	1	0	9	0	0	1	0	0	1	0	0	0	0	0	0	0	0	1	2	0	0	0	0	1	2	48	0	0	0	0	AST
NOA	1	0	1	0	5	0	5	0	0	0	1	3	0	0	16	0	7	1	0	14	1	1	0	0	15	0	1	0	0	0	0	NOA
EXC	1	1	4	3	3	4	5	8	2	0	6	30	2	1	9	2	21	12	2	3	2	5	1	0	19	3	63	2	0	1	1	EXC
EU	1	0	19	0	7	18	20	11	7	0	27	146	8	3	49	8	104	57	0	12	8	21	6	0	95	0	2	7	2	4	2	EU
	AL	AM	AT	AZ	BA	BE	BG	BY	CH	CY	CZ	DE	DK	EE	ES	FI	FR	GB	GE	GR	HR	HU	IE	IS	IT	KG	KZT	LT	LU	LV	MD	

Table C.13 Cont.: 2014 country-to-country blame matrices for **PM2.5**.
Units: ng/m^3 per 15% emis. red. of PPM, SO_x, NO_x, NH_3 and VOC. **Emitters →, Receptors ↓.**

	ME	MK	MT	NL	NO	PL	PT	RO	RS	RUE	SE	SI	SK	TJ	TM	TR	UA	UZ	ATL	BAS	BLS	MED	NOS	AST	NOA	BIC	DMS	VOL	EXC	EU	
AL	40	81	0	0	0	19	0	16	138	5	0	1	4	0	0	9	15	0	1	0	1	84	1	0	6	11	5	53	870	231	AL
AM	0	1	0	0	0	1	0	1	1	20	0	0	0	0	18	149	5	15	0	0	1	2	0	96	2	11	0	10	545	7	AM
AT	1	1	0	3	0	68	0	16	28	8	1	56	26	0	0	4	20	0	1	1	0	10	4	0	1	11	1	10	1039	946	AT
AZ	0	0	0	0	0	2	0	1	1	94	0	0	0	0	45	42	16	36	1	0	1	1	0	102	0	12	0	22	826	10	AZ
BA	33	7	0	1	0	44	0	20	144	8	0	4	14	0	0	6	27	0	1	0	1	23	1	0	3	8	2	17	977	299	BA
BE	0	0	0	150	3	44	1	4	3	9	3	1	3	0	0	2	10	0	27	7	0	6	108	0	1	40	15	16	1855	1810	BE
BG	3	24	0	0	0	21	0	141	77	54	0	1	5	0	1	119	110	2	0	0	18	18	1	1	3	13	1	23	1162	741	BG
BY	1	1	0	3	1	117	0	28	9	219	3	1	7	0	2	18	215	3	1	6	2	2	4	1	0	10	2	33	1080	269	BY
CH	0	0	0	5	0	10	0	1	1	1	0	2	1	0	0	1	2	0	3	1	0	7	6	0	1	14	1	10	980	564	CH
CY	1	7	0	0	0	3	0	4	6	15	0	0	1	0	0	1018	30	1	1	0	7	209	0	48	16	16	29	66	1242	154	CY
CZ	1	3	0	8	1	222	0	34	46	19	2	16	86	0	0	9	38	0	3	3	1	7	9	0	1	16	3	15	1615	1460	CZ
DE	0	1	0	63	2	128	1	10	10	17	4	3	9	0	0	5	26	0	10	18	0	5	50	0	1	29	8	15	1766	1661	DE
DK	0	1	0	57	10	116	0	7	4	32	29	1	3	0	0	7	26	0	11	77	0	1	102	0	0	21	17	20	1104	1000	DK
EE	0	0	0	6	2	63	0	7	2	113	13	0	3	0	1	3	36	1	2	24	0	0	7	0	0	8	6	26	581	366	EE
ES	0	0	0	2	0	3	27	1	1	1	0	0	0	0	0	0	2	0	29	0	0	59	3	0	7	23	9	7	422	416	ES
FI	0	0	0	2	3	17	0	2	1	41	13	0	1	0	0	1	9	0	2	9	0	0	4	0	0	7	8	26	240	169	FI
FR	0	0	0	23	1	14	1	2	2	2	1	1	1	0	0	0	4	0	29	2	0	22	39	0	3	15	13	19	946	915	FR
GB	0	0	0	32	2	12	1	1	1	4	2	0	1	0	0	1	4	0	43	4	0	1	52	0	0	17	21	29	841	825	GB
GE	0	1	0	0	0	2	0	2	1	50	0	0	0	0	14	87	13	12	0	0	5	2	0	28	1	9	0	9	624	11	GE
GL	0	0	0	-0	0	0	0	0	0	0	0	0	0	0	0	0	0	0	0	0	0	0	0	0	0	32	1	13	1	0	GL
GR	5	63	1	0	0	12	0	23	43	20	0	1	2	0	0	77	40	1	1	0	5	122	0	0	8	12	8	61	764	482	GR
HR	7	5	0	1	0	75	0	34	155	13	1	41	24	0	0	7	38	0	1	1	1	40	2	0	3	9	3	18	1150	772	HR
HU	6	11	0	3	0	146	0	196	182	28	1	20	108	0	1	19	89	1	1	1	2	14	3	0	2	13	2	17	1626	1221	HU
IE	0	0	0	8	1	3	1	0	0	2	1	0	0	0	0	0	1	0	54	1	0	0	16	0	0	11	29	31	414	408	IE
IS	0	0	0	0	1	1	0	0	0	1	0	0	0	0	0	1	1	0	6	0	0	0	1	0	0	8	13	79	100	9	IS
IT	1	1	1	1	0	21	1	7	14	3	0	19	5	0	0	2	9	0	3	0	0	123	1	0	9	22	8	54	1369	1309	IT
KG	0	0	0	0	0	0	0	0	0	9	0	0	0	33	4	2	0	455	0	0	0	0	0	40	0	14	0	9	816	2	KG
KZT	0	0	0	0	0	2	0	1	0	162	0	0	0	2	11	2	13	53	0	0	0	0	0	15	0	12	0	40	580	7	KZT
LT	0	1	0	7	2	214	0	19	7	157	8	1	9	0	1	12	101	2	2	19	1	1	9	1	0	10	5	30	1088	642	LT
LU	0	0	0	70	2	41	1	4	3	6	2	1	4	0	0	1	10	0	17	4	0	7	48	0	2	27	9	13	1709	1664	LU
LV	0	1	0	6	2	110	0	12	5	135	9	1	5	0	1	7	69	1	2	17	1	1	7	0	0	9	5	26	812	481	LV
MD	1	2	0	1	0	61	0	252	11	128	1	1	5	0	3	79	432	4	1	1	14	5	1	1	1	12	1	25	1317	425	MD
ME	288	16	0	0	0	21	0	13	145	4	0	1	5	0	0	6	14	0	0	0	0	33	0	0	4	9	3	24	721	138	ME
MK	8	441	0	0	0	19	0	27	187	10	0	1	5	0	0	21	26	0	1	0	2	25	0	0	5	11	2	26	1106	341	MK
MT	2	4	160	1	0	8	1	4	10	2	0	2	2	0	0	3	6	0	3	0	0	393	2	0	34	19	26	99	447	405	MT
NL	0	0	0	416	3	81	2	7	4	17	5	1	5	0	0	3	18	0	27	17	0	5	176	0	1	50	16	17	1943	1878	NL
NO	0	0	0	2	41	9	0	0	1	9	8	0	0	0	0	2	4	0	5	3	0	0	7	0	0	8	15	28	113	54	NO
PL	1	2	0	11	2	814	0	40	26	64	4	4	43	0	1	13	116	1	3	10	1	3	10	0	1	15	5	22	1587	1297	PL
PT	0	0	0	1	0	2	304	0	0	1	0	0	0	0	0	0	1	0	93	0	0	10	2	0	3	25	15	4	467	464	PT
RO	3	9	0	1	0	50	0	714	61	60	1	2	11	0	1	52	177	2	1	1	11	7	1	1	1	11	1	23	1358	946	RO
RS	30	72	0	1	0	56	0	137	669	22	1	2	21	0	0	18	61	1	1	1	3	16	2	0	3	11	1	21	1439	482	RS
RUE	0	0	0	0	0	4	0	1	0	241	1	0	0	0	2	2	19	3	0	1	0	0	0	1	0	11	4	17	326	17	RUE
SE	0	0	0	7	9	34	0	2	2	21	59	0	1	0	0	2	13	0	3	15	0	0	12	0	0	8	7	28	279	218	SE
SI	1	2	0	1	0	72	0	25	60	9	1	478	17	0	0	5	26	0	1	1	1	41	2	0	2	11	2	14	1420	1281	SI
SK	3	6	0	3	1	238	0	108	86	26	1	8	441	0	0	17	83	1	1	2	1	7	3	0	1	13	2	15	1523	1254	SK
TJ	0	0	0	0	0	0	0	0	0	7	0	0	0	314	24	4	1	384	0	0	0	0	0	57	0	17	0	7	805	2	TJ
TM	0	0	0	0	0	1	0	0	0	61	0	0	0	14	251	9	10	250	0	0	0	0	0	56	0	18	0	38	740	6	TM
TR	1	4	0	0	0	4	0	7	5	25	0	0	1	0	1	1235	36	1	0	0	10	33	0	32	6	15	4	29	1376	52	TR
UA	0	1	0	1	1	65	0	65	8	228	1	1	5	0	5	51	678	6	1	2	8	3	1	2	0	12	1	26	1252	201	UA
UZ	0	0	0	0	0	1	0	0	0	70	0	0	0	51	66	5	9	740	0	0	0	0	0	23	0	21	0	33	1199	7	UZ
ATL	0	0	0	1	1	1	1	0	0	6	0	0	0	0	0	0	1	0	17	0	0	0	3	0	0	16	34	16	50	39	ATL
BAS	0	0	0	16	4	131	0	8	5	58	39	1	4	0	0	5	33	0	4	44	0	1	21	0	0	11	9	27	679	536	BAS
BLS	1	3	0	0	0	14	0	41	10	165	0	0	1	0	5	344	207	6	0	0	57	9	0	5	1	12	1	24	913	114	BLS
MED	4	6	2	1	0	11	1	7	14	9	0	2	2	0	0	157	19	0	3	0	3	316	1	8	28	17	26	101	481	251	MED
NOS	0	0	0	52	10	31	1	2	1	11	8	0	1	0	0	3	9	0	20	13	0	1	67	0	0	14	24	34	619	576	NOS
AST	0	0	0	0	0	1	0	1	0	27	0	0	0	4	23	74	7	39	0	0	0	8	0	218	2	22	2	16	244	8	AST
NOA	1	4	1	0	0	4	1	2	6	2	0	0	1	0	0	28	5	0	1	0	1	86	0	2	62	32	11	60	129	75	NOA
EXC	1	2	0	4	1	25	2	14	8	151	2	1	3	4	9	49	40	33	3	2	1	6	4	6	1	14	4	22	566	182	EXC
EU	1	4	0	18	2	102	10	56	20	25	9	7	16	0	0	13	36	0	15	7	1	26	19	0	3	16	9	24	959	828	EU
	ME	MK	MT	NL	NO	PL	PT	RO	RS	RUE	SE	SI	SK	TJ	TM	TR	UA	UZ	ATL	BAS	BLS	MED	NOS	AST	NOA	BIC	DMS	VOL	EXC	EU	

Table C.14: 2014 country-to-country blame matrices for **fine EC**.
Units: 0.1 ng/m^3 per 15% emis. red. of PPM. **Emitters →, Receptors ↓.**

	AL	AM	AT	AZ	BA	BE	BG	BY	CH	CY	CZ	DE	DK	EE	ES	FI	FR	GB	GE	GR	HR	HU	IE	IS	IT	KG	KZT	LT	LU	LV	MD	
AL	255	0	1	0	2	0	2	0	0	0	1	1	0	0	1	0	2	0	0	21	4	2	0	0	16	0	0	0	0	0	0	AL
AM	0	55	0	48	0	0	0	0	0	0	0	0	0	0	0	0	0	0	20	0	0	0	0	0	0	0	1	0	0	0	0	AM
AT	0	0	217	0	1	1	1	0	4	0	16	42	0	0	0	0	6	1	0	0	16	15	0	0	31	0	0	0	0	0	0	AT
AZ	0	4	0	182	0	0	0	0	0	0	0	0	0	0	0	0	0	0	26	0	0	0	0	0	0	0	3	0	0	0	0	AZ
BA	3	0	4	0	118	0	3	0	0	0	3	4	0	0	0	0	2	0	0	1	64	8	0	0	16	0	0	0	0	0	0	BA
BE	0	0	2	0	0	385	0	0	2	0	3	74	1	0	2	0	197	30	0	0	0	1	2	0	2	0	0	0	16	0	0	BE
BG	1	0	1	0	1	0	362	1	0	0	1	2	0	0	0	0	1	0	0	17	1	3	0	0	3	0	0	0	0	0	2	BG
BY	0	0	1	0	0	0	2	120	0	0	2	4	1	0	0	1	1	1	0	0	1	2	0	0	1	0	1	9	0	2	2	BY
CH	0	0	10	0	0	1	0	0	190	0	1	37	0	0	1	0	52	1	0	0	0	0	0	0	58	0	0	0	0	0	0	CH
CY	0	0	0	0	0	0	2	0	0	36	0	0	0	0	1	0	1	0	0	6	0	0	0	0	4	0	0	0	0	0	0	CY
CZ	0	0	33	0	1	2	3	1	2	0	216	67	1	0	0	0	13	3	0	0	11	21	0	0	7	0	0	0	0	0	0	CZ
DE	0	0	19	0	0	14	0	1	8	0	16	375	2	0	1	0	47	9	0	0	1	3	1	0	4	0	0	0	4	0	0	DE
DK	0	0	1	0	0	7	0	3	0	0	2	42	115	0	0	1	15	16	0	0	0	1	1	0	0	0	0	2	1	1	0	DK
EE	0	0	0	0	0	1	0	9	0	0	1	6	2	38	0	11	2	2	0	0	0	1	0	0	0	0	0	11	0	18	0	EE
ES	0	0	0	0	0	0	0	0	0	0	0	1	0	0	152	0	11	1	0	0	0	0	0	0	2	0	0	0	0	0	0	ES
FI	0	0	0	0	0	0	0	2	0	0	0	2	1	2	0	60	1	1	0	0	0	0	0	0	0	0	0	2	0	2	0	FI
FR	0	0	1	0	0	9	0	0	5	0	1	22	0	0	8	0	348	12	0	0	0	0	1	0	9	0	0	0	2	0	0	FR
GB	0	0	0	0	0	4	0	0	0	0	1	8	1	0	1	0	18	275	0	0	0	0	8	0	0	0	0	0	0	0	0	GB
GE	0	4	0	25	0	0	0	0	0	0	0	0	0	0	0	0	0	0	236	0	0	0	0	0	0	0	1	0	0	0	0	GE
GL	0	0	0	0	0	0	0	0	0	0	0	0	0	0	0	0	0	0	0	0	0	0	0	0	0	0	0	0	0	0	0	GL
GR	8	0	1	0	0	0	21	0	0	0	0	1	0	0	1	0	1	0	0	189	1	1	0	0	9	0	0	0	0	0	0	GR
HR	2	0	13	0	27	0	5	1	0	0	7	8	0	0	0	0	4	1	0	1	327	21	0	0	38	0	0	0	0	0	0	HR
HU	1	0	19	0	5	1	8	1	1	0	11	12	0	0	0	0	4	1	0	1	45	205	0	0	14	0	0	1	0	0	1	HU
IE	0	0	0	0	0	1	0	0	0	0	0	2	0	0	0	0	5	33	0	0	0	0	99	0	0	0	0	0	0	0	0	IE
IS	0	0	0	0	0	0	0	0	0	0	0	0	0	0	0	0	0	1	0	0	0	0	0	0	0	0	0	0	0	0	0	IS
IT	0	0	6	0	1	0	0	0	3	0	1	3	0	0	2	0	15	0	0	0	6	2	0	0	605	0	0	0	0	0	0	IT
KG	0	0	0	0	0	0	0	0	0	0	0	0	0	0	0	0	0	0	0	0	0	0	0	0	0	53	27	0	0	0	0	KG
KZT	0	0	0	0	0	0	0	0	0	0	0	0	0	0	0	0	0	0	0	0	0	0	0	0	0	2	88	0	0	0	0	KZT
LT	0	0	1	0	0	1	1	38	0	0	3	10	2	1	0	2	3	2	0	0	1	2	0	0	1	0	1	145	0	10	1	LT
LU	0	0	4	0	0	77	0	0	3	0	4	137	0	0	2	0	254	15	0	0	0	1	1	0	3	0	0	0	228	0	0	LU
LV	0	0	1	0	0	1	1	23	0	0	2	8	2	3	0	3	3	2	0	0	1	1	0	0	1	0	1	40	0	76	1	LV
MD	0	0	1	0	0	0	18	4	0	0	1	3	0	0	0	0	1	1	1	1	1	2	0	0	1	0	2	1	0	0	96	MD
ME	30	0	1	0	13	0	2	0	0	0	1	1	0	0	1	0	2	0	0	2	7	3	0	0	12	0	0	0	0	0	0	ME
MK	30	0	1	0	1	0	27	0	0	0	1	1	0	0	1	0	1	0	0	50	2	3	0	0	5	0	0	0	0	0	0	MK
MT	1	0	1	0	0	0	1	0	0	0	0	2	0	0	5	0	15	1	0	2	1	0	0	0	48	0	0	0	0	0	0	MT
NL	0	0	2	0	0	108	0	1	1	0	4	132	2	0	1	0	80	36	0	0	0	1	2	0	1	0	0	0	3	0	0	NL
NO	0	0	0	0	0	0	0	0	0	0	0	1	1	0	0	1	1	2	0	0	0	0	0	0	0	0	0	0	0	0	0	NO
PL	0	0	4	0	1	2	2	11	0	0	19	30	2	0	0	1	6	3	0	0	4	8	0	0	3	0	0	3	0	1	1	PL
PT	0	0	0	0	0	0	0	0	0	0	0	1	0	0	48	0	4	1	0	0	0	0	0	0	1	0	0	0	0	0	0	PT
RO	1	0	2	0	1	0	31	1	0	0	2	3	0	0	0	0	1	0	0	2	2	8	0	0	4	0	1	0	0	0	7	RO
RS	9	0	3	0	8	0	28	1	0	0	3	4	0	0	0	0	2	0	0	6	14	15	0	0	7	0	0	0	0	0	1	RS
RUE	0	0	0	0	0	0	0	1	0	0	0	0	0	0	0	1	0	0	0	0	0	0	0	0	0	0	5	0	0	0	0	RUE
SE	0	0	0	0	0	1	0	2	0	0	1	6	4	1	0	4	3	3	0	0	0	0	0	0	0	0	0	2	0	1	0	SE
SI	0	0	56	0	2	0	2	0	1	0	6	10	0	0	0	0	4	1	0	0	126	13	0	0	81	0	0	0	0	0	0	SI
SK	0	0	12	0	2	1	4	1	0	0	20	12	0	0	0	0	4	1	0	1	10	64	0	0	6	0	0	1	0	0	1	SK
TJ	0	0	0	0	0	0	0	0	0	0	0	0	0	0	0	0	0	0	0	0	0	0	0	0	0	3	5	0	0	0	0	TJ
TM	0	0	0	2	0	0	0	0	0	0	0	0	0	0	0	0	0	0	1	0	0	0	0	0	0	0	13	0	0	0	0	TM
TR	0	1	0	1	0	0	2	0	0	0	0	0	0	0	0	0	0	0	1	2	0	0	0	0	1	0	0	0	0	0	0	TR
UA	0	0	1	1	0	0	4	6	0	0	1	3	0	0	0	0	1	1	1	1	1	2	0	0	1	0	2	1	0	0	5	UA
UZ	0	0	0	1	0	0	0	0	0	0	0	0	0	0	0	0	0	0	0	0	0	0	0	0	0	6	35	0	0	0	0	UZ
ATL	0	0	0	0	0	0	0	0	0	0	0	0	0	0	1	0	2	3	0	0	0	0	1	0	0	0	0	0	0	0	0	ATL
BAS	0	0	1	0	0	2	0	6	0	0	2	21	13	4	0	15	5	5	0	0	1	1	0	0	1	0	0	8	0	8	0	BAS
BLS	0	0	0	1	0	0	10	1	0	0	0	1	0	0	0	0	0	0	16	2	0	1	0	0	1	0	1	0	0	0	2	BLS
MED	2	0	1	0	1	0	3	0	0	0	1	2	0	0	9	0	17	1	0	10	4	1	0	0	48	0	0	0	0	0	0	MED
NOS	0	0	0	0	0	7	0	1	0	0	1	16	6	0	1	0	24	51	0	0	0	0	2	0	0	0	0	1	0	0	0	NOS
AST	0	0	0	3	0	0	0	0	0	0	0	0	0	0	0	0	0	0	0	0	0	0	0	0	0	0	5	0	0	0	0	AST
NOA	0	0	0	0	0	0	1	0	0	0	0	0	0	0	3	0	3	0	0	2	0	0	0	0	6	0	0	0	0	0	0	NOA
EXC	1	0	2	1	0	1	3	2	1	0	2	8	0	0	4	1	11	4	1	1	2	2	0	0	9	1	14	1	0	1	0	EXC
EU	0	0	8	0	1	7	12	2	2	0	8	43	2	1	20	5	55	20	0	6	7	8	2	0	47	0	0	4	1	2	1	EU
	AL	AM	AT	AZ	BA	BE	BG	BY	CH	CY	CZ	DE	DK	EE	ES	FI	FR	GB	GE	GR	HR	HU	IE	IS	IT	KG	KZT	LT	LU	LV	MD	

Table C.14 Cont.: 2014 country-to-country blame matrices for **fine EC**.
Units: 0.1 ng/m^3 per 15% emis. red. of PPM. **Emitters →, Receptors ↓.**

	ME	MK	MT	NL	NO	PL	PT	RO	RS	RUE	SE	SI	SK	TJ	TM	TR	UA	UZ	ATL	BAS	BLS	MED	NOS	AST	NOA	BIC	DMS	VOL	EXC	EU	
AL	12	17	0	0	0	3	0	5	50	1	0	0	1	0	0	1	1	0	0	0	0	14	0	0	1	0	0	0	398	59	AL
AM	0	0	0	0	0	0	0	0	0	3	0	0	0	0	1	28	0	1	0	0	0	0	0	8	0	0	0	0	159	1	AM
AT	0	0	0	0	0	13	0	5	3	1	0	26	12	0	0	0	2	0	0	0	0	1	0	0	0	0	0	0	416	404	AT
AZ	0	0	0	0	0	0	0	0	0	22	0	0	0	0	4	5	1	4	0	0	0	0	0	32	0	0	0	0	252	1	AZ
BA	8	1	0	0	0	9	0	7	25	1	0	2	4	0	0	0	3	0	0	0	0	4	0	0	0	0	0	0	288	129	BA
BE	0	0	0	38	0	7	0	1	0	1	0	0	1	0	0	0	1	0	2	1	0	1	25	0	0	0	0	0	768	763	BE
BG	0	4	0	0	0	4	0	66	19	10	0	0	1	0	0	17	14	0	0	0	5	4	0	0	0	0	0	0	534	464	BG
BY	0	0	0	0	0	33	0	13	1	52	1	0	2	0	0	2	33	0	0	1	0	0	1	0	0	0	0	0	293	80	BY
CH	0	0	0	0	0	1	0	0	0	0	0	0	0	0	0	0	0	0	0	0	0	1	0	0	0	0	0	0	356	165	CH
CY	0	0	0	0	0	0	0	1	1	3	0	0	0	0	0	64	3	0	0	0	1	37	0	3	2	0	0	0	124	52	CY
CZ	0	0	0	1	0	73	0	12	6	3	0	5	34	0	0	1	4	0	0	0	0	1	1	0	0	0	0	0	519	501	CZ
DE	0	0	0	10	0	34	0	3	1	3	1	1	2	0	0	0	2	0	1	4	0	0	7	0	0	0	0	0	566	550	DE
DK	0	0	0	7	2	30	0	2	0	6	6	0	1	0	0	0	3	0	1	25	0	0	19	0	0	0	0	0	267	251	DK
EE	0	0	0	1	1	17	0	3	0	35	3	0	1	0	0	0	5	0	0	9	0	0	1	0	0	0	0	0	172	120	EE
ES	0	0	0	0	0	0	13	0	0	0	0	0	0	0	0	0	0	0	5	0	0	13	0	0	1	0	0	0	183	182	ES
FI	0	0	0	0	1	4	0	1	0	12	3	0	0	0	0	0	1	0	0	3	0	0	1	0	0	0	0	0	97	81	FI
FR	0	0	0	3	0	2	0	0	0	0	0	0	0	0	0	0	0	0	3	0	0	5	6	0	0	0	0	0	426	420	FR
GB	0	0	0	3	0	2	0	0	0	1	0	0	0	0	0	0	0	0	7	1	0	0	14	0	0	0	0	0	326	324	GB
GE	0	0	0	0	0	0	0	0	0	19	0	0	0	0	1	15	1	1	0	0	1	0	0	3	0	0	0	0	304	2	GE
GL	0	0	0	0	0	0	0	0	0	0	0	0	0	0	0	0	0	0	0	0	0	0	0	0	0	0	0	0	0	0	GL
GR	0	9	0	0	0	2	0	7	8	4	0	0	1	0	0	11	4	0	0	0	1	27	0	0	1	0	0	0	281	235	GR
HR	1	1	0	0	0	15	0	12	29	2	0	24	6	0	0	0	4	0	0	0	0	10	0	0	0	0	0	0	549	482	HR
HU	1	1	0	0	0	33	0	97	42	5	0	9	42	0	0	1	10	0	0	0	0	2	0	0	0	0	0	0	570	502	HU
IE	0	0	0	1	0	0	0	0	0	0	0	0	0	0	0	0	0	0	10	0	0	0	2	0	0	0	0	0	143	142	IE
IS	0	0	0	0	0	0	0	0	0	0	0	0	0	0	0	0	0	0	1	0	0	0	0	0	0	0	0	0	3	2	IS
IT	0	0	0	0	0	3	0	2	1	0	0	6	1	0	0	0	1	0	0	0	0	25	0	0	1	0	0	0	660	654	IT
KG	0	0	0	0	0	0	0	0	0	1	0	0	0	13	1	0	0	119	0	0	0	0	0	3	0	0	0	0	213	0	KG
KZT	0	0	0	0	0	0	0	0	0	25	0	0	0	1	2	0	1	16	0	0	0	0	0	1	0	0	0	0	138	1	KZT
LT	0	0	0	1	0	64	0	8	1	37	2	0	3	0	0	1	13	0	0	3	0	0	1	0	0	0	0	0	355	262	LT
LU	0	0	0	8	0	7	0	1	0	1	0	0	1	0	0	0	1	0	1	0	0	1	6	0	0	0	0	0	749	744	LU
LV	0	0	0	1	1	31	0	5	1	36	2	0	2	0	0	0	9	0	0	4	0	0	1	0	0	0	0	0	255	184	LV
MD	0	0	0	0	0	14	0	132	2	28	0	0	2	0	0	11	80	0	0	0	4	1	0	0	0	0	0	0	404	181	MD
ME	149	2	0	0	0	4	0	4	42	1	0	0	1	0	0	0	1	0	0	0	0	7	0	0	0	0	0	0	280	41	ME
MK	1	192	0	0	0	4	0	9	67	2	0	0	1	0	0	2	2	0	0	0	0	4	0	0	0	0	0	0	405	107	MK
MT	0	0	98	0	0	1	0	1	1	0	0	1	0	0	0	0	0	0	0	0	0	146	0	0	6	0	0	0	183	179	MT
NL	0	0	0	215	0	15	0	2	0	2	0	0	1	0	0	0	1	0	2	2	0	0	56	0	0	0	0	0	613	607	NL
NO	0	0	0	0	23	2	0	0	0	2	3	0	0	0	0	0	0	0	1	1	0	0	2	0	0	0	0	0	39	13	NO
PL	0	0	0	1	0	427	0	17	3	13	1	1	15	0	0	1	17	0	0	2	0	0	2	0	0	0	0	0	597	548	PL
PT	0	0	0	0	0	0	219	0	0	0	0	0	0	0	0	0	0	0	22	0	0	2	0	0	0	0	0	0	276	275	PT
RO	0	1	0	0	0	10	0	469	12	11	0	1	3	0	0	6	23	0	0	0	2	1	0	0	0	0	0	0	604	539	RO
RS	7	14	0	0	0	10	0	59	338	4	0	1	5	0	0	1	6	0	0	0	0	2	0	0	0	0	0	0	549	160	RS
RUE	0	0	0	0	0	1	0	0	0	62	0	0	0	0	0	0	3	0	0	0	0	0	0	0	0	0	0	0	77	4	RUE
SE	0	0	0	1	4	10	0	1	0	5	24	0	0	0	0	0	1	0	0	5	0	0	3	0	0	0	0	0	74	62	SE
SI	0	0	0	0	0	12	0	8	6	1	0	350	4	0	0	0	2	0	0	0	0	7	0	0	0	0	0	0	688	674	SI
SK	0	1	0	0	0	82	0	48	13	4	0	3	229	0	0	1	12	0	0	0	0	1	0	0	0	0	0	0	536	500	SK
TJ	0	0	0	0	0	0	0	0	0	1	0	0	0	201	4	0	0	101	0	0	0	0	0	29	0	0	0	0	316	0	TJ
TM	0	0	0	0	0	0	0	0	0	8	0	0	0	5	103	1	1	72	0	0	0	0	0	24	0	0	0	0	204	1	TM
TR	0	0	0	0	0	0	0	2	1	4	0	0	0	0	0	265	3	0	0	0	2	6	0	2	1	0	0	0	286	10	TR
UA	0	0	0	0	0	18	0	33	1	56	0	0	2	0	1	7	188	1	0	0	2	1	0	0	0	0	0	0	339	70	UA
UZ	0	0	0	0	0	0	0	0	0	9	0	0	0	22	19	0	1	369	0	0	0	0	0	8	0	0	0	0	462	1	UZ
ATL	0	0	0	0	0	0	1	0	0	1	0	0	0	0	0	0	0	0	4	0	0	0	1	0	0	0	0	0	11	10	ATL
BAS	0	0	0	2	1	42	0	3	1	17	11	0	1	0	0	0	4	0	0	25	0	0	4	0	0	0	0	0	177	147	BAS
BLS	0	0	0	0	0	3	0	16	2	49	0	0	0	0	0	82	33	1	0	0	20	3	0	0	0	0	0	0	224	37	BLS
MED	0	0	1	0	0	2	1	2	2	2	0	1	0	0	0	17	2	0	0	0	0	87	0	1	6	0	0	0	131	104	MED
NOS	0	0	0	8	5	7	0	1	0	2	2	0	0	0	0	0	1	0	3	3	0	0	36	0	0	0	0	0	138	129	NOS
AST	0	0	0	0	0	0	0	0	0	5	0	0	0	1	4	8	1	6	0	0	0	1	0	46	0	0	0	0	35	1	AST
NOA	0	0	0	0	0	0	0	1	1	0	0	0	0	0	0	2	0	0	0	0	0	14	0	0	13	0	0	0	23	19	NOA
EXC	0	0	0	1	1	9	1	8	2	36	1	1	1	2	3	10	8	12	0	0	0	1	1	1	0	0	0	0	170	74	EXC
EU	0	0	0	4	1	42	6	33	3	5	3	3	6	0	0	1	4	0	2	2	0	5	4	0	0	0	0	0	377	355	EU
	ME	MK	MT	NL	NO	PL	PT	RO	RS	RUE	SE	SI	SK	TJ	TM	TR	UA	UZ	ATL	BAS	BLS	MED	NOS	AST	NOA	BIC	DMS	VOL	EXC	EU	

Table C.15: 2014 country-to-country blame matrices for **coarse EC**.
Units: 0.1 ng/m^3 per 15% emis. red. of PPM. **Emitters →, Receptors ↓**.

	AL	AM	AT	AZ	BA	BE	BG	BY	CH	CY	CZ	DE	DK	EE	ES	FI	FR	GB	GE	GR	HR	HU	IE	IS	IT	KG	KZT	LT	LU	LV	MD	
AL	1	0	0	0	0	0	0	0	0	0	0	0	0	0	0	0	0	0	0	0	0	0	0	0	0	0	0	0	0	0	0	AL
AM	0	1	0	0	0	0	0	0	0	0	0	0	0	0	0	0	0	0	0	0	0	0	0	0	0	0	0	0	0	0	0	AM
AT	0	0	4	0	0	0	0	0	0	0	0	13	0	0	0	0	0	0	0	0	0	0	0	0	0	0	0	0	0	0	0	AT
AZ	0	0	0	2	0	0	0	0	0	0	0	0	0	0	0	0	0	0	0	0	0	0	0	0	0	0	0	0	0	0	0	AZ
BA	0	0	0	0	0	0	0	0	0	0	0	1	0	0	0	0	0	0	0	0	0	0	0	0	0	0	0	0	0	0	0	BA
BE	0	0	0	0	0	5	0	0	0	0	0	34	0	0	0	0	1	1	0	0	0	0	0	0	0	0	0	0	0	0	0	BE
BG	0	0	0	0	0	0	0	0	0	0	0	0	0	0	0	0	0	0	0	0	0	0	0	0	0	0	0	0	0	0	0	BG
BY	0	0	0	0	0	0	0	1	0	0	0	1	0	0	0	0	0	0	0	0	0	0	0	0	0	0	0	0	0	0	0	BY
CH	0	0	0	0	0	0	0	0	20	0	0	15	0	0	0	0	0	0	0	0	0	0	0	0	0	0	0	0	0	0	0	CH
CY	0	0	0	0	0	0	0	0	0	3	0	0	0	0	0	0	0	0	0	0	0	0	0	0	0	0	0	0	0	0	0	CY
CZ	0	0	0	0	0	0	0	0	0	0	2	28	0	0	0	0	0	0	0	0	0	0	0	0	0	0	0	0	0	0	0	CZ
DE	0	0	0	0	0	0	0	0	1	0	0	166	0	0	0	0	0	0	0	0	0	0	0	0	0	0	0	0	0	0	0	DE
DK	0	0	0	0	0	0	0	0	0	0	0	12	1	0	0	0	0	1	0	0	0	0	0	0	0	0	0	0	0	0	0	DK
EE	0	0	0	0	0	0	0	0	0	0	0	2	0	1	0	0	0	0	0	0	0	0	0	0	0	0	0	0	0	0	0	EE
ES	0	0	0	0	0	0	0	0	0	0	0	0	0	0	1	0	0	0	0	0	0	0	0	0	0	0	0	0	0	0	0	ES
FI	0	0	0	0	0	0	0	0	0	0	0	1	0	0	0	2	0	0	0	0	0	0	0	0	0	0	0	0	0	0	0	FI
FR	0	0	0	0	0	0	0	0	0	0	0	9	0	0	0	0	2	0	0	0	0	0	0	0	0	0	0	0	0	0	0	FR
GB	0	0	0	0	0	0	0	0	0	0	0	3	0	0	0	0	0	13	0	0	0	0	0	0	0	0	0	0	0	0	0	GB
GE	0	0	0	0	0	0	0	0	0	0	0	0	0	0	0	0	0	0	2	0	0	0	0	0	0	0	0	0	0	0	0	GE
GL	0	0	0	0	0	0	0	0	0	0	0	0	0	0	0	0	0	0	0	0	0	0	0	0	0	0	0	0	0	0	0	GL
GR	0	0	0	0	0	0	0	0	0	0	0	0	0	0	0	0	0	0	0	1	0	0	0	0	0	0	0	0	0	0	0	GR
HR	0	0	0	0	0	0	0	0	0	0	0	2	0	0	0	0	0	0	0	0	1	0	0	0	0	0	0	0	0	0	0	HR
HU	0	0	0	0	0	0	0	0	0	0	0	3	0	0	0	0	0	0	0	0	0	1	0	0	0	0	0	0	0	0	0	HU
IE	0	0	0	0	0	0	0	0	0	0	0	1	0	0	0	0	0	1	0	0	0	0	1	0	0	0	0	0	0	0	0	IE
IS	0	0	0	0	0	0	0	0	0	0	0	0	0	0	0	0	0	0	0	0	0	0	0	0	0	0	0	0	0	0	0	IS
IT	0	0	0	0	0	0	0	0	0	0	0	1	0	0	0	0	0	0	0	0	0	0	0	0	2	0	0	0	0	0	0	IT
KG	0	0	0	0	0	0	0	0	0	0	0	0	0	0	0	0	0	0	0	0	0	0	0	0	0	1	0	0	0	0	0	KG
KZT	0	0	0	0	0	0	0	0	0	0	0	0	0	0	0	0	0	0	0	0	0	0	0	0	0	0	1	0	0	0	0	KZT
LT	0	0	0	0	0	0	0	0	0	0	0	3	0	0	0	0	0	0	0	0	0	0	0	0	0	0	0	0	0	0	0	LT
LU	0	0	0	0	0	1	0	0	0	0	0	61	0	0	0	0	1	1	0	0	0	0	0	0	0	0	0	0	4	0	0	LU
LV	0	0	0	0	0	0	0	0	0	0	0	2	0	0	0	0	0	0	0	0	0	0	0	0	0	0	0	0	0	0	0	LV
MD	0	0	0	0	0	0	0	0	0	0	0	1	0	0	0	0	0	0	0	0	0	0	0	0	0	0	0	0	0	0	1	MD
ME	0	0	0	0	0	0	0	0	0	0	0	0	0	0	0	0	0	0	0	0	0	0	0	0	0	0	0	0	0	0	0	ME
MK	0	0	0	0	0	0	0	0	0	0	0	0	0	0	0	0	0	0	0	0	0	0	0	0	0	0	0	0	0	0	0	MK
MT	0	0	0	0	0	0	0	0	0	0	0	1	0	0	0	0	0	0	0	0	0	0	0	0	0	0	0	0	0	0	0	MT
NL	0	0	0	0	0	1	0	0	0	0	0	55	0	0	0	0	0	1	0	0	0	0	0	0	0	0	0	0	0	0	0	NL
NO	0	0	0	0	0	0	0	0	0	0	0	0	0	0	0	0	0	0	0	0	0	0	0	0	0	0	0	0	0	0	0	NO
PL	0	0	0	0	0	0	0	0	0	0	0	10	0	0	0	0	0	0	0	0	0	0	0	0	0	0	0	0	0	0	0	PL
PT	0	0	0	0	0	0	0	0	0	0	0	0	0	0	0	0	0	0	0	0	0	0	0	0	0	0	0	0	0	0	0	PT
RO	0	0	0	0	0	0	0	0	0	0	0	1	0	0	0	0	0	0	0	0	0	0	0	0	0	0	0	0	0	0	0	RO
RS	0	0	0	0	0	0	0	0	0	0	0	1	0	0	0	0	0	0	0	0	0	0	0	0	0	0	0	0	0	0	0	RS
RUE	0	0	0	0	0	0	0	0	0	0	0	0	0	0	0	0	0	0	0	0	0	0	0	0	0	0	0	0	0	0	0	RUE
SE	0	0	0	0	0	0	0	0	0	0	0	2	0	0	0	0	0	0	0	0	0	0	0	0	0	0	0	0	0	0	0	SE
SI	0	0	1	0	0	0	0	0	0	0	0	3	0	0	0	0	0	0	0	0	0	0	0	0	0	0	0	0	0	0	0	SI
SK	0	0	0	0	0	0	0	0	0	0	0	4	0	0	0	0	0	0	0	0	0	0	0	0	0	0	0	0	0	0	0	SK
TJ	0	0	0	0	0	0	0	0	0	0	0	0	0	0	0	0	0	0	0	0	0	0	0	0	0	0	0	0	0	0	0	TJ
TM	0	0	0	0	0	0	0	0	0	0	0	0	0	0	0	0	0	0	0	0	0	0	0	0	0	0	0	0	0	0	0	TM
TR	0	0	0	0	0	0	0	0	0	0	0	0	0	0	0	0	0	0	0	0	0	0	0	0	0	0	0	0	0	0	0	TR
UA	0	0	0	0	0	0	0	0	0	0	0	1	0	0	0	0	0	0	0	0	0	0	0	0	0	0	0	0	0	0	0	UA
UZ	0	0	0	0	0	0	0	0	0	0	0	0	0	0	0	0	0	0	0	0	0	0	0	0	0	0	0	0	0	0	0	UZ
ATL	0	0	0	0	0	0	0	0	0	0	0	0	0	0	0	0	0	0	0	0	0	0	0	0	0	0	0	0	0	0	0	ATL
BAS	0	0	0	0	0	0	0	0	0	0	0	6	0	0	0	0	0	0	0	0	0	0	0	0	0	0	0	0	0	0	0	BAS
BLS	0	0	0	0	0	0	0	0	0	0	0	0	0	0	0	0	0	0	0	0	0	0	0	0	0	0	0	0	0	0	0	BLS
MED	0	0	0	0	0	0	0	0	0	0	0	1	0	0	0	0	0	0	0	0	0	0	0	0	0	0	0	0	0	0	0	MED
NOS	0	0	0	0	0	0	0	0	0	0	0	5	0	0	0	0	0	2	0	0	0	0	0	0	0	0	0	0	0	0	0	NOS
AST	0	0	0	0	0	0	0	0	0	0	0	0	0	0	0	0	0	0	0	0	0	0	0	0	0	0	0	0	0	0	0	AST
NOA	0	0	0	0	0	0	0	0	0	0	0	0	0	0	0	0	0	0	0	0	0	0	0	0	0	0	0	0	0	0	0	NOA
EXC	0	0	0	0	0	0	0	0	0	0	0	4	0	0	0	0	0	0	0	0	0	0	0	0	0	0	0	0	0	0	0	EXC
EU	0	0	0	0	0	0	0	0	0	0	0	18	0	0	0	0	0	1	0	0	0	0	0	0	0	0	0	0	0	0	0	EU
	AL	AM	AT	AZ	BA	BE	BG	BY	CH	CY	CZ	DE	DK	EE	ES	FI	FR	GB	GE	GR	HR	HU	IE	IS	IT	KG	KZT	LT	LU	LV	MD	

Table C.15 Cont.: 2014 country-to-country blame matrices for **coarse EC**.
Units: 0.1 ng/m^3 per 15% emis. red. of PPM. **Emitters →, Receptors ↓.**

	ME	MK	MT	NL	NO	PL	PT	RO	RS	RUE	SE	SI	SK	TJ	TM	TR	UA	UZ	ATL	BAS	BLS	MED	NOS	AST	NOA	BIC	DMS	VOL	EXC	EU	
AL	0	0	0	0	0	0	0	0	0	0	0	0	0	0	0	0	0	0	0	0	0	1	0	0	0	0	0	0	2	1	AL
AM	0	0	0	0	0	0	0	0	0	0	0	0	0	0	0	3	0	0	0	0	0	0	0	6	0	0	0	0	5	0	AM
AT	0	0	0	0	0	2	0	0	0	0	0	0	0	0	0	0	0	0	0	0	0	0	0	0	0	0	0	0	20	19	AT
AZ	0	0	0	0	0	0	0	0	0	0	0	0	0	0	0	0	0	0	0	0	0	0	0	46	0	0	0	0	3	0	AZ
BA	0	0	0	0	0	1	0	0	0	0	0	0	0	0	0	0	0	0	0	0	0	0	0	0	0	0	0	0	3	3	BA
BE	0	0	0	1	0	1	0	0	0	0	0	0	0	0	0	0	0	0	0	0	0	0	2	0	0	0	0	0	43	43	BE
BG	0	0	0	0	0	1	0	0	0	0	0	0	0	0	0	2	0	0	0	0	0	0	0	0	0	0	0	0	4	1	BG
BY	0	0	0	0	0	6	0	0	0	0	0	0	0	0	0	0	0	0	0	0	0	0	0	0	0	0	0	0	8	7	BY
CH	0	0	0	0	0	0	0	0	0	0	0	0	0	0	0	0	0	0	0	0	0	0	0	0	0	0	0	0	35	15	CH
CY	0	0	0	0	0	0	0	0	0	0	0	0	0	0	0	7	0	0	0	0	0	2	0	3	0	0	0	0	10	3	CY
CZ	0	0	0	0	0	15	0	0	0	0	0	0	0	0	0	0	0	0	0	0	0	0	0	0	0	0	0	0	46	46	CZ
DE	0	0	0	0	0	7	0	0	0	0	0	0	0	0	0	0	0	0	0	0	0	0	0	0	0	0	0	0	175	174	DE
DK	0	0	0	0	0	6	0	0	0	0	0	0	0	0	0	0	0	0	0	2	0	0	1	0	0	0	0	0	21	20	DK
EE	0	0	0	0	0	3	0	0	0	0	0	0	0	0	0	0	0	0	0	1	0	0	0	0	0	0	0	0	6	6	EE
ES	0	0	0	0	0	0	0	0	0	0	0	0	0	0	0	0	0	0	0	0	0	1	0	0	0	0	0	0	2	2	ES
FI	0	0	0	0	0	1	0	0	0	0	0	0	0	0	0	0	0	0	0	0	0	0	0	0	0	0	0	0	3	3	FI
FR	0	0	0	0	0	0	0	0	0	0	0	0	0	0	0	0	0	0	0	0	0	0	0	0	0	0	0	0	13	13	FR
GB	0	0	0	0	0	0	0	0	0	0	0	0	0	0	0	0	0	0	0	0	0	0	1	0	0	0	0	0	16	16	GB
GE	0	0	0	0	0	0	0	0	0	0	0	0	0	0	0	2	0	0	0	0	0	0	0	3	0	0	0	0	4	0	GE
GL	0	0	0	0	0	0	0	0	0	0	0	0	0	0	0	0	0	0	0	0	0	0	0	0	0	0	0	0	0	0	GL
GR	0	0	0	0	0	0	0	0	0	0	0	0	0	0	0	1	0	0	0	0	0	2	0	0	0	0	0	0	3	2	GR
HR	0	0	0	0	0	2	0	0	0	0	0	0	0	0	0	0	0	0	0	0	0	1	0	0	0	0	0	0	7	6	HR
HU	0	0	0	0	0	5	0	0	0	0	0	0	0	0	0	0	0	0	0	0	0	0	0	0	0	0	0	0	11	11	HU
IE	0	0	0	0	0	0	0	0	0	0	0	0	0	0	0	0	0	0	1	0	0	0	0	0	0	0	0	0	3	3	IE
IS	0	0	0	0	0	0	0	0	0	0	0	0	0	0	0	0	0	0	0	0	0	0	0	0	0	0	0	0	0	0	IS
IT	0	0	0	0	0	0	0	0	0	0	0	0	0	0	0	0	0	0	0	0	0	2	0	0	0	0	0	0	3	3	IT
KG	0	0	0	0	0	0	0	0	0	0	0	0	0	2	0	0	0	14	0	0	0	0	0	1	0	0	0	0	17	0	KG
KZT	0	0	0	0	0	0	0	0	0	0	0	0	0	0	0	0	0	2	0	0	0	0	0	1	0	0	0	0	3	0	KZT
LT	0	0	0	0	0	12	0	0	0	0	0	0	0	0	0	0	0	0	0	0	0	0	0	0	0	0	0	0	16	15	LT
LU	0	0	0	0	0	1	0	0	0	0	0	0	0	0	0	0	0	0	0	0	0	0	0	0	0	0	0	0	69	68	LU
LV	0	0	0	0	0	6	0	0	0	0	0	0	0	0	0	0	0	0	0	0	0	0	0	0	0	0	0	0	9	8	LV
MD	0	0	0	0	0	2	0	0	0	0	0	0	0	0	0	1	1	0	0	0	0	0	0	0	0	0	0	0	6	3	MD
ME	0	0	0	0	0	1	0	0	0	0	0	0	0	0	0	0	0	0	0	0	0	0	0	0	0	0	0	0	2	1	ME
MK	0	1	0	0	0	0	0	0	0	0	0	0	0	0	0	0	0	0	0	0	0	0	0	0	0	0	0	0	3	1	MK
MT	0	0	2	0	0	0	0	0	0	0	0	0	0	0	0	0	0	0	0	0	0	11	0	0	0	0	0	0	3	3	MT
NL	0	0	0	4	0	3	0	0	0	0	0	0	0	0	0	0	0	0	0	0	0	0	4	0	0	0	0	0	64	64	NL
NO	0	0	0	0	0	0	0	0	0	0	0	0	0	0	0	0	0	0	0	0	0	0	0	0	0	0	0	0	1	1	NO
PL	0	0	0	0	0	95	0	0	0	0	0	0	0	0	0	0	0	0	0	0	0	0	0	0	0	0	0	0	106	105	PL
PT	0	0	0	0	0	0	1	0	0	0	0	0	0	0	0	0	0	2	0	0	0	0	0	0	0	0	0	0	1	1	PT
RO	0	0	0	0	0	1	0	0	0	0	0	0	0	0	0	1	0	0	0	0	0	0	0	0	0	0	0	0	4	3	RO
RS	0	0	0	0	0	1	0	0	3	0	0	0	0	0	0	0	0	0	0	0	0	0	0	0	0	0	0	0	6	3	RS
RUE	0	0	0	0	0	0	0	0	0	1	0	0	0	0	0	0	0	0	0	0	0	0	0	0	0	0	0	0	1	0	RUE
SE	0	0	0	0	0	2	0	0	0	0	2	0	0	0	0	0	0	0	0	0	0	0	0	0	0	0	0	0	5	5	SE
SI	0	0	0	0	0	2	0	0	0	0	0	2	0	0	0	0	0	0	0	0	0	0	0	0	0	0	0	0	8	8	SI
SK	0	0	0	0	0	15	0	0	0	0	0	0	1	0	0	0	0	0	0	0	0	0	0	0	0	0	0	0	21	21	SK
TJ	0	0	0	0	0	0	0	0	0	0	0	0	0	29	0	0	0	12	0	0	0	0	0	13	0	0	0	0	42	0	TJ
TM	0	0	0	0	0	0	0	0	0	0	0	0	0	0	17	0	0	9	0	0	0	0	0	15	0	0	0	0	27	0	TM
TR	0	0	0	0	0	0	0	0	0	0	0	0	0	0	0	36	0	0	0	0	0	0	0	1	0	0	0	0	36	0	TR
UA	0	0	0	0	0	3	0	0	0	0	0	0	0	0	0	1	2	0	0	0	0	0	0	0	0	0	0	0	7	4	UA
UZ	0	0	0	0	0	0	0	0	0	0	0	0	0	3	3	0	0	56	0	0	0	0	0	4	0	0	0	0	62	0	UZ
ATL	0	0	0	0	0	0	0	0	0	0	0	0	0	0	0	0	0	0	0	0	0	0	0	0	0	0	0	0	0	0	ATL
BAS	0	0	0	0	0	8	0	0	0	0	1	0	0	0	0	0	0	0	0	2	0	0	0	0	0	0	0	0	16	16	BAS
BLS	0	0	0	0	0	0	0	0	0	0	0	0	0	0	0	10	0	0	0	0	1	0	0	0	0	0	0	0	11	1	BLS
MED	0	0	0	0	0	0	0	0	0	0	0	0	0	0	0	2	0	0	0	0	0	6	0	1	0	0	0	0	3	1	MED
NOS	0	0	0	0	0	1	0	0	0	0	0	0	0	0	0	0	0	0	0	0	0	0	3	0	0	0	0	0	9	9	NOS
AST	0	0	0	0	0	0	0	0	0	0	0	0	0	0	1	1	0	1	0	0	0	0	0	31	0	0	0	0	2	0	AST
NOA	0	0	0	0	0	0	0	0	0	0	0	0	0	0	0	0	0	0	0	0	0	1	0	0	0	0	0	0	0	0	NOA
EXC	0	0	0	0	0	2	0	0	0	0	0	0	0	0	0	1	0	2	0	0	0	0	0	1	0	0	0	0	10	6	EXC
EU	0	0	0	0	0	9	0	0	0	0	0	0	0	0	0	0	0	0	0	0	0	0	0	0	0	0	0	0	30	29	EU
	ME	MK	MT	NL	NO	PL	PT	RO	RS	RUE	SE	SI	SK	TJ	TM	TR	UA	UZ	ATL	BAS	BLS	MED	NOS	AST	NOA	BIC	DMS	VOL	EXC	EU	

APPENDIX D

Explanatory note on country reports for 2014

For many years, country reports have been issued as a supplement to the EMEP status reports.

The country reports issued by EMEP MSC-W focus on chemical species that are relevant to eutrophication, acidification and ground level ozone, but also information on particulate matter is given. More specifically, these country reports provide for each country:

- horizontal maps of emissions, and modelled air concentrations and depositions in 2014
- emission trends for the years 2000 to 2014, and emissions in the year 2020 according to the revised Gothenburg Protocol
- modelled trends of air concentrations and depositions for the years 2000 to 2014
- maps and charts on transboundary air pollution in 2014, visualizing the effect of the country on its surroundings, and vice versa
- frequency analysis of air concentrations and depositions, based on measurements and model results for 2014, along with a statistical analysis of model performance
- maps on the risk of damage from ozone and particulate matter in 2014

EMEP MSC-W issues these country reports for 47 Parties to the Convention, and for Tajikistan, Turkmenistan and Uzbekistan. For the Russian Federation, the country report includes the territory of the Russian Federation, which is covered by the extended EMEP domain (see Figure 1.1b).

All 50 country reports are written in English. For the 12 EECCA countries, the reports are made available also in Russian. All country reports can be downloaded in pdf format from the MSC-W report page on the EMEP website `http://emep.int/mscw/mscw_publications.html`

This year, the country reports are found under the header 'MSC-W Data Note 1/2016'. The reports for each country can be selected conveniently from a drop-down menu.

APPENDIX E

Model Evaluation

The EMEP MSC-W model is regularly evaluated against various kinds of measurements, including ground-based, airborne and satellite measurements. As the main application of the EMEP MSC-W model within the LRTAP Convention is to assess the status of air quality on regional scales and to quantify long-range transboundary air pollution, the focus of the evaluation performed for the EMEP status reports is on the EMEP measurement sites.

Only parts of this evaluation are included in the printed version of the EMEP status report (see 2). A comprehensive collection of maps, graphs and statistical analyses, including a more detailed discussion of model performance, are freely available as supplementary material from the MSC-W report page on the EMEP website `http://emep.int/mscw/mscw_publications.html`

This year, the evaluation report is found under the link 'Supplementary material to EMEP Status Report 1/2016'. It contains a comprehensive evaluation of the EMEP MSC-W model for air concentrations and depositions in 2014. The report is divided into three chapters, dealing with pollutants responsible for eutrophication and acidification (Gauss et al. 2016b), ground level ozone and nitrogen dioxide (Gauss et al. 2016a), and particulate matter (Tsyro et al. 2016), respectively.

The agreement between model and measurements in 2014 is visualized as:

- scatter plots for the EMEP MSC-W model domain
- time series for individual EMEP stations
- horizontal maps combining model results and EMEP measurement data

Tables summarize common statistical measures of model score, such as bias, root mean square error, temporal and spatial correlations and the index of agreement (see Chapter 1).

This type of model evaluation is performed on an annual basis and can be downloaded from the same web page also for previous years.

References

Gauss, M., Hjellbrekke, A.-G., and Solberg, S.: Ozone, Supplementary material to EMEP Status Report 1/2016, available online at www.emep.int, The Norwegian Meteorological Institute, Oslo, Norway, 2016a.

Gauss, M., Tsyro, S., Fagerli, H., Benedictow, A. C., Hjellbrekke, A.-G., and Aas, W.: Acidifying and eutrophying components, Supplementary material to EMEP Status Report 1/2016, available online at www.emep.int, The Norwegian Meteorological Institute, Oslo, Norway, 2016b.

Tsyro, S., Gauss, M., and Hjellbrekke, A.-G.: PM10, PM2.5 and individual aerosol components, Supplementary material to EMEP Status Report 1/2016, available online at www.emep.int, The Norwegian Meteorological Institute, Oslo, Norway, 2016.

emep

Meteorological Synthesizing Centre – West
Norwegian Meteorological Institute
P.O.Box 43 – Blindern, NO-0313 Oslo, Norway

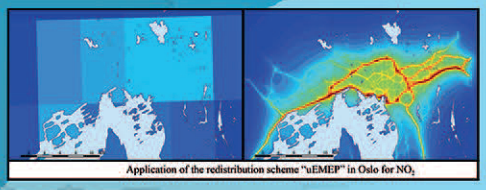

Application of the redistribution scheme "uEMEP" in Oslo for NO_2

ccc
NILU
Norwegian Institute for Air Research
P.O. Box 100
NO-2027 Kjeller
Norway
Phone: +47 63 89 80 00
Fax: +47 63 89 80 50
E-mail: kjetil.torseth@nilu.no
Internet: www.nilu.no

ciam
International Institute for
Applied Systems Analysis
(IIASA)
Schlossplatz 1
A-2361 Laxenburg
Austria
Phone: +43 2236 807 0
Fax: +43 2236 71 313
E-mail: amann@iiasa.ac.at
Internet: www.iiasa.ac.at

ceip
Umweltbundesamt GmbH
Spittelauer Lände 5
1090 Vienna
Austria
Phone: +43-(0)1-313 04
Fax: +43-(0)1-313 04/5400
E-mail:
emep.emissions@umweltbundesamt.at
Internet:
http://www.umweltbundesamt.at/

msc-e
Meteorological Synthesizing
Centre-East
2nd Roshchinsky proezd,
8/5, room 207
115419 Moscow
Russia
Phone +7 926 906 91 78
Fax: +7 495 956 19 44
E-mail: msce@msceast.org
Internet: www.msceast.org

msc-w
Norwegian Meteorological
Institute (MET Norway)
P.O. Box 43 Blindern
NO-0313 OSLO
Norway
Phone: +47 22 96 30 00
Fax: +47 22 96 30 50
E-mail: emep.mscw@met.no
Internet: www.emep.int